Role of Hypoxia-Inducible Factor 1A and Erythropoietin in Retinal Physiology and Development

---

Dissertation

zur

Erlangung der naturwissenschaftlichen Doktorwürde

(Dr. sc. nat.)

vorgelegt der

Mathematisch-naturwissenschaftlichen Fakultät der

Universität Zürich

von

Christian Caprara

von Biasca, TI

Promotionskomitee

Prof. Dr. Christian Grimm (Vorsitz und Leitung der Dissertation)

Prof. Dr. Stephan Neuhauss

Prof. Dr. Max Gassmann

Dr. Botond Roska

Zürich, 2014

Summary

Photoreceptors and other retinal cells require a considerable amount of energy in form of ATP to generate visual signals that can be decoded by the brain. To generate enough ATP for retinal function and survival, oxygen needs to be delivered efficiently to the tissue via a constant blood flow through the retinal and choroidal vascular systems. Inefficient supply of oxygen and nutrients to the retina results in tissue hypoxia or ischemia, with severe consequences on retinal function and cell survival. Consequently, cells require adjusting and responding adequately to ischemic/hypoxic conditions to preserve viability and function. Hypoxia-inducible factor 1A (HIF1A) is one of the most important transcription factors that regulate tissue response to hypoxia. It drives the expression of a large number of genes that play a role in angiogenesis, cell survival and metabolism. Protein levels of HIF1A accumulate in the early post-natal mouse retina, but the precise roles of this transcription factor in retinal development and physiology are not yet fully elucidated.

In the first part of my thesis, I show that HIF1A is not strictly necessary for the survival of the retina but is required for the complete and correct development of the retinal vasculature. The intermediate plexus of the retinal vasculature did not develop in a mouse model with a CRE-mediated *Hif1a* knockdown in the peripheral retina, despite normal tissue morphology and absence of retinal degeneration. The *Hif1a* knockdown did not affect expression of angiogenesis-related genes such as vascular endothelial growth factor a (*Vegfa*), but influenced the expression of netrin (*Ntn*) family members and components of WNT signalling. In addition, *Hif1a* knockdown robustly induced expression of erythropoietin (*Epo*), most probably by inducing the stabilization of endothelial PAS domain-containing protein 1 (hypoxia-inducible factor 2A) (EPAS1 (HIF2A)). These results suggest that HIF1A is directly or indirectly necessary for the normal development of the retinal vasculature, particularly of the intermediate plexus.

Blinding diseases, such as retinitis pigmentosa and age-related macular degeneration have harmful effects on vision due to the apoptosis of photoreceptor cells. Hypoxic preconditioning protects photoreceptors from light-induced apoptosis. Tissue protective factors such as EPO have been shown to be part of this defensive response. Due to the various neuro- and vaso-protective activities mediated in the retina, EPO has gained attention as potential therapeutic factor for

retinal degenerative diseases. However, the precise mechanisms of EPO-mediated neuroprotection of photoreceptors are still largely unknown. Also, the precise contribution of endogenously secreted EPO and downstream signalling through the EPO receptor (EPOR) in the retina has not yet been clarified.

In the second part of my thesis, I show that *EpoR* is strongly expressed by cells located in the inner and ganglion cell layer, while photoreceptors seem to express only very low levels of *EpoR*. CRE-mediated *EpoR* knockdown in rod photoreceptors or in the peripheral retina does not cause developmental defects or show signs of degeneration in adult mice. *EpoR* knockdown caused only minor but unexpected changes in gene expression and in the activation/deactivation of EPOR downstream signalling pathways. Taken together, these results suggest that EPOR downstream signalling is not necessary for correct retinal development and survival of this neural tissue.

Zusammenfassung

Photorezeptoren und andere Zellen der Netzhaut erfordern eine erhebliche Menge an Energie in Form von ATP, um optische Signale zu erzeugen, die vom Gehirn decodiert werden können. Um genügend ATP für die Funktion und den Erhalt der Netzhaut zu erzeugen, muss Sauerstoff über eine konstante Durchblutung der Netz- sowie der Aderhaut effizient zugeführt werden. Eine eingeschränkte Zufuhr von Sauerstoff und Nährstoffen führt zu Hypoxie oder Ischämie, mit schweren Folgen für die Funktion und die Integrität der Netzhaut. Daher benötigen Zellen entsprechende Möglichkeiten, um auf ischämische bzw. hypoxische Bedingungen reagieren zu können und um das Überleben und den Erhalt der Netzhautfunktion gewährleisten. Hypoxia-inducible Factor 1A (HIF1A) ist einer der wichtigsten Transkriptionsfaktoren, welche die Reaktion des Gewebes auf Hypoxie regulieren. HIF1A steuert die Expression einer Vielzahl von Genen, die z.B. in der Regulation von Angiogenese und des Stoffwechsels, sowie für das Überleben der Zelle eine wichtige Rolle spielen. Das HIF1A Protein akkumuliert in der Netzhaut der neugeborenen Maus, aber die genaue Rolle dieses Transkriptionsfaktors in Entwicklung und Physiologie der Netzhaut ist noch nicht vollständig aufgeklärt.

Im ersten Teil meiner Arbeit zeige ich, dass HIF1A für die normale Entwicklung des Gefäßsystems der Netzhaut essentiell ist, nicht jedoch für die Differenzierung und das Überleben der Zellen in der Netzhaut. , Der Knockdown von *Hif1a* in der peripheren Netzhaut verhindert die Entwicklung des intermediären Plexus des retinales Gefäßsystems, trotz einer normalen Gewebemorphologie. Der Knockdown von *Hif1a* hat keinen Einfluss auf die Expression von Angiogenese-relevanten Genen, wie Vascular Endothelial Growth Factor a (*Vegfa*), beeinflusst aber die Expression von Mitgliedern der Netrin (*Ntn*) Genfamilie und von Komponenten des WNT Signalwegs. Außerdem induziert der Knockdown von *Hif1a* die Expression von Erythropoietin (*Epo*), höchstwahrscheinlich durch die Stabilisierung von Endothelial PAS Domain-containing Protein 1 (Hypoxia-inducible Factor 2A) EPAS1 (HIF2A). Die Ergebnisse zeigen, dass HIF1A direkt oder indirekt für die normale Entwicklung des retinalen Gefäßsystems, insbesondere des intermediären Plexus notwendig ist.

Krankheiten wie Retinitis Pigmentosa und altersbedingter Makuladegeneration beinträchtigen die Sehkraft aufgrund des Verlusts von Photorezeptoren durch einen apoptotischen Zelltod. Hypoxische Präkonditionierung schützt Photorezeptoren in einem Degenerationsmodel vor Licht-induzierter Apoptose. Es wurde gezeigt, dass Faktoren wie EPO Teil dieser Schutzreaktion sind. Aufgrund der verschiedenen protektiven Aktivitäten in der Netzhaut, hat EPO die Aufmerksamkeit als möglicher therapeutischer Faktor für degenerative Netzhauterkrankungen erlangt. Allerdings sind die genauen Mechanismen der EPO-vermittelten Neuroprotektion von Photorezeptoren noch weitgehend unbekannt - besonders die spezifische Rolle des endogen produzierten und des sezernierten EPOs sowie die Signalwege über den EPO-Rezeptor (EPOR) in der Netzhaut.

Im zweiten Teil meiner Arbeit zeige ich, dass *EpoR* von Zellen in der inneren Körnerschicht und in der Ganglienzellschicht stark exprimiert wird, während Photorezeptoren *EpoR* nur auf sehr niedrigem Niveau exprimieren. Der zellspezifische Knockdown von *EpoR* in Stäbchen-Photorezeptoren oder in der den meisten Zellen der peripheren Netzhaut durch das Cre-lox System führt weder zu Entwicklungsstörungen noch zu einer Degeneration der Netzhaut. Zudem verursacht der Knockdown von *EpoR* nur geringfügige Veränderungen in der Expression von Genen welche für das EPO/EPOR Signaling relevant sind. Zusammenfassend deuten diese Ergebnisse darauf hin, dass EPOR Signaling weder für die korrekte Entwicklung der Netzhaut noch für das Überleben dieses neuronalen Gewebes notwendig ist.

Table of Contents

Summary ... **1**

Zusammenfassung ... **3**

1 Introduction ... **7**
1.1 The Retina ... 9
1.1.1 Photoreceptors ... *11*
1.1.2 Phototransduction ... *13*
1.1.3 Retinal Circuits ... *17*
1.1.4 The Retinal Pigment Epithelium ... *19*
1.1.5 The Retinoid Cycle of Vision ... *20*
1.1.6 Müller Cells ... *20*
1.1.7 Astrocytes ... *23*
1.1.8 Microglia ... *24*
1.2 Retinal Diseases ... 25
1.2.1 Age-related Macular Degeneration ... *26*
1.2.2 Retinitis Pigmentosa ... *28*
1.2.3 Mouse Models for Retinal Degeneration ... *29*
1.2.3.1 Models for Inherited Retinal Degeneration ... *29*
1.2.3.2 Light Exposure as Model for Induced Retinal Degeneration ... *30*
1.3 Oxygen in the Retina ... 32
1.3.1 The Retinal and Choroidal Vasculature ... *32*
1.3.2 The Blood-Retina Barrier ... *34*
1.3.3 Intraretinal Oxygen Profile ... *36*
1.3.4 Hypoxic Events in Retinal Development ... *37*
1.3.5 Hypoxia and Retinal Angiogenesis ... *38*
1.4 Hypoxia Inducible Factors ... 41
1.4.1 HIFs in the Retina ... *45*
1.5 Hypoxic Preconditioning ... 46
1.6 Erythropoietin ... 48
1.6.1 The Erythropoietin Receptor ... *49*
1.6.2 Tissue Protective Effects ... *51*
1.6.3 Neuroprotection in the Retina ... *52*
1.6.3.1 Protection of Retinal Ganglion Cells ... *52*
1.6.3.2 Protection of Photoreceptors ... *52*
1.6.4 Beneficial Effects in the Diabetic Retina ... *53*
1.6.5 EPO as Angiogenic Factor ... *53*

2 Aims of the thesis ... **54**

3 Materials and Methods ... **55**
3.1 Buffers and Solutions ... 55
3.2 Mice and Genotyping ... 55
3.3 RNA Isolation and cDNA Synthesis ... 57
3.4 Semi-quantitative Real-time Polymerase Chain Reaction ... 57
3.5 Western Blot Analysis ... 58
3.6 Histological Analysis and Light Microscopy ... 59
3.7 Immunofluorescence on Retinal Cryosections ... 60
3.8 Flatmount Immunofluorescence ... 61
3.9 Quantification of Vascular Coverage ... 62
3.10 Electroretinography ... 62
3.11 Hypoxic Exposure ... 62
3.12 Laser Capture Microdissection ... 63
3.13 Rhodopsin Measurements ... 63
3.14 Light Exposure and rhEPO Injections ... 64
3.15 Confocal Scanning Laser Ophthalmoscopy ... 64
3.16 Micron III Ophthalmoscopy ... 65
3.17 Spectral Domain Optical Coherence Tomography ... 65
3.18 Statistical Analysis ... 66

4 Results ... **67**
4.1 Expression of *Cre* Recombinase in *α-Cre*, *Opn-Cre*, and *Pdgfra-Cre* Mice ... 67
4.2 Genes Encoding for HIFs Are Expressed in the Mouse Retina ... 73
4.3 *Hif1a* Knockdown in the Retinal Periphery Does Not Alter Retinal Development and Survival ... 74

4.4 Knockdown of *Hif1a* in the Retinal Periphery Results in an Incomplete Development of the Retinal Vasculature ... 82
4.5 Normal Retinal Function in the Absence of HIF1A in the Retinal Periphery ... 89
4.6 *Epo* Is Upregulated in *Hif1a* Knockdown Mice ... 90
4.7 Double Knockdown of *Hif1a* and *EpoR* in the Peripheral Retina Does not Lead to Retinal Degeneration ... 92
4.8 Knockdown of *Hif1a* in Retinal Glia Does not Affect Retinal Morphology, Angiogenesis, and Resistance to Hypoxia ... 98
4.9 *Epo*, *EpoR* and *Csf2rb (βCR)* Are Expressed in Retina ... 102
4.10 Knockdown of *EpoR* in Rod Photoreceptors or in the Peripheral Retina Has no Effects on Retinal Development and Function ... 103
4.11 Intracellular Signalling and Gene Expression Upon *EpoR* Knockdown ... 111
4.12 Ablation of *EpoR* in Rods or the Peripheral Retina Does not Affect Retinal Angiogenesis ... 118
4.13 $EpoR^{flox/flox}$*;Opn-Cre* Retinas Are Constitutively Protected Against Light-induced Photoreceptor Apoptosis ... 120

5 Discussion ... 122
5.1 CRE-mediated Recombination in *α-Cre*, *Opn-Cre*, and *Pdgfra-Cre* Mice ... 122
5.2 Transcription of *Hif* Genes May Be Regulated by Hypoxia ... 125
5.3 HIF1A is Essential for the Development of the Retinal Vascular Intermediate Plexus ... 127
5.4 Search for the Molecular Basis of the Lack of the Retinal Vascular Intermediate Plexus ... 129
5.5 HIFs as Therapeutic Targets to Inhibit Pathological Retinal Angiogenesis ... 134
5.6 The Viability of the Retina Is Preserved in the Absence of HIF1A ... 136
5.7 Double Knockdown of *Hif1a* and *EpoR* in the Peripheral Retina Does not Lead to Retinal Degeneration ... 139
5.8 *Epo*, *EpoR*, and *Csf2rb (βCR)* Are Expressed in The Retina ... 140
5.9 Absence of *EpoR* Does not Affect Retinal Development, Function and Tissue Survival ... 142
5.10 Increased EPOR Signalling May Be Present in the Retina of $EpoR^{flox/flox}$*;α-Cre* Mice ... 144
5.11 Lack of *EpoR* in Retinal Glia and Neurons Does not Affect Retinal Angiogenesis ... 148
5.12 $EpoR^{flox/flox}$*;Opn-Cre* Mice Are Not Susceptible to Light-induced Retinal Degeneration ... 149

6 Concluding Remarks and Outlook ... 152

7 References ... 154

8 List of Abbreviations ... 178

9 Rights and Permissions ... 181

10 First Author Publications ... 182
10.1 HIF1A Is Essential for the Development of the Intermediate Plexus of the Retinal Vasculature ... 182
10.2 From Oxygen to Erythropoietin: Relevance of Hypoxia for Retinal Development, Health and Disease ... 192

11 Additional Publications ... 224
11.1 Retina-specific Activation of a Sustained Hypoxia-like Response Leads to Severe Retinal Degeneration and Loss of Vision ... 224
11.2 Normoxic Activation of Hypoxia-inducible Factors in Photoreceptors Provides Transient Protection Against Light-induced Retinal Degeneration ... 237
11.3 Intrinsically Photosensitive Retinal Ganglion Cells Are Resistant to N-methyl-D-aspartic Acid Excitotoxicity ... 247
11.4 CDC42 Is Required for Tissue Lamination and Cell Survival in the Mouse Retina ... 262
11.5 p38 MAPK Signalling Acts Upstream of LIF-dependent Neuroprotection During Photoreceptor Degeneration ... 276

Curriculum Vitae ... 287

Acknowledgements ... 291

1 Introduction

Organisms ranging from bacteria to humans adjust their behaviours in response to specific environmental inputs. Accordingly, for a great proportion of time, organisms actively explore the surroundings perceiving a plethora of sensory signals, which include, among others, light, sound, chemicals, and temperature. Living organisms have a varied set of tools to sense environmental clues. The ability to process sensory information is crucial for survival and for organism-environment interactions. Indeed, without this ability, the search for food, mating partners, and the ability to avoid predators would not be possible.

Vision can be considered as the most important of our senses. In fact, it has been estimated that visual inputs provide about 80% of our sensory information (Sharma and Ehinger, 2003). To allow the interaction of an organism with the outside world, vision has to function efficiently and optimally under different conditions. Blinding diseases represent therefore a tragedy for affected individuals, as their interaction with the outside world becomes dramatically impaired. The eye is the organ that is responsible for the initiation of the process of vision. It detects light stimuli and converts them into neuronal electrochemical signals by the process of phototransduction. These neural outputs are then sent, through the optic nerve, to different brain regions where the visual image gets processed. The vertebrate eye represents a spectacular product of billion of years of evolution. Charles Darwin himself realized that it seemed impossible that the process of evolution though natural selection could explain the perfection and complexity of eye anatomy and vision. The retina is the crucial tissue responsible for phototransduction, even though all anatomical parts of the eye are necessary for the process of vision. Developmentally part of the central nervous system (CNS), the retina is a multilayered neuronal tissue lining the inner part of the eyeball. The cornea and the lens, which build up the optics of the eye, focus and project an image of the visual world on the retina, which provides a similar function as a light-sensitive film in a camera. In fact, this neural tissue is able to capture incident photons and convert these inputs into electrochemical signals that can be processed by the brain. Besides acting as a light receiver, the retina also performs the first steps of image processing through neural circuits that involve different types of cells.

The nervous system needs a disproportionate large fraction of the energy production of an organism. In humans, the brain represents only 2% of the body mass, but consumes up to 20% of the oxygen required by the body under resting conditions (Mink et al., 1981). As a component of the nervous system, the retina possesses even higher energy requirements, and on a per gram basis, its oxygen consumption is higher than that of the brain (Anderson and Saltzman, 1964; Ames, 1992). But, how is this energy generated, and how can this fundamental process be potentially impaired? Cellular respiration, better known as oxidative phosphorylation, is a metabolic pathway that uses the energy gained by oxidation of nutrients to generate adenosine triphosphate (ATP): the energy currency of a cell that is required to perform its various functions (Bonora et al., 2012). Oxidative phosphorylation obtained a widespread evolutionary success because of its higher efficiency in the production of ATP compared to other metabolic pathways, such as glycolysis. The redox reactions involved in cellular respiration require an electron acceptor, usually oxygen. The concentration of oxygen found in the terrestrial atmosphere is about 21%. Under these conditions – defined as "normoxic" – generation of ATP through cellular respiration is highly efficient, and not compromised. Yet, ambient oxygen levels can vary significantly on earth, and oxygen-limited environments are not infrequent. Similarly, oxygen tension found in different tissues can be adequate for its needs or not be enough because of a higher oxygen demand compared to its supply. The organism or tissue is defined as "hypoxic" when oxygen demand exceeds its availability, while an oxygen-deprived tissue or organism is defined as "anoxic". Hypoxia, or in extreme cases anoxia, usually arises as a consequence of pathological conditions such as ischemia, haemorrhages, stroke, and others. Ischemia is defined as restriction in blood supply to tissues caused by vascular deficits. Ischemia leads to a deficiency of oxygen delivery – i.e. hypoxia or anoxia in extreme cases - and nutrients supply together with an insufficient waste removal from the extracellular space.

The aim of the introduction is to drive the reader into the fascinating field of retinal anatomy, physiology, function and disease with special regard to the contribution of oxygen, particularly hypoxia, to these processes. Special focus will be put on the cellular mechanisms involved in sensing tissue oxygenation and the reactions to hypoxia in the retina. Also, the consequences of oxygen deprivation on the function and survival of the retinal tissue will be discussed.

1.1 The Retina

The elucidation of the intricate organization of the vertebrate retina has been the scope of many vision scientists over the years. Already around 300 BC, Herophilus of Chalcedon provided the first description of the retina, which was named as such by Rufos of Ephesus (110 AD) due to its net-like appearance to hold the vitreous humour. In the 19th century, Ramon y Cajal presented the first detailed neuroanatomical descriptions of the cells that populate the retina by using the Golgi's silver nitrate staining method. Today, it is known that the retina is composed of more than 60 distinct types of neurons (Masland, 2001, 2012) that are subdivided into five main classes: photoreceptors, bipolar cells, amacrine cells, horizontal cells, and ganglion cells (Fig 1). The neural circuitry build up by neuronal cells is involved in image generation and processing by capturing incident photons and amplifying, extracting, and compressing the resulting neural signals to preserve appropriate information to be sent to higher brain regions of the visual system. These components of the visual system include parts of the midbrain, the lateral geniculate nucleus (LGN) and superior colliculus of the thalamus, the visual cortex and other cortical regions. While midbrain regions collectively process information to control eye movement, circadian photoentrainment and pupil size, the inputs to the LGN are processed for visual perception and sent to the visual cortex. Here, information about colour, shade, motion, and depth is combined to result in what we define as visual experience. In addition to neurons, glial cells that include Müller cells, astrocytes and microglia, populate the retina and are essential to support the function and survival of the tissue.

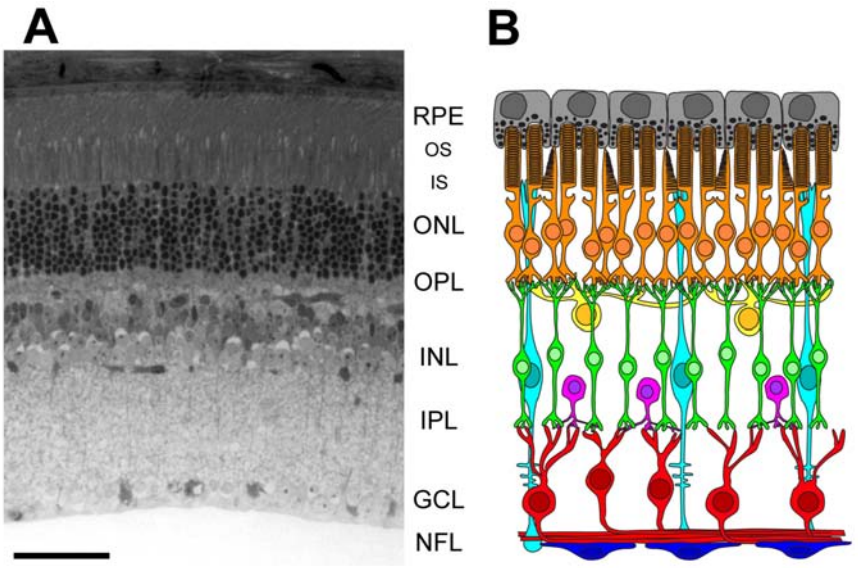

Figure 1 Simple anatomy of the mammalian retina. (A) Micrograph of a mouse retina, contrasted with osmium tetroxide and stained with toluidine blue. Scale bar: 50 µm. **(B)** Schematic and simplified representation of the major cell types populating the mammalian retina. Shown are ganglion cells (red), amacrine cells (purple), bipolar cells (green), horizontal cells (yellow), photoreceptors (orange), pigment epithelial cells (grey), Müller cells (light blue), and astrocytes (dark blue). Microglia, intrinsically photosensitive ganglion cells, and cells of the vascular system are not shown. NFL: nerve fibre layer. GCL: ganglion cell layer. IPL: inner plexiform layer. INL: inner nuclear layer. OPL: outer plexiform layer. ONL: outer nuclear layer. IS: inner segments. OS: outer segments. RPE: retinal pigment epithelium. (Figure: Caprara and Grimm, unpublished)

The mammalian retina is an orderly laminated tissue that consists of three layers of cell nuclei and somata, and two synaptic layers. The outermost retinal layer is the outer nuclear layer (ONL), which is composed of nuclei of photoreceptors: rods and cones. The inner nuclear layer (INL) is an assembly of nuclei of bipolar, horizontal, amacrine, and Müller cells. The vitreous-facing ganglion cell layer (GCL) is in turn composed of nuclei of retinal ganglion cells (RGCs) and displaced amacrine cells. The plexiform layers are the anatomical result of synapses between retinal neurons. The outer plexiform layer (OPL) is the assembly of synaptic contacts between photoreceptors, horizontal cells and bipolar cells. The inner plexiform layer (IPL) acts as a relay station for bipolar cells to connect to amacrine cells and RGCs. Furthermore, horizontally and vertically aligned amacrine cells interact in networks with both bipolar cells and RGCs. Above the inner limiting membrane (ILM) at the innermost side of the retina, RGC axons bundle to form the nerve fibre layer (NFL) (Fig. 1). These axons from all parts of the retina converge and leave the eye at the optic nerve head (ONH) to form the optic nerve.

1.1.1 Photoreceptors

Two major types of retinal neurons carry out the process of phototransduction: rod and cone photoreceptors. Rods and cones have a basic structure consisting of a cell body located in the ONL, synaptic connections to second-order neurons in the OPL, and specialized ciliary structures: inner and outer segment (IS and OS) (Fig. 2).

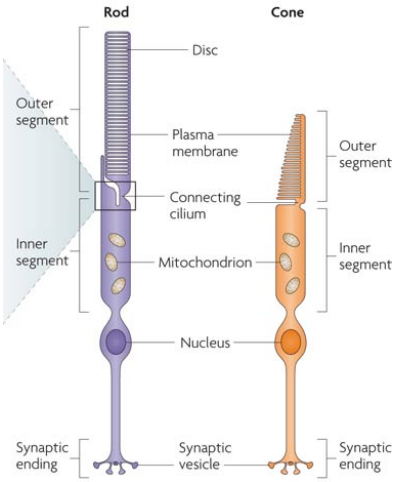

Figure 2 Rod and cone photoreceptor. Schematic representation of the structural features of a rod (left) and cone (right) photoreceptor. Outer segments are composed of disc membrane-like structures. The connecting cilium connects the outer segments to the inner segments. Inner segments contain mitochondria and the machinery to synthesize new proteins. Downstream retinal neurons synapse at the synaptic ending. (Figure: adapted from (Wright et al., 2010))

The ciliary structures fill the subretinal space and are oriented towards the RPE. Phototransduction begins in rod and cone OS, where a photon is absorbed by a molecule of visual pigment. The visual pigments are composed of an opsin protein and a chromophore – 11-*cis*-retinal - derived from vitamin A. Rods express rhodopsin (RHO) and are sensitive to blue-green light with a peak wavelength around 500 nm (Govardovskii et al., 2000). Rod photoreceptors are highly sensitive to light, being able to detect even a single photon (Baylor et al., 1979). This makes them useful for vision at low light intensities (scotopic vision), i.e. at luminance levels of 10^{-2} to 10^{-6} cd/m^2. Cone photoreceptors require higher light intensities and are thus ideal for daylight (photopic) vision that occurs at a range above roughly 3 cd/m^2. Mesopic vision, occurring at light intensities of approximately 0.001 to 3 cd m^{-2}, is a combination of scotopic and

photopic vision carried out by both the rod and cone system (Peichl, 2005). While a single type of rod photoreceptor populates the mammalian retina, two or three types of cone photoreceptors can be found. The majority of the mammalian species, excluding primates, possess dichromatic colour vision. This type of vision is based on two types of cone photoreceptors with spectrally different visual pigments: a short-wavelength-sensitive (S-) cone, and a long-wavelength-sensitive (L-) cone (Calderone and Jacobs, 1995). The primate retina is populated by an additional type of cone photoreceptor that expresses an opsin gene that evolved through the duplication of the LWS opsin gene. This gave rise to two spectrally discrete LWS opsins: M-opsin and L-opsin, expressed in M- and L-cones respectively (Wikler and Rakic, 1990; Jacobs, 1993). In the human retina, S-cones are maximally sensitive to wavelengths peaking at 437 nm (blue), M-cones at 533 nm (green), and L-cones at 564 nm (red) (Govardovskii et al., 2000). Most mammals have rod-dominant retinas, i.e. their retinas are populated predominantly by rods, with relatively few cones. For instance, the ratio of rods to cones in the mouse retina is 97:3 (Carter-Dawson and LaVail, 1979), and 95:5 in the human retina (Curcio et al., 1990). However, exclusively cones are found in the fovea, i.e. the central area of the human retina (Curcio et al., 1990).

While rod photoreceptors are more sensitive to light and function optimally under scotopic conditions, they are easily saturated and lose their sensitivity even under moderately bright conditions (Kraft et al., 1993). Rod responses to light are slow and they have a long refractory period following exposure to bright light (Gaunt, 1968; Leibovic and Pan, 1994). In contrast to rods, cones are less light sensitive, and function under bright light. However, cone responses are fast and they recover rapidly following exposure to bright light (Finkelstein and Hood, 1981; Naarendorp et al., 2010). This difference in sensitivity of rods and cones is partially caused by their different biochemical properties, such as different amounts of visual pigment and amplification factors of the phototransduction cascade (Peichl, 2005). These functional differences can also be attributed to differences in the structure of the OS (Yau, 1994; Mustafi et al., 2009). The higher light sensitivity of rods is increased further by a high convergence of the rod system onto RGCs, thereby improving the signal-to-noise ratio (van Rossum and Smith, 1998). This is possible because many rods contact a single rod bipolar cell that conveys this convergent signal to RGCs though amacrine cells (Sterling et al., 1988). A higher degree of

convergence renders the rod system an enhanced light detector, despite reducing spatial resolution. Cones have instead a close to one-to-one relationship to cone bipolar cells and RGCs, resulting in higher visual acuity (Enroth-Cugell et al., 1974, 1977). In addition, the different arrangement of the circuits that transmit rod and cone information to RGCs contributes to the different characteristics of scotopic and photopic vision.

1.1.2 Phototransduction

The OS of rods and cones are highly specialized cilia that contain the protein machinery necessary for phototransduction (Fig. 3). Rod OS enclose membranous disks stacked on top of each other. This increases the membrane surface area by about 1500-fold when compared to the plasma membrane alone, and allows photons to be efficiently absorbed as they pass through the OS (Mayhew and Astle, 1997). Cone OS differ from rod OS in several aspects. For example, cone OS are shorter and more conical than rod OS, and their discs are connected to the plasma membrane, thus making them open to the extracellular space (Braekevelt, 1983). The catalytic reactions involved in the phototransduction cascade occur at the interface of disk membranes and the OS plasma membrane. Visual pigment molecules are found at high density in OS. In rods, RHO occupies about half the membrane volume within the disks of the OS (Filipek et al., 2003).

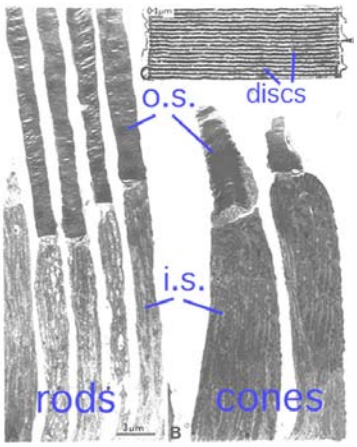

Figure 3 Inner and outer segments. Shown is an electron microscopy picture of monkey rod and cone inner (i.s.) and outer (o.s.) segments. An enlarged picture of the outer segment discs is also shown (top). (Figure: http://webvision.med.utah.edu)

Under dark conditions, rod and cone photoreceptors maintain a circulating ionic current that flows along the extracellular space from the IS to the OS (Hagins et al., 1970). This current consists of an outward K^+ ion flux across the IS membrane mediated by voltage-gated K^+ channels (Hestrin, 1987; Maricq and Korenbrot, 1990), and an inward Na^+ and Ca^{2+} ion flux across the OS membrane mediated by cyclic GMP (cGMP)-gated ion channels (Fesenko et al., 1985). This constitutes a "dark current" that partially depolarizes the photoreceptor cell (Hagins et al., 1970). As a consequence, in the absence of light, the depolarized photoreceptor cell steadily releases the neurotransmitter glutamate from its synaptic terminals.

In order to overcome an intrinsically noisy background, the signal from activated visual pigments (RHO or cone opsins) needs to be adequately amplified. The phototransduction cascade, a G-protein-based signal transduction pathway, accomplishes this task. Phototransduction starts when a photon causes *cis-trans*-isomerization of the opsin chromophore 11-*cis*-retinal in the OS, thereby inducing a conformational change of the opsin, leading to the active form R* (Rafferty, 1977; Green et al., 1977). The active form R* activates transducin, a heterotrimeric G protein, by catalyzing the exchange of guanosine diphosphate (GDP) for guanosine triphosphate (GTP) on the G protein α-subunit ($G\alpha_t$) (Fung et al., 1981; Bornancin et al., 1989). As a consequence $G\alpha_t$-GTP dissociates from the transducin $\beta\gamma$-subunits and binds to the γ-subunit of the effector protein cGMP phosphodiesterase (PDE), thereby releasing the inhibitory constraint of PDE γ-subunit on the catalytic α- and β-subunits of PDE (Stryer, 1983). The activated PDE then rapidly hydrolyzes cGMP, thereby reducing its concentration in the cytoplasm and causing cGMP-gated ion channels to close (Fig. 4). The light-induced closure of cGMP-gated ion channels reduces the inward cation current, resulting in membrane hyperpolarisation, and a transient photoresponse generated in a millisecond timeframe (Hughes and Brand, 1985). Upon closure of the cGMP-gated ion channels, the resulting hyperpolarisation decreases or shuts off the release of glutamate at the photoreceptor synaptic terminal (Nawy and Jahr, 1991). The reduced glutamate release leads to the activation of ON-bipolar cells and the inhibition of OFF-bipolar cells through excitatory or inhibitory glutamate receptors, respectively (Chapter 1.1.3) (Westheimer, 2007).

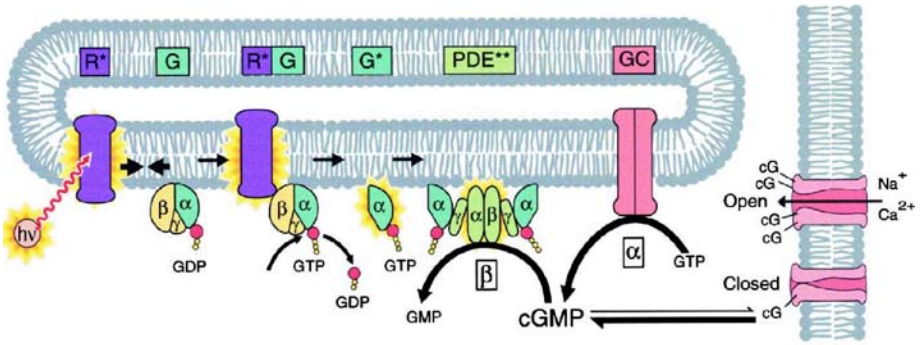

Figure 4 The phototransduction cascade. Shown is a schematic diagram of the signalling cascade activated after absorption of a photon by rhodopsin (R*). R* activates transducin (G) α-subunit by GDP/GTP exchange. The activated subunit (G*) binds to the γ-subunits phosphodiesterase (PDE**). The PDE α- and β-subunit get activated and trigger the processing of cGMP to GMP. This causes the closure of cGMP-gated cation-channels and results in the hyperpolarisation of the photoreceptor cell. cGMP is restored by the Guanylyl cyclase (GC). (Figure: adapted from (Leskov et al., 2000))

A highly significant feature of phototransduction is the enormous degree of signal amplification that takes place through the subsequent steps of the biochemical cascade. For instance, a single activated rhodopsin molecule can activate 800 transducin molecules. Each transducin molecule activates only one PDE molecule, but each of these is in turn able of catalyzing the breakdown of as many as six cGMP molecules. Eventually, the absorption of a single photon by a rhodopsin molecule leads to the closure of approximately 200 cGMP-gated ion channels. This causes a net change in the membrane potential of about 1 mV (Chen, 2005).

After light stimulation, an appropriate recovery of the photoreceptor is indispensable to respond anew to incoming photons and to be able to signal rapid changes in illumination. First, the bleached visual pigment has to be regenerated in the visual cycle (Chapter 1.1.5) and second, the photoresponse has to be rapidly terminated through the action of one or more regulatory enzymes. One of these enzymes, rhodopsin kinase, phosphorylates each active form R* at multiple C-terminal sites, with each added phosphate partially reducing the rate with which the active form R* can activate transducin (Maeda et al., 2003). After the addition of three phosphates, arrestin binds to the active form R* with high affinity, completely blocking subsequent transducin activation (Kuhn and Wilden, 1987). Likewise, transducin and PDE remain active until transducin hydrolyzes GTP, a step catalyzed by the RGS9 protein complex (He et al., 1998; Anderson et al., 2009). Finally, cGMP levels are restored through the action of

guanylate cyclase (GC) allowing the cGMP-gated ion channels to reopen (Kawamura and Murakami, 1989) (Fig. 4).

Equally crucial is the fact that the weight of phototransduction amplification varies with the level of illumination, a phenomenon known as light adaptation. Even though the phototransduction cascade possesses high sensitivity at low light levels, incident photons must continue to generate useful signals also when the mean light level increases by many orders of magnitude. If the sensitivity would be constant, the response amplitude would reach the maximal level at relatively modest light levels. Indeed, increasing illumination is accompanied by a decreasing sensitivity. This phenomenon deeply extends the range of light intensities over which photoreceptors can operate. These incremental responses vary linearly with the increment of light intensity, and thus, under natural conditions, phototransduction continues to operate linearly in this sense (Vu et al., 1997). The drop in intracellular Ca^{2+} concentration upon light exposure helps to coordinate light adaptation. Several Ca^{2+}-binding proteins sense the reduction of intracellular Ca^{2+} concentration. Among these, GC-activating proteins (GCAP) stimulate cGMP synthesis by GC when Ca^{2+} concentration falls, thus creating a feedback mechanism by which cGMP synthesis increases as the Ca^{2+} concentration is reduced. This eventually helps the cGMP-sensitive channels to rapidly reopen (Stephen et al., 2008). A second calcium-binding protein is recoverin. Ca^{2+}-bound recoverin inhibits the ability of rhodopsin kinase to phosphorylate the active form R* (Klenchin et al., 1995; Chen et al., 1995). The third mechanism is represented by the sensitivity of cGMP-gated channels to calmodulin or calmodulin-like proteins. When Ca^{2+} levels fall in light, calmodulin dissociates from the channel and thereby increases the channel sensitivity to cGMP, thus allowing the channel to operate at a lower cGMP concentration under light exposure than under dark conditions (Hsu and Molday, 1993; Chen et al., 2010a). Another different type of adaptation mechanism induced by sustained light involves translocation of several phototransduction proteins between the OS and the rest of the photoreceptor cell. Upon light exposure, and over a time course of several minutes, significant fractions of transducin and recoverin exit rod OS while arrestin translocates into the rod OS (Artemyev, 2008; Slepak and Hurley, 2008).

1.1.3 Retinal Circuits

Light-evoked signals from rod and cone photoreceptors are transferred onto bipolar cells. In general, two types of bipolar cells exist: ON (ON-center) and OFF (OFF-center) bipolar cells. This categorization (valid also for RGCs, see below) refers to the receptive field, i.e. the region in space in which a stimulus can alter the firing of a neuron. ON bipolar cells depolarize (are activated) when light is in their receptive field and hyperpolarize (are deactivated) when light is in the surrounding region. On the contrary, OFF bipolar cells hyperpolarize (are deactivated) when light is in the center of their receptive field and depolarize (are activated) when light is in the surround (Berntson and Taylor, 2000).

A further step in early processing of the light stimulus is performed by horizontal cells, which provide lateral interaction in the outer retina. They exert lateral inhibition on neighbouring bipolar cells that surround the central region of highest response to light. This inhibition plays important roles in early image processing, such as the generation of center-surround receptive fields that increase spatial discrimination (Thoreson and Mangel, 2012).

Rod photoreceptors synapse one type of bipolar cell. The rod bipolar cells are ON bipolar cells, express the metabotropic glutamate receptor 6 (*mGluR6*) (Vardi and Morigiwa, 1997), and are depolarized by a light stimulus (Euler and Masland, 2000). Rod bipolar cells do not send signals directly into RGCs but synapse with AII and A17 amacrine cells, which integrate inputs from many rod bipolar cells (Bloomfield and Dacheux, 2001). AII amacrine cells form gap junctions onto ON cone bipolar cells and inhibitory synapses onto OFF cone bipolar cells. In turn, these cone bipolar cells synapse onto RGCs (Vardi and Smith, 1996). A17 amacrine cells are required to modulate and amplify the signal from AII amacrines (Menger and Wassle, 2000). This wiring map is the “classical rod pathway” of the mammalian retina (DeVries and Baylor, 1995) (Fig. 5). However, recent advances in the field have demonstrated that alternative routes can transmit the rod signal, for example through gap junctions between rods and cone pedicles (DeVries and Baylor, 1995).

In contrast to rods, transmission of the cone signal involves two classes of cone bipolar cells: ON and OFF bipolar cells. OFF cone bipolar cells express ionotropic (AMPA (-amino-3-hydroxy-5-methyl-4-isoxazole propionic acid) and kainate) glutamate receptors, while ON cone

bipolar cells express the metabotropic glutamate receptor *mGluR6* (Nomura et al., 1994; Vardi et al., 2000). OFF cone bipolar cells are hyperpolarized by light stimuli, and ON cone bipolar cells are depolarized. OFF cone bipolar cells transfer their signals onto OFF RGCs, whereas ON cone bipolar cells synapse onto ON RGCs (Fig. 5). Consequently, OFF RGCs are excited by stimuli that are darker than the background, and ON RGCs spike by stimuli that are brighter than the background (Balasubramanian and Sterling, 2009). The ON and OFF pathways have evolved to rapidly process images that become visible as a consequence of either light increment or light decrement. The ON pathway processes images that become visible following light augmentation and the OFF pathway processes images that become visible after light decrement (Schiller, 2010).

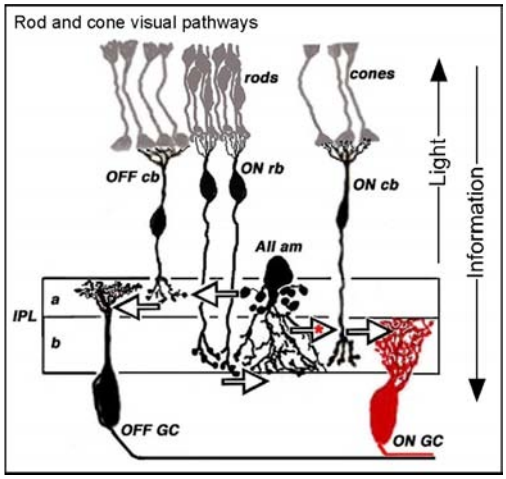

Figure 5 Transmission of the rod and cone signal. Schematic diagram representing the rod and cone pathway through the retina. OFF cone bipolar (cb) cells synapse with OFF ganglion cells (GC) at the inner plexiform layer (IPL) strata a. ON cone bipolar cells synapse with ON ganglion cells at IPL strata b. ON rod bipolar (rb) relay light information through gap junctions (white arrow with red star) between AII amacrine (AII) and ON cb cells, to ON ganglion cells. White arrows represent the chemical synapses between different neurons in the IPL. (Figure: adapted from Nelson R and Kolb H Visual Neurosciences Vol 1 [31]).

Beside the classification of RGCs to either the ON or OFF pathways, a classification based onto dendritic morphology identifies additional RGC subclasses. For instance, M-type RGCs (also known as alpha or parasol RGCs) have bigger cell bodies and larger receptive fields than other RGC subtypes (Dacey, 1993; Silveira et al., 2004). M-type RGCs are responsible for motion detection (Schiller et al., 1990), are more sensitive to contrast stimuli (Kaplan and Shapley, 1986), and are responsive to visual inputs that change rapidly over time by responding with a

transient burst of action potentials (Hicks et al., 1983). P-type RGCs (also known as beta or midget RGCs) have smaller cell bodies and smaller receptive fields than M-type cells. P-type RGCs mediate visual acuity and colour detection (Merigan, 1989; Merigan et al., 1991). They are sensitive to high-frequency spatial stimuli and respond with a sustained discharge of action potentials as long as the stimulus is present (Hicks et al., 1983; Silveira et al., 2004).

Beside rods and cones, the mammalian retina contains a third class of photoreceptor: the intrinsically photosensitive retinal ganglion cell (ipRGC). These photosensitive RGCs express the photopigment melanopsin (encoded by the *Opn4* gene) and transmit irradiance information to the brain, influencing several functions such as circadian photoentrainment, pupillary light reflex, sleep and possibly some aspects of vision (Munch and Kawasaki, 2013).

1.1.4 The Retinal Pigment Epithelium

The retinal pigment epithelium (RPE) is a single layer of hexagonal cells that is located between the OS of photoreceptors and the choroid. RPE cells are heavily pigmented as a consequence of the production of melanin. The main and most obvious function of RPE pigmentation is the absorption of scattered light (Sarna, 1992). However, melanin granules also contribute as line of defence against free radicals produced by the phagocytosis of photoreceptor OS, photo-oxidative exposure, and light energy (Winkler et al., 1999; Beatty et al., 2000).

The RPE is also involved in the recycling of retinoids. For example, it is essential for the regeneration of 11-*cis* retinal in the visual cycle, a fundamental duty to enable a continuous visual experience. For this intention, all-*trans* retinal is delivered from rod photoreceptors to RPE cells, re-isomerised to 11-*cis* retinal, and transported back to photoreceptors (Chapter 1.1.5) (Baehr et al., 2003). In addition, RPE cells are also responsible for the phagocytosis of the OS of photoreceptors, which go through a constant cycle of shedding and renewing to prevent overaccumulation of lipid and protein damage due to photo-oxidation (LaVail, 1976, 1983). Another role of the RPE is the establishment of the outer blood-retina barrier (BRB) through tight junctions between neighbouring RPE cells (Chapter 1.3.2).

1.1.5 The Retinoid Cycle of Vision

When the visual pigment gets exposed to intense or prolonged levels of light, a significant amount of it gets "bleached", i.e. activated, and can no longer absorb an additional photon. It can then take tens of minutes for the visual sensitivity to return under normal conditions (Lamb and Pugh, 2004). This very slow retrieval of visual sensitivity is known as "dark adaptation", to distinguish it from the faster process of light adaptation. The recovery of visual sensitivity is associated with the retinoid cycle of regeneration of the visual pigment. In order to detect an additional photon, the opsin molecule needs to replace the all-*trans* retinoid by a new molecule of 11-*cis* retinal (Pepperberg et al., 1976). After being released from the opsin moiety, the isomerised all-*trans* retinoid undergoes a series of reactions inside and outside the photoreceptor cell to eventually be reconverted back into the 11-*cis* isomer, which can then recombine with the opsin protein moiety to catch an additional photon. The retinoid cycle involves a series of reactions catalyzed by membrane-bound enzymes found in rod and cone OS and eventually in the RPE, where 11-*cis* retinal is regenerated (for a detailed description of the retinoid cycle and enzymes involved in the process see (Tang et al., 2013) and (Saari, 2012)). A growing body of evidences suggests that for cones an alternative and slightly different visual cycle exists that involves Müller cells (Schonthaler et al., 2007).

1.1.6 Müller Cells

Müller cells represent the main glia population of the retina. Their nuclei are found in the INL while their radial processes span the entire retina, and thus provide architectural support to the tissue (Fig. 6). Towards the vitreous, the basal lamina of Müller cell endfeet forms the ILM, and junctional complexes at their extensions at the basis of photoreceptor inner segments build the outer limiting membrane (OLM). Moreover, Müller cell processes also project laterally to surround retinal neurons (Bringmann et al., 2006).

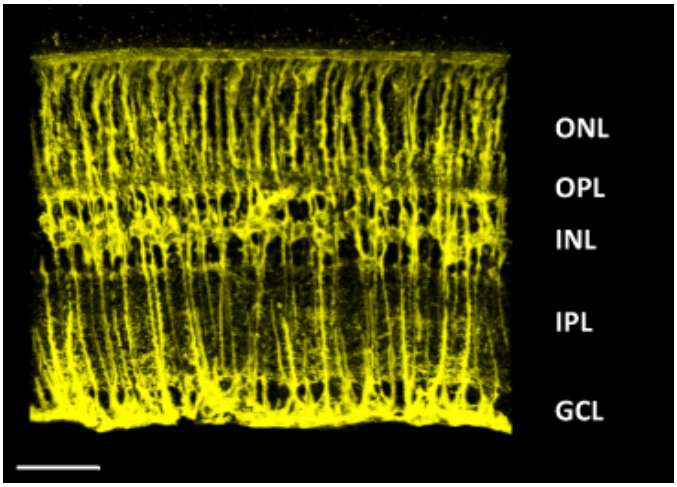

Figure 6 Müller cells. Shown is an immunostaining for GLUL (GS) (yellow) on a cryosection from a mouse retina, staining Müller cells. ONL: outer nuclear layer; OPL: outer plexiform layer, INL: inner nuclear layer; IPL: inner plexiform layer; GCL: ganglion cell layer. Scale bar: 50 μm (Figure: Caprara, unpublished)

Müller cells are in a symbiotic connection with neurons, and are vital to their health and function. The glial supportive functions are carried out in many different ways. For example, Müller cells contain glycogen stores and can therefore supply end products of anaerobic metabolism through breakdown of glycogen, in order to increase aerobic metabolism in neurons (Magalhaes and Coimbra, 1970; Reichenbach et al., 1993). In fact, Müller cells have a specialized energy metabolism, which is very different from neurons that mainly rely on oxidative phosphorylation (Magistretti and Pellerin, 1999). As other glia cells, Müller cells use mainly glycolysis for the generation of ATP, even in the presence of sufficient oxygen (Poitry-Yamate et al., 1995; Pellerin et al., 2007). Intriguingly, this different metabolism of Müller glia versus neurons results in a so-called "metabolic symbiosis". The glycolytic metabolism of Müller cells results in the production and release of lactate, which is converted into pyruvate and used by neurons as substrate in the Krebs cycle (Poitry-Yamate et al., 1995; Tsacopoulos et al., 1998). This is a beneficial interaction between neurons and glia, as Müller cells can get rid of an end product of their metabolism – lactate – by feeding neurons, and neuronal cells can rely on Müller cells to inactivate the end product of neuronal metabolism – CO_2 – by the action of carbonic anhydrase (Sarthy and Lam, 1978; Deitmer, 2002).

Müller glia also support neurons by maintaining a correct local microenvironment. This is achieved by controlling tissue homeostasis, for instance, by buffering extracellular CO_2 variations (Newman, 1994), by taking up extracellular potassium and redistributing it (Bringmann et al.,

1997; Kofuji et al., 2002; Skatchkov et al., 2006), by regulating retinal water homeostasis (Bringmann et al., 2004), and by clearing up neuronal waste products, such as ammonia (Marcaggi and Coles, 2001). In addition to molecular waste products, Müller cells also clear up debris from dead neurons by phagocytosis (Francke et al., 2001). A vital neuroprotective role of Müller glia is represented by their contribution to the defence against free radicals. Müller cells synthesize glutathione from glutamate, cysteine, and glycine (Pow and Crook, 1995; Reichelt et al., 1997). Reduced glutathione is delivered to neurons to act as a scavenger of free radicals and reactive oxygen species (ROS) (Schutte and Werner, 1998). An important observation is that during hypoxia the glutathione levels in Müller cells decrease very strongly (Huster et al., 2000). This lack of glutathione may boost the intraretinal concentration of oxygen-derived free radicals (Burstedt et al., 2009).

The supportive contributions of retinal radial glia are also fundamental for optimal function of the retina. Müller cells are mediators of the removal and recycling of different neurotransmitters (Bringmann et al., 2009), e.g. γ-aminobutyric acid (GABA) (Sarthy, 1982) and glutamate (White and Neal, 1976). Removal of excessive glutamate is accomplished through the expression of glutamate transporters (Peng et al., 1995) and high levels of glutamine synthetase (GS, expressed by the *Glul* gene in the mouse) (Fig. 6), the enzyme that converts glutamate into glutamine (Riepe and Norenburg, 1977). This task is fundamental, as excessive extracellular accumulation of glutamate can lead to excitotoxicity, in particular to RGCs (Ferreira et al., 1996; Izumi et al., 2002).

Müller cells express intermediate filaments, which are immunoreactive for vimentin, and to some degree also to glial fibrillary acidic protein (GFAP). Under various pathological conditions, both vimentin and GFAP are strongly upregulated and distributed throughout the glial cell body (Guerin et al., 1990; Erickson et al., 1992). This is part of the so-called “gliosis”: a general response to nearly every pathological alteration of the retina, under which glia cells become “activated”. Here, Müller cells can produce pro-inflammatory cytokines and in this way can act as modulators of immune and inflammatory responses (Caspi and Roberge, 1989; Drescher and Whittum-Hudson, 1996). Early after injury, gliosis is thought to be neuroprotective, as a result of the release of neurotrophic factors and antioxidants (Schutte and Werner, 1998;

Frasson et al., 1999). However, at later stages gliosis can become detrimental for neuronal cell survival (Bringmann et al., 2006).

1.1.7 Astrocytes

Astrocytes are the second main glia population found in the retina. They have a morphology characterized by a flattened cell body and radial processes filled by intermediate filament proteins such as GFAP (Schnitzer, 1988b) (Fig. 7). These glia invade the retina through the optic nerve during development (Watanabe and Raff, 1988), and eventually become restricted to the NFL, where they surround RGCs, nerve fibres, and superficial retinal blood vessels (Provis, 2001) (Fig. 7). Astrocyte density and morphology vary through the retina. Their density peaks at the ONH, where they have an elongated cell shape. Their abundance uniformly declines towards the retinal periphery were they assume a symmetrically stellate morphology (Schnitzer and Karschin, 1986; Karschin et al., 1986). They are not present in the avascular fovea of the human retina (Schnitzer, 1988a).

The close association of astrocytes to RGC axons and blood vessels suggests that these cells form axonal and vascular glial sheaths and contribute to the formation of the BRB (Gardner et al., 1997; Makarov et al., 2000) (Chapter 1.3.2). In addition, astrocytes are thought to play a crucial role in the development of the retinal vasculature in rodents (Fruttiger, 2007) and primates (Gariano et al., 1996). At the functional level, astrocytes share many common roles with Müller cells. For example, astrocytes play a role in ionic homeostasis by the regulation of extracellular K^+ levels (Bay and Butt, 2012). They are also known to contain abundant stores of glycogen and may support retinal physiology by providing glucose to neurons (Pfeiffer-Guglielmi et al., 2005).

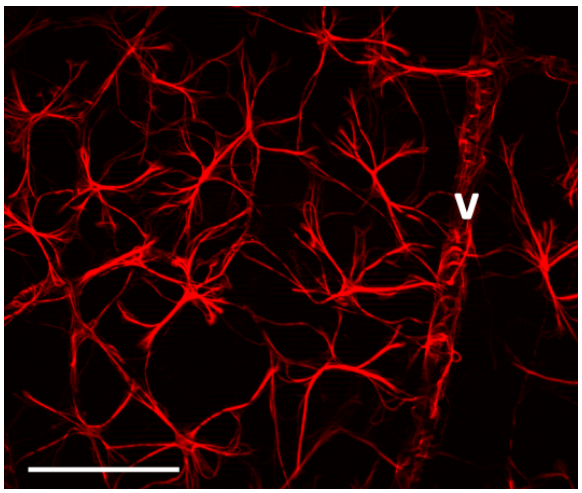

Figure 7 Retinal astrocytes. Shown is an immunostaining for GFAP (red) on a retinal flatmount, staining astrocytes found on the NFL. Note glial processes wrapping a retinal vessel (v). Scale bar.100 μm. (Figure: Caprara, unpublished)

1.1.8 Microglia

Microglia are the third glia cell population resident in the retina, and are characterized by a multipolar and ramified morphology, with relatively small cell bodies and irregular processes (Kohno et al., 1982). Microglia precursors are of mesodermal origin and migrate into the retina during late embryonic development and in the early post-natal stage (Barron, 1995). During this developmental time, microglia migrate in a central-to-peripheral fashion in the NFL, to then translocate intraretinally and form a dense network mainly localized in the plexiform layers (Hume et al., 1983). Nowadays, microglia cells are considered to be part of the phagocyte system of the CNS, including the retina (Oehmichen, 1982), and play important functions in immune surveillance and neuronal homeostasis (Hanisch, 2002; Streit, 2002; Hanisch and Kettenmann, 2007). Ramified "resting" microglia constantly survey their microenvironment carrying out active tissue scanning, monitoring the retinal environment with their very motile protrusions to get rid of metabolic products and neuronal debris (Nimmerjahn et al., 2005) (Fig. 8). "Resting" microglia in the healthy retina express low levels of co-stimulatory molecules and show a relatively low phagocytic activity (Dick et al., 2003). However, following a very large array of retinal injuries and neurodegenerative pathologies, microglia become activated (Schuetz and Thanos, 2004). Following activation, microglia undergo a morphological transition from ramified cells to amoeboid phagocytes (Fig. 8). This is accompanied by a strong proliferation, enhanced

migration, phagocytosis, expression of macrophage markers (e.g. F4/80), and production of different biologically active molecules, including cytokines, chemokines and inflammatory molecules (Hume et al., 1983; Streit, 2002; Hanisch, 2002; van Rossum and Hanisch, 2004; Zeng et al., 2005). Under pathological conditions, microglia may be involved significantly in the initiation and perpetuation of neurodegeneration (Zeng et al., 2005).

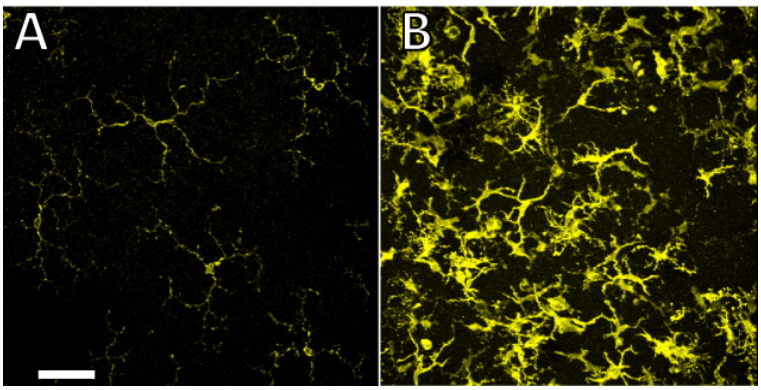

Figure 8 "Resting" and activated microglia. Shown is an immunostaining for the microglial marker ionized calcium-binding adapter molecule 1 (IBA1) on retinal flatmounts from dark-adapted **(A)** and light exposed **(B)** mice at 5 days after light exposure. Note the extended ramified morphology of microglia in the unexposed retina compared to the rounded morphology after light damage, in addition to the accumulation of microglia at the site of damage. Scale bar: 100µm (Figure: Caprara, unpublished).

1.2 Retinal Diseases

The retina is a complex tissue and the process of vision involves a multitude of different proteins. Hence, much can go wrong and have dramatic effects for vision. Human blinding diseases are an increasing global problem. Population-based surveys have shown an increase in the number of blind people worldwide from 28 million to 45 million in a time frame of 17 years from 1978 to 1995 (Foster and Resnikoff, 2005). The major blinding diseases in the world are cataract, glaucoma, diabetic retinopathy (DR), and age-related macular degeneration (AMD) (Rosenberg and Sperazza, 2008).

Cataract is the most common cause of blindness worldwide (Foster and Johnson, 1990). This disease refers to lens opacities that interfere with visual function. Opacification of the lens

obstructs light from passing and being focused on the retina, and can lead to loss of vision (Quillen, 1999). Glaucoma is the second principal cause of blindness worldwide (Quigley and Broman, 2006). This disease is a progressive optic neuropathy characterized by loss of RGCs and thinning of the NFL. Increased IOP is often found in glaucoma and is a known cause of RGC degeneration, but normal-tension glaucoma with RGC loss is also frequently observed. DR is the leading cause of loss of sight in the western world and is a secondary cause of diabetes mellitus. DR develops as a consequence of vasoregression induced by hyperglycemia and results in retinal hypoxia. This eventually leads to the activation of angiogenic genes and subsequent neovascularisation in the retina (Aiello et al., 1994; Chen et al., 2013). In contrast to the aforementioned retinal diseases, AMD and retinitis pigmentosa (RP) are mainly characterized by loss of vision due to photoreceptor cell death.

Here, I will address AMD and RP in more detail since these are diseases of most interest in our lab.

1.2.1 Age-related Macular Degeneration

AMD is the primary cause of vision loss in the elderly (Gehrs et al., 2006). Many risk factors have been associated with AMD, including aging (Klein et al., 2010), smoking (Smith et al., 1996), genetic predisposition (Edwards et al., 2005; Tolppanen et al., 2009), obesity (Adams et al., 2011), hypertension (van Leeuwen et al., 2003), hypercholesterolemia (Reynolds et al., 2010), and light exposure (Cruickshanks et al., 1993). AMD pathogenesis is characterized by a progressive loss of central vision due to degenerative and neovascular changes in the macula that result in disturbance of fine and colour vision. AMD can be separated into an early and late phase, as well as into dry and exudative forms (Bressler et al., 1988). The dry stage of AMD is characterized by the accumulation of soft and hard drusen and geographic atrophy (Fig. 9). Oxidative stress, as a result of increased ROS production, may damage lysosomal membranes in RPE cells, impairing their phagocytotic capacity and leading to the (over)accumulation of lipofuscin in senescent RPE cells (Terman and Brunk, 2004; Kurz et al., 2008). Since lipofuscin may augment ROS production on its own, its accumulation may lead to a vicious cycle accelerating AMD progression (Boulton et al., 1993; Sparrow et al., 2003)(reviewed in

(Khandhadia and Lotery, 2010)). Altogether, these events may ultimately lead to the neovascular/exudative form of AMD, which is most harmful for patients (Bressler et al., 1988). The neovascular/exudative stage of AMD is characterized by the process of choroidal neovascularisation (CNV), i.e. the growth of new, leaky vessels that penetrate Bruch's membrane from choroidal capillaries and grow into the RPE and the neural retina (Bressler et al., 1988) (Fig. 9). Disturbed ocular and retinal hemodynamics have been described in both phases of AMD (Friedman et al., 1995) (reviewed in (Harris et al., 1999)), and reduction in choroidal blood flow has been correlated to increased severity of the disease (Grunwald et al., 1998, 2005). This is thought to result in tissue hypoxia and activation of gene expression that may contribute to CNV (Grunwald et al., 2005; Metelitsina et al., 2008; Pournaras et al., 2008).

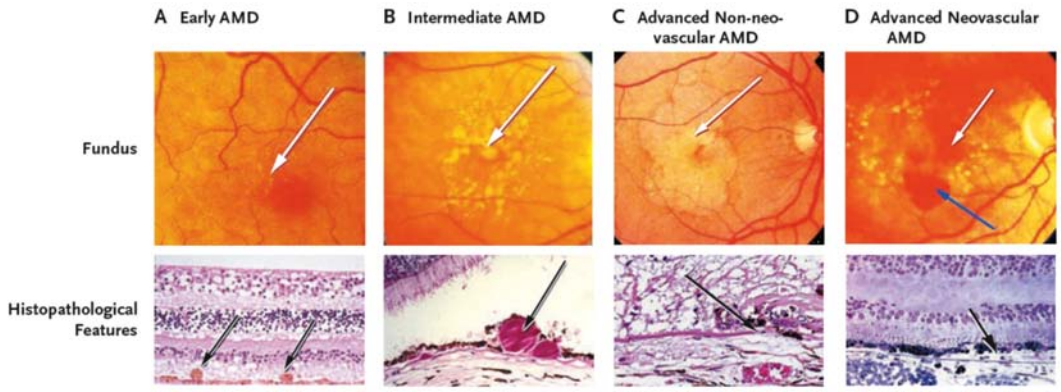

Figure 9 Stages of AMD Shown are fundus and histology images of different clinical stages of AMD. During early AMD **(A)** small and medium-sized drusen can be noticed (white and black arrows). During intermediate AMD **(B)** large drusen are formed (black arrow). These appear as enlarged yellowish dots in the fundus (white arrow). Dry AMD **(C)** is characterized by geographic atrophy (white arrow) in the center of the macula and the loss of Bruch's membrane (black arrow). In neovascular (wet) AMD **(D)** neovascular growth of leaky vessels (white and black arrow) causes haemorrhages (blue arrow). (Figure: reproduced with permission from (Jager et al., 2008), Copyright Massachusetts Medical Society).

Nowadays, several strategies are employed to reduce AMD symptoms and disease progression. A low fat diet accompanied by antioxidant supplementation may delay the transition into advanced stages of the disease (Jager et al., 2008). The majority of therapeutical products on the market today are designed for the treatment of wet AMD. The most recent approaches involve intravitreal injection of antiangiogenic components targeting vascular

endothelial growth factor A (VEGFA), such as ranibizumab (Lucentis, Genentech) and bevacizumab (Avastin, Genentech) (Kodjikian et al., 2013).

1.2.2 Retinitis Pigmentosa

RP is a heterogeneous group of inherited retinal diseases that result in photoreceptor apoptosis, leading to severe vision impairment and often blindness. RP has been estimated to be responsible for vision loss in 1 in 4000 people worldwide (Sung and Chuang, 2010). The various modes of inheritance include autosomal-dominant, autosomal-recessive, X-linked, as well as mitochondrial (Hamel, 2006). Autosomal dominant RP (adRP) accounts for 30%–40% of all cases of RP, and is therefore the most common mode of inheritance (Dinculescu et al., 2005). Mutations in more than 60 genes have been identified and play a causative role in RP (a list of genes can be found in http://ghr.nlm.nih.gov/condition/retinitis-pigmentosa). Mutations in the *RHO* gene, in the usher syndrome 2A gene (*USH2A*) and in the retinitis pigmentosa GTPase regulator gene (*RPGR*) account for 30% of all RP cases (Hartong et al., 2006). About one fourth of all patients suffer from associated, non-ocular diseases. These are described by more than 30 different syndromes. The two main forms are Usher and Bardet-Biedl syndrome (Hartong et al., 2006).

The genetic heterogeneity of RP is also reflected by differences in disease onset, progression rate and severity. RP initially starts as an apoptotic degeneration of rod photoreceptors and the main symptoms include progressive loss of visual function leading to night blindness, reduced peripheral vision and narrowing of the visual field (Fig. 10). Most forms of RP involve degeneration of both rod and cone photoreceptors, and usually loss of rods precedes loss of cones. In some cases, rods and cones are lost simultaneously, while in cone-rod dystrophies cone degeneration precedes loss of rods (Birch et al., 1999). After the initial stages, diffusion of pigmentary deposits, thinning of retinal vessels, and decrease in retinal function are observed (Hamel, 2007, 2006).

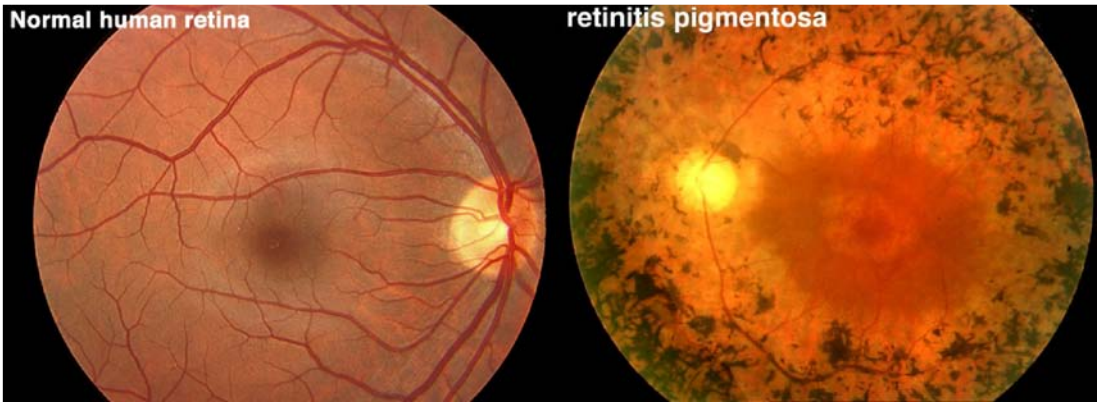

Figure 10 Fundus image of RP patient Shown is the fundus photography of a healthy patient (left panel) and a patient affected by RP (right panel). The dark lesions in the fundus of RP patient represent the pigment of RPE cells that migrate in degenerated regions due to the absence of photoreceptor cells. (Figure: adapted from http://webvision.med.utah.edu)

Nowadays, RP is still considered as an incurable disease. Nevertheless, several strategies are being used or are being developed to slow the progression, or eventually treat this pathology. Among them, dietary supplementation with Vitamin A palmitate has shown to reduce the progression rate of the disease (Berson et al., 1993). Other strategies, including gene therapy, and treatments with trophic factors are in clinical trials (Cideciyan et al., 2008). Further promising approaches, including cell transplantation, retinal prostheses, and optogenetics, are under investigation (Lund et al., 2003; Weiland et al., 2011; Lagali et al., 2008).

1.2.3 Mouse Models for Retinal Degeneration

The majority of the knowledge and understanding about the molecular mechanisms involved in the pathophysiology of different retinal diseases has come from studies performed in animals. Several models are available and can be subdivided into two major groups: induced and inherited models for retinal degeneration.

1.2.3.1 Models for Inherited Retinal Degeneration

The need for an efficient therapy for RP has led to the identification of animals with spontaneous mutations and the creation of several mammalian models mimicking this disease and revealing the molecular mechanisms at the basis of inherited photoreceptor degeneration.

Mouse models of RP include, among others, retinal degeneration (*rd*)1 (Bowes et al., 1990), *rd10* (Chang et al., 2007), *VPP* (Naash et al., 1993), and retinal degeneration slow *(rds)* mouse (Travis et al., 1989). *Rd1* and *rd10* mice carry a recessive nonsense or missense mutation, respectively, in the β-subunit of the *Pde* gene, resulting in either a rapid degeneration with early onset (*rd1*) or slower retinal degenerative process at later onset (*rd10*). The *VPP* mouse expresses a rhodopsin transgene encoding a dominant mutant protein with three amino acid substitutions (V20G, P23H, P27L), resulting in photoreceptor apoptosis beginning at two weeks after birth and progressing over several weeks. The *rds* mouse contains a 10 kb insertion in the middle of the peripherin/rds gene and OS in these mice appear abnormal and shortened resulting in a progressive death of photoreceptors, starting around two/three weeks after birth (Ma et al., 1995).

It is relatively difficult to find appropriate models mimicking AMD. In fact, a human-like macula can be found only in primates, and animals need to survive for a long lifespan to develop an age-related disease such as AMD. Nevertheless, a limited number of mouse models partially mimicking some features of the disease exist. For example, transgenic mice that express a mutant form of human elongation of very long chain fatty acids protein 4 *(ELOVL4)* show RPE changes, including vacuolization, accumulation of debris in the subretinal space, and pigment granule deposits (Karan et al., 2005).

1.2.3.2 Light Exposure as Model for Induced Retinal Degeneration

Retinal degeneration can be induced by many different exogenous stimuli, including among others *N*-methyl-*N*-nitrosourea (MNU), iron, led or calcium overload, or treatment with autoantibodies (Samardzija et al., 2010).

Light damage is an experimental model used to induce apoptosis of photoreceptors (Portera-Cailliau et al., 1994). Compared to the many genetic models mimicking RP, the light damage model has the advantage that the timing and intensity of the stimulus triggering retinal degeneration can be adjusted to meet experimental needs. This allows the induction of the degeneration at the age of choice and the control of the extent of photoreceptor death. Furthermore, exposure to toxic levels of light induces a synchronized burst of photoreceptor apoptosis, facilitating the analysis of the molecular events of the initiation, progression and

termination of the degeneration. The cell death program initiated by light exposure can be divided into 4 phases: induction, death signal propagation, execution and clearance of photoreceptor debris. At 12 hours after light exposure, pyknotic nuclei appear, and the peak of photoreceptor apoptosis is approximately after 36 hours (Wenzel et al., 2005). After induction of apoptosis, activated retinal microglia and blood-derived macrophages invade the retina and clear photoreceptor debris (Joly et al., 2009). By 10 days after light exposure, almost no photoreceptor nucleus is left in the damaged area (Fig. 11).

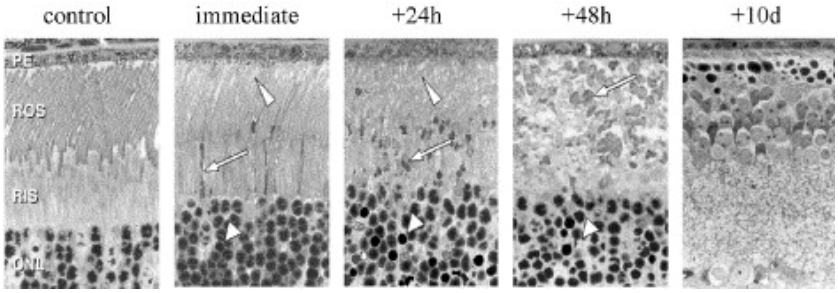

Figure 11 Light-induced retinal degeneration. The time course of morphological changes in photoreceptors after exposure to intense toxic levels of white light is shown. Already immediately after light exposure, first pyknotic nuclei (short arrowheads) and condensed inner segments or apoptotic bodies (arrows) are noticed. Rod outer segments are vesiculated (long arrowheads). More pyknotic nuclei appear and rod outer and inner segments disintegrate with increasing time after light exposure. 10 days following light exposure, photoreceptor cells are mostly cleared from the retina. PE: pigment epithelium, ROS: rod outer segments, RIS: rod inner segments, ONL: outer nuclear layer. (Figure: (Wenzel et al., 2005)):

Studies investigating the molecular mechanisms of light-induced photoreceptor apoptosis revealed that light damage depends on the visual cycle. In fact, *Rpe65*$^{-/-}$ (retinal pigment epithelium 65) mice have a compromised visual cycle and are resistant to light-induced photoreceptor apoptosis (Grimm et al., 2000). Mice carrying a methionine instead of leucine at position 450 of the *Rpe65* gene, have a slower rhodopsin regeneration kinetic and are less sensitive to light damage (Wenzel et al., 2001). In addition, mice anesthetized with halothane are resistant to light-induced photoreceptor apoptosis. This is due to prevention of rhodposin regeneration by the competition of halothane with 11-*cis*-retinal for binding to the opsin molecule (Keller et al., 2001).

1.3 Oxygen in the Retina

Photoreceptors consume much of the energy required for the process of vision. Preservation of the correct ion gradients, by extrusion of Na^+ ions in OS, and Na^+ and Ca^{2+} in the IS, depletes most of ATP stores and leads to a single rod consuming up to 10^8 ATP s^{-1} under dark conditions (Okawa et al., 2008). Photoreceptors mainly generate ATP through the process of oxidative phosphorylation (Ames et al., 1992). Therefore the retina demands high levels of oxygenation and prompt delivery of nutrients to generate sufficient ATP for proper photoreceptor function, especially under dark conditions when the highest rate of ion pumping is needed (Stefansson et al., 1983; Haugh et al., 1990). As a consequence, the retina is one of the tissues with the highest metabolic rate (Ames et al., 1992), and its rate of oxygen consumption is faster than that of any other tissue (Kimble et al., 1980; Weiter and Zuckerman, 1980; Anderson and Saltzman, 1964; Ames, 1992). The levels of energy expenditure are very different under photopic conditions, where, as a result of the decreased ion influx, photoreceptors reduce their rate of ion pumping and require much less ATP. In fact, the total consumption of ATP drops by more than 75% when a retina gets exposed to bright light (Okawa et al., 2008).

1.3.1 The Retinal and Choroidal Vasculature

A tightly balanced and constant blood flow through a vascular system is of fundamental importance to ensure an appropriate delivery of oxygen and nutrients to a tissue. For this reason, it is not surprising that the high energy-demanding retinal tissue is supplied by very sophisticated vascular beds, providing adequate blood perfusion to meet the metabolic needs of the retina. In vascularised retinas, oxygen and nutrients are delivered through two separate systems: the choroidal and the retinal vasculature. The ophthalmic artery delivers blood to the choroidal vessels, which are responsible for the nourishment of the outer retina. The central retinal artery and the short posterior ciliary arteries supply the retinal vasculature that delivers oxygen and nutrients to the inner retina. Venous ocular outflow occurs predominantly via the vortex veins and the central retinal vein.

The extent of vascular coverage is variable among mammalian species. For example, the retina of rodents, primates, and cats is highly vascularised, while rabbits possess a partially

vascularised and guinea pigs a completely avascular retina. Avascular retinas rely only upon the choroidal vasculature for the diffusion of oxygen to the inner retina. In addition, the number of parallel intraretinal capillary plexi found in vascularised retinas can differ among species. For instance, in the primate and rat retina, a superficial vascular plexus is found on the NFL/GCL and is interconnected with a deep capillary plexus in the OPL (Kur et al., 2012). The mouse retina instead has an additional intermediate capillary plexus found at the inner margin of the INL (Fruttiger, 2007) (Fig. 12). In addition, the primate retina is avascular in the fovea, in order to permit undisturbed light penetration in this region of high acuity vision (Gariano, 2010).

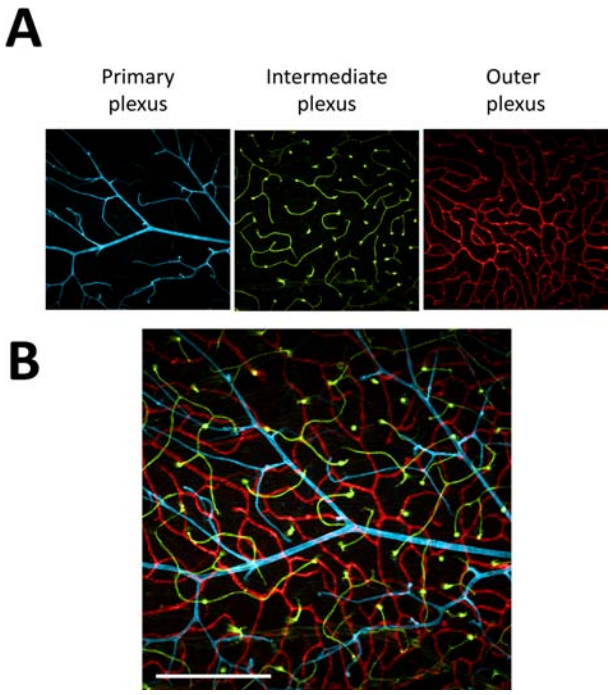

Figure 12 Capillary plexi of the mouse retinal vasculature. Immunostaining of vessels on a retinal flatmount from 129S6/Tac wt mice, stained with isolectin IB_4. **(A)** Images of the different capillary plexi in flatmounts were taken by adjusting the focal plane of the confocal microscope accordingly. Vessels of the different vascular plexi are highlighted by artificial colouring (primary plexus: blue; intermediate plexus: green; outer plexus: red). **(B)** Merged picture from (A). Scale bar: 200 μm. (Figure: Caprara and Grimm, unpublished)

The circulation properties of the choroidal and retinal vascular beds have significant differences. The retinal vasculature has sophisticated autoregulatory mechanisms to oxygen fluctuations (Flammer and Mozaffarieh, 2008), and a high arteriovenous oxygen gradient. The highly vascularised choroid has limited autoregulatory responses, and has only a minor difference in the arteriovenous oxygen concentration (Pournaras et al., 2008).

1.3.2 The Blood-Retina Barrier

A tight homeostatic regulation of the retinal microenvironment is fundamental for an optimal tissue function, as well as for cell survival. A misregulated tissue milieu may be causative or contributory to the etiology of different disease of the retina. The BRB represents a central player in the control of the local homeostasis of the neural tissue of the eye. Like its cerebral counterpart - the blood-brain barrier (BBB) – the BRB controls fluid and molecular movement between the vasculature and the tissue microenvironment. This prevents the potentially harmful leakage of macromolecules and damaging agents into the retina, and regulates the removal of waste products. The BRB can be subdivided into an internal component – the inner BRB (iBRB) – formed by tight junctions between capillary endothelial cells of retinal vessels (Shakib and Cunha-Vaz, 1966), and an outer component – the outer BRB (oBRB) - where tight junctions are formed between RPE cells (Cunha-Vaz, 1979). Capillary endothelial cells of the retinal vascular bed are surrounded by a basal lamina that separates them from pericytes, astrocytes and processes of Müller cells, all cells that are thought to contribute to iBRB integrity (Ashton, 1965; Reichenbach et al., 2007). Among them, pericytes maintain the capillary structure, support and communicate to endothelial cells, and regulate vascular tone and regional blood flow (Sims, 1991; Frank et al., 1990; Bandopadhyay et al., 2001). The pericyte coverage density of retinal capillaries has been reported to be higher than in other parts of the CNS (Frank et al., 1990). Furthermore, the ratio of pericytes to endothelial cells in the retina is higher than in any other vascular bed (Balabanov and Dore-Duffy, 1998).

The oBRB is an important physiological barrier that regulates the otherwise free flow of molecules between the permeable choriocapillaries and the outer retina. RPE cells and the Bruch's membrane separate fenestrated choriocapillaries from the neuroretina (Cunha-Vaz, 1978). The barrier function includes the isolation of the retina from systemic influences at the side of the choroid, thus representing an important contribution to the immune privilege of the eye (Benhar et al., 2012). It also controls a highly selective and regulated transverse transport of molecules between the choroidal side and the subretinal space. This epithelial transport provides nutrients to photoreceptors (Ban and Rizzolo, 2000), manages the ion homeostasis in the

subretinal space (Wimmers et al., 2007) and removes water and metabolites from the retina (Hamann, 2002).

The stability of the BRB depends on the correct function and viability of its cellular components. For that reason, the integrity of the BRB can be lost under ischemic / hypoxic conditions, when cell function and survival are put under pressure (Kaur et al., 2008). Loss of pericytes, and the consequent disruption of the iBRB, is an early event in DR (Ejaz et al., 2008). Also, dysfunction of Müller cells may contribute to a BRB breakdown in different pathological conditions (Tretiach et al., 2005). Under hypoxic conditions, the iBRB is disrupted (Kaur et al., 2007) and vascular permeability is enhanced (Josko and Knefel, 2003), eventually leading to oedema. The enhanced secretion of the vascular permeability factor VEGFA by Müller cells is a main determinant of BRB breakdown and vascular leakage (Eichler et al., 2000; Tretiach et al., 2005). This is exacerbated by a reduced production of pigment epithelium-derived growth factor (PEDF, encoded by the *Serpinf1* gene in mice), a VEGFA antagonist secreted by Müller glia in hypoxia (Duh et al., 2002). In addition, under hypoxic and ischemic conditions, astrocyte and Müller cell swelling occurs as a result of altered ionic homeostasis, production of free radicals and energy failure (Bringmann et al., 2005). Swelling of glial cells is associated with vascular leakage in the hypoxic retina (Stepinac et al., 2005). Additionally, also increased nitric oxide (NO) production by upregulation of inducible NO synthase (iNOS, encoded by the *Nos2* gene in mice) under hypoxic conditions correlates with disruption of the iBRB (El-Remessy et al., 2003; Kaur et al., 2006).

In contrast to the iBRB, the oBRB seems to be much more resistant to ischemic / hypoxic insults. No appreciable changes can be seen in tight junctions of the oBRB, although RPE cellular changes are observed under reduced oxygen tension (Johnson and Foulds, 1978; Kaur et al., 2007). Even though the oBRB appears to be resistant to hypoxia, the barrier becomes unstable when other factors such as oxidative stress are involved (Jiang et al., 2000). This has been reported in macular oedema in AMD (Vinores et al., 1999).

1.3.3 Intraretinal Oxygen Profile

Oxygen tension profiles in the retina reflect the spatial arrangement of the retinal and choroidal vascular bed, the degree of perfusion, and the oxygen utilization rates of different cell types. The intraretinal oxygen distribution in mammalian species with vascularised retinas, such as pigs (Pournaras et al., 1989), cats (Alder et al., 1983), rats (Cringle et al., 1991; Yu et al., 1994), and monkeys (Ahmed et al., 1993; Yu et al., 2005) have been measured using oxygen-sensitive microelectrodes and appear very similar among each other. For example, in rats the profile of oxygen distribution across the retinal layers and the choroid is heterogeneous. Here, the highest oxygen tension is found in the choroid, showing a considerable drop throughout the photoreceptor layer, with an almost vertical gradient towards the IS. This steep gradient reflects the high oxygen consumption rate of these neurons together with the localization of mitochondria in photoreceptor IS (Linsenmeier, 1986; Yu et al., 1994; Cringle et al., 2002). The two plexiform layers are the dominant oxygen consuming layers in the inner retina, as they also contain a high number of mitochondria (Yu et al., 2007; Yu and Cringle, 2001). As a consequence, the high-energy demand in these synaptic layers causes the oxygen tension profile to drop. The presence of the primary vascular plexus towards the vitreal side of the retina causes oxygen tension to finally increase again at the GCL (Yu et al., 1994) (Fig. 13).

This general picture can vary to some degree, and the control of oxygen supply to the outer retina can be dynamic, especially under conditions of highest ATP consumption by photoreceptors, e.g. in darkness (Linsenmeier, 1986). Under these circumstances, the high oxygen consumption rate of photoreceptors significantly increases the risk of hypoxia, especially under pathological conditions, such as disturbed oxygen diffusion from the choroid, as in AMD (Stefansson et al., 2011).

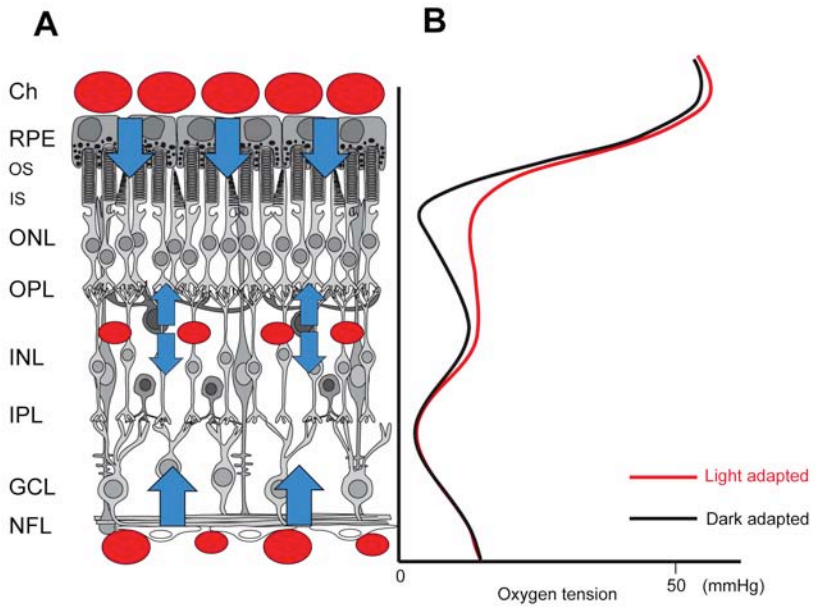

Figure 13 Oxygen distribution profile of the rat retina. (A) Schematic illustration of the position of the capillary plexi (red) - the superficial plexus (found in the NFL) and the deeper capillary plexus (located at the outer boundary of the INL) - and the directions of oxygen diffusion (blue arrows). Ch: Choroid, RPE: retinal pigment epithelium, photoreceptor outer (OS) and inner (IS) segments, ONL: outer nuclear layer, OPL: outer plexiform layer, INL: inner nuclear layer, IPL: inner plexiform layer, GCL: ganglion cell layer, NFL: nerve fibre layer. **(B)** Intraretinal oxygen distribution profile of a rat retina. The oxygen distribution profiles of a light-adapted (red line) and a dark-adapted (black line) rat retina are shown. The y-axis follows the section through the retina shown in A). (Figure: (Caprara and Grimm, 2012))

To maintain sufficient oxygenation, photoreceptors may increase oxygen exploitation from the intraretinal capillaries and/or use the autoregulatory ability of the retinal vasculature to compensate for the increased oxygen demand in times of high ATP consumption (Feke et al., 1983).

1.3.4 Hypoxic Events in Retinal Development

Photoreceptors are the major cell population in the retina and their demand for oxygen is extremely elevated (Chapter 1.3). In rodents, photoreceptors are generated post-natally from retinal progenitor cells (RPCs) and retinal activity begins only after lamination and synaptic connectivity is completed (Reese, 2011). Retinal activity is linked to an increase in oxidative metabolism, an event that occurs before the retinal vasculature has fully developed (Graymore, 1959), hence before the optimal supply of oxygen can be guaranteed. As a consequence, the retina may experience a physiological period of chronic hypoxia during post-natal development,

timely limited to the period of the start of neuronal function and the end of retinal angiogenesis (Chan-Ling et al., 1995). Therefore, the ratio between oxygen consumption and supply can vary considerably depending upon on the developmental stage and age of the retinal tissue.

1.3.5 Hypoxia and Retinal Angiogenesis

The vascular system that feeds the inner retina has to undergo remarkable reorganization during development in order to support neuronal survival and to meet the increased demand for oxygen as retinal neural activity begins. The embryonic inner retina is nourished by the hyaloid vasculature that fills the interior of the optic cup. This embryonic vascular system is replaced by the retinal vasculature during development (Saint-Geniez and D'Amore, 2004). In the human foetus, this switch takes place at around 18 weeks of gestation. In mice, rats and other non-primate mammals, the retinal vasculature develops post-natally. Therefore, the mouse and rat retina have become an attractive model tissue to study angiogenic processes. In fact, the retina in newborns is an easy accessible tissue for both imaging and experimentation, in contrast to embryonic studies, which are *per se* more experimentally challenging (Stahl et al., 2010).

Preceding the development of the retinal vasculature, astrocytes migrating from the ONH invade the retina, proliferate and spread in a radial fashion across the NFL towards the retinal periphery (Stone and Dreher, 1987; Watanabe and Raff, 1988; Ling et al., 1989). As an end result, an astrocytic meshwork is generated that eventually acts as a template for the development of the vessels of the primary plexus by providing a glial template to guide the migration of vascular endothelial cells (Stone et al., 1995; Jiang et al., 1995; Zhang and Stone, 1997; Fruttiger et al., 1996; Dorrell et al., 2002). Accordingly, the vessels of the primary plexus also grow in a centrifugal manner from the ONH, reaching the periphery within the first post-natal week in mice (Connolly et al., 1988). The emergent “physiological hypoxia” that occurs in the developing retina (see above) is a crucial event regulating the development of the retinal vasculature. Three lines of evidence support an oxygen-dependent regulation of angiogenesis in the retina. First, the timing and central-to-peripheral course of the angiogenic wave match the developmental processes of retinal neurons that apparently result in locally reduced oxygen tension. Indeed, the centrifugal waves of neuronal proliferation, differentiation, synaptic connectivity and eventually neuronal

activity, start in the central retina and then expand towards the retinal periphery (Neumann and Nuesslein-Volhard, 2000). This observation suggests that the metabolic demand of neurons, and the resulting "physiological hypoxia", induce vascularisation of the tissue (Chan-Ling et al., 1995). Second, in several ocular diseases, retinal ischemia induces the pathological growth of new vessels by angiogenesis (Grimm and Willmann, 2012)). Third, the expression of a number of pro- and anti-angiogenic factors is regulated by oxygen tension. The emerging tissue hypoxia during development leads to an increased expression of *Vegfa,* which forms a concentration gradient with high levels in the avascular retina, and reduced expression in the regions where the retina is vascularised, and hypoxia is relieved (Stone et al., 1995; Pierce et al., 1996; West et al., 2005). The growth of the vessels of the primary plexus is believed to be induced by this central-to-peripheral VEGFA gradient. VEGFAs are growth factors expressed in several splice variants with different lengths (reviewed in (Holmes and Zachary, 2005)). VEGFA isoforms bind to two high-affinity VEGF receptors (VEGFR), i.e. VEGFR1 (de Vries et al., 1992) and VEGFR2 (Millauer et al., 1993), which leads to an increased vascular permeability and the proliferation of endothelial cells (Miller et al., 1994). VEGFR signalling also assists the growth of the developing blood vessels by increasing the production of matrix metalloproteinases (MMPs) (Yancopoulos et al., 2000). The distinct VEGFA isoforms are thought to have distinct roles in vascular patterning in the retina. The guidance signals from VEGF164 and VEGF188 isoforms, which are more cell- and matrix-bound and thus less diffusible, present a track along which retinal vessels can properly grow. On the other hand, the more diffusible VEGF120 isoform does not offer this spatial information, and its secretion results in reduced vessel branching (Stalmans et al., 2002).

Considerable effort has been made over the past years to identify the cellular origin of VEGFA production during retinal angiogenesis. Retinal astrocytes have been proposed to be the source of VEGFA secretion in the avascular retina of the newborn mouse (Chan-Ling et al., 1995; Stone et al., 1995; Pierce et al., 1996; Dorrell et al., 2002; Gerhardt et al., 2003; West et al., 2005). However, recent advances have questioned this notion. In fact, the vasculature develops quite normally when the *Vegfa* gene is ablated in astrocytes (Weidemann et al., 2010). Thus, RGCs are discussed as an alternative source of VEGFA for regulation of developmental angiogenesis (Stone et al., 1996; Sapieha et al., 2008; Kim et al., 2010). The exact contribution of astrocytes, RGCs or additional, yet unidentified cellular sources of hypoxia-mediated production and release of pro-

angiogenic factors needs to be clarified.

Developmental angiogenesis is a process not only regulated by VEGFA isoforms and their receptors, but also by the interaction of endothelial-specific receptor tyrosine kinase (TIE2, encoded by the *Tek* gene in mice) (Dumont et al., 1994; Puri et al., 1995) with its ligands angiopoietin 1 (ANG1) (Suri et al., 1996), and angiopoietin 2 (ANG2) (Hackett et al., 2002). It is imperative to note that a tightly balanced expression of additional pro- and anti-angiogenic factors is required for the angiogenic process. Advances in the field have shown the involvement of, among others, insulin-like growth factor 1 (IGF1) (Hellstrom et al., 2001), placental growth factor (PIGF) (Feeney et al., 2003), norrin (NDP) (Zuercher et al., 2012), platelet-derived growth factor (PDGF) (Fruttiger et al., 1996; Lindblom et al., 2003), fibroblast growth factor 2 (FGF2) (Friedlander et al., 1995; Rousseau et al., 2000), PEDF (Huang et al., 2008), and leukemia inhibitory factor (LIF) (Kubota et al., 2008).

Before the primary plexus reaches the retinal periphery, the deeper capillary plexi start to grow by angiogenic sprouting from the primary plexus, a process that occurs independently of retinal astrocytes (Gariano et al., 1994; Provis, 2001). In rodents, angiogenic sprouts emerge from blood vessels of the primary plexus and penetrate the retina along Müller cell processes (Engerman and Meyer, 1965; Stahl et al., 2010). In the mouse retina, when the growing sprouts reach the inner and outer boundaries of the INL, they form the outer and intermediate capillary plexi (Stahl et al., 2010). This process starts in the center, expands towards the retinal periphery, and is preceded by a transient and hypoxia-driven expression of *Vegfa* transcripts in the INL (Stone et al., 1995; Sandercoe et al., 2003), presumably by Müller glia, which are known to boost VEGFA production upon hypoxia in the adult retina (Pierce et al., 1995). As for the formation of the primary plexus, additional proteins besides VEGFA regulate the growth also of the deep capillary plexi. For instance, activation of WNT signalling by NDP has been recognized to be essential for the formation of the intraretinal capillary plexi by sprouting angiogenesis (Luhmann et al., 2005). For a more detailed description of the mechanisms of retinal angiogenesis, I refer to excellent reviews by Fruttiger (Fruttiger, 2007) and Stahl and co-workers (Stahl et al., 2010).

1.4 Hypoxia Inducible Factors

The retina is a tissue with a very heterogeneous distribution of oxygen through its layers. Especially photoreceptor and synaptic layers experience a "borderline hypoxia", particularly under conditions of elevated neural activity, e.g. in dark conditions (Chapter 1.3.3). Additionally, the retina may experience hypoxia during development, aging and under pathological circumstances. Therefore, retinal cells must be able to respond to fluctuations in oxygen tension to safeguard viability and function. A family of heterodimeric transcription factors - the hypoxia-inducible factors (HIFs) - are the "master regulators" of the cellular hypoxic response by regulating the expression of target genes involved in a large number of biological events. These include angiogenesis, regulation of the vascular tone, changes in metabolism (e.g. glycolysis and mitochondrial function), erythropoiesis, metal transport, cell growth and survival (Majmundar et al., 2010).

HIF heterodimers are composed of a 120 kDa alpha subunit (HIFA) and a 91-94 kDa beta subunit (HIFB, also known as aryl hydrocarbon receptor nuclear translocator (ARNT)) (Semenza, 2001; Maxwell et al., 2001; Harris, 2002). Three *Hifa* isoforms are found in mammals: hypoxia-inducible factor 1a *(Hif1a)* (Wang et al., 1995a), endothelial PAS domain-containing protein 1 / hypoxia-inducible factor 2a *(Epas1 (Hif2a))* (Tian et al., 1997; Ema et al., 1997; Flamme et al., 1997), and hypoxia-inducible factor 3a *(Hif3a)* (Hara et al., 2001; Heidbreder et al., 2003; Makino et al., 2001, 2002). In addition, three paralogues of the gene encoding for the HIFB subunit (*Arnt1*, *Arnt2*, and *Arnt3)* have been identified up to date (Hirose et al., 1996; Ikeda and Nomura, 1997; Hogenesch et al., 1998, 2000). HIF transcription factors are members of the basic helix-loop-helix (bHLH) family and are PER-ARNT-SIM (PAS) domain-containing transcription factors (Wang et al., 1995a). At the structural level, HIFs contain a PAS domain, involved in protein-protein interactions, and a bHLH domain that contributes to both HIF subunit heterodimerisation and DNA binding (Jiang et al., 1996). In addition, HIF1A and EPAS1 (HIF2A) subunits have an oxygen-dependent degradation domain (ODDD), and two transactivation domains (TAD): the N-terminal TAD, involved in target gene specificity, and the C-terminal TAD, which contributes to the regulation of the majority of HIF target genes (Dayan et al., 2006; Hu et al., 2007) (Fig. 14).

Although HIF1 and HIF2 share several common target genes, e.g. *Vegfa*, they seem to regulate their own specific sets of targets by the contribution of their TAD domains (Loboda et al., 2010).

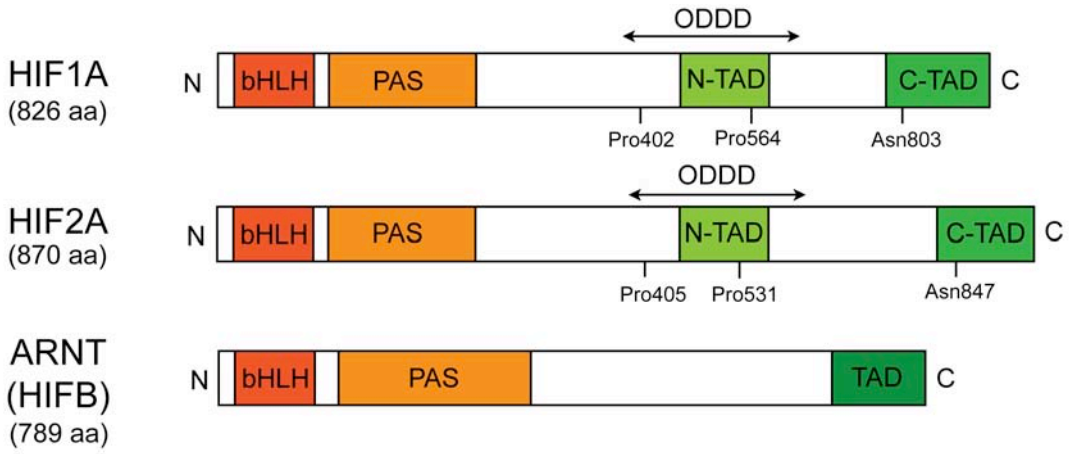

Figure 14 Structure of human HIF1A, HIF2A, and HIFB. Shown are schematic representations of the main domains of HIF isoforms, including the PER-ARNT-SIM (PAS) domain, the basic helix-loop-helix (bHLH) domain, the oxygen-dependent degradation domain (ODDD) containing proline (Pro) residues that are hydroxylated under normoxic conditions, the N-terminal transactivation domain (N-TAD), and the C- terminal transactivation domain (C-TAD) (Figure: (Caprara and Grimm, 2012)).

Expression of *Hif1a* has been detected in virtually each cell type in every tissue, while *Epas1 (Hif2a)* is highly expressed particularly in the endothelium of blood vessels (Jain et al., 1998) and in distinct cell types of most organs, including brain, heart, lung, kidney, liver, pancreas, and intestine (Wiesener et al., 2003). Expression of both *Hif1a* and *Epas1 (Hif2a)* has also been reported in the retina (Thiersch et al., 2009; Caprara et al., 2011; Mowat et al., 2010). Analysis of the expression of the HIFB paralogues suggest that *Arnt1* is transcribed virtually in every tissue, *Arnt2* is found predominantly in brain and kidney, while *Arnt3* is highly expressed in brain, thymus and muscle (Aitola and Pelto-Huikko, 2003; Hogenesch et al., 1998). Both HIF1A and EPAS1 (HIF2A) isoforms form functional heterodimers with ARNT1 and ARNT2, which seem to have a partial functional redundancy in the hypoxic response *in vivo* (Maltepe et al., 1997, 2000; Keith et al., 2001; Powell and Hahn, 2002). Conversely, ARNT3 has been suggested not to provide an important contribution to the induction of hypoxic gene expression (Cowden and Simon, 2002). The HIF3A isoform lacks a transactivation domain (Gu et al., 1998), and was proposed not to form functional transcription factors but instead to inhibit HIF1- and HIF2-

mediated gene regulation in a dominant negative manner by binding and scavenging HIFB subunits (Makino et al., 2001).

At the protein level, both HIFA and HIFB subunits are constitutively expressed under normoxic conditions. However, while HIFB is stable, HIFA is rapidly degraded in the presence of adequate oxygen levels (Huang et al., 1996). The stability of the alpha subunits is regulated by several oxygen-dependent and –independent mechanisms. The most important regulation occurs by a fast oxygen-dependent degradation. This is achieved by the posttranslational hydroxylation of proline (Pro) residues within the ODDD of the HIFA subunit (Pro 402 and 564 for human HIF1A, and Pro 405 and 531 for human HIF2A) by members of the prolyl-4-hydroxylase (PHD) family of proteins. Among these hydroxylases, PHD1, PHD2, and PHD3 regulate the stability of HIFA proteins (Epstein et al., 2001). The degree of HIFAs protein hydroxylation is directly proportional to oxygen availability, since PHDs are Fe(II) dependent dioxygenases that require oxygen and the tricarboxylic acid (TCA) cycle intermediate 2-oxoglutarate as substrates (Hewitson et al., 2003; McNeill et al., 2002b). Thus, PHDs have been named as "cellular oxygen sensors", directly coupling cellular oxygen concentration to the extent of HIFA protein hydroxylation, and thus HIFA stability. In fact, once hydroxylated, HIFA proteins become substrates for poly-ubiquitinylation by the von Hippel-Lindau protein (VHL) complex, which contains an E3 ubiquitin ligase. Poly-ubiquitinylation of hydroxylated HIFA proteins eventually targets them for rapid proteasomal degradation (Maxwell et al., 1999; Jaakkola et al., 2001). Even though the constitutive expression of HIFA subunits and continuous degradation under normoxic conditions might appear as a wasteful process, it allows a very rapid accumulation and thus activation of these transcription factors once their degradation is reduced or interrupted. In fact, under hypoxic conditions, PHDs lack oxygen as a cofactor, their activity is significantly reduced, and the extent of HIFA hydroxylation strongly decreases proportionally to the drop in oxygen availability. As a consequence, HIFA proteins avoid proteasomal degradation, accumulate and translocate to the nucleus, heterodimerize with HIFB and recruit transcriptional co-activators such as p300/CREB binding protein (CBP) (Arany et al., 1996) (a description of some co-activators for HIF1A or EPAS1 (HIF2A) can be found in (Loboda et al., 2010)). Finally, active HIF heterodimers and co-factors bind to hypoxia response elements (HREs) within promoters of HIF target genes to regulate gene expression (Chilov et al., 1999a; Gradin et al., 1996; Kallio et al.,

1997; Wenger et al., 2005). A degree of regulation of the activity of HIFA proteins is mediated by factor inhibiting HIF (FIH) that hydroxylates HIFAs at an asparagine (Asn) residue (Asn803 for human HIF1A and Asn847 for human HIF2A) in the C-terminal TAD. This hydroxylation step prevents the interaction with the transcriptional co-activator p300/CBP, and therefore prevents the HIFA subunits that do not get efficiently hydroxylated by PHDs to induce gene expression under normoxia (McNeill et al., 2002a; Lando et al., 2002a; Mahon et al., 2001; Lando et al., 2002b) (Fig. 15). Beside this basic mechanism regulating the stability of HIFA proteins, HIF1A and EPAS1 (HIF2A) have been proposed to be differentially stabilized depending on the duration and extent of a hypoxic event. Experimental evidence suggests that HIF1A is transiently stabilized in acute hypoxia, while EPAS1 (HIF2A) may induce a long-lasting change in target gene expression under conditions of chronic hypoxia (Wiesener et al., 1998; Holmquist-Mengelbier et al., 2006; Bracken et al., 2006).

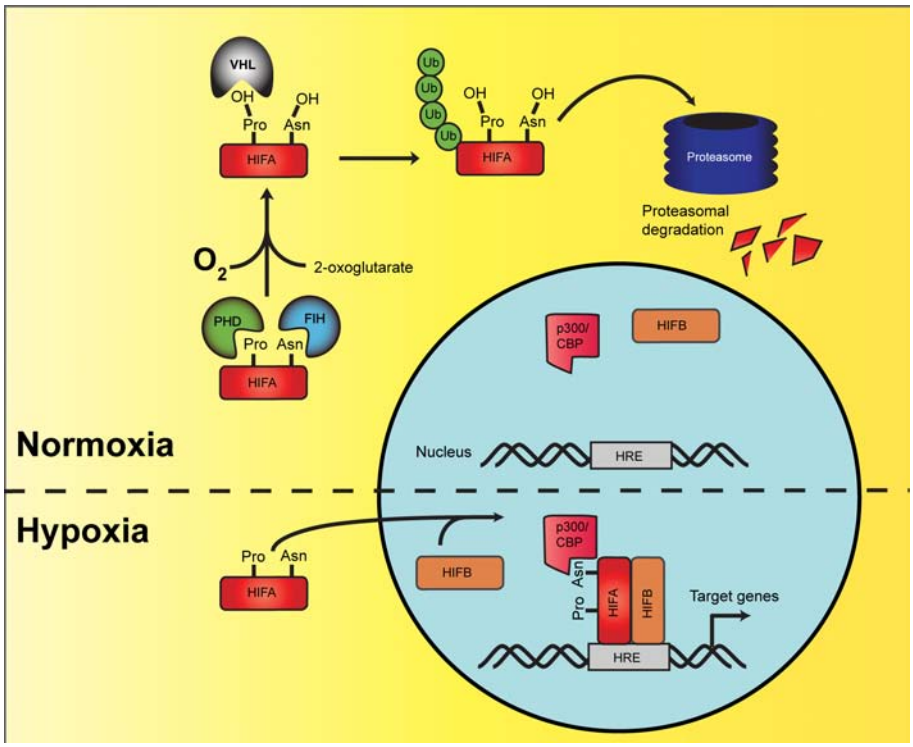

Figure 15 Oxygen-dependent regulation of HIFA stability. Representation of the oxygen-dependent regulation of HIFA proteins. In normoxia, HIFA isoforms undergo proteasomal degradation by a mechanism involving hydroxylation of Pro residues in the ODDD of HIFA by PHD enzymes. Consequently, pVHL E3 ubiquitin ligase complex poly-ubiquitinylates hydroxylated HIFAs. Additional hydroxylation of an asparagine (Asn) residue of HIFA by factor inhibiting HIF (FIH) abrogates HIFA interaction with the p300/CBP transcriptional co-activator. Hydroxylation mediated by PHD enzymes requires oxygen and 2-oxoglutarate as substrates. In hypoxia, when oxygen availability is limited, HIFA escapes

hydroxylation by PHD and FIH, translocates to the nucleus where it heterodimerizes with HIFB, complexes with p300/CBP and accessory transcriptional co-activators, binds hypoxia response elements (HREs) and drives transcription of target genes (Figure: (Caprara and Grimm, 2012)).

Beside the dependency on oxygen availability for the regulation of HIFA stability, other oxygen-independent mechanisms are known to control the process in both normoxic and hypoxic conditions. These include cytokine and growth factor-dependent signalling pathways (reviewed in (Bardos and Ashcroft, 2005; Majmundar et al., 2010)) and the interaction with the chaperone heath shock protein 90 (HSP90) (Neckers and Ivy, 2003). Recent evidence also proposes that mitochondria-produced ROS may be involved in the regulation of HIF activity, possibly by the inhibition of HIFA hydroxylation by PHDs under normoxic conditions (Cash et al., 2007; Yuan et al., 2008; Frede et al., 2009).

The characterization of knockout animals strongly suggests that HIFA subunits predominantly play non-redundant and specific roles in cellular physiology, particularly during development. Indeed, *Hif1a* knockout mice are not viable due to cardiac and vascular malformations, leading to death at embryonic day 10.5 (E10.5) (Ryan et al., 1998; Kotch et al., 1999). On the other hand, various phenotypes have been reported for systemic *Epas1 (Hif2a)* knockouts, including embryonic lethality with vascular abnormalities (Peng et al., 2000), perinatal lethality due to impairment in catecholamine production (Tian et al., 1998) or respiratory distress syndrome (Compernolle et al., 2002), post-natal lethality caused by progressive multiorgan failure (Scortegagna et al., 2003a), and viability into adulthood (Ding et al., 2005). The reasons for the different phenotypes are unclear yet, but may involve differences in genetic background and gene targeting strategies.

1.4.1 HIFs in the Retina

Experimental evidence shows that mammalian embryos experience a general hypoxic environment during development (human 3% O_2, rabbit 8.7% O_2, and monkey 1.5% O_2,) (Burton and Jaunaiux, 2001; Fischer and Bavister, 1993). Accordingly, hypoxic areas are found throughout the embryonic retina of the mouse and persist into early post-natal periods (Kurihara et al., 2010). In line with this, HIF1A protein accumulates in all layers of the embryonic and

newborn retina (Fig. 16). Interestingly, low but detectable HIF1A basal levels persist even in the adult retina, reflecting the borderline hypoxia found in the tissue (Ozaki et al., 1999; Grimm et al., 2005; Kurihara et al., 2010).

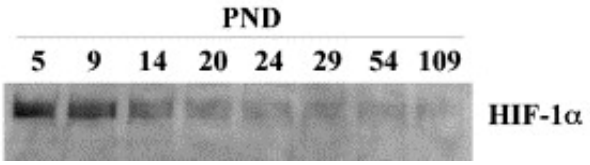

Figure 16 HIF1A protein stabilization in the post-natal retina. Total protein was prepared from retinas isolated at different post-natal days (PND) as indicated. HIF1A levels were tested by Western blotting using a specific antibody. (Figure: adapted from (Grimm et al., 2005))

Similar to the embryonic brain (Jain et al., 1998), EPAS1 (HIF2A) was described to be stabilized principally in vascular endothelial cells of the hyaloid vasculature of the embryonic retina (Kurihara et al., 2010). In the adult retina, *Epas1 (Hif2a)* is expressed by cells located in the GCL, INL, and RPE, in addition to vascular endothelial cells (Ding et al., 2005). Taken together, these observations highlight the responsiveness of the retinal tissue to hypoxic events during development via stabilization of HIFA proteins. However, each isoform seems to have specific spatio-temporal accumulation and expression patterns, pointing to distinct roles for HIF1A and EPAS1 (HIF2A) during retinal development and probably adulthood.

1.5 Hypoxic Preconditioning

A cell exposed to damaging stimuli or harmful molecules has a high risk of undergoing programmed cell death. However, cells respond to noxious insults by producing a plethora of protective factors, and only undergo apoptosis when a point of no return is reached (Loos and Engelbrecht, 2009). This knowledge has been used over the past years in the field of biomedical research to activate endogenous protective mechanisms in a tissue as an alternative to the application of exogenous molecules with its potential side effects. This treatment, known as "preconditioning", describes the capability of cells, or a tissue, to better cope with a noxious stimulus if they where previously exposed to a brief and non-damaging period of stress. Both

ischemia and hypoxia, especially under chronic conditions, can represent a threat for cell survival (Guo et al., 2011). But, short and controlled periods of ischemia or hypoxia protect retinal cells against damage by a subsequent insult. Two types of preconditioning protocols based on the modification of oxygen tension in the retina are frequently used in vision research. Ischemic preconditioning (IPC) involves a transient interruption of ocular blood flow by the occlusion of the central retinal artery (Roth et al., 1998), or by a raise of the intraocular pressure (IOP) (Zhang et al., 2002). Hypoxic preconditioning (HP) is a similar approach that involves the exposure of organisms, tissues or cells to air with reduced oxygen concentrations, usually in a "hypoxic chamber". Both IPC and HP result in the induction of systemic alterations as well as a strong protective effect in the retina (see below). In the past years, IPC was predominantly applied to laboratory rodents to study mechanisms of RGC survival, while HP was applied to obtain protection of photoreceptors (Fig. 17). However, both IPC and HP caused "ischemic tolerance", thereby preventing injury of retinal cells due to ischemia-reperfusion (Roth et al., 1998; Zhu et al., 2002). Both preconditioning protocols also provided protection of photoreceptors from apoptosis induced by exposure to bright light (Grimm et al., 2002; Casson et al., 2003). The tissue protective effects mediated by IPC or HP are thought to arise from the expression of specific protective factors, which control and activate endogenous survival mechanisms and inhibit apoptotic signalling (Kirino et al., 1991). In general, the effects of preconditioning can be divided into three steps. First, activation or deactivation of signalling pathways results in changes in second messenger levels and in an activation or repression of specific transcription factors. This leads to the second step: the upregulation of pro-survival genes or the downregulation of pro-apoptotic genes, which mediate the cytoprotective actions against damaging insults in the third step. Elucidating these mechanisms may give insights into relevant biochemical pathways and cytoprotective proteins that could potentially be translated into therapeutic options for the preservation of vision in patients.

As would be expected, HIFs might be the central mediators of the protective effects of HP. Upon HP, a direct relationship between protection of photoreceptors from light-induced degeneration and HIF1A protein stabilization suggests that hypoxia-induced HIF1-target genes may contribute to the protective mechanisms induced by HP (Grimm et al., 2002). Erythropoietin (EPO) is a candidate protective factor that is upregulated upon HP (Grimm et al., 2002) and has

been shown to protect photoreceptors and other cells even when applied exogenously (Chapter 1.6.3) (Fig. 17).

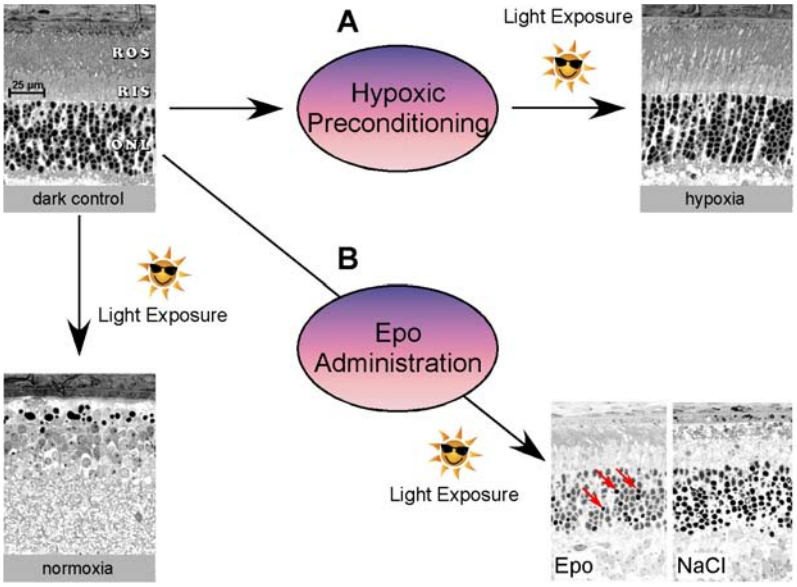

Figure 17 Hypoxic preconditioning and EPO protect against light-induced retinal degeneration Dark control mice have healthy photoreceptor cells with correctly structured outer and inner segments. Normoxic mice exposed to toxic levels of light almost completely lose photoreceptor cells 10 days after light exposure. **(A)** Hypoxic preconditioning completely protects the retina against light damage. **(B)** EPO administration partially protects the retina against light damage. Some pycnotic nuclei (red arrows) are present 36 hours after light exposure. Retinas injected with sodium chloride (NaCl) as control were damaged after illumination. (Figure: Thiersch and Grimm)

1.6 Erythropoietin

EPO is a secreted glycosylated protein belonging to the type I cytokine family that systemically acts as an erythropoiesis-stimulating hormone. EPO is mainly produced in the kidney (Koury et al., 1993) and secreted into the blood circulation to reach the primary site of erythropoiesis, i.e. the bone marrow. Here it binds to the cognate EPO receptor (EPOR) on erythroid progenitor cells preventing their apoptotic death and stimulating their differentiation and maturation into erythrocytes (Koury and Bondurant, 1988). The gene expression of *Epo* is robustly oxygen-regulated, and thus is induced significantly under conditions that result in systemic hypoxia (Bondurant and Koury, 1986). Hence, EPO secretion into the bloodstream

increases under hypoxic conditions, eventually resulting in a rise of the hematocrit. This ameliorates the ability of the blood to transport oxygen and ultimately reliefs the hypoxic insult (reviewed in (Jelkmann, 2004)).

About 10% of EPO in the bloodstream is of non-renal origin (Fried et al., 1969). The brain, spleen, lung, placenta, uterus, testis, and retina have been identified as EPO-secreting tissues apart from kidney (reviewed in (Fandrey, 2004)). The expression of both *Epo* and *EpoR* mRNA has been reported in both the human and rodent retina (Juul et al., 1998; Xie et al., 2007; Grimm et al., 2002; Chen et al., 2009). Yet, the cellular origin of *Epo* expression in the retina deserves further investigation. In fact, reports suggest either Müller cells (Fu et al., 2008) or cells found in the GCL (Scheerer et al., 2010) to be the source of *Epo* expression, but definitive proof is still lacking.

The presence of an HRE in the 3' regulatory region of the *Epo* gene strongly points to a HIF-dependent transcriptional regulation under hypoxia (Semenza et al., 1991; Semenza and Wang, 1992; Wang et al., 1995a). Over the years, both HIF1 and HIF2 have been implicated in the hypoxic induction of *Epo* expression, but the latest *in vivo* and *in vitro* evidence suggest that HIF2 could be the main inducer of *Epo* gene expression in kidney (Semenza and Wang, 1992; Tian et al., 1997; Gruber et al., 2007; Morita et al., 2003; Rankin et al., 2007; Scortegagna et al., 2005, 2003b; Warnecke et al., 2004; Gruber et al., 2007), brain (Chavez et al., 2006; Yeo et al., 2008) and retina (Morita et al., 2003). Nevertheless, other factors, e.g. hepatocyte nuclear factor 4 (HNF4) and GATA proteins, regulate tissue-specific *Epo* gene expression (reviewed in (Weidemann and Johnson, 2009)).

1.6.1 The Erythropoietin Receptor

The EPOR is a single chain cell surface receptor belonging to the cytokine receptor superfamily (Bazan, 1990). The pro-survival activity of EPO on erythroid progenitor cells is mediated by binding to the EPOR homodimer, leading to a conformational change of the receptor that results in its transphosphorylation and activation of intracellular signalling pathways that include Janus kinase 2 (JAK2) / signal transducer and activator of transcription 3/5 (STAT3/5), phosphatidylinositide 3-kinases (PI3K)/AKT, and mitogen-activated protein kinases (MAPK)

(Witthuhn et al., 1993; Livnah et al., 1999; Constantinescu et al., 1999; Marzo et al., 2008)(Fig. 18). Activation of these signalling pathways leads to cellular proliferation and inhibition of apoptosis of hematopoietic cells (Neubauer et al., 1998).

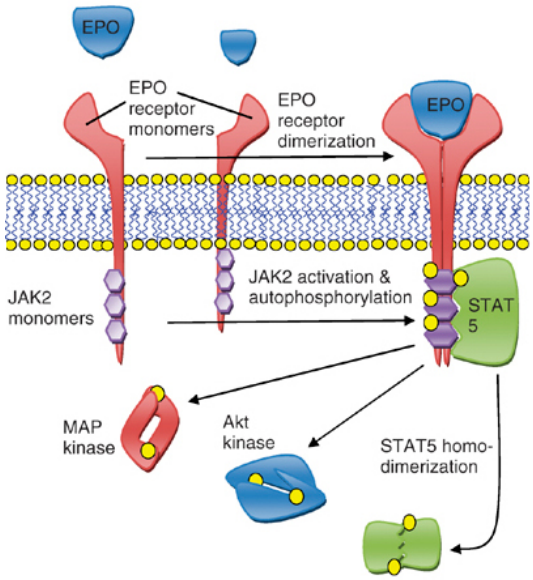

Figure 18 Erythropoietin receptor signalling in erythroid progenitor cells. Binding of EPO to EPOR results in receptor homodimerisation and autophosphorylation of JAK2. Phosphorylated JAK2 mediates phosphorylation of tyrosine residues on the cytoplasmic region of EPOR, which serve as docking sites for downstream effectors. These include STAT5 and PI3K/AKT, and MAPK. (Figure: adapted from (Patnaik and Tefferi, 2009))

As suggested by the diverse tissue origin of *Epo* expression, also expression of *EpoR* is broader than initially recognized. Expression of the receptor has been identified, among others, in the heart, brain, liver, uterus (Farrell and Lee, 2004), and retina (Juul et al., 1998). Similarly to its ligand, the precise cellular location of retinal *EpoR* expression needs further investigation but may include Müller cells (Zhu et al., 2008; Wang et al., 2010; Hu et al., 2011), RGCs (Kilic et al., 2005b; Zhong et al., 2007; Fu et al., 2008), and photoreceptors (Grimm et al., 2002; Zhong et al., 2007). However, the unreliability of the commercially available anti-EPOR antibodies (Elliott et al., 2006; Kirkeby et al., 2007), demands further experimentation to corroborate these studies. On the other hand, *in situ* hybridization analysis on retinal sections suggests that *EpoR* transcripts are found in cells of the INL and GCL (Colella et al., 2011).

Interestingly, the EPOR can be expressed through alternative splicing as both a membrane-bound (mEPOR) and soluble form (sEPOR), which corresponds to the extracellular

domain of the mEPOR (Nagao et al., 1992; Harris and Winkelmann, 1996; Westphal et al., 2002). Very limited knowledge has been gathered on the function of sEPOR, but in the brain this isoform seems to be important for ventilatory acclimatization to hypoxia, and acts as a negative regulator of EPO binding to the EPOR (Soliz et al., 2007). Both the roles and expression of this isoform have not been yet reported in the retina.

1.6.2 Tissue Protective Effects

Beside the "traditional" anti-apoptotic properties on erythroid progenitors, over the last 15 years EPO has shown to have cytoprotective effects in different tissues against various damaging insults. In kidney and heart for example, EPO protects against injury by ischemia/reperfusion (Patel et al., 2004; Cai et al., 2003; Parsa et al., 2003). Other results suggest a general neuroprotective capacity of EPO, thus stimulating growing interest in its use as a potential therapeutic drug for neurodegenerative diseases. For example, in cell culture systems, application of recombinant human EPO (rhEPO) protected neurons from various cytotoxic conditions (Lewczuk et al., 2000; Morishita et al., 1997; Siren et al., 2001a). In animal models, systemic delivery of rhEPO has shown to ameliorate experimental brain injury (Brines et al., 2000; Yatsiv et al., 2005), ischemic damage and stroke (Sakanaka et al., 1998; Bernaudin et al., 1999), experimental Parkinson's disease (Genc et al., 2001), multiple sclerosis (Sattler et al., 2004), spinal cord injury (Celik et al., 2002; Gorio et al., 2002), and retinal degeneration (see below).

It was observed that EPO binds to erythrocyte precursors with different affinity than to cells with neuronal characteristics (Masuda et al., 1993), and that non-hematopoietic EPO variants still retain tissue-protective abilities without binding to EPOR homodimers (Leist et al., 2004). Hence, the involvement of another receptor in neuronal signalling and neuroprotection has been considered. EPOR has been previously reported to physically (Jubinsky et al., 1997) and functionally (Blake et al., 2002) interact with the common β receptor (βCR, encoded by *Csf2rb* in mouse), also known as CD131. Since protection by EPO was abolished in mice lacking βCR, Brines and colleagues proposed that neuroprotection might be mediated through an EPOR/βCR heteroreceptor complex (Brines et al., 2004). However, the contribution of βCR to EPO signalling

has been challenged by experiments showing that EPO also protected neuroblastoma cells that do not detectably express βCR (Um et al., 2007), and hippocampus cells which express only very low levels of βCR (Nadam et al., 2007).

1.6.3 Neuroprotection in the Retina

In the past years, EPO was shown to exert neuroprotective effects on two major retinal cell populations: RGCs and photoreceptors.

1.6.3.1 Protection of Retinal Ganglion Cells

Application of rhEPO protected RGCs from glutamate-induced excitotoxicity (Yamasaki et al., 2005). Similar to the *in vitro* situation, EPO showed protective effects against axotomy-induced RGC apoptosis *in vivo* (Fu et al., 2008). The neuroprotective potential was also confirmed in models of mild (Tsai et al., 2005) and chronic ocular hypertension (Fu et al., 2008), as well as in the DBA/2J mouse (Zhong et al., 2007).

Besides preventing RGC apoptosis, EPO has revealed an additional attractive property that may be of particular interest in diseases that are associated with axonal degeneration. Here, EPO supported axonal regeneration and outgrowth of neurites in RGCs *in vivo* after axotomy of the optic nerve (King et al., 2007), in cultured retinal explants (Bocker-Meffert et al., 2002), and different retinal cell culture models (Kretz et al., 2004, 2005).

1.6.3.2 Protection of Photoreceptors

The ability of EPO to counteract apoptosis of photoreceptors has emerged as this cytokine has been implicated in the protective effects of HP in the retina (Grimm et al., 2002). Application of rhEPO partially mimicked these effects in different models of light-induced photoreceptor apoptosis (Grimm et al., 2002; Ranchon Cole et al., 2007). Furthermore, intramuscular adeno-associated virus (AAV)-mediated delivery of an *Epo* transgene resulted in its systemic overexpression and protected photoreceptors from light-induced apoptosis (Rex et al., 2004). Likewise, systemic overexpression of a human *Epo* transgene (Ruschitzka et al., 2000) that resulted in a 20-fold increased level of EPO protein in the retina, supported photoreceptor

viability in the light-damage model (Grimm et al., 2004). This led to the fascinating possibility to use EPO as therapeutical agent for the treatment of RP patients.

However, while it seems clear that EPO can protect photoreceptor cells against phototoxic stress, protection against inherited photoreceptor degeneration seems to depend on the model and thus on the particular molecular pathway that causes cell death. In fact, neither transgenic *Epo* overexpression nor repetitive intraperitoneal injections of rhEPO in *rd1*, *rd10* and *VPP* mice rescued photoreceptor cells (Grimm et al., 2004; Rex et al., 2004). However, the same approach significantly prevented degeneration in the *rds* mouse (Rex et al., 2004, 2009).

1.6.4 Beneficial Effects in the Diabetic Retina

The beneficial effects of EPO in the retina are not restricted to neuroprotection of RGCs and photoreceptors. Several studies have shed light on the potential of this cytokine to counteract retinal complications associated with diabetes. In fact, EPO has shown to exert protective effect on retinal pericytes and vascular endothelial cells, and to ameliorate the stability of the BRB in the diabetic retina (Wang et al., 2011b; Zhang et al., 2008, 2010; Wang et al., 2011b). In addition, also decreased neuronal apoptosis and reduced functional damage have been reported (Wang et al., 2011b; Zhu et al., 2008). Applications of rhEPO attenuated the secretion of tumour necrosis factor A (TNFA) and interleukin 1B (IL1B) in the diabetic rat retina (Lei et al., 2011) and repressed osmotic swelling of retinal glial cells *in vitro* (Krugel et al., 2010).

1.6.5 EPO as Angiogenic Factor

EPO has long been recognized to exert pro-angiogenic activities (Anagnostou et al., 1990a; Ribatti et al., 2003). Deletion of *Epo* or *EpoR* in mice had a strong effect on angiogenesis, resulting in a decreased complexity of the vascular network, a phenotype that included constricted vessel diameter and reduced vascular branching (Kertesz et al., 2004). It is thought that the angiogenic effects of EPO are due to its ability to stimulate endothelial progenitor cell mobilization or proliferation (Heeschen et al., 2003). Due to this angiogenic properties, the potential of EPO as therapeutic agent must be considered critically. In fact, the angiogenic effects of this cytokine may contribute to the progression of retinal diseases into a neovascular phase.

2 Aims of the thesis

The reduction of tissue oxygenation that occurs under hypoxic conditions has deep consequences on both retinal function and cell survival (Caprara and Grimm, 2012). Hence, cells require an adaptational response to cope with hypoxic episodes occurring during development and in the adult tissue. Central to this response is HIF1A, a transcription factor that accumulates when oxygen is limited and induces the expression of a large assortment of target genes involved in angiogenesis, cell survival and metabolism (Chapter 1.4). Prominent among these factors are VEGFA and EPO, which may contribute to angiogenesis during retinal development. In mice, retinal angiogenesis occurs post-natally, and reduction in tissue oxygenation is expected to occur until tissue vascularisation is completed (Chapter 1.3.5). HIF1A protein levels are elevated in the post-natal mouse retina and decrease as the retinal vasculature develops (Grimm et al., 2005). Nevertheless, the roles of HIF1A in both retinal development and angiogenesis have not yet been fully elucidated. Beside the negative effects of chronic hypoxia on retinal cell survival and function, the protective reactions induced in a tissue by short periods of hypoxia can be exploited for clinical purposes. In fact, hypoxic preconditioning has revealed the ability of the retina to activate endogenous survival mechanisms, which protect photoreceptors against light-induced apoptosis (Grimm et al., 2002). The local production of protective factors such as EPO is part of these mechanisms, and exogenous applications of rhEPO mimic the protective effects of hypoxic preconditioning (Grimm et al., 2002). Despite the attractiveness of EPO as potential therapeutic factor for retinal degenerative diseases, the roles of endogenous EPO-EPOR signalling in the developing and adult retina are still unknown.

The main aims of my thesis are to investigate the roles of HIF1A and endogenous EPO-EPOR signalling in development, maturation and angiogenesis of the retina, as well as to elucidate their involvement in the survival of the aging retina. Furthermore, I aim to clarify the participation of EPO-EPOR signalling in the neuroprotective effects mediated by rhEPO applications.

3 Materials and Methods

3.1 Buffers and Solutions

Buffer/Solution	Composition (final conc.)	Application
4% Paraformaldehyde (PFA)	4 g PFA, 50 mL H_2O, 50 mL 0.2 M PB, pH: 7.4	IF
0.2 M Phosphate Buffer (PB)	5.244 g NaH_2PO_4 x H_2O, 23 g Na_2HPO_4 in 1 L H_2O, pH: 7.4	IF
0.1 M Phosphate Buffered Saline (PBS)	4 g NaCl, 0.1 g KCl, 250 mL 0.2 M PB, 250 mL H_2O, pH:7.4	IF
30% sucrose	30 g Sucrose in 100 mL PBS, pH: 7.4	IF
2.5% Glutaraldehyde	250 mL 0.4 M Na-cacodylate Buffer, 100 mL 25% Glutaraldehyde, 50 mg $CaCl_2$, 100 mg $MgCl_2$ x H_2O, 650 mL H_2O, pH: 7.2-7.4	Morph
Epon embedding media	147 mL EPON812, 100 mL $C_{16}H_{26}O_3$, 90 mL $C_{10}H_{10}O_3$, 6.74 mL BDMA	Morph
0.4M Na-cacodylate Buffer	171.2 g Na-cacodylate, 38.4 mL 1M HCl, ad 2000 mL H_2O, pH: 7.2-7.4	Morph
1% Osmium tetroxide (OsO_4)	1 g OsO_4, 1000 mL H_2O	Morph
10X Tris-Buffered Saline (TBS)	10 mM Tris/HCl [pH 8.0], 150 mM NaCl	WB
10X TBS-Tween20 (TBST)	10 mM Tris/HCl [pH 8.0], 150 mM NaCl, 0.05% Tween-20	WB
10X RIPEA	20 mM Tris/HCl [pH 7.5], 60 mM NaCl, 2 mM EDTA, 0.4% Triton X-100; 0.4% SDS, 0.4% Sodium Deoxycholat	WB
5X PAGE Running Buffer	25 mM Tris Base, 190 mM Glycine, 0.1% SDS	SDS-PAGE
1X PAGE Transfer Buffer	48 mM Tris Base, 39 mM Glycine, 0.038% SDS, 20% MeOH	SDS-PAGE/WB
4X sodium dodecylsulfate (SDS) sample buffer	62.5 mM Tris/HCl [pH 6.8], 10% Glycerol, 2.3% SDS, 0.1% Bromphenolblue, 5% 2-Mercaptoethanol	WB
5X TBE	450 mM Tris Base, 450 mM Boric Acid, 10 mM EDTA	Agarose gel electrophoresis
10X Tissue Homogenization Buffer (THB)	100 mM Tris/HCl [pH 8.0], 500 mM KCl; 0.1 mg/mL gelatin; 0.45% NP-40; 0.45% Tween-20	Genotyping

Table 1 Composition of buffers and solutions. The composition of buffers and solutions for the experiments in this thesis is shown. Also, the application for each solution is listed. IF: immunofluorescence, WB: Western blot, SDS-PAGE: SDS polyacrylamide gel electrophoresis, Morph: histology.

3.2 Mice and Genotyping

Mice were treated and procedures were performed in accordance with the regulations of the Veterinary Authority of Zurich and the statement of the Association for Research in Vision and Ophthalmology (ARVO) for the use of animals in research. All mice were kept at the animal facility of the University Hospital Zurich in a dark-light cycle (12 Hr : 12 Hr). During the light cycle, the light level was maintained at 60 lux at cage level with food and water *ad libitum*. Mice

were euthanized by a CO_2 overdose followed by cervical dislocation. All experiments were done with a minimum of N = 3 mice for each time point and condition.

To knockdown genes of interest in specific retinal cells, the Cre-loxP recombination approach was used. Mice carrying *loxP*-targeted sequences in the gene of interest were crossed to mice expressing *Cre* recombinase in specific retinal cells (Table 2). Wild-type animals used for the analysis of post-natal gene expression were C57BL/6 mice. Except C57BL/6 mice, all animals were homozygous for *Rpe65*^{450Leu} (Wenzel et al., 2003).

Knockdown	loxP-flanked gene	*Cre* expressing mouse
Hif1a in peripheral retina (*Hif1a*$^{flox/flox}$*;α-Cre*)	*Hif1a*^{flox} (Ryan et al., 2000)	*α-Cre* (Marquardt et al., 2001)
EpoR in peripheral retina (*EpoR*$^{flox/flox}$*;α-Cre*)	*EpoR*^{flox} (Tsai et al., 2006)	*α-Cre* (Marquardt et al., 2001)
EpoR in rod photoreceptors (*EpoR*$^{flox/flox}$*;Opn-Cre*)	*EpoR*^{flox} (Tsai et al., 2006)	*Opn-Cre* (Le et al., 2006)
Hif1a and *EpoR* in peripheral retina (*Hif1a*$^{flox/flox}$*;EpoR*$^{flox/flox}$*;α-Cre*)	*Hif1a*^{flox} (Ryan et al., 2000) *EpoR*^{flox} (Tsai et al., 2006)	*α-Cre* (Marquardt et al., 2001)
Hif1a in retinal glia (*Hif1a*$^{flox/flox}$*;Pdgfra-Cre*)	*Hif1a*^{flox} (Ryan et al., 2000)	*Pdgfra-Cre* (Roesch et al., 2008)

Table 2 *Hif1a* and *EpoR* knockdown mice. Shown are the mouse lines used for experiments in this theses, accompanied by the original research article where the mouse line was presented for the first time.

To investigate the spatial expression pattern of *Cre* recombinase, *α-Cre* and *Pdgfra-Cre* mice were crossed with the *Ai6* reporter mouse (Madisen et al., 2010) (a gift from Dr. Botond Roska, FMI, Basel, Switzerland) that expresses a green fluorescent protein (ZSGREEN) following CRE-mediated deletion of a floxed STOP cassette. *Opn-Cre* mice were bred to the *ROSA-flox-RFP* reporter line (Luche et al., 2007) (a gift from Hans Joerg Fehling, University Clinics Ulm, Germany), that expresses a red fluorescence protein (RFP) upon CRE-mediated deletion of a floxed STOP cassette.

Mice were genotyped using genomic DNA isolated from ear biopsies by conventional PCR conditions: initial denaturation (95°C, 5 min); 35 cycles of denaturation (95°C, 45 s), annealing (see conditions in Table 3) and elongation (72°C, 45 s); final extension (72°C, 10 min). PCR products were run on a 1.5% agarose gel for size detection.

Mouse/Gene	Forward Primer (5'-3')	Reverse Primer (5'-3')	Annealing Temperature (°C)
Hif1a^{flox}	GCAGTTAAGAGCACTAGTTG	GGAGCTATCTCTCTAGACC	62
EpoR^{flox}	CTCCAGCCCAGTCCACCAACTGGG	GGCGGGTAGTGGTACAGCACTTGCC CCCGTTCTTGGCTCAAAGCCAATC	67
Rpe65^{450}	CACTGTGGTCTCTGCTATCTTC	GGTGCAGTTCCACTTCAGTT	58
Cre	GGACATGTTCAGGGATCGCCAGGCG	GCATAACCAGTGAAACAGCATTGCTG	67
Ai6	(WT for) AAGGGAGCTGCAGTGGAGTA (MUT for) AACCAGAAGTGGCACCTGAC	(WT rev)CCGAAAATCTGTGGGAAGTC (MUT rev)GGCATTAAAGCAGCGTATCC	62
ROSA-flox-RFP	(WT for) GGAGCGGGAGAAATGGATATG (MUT for) GCGAAGAGTTTGTCCTCAACC	AAAGTCGCTCTGAGTTGTTAT	62

Table 3 Primers used for genotyping. Shown are forward and reverse primers (5'-3' orientation) used for genotyping, together with annealing temperatures.

3.3 RNA Isolation and cDNA Synthesis

Retinas were isolated through a corneal incision and immediately snap frozen in liquid nitrogen. Total RNA was isolated using the RNeasy isolation kit (RNeasy, Cat-nr: 74104, Qiagen, Hilden, Germany) or the High Pure RNA isolation kit (Roche Diagnostics, Cat-nr: 11828665001, Basel, Switzerland). Residual genomic DNA was removed by an incubation step with DNase. Identical amounts of RNA (650 or 1000 ng) were reverse transcribed using oligo(dT) and M-MLV reverse transcriptase (Promega, Cat-nr: M1701, Madison, WI, USA). The obtained first-strand cDNA was diluted to 5 ng/µl for gene expression analysis by semi-quantitative real-time PCR.

3.4 Semi-quantitative Real-time Polymerase Chain Reaction

Relative quantification of cDNA was performed by real-time PCR using a LightCycler 480 instrument (Roche Diagnostics, Basel, Switzerland), a LightCycler 480 SYBR Green I Master kit (Roche Diagnostics, Cat-nr: 04887352001, Basel, Switzerland), and specific primer pairs (Table 4). Primer pairs were designed to span large intronic sequences or to cover exon-exon boundaries. Gene expression was normalized to *Actb* (β-actin) and relative quantification was

calculated using the comparative threshold method ($\Delta\Delta C_T$) and Light Cycler 480 software (Roche Diagnostics, Basel, Switzerland).

Gene	Forward Primer	Reverse Primer	Annealing Temperature (°C)	Product Size (bp)
Actb	CGACATGGAGAAGATCTGGC	CAACGGCTCCGGCATGTGC	62	153
Adm	TTCGCAGTTCCGAAAGAAGT	GGTAGCTGCTGGATGCTTGTA	62	77
Ang2	AGAATACAAAGAGGGCTTCGGG	GTGCTAAAATCACTTCCTGGTTGGC	60	255
Apaf1	TGAGTACGTGGCATTCGGAG	TGTCTGCCAATTCCATACCTGA	60	184
Bcl2	TGCACCTGACGCCCTTCAC	AGACAGCCAGGAGAAATCAAACAG	62	293
Bcl2l1(Bcl$_{XL}$)	GCGGCTGGGACACTTTTGTGG	TGAGCCCAGCAGAACCACACC	60	128
Bdnf	CACTGAGTCTCCAGGACAGC	GTCAGACCTCTCGAACCTGC	60	223
Casp1	GGCAGGAATTCTGGAGCTTCAA	GTCAGTCCTGGAAATGTGCC	60	138
Cebp/d	CTTTTAGGTGGTTGCCGAAG	GCAACGAGGAATCAAGTTTCA	60	70
Csf2rb (βCR)	ACTACTACTCCTTCCGGCCA	AGCTGATGCTGACGTTCTTG	62	102
Edn2	AGACCTCCTCCGAAAGCTG	CTGGCTGTAGCTGGCAAAG	60	64
Epas 1 (Hif2a)	GGAGCTCAAAAGGTGTCAGG	CAGGTAAGGCTCGAACGATG	62	61
Epo	GCCCTGCTAGCCAATTCC	GCCCTGCTAGCCAATTCC	60	128
EpoR	GTCCTCATCTCGCTGTTGCT	CAGGCCAGATCTTCTGCTG	62	76
Fgf2	TGTGTCTATCAAGGGAGTGTGTGC	ACCAACTGGAGTATTTCCGTGACCG	62	158
Fzd4	CTACAAGCTGACCAACATGC	GGGAATTTGCTGCAGTTCAG	62	277
Gata2	TGGCAGCAGTCTCTTCCATC	CACAGGCATTGCACAGGTAG	60	179
Gfap	CCACCAAACTGGCTGATGTCTAC	TTCTCTCCAAATCCACACGAGC	62	240
Gnat1	GAGGATGCTGAGAAGGATGC	TGAATGTTGAGCGTGGTCAT	58	209
Gnat2	GCATCAGTGCTGAGGACAAA	CTAGGCACTCTTCGGGTGAG	58	192
Hif1a	TCATCAGTTGCCACTTCCCCAC	CCGTCATCTGTTAGCACCATCAC	62	198
Hif1b	TCCACTGCACAGGCTACATC	TCATCATCTGGGAGGGAGAC	60	61
Hif3a	CTGCAAGGTCGACAACTCCT	AGCAGCGAGGGAGCTAGG	60	92
Hnf4a	AAGTGCTTCCGGGCTGGCAT	ATGGGAGAGGTGATCTGCTGGGA	62	152
Il1b	GCTATGGCAACTGTTCCTGA	GATGTGCTGCTGCGAGATT	62	171
Lif	AATGCCACCTGTGCCATACG	CAACTTGGTCTTCTCTGTCCCG	60	216
Lrp5	TGTGGACCTGCGGTTACGCT	ATGAGGACACACTGGCCGCT	60	123
mEpoR	GCTACACCTTCGCTGTTCGAG	TGAGAGGGTCCAGGTCGCTA	60	111
Mt1	GAATGGACCCCAACTGCTC	GCAGCAGCTCTTCTTGCAG	62	104
Mt2	TGTACTTCCTGCAAGAAAAGCTG	ACTTGTCGGAAGCCTCTTTG	62	94
Ndp	AAGGAGCCCTGCGTTTCCCC	AAGGCTGCCGCTTTCTGGTTG	60	120
Nos2 (iNos)	GGGCTGTCACGGAGATCA	CCATGATGGTCACATTCTGC	60	66
Ntn1	TTGCAAAGCCTGTGATTGCC	AATCTTGATGCAAGGGGCGA	60	163
Ntn4	TGCACCGGAGGAGAGGTTATT	GGTTTTGCGTTCAGGTCGTT	62	164
Opn4	CCAGCTTCACAACCAGTCCT	CAGCCTGATGTGCAGATGTC	60	111
Pou4f1 (Brn3a)	CGCCGCTGCAGAGCAACCTCTT	TGGTACGTGGCGTCCGGCTT	60	130
Rho	CTTCACCTGGATCATGGCGTT	TTCGTTGTTGACCTCAGGCTTG	62	130
sEpoR	TGAAGTGGACGTGTCGGCAG	GGAACTAGGGCCTCACCGCT	60	216
Serpin 1f (Pedf)	TCCACAGCACCTACAAGGAG	TAAGCCACGCCAAGGAGAAG	60	280
Stat3	CAAAACCCTCAAGAGCCAAGG	TCACTCACAATGCTTCTCCGC	62	133
Tek (Tie2)	CCATCACCATAGGAAGGGACTTTG	TAGGAAGGACGCTTGTTGACGCATC	60	215
Tnfa	CCACGCTCTTCTGTCTACTGA	GGCCATAGAACTGATGAGAGG	62	92
Tspan12	TTGCGCTGCTTGCTCTACGC	GGGGTGAACCACGGGGAAGTAA	60	168
Vegfa	ACTTGTGTTGGGAGGAGGATGTC	AATGGGTTTGTCGTGTTTCTGG	60	171
Vsx2 (Chx10)	CCAGAAGACAGGATACAGGTG	GGCTCCATAGAGACCATACT	62	111

Table 4 Primers for semi-quantitative real-time PCR. Shown is a list of primer pair sequences for genes of interest. Primer sequences of forward/reverse primers are shown in 5'-3' orientation, together with annealing temperatures and size of the obtained amplicon.

3.5 Western Blot Analysis

Proteins from isolated retinas were extracted in 0.1 M Tris-HCL (pH 8.0) by sonication at 4°C and protein content was determined with a Bradford assay. Protein extracts were mixed with sodium dodecylsulfate (SDS) sample buffer and incubated for 10 minutes at 75°C. Proteins were separated by SDS polyacrylamide gel electrophoresis (SDS-PAGE) and transferred to

nitrocellulose membranes. Membranes were blocked with 5% nonfat dry milk (Bio-Rad, Cat-nr: 170-6404XTU, Munich, Germany) in TBST for 1 Hr at room temperature. Membranes were incubated in 5% milk in TBST containing a respective primary antibody (Table 5) overnight at 4°C. The membranes were incubated with horseradish peroxidase–labeled secondary antibodies for 1 hour at room temperature. After antibody incubation, the membranes were washed once in RIPEA for 10 minutes and twice in TBST, 10 minutes each. The protein bands were visualized by the application of a chemiluminescent substrate (PerkinElmer, Boston, MA) and Fusion FX7 Advance imaging system with a CDD camera (Vilber Lourmat, Torcy, France) was used for digital signal detection. Recordings were obtained at the dynamic range of exposure without binning. Calculations for signal quantification were obtained using BioD1 software (Vilber Lourmat, Torcy, France). Alternatively, signal was detected by exposure of the membrane to autoradiograph film (Super RX; Fujifilm, Dielsdorf, Switzerland).

Protein	Host	Supplier	Cat-nr	Dilution
ACTB	mouse	Santa Cruz Biotechnology; Santa Cruz, CA, USA	sc1616	1:10000
AKT	rabbit	Cell Signalling Technology, Beverly, MA, USA	9272	1:2500
CASP1	rabbit	kindly provided by P. Vandenabeele, Ghent University, Belgium	-	1:10000
EPAS1 (HIF2A)	rabbit	Novus Biologicals; Littleton, CO, USA	100-480	1:500
ERK1/2	rabbit	Cell Signalling Technology, Beverly, MA, USA	9102	1:1000
GFAP	mouse	Sigma, St. Louis, MO, USA	G3893	1:500
HIF1A	rabbit	Novus Biologicals; Littleton, CO, USA	100-479	1:1000
p-AKT	rabbit	Cell Signalling Technology, Beverly, MA, USA	9271	1:1000
p-ERK1/2	rabbit	Cell Signalling Technology, Beverly, MA, USA	9101	1:1000
p-STAT3	rabbit	Cell Signalling Technology, Beverly, MA, USA	9131	1.250
STAT3	rabbit	Cell Signalling Technology, Beverly, MA, USA	9132	1:1000

Table 5 Antibodies for Western blot analysis. Shown is a list of primary antibodies used, with specifications for the host immunized to obtain the desired antibody, the supplier and catalogue number of the product, and the dilution used for western blot analysis.

3.6 Histological Analysis and Light Microscopy

To analyze retinal morphology by light microscopy, eyes were enucleated and fixed in 2.5% glutaraldehyde in 0.1 M cacodylate buffer (pH 7.3) at 4 °C overnight. After fixation, cornea

and lens were removed and the eyecup separated into a superior and an inferior half by cutting through the optic nerve. Tissue was washed in cacodylate buffer, contrasted with osmium tetroxide (1%, 1 Hr, room temperature), dehydrated by incubation in increasing ethanol concentrations, and embedded in Epon 812. Semi-thin sections (0.5 µm) were prepared and counterstained with toluidine blue. A digitalized microscope (Axiovision; Carl Zeiss Meditec, Jena, Germany) was used to examine the slides. Retinal thickness was measured at fixed distances from the ONH using ImageJ (ver. 1.43; developed by Wayne Rasband, National Institutes of Health, Bethesda, MD; available at http://rsb.info.nih.gov/ij/index.html).

3.7 Immunofluorescence on Retinal Cryosections

For immunofluorescence, eyes were enucleated and fixed in 4% PFA at 4°C overnight. Cornea and lens were removed and eyecups were incubated in 30% sucrose in PBS for cryoprotection until the tissue sunk to the bottom of the tube. Tissue was then embedded in tissue cryoprotective medium (Leica Microsystems Nussloch GmbH, Cat-nr: 14020108926, Nussloch, Germany) and rapidly frozen in a 2-methylbutane bath cooled with liquid nitrogen. 12 µm thick sections were cut through the optic nerve head on a Cryostat (Leica, Germany), air-dried and stored at −80 °C until further use. Sections on slides were incubated with blocking solution (3% horse serum in PBS; 0.3% Triton X-100) for 1 Hr at RT. Primary antibodies were applied in blocking solution overnight at 4 °C (Table 6). Slides were washed 3 times with PBS and incubated with Cy2- or Cy3-conjugated secondary antibodies (Jackson ImmunoResesarch, Soham, UK) in blocking solution (dilution 1:500) for 1 Hr at room temperature. After 3 washing steps in PBS, cell nuclei were stained with DAPI and slides were mounted with anti-fade medium (10% Mowiol 4–88; vol/vol; Calbiochem, San Diego, CA, USA), in 100 mM Tris (pH 8.5), 25% glycerol (wt/vol), 0.1% 1,4-diazabicyclo [2.2.2] octane (DABCO)). Immunofluorescently labeled proteins were visualized using a fluorescence microscope (Axioplan, Zeiss, Switzerland).

Protein	Host	Supplier	Cat-nr	Dilution
CALB1	rabbit	Chemicon, Billerica, MA, USA	1778	1:500
CALB2	rabbit	Chemicon, Billerica, MA, USA	5054	1:1000
GFAP	mouse	Sigma, St. Louis, MO, USA	G3893	1:500
GNAT1	rabbit	Santa Cruz Biotechnology; Santa Cruz, CA, USA	sc-389	1:500
GNAT2	rabbit	Santa Cruz Biotechnology; Santa Cruz, CA, USA	sc-390	1:500
GLUL (GS)	mouse	Millipore, Billerica, MA	B302	1:500
IBA1	rabbit	Wako, Neuss, Germany	019-19741	1:500
PKCA	rabbit	Sigma, St. Louis, MO, USA	4334	1:1000
POU4F1 (BRN3A)	mouse	Chemicon, Billerica, MA, USA	1585	1:100
RPE65	rabbit	Pineda Antibodies, Berlin, Germany	Pin-5	1.500
SYP	mouse	Novocastra, Newcastle, UK	299	1:100
VSX2 (CHX10)	rabbit	generous gift of C. Cepko, Harvard University, MA, USA	-	1:500

Table 6 Antibodies for immunofluorescence on retinal cryosections. Shown is a list of primary antibodies used, with specifications for the host immunized to obtain the desired antibody, the supplier and catalogue number of the product, and the dilution used for immunofluorescence analysis.

3.8 Flatmount Immunofluorescence

Eyes were enucleated and incubated in 2% PFA in PBS for 5 minutes. Subsequently, cornea and lens were removed and the retina carefully separated from the eyecup. The retina was cut into a “clover-leaf” shape and post-fixed in 4% PFA in PBS for 10 minutes. Flat mounted retinas were washed briefly with PBS and placed in blocking solution (1% fetal calf serum, 0.1% Triton X-100 in PBS) for 1 Hr. Retinas were incubated overnight at 4°C with *G. simplicifolia* isolectin IB_4-Alexa594 (Invitrogen, Basel, Switzerland) in blocking solution. Retinal flatmounts were washed with PBS and mounted using anti-fade medium (10% Mowiol 4–88; vol/vol; Calbiochem, San Diego, CA, USA), in 100 mM Tris (pH 8.5), 25% glycerol (wt/vol), 0.1% 1,4-diazabicyclo [2.2.2] octane (DABCO)). Imaging was performed using a digitalized light microscope (Axiovision, Zeiss, Switzerland) or a SP5 confocal microscope (Leica Microsystems, Wetzlar, Germany). The Imaris software (Bitplane AG, Zurich, Switzerland) was used to analyze z-stacks and to generate xz-projections.

3.9 Quantification of Vascular Coverage

For quantification of vascular coverage, three regions (770 μm^2) at a distance of 2000 µm from the ONH were analyzed for each flatmounted retina by laser scanning confocal microscopy. The image-analysis software Imaris (Bitplane AG, Zurich, Switzerland) was used to analyze confocal microscope z-stacks and to generate xy-sections for each vascular layer. The images were then post-processed (thresholded and binarized) with ImageJ to obtain binary data from which vascular coverage was determined (ratio of black pixels to total pixels).

3.10 Electroretinography

ERGs were recorded according to previously described procedures (Seeliger et al., 2001; Tanimoto et al., 2009). The ERG equipment consisted of a Ganzfeld bowl, a direct current amplifier, and a PC-based control and recording unit (Multiliner Vision; VIASYS Health Care GmbH, Hoechberg, Germany). Mice were dark adapted overnight and anesthetized with ketamine (66.7 mg/kg body weight) and xylazine (11.7 mg/kg body weight). Pupils were dilated and single-flash ERG responses were obtained under dark-adapted (scotopic) and light-adapted (photopic) conditions. Light adaptation was accomplished with a background illumination of 30 cd/m^2 starting 10 minutes before recording. Single white-flash stimulus intensity ranged from –3.7 to 1.9 log cd · s/m^2 under scotopic and from –0.6 to 2.9 log cd · s/m^2 under photopic conditions, divided into 10 and 8 steps, respectively. Ten responses were averaged with an interstimulus interval (ISI) of either 4.95 seconds (for –3.7, –3, –2.6, –2, -1.6, –1, –0.6, -0.02, 0.4, and 0.9 log cd · s/m^2) or 16.95 seconds (for 1.4, 1.9, 2.4, and 2.9 log cd · s/m^2).

3.11 Hypoxic Exposure

Mice were exposed to reduced oxygen levels in a hypoxic chamber (Coy Laboratory Products, In Vivo cabinet Model 30, Grass Lake, MI, USA) containing food and water *ad libitum*. By altering the O_2:N_2 ratio, O_2 was reduced to the desired concentration in steps of 2% over a time period of 1 Hr. Mice were kept at 7% O_2 levels for 6 Hrs. For the analysis of gene and protein

expression, the retinas were isolated immediately following the hypoxic exposure and processed for further analyisis. To investigate retinal morphology, the eyes were enucleated 12 days after the hypoxic exposure.

3.12 Laser Capture Microdissection

After mice were euthanized, eyes were enucleated, immediately embedded in tissue freezing medium (Leica Microsystems Nussloch GmbH, Cat-nr: 14020108926, Nussloch, Germany), and frozen in a 2-methylbutane bath cooled with liquid nitrogen. Retinal sections (20 µm) were fixed (5 minutes in acetone), air dried (5 minutes), and dehydrated (30 seconds in 100% ethanol, 5 minutes in xylene). Microdissection was performed using an Arcturus XT Laser capture device (Molecular Devices, Sunnyvale, CA, USA). RNA was isolated using the Arcturus kit for RNA isolation (Molecular Devices, Cat-nr: KIT0204, Sunnyvale, CA, USA) according to the manufacturer's directions including a DNase treatment to digest residual genomic DNA. Equal amounts of RNA were used for reverse transcription using oligo(dT) and M-MLV reverse transcriptase (Promega, Cat-nr: M1701, Madison, WI, USA).

3.13 Rhodopsin Measurements

Mice were dark adapted overnight. Retinas of euthanized mice were removed through a slit in the cornea under dim red light and placed in 1 mL of distilled H_2O for 1 minute. After 3 minutes of centrifugation at 15'000 g, the supernatant was discarded and 700 µL of 1% hexadecyltrimethylammonium bromide (Sigma-Aldrich, Cat-nr: H6269, Buchs, SG, Switzerland) in H_2O was added to the pellet. Retinas were mechanically homogenized with a polytron (10 seconds, 3'000 rpm), centrifuged for 3 minutes at 15'000 g, and the supernatant was collected. The absorption at 500 nm was measured before and after exposure to bright white light (20'000 lux for 1 minute). The amount of rhodopsin present per retina was calculated using the following formula derived from the Lambert-Beer equation: $\rho = vol \times c = vol \times \Delta abs500/(E500 \times l \times n)$. ρ is the amount of rhodopsin per retina (in moles); vol is the volume of the sample (in liters); c is the concentration of rhodopsin per retina (M); $\Delta abs500$ is the difference between absorption of the

sample at 500 nm before and after bleaching; E500 is the extinction coefficient of rhodopsin at 500 nm (4.2×10^4 cm × M); l is the path length of the cuvette (in cm); and n is the number of retinas.

3.14 Light Exposure and rhEPO Injections

Mice were dark adapted overnight and pupils dilated with 1% ophthalmic solution (Cyclogyl; Alcon, Cham, Switzerland) and 5% phenylephrine (Ciba Vision, Cat-nr: Niederwangen, Switzerland) 1 Hr before exposure to white fluorescent light (17'000 lux) for 2 Hrs. After light exposure, mice were placed in darkness overnight. Thereafter, mice were kept in normal cyclic light until they were killed. Intraperitoneal injections were performed under dark conditions 1 Hr prior to light exposure. Injections consisted of 50 μL of a 2 IU/μL solution of rhEPO (Epogen, Amgen, USA), or PBS as control.

3.15 Confocal Scanning Laser Ophthalmoscopy

Confocal scanning laser ophthalmoscopy (cSLO) analysis was performed as previously described (Seeliger et al., 2005). Briefly, mice were anaesthetized by a subcutaneous injection of ketamine (66.7 mg/kg) and xylazine (11.7 mg/kg). Pupils were dilated in anaesthesia with tropicamide eye drops (Mydriaticum Stulln, Pharma Stulln, Stulln, Germany). cSLO imaging was performed using a Heidelberg Retina Angiograph (HRA I) equipped with an argon laser featuring two wavelengths (488 nm and 514 nm) in the short wavelength range and two infrared diode lasers (795 nm and 830 nm) in the long wavelength range. The 488-nm and the 795-nm lasers were used for fluorescein (FL) and indocyanine green (ICG) angiography, respectively. FL angiography was performed using a subcutaneous injection of 75 mg/kg body weight fluorescein-Na (University pharmacy, University of Tuebingen, Germany), and ICG angiography following an s.c. injection of 50 mg/kg body weight ICG (ICG-Pulsion, Pulsion Medical Systems AG, Munich, Germany).

3.16 Micron III Ophthalmoscopy

Pupils of mice were dilated with 1% ophthalmic solution (Cyclogyl; Alcon, Cham, Switzerland) and 5% phenylephrine (Ciba Vision, Cat-nr: Niederwangen, Switzerland) 1 Hr before Micron III ophthalmoscopy. Mice were anaesthetized with 2.2 µL/g body weight of a ketamine/xylazine mix (51/6 mix, subcutaneous injection) 5-10 minutes before Micron III ophthalmoscopy. Eyes were kept moisturized with hydroxypropylmethylcellulose (Methocel 2%, Omnivision, Puchheim, Germany) to prevent cataract. Funduscopy and FL angiography were performed with Micron III retinal imaging system (Phoenix Research Labs, Pleasanton, USA). For FL angiography, 50 µL of 0.2% FL solution (AK Fluor, Akorn, Lake Forest, USA) were injected intraperitoneally.

3.17 Spectral Domain Optical Coherence Tomography

Spectral domain optical coherence tomography (SD-OCT) was performed as previously described (Fischer et al., 2009). Briefly, mice were anaesthetized by a subcutaneous injection of ketamine (66.7 mg/kg) and xylazine (11.7 mg/kg). Pupils were dilated in anaesthesia with tropicamide eye drops (Mydriaticum Stulln, Pharma Stulln, Stulln, Germany). Mouse eyes were subjected to SD-OCT using the commercially available Spectralis HRA+SD-OCT device (Heidelberg Engineering, Heidelberg, Germany) featuring a broadband superluminescent diode at λ = 870 nm as low coherent light source. Each two-dimensional B-Scan recorded at 30° field of view consists of 1536 A-Scans, which are acquired at a speed of 40'000 scans per second. Optical depth resolution is around 7 µm with digital resolution reaching 3.5 µm (Huber et al., 2009). Imaging was performed using the proprietary software package Eye Explorer version 3.2.1.0. The combination of scanning laser retinal imaging and SD-OCT allows for real-time tracking of eye movements and real-time averaging of SD-OCT scans, reducing speckle noise in the SD-OCT images considerably (Huber et al., 2009).

3.18 Statistical Analysis

Statistical analysis was performed using Prism4 software (GraphPad Inc., San Diego, USA). All data are presented as mean values ± standard deviations (SD). The number of samples (*N*) used for individual experiments is given in figure legends. Unless stated otherwise, statistical differences of means were calculated using Student's t-test. Differences with *P*-values below 0.05 were considered significant.

4 Results

4.1 Expression of *Cre* Recombinase in *α-Cre*, *Opn-Cre*, and *Pdgfra-Cre* Mice

To characterize the subset of retinal cells expressing *Cre* recombinase, we bred the *Cre*-expressing mice used in this thesis with reporter strains (*Ai6* or *ROSA-flox-RFP*, see below). These reporter strains are engineered to express a reporter protein following the ablation of a *loxP*-flanked STOP cassette, hence marking cell lineages that can be targeted with a given *Cre* line (Novak et al., 2000; Muzumdar et al., 2007). We bred the *α-Cre* mouse (Ashery-Padan et al., 2000) with the *Ai6* reporter mouse that expresses the green fluorescent protein ZSGREEN upon CRE-mediated recombination (Madisen et al., 2010). At PND 15, localization of ZSGREEN on retinal cryosections was observed in a large cell population of the retinal periphery and a smaller subset of cells in the central retina (Fig. 19). Analysis of ZSGREEN distribution on retinal flatmounts revealed a reduced ZSGREEN expression in the central retina and a lack of CRE activity in the dorsal retina (Fig. 19B). Detailed investigation of the ZSGREEN distribution throughout the retinal layers revealed the heterogeneity of retinal cell populations expressing *Cre* recombinase (Fig. 19C).

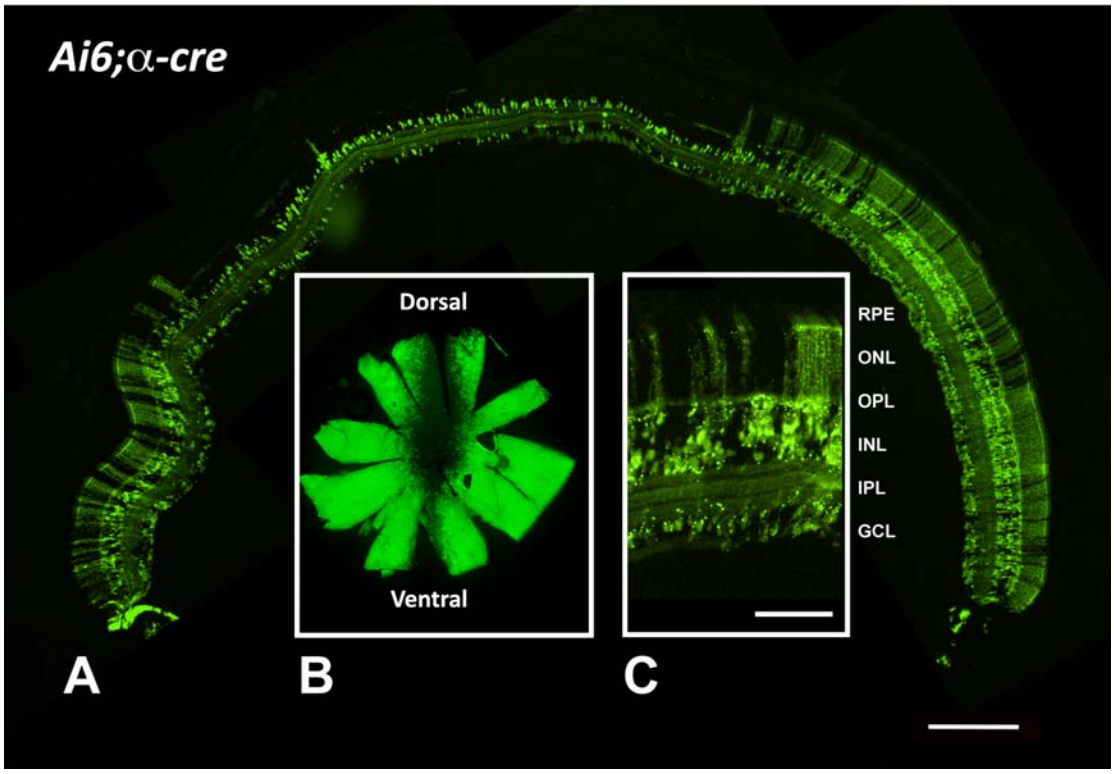

Figure 19 Localization of CRE activity in *Ai6;α-Cre* double mutant reporter mouse. **(A)** Shown is a retinal cryosection (cut naso-temporal) presenting native ZSGREEN fluorescence (green, only expressed where CRE activity is present) at PND 15. **(B)** Retinal flatmount showing the distribution of native ZSGREEN fluorescence. **(C)** Higher magnification of the retinal cryosection shown in (A) presenting the distribution of ZSGREEN through the retinal layers (shown is the transition zone between central and peripheral retina). Scale bar: 200 μm (A), 50 μm (B). (RPE: retinal pigment epithelium; ONL: outer nuclear layer; OPL: outer plexiform layer; INL: inner nuclear layer; IPL: inner plexiform layer; GCL: ganglion cell layer; D: dorsal; V: ventral) (Figure: Caprara and Grimm, unpublished)

Immunostainings with antibodies specific for different retinal cell markers revealed co-localization of GLUL (GS) with ZSGREEN, suggesting that Müller cells express *Cre* recombinase in the *α-Cre* mouse (Fig 20). ZSGREEN was also detectable in rod photoreceptors, as revealed by the localization of ZSGREEN in rod cell bodies and inner segments. A weak co-localization was also observed for both calbindin 1 (CALB1) and calbindin 2 (CALB2) with ZSGREEN, suggesting that horizontal, amacrine, and a subset of ganglion cells may also express *Cre* recombinase (Fig. 20).

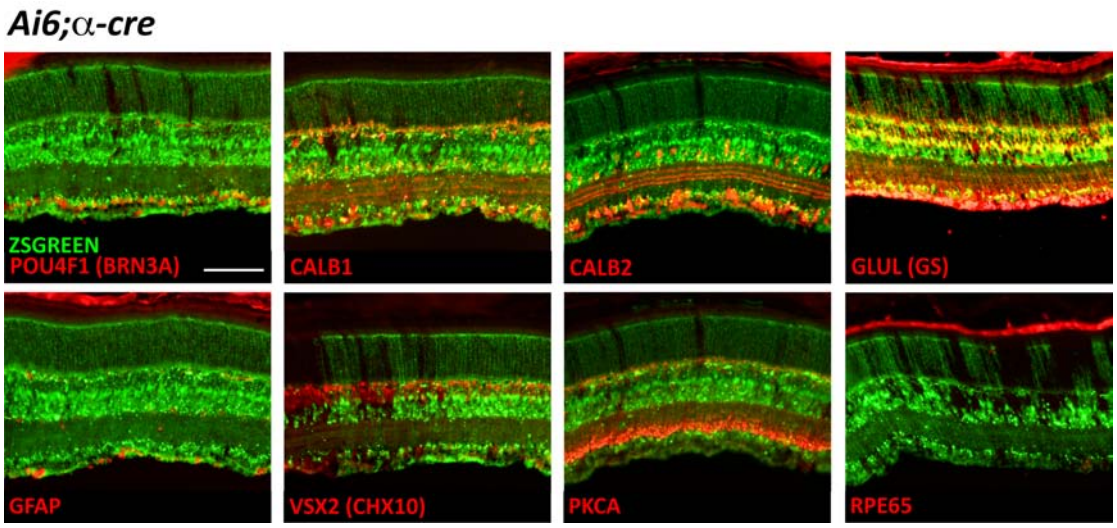

Figure 20 Detection of *Cre* expression in retinal cells of the *α-Cre* mouse as indicated by the co-localization of ZSGREEN and different cell markers in *Ai6;α-Cre* mice at PND 15. Shown are retinal cryosections presenting native ZSGREEN fluorescence (green, only expressed where CRE activity is present) at PND 15 and immunostainings for different retinal cells markers (red). POU4F1 (BRN3A) (brain-specific homeobox/POU domain protein 3A; retinal ganglion cells); CALB1 (calbindin1; horizontal cells and amacrine cell subset); CALB2 (calbindin 2/calretinin, amacrine cells, ganglion cell subset); GLUL (GS) (glutamate-ammonia ligase/glutamine synthetase, Müller cells), GFAP (glial fibrillary acidic protein; astrocytes and activated Müller cells); VSX2 (CHX10) (visual system homeobox 2/Chx10, bipolar cells); PKCA (protein kinase Ca; rod bipolar cells); RPE65 (retinal pigment epithelium-specific 65 kDa protein; retinal pigment epithelium). Scale bar: 100 μm. (Figure: Caprara and Grimm, unpublished)

Even though a clear co-localization of ZSGREEN and POU4F1 (BRN3A) was not found, cells whose nucleus was labelled by the RGC-specific transcription factor showed expression of ZSGREEN in their cytoplasm (Fig. 21). On the contrary, no co-localization of ZSGREEN with bipolar cell markers visual system homeobox 2 (VSX2 (CHX10)), protein kinase Ca (PKCA), or the RPE marker RPE65 were detected (Fig. 20).

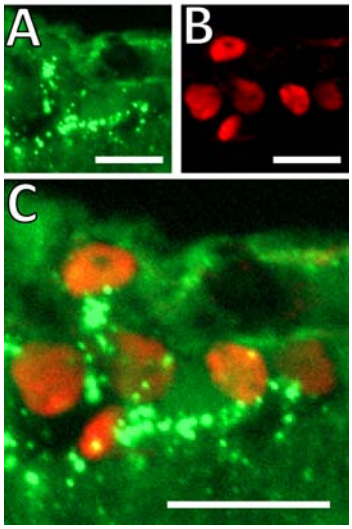

Figure 21 ZSGREEN is expressed in RGCs. ZSGREEN protein (**A,** green, only expressed where CRE activity is present) is expressed in the cytoplasm of POU4F1 (BRN3A)-positive RGCs (**B**, red). Co-localization is not visible due to the different intracellular localization of ZSGREEN and POU4F1 (BRN3A) (**C**, merge of A and B). Scale bar: 20 µm. (Figure: Caprara and Grimm, unpublished)

Next, we analysed the *Pdgfra-Cre* mouse, which was reported to express *Cre* recombinase in Müller cells (Roesch et al., 2008). We bred the *Ai6* reporter mouse (see above) to the *Pdgfra-Cre* mouse and investigated the pattern of *Cre* expression at PND 15. Analysis of native ZSGREEN fluorescence on retinal cryosections revealed a broad distribution of the green fluorescent protein from central to peripheral retina and throughout the retinal layers (Fig. 22). ZSGREEN was also observed uniformly distributed in the whole retina on flatmount preparations (Fig. 22B).

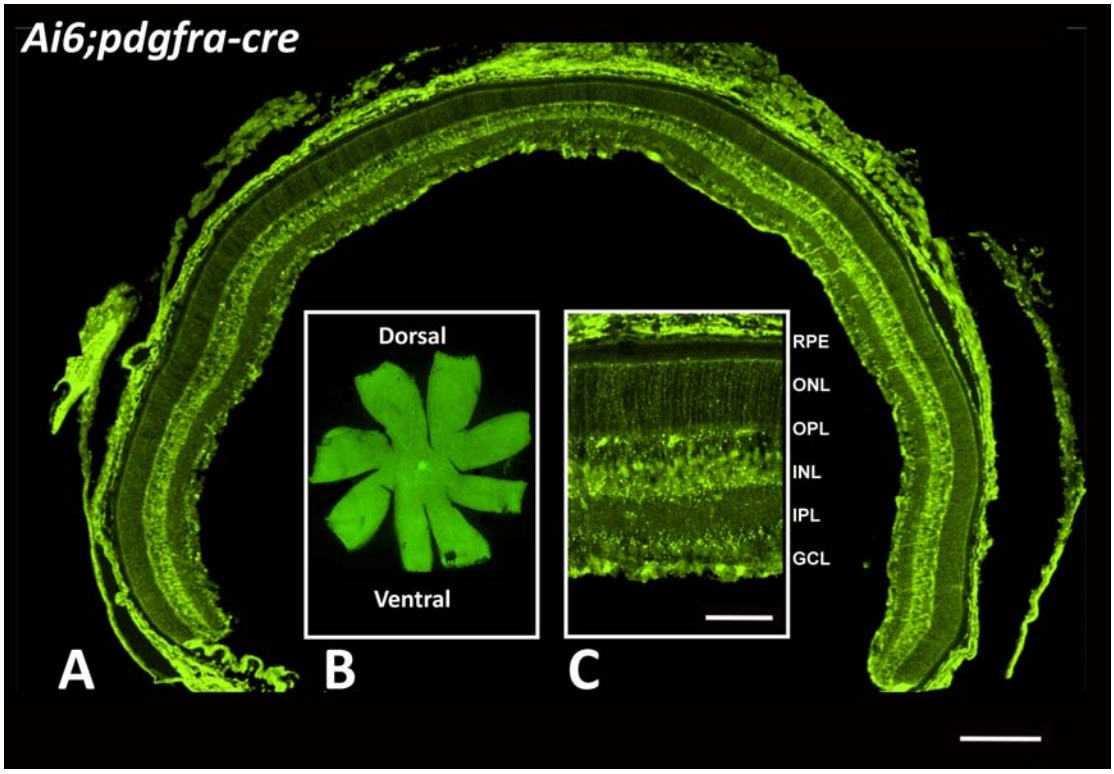

Figure 22 Localization of CRE activity in *Ai6;Pdgfra-Cre* double mutant reporter mouse. **(A)** Shown is a retinal cryosection presenting native ZSGREEN fluorescence (green, only expressed where CRE activity is present) at PND 15. **(B)** Retinal flatmount showing the distribution of native ZSGREEN fluorescence. **(C)** Higher magnification of the retinal cryosection shown in (A) presenting the distribution of ZSGREEN through the retinal layers (shown is a picture from the central retina). Scale bar: 200 μm (A), 50 μm (C). (RPE: retinal pigment epithelium; ONL: outer nuclear layer; OPL: outer plexiform layer; INL: inner nuclear layer; IPL: inner plexiform layer; GCL: ganglion cell layer; D: dorsal; V: ventral). (Figure: Caprara and Grimm, unpublished)

Immunofluorescence co-localization studies on retinal cryosections of the *Ai6;Pdgfra-Cre* mouse at PND 15 revealed a clear co-localization of both GLUL (GS) and GFAP with ZSGREEN, thus supporting the previously reported expression of *Cre* recombinase in Müller cells, but suggesting that astrocytes may also express *Cre* recombinase (Fig. 23). Weak co-localization of CALB1 and ZSGREEN was also observed in the OPL, implying that also horizontal cells express *Cre* recombinase in the *Pdgfra-Cre* mouse. Absence of co-localization of ZSGREEN with POU4F1 (BRN3A), CALB2, VSX2 (CHX10), PKCA, or RPE65 points to the absence of CRE-mediated recombination in RGCs, amacrine, bipolar, and RPE cells, respectively (Fig. 23). It is important to note that in the *Pdgfra-Cre* mouse, *Cre* transcription is not restricted to the retina. Even though a detailed analysis was not performed, ZSGREEN was detected in the sclera, choroid (Fig. 22) and in extraocular tissues, such as the skin of the limbs. This broad expression pattern of CRE may cause systemic and unwanted effects after the deletion of specific genes.

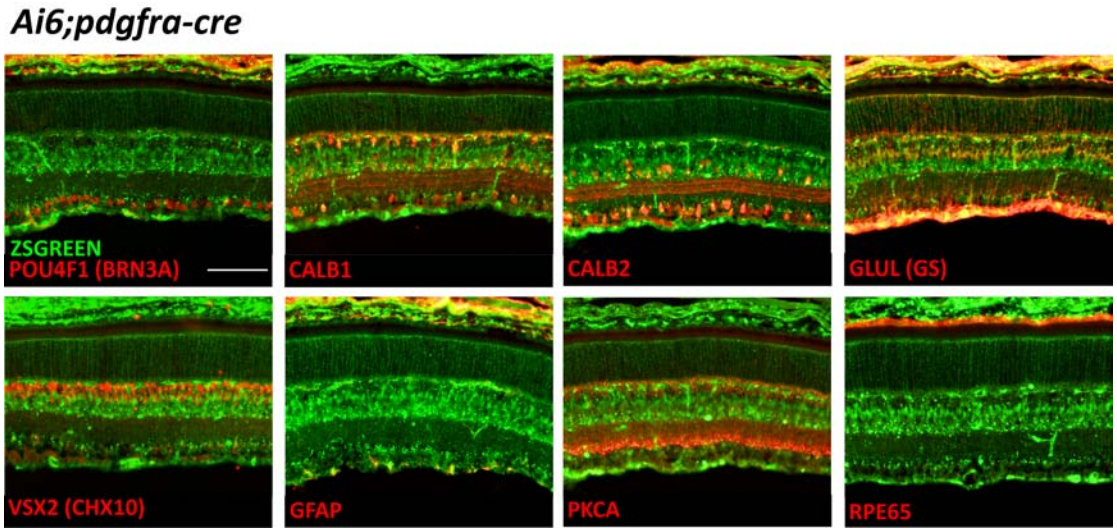

Figure 23 Detection of *Cre* expression in retinal cells of the *Pdgfra-Cre* mouse as indicated by the co-localization of ZSGREEN and different cell markers in *Ai6;Pdgfra-Cre* mice at PND 15. Shown are retinal cryosections presenting native ZSGREEN fluorescence (green, only expressed where CRE activity is present) at PND 15 and immunostainings for different retinal cells markers (red). POU4F1 (BRN3A) (brain-specific homeobox/POU domain protein 3A; retinal ganglion cells); CALB1 (calbindin1; horizontal cells and amacrine cell subset); CALB2 (calbindin 2/calretinin, amacrine cells, ganglion cell subset); GLUL (GS) (glutamate-ammonia ligase/glutamine synthetase, Müller cells), GFAP (glial fibrillary acidic protein; astrocytes and activated Müller cells); VSX2 (CHX10) (visual system homeobox 2/Chx10, bipolar cells); PKCA (protein kinase Ca; rod bipolar cells); RPE65 (retinal pigment epithelium-specific 65 kDa protein; retinal pigment epithelium). Scale bar: 100 μm. (Figure: Caprara and Grimm, unpublished)

The *Opn-Cre* mouse was reported to express *Cre* recombinase in rod photoreceptors starting approximately at PND 7 and increasing up to 6 weeks of age (Le et al., 2006). We analyzed for rod-specific *Cre* expression by breeding the reporter strain *ROSA-flox-RFP,* expressing red fluorescence protein (RFP), to the *Opn-Cre* mouse. The retinas were prepared for analysis when the animals were 10-week old. In fact, based on our observations, recombination is efficient only from this age onwards in the *Opn-Cre* mouse (data not shown). Distribution of RFP in retinal cryosections of 10-week old *ROSA-flox-RFP;Opn-Cre* mice revealed localization of CRE in rods, but also revealed a patchy pattern of expression in roughly 40% of the total rod population (estimation not based on quantitative measurements)(Fig. 24).

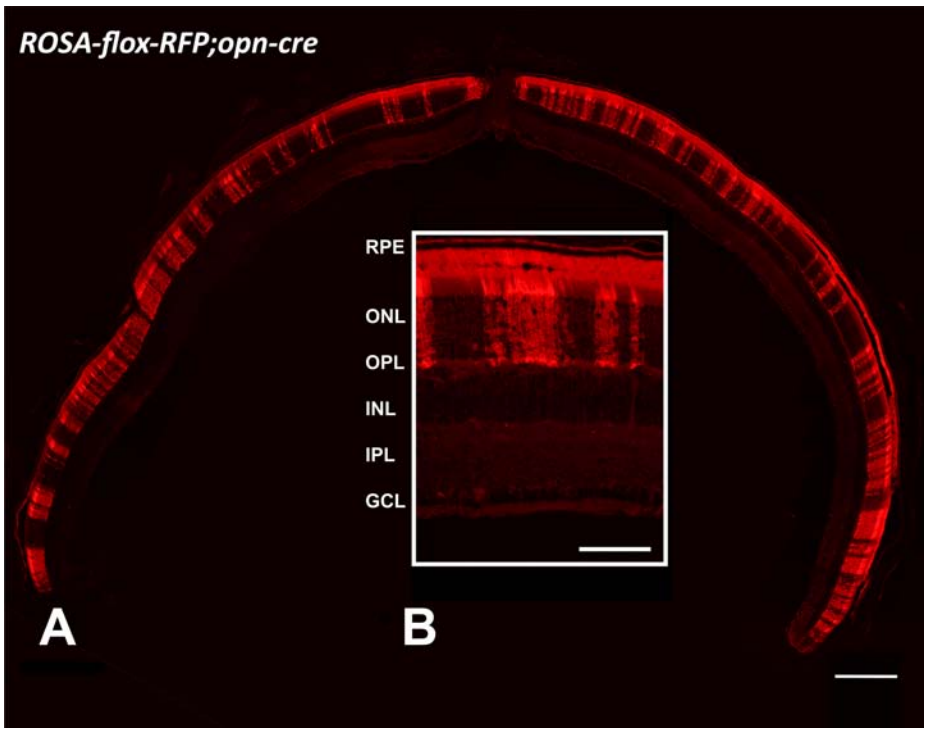

Figure 24 Detection of *Cre* expression pattern in the *Opn-Cre* mouse as indicated by the distribution of RFP in *ROSA-flox-RFP;Opn-Cre* mice at PND 70. **(A)** Shown is a naso-temporal cryosection through the optic nerve head with RFP fluorescence **(B)** Higher magnification of the retinal cryosection shown in (A) presenting the distribution of RFP through the retinal layers. Scale bar: 200 μm (A), 50 μm (B). (RPE: retinal pigment epithelium; ONL: outer nuclear layer; OPL: outer plexiform layer; INL: inner nuclear layer; IPL: inner plexiform layer; GCL: ganglion cell layer) Scale bar 200 μm (Figure: Lange *et al,* 2011)

4.2 Genes Encoding for HIFs Are Expressed in the Mouse Retina

To address the roles of HIFs in the retina, we first measured the expression profile of genes encoding for these transcription factors during post-natal development and in the adult retina of BL6/JFue mice. The expression profiles of *Hif1a* and *Epas1 (Hif2a)* were remarkably similar. Both genes were transcribed at relatively low levels up to PND 10, the time-point when the expression increased by 6-fold and was maintained at constant level in the adult retina, with a slight tendency for increased mRNA levels towards 6 months of age (Fig. 25A, B). A similar strong upregulation and a peak of expression at PND 10 were measured for *Hif3a*, which however showed a trend towards a decline of expression in the adult retina (Fig 25C). The gene expression pattern of *Hif1b* showed a comparable profile as *Hif1a* and *Epas1 (Hif2a)* (Fig. 25D).

Nevertheless, the increase in the expression of *Hif1b* at PND 10 was modest (3-fold) when compared to *Hif1a* and *Epas1 (Hif2a)* (6-fold).

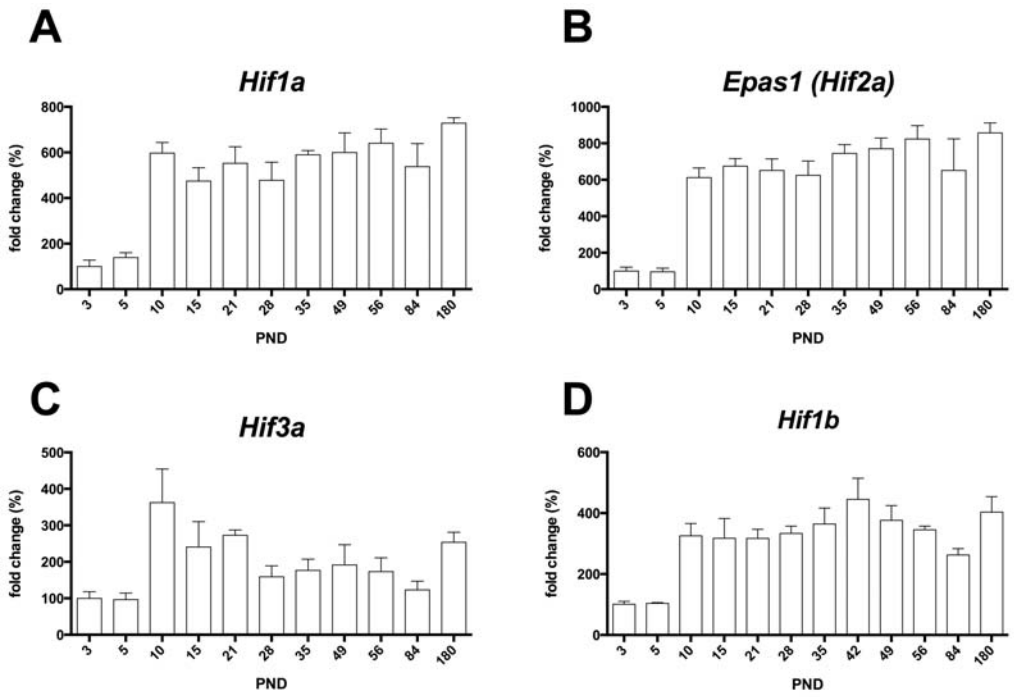

Figure 25 Expression profile of *Hif* genes in the post-natal retina of BL6/JFue mice. Expression of *Hif1a* (hypoxia-inducible factor 1a) **(A)**, *Epas1 (Hif2a)* (endothelial PAS domain protein 1 / hypoxia-inducible factor 2a) **(B)**, *Hif3a* (hypoxia-inducible factor 3a) **(C)**, and *Hif1b* (hypoxia-inducible factor 1b) **(D)** as measured by semi-quantitative real-time PCR on cDNA samples prepared from BL6/JFue animals at different post-natal days (PND). All values were normalized to *Actb* and the value at PND 3 was set as 100%. Shown are mean values of N=3 animals with SD. (Figure: Caprara and Grimm, unpublished)

4.3 *Hif1a* Knockdown in the Retinal Periphery Does Not Alter Retinal Development and Survival

To address the role of HIF1A in the developing and adult retina, we generated *Hif1a*$^{flox/flox}$*;α-Cre* mice. Ablation of the floxed exon 2 of the *Hif1a* gene upon expression of *Cre* recombinase was expected in rods, Müller cells and a subset of amacrine, horizontal and ganglion cells of the peripheral retina. In the central and throughout the dorsal retina, *Cre* expression is restricted to a subset of amacrine and ganglion cells (Fig. 19, 20, 21). Quantification of *Hif1a* mRNA levels in *Hif1a*$^{flox/flox}$*;α-Cre* knockdown mice showed a reduced expression, when compared to *Hif1a*$^{flox/flox}$ control littermates, as early as PND 5 and persisting up to PND 60, the last time-

point measured (Fig. 26A). Correspondingly, the levels of HIF1A protein under normoxia at PND 10 detected by immunoblotting were strongly reduced in the retina of knockdown mice (Fig. 26B). The relatively strong reduction of HIF1A in knockdown mice is conceivable with incomplete retinal angiogenesis at PND 10, in particular in the peripheral retina. This results in the hypoxic stabilization of HIF1A in the avascular retinal periphery (Fig. 16 (Stahl et al., 2010; Grimm et al., 2005). However, this cannot occur in the peripheral retina of the knockdown mice, where CRE-mediated deletion of *Hif1a* occurs.

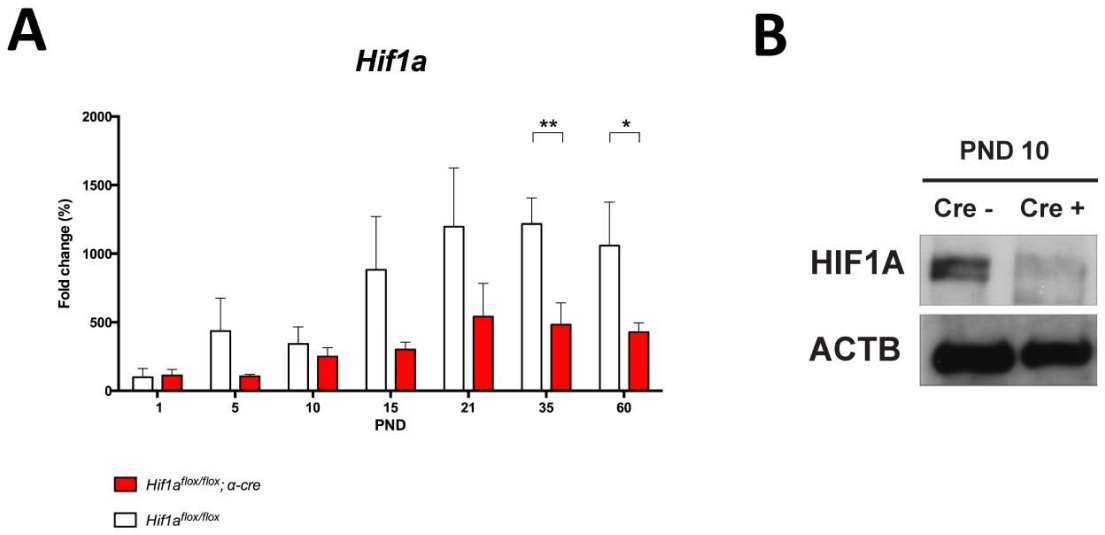

Figure 26 Knockdown of *Hif1a* gene and protein expression in retinas of *Hif1a*$^{flox/flox}$;*α-Cre* mice. (A) Semi-quantitative real-time PCR of *Hif1a* (hypoxia-inducible factor 1a) gene expression in retinas of *Hif1a*$^{flox/flox}$ mice which served as wild-type controls (white columns) and of *Hif1a* knockdown (red columns) mice. cDNAs were prepared from total retinal RNA isolated at post-natal days as indicated on the X-axis. Given are mean values ± SD of N = 3 retinas per time point and genotype, amplified in duplicates. Values were normalized to *Actb* and expressed relatively to PND 1 in *Hif1a*$^{flox/flox}$ mice, which was set to 100%. Differences in gene expression levels between knockdown and control mice at individual time points were tested for significance using a Students t-test *: $P < 0.05$; **: $P < 0.01$. **(B)** Western blot showing retinal HIF1A protein levels under normoxic conditions at PND 10 in *Hif1a*$^{flox/flox}$ mice without (Cre –) or with (Cre +) *α-Cre*. ACTB served as loading control (Figure: adapted from (Caprara et al., 2011)).

In spite of the successful knockdown of *Hif1a*, histological analysis by light microscopy of retinal tissue morphology did not reveal any appreciable abnormality or degeneration in *Hif1a*$^{flox/flox}$;*α-Cre* mice during post-natal development and in the aging retina (Fig. 27). The retinal structure of the *Hif1a* knockdown retina at PND 10 appeared to be unaffected in the periphery where knockdown of *Hif1a* occurs. Maturation of the retina also advanced normally (Fig. 27), and up to 1 year of age the retinal morphology of *Hif1a* knockdowns was indistinguishable from control *Hif1a*$^{flox/flox}$ mice (data not shown).

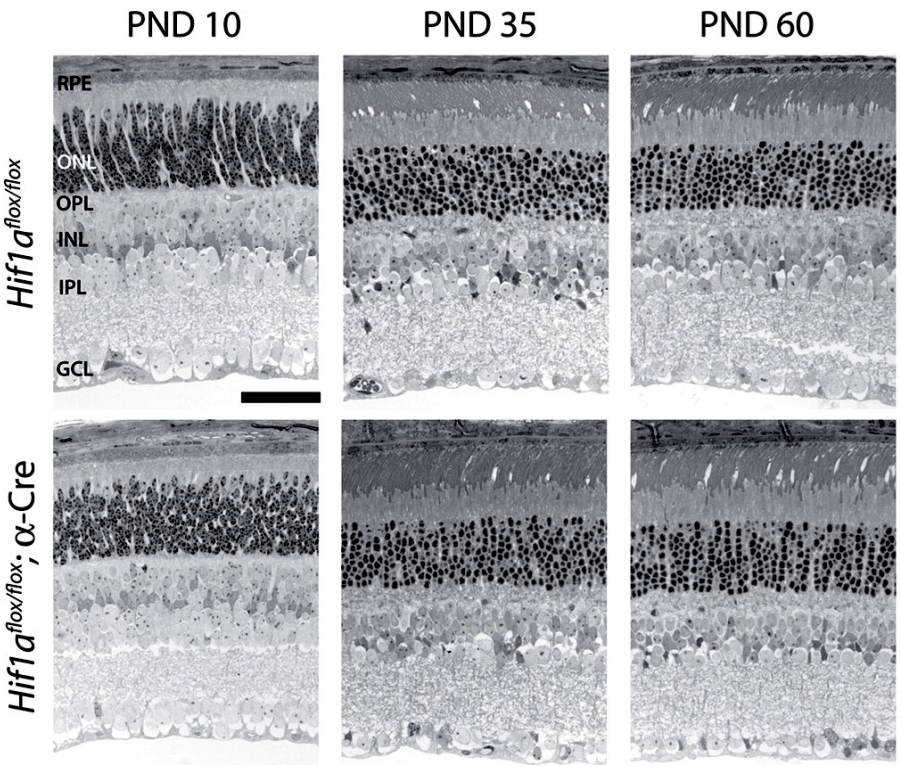

Figure 27 Normal morphology and absence of retinal degeneration in *Hif1a*$^{flox/flox}$*;α-Cre* mice. Retinal morphology of *Hif1a*$^{flox/flox}$*;α-Cre* mice, and *Hif1a*$^{flox/flox}$ littermates at PND 10, 35, 60, was analyzed. Shown are representative sections of the retinal periphery of at least three animals per time point. RPE, retinal pigment epithelium; ONL, outer nuclear layer; OPL, outer plexiform layer; INL, inner nuclear layer; IPL, inner plexiform layer; GCL, ganglion cell layer. Scale bar: 50µm. (Figure: adapted from (Caprara et al., 2011)).

The histological observations were confirmed *in vivo* by fundus and SD-OCT imaging in 3 month-old animals. Analysis by these techniques revealed that retinal tissue architecture of *Hif1a* knockdown mice was comparable to control animals (Fig. 28).

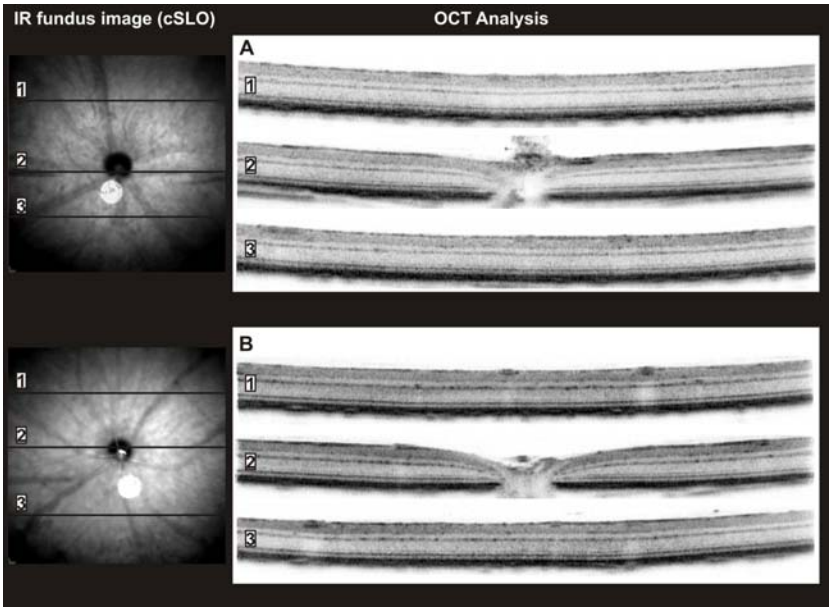

Figure 28 ***In vivo*** **fundus and SD-OCT imaging** of *Hif1a*$^{flox/flox}$ **(A)** and *Hif1a*$^{flox/flox}$*;α-Cre* **(B)** mice at 3 months of age. Solid lines in the fundus image indicate the position where the OCT scans were taken. Shown are representative images of N=3 mice per genotype (Figure: Caprara, Seeliger and Grimm, unpublished).

In addition, quantitative measurements of retinal thickness supported the qualitative observations of retinal morphology of *Hif1a* knockdowns. In fact, a similar thickness of the retina and of the photoreceptor layer at PND 60 was measured in knockdown and wild-type mice both *in vivo* by SD-OCT (Fig. 29A) and in retinal histological preparations (Fig. 29B).

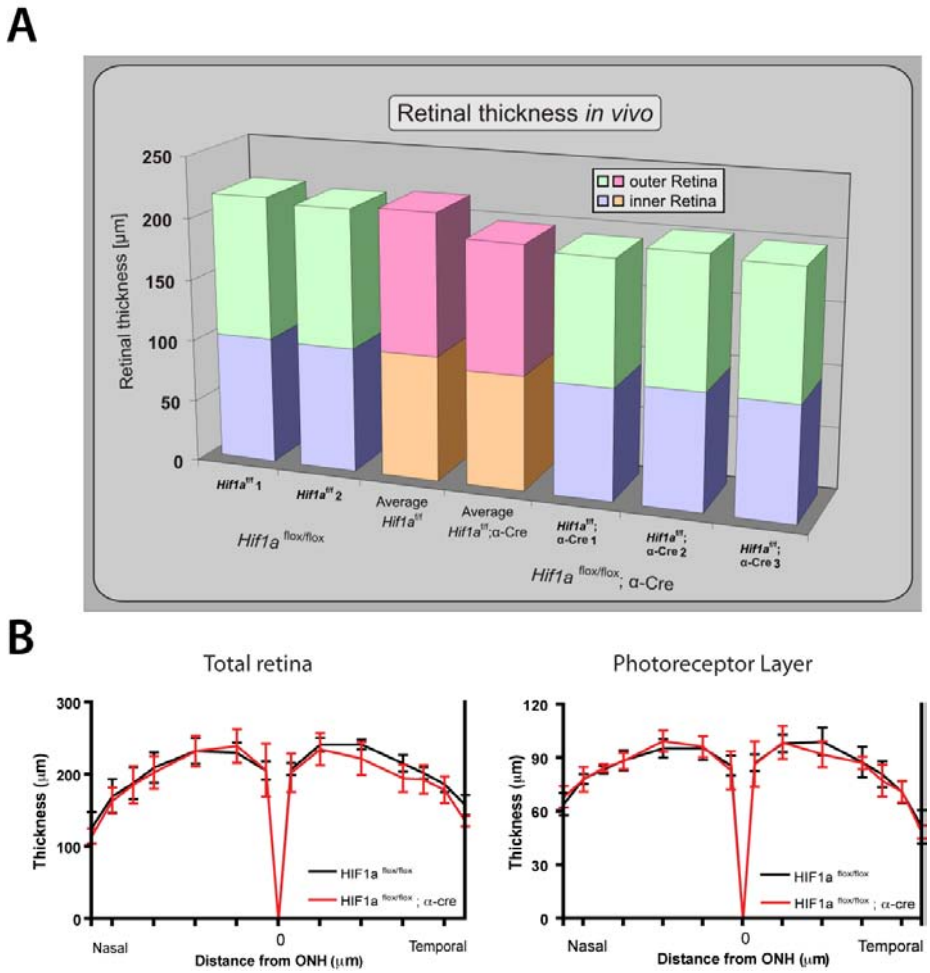

Figure 29 Retinal thickness in *Hif1a*$^{flox/flox}$*;α-Cre* mice. (A) Thickness of the retinal tissue, outer and inner retina, *in vivo* as measured by SD-OCT. Shown are three *Hif1a* knockdown mice and two control littermates at PND 90. **(B)** Thickness of the total retina (left graph) and photoreceptor layer (right graph) measured in histological preparations from *Hif1a* knockdown mice (red lines) and control littermates (black lines) at PND 60. Thickness was measured at 0, 150, 500, 1000, 1500, 1750, 2000, and 2250 µm from the optic nerve head (ONH) in both nasal and temporal hemispheres, as indicated. Shown are means ± SD; N = 3. Ticks on the x-axis correspond to 500 µm. (Figure: A**:** Caprara, Seeliger and Grimm, unpublished; B: adapted from (Caprara et al., 2011)).

A more detailed inspection by immunofluorescence analysis on retinal cryosections revealed no appreciable differences in the localization and spatial arrangement of the main neuronal and glial cell populations between *Hif1a* knockdown and control retinas (Fig. 30), in line with the observations made on histological sections. Notably, in the 3-month old retinas analyzed, the expression of GFAP was not upregulated in Müller cells of *Hif1a*$^{flox/flox}$*;α-Cre* mice, thus suggesting that *Hif1a* knockdown does not lead to retinal stress or injury which would result in gliosis. Furthermore, the distribution of synaptophysin (SYP) immunostaining appeared

undistinguishable in both knockdown and control retinas (Fig. 30), signifying that the formation of synapses in the plexiform layers was unaffected by *Hif1a* ablation.

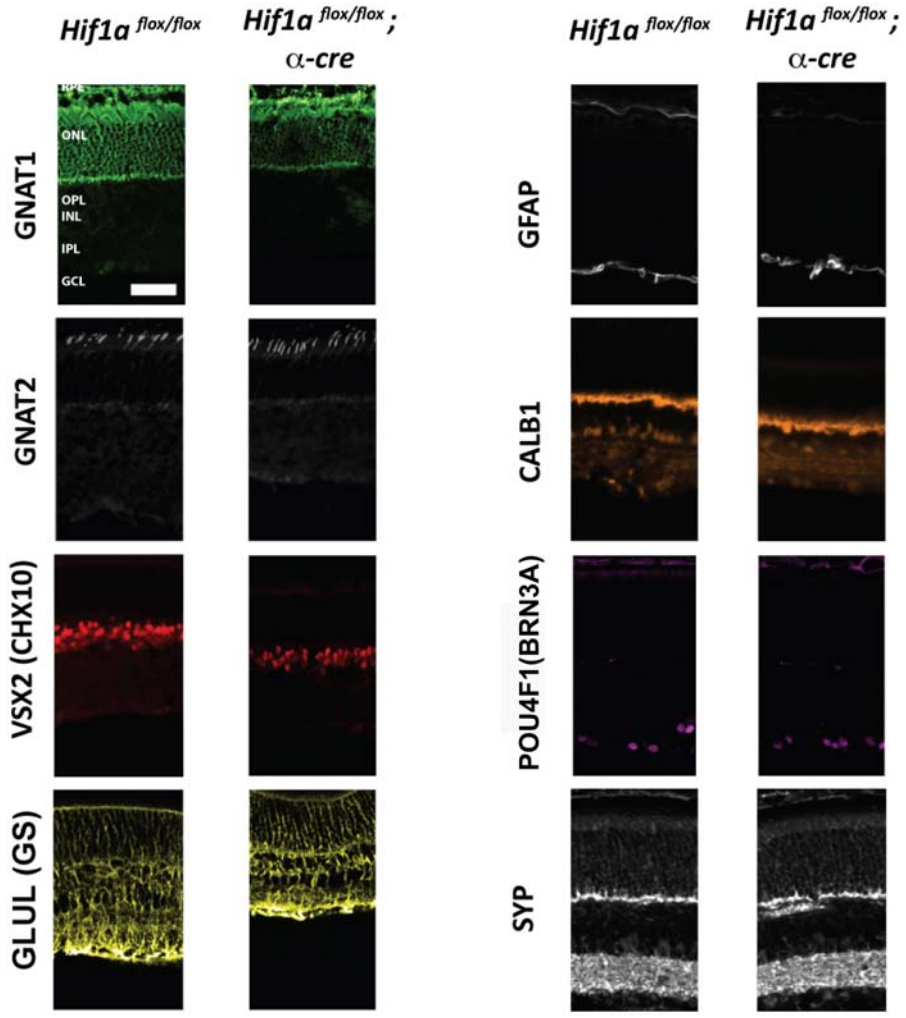

Figure 30 Normal distribution of major retinal cell types in *Hif1a* knockdown mice. Immunostainings of rods (GNAT1: rod transducin, green), cones (GNAT2: cone transducin, white), bipolar cells (VSX2 (CHX10): visual system homeobox 2, red), Müller cells (GLUL (GS): glutamine synthase, yellow), astrocytes and Müller cell endfeet (GFAP: glial fibrillary acid protein, white), horizontal cells (CALB1: calbindin, orange), ganglion cells (POU4F1 (BRN3A): POU domain, class 4, transcription factor 1, purple), and synapses in the inner plexiform and outer plexiform layer (SYP: synaptophysin, white) in *Hif1a*$^{flox/flox}$*;α-Cre* mice, and *Hif1a*$^{flox/flox}$ littermates at PND 90. Note that the mice used for this study were light-adapted which caused the redistribution of rod transducin to rod inner segments and cell bodies. Shown are stainings for the peripheral retina. Scale bar: 50 µm. (Figure: (Caprara et al., 2011))

Semi-quantitative analysis of gene expression up to PND 60 of selected marker genes for rod photoreceptors (*Rho*), cone photoreceptors (*Gnat2*), bipolar cells *(Vsx2 (Chx10)),* and ipRGCs (*Opn4*) confirmed the qualitative observations obtained by immunofluorescence (Fig. 31).

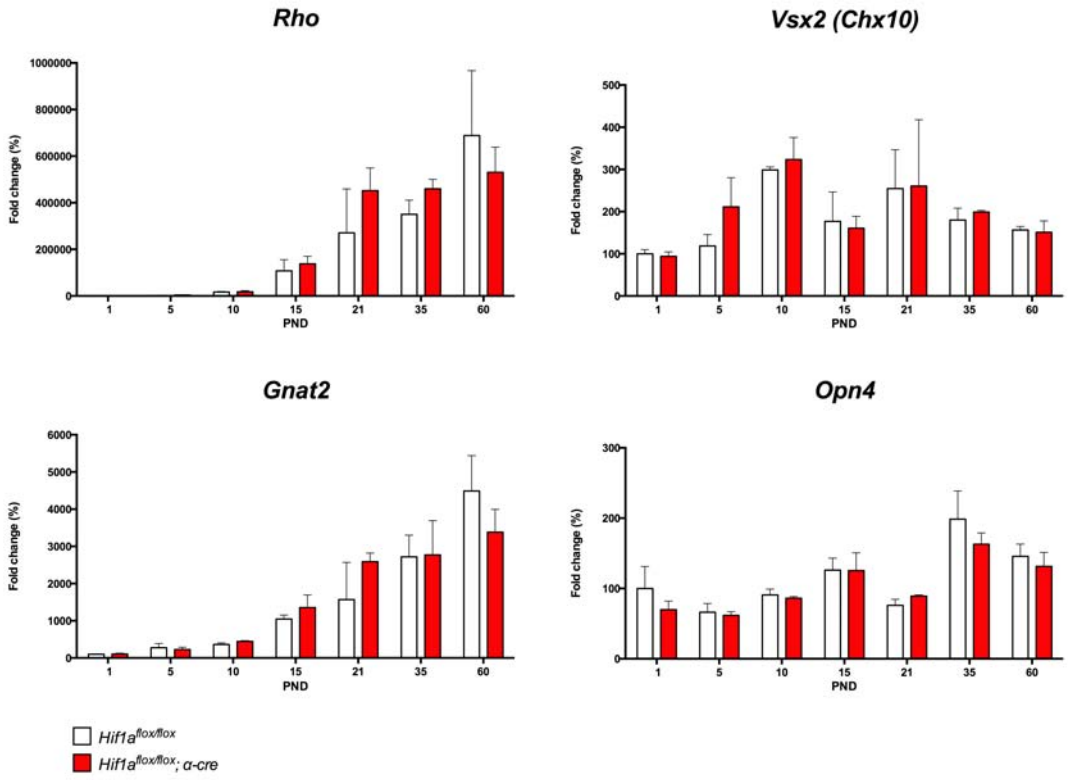

Figure 31 Expression of retinal cell markers upon *Hif1a* ablation in the peripheral retina. Relative quantification of *Rho* (rhodopsin; rod photoreceptors), *Vsx2 (Chx10)* (visual system homeobox 2/Chx10; bipolar cells), *Gnat2* (cone transducin; cone photoreceptors), and *Opn4* (melanopsin; ipRGCs) gene expression in retinas of *Hif1a*$^{flox/flox}$*;α-Cre* mice (red bars) compared to *Hif1a*$^{flox/flox}$ control littermates (white bars) by real-time PCR. cDNAs were prepared from total retinal RNA isolated at time points indicated in the x-axis. Given are mean values ± SD of N = 3 retinas for each genotype and time point, amplified in duplicates. Values were normalized to *Actb* and expressed relatively to *Hif1a*$^{flox/flox}$ control littermates at PND 1, which was set to 100%. Differences in gene expression levels between knockdown and control mice at individual time points were tested for significance using a Students t-test. (Figure: Caprara and Grimm, unpublished)

In various mouse models for retinal degeneration, the cytokine LIF is induced in a subset of Müller glia cells (Samardzija et al., 2006; Joly et al., 2008), and controls a neuroprotective signalling cascade, which culminates in an increased expression of *Fgf2* and endothelin 2 *(Edn2)* (Samardzija et al., 2012). In addition, several genes involved in gliosis, including *Gfap*, are induced in different models of retinal degeneration (Grosche et al., 1997; Samardzija et al., 2012). To assess whether the aforementioned signalling pathway transiently or continuously supports the survival of retinal neurons upon *Hif1a* knockdown, we measured gene expression of *Lif*, *Fgf2*, *Edn2*, and *Gfap* in the retina of *Hif1a*$^{flox/flox}$*;α-Cre* mice at different post-natal stages. While *Lif* was upregulated three-fold ($p<0.001$) at PND 21 in *Hif1a* knockdown retinas, accompanied by a two-fold increase in *Edn2* mRNA expression at PND 35, over a longer time span, this pro-survival signalling pathway did not show signs of induction (Fig. 32). Along with the absence of GFAP

upregulation in Müller cells at PND 90 (Fig. 30), no increase in *Gfap* expression was observed in *Hif1a*$^{flox/flox}$;*α-Cre* mice (Fig. 32).

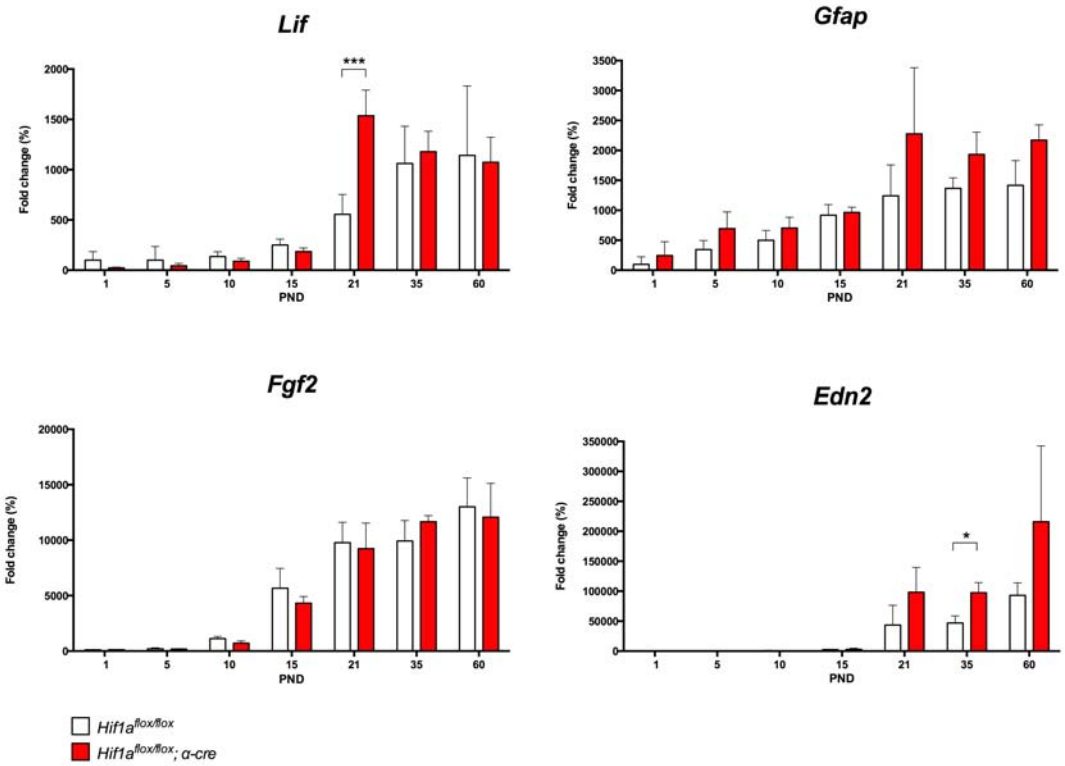

Figure 32 Expression of retinal stress genes upon *Hif1a* ablation in the peripheral retina. Relative quantification of *Lif* (leukemia inhibitory factor), *Gfap* (glial fibrillary acidic protein), *Fgf2* (fibroblast growth factor 2), and *Edn2* (endothelin 2) gene expression in retinas of *Hif1a*$^{flox/flox}$;*α-Cre* mice (red bars) compared to *Hif1a*$^{flox/flox}$ control littermates (white bars) by real-time PCR. cDNAs were prepared from total retinal RNA isolated at time points indicated on the x-axis. Given are mean values ± SD of N = 3 retinas for each genotype and time point, amplified in duplicates. Values were normalized to *Actb* and expressed relatively to *Hif1a*$^{flox/flox}$ control littermates at PND 1, which was set to 100%. Differences in gene expression levels between knockdown and control mice at individual time points were tested for significance using a Students t-test. *: $p<0.05$; ***: $p<0.001$ (Figure: adapted from (Caprara et al., 2011))

Altogether, these results show that knockdown of *Hif1a* did not cause evident alterations in the post-natal development and aging retina. The survival of the major types of retinal neurons and glia was not affected and any sign of gliosis was detected in the retina of *Hif1a*$^{flox/flox}$;*α-Cre* mice.

4.4 Knockdown of *Hif1a* in the Retinal Periphery Results in an Incomplete Development of the Retinal Vasculature

In the early post-natal retina, HIF1A protein is stabilized due to the hypoxic event preceding and driving retinal angiogenesis. Afterwards, HIF1A protein levels decrease as the retina becomes vascularised (Fig. 16) (Grimm et al., 2005). We therefore investigated the time course of retinal angiogenesis by analyzing the vasculature in retinal flatmounts of *Hif1a* knockdown and wild-type mice. At PND 5, the primary plexus reached about two thirds of the retinal surface in both experimental groups. The primary plexus grew with similar kinetics and reached the periphery around PND 10 in both *Hif1a* knockdown and control mice (Fig. 33).

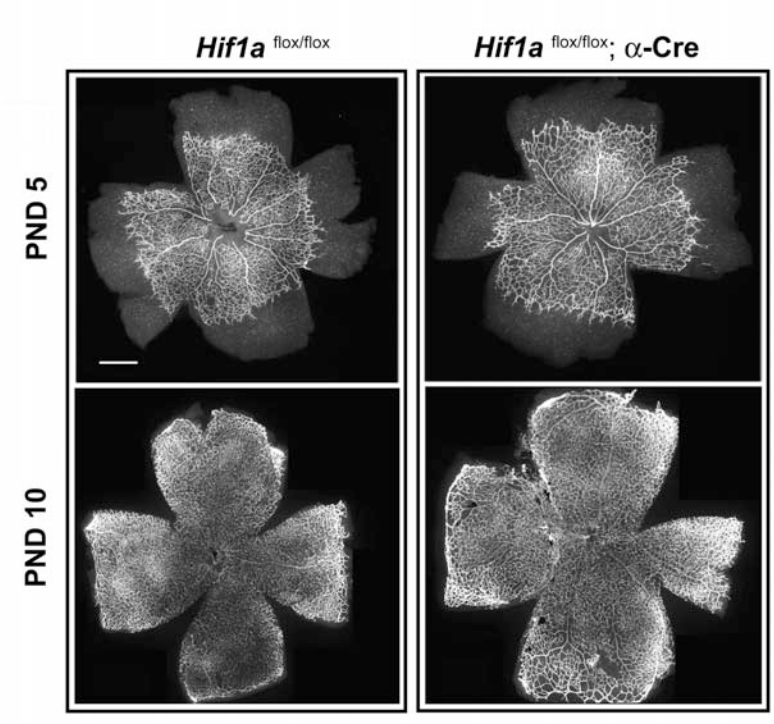

Figure 33 Development of the primary plexus in *Hif1a* knockdown mice. Retinal flatmounts of *Hif1a*$^{flox/flox}$;α-*Cre* mice (right), and *Hif1a*$^{flox/flox}$ littermates (left) at PND 5 (top) and PND 10 (bottom). Vessels were stained with isolectin IB_4 (white) coupled to Alexa594. Shown are representative retinas of N = 3 mice. Scale bar: 500 µm (Figure: (Caprara et al., 2011))

Despite the apparently normal kinetics of development of the primary plexus, when we analyzed the intraretinal vasculature in more detail by confocal microscopy of flatmounted retinas and cryosections, *Hif1a*$^{flox/flox}$;*α-Cre* mice presented a strongly reduced vascular coverage at the level of the intermediate plexus in the peripheral retina at PND 21 (Fig. 34A). On the

contrary, the development of the primary and outer capillary plexi did not appear to be affected. In the central retina of *Hif1a*$^{flox/flox}$*;α-Cre* mice, both deeper plexi were present and showed a pattern comparable to control mice, in line with the low expression of *Cre* recombinase in this region (Fig. 34A). The incomplete capillary coverage in the periphery persisted at least until PND 60 (the last time point analyzed). In fact, the retinal vasculature of *Hif1a*$^{flox/flox}$ control animals at PND 60 showed the dense capillary network of the intermediate plexus. However, in *Hif1a* knockdown mice, the capillary network of the intermediary plexus was largely absent and only vessels connecting the primary to the outer plexus were distinguishable in the peripheral retina (Fig. 34B). Hence, the absence of the intermediate plexus is not a transient phenotype due to a delayed angiogenesis, but persists into adulthood. When the extent of vascular coverage in 21-day old retinas was quantified for each individual plexus, knockdown mice showed a reduction of 75% ± 6% ($P<0.01$) in the extent of vascularisation of the intermediate plexus compared to controls. A mildly increased vascular density, corresponding to 130% ± 11% ($P<0.05$) of that of control littermates, was observed for the primary plexus in *Hif1a*$^{flox/flox}$*;α-Cre* mice. At the level of the outer plexus, no significant differences were detected.

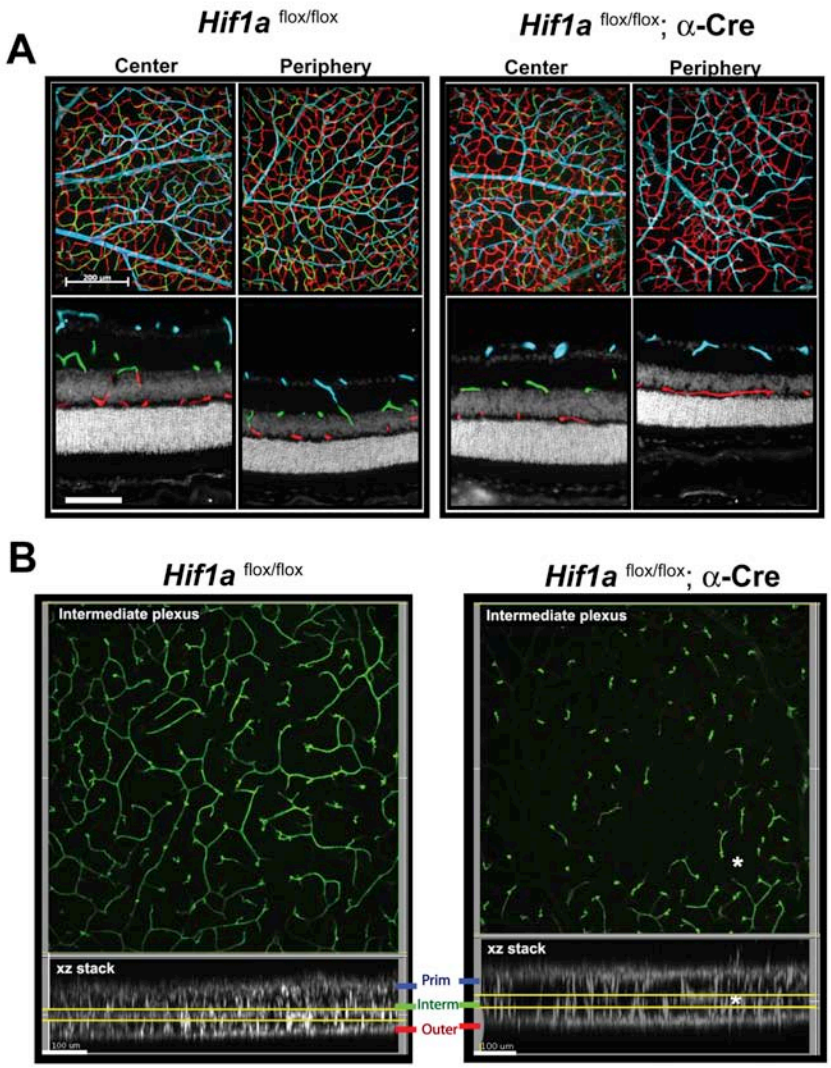

Figure 34 Lack of the intermediate plexus in the peripheral retina of *Hif1a* knockdown mice. (A) Immunostainings of blood vessels (isolectin IB_4, coupled to Alexa594) in *Hif1a*$^{flox/flox}$ littermates (left) and *Hif1a*$^{flox/flox}$*;α-Cre* mice (right). Shown are flatmounts (top) and retinal cryosections (bottom) at PND 21. Pictures of the vascular layers in flatmounts were taken by adjusting the focal plane of the confocal microscope accordingly. Vessels were highlighted by artificial colouring (primary plexus: blue; intermediate plexus: green; outer plexus: red). Scale bar: 200 µm (flatmounts); 100 µm (sections). **(B)** Representative pictures of the intermediate plexus in flatmounts of *Hif1a*$^{flox/flox}$ littermates (left), and *Hif1a*$^{flox/flox}$*;α-Cre* mice (right) at PND 60. The focal plane was adjusted to visualize exclusively the intermediate plexus (top). XZ-stacks (bottom) are artificial sections and show the sum of all signals (including signals in the primary (Prim), the intermediate (Inter) and the outer (Outer) plexus) of the area shown in the flatmount panels above the stacks. For better recognition of the different plexi, the z-value of the z-stacks was increased 5 times (x=1; y=1; z=5). Yellow lanes depict the focal planes used for the flatmount pictures. *: depicts the more central retina. Scale bar: 100 µm (Figure: (Caprara et al., 2011)).

The absence of the intermediate plexus in the retinal periphery of *Hif1a*$^{lox/flox}$*;α-Cre* mice raises questions about the stability of the BRB, and the ability of the existing capillary network to provide an adequate perfusion of the tissue. Aberrant development of the retinal vasculature can be accompanied by functional deficits of blood vessels, which may lead to leakage or

haemorrhage also under physiological conditions (Kaur et al., 2008; Pournaras et al., 2008). To analyze the solidity of the retinal hemodynamics in the *Hif1a*$^{lox/flox}$;*α-Cre* mice, we tested for vascular stability and possible leakage with cSLO in combination with FL and ICG. ICG angiography highlights both retinal and choroidal vascular structures, whereas FL angiography imaging yields particularly detailed information about the retinal capillary beds, but not the choroidal vasculature (Seeliger et al., 2005). Both ICG and FL angiography in the retina of 3-month old *Hif1a* knockdowns did not reveal any vascular leakage and showed a normal blood perfusion of the whole neural tissue of the eye (Fig. 35). Nevertheless, fundus images uncovered abnormalities (lesions) in the retina of *Hif1a* knockdown mice that were not seen in control littermates. In addition, these abnormal lesions were visible also with ICG and FL angiography, thus pointing to vascular defects in the deep capillary beds (Fig. 35C-F). Taken together, these results show that in spite of the inhibitory effect of *Hif1a* knockdown on the development of the intermediate plexus, functional capillaries interconnecting the primary to the outer plexus can guarantee the perfusion of the retina. No obvious effects on the stability of the BRB, such as leakage or haemorrhage, could be observed. Furthermore, the presence of vascular lesions in the retina of adult *Hif1a* knockdown mice suggests for abnormalities in vascular proliferation persisting into adulthood.

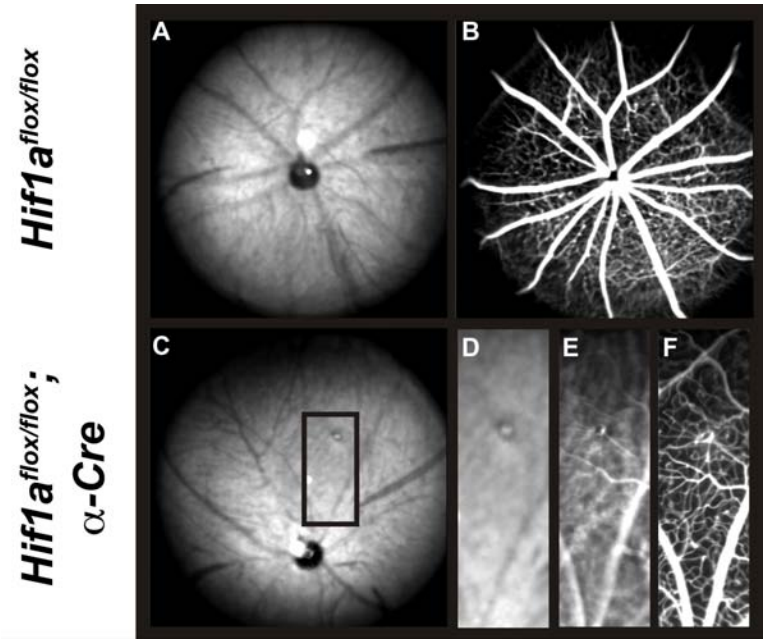

Figure 35 Normal vascular perfusion and presence of vascular lesions in the retina of *Hif1a*$^{flox/flox}$;*α-Cre* mice. Control and *Hif1a* knockdown mouse retinas were examined with cSLO imaging (**A**: control; vs. **C, D**: knockdown), fluorescein angiography (**B**: control; **E, F**: knockdown), and indocyanine green angiography (**E**: knockdown). Fundus

images at 830 nm revealed some alterations in the eye of *Hif1a*$^{flox/flox}$*;α-Cre* mice in comparison to the unaffected control (compare **A** to **C, D**). This lesion was also detectable with indocyanine green and fluorescein angiography (**E, F**), indicating some abnormalities in the deep capillary plexi. (Figure: Caprara, Seeliger and Grimm, unpublished)

Many gene products have been implicated in the complex and multi-stage process of retinal angiogenesis. Analysis of the time-course of expression of these genes by semi-quantitative real-time PCR may give hints about their involvement in the vascular phenotype of *Hif1a* knockdown retinas. The most notable and investigated pro-angiogenic gene is *Vegfa*, whose expression is upregulated in the hypoxic avascular retina, and thus drives post-natal angiogenesis (Fruttiger, 2007). Upregulation of *Vegfa* transcripts have also been described in the INL of the rat retina in a time window preceding the growth of the deep capillary plexus (Stone et al., 1995). In spite of this, no notable and significant alterations of *Vegfa* mRNA expression in the retina were observed up to PND 60 upon *Hif1a* ablation (Fig. 36).

Not only reduced expression of pro-angiogenic genes may explain the vascular phenotype of *Hif1a*$^{flox/flox}$*;α-Cre* retinas, but also an increased production of anti-angiogenic factors such as *Serpinf1 (Pedf)* may underlie this phenomenon (Eichler et al., 2004). As for *Vegfa* expression, also *Serpinf1 (Pedf)* mRNA levels were unchanged upon *Hif1a* knockdown in the retinal periphery (Fig. 36).

ANG2 is a natural antagonist of TEK (TIE2), an endothelial-specific tyrosine kinase receptor that plays an important role in the regulation of physiological vascular growth (Maisonpierre et al., 1997). *Ang2* expression was slightly but not significantly increased at PND 5-10 in *Hif1a* knockdown mice. Interestingly, *Tek (Tie2)* expression at PND 21 was significantly increased by two-fold ($p<0.001$) (Fig. 36).

Members of the netrin protein family have recently been postulated to contribute to retinal developmental and pathological angiogenesis (Xu et al., 2012; Lange et al., 2012). Interestingly, upon *Hif1a* ablation in the retinal periphery, both netrin 1 *(Ntn1)* and netrin 4 *(Ntn4)* mRNA levels were slightly but significantly reduced ($p<0.5$) at PND 10 when compared to wild-type littermates. Gene expression of *Ntn1* was also strongly decreased in the adult retina of *Hif1a*$^{flox/flox}$*;α-Cre* mice when compared to control animals, even though the downregulation was not statistically significant (Fig. 36).

Loss of norrin (NDP), the ligand of a receptor complex composed of frizzled 4 (FZD4), low-density lipoprotein receptor-related protein 5 (LRP5), and tetraspanin 12 (TSPAN12), causes acute developmental blood vessel defects in the retina, including the absence of both the outer and intermediate retinal capillary beds (Ohlmann and Tamm, 2012). Gene expression analysis by real-time PCR did not reveal statistically significant decreased expression of *Ndp* but showed significantly reduced expression of the receptor components *Fzd4* and *Tspan12* at PND 10 in *Hif1a*$^{flox/flox}$*;α-Cre* retinas, the approximate time window for the development of the intermediate plexus (Fig. 36).

Adrenomedullin (ADM) is a molecule expressed in the retina that is involved in the regulation of vascular tone by inducing vasodilation (Kitamura et al., 1993). In addition, *Adm* gene expression has been shown to be induced by hypoxia in the retina (Thiersch et al., 2008). In the retinas of *Hif1a*$^{flox/flox}$*;α-Cre* mice, expression of *Adm* was significantly increased two-fold at PND 15 ($p<0.01$) and PND 21 ($p<0.5$) when compared to control mice (Fig. 36).

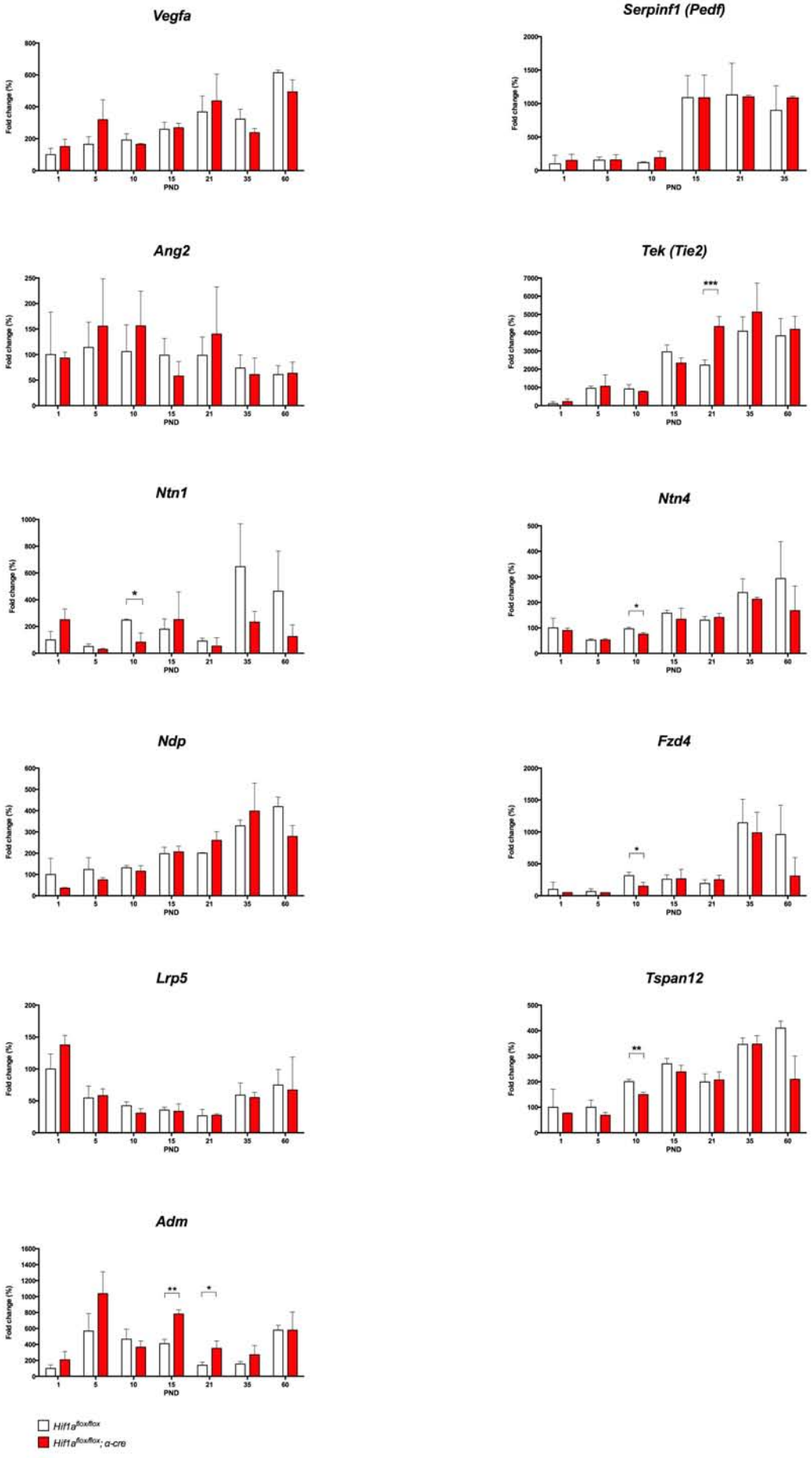
Vegfa
Serpinf1 (Pedf)
Ang2
Tek (Tie2)
Ntn1
Ntn4
Ndp
Fzd4
Lrp5
Tspan12
Adm
Fold change (%)
PND
1
5
10
15
21
35
60
*
**
***
Hif1a^floxflox
Hif1a^floxflox; α-cre

Figure 36 Expression of angiogenic genes upon *Hif1a* ablation in the peripheral retina. Relative quantification of *Vegfa* (vascular endothelial growth factor a), *Serpinf1* (serine (or cysteine) peptidase inhibitor, clade F, member 1/Pedf), *Ang2* (angiopoietin 2), *Tek* (endothelial-specific receptor tyrosine kinase/Tie 2), *Ntn1* (netrin 1), *Ntn4* (netrin 4), *Ndp* (Norrie disease pseudoglioma), *Fzd4* (frizzled homolog 4), *Lrp5* (low density lipoprotein receptor-related protein 5), *Tspan12* (tetraspanin 12), and *Adm* (adrenomedullin) gene expression in retinas of $Hif1a^{flox/flox}$;*α-Cre* mice (red bars) compared to $Hif1a^{flox/flox}$ control littermates (white bars) by real-time PCR. cDNAs were prepared from total retinal RNA isolated at time points indicated on the x-axis. Given are mean values ± SD of N = 3 retinas for each genotype and time point, amplified in duplicates. Values were normalized to *Actb* and expressed relatively to $Hif1a^{flox/flox}$ control littermates at PND 1, which was set to 100%. Differences in gene expression levels between knockdown and control mice at individual time points were tested for significance using a Students t-test. *: $P < 0.05$; **: $P < 0.01$; ***: $P < 0.001$ (Figure: Caprara and Grimm, unpublished)

In conclusion, in spite of the absence of significant modifications in the expression of *Vegfa* upon *Hif1a* ablation, the mRNA levels of *Ntn* family members, as well as components of WNT signalling (*Fzd4* and *Tspan12*) are reduced in the $Hif1a^{flox/flox}$;*α-Cre* mouse retina in a time-window when retinal angiogenesis occurs. Also, the increased expression of *Adm* hints to a possible induction of vasodilation in the retina of *Hif1a* knockdowns.

4.5 Normal Retinal Function in the Absence of HIF1A in the Retinal Periphery

Alterations in the delivery of oxygen and nutrients have harmful consequences on cellular metabolism and also affect neuronal function. Data obtained by ERG recordings show that ischemia and hypoxia reduce retinal function, primarily affecting b-wave amplitude (Brown et al., 1957; Coleman et al., 1990; Tinjust et al., 2002). The reduced vascular coverage in the inner retina of *Hif1a* knockdown mice may result in local retinal hypoxia, and could therefore affect function of the tissue. To test this hypothesis, we measured retinal function under scotopic and photopic conditions by ERG in both *Hif1a* knockdown and control mice at PND 90. ERG recordings did not underline statistically significant differences between the two experimental groups, even though the b-wave amplitude of *Hif1a* knockdowns was decreased under both scotopic and photopic conditions (Fig. 37).

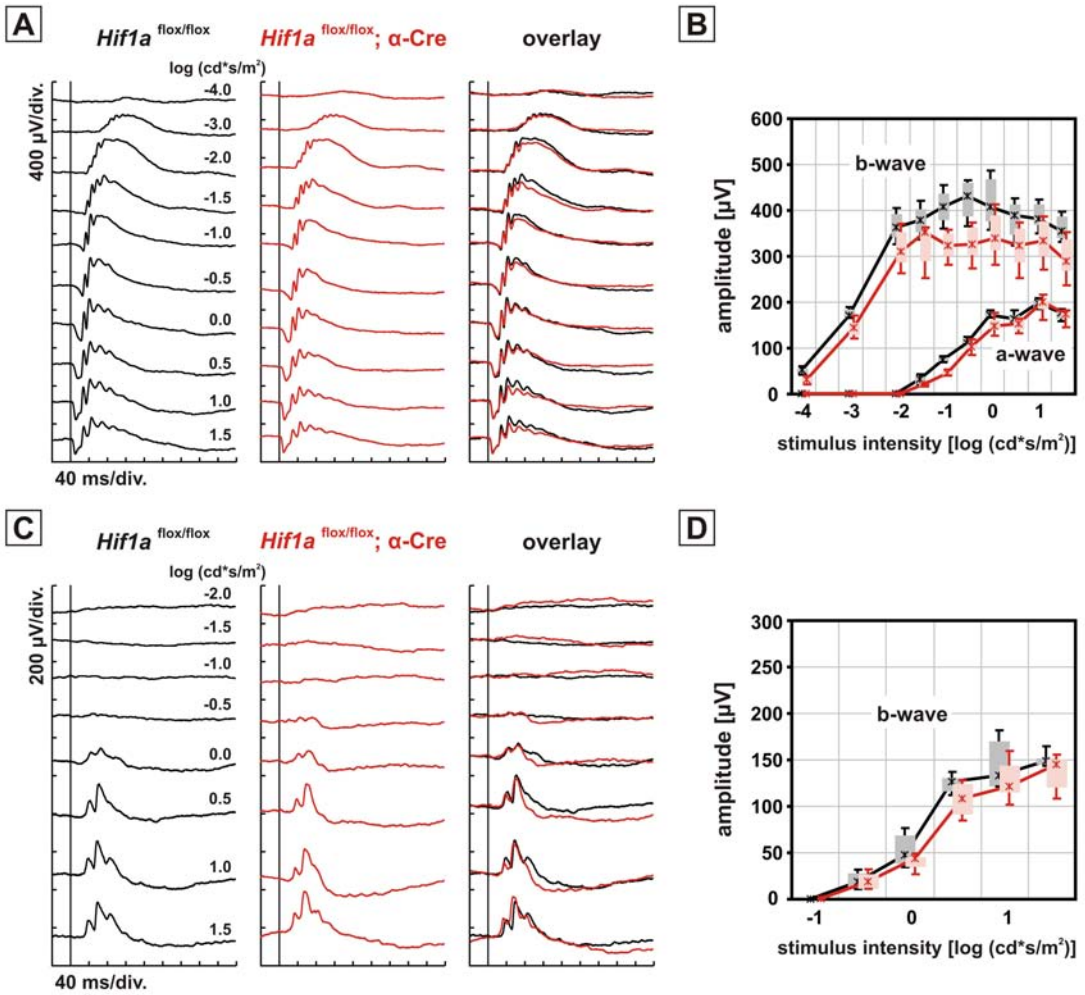

Figure 37 ERG recordings in *Hif1a*$^{flox/flox}$*;α-Cre* mice are comparable to control littermates. Scotopic **(A and B)** and photopic **(C and D)** ERG recordings in *Hif1a*$^{flox/flox}$*;α-Cre* (red lines) and *Hif1a*$^{flox/flox}$ control littermates (black lines). a- and b-wave amplitudes under scotopic conditions **(B)** and b-wave amplitude under photopic conditions **(D)** are shown. N = 3. (Figure: Caprara, Seeliger and Grimm, unpublished)

4.6 *Epo* Is Upregulated in *Hif1a* Knockdown Mice

Despite knockdown of *Hif1a*, a known inducer of *Epo* transcription in hypoxia (Wang and Semenza, 1996), semi-quantitative real-time PCR analysis revealed a strong and significant upregulation of *Epo* expression starting at PND 15, and persisting up to PND 60, the last time point analyzed (Fig. 38A). The induction of *Epo* transcription in retinas of *Hif1a*$^{flox/flox}$*;α-Cre* mice may have been regulated by EPAS1 (HIF2A) (Chavez et al., 2006). Interestingly, *Epas1 (Hif2a)* mRNA levels appeared upregulated at PND 21 in *Hif1a*$^{flox/flox}$*;α-Cre* mice (Fig. 38A), and EPAS1 (HIF2A) was present at increased levels in *Hif1a* knockdown mice at the time when *Epo*

upregulation started (PND 15) and persisted up to PND 75 (Fig. 38B). In contrast, EPAS1 (HIF2A) levels were very low in both *Hif1a* knockdown and control mice at PND 10. At this time point, also *Epo* was expressed at similar low levels in both knockdown and control mice (Fig. 38A).

Beside EPAS1 (HIF2A), also GATA2 (Obara et al., 2008) and HNF4A (Zhang et al., 1999) are known regulators of *Epo* gene expression. Nevertheless, in our mouse model, neither *Gata2* nor *Hnf4a* gene expression was altered by *Hif1a* knockdown (Fig. 38A).

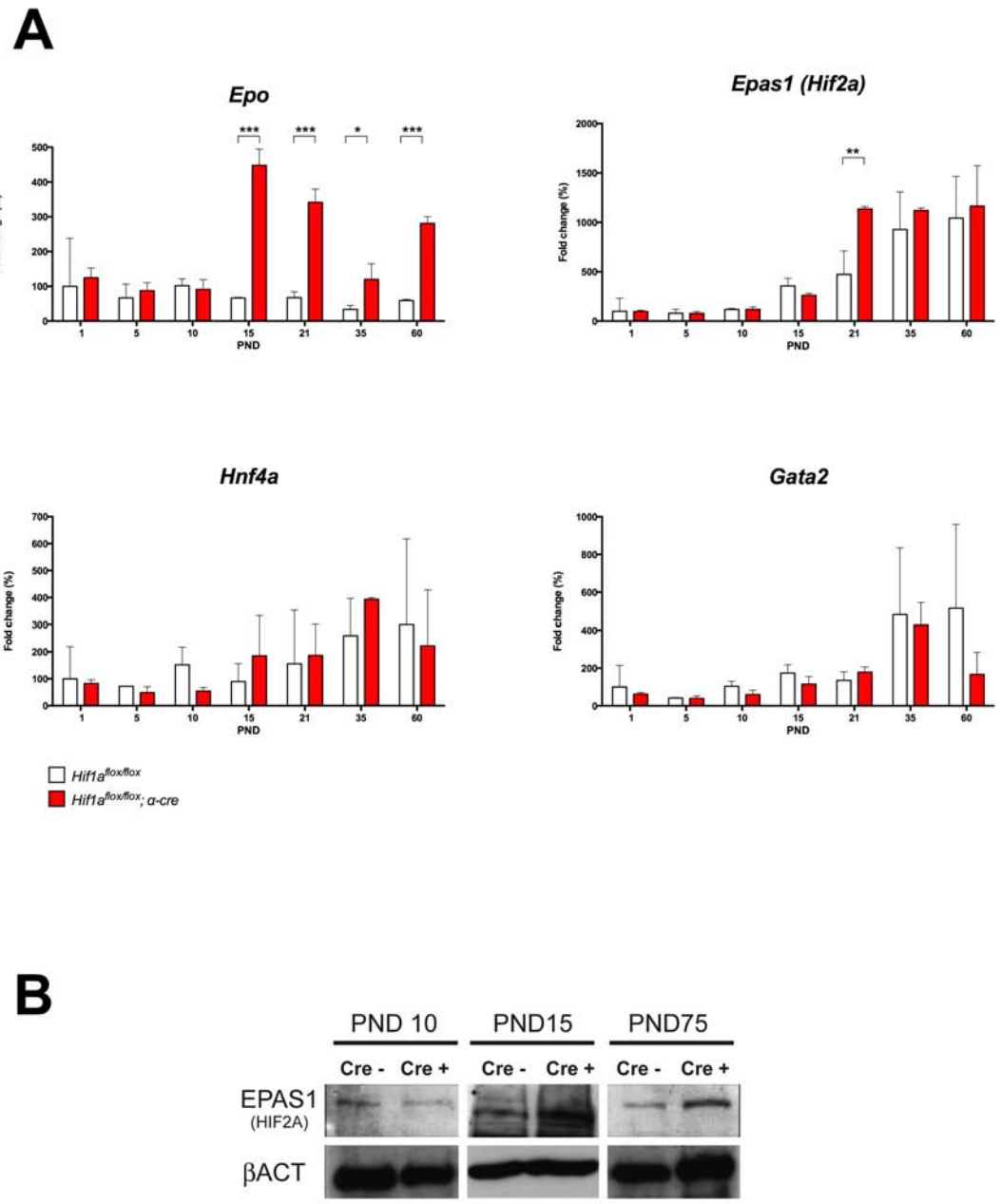

Figure 38 Increased expression of *Epo* mRNA and elevated protein levels of EPAS1 (HIF2A) in *Hif1a*$^{flox/flox}$;*α-Cre* retinas. (A) Relative quantification of *Epo* (erythropoietin), *Epas1 (Hif2a)* (endothelial PAS domain protein 1/*Hif2a*),

Hnf4a (hepatic nuclear factor 4a), *Gata2* (GATA binding protein 2), gene expression in retinas of *Hif1a*$^{flox/flox}$*;α-Cre* mice (red bars) compared to *Hif1a*$^{flox/flox}$ control littermates (white bars) by semi-quantitative real-time PCR. cDNAs were prepared from total retinal RNA isolated at time points indicated on the x-axis. Given are mean values ± SD of N = 3 retinas for each genotype and time point, amplified in duplicates. Values were normalized to *Actb* and expressed relatively to *Hif1a*$^{flox/flox}$ control littermates at PND 1, which was set to 100%. Differences in gene expression levels between knockdown and control mice at individual time points were tested for significance using a Students t-test. *: P < 0.05; **: P < 0.01; ***: P < 0.001**. (B)** Western blot analysis of total retinal extracts at PND 10, PND 15 and PND 75 of *Hif1a*$^{flox/flox}$ mice without (Cre –) or with *α-Cre* (Cre +) as indicated. ACTB served as loading control. Shown are representative blots of N=3 animals per time point and genotype (Figure: adapted from (Caprara et al., 2011)).

4.7 Double Knockdown of *Hif1a* and *EpoR* in the Peripheral Retina Does not Lead to Retinal Degeneration

Elevated expression of *Epo* may contribute to neuronal survival in particular in the senescent retina due to the tissue-protective abilities of this cytokine (Chapter 1.6.2). The absence of noticeable signs of retinal degeneration, in spite of the vascular phenotype described in *Hif1a* knockdown retinas, may thus be the consequence of increased secretion of EPO. To investigate on a possible pro-survival activity of EPO-EPOR signalling in *Hif1a*$^{flox/flox}$*;α-Cre* mice, we ablated *EpoR* concomitantly with *Hif1a* in the retinal periphery by generating *Hif1a*$^{flox/flox}$; *EpoR*$^{flox/flox}$*;α-Cre* mice. At 6 months of age, retinal expression of *Hif1a* mRNA was significantly reduced by about 70% ($p<0.01$) in *Cre* expressing mice as compared to control littermates. This was accompanied by a significant decrease of *EpoR* mRNA by 40% ($p<0.05$) (Fig. 39). The reduction of *EpoR* transcripts was a result of CRE-mediated excision of the *loxP*-flanked *EpoR* genomic sequence (exons 1-4), as revealed by the appearance of a 220bp fragment upon PCR analysis of retinal genomic DNA of *Hif1a*$^{flox/flox}$; *EpoR*$^{flox/flox}$*;α-Cre* mice (data not shown, see Chapter 4.10).

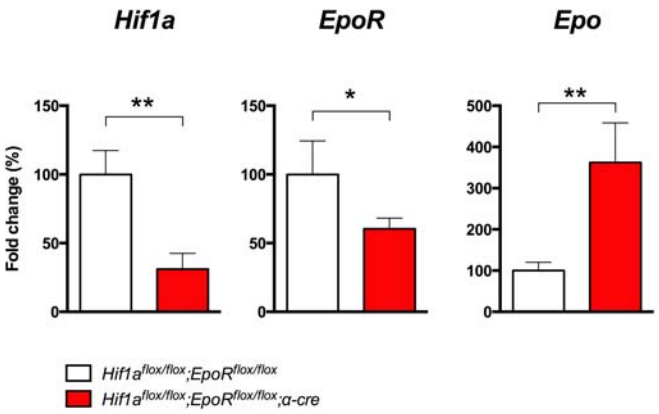

Figure 39 Knockdown of *Hif1a, EpoR* and overexpression of *Epo* in retinas of *Hif1a$^{flox/flox}$; EpoR$^{flox/flox}$;α-Cre* mice. Relative quantification of *Hif1a* (hypoxia-inducible factor 1a), *EpoR* (erythropoietin receptor) and *Epo* (erythropoietin) gene expression in retinas of *Hif1a$^{flox/flox}$; EpoR$^{flox/flox}$;α-Cre* mice (red bars) compared to *Hif1a$^{flox/flox}$; EpoR$^{flox/flox}$* control littermates (white bars) by semi-quantitative real-time PCR. cDNAs were prepared from total retinal RNA isolated at 6 months of age. Given are mean values ± SD of N = 4 retinas for *Hif1a$^{flox/flox}$; EpoR$^{flox/flox}$;α-Cre* animals and N = 3 retinas for controls, amplified in duplicates. Values were normalized to *Actb* and expressed relatively to *Hif1a$^{flox/flox}$; EpoR$^{flox/flox}$* control littermates, which was set to 100%. Differences in gene expression levels between knockdown and control mice at individual time points were tested for significance using a Students t-test *: $P < 0.05$; **: $P < 0.01$ (Figure: Caprara and Grimm, unpublished)

Similarly as observed upon ablation of *Hif1a* in the retinal periphery (Fig. 38A), simultaneous deletion of *Hif1a* and *EpoR* resulted in significantly elevated ($p<0.01$) *Epo* mRNA by about 3.5 fold as compared to control littermates (Fig. 39). Despite deletion of both *Hif1a* and *EpoR* in the peripheral retina, long-term analysis revealed a normal preservation of retinal morphology with any appreciable signs of ongoing tissue degeneration up to PND 400, the last time point analyzed (Fig. 40).

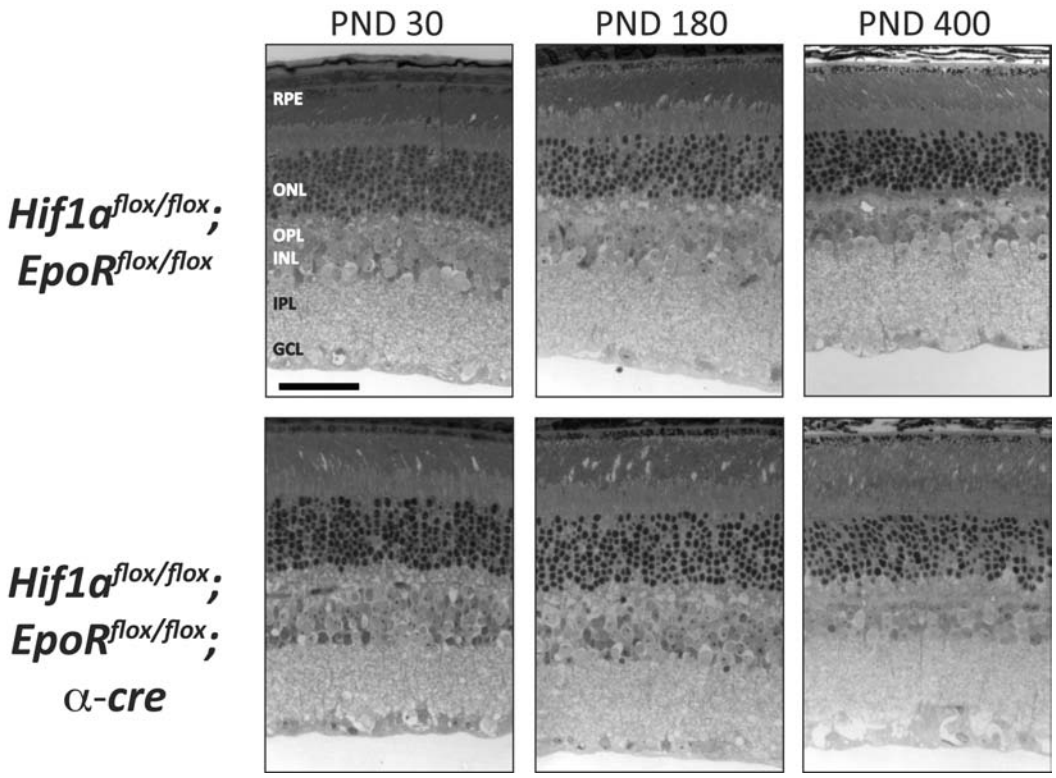

Figure 40 Normal morphology and absence of retinal degeneration in *Hif1a*$^{flox/flox}$; *EpoR*$^{flox/flox}$;*α-Cre* mice. Retinal morphology of *Hif1a*$^{flox/flox}$; *EpoR*$^{flox/flox}$;*α-Cre* mice, and *Hif1a*$^{flox/flox}$; *EpoR*$^{flox/flox}$ littermates at PND 30, 180, and 400 were analyzed. Shown are representative sections of the retinal periphery of at least three animals per time point. RPE, retinal pigment epithelium; ONL, outer nuclear layer; OPL, outer plexiform layer; INL, inner nuclear layer; IPL, inner plexiform layer; GCL, ganglion cell layer. Scale bar: 50µm. (Figure: Caprara and Grimm, unpublished)

Analysis of the survival of the main retinal cell populations was performed by quantification of mRNA levels of different marker genes by semi-quantitative real-time PCR. In double knockdown mice and control littermates, mRNA expression of *Gnat1* and *Gnat2* suggested a comparable survival of rod and cone photoreceptors, respectively. Similarly, expression of *Vsx2 (Chx10)* and *Glul (GS)* transcripts, as marker for bipolar cells and Müller cells, respectively, was unaltered upon simultaneous ablation of *Hif1a* and *EpoR*. The ganglion cell survival in the retina of knockdown mice was not impaired, as suggested by mRNA expression of the "traditional" ganglion cell marker *Pou4f1 (Brn3a)* and *Opn4*, the gene encoding for melanopsin, which is expressed by ipRGCs (Fig. 41).

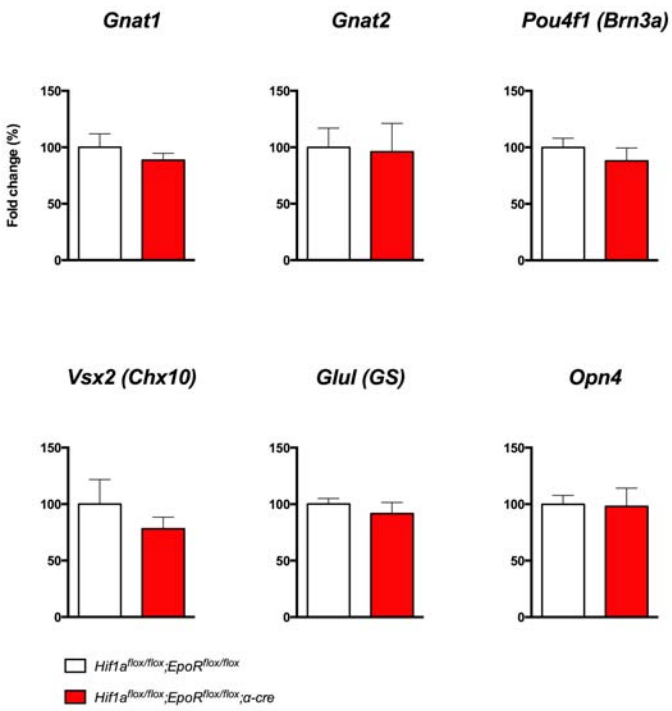

Figure 41 Expression of retinal cell markers in retinas of *Hif1a*$^{flox/flox}$; *EpoR*$^{flox/flox}$;*α-Cre* mice. Relative quantification of *Gnat1* (rod transducin, rods), *Gnat2* (cone transducin, cones), *Pou4f1 (Brn3a)* (POU domain, class 4, transcription factor 1, RGCs), *Vsx2 (Chx10)* (visual system homeobox 2, bipolar cells), *Glul (GS)* (glutamine synthase, Müller cells), and *Opn4* (melanopsin, ipRGCs) gene expression in retinas of *Hif1a*$^{flox/flox}$; *EpoR*$^{flox/flox}$;*α-Cre* mice (red bars) compared to *Hif1a*$^{flox/flox}$; *EpoR*$^{flox/flox}$ control littermates (white bars) by semi-quantitative real-time PCR. cDNAs were prepared from total retinal RNA isolated at 6 months of age. Given are mean values ± SD of N = 4 retinas for *Hif1a*$^{flox/flox}$; *EpoR*$^{flox/flox}$;*α-Cre* animals and N = 3 retinas for controls, amplified in duplicates. Values were normalized to *Actb* and expressed relatively to *Hif1a*$^{flox/flox}$; *EpoR*$^{flox/flox}$ control littermates, which was set to 100%. Differences in gene expression levels between knockdown and control mice at individual time points were tested for significance using a Students t-test (Figure: Caprara and Grimm, unpublished)

Rex and co-workers emphasized a contribution of EPO in the regulation of the expression of stress-related genes, such as *Gfap* (Rex et al., 2009). Measurement of *Gfap* mRNA levels by semi-quantitative real-time PCR revealed a significant ($p<0.05$) 1.8-fold increased mRNA expression of *Gfap* in the retina of double knockdown mice at 6 months of age (Fig. 42). Increased expression of this gene can be a sign of ongoing retinal gliosis, which upon injurious insults is accompanied by the production of inflammatory molecules (Wang et al., 2011a). However, the mediators of the inflammatory response *Tnfa* and *Il1b* did not show statistically significant upregulation in double knockdown mice when compared to control animals at 6 months of age (Fig. 42).

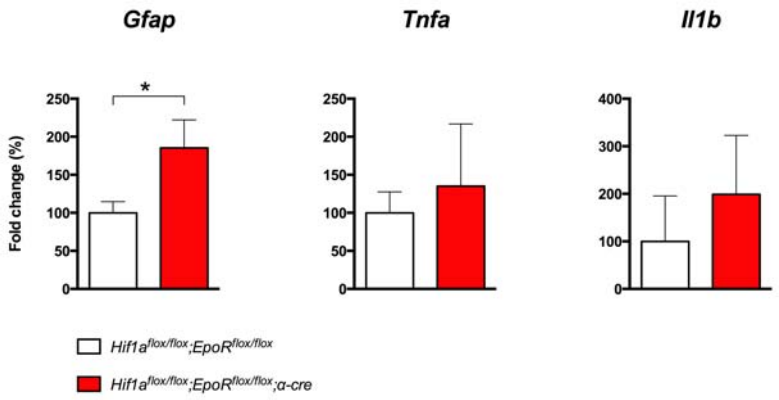

Figure 42 Expression of stress-related genes in retinas of *Hif1a$^{flox/flox}$; EpoR$^{flox/flox}$;α-Cre* mice at 6 months of age. Relative quantification of *Gfap* (glial fibrillary acidic protein), *Tnfa* (tumour necrosis factor a), and *Il1b* (interleukin 1b) gene expression in retinas of *Hif1a$^{flox/flox}$; EpoR$^{flox/flox}$;α-Cre* mice (red bars) compared to *Hif1a$^{flox/flox}$; EpoR$^{flox/flox}$* control littermates (white bars) by semi-quantitative real-time PCR. cDNAs were prepared from total retinal RNA isolated at 6 months of age. Given are mean values ± SD of N = 4 retinas for *Hif1a$^{flox/flox}$; EpoR$^{flox/flox}$;α-Cre* animals and N = 3 retinas for controls, amplified in duplicates. Values were normalized to *Actb* and expressed relatively to *Hif1a$^{flox/flox}$; EpoR$^{flox/flox}$* control littermates, which was set to 100%. Differences in gene expression levels between knockdown and control mice at individual time points were tested for significance using a Students t-test *: $P < 0.05$ (Figure: Caprara and Grimm, unpublished).

Analysis by immunostaining on retinal cryosections at 6 months of age revealed that the distribution of GFAP across retinal layers was restricted to astrocytes and did not show upregulation of the fibrillary protein in Müller cells, thereby excluding development of gliosis in *Hif1a$^{flox/flox}$; EpoR$^{flox/flox}$;α-Cre* mice. Noteworthy, the protein levels of GFAP in astrocytes appeared to be upregulated in knockdown animals. Also, the normally stellate astrocytic morphology was altered in knockdown retinas with a reduction in the extent of glial processes (Fig. 43).

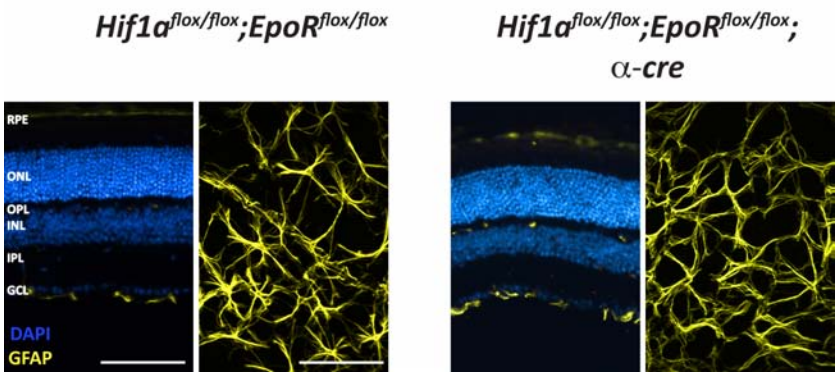

Figure 43 GFAP distribution in retinas of *Hif1a$^{flox/flox}$; EpoR$^{flox/flox}$;α-Cre* mice. Immunostainings of astrocytes / Müller cell endfeet (GFAP: glial fibrillary acid protein, yellow) and staining of cell nuclei (DAPI, blue) on retinal cryosections (left panels) and retinal flatmounts (right panels) of *Hif1a$^{flox/flox}$; EpoR$^{flox/flox}$;α-Cre* mice, and *Hif1a$^{flox/flox}$; EpoR$^{flox/flox}$* littermates

at PND 180. GFAP signal detected within the choroid and OPL is unspecific and derived from secondary antibody. Scale bar: 100µm. (Figure: Caprara and Grimm, unpublished)

Over the past years, treatments with rhEPO have been shown to ameliorate the stability of retinal vessels (Chen et al., 2008), and to possess pro-angiogenic properties (Kertesz et al., 2004). To test whether concomitant deletion of *Hif1a* and *EpoR* could aggravate the vascular phenotype observed in *Hif1a*$^{flox/flox}$*;α-Cre,* we stained 1-month old retinal flatmounts with isolectin IB_4 to highlight the vasculature. The vascular phenotype in *Hif1a*$^{flox/flox}$*;EpoR*$^{flox/flox}$*;α-Cre* mice did not diverge from the one reported in *Hif1a*$^{flox/flox}$*;α-Cre* retinas, where the development of the intermediate capillary plexus was strongly reduced in the periphery (Fig. 44).

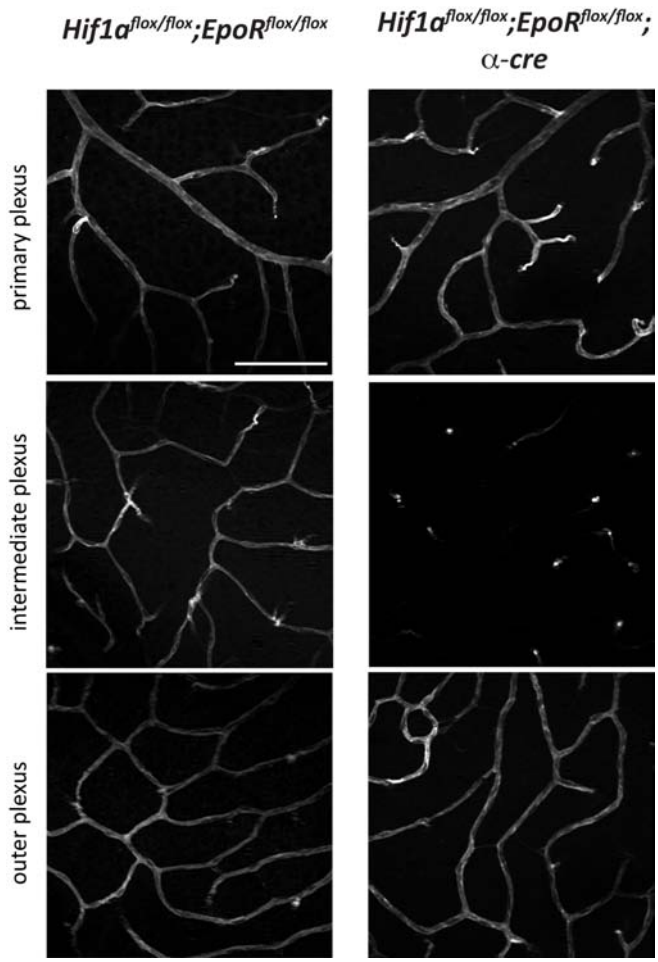

Figure 44 Lack of the intermediate plexus in the peripheral retina of *Hif1a*$^{flox/flox}$*; EpoR*$^{flox/flox}$*;α-Cre* mice. Stainings of blood vessels (isolectin IB_4, coupled to Alexa594) in *Hif1a*$^{flox/flox}$*; EpoR*$^{flox/flox}$*;α-Cre* mice and *Hif1a*$^{flox/flox}$*; EpoR*$^{flox/flox}$ littermates. Shown are flatmounts at PND 30. Pictures of the different vascular plexi in the periphery of retinal flatmounts were taken by adjusting the focal plane of the confocal microscope accordingly. Scale bar: 100 µm. (Figure: Caprara and Grimm, unpublished)

Taken together, data obtained from the analysis of the *Hif1a*$^{flox/flox}$*;EpoR*$^{flox/flox}$*;α-Cre* mouse retina demonstrate that the absence of EPOR (in *Cre*-expressing cells) does not affect the long-term survival of the retina and angiogenesis, in spite of the presence of increased *Epo* transcripts.

4.8 Knockdown of *Hif1a* in Retinal Glia Does not Affect Retinal Morphology, Angiogenesis, and Resistance to Hypoxia

The heterogeneity of *Cre*-expressing cells in the retina of *Hif1a*$^{flox/flox}$*;α-Cre* mice renders it difficult to assign changes of the expression of a particular gene to a specific retinal cell type. The vascular phenotype we observed in the retina of *Hif1a*$^{flox/flox}$*;α-Cre* mice (Fig. 34) may have been caused by alterations in the transcription of specific HIF1A-induced genes in Müller cells. To inquire on this possibility, we ablated *Hif1a* in retinal glia by generating *Hif1a*$^{flox/flox}$*;Pdgfra-Cre* animals. The *Pdgfra-Cre* mouse expresses *Cre* recombinase in Müller cells, astrocytes and a subset of CALB1-positive cells in the OPL, presumably horizontal cells (Fig. 22, 23). Analysis of the mRNA levels *Hif1a* in the retina of *Hif1a*$^{flox/flox}$*;Pdgfra-Cre* mice at 8 weeks of age showed a statistically significant ($p<0.05$) reduction corresponding to approximately 65% when compared to control littermates, thus validating the knockdown strategy (Fig. 45A). Ablation of *Hif1a* did not result in aberrant lamination of the retina or degeneration up to 1 year of age, the last time-point analyzed (Fig. 45B). In line with these results, the expression levels of *Rho*, *Pou4f1 (Brn3a)*, and *Vsx2 (Chx10)* were similar between 8-week old *Hif1a* knockdown mice and control littermates, thus suggesting that the total cell number of rod photoreceptors, RGCs, and bipolar cells, respectively, was not influenced by deletion of *Hif1a* in retinal glia (Fig. 45C). The absence of noticeable signs of retinal degeneration was confirmed by a similar thickness of the retina between *Hif1a*$^{flox/flox}$*;Pdgfra-Cre* and control mice at 1 year of age (Fig. 45D). Furthermore, thickness of the ONL, INL, and GCL was not influenced by ablation of *Hif1a* in retinal glia (data not shown). Also, expression of *Gfap* did not suggest for the presence of a gliotic response (Fig. 45C).

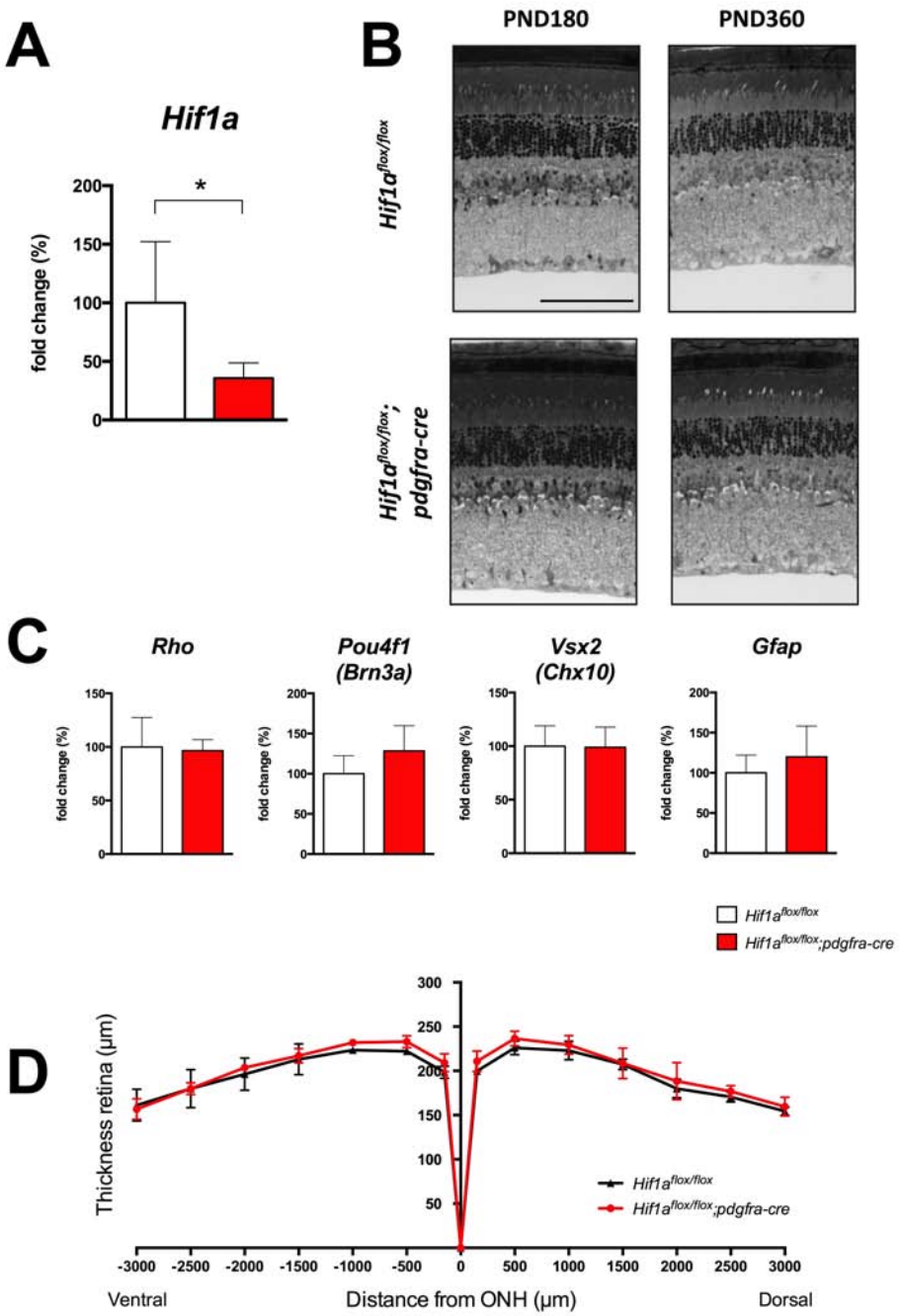

Figure 45 Normal retinal morphology upon ablation of *Hif1a* in retinal glia. (A) Quantification of *Hif1a* (hypoxia-inducible factor 1a) mRNA expression under normoxic conditions by real-time PCR. cDNAs were prepared from total retinal RNA isolated at 8 weeks of age. Given are mean values ± SD of N = 4 retinas for *Hif1a$^{flox/flox}$; Pdgfra-Cre* animals and for controls, amplified in duplicates. Values were normalized to *Actb* and expressed relatively to *Hif1a$^{flox/flox}$* control littermates, which was set to 100%. The difference in gene expression levels between knockdown and control mice was tested for significance using a Students t-test *: P < 0.05. **(B)** Retinal morphology of *Hif1a$^{flox/flox}$;Pdgfra-Cre* mice, and *Hif1a$^{flox/flox}$;* littermates at PND 180, and PND 360. Shown are representative sections of the central retina of three animals per time point. Scale bar: 100µm. **(C)** Relative quantification of *Rho* (rhodopsin, rods), *Pou4f1 (Brn3a)* (POU domain, class 4, transcription factor 1, RGCs), *Vsx2 (Chx10)* (visual system homeobox 2, bipolar cells), and *Gfap* (glial fibrillary acidic protein, astrocytes, activated Müller cells) gene expression in retinas of *Hif1a$^{flox/flox}$;Pdgfra-Cre* mice compared to *Hif1a$^{flox/flox}$* control littermates by real-time PCR. cDNAs were prepared from total retinal RNA isolated at 8 weeks of age Given are mean values ± SD of N = 4 retinas for *Hif1a$^{flox/flox}$; Pdgfra-Cre* animals and for controls, amplified in duplicates.

Values were normalized to *Actb* and expressed relatively to *Hif1a*$^{flox/flox}$ control littermates, which was set to 100%. Differences in gene expression levels between knockdown and control mice at individual time points were tested for significance using a Students t-test. **(D)** Thickness of the retina in 1 year-old *Hif1a*$^{flox/flox}$*;Pdgfra-Cre* mice and *Hif1a*$^{flox/flox}$ control littermates. Thickness was measured at 0, 150, 500, 1000, 1500, 2000, 2500, and 3000 µm from the optic nerve head (ONH) in both dorsal and ventral hemispheres, as indicated. Mean ± SD; N = 3. (Figure: Caprara and Grimm, unpublished).

Since absence of HIF1A in Müller cells may be involved in the vascular phenotype of *Hif1a*$^{flox/flox}$*;α-Cre* mice, we analyzed the retinal vasculature of *Hif1a*$^{flox/flox}$*;Pdgfra-Cre* mice. At 1 month of age, the primary, intermediate and outer plexus of *Hif1a*$^{flox/flox}$*;Pdgfra-Cre* animals were comparable to control littermates. In particular, the intermediate plexus was completely and correctly developed (Fig. 46).

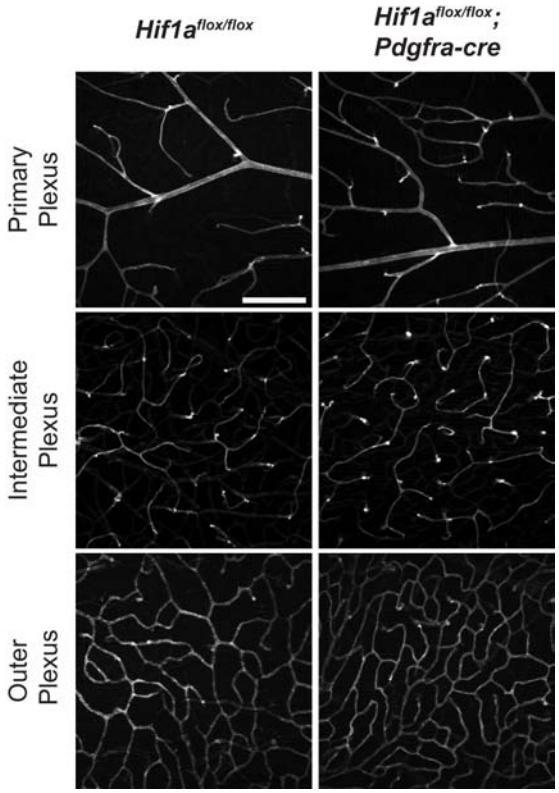

Figure 46 Normal development of the intermediate plexus in the peripheral retina of *Hif1a*$^{flox/flox}$*; Pdgfra-Cre* mice. Stainings of blood vessels (isolectin IB_4, coupled to Alexa594) in *Hif1a*$^{flox/flox}$*; Pdgfra-Cre* mice and *Hif1a*$^{flox/flox}$ littermates. Shown are flatmounts at PND 30. Pictures of the different vascular plexi in the periphery of retinal flatmounts were taken by adjusting the focal plane of the confocal microscope accordingly. Scale bar: 200 µm. (Figure: Caprara and Grimm, unpublished).

Hypoxia can result in cellular dysfunction and / or cell death in different tissues (Shimizu et al., 1996; Azad et al., 2008; Zheng et al., 2012). In spite of this, exposure of wild-type mice to

reduced oxygen tension (6 Hrs, /7% O_2) does not affect retinal cell viability (Grimm et al., 2002). HIF1A may be the essential factor that provides resistance to the retina against hypoxic damage. This could occur by a paracrine mechanism in which HIF1A-induced expression of protective factors by retinal glia may sustain the survival of retinal neurons. Concomitantly, HIF1A could be crucial for the survival of Müller cells and astrocytes under conditions of oxygen deficiency. To test this hypothesis, we exposed *Hif1a$^{flox/flox}$;Pdgfra-Cre* mice to hypoxia and analyzed retinal morphology 12 days after the hypoxic insult for the presence of any symptom of degeneration. In line with previous reports (Thiersch et al., 2009), retinal morphology of or *Hif1a$^{flox/flox}$* mice did not shown signs of damage following a hypoxic exposure. Absence of HIF1A in retinal glia did not result in retinal degeneration caused by hypoxic damage (Fig. 47).

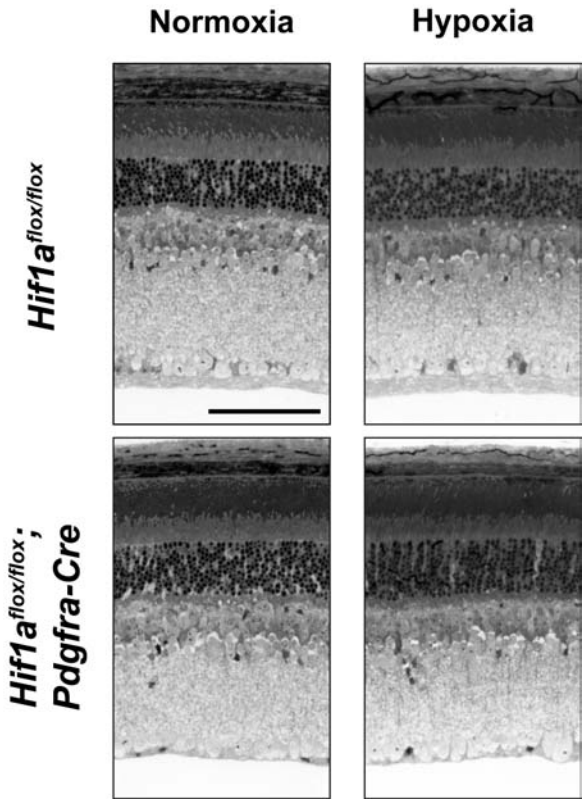

Figure 47 Absence of HIF1A in retinal glia does not result in hypoxic damage to the retina. Retinal morphology of *Hif1a$^{flox/flox}$;Pdgfra-Cre* mice, and *Hif1a$^{flox/flox}$;* littermates was analyzed 12 days after exposure to hypoxia (6 Hrs, 7% O_2) and compared to animals maintained under normoxic conditions. Shown are representative sections of the central retina of three animals per time point. Scale bar: 100µm. (Figure: Caprara and Grimm, unpublished)

Taken together, these results suggest that the absence of HIF1A in Müller cells does not affect angiogenesis and is therefore not the cause for the lack of the intermediate plexus in the

retinal periphery of *Hif1a*$^{flox/flox}$*;α-Cre* mice. In addition, *Hif1a* knockdown in Müller glia has no consequences on the development of the retina, and its ability to survive to hypoxic episodes.

4.9 *Epo*, *EpoR* and *Csf2rb (βCR)* Are Expressed in Retina

To acquire first hints on the possible roles of *Epo*, *EpoR*, and the cytokine co-receptor *Csf2rb (βCR)* in retinal development and physiology, we analyzed the expression profile of these genes in the post-natal and adult retina of BL6/JFue mice. The expression of *Epo* augmented by two-fold gradually starting from PND 10 to reach an approximately steady-state level in adulthood, with a tendency towards higher expression in older animals (Fig. 48A). Intriguingly, expression of *EpoR* was maintained at relatively low levels until PND 10, the time-point when its expression increased by 7-fold and progressively reached a 14-fold increase at 6 months of age, when compared to PND 3 (Fig. 48B). On the contrary, expression of the *Csf2rb (βCR)* was stable and did not show significant oscillations over time (Fig. 48C).

In semi-quantitative real-time PCR, monitoring of reaction kinetics by inclusion of fluorescent probes enables the measurement of a crossing point (C_P) (or cycle threshold (C_T)) value, at a cycle number at which fluorescence becomes measurable above background signal (Higuchi et al., 1993). C_P values are directly proportional to the number of gene transcripts in an inverse logarithmic relationship (Heid et al., 1996). Thus, high C_P values are a sign of low transcript abundance, while low C_P values indicate that a gene is highly expressed. In respect to the analysis of *Epo* and *EpoR* gene expression, it is important to mention that C_P values for both gene transcripts were particularly elevated. In the case of *Epo*, C_P value was set around cycle 34 in normoxia (cycle 30 in hypoxia), while *EpoR* transcripts were detected at cycle 29 in both normoxia and hypoxia. A highly expressed gene in the retina, such as *Rho*, shows C_P values of 14 when transcripts are amplified (data not shown). This observation highlights the low abundance of *EpoR* and particularly *Epo* transcripts in the retina.

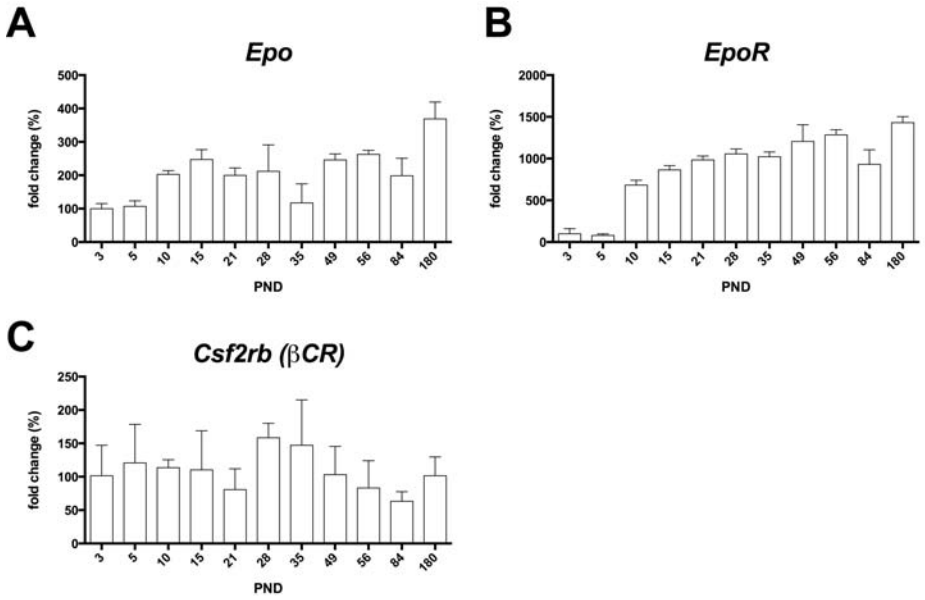

Figure 48 Gene expression profile of *Epo, EpoR, and Csf2rb (βCR)* in the post-natal retina of BL6/JFue mice. Expression of *Epo* (erythropoietin) **(A)**, *EpoR* (erythropoietin receptor) **(B)**, and *Csf2rb (βCR)* (beta common receptor) **(C)** as measured by semi-quantitative real-time PCR on cDNA samples prepared from BL6/JFue animals at different post-natal days (PND). All values were normalized to *Actb* and PND 3 was set as 100%. Shown are mean values ± SD of N = 3 animals. (Figure: Caprara and Grimm, manuscript in preparation)

4.10 Knockdown of *EpoR* in Rod Photoreceptors or in the Peripheral Retina Has no Effects on Retinal Development and Function

To explore the role of EPOR in the retina, we ablated the *EpoR* genomic sequence either in rod photoreceptors, by generating $EpoR^{flox/flox}$*;Opn-Cre* mice, or in the peripheral retina by breeding $EpoR^{flox/flox}$*;α-Cre* mice. CRE-mediated recombination in the *Opn-Cre* mouse is considered to be efficient after approximately 10 weeks of age, and occurs in approximately 40% of rod photoreceptors (Fig. 24). On the other hand, expression of *Cre* in the *α-Cre* mouse begins embryonically, and is eventually restricted to a heterogeneous cell population of the peripheral retina (Fig. 19, 20). Upon excision of *loxP*-flanked exons 1-4 in the *EpoR* gene, a 220bp fragment is generated when using specific primers for PCR (Tsai et al., 2006). Appearance of the 220bp fragment revealed a successful recombination in both $EpoR^{flox/flox}$*;Opn-Cre* and $EpoR^{flox/flox}$*;α-Cre* mouse retinas (Fig. 49A1, B1). A decrease in *EpoR* expression of approximately 35% ($p<0.05$) was measured in the retina of $EpoR^{flox/flox}$*;α-Cre* mice kept under normoxic conditions (Fig. 49B2),

thus validating the knockdown strategy. In contrast, no significant knockdown was observed when *EpoR* mRNA levels where measured in total retinal extracts from *EpoR$^{flox/flox}$;Opn-Cre* mice (Fig. 49A2). This was an unexpected result, as the validity of the *Opn-Cre* mouse was confirmed before (Le et al., 2006).

Siren and co-workers suggested that the transcription of *EpoR* might be induced by hypoxia in the brain (Siren et al., 2001b). To investigate the expression of *EpoR* under hypoxic conditions in the retina, animals were kept for 6 Hrs at 7% O_2 in a hypoxic chamber and retinas were collected immediately after the exposure for analysis. In both *EpoR* knockdown mouse lines and control littermates, exposure to hypoxia did not cause any statistically significant increase in *EpoR* transcripts (Fig. 49A2, B2).

We also investigated the mRNA levels of *mEpoR* (membrane-bound *EpoR*) and *sEpoR* (soluble *EpoR*), in the retina of 2.5 and 7.5 month-old mice. Expression of the two *EpoR* splice variants was unaltered in *EpoR$^{flox/flox}$;Opn-Cre* retinas (Fig. 49A3). On the contrary, expression of *sEpoR* was statistically significantly ($p<0.001$) reduced by roughly 60% in the retina of 2.5 month-old *EpoR$^{flox/flox}$;α-Cre* mice when compared to wild-type mice (Fig. 49B3).

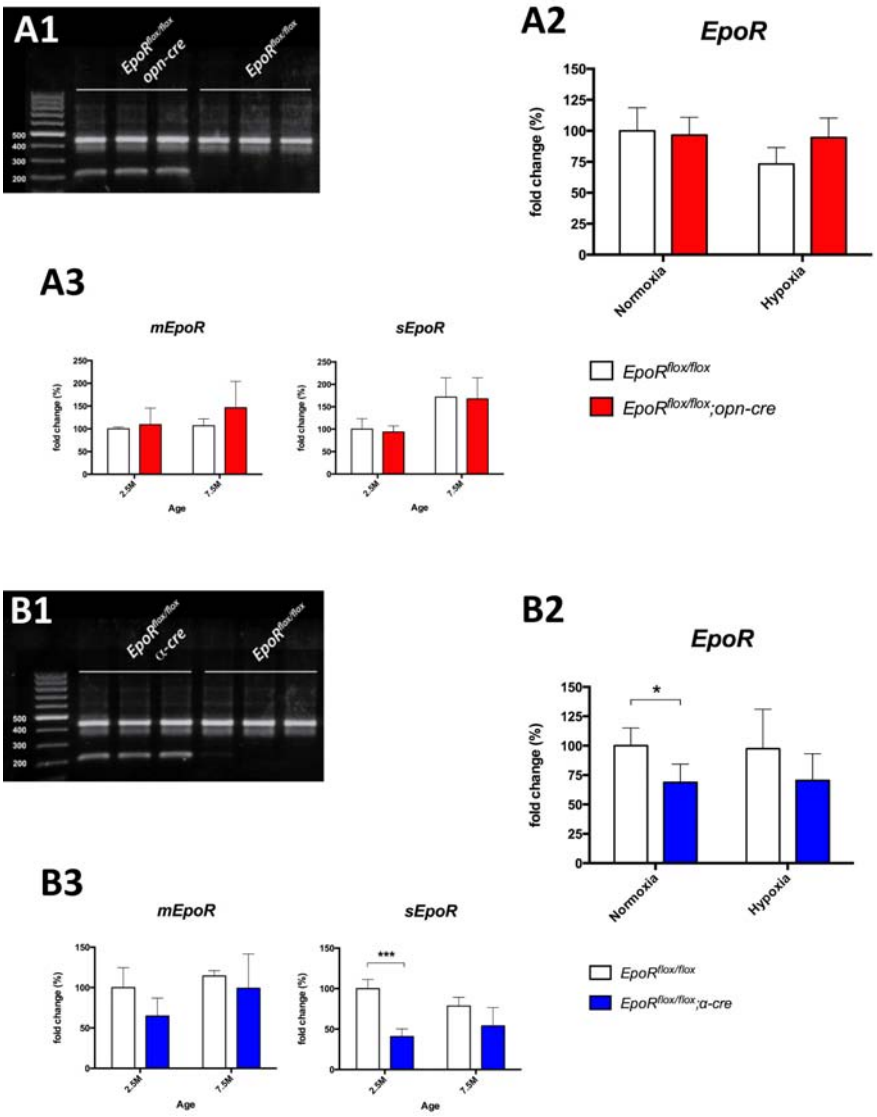

Figure 49 Knockdown of *EpoR* in *EpoR$^{flox/flox}$;Opn-Cre* and *EpoR$^{flox/flox}$;α-Cre* retinas. PCR amplification of genomic DNA from total retinal extract of three different *EpoR$^{flox/flox}$* and *EpoR$^{flox/flox}$;Opn-Cre* mice **(A1)** or three different *EpoR$^{flox/flox}$* and *EpoR$^{flox/flox}$; α-Cre* mice **(B1)** at 12 weeks of age. The amplified fragment from the *loxP*-flanked *EpoR* sequence has a length of 420 bp. CRE-mediated recombination results in the appearance of a 220bp fragment. Semi-quantitative real-time PCR analysis of the expression of *EpoR* (erythropoietin receptor) in total retinal extracts of 12 week-old *EpoR$^{flox/flox}$;Opn-Cre* mice (red bars) **(A2)** or *EpoR$^{flox/flox}$α-Cre* mice (blue bars) **(B2)** in normoxia (21% O_2) and hypoxia (6 Hrs, 7% O_2). Values were normalized to *Actb*, and *EpoR$^{flox/flox}$* normoxic value (white bars) was set as 100%. Shown are mean values ± SD of N = 4 animals. Semi-quantitative real-time PCR analysis of the expression of *mEpoR* (membrane-bound EpoR) and *sEpoR* (soluble EpoR) in total retinal extracts of 12 week-old *EpoR$^{flox/flox}$;Opn-Cre* mice (red bars) **(A3)** or *EpoR$^{flox/flox}$; α-Cre* mice (blue bars) **(B3)** at 2.5 and 7.5 months of age. Values were normalized to *Actb*, and *EpoR$^{flox/flox}$* at 2.5 months (white bars) was set as 100%. Shown are mean values ± SD of N = 3 animals. Differences in gene expression levels between knockdown and control mice at individual time points were tested for significance using a Students t-test. *:p<0.05; ***: p<0.001. (Figure: Caprara and Grimm, manuscript in preparation)

The absence of a measurable knockdown in total retinal extracts of *EpoR$^{flox/flox}$;Opn-Cre* mice could result either from absence or low expression of EpoR in the ONL or increased

transcription of *EpoR* in cells other than rod photoreceptors. To test this possibility, we isolated RNA from the three different retinal nuclear layers by laser capture microdissection. Analysis of the expression of marker genes for the ONL (*Gnat1*), INL (*Vsx2 (Chx10)*), and GCL (*Pou4f1 (Brn3a)*) showed a low level of cross contamination between the different nuclear layers (Fig. 50A). Semi-quantitative real-time PCR analysis revealed a decrease of *EpoR* expression (35%) in the ONL of *EpoR*$^{flox/flox}$*;Opn-Cre* mice compared to control littermates, even though the reduction did not reach statistical significance. Interestingly, the mRNA levels of *EpoR* in the ONL of control mice were markedly lower than the INL and GCL, thus suggesting for a low expression of *EpoR* in photoreceptors (Fig. 50B).

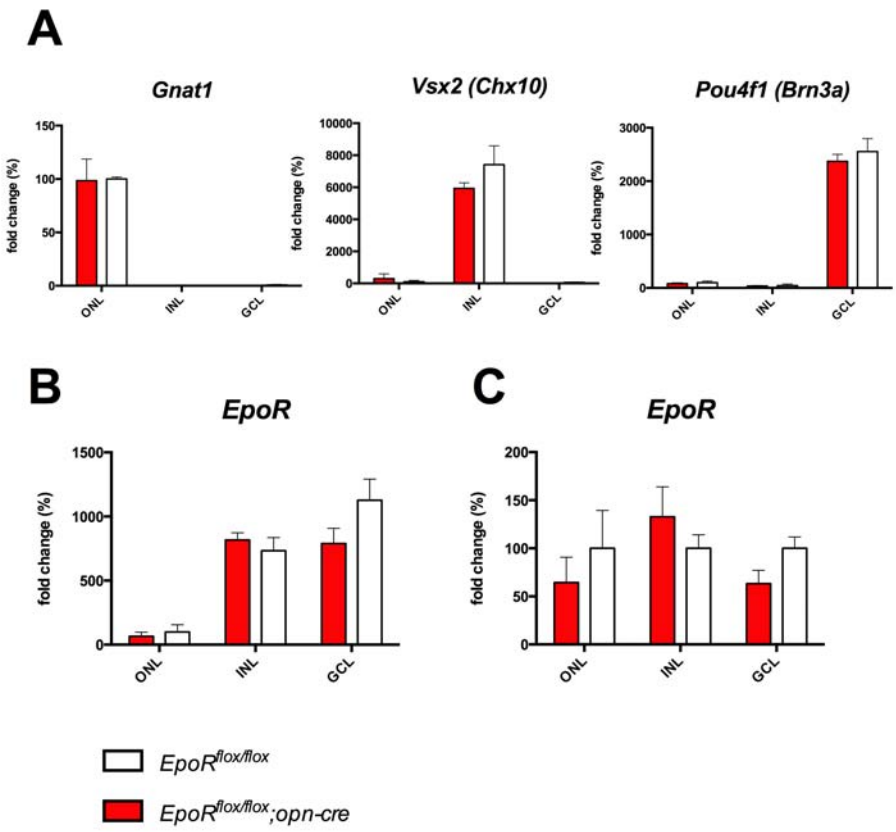

Figure 50 Expression of *EpoR* in retinal nuclear layers of *EpoR*$^{flox/flox}$*;Opn-Cre* mice. (A) Semi-quantitative real-time PCR after laser capture microdissection showing relative *Gnat1* (rod transducin, rods), *Vsx2 (Chx10)* (visual system homeobox 2, bipolar cells), and *Pou4f1 (Brn3a)* (POU domain, class 4, transcription factor 1, RGCs), levels in the different retinal layers (as indicated) of *EpoR*$^{flox/flox}$ (white bars) and *EpoR*$^{flox/flox}$*;Opn-Cre* mice (red bars). Values were normalized to *Actb* and expressed relatively to the value of *EpoR*$^{flox/flox}$ ONL, which was set to 100%. **(B, C)** Semi-quantitative real-time PCR after laser capture microdissection showing relative *EpoR* (erythropoietin receptor) mRNA levels in the different retinal layers (as indicated) of *EpoR*$^{flox/flox}$ (white bars) and *EpoR*$^{flox/flox}$*;Opn-Cre* mice (red bars). Values were normalized to *Actb* and expressed relatively to the value of *EpoR*$^{flox/flox}$ ONL, which was set to 100% in (B) or respective to the value of

EpoR$^{flox/flox}$ mice for each layer, which were set to 100% in (C). Shown are mean values ± SD of at least 2 different mice amplified in duplicates. ONL, outer nuclear layer; INL, inner nuclear layer; GCL, ganglion cell layer. Differences in gene expression levels between knockdown and control mice at individual time points were tested for significance using a Students t-test (Figure: Caprara and Grimm, manuscript in preparation)

The successful knockdown of *EpoR* in the retina of *EpoR*$^{flox/flox}$*;α-Cre* mice prompted us to analyze the consequences of the lack of EPOR for development and maturation of the retina. The importance of EPO-EPOR signalling in neural development has been revealed in recent years. Absence of EPOR has shown to result in increased apoptosis in the embryonic CNS (Yu et al., 2002). Hence, signs of developmental defects may be seen in the adult by analyzing tissue morphology. Conversely, the reduced expression of *EpoR* in the ONL suggests that the EPOR does not play significant roles in photoreceptor physiology and survival. Nevertheless, a possible role of EPOR in photoreceptors cannot be excluded based exclusively on the extent of *EpoR* gene expression. In fact, EPOR protein levels may be present at elevated levels in photoreceptors, despite low presence of *EpoR* transcripts in these cells.

Despite successful knockdown of *EpoR* in the peripheral retina of *EpoR*$^{flox/flox}$*;α-Cre* mice, and a reduced *EpoR* expression in the ONL of *EpoR*$^{flox/flox}$*;Opn-Cre* mice, histological analysis of the retinal tissue by did not reveal signs of developmental defects. In fact, the lamination and integrity of the retina were comparable to wild-type mice (Fig. 51).

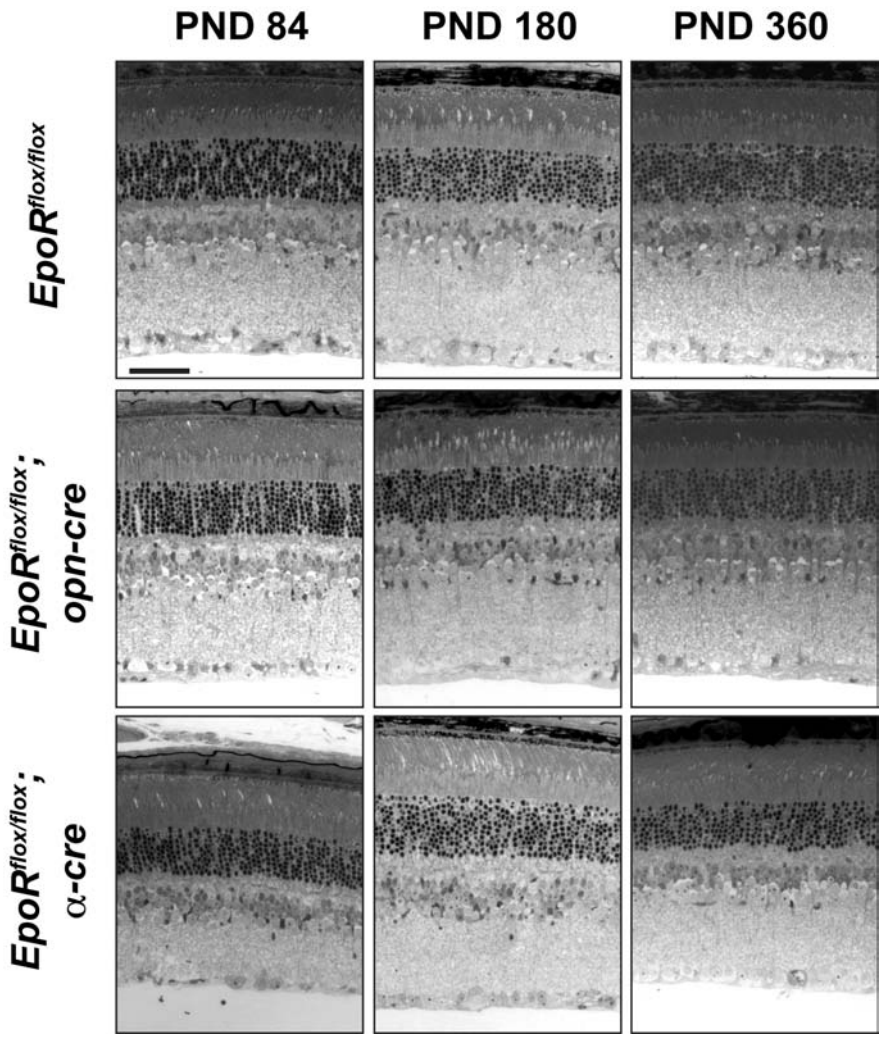

Figure 51 Normal retinal morphology upon ablation of *EpoR* in rod photoreceptors or the peripheral retina. Retinal morphology of *EpoR*$^{flox/flox}$*;Opn-Cre* mice, *EpoR*$^{flox/flox}$*;α-Cre* mice and *EpoR*$^{flox/flox}$ mice at PND 84, 180, and 360 were analyzed. Shown are representative sections of the central retina (*EpoR*$^{flox/flox}$*;Opn-Cre,* and *EpoR*$^{flox/flox}$) or peripheral retina (*EpoR*$^{flox/flox}$*;α-Cre*) of at least three animals per time point. Scale bar: 50µm. (Figure: Caprara and Grimm, manuscript in preparation)

Analysis of the expression of *Rho, Gnat2, Vsx2 (Chx10),* and *Pou4f1 (Brn3a)* suggested that the total amount of rods, cones, bipolar cells, and RGCs respectively, was not affected by ablation of *EpoR* (Fig. 52). Furthermore, a long-term analysis of retinal histology did also not show noticeable symptoms of retinal degeneration in 1 year-old retina of *EpoR* knockdown mice (Fig. 51).

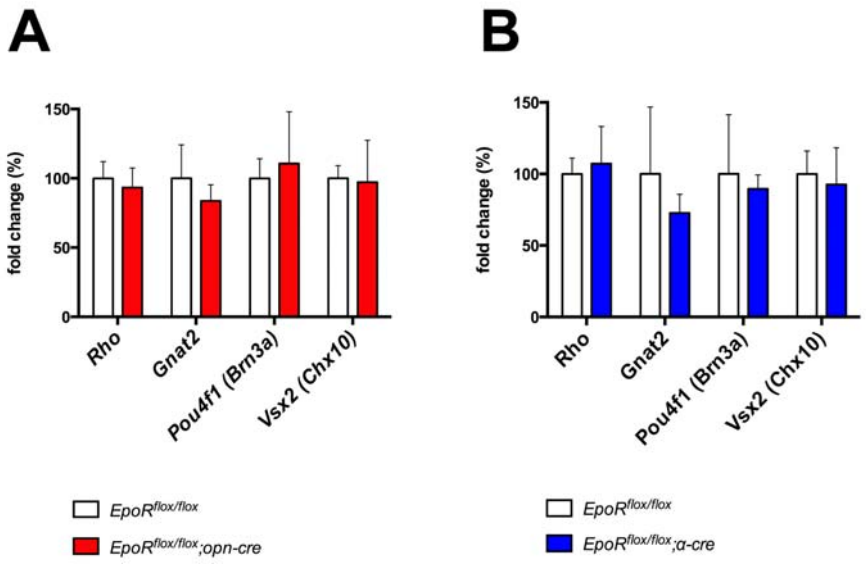

Figure 52 Absence of retinal degeneration upon ablation of *EpoR* in rod photoreceptors or the peripheral retina. Relative quantification by semi-quantitative real-time PCR of *Rho* (rhodopsin, rods), *Gnat2* (cone transducin, cones), *Pou4f1 (Brn3a)* (POU domain, class 4, transcription factor 1, RGCs), *Vsx2 (Chx10)* (visual system homeobox 2, bipolar cells), gene expression at 7.5 months of age in retinas of $EpoR^{flox/flox}$;*Opn-Cre* (red bars) **(A)**, and $EpoR^{flox/flox}$;*α-Cre* (blue bars) **(B)** mice compared to $EpoR^{flox/flox}$ control littermates (white bars). cDNAs were prepared from total retinal RNA isolated at 7.5 months of age. Given are mean values ± SD of N = 4 retinas, amplified in duplicates. Values were normalized to *Actb* and expressed relatively to $EpoR^{flox/flox}$ control littermates, which was set to 100%. Differences in gene expression levels between knockdown and control mice at individual time points were tested for significance using a Students t-test (Figure: Caprara and Grimm, manuscript in preparation).

An additional confirmation for the absence of tangible consequences on retinal physiology resulting from the lack of EPOR comes from the analysis of retinal function by ERG. The retinas of knockdown mice were fully functional, and neither $EpoR^{flox/flox}$;*Opn-Cre* nor $EpoR^{flox/flox}$;*α-Cre* showed significant changes in their a- and b-wave amplitudes under both scotopic and photopic conditions when compared to wild-type mice (Fig. 53).

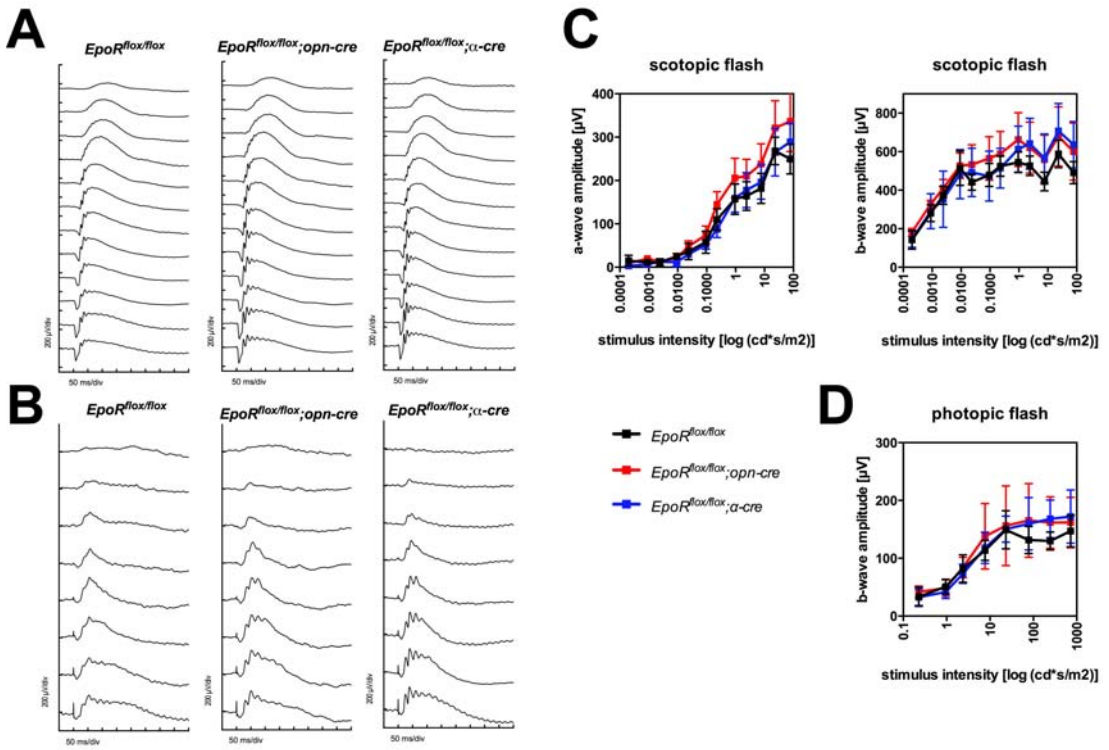

Figure 53 ERG recordings in *EpoR$^{flox/flox}$;Opn-Cre* and *EpoR$^{flox/flox}$;α-Cre* mice are comparable to control littermates. Scotopic **(A)** and photopic **(B)** ERG recordings in *EpoR$^{flox/flox}$;Opn-Cre* (red line), *EpoR$^{flox/flox}$;α-Cre* mice (blue line) and *EpoR$^{flox/flox}$* control littermates (black line). Shown are a- and b-wave amplitudes under scotopic conditions **(C)** and b-wave amplitudes under photopic conditions **(D)**. Mean values ± SD of N = 3 animals per genotype are presented. (Figure: Caprara and Grimm, manuscript in preparation)

In conclusion, ablation of the *EpoR* genomic sequence was successful in both knockdown strains. However, only *EpoR$^{flox/flox}$;α-Cre* showed a significant reduction of *EpoR* expression, in particular of the *sEpoR* isoform. Knockdown in the ONL of *EpoR$^{flox/flox}$;Opn-Cre* mouse retina did not reach statistical significance but, most importantly, analysis of the expression of *EpoR* throughout the retina demonstrated that photoreceptors express low levels of *EpoR* compared to the inner retinal layers. Regardless of the reduction in *EpoR* expression in both knockdown strains, the development, function and survival of the retina were not disturbed.

4.11 Intracellular Signalling and Gene Expression Upon *EpoR* Knockdown

EPO-EPOR downstream signalling results in the activation of numerous signal transduction pathways that may eventually modulate the expression of target genes involved in multiple biological processes, such as cell growth or apoptosis (Chateauvieux et al., 2011). In order to study the effects of EPO-EPOR signalling in the retina, including changes in the expression of target genes, we exposed mice to hypoxia (7% O_2, 6 Hrs). We isolated retinas immediately after the hypoxic exposure for analysis of gene and protein expression. Upon exposure of mice to hypoxia, *Epo* transcripts are increased in the retina (Grimm et al., 2006), and therefore EPO-EPOR signalling is expected to be active at this time. The validity of the experimental procedure for the manipulation of oxygen tension was confirmed by the increased transcription of *Adm*, a gene that is upregulated in the hypoxic retina (Thiersch et al., 2008). As expected, transcription of *Epo* was increased immediately after hypoxia in the *EpoR$^{flox/flox}$;Opn-Cre* and *EpoR$^{flox/flox}$;α-Cre* mouse retinas. However, ablation of *EpoR* did not alter the expression of *Epo* when compared to control mice (Fig. 54). The absence of *EpoR* could have led to a compensatory upregulation of *Csf2rb (βCR)*, the gene encoding for a co-receptor interacting with EPOR (Jubinsky et al., 1997; Blake et al., 2002). Yet, retinal expression of *Csf2rb (βCR)* under both normoxic and hypoxic conditions was unaffected by *EpoR* knockdown (Fig. 54).

The absence of EPOR in specific retinal cell populations may result in biologically relevant changes in the expression of target genes. For this reason, we measured the mRNA levels of genes previously reported to be either induced or repressed by treatments with rhEPO.

EPO may increase NO production by increasing the mRNA levels of *Nos2 (iNos)* (Beleslin-Cokic et al., 2011). The expression of *Nos2* (*iNos*) was significantly ($p<0.05$) increased 3-fold in the *EpoR$^{flox/flox}$;Opn-Cre* mouse retina under hypoxic conditions (Fig. 54A).

EPO has also been reported to induce the expression of metallothionein 1 *(Mt1)* and 2 *(Mt2) in vitro* (Abdel-Mageed et al., 2003) and *in vivo* (Wakida et al., 2007). Both *Mt1* and *Mt2* are highly expressed in hypoxia in the mouse retina (Thiersch et al., 2008). In both *EpoR* knockdown lines and control mice, mRNA levels of *Mt1* and *Mt2* were increased after the hypoxic exposure. Interestingly, ablation of *EpoR* in rod photoreceptors resulted in a significant ($p<0.05$) reduction

of *Mt2* expression (approximately 40%) under hypoxic conditions when compared to control littermates (Fig. 54A).

Many reports have pointed to the ability of EPO to increase VEGFA secretion in different experimental models (Westenbrink et al., 2010). In our hands, ablation of *EpoR* in rod photoreceptors resulted in a statistically significant ($p<0.05$) 30% increase of *Vegfa* transcripts under hypoxia compared to control mice (Fig. 54A).

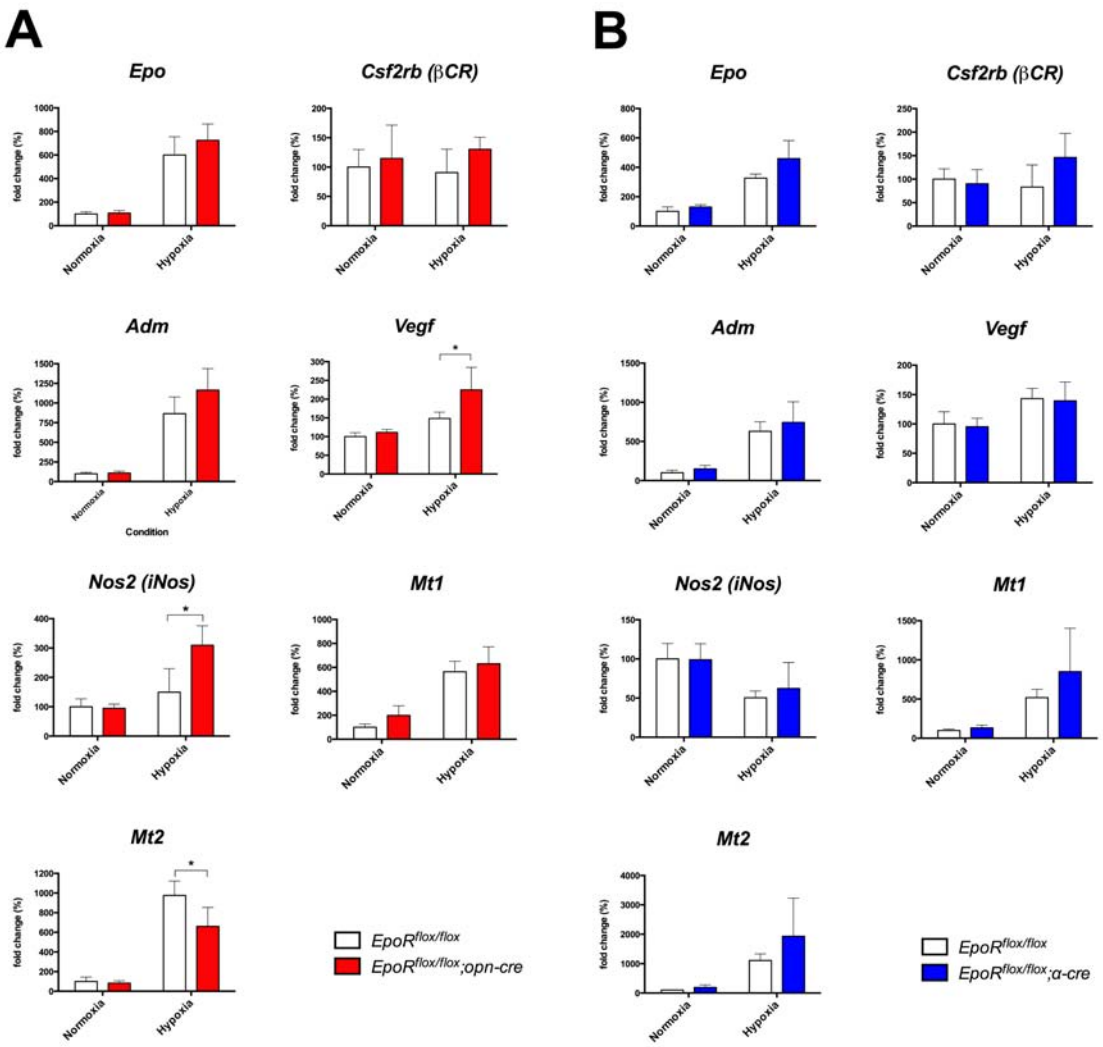

Figure 54 Expression of a selection of genes in retinas of *EpoR* knockdown mice. Relative quantification of *Epo* (erythropoietin), *Csf2rb (βCR)* (beta common receptor), *Adm* (adrenomedullin), *Vegfa* (vascular endothelial growth factor a), *Nos2(iNos)* (nitric oxide synthase 2), *Mt1* (metallothionein 1), and *Mt2* (metallothionein 2) gene expression in retinas of $EpoR^{flox/flox}$*;Opn-Cre* (**A**, red bars), and $EpoR^{flox/flox}$*;α-Cre* mice (**B**, blue bars) compared to $EpoR^{flox/flox}$ control littermates (white bars) by semi-quantitative real-time PCR. cDNAs were prepared from total retinal RNA isolated at 12 weeks of age. Animals were kept under normoxic or hypoxic (6 Hrs, 7% O_2) conditions and retinas were isolated immediately after the experimental treatment. Given are mean values ± SD of N = 4 retinas, amplified in duplicates. Values were normalized to *Actb* and expressed relatively to $EpoR^{flox/flox}$ control littermates under normoxic conditions, which were set to 100%.

Differences in gene expression levels between knockdown and control mice at individual time points were tested for significance using a Students t-test *: P < 0.05 (Figure: Caprara and Grimm, manuscript in preparation)

The expression of many genes associated with the apoptotic pathway is influenced by treatments with rhEPO (Chateauvieux et al., 2011). B-cell lymphoma 2 *(Bcl2)* and Bcl-2-like 1 *(Bcl2l1 (Bcl_{XL}))* are two examples of anti-apoptotic genes that are induced by rhEPO (Wen et al., 2002; Renzi et al., 2002). However, in both *EpoR* knockdown mouse models, the expression of *Bcl2* and *Bcl2l1* (Bcl_{XL}) was not affected upon normoxic or hypoxic exposure (Fig. 55).

Also, reduced expression of the pro-apoptotic gene *Casp1* has been previously linked to the protective activity of EPO (Grimm et al., 2002). Unexpectedly, upon *EpoR* knockdown in the peripheral retina, *Casp1* expression was significantly ($p<0.05$) reduced (approximately 40%) under hypoxic conditions (Fig. 55B).

Apoptotic protease activating-factor 1 *(Apaf1)* encodes for a protein that acts as central initiator of the apoptotic cascade (Bratton and Salvesen, 2010), and its expression has been previously reported to be influenced by treatments with rhEPO (Chong et al., 2003b; Shang et al., 2011b). Knockdown of *EpoR* in the retinal periphery caused a decrease in *Apaf1* expression of about 50% under both normoxic and hypoxic conditions. However, the changes in expression were statistically significant ($p<0.01$) only under hypoxic conditions (and thus in the presence of increased *Epo* mRNA) when compared to control mice (Fig. 55B).

Beside the regulation of the expression of pro- and anti-apoptotic genes, treatments with rhEPO have shown to induce the transcription of neurotrophic factors, such as *Bdnf* (Hu et al., 2011). We expected a reduction in expression of *Bdnf* upon *EpoR* knockdown. However, in the retina of $EpoR^{flox/flox}$;*α-Cre* mice, hypoxia increased *Bdnf* transcript levels and this upregulation was significantly ($p<0.01$) higher than control littermates (roughly 250%) (Fig. 55B).

CCAAT/enhancer-binding protein delta *(Cebp/d)* is a gene encoding for a transcription factor regulating the expression of genes involved in inflammation (Valente et al., 2013), cell growth (Yu et al., 2010), and other cellular processes. As reported before (Min et al., 2011), exposure of mice to hypoxia increased expression of *Cebp/d* (Fig. 55). Ablation of *EpoR* in the retinal periphery resulted in a statistically significant ($p<0.05$) 30% increase in the expression of *Cebp/d* under normoxic conditions, when compared to control littermates (Fig. 55B).

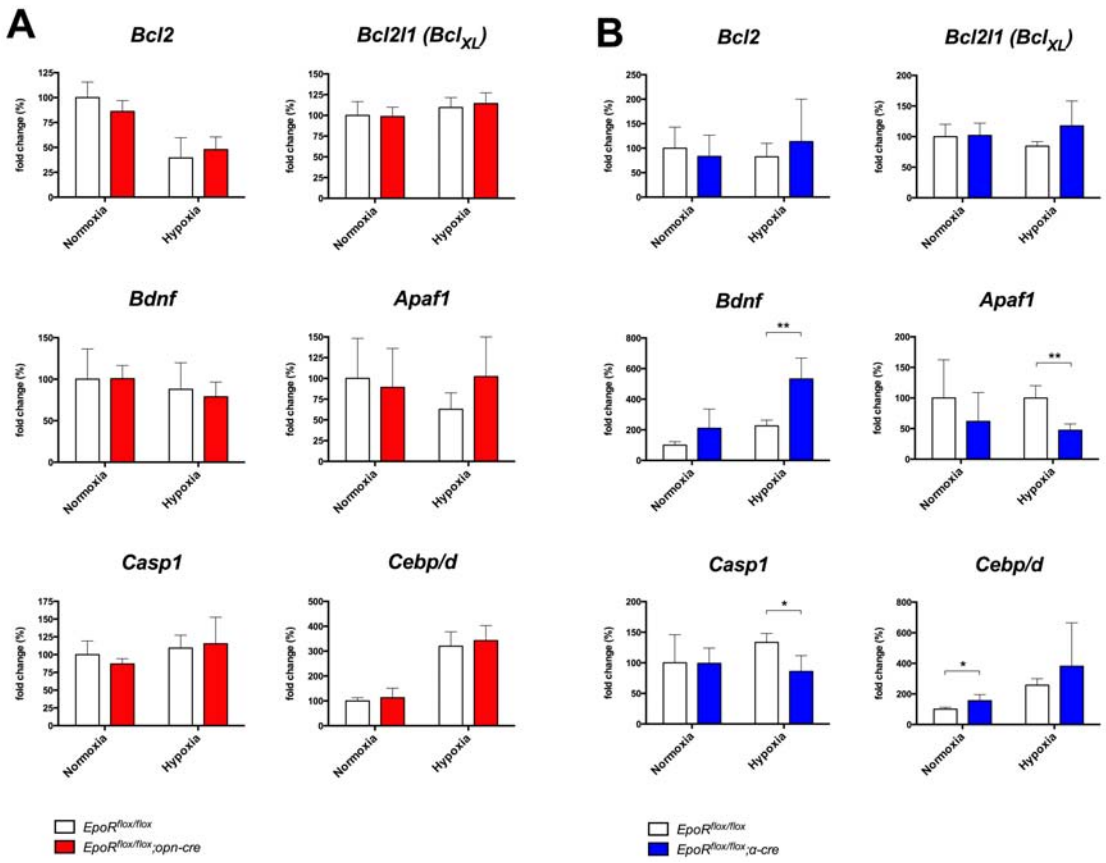

Figure 55 Expression of a selection of anti- or pro-apoptotic genes in retinas of *EpoR* knockdown mice. Relative quantification of *Bcl2* (B cell lymphoma 2), *Bcl2l1(Bcl$_{XL}$)* (Bcl2-like 1), *Bdnf* (brain-derived neurotrophic factor), *Apaf1* (apoptotic protease activating factor 1), *Casp1* (caspase 1), and *Cebp/d* (CCAAT/enhancer-binding protein delta) gene expression in retinas of *EpoR$^{flox/flox}$Opn-Cre* (**A**, red bars), and *EpoR$^{flox/flox}$;α-Cre* mice (**B**, blue bars) compared to *EpoR$^{flox/flox}$* control littermates (white bars) by semi-quantitative real-time PCR. cDNAs were prepared from total retinal RNA isolated at 12 weeks of age. Animals were kept under normoxic or hypoxic (6 Hrs, 7% O_2) conditions and retinas were isolated immediately after the experimental treatment. Given are mean values ± SD of N = 4 retinas, amplified in duplicates. Values were normalized to *Actb* and expressed relatively to *EpoR$^{flox/flox}$* control littermates under normoxic conditions, which was set to 100%. Differences in gene expression levels between knockdown and control mice at individual time points were tested for significance using a Students t-test *: $P < 0.05$; **: $P < 0.01$ (Figure: Caprara and Grimm, manuscript in preparation)

Exogenously applied rhEPO has demonstrated to provide beneficial effects in part by reducing the gliotic response, and thus the expression of *Gfap* (Hu et al., 2011). Unexpectedly, knockdown of *EpoR* (which should result in decreased EPOR signalling) in the peripheral retina led to significant ($p<0.05$) reduction of the expression of *Gfap* (about 50%) in both normoxia and hypoxia (Fig 56B).

A retinal endogenous protective pathway, that includes protein expressed by genes such as *Lif, Edn2* and *Fgf2,* is activated upon inherited (Samardzija et al., 2012) or induced (Burgi et al.,

2009) photoreceptor degeneration. Transcripts of *Lif*, *Edn2*, and *Fgf2* were increased in *EpoR*$^{flox/flox}$*;Opn-Cre* mouse retinas in hypoxia, even though the changes in gene expression were not statistically significant (Fig 56A). In contrast, *EpoR*$^{flox/flox}$*;α-Cre* mice showed a trend towards a reduced expression of *Lif*, *Edn2*, and *Fgf2* in the retina under both normoxic and hypoxic conditions. Here again, the changes of the mRNA levels were not statistically significant but involved all three members of this protective pathway (Fig. 56B). Also, expression of *Stat3* has been reported to increase upon retinal degeneration (Joly et al., 2008). In the retina of *EpoR*$^{flox/flox}$*;α-Cre* mice, the expression of *Stat3* was significantly reduced ($p<0.05$) by roughly 20% under hypoxic conditions in comparison to control mice (Fig. 56B).

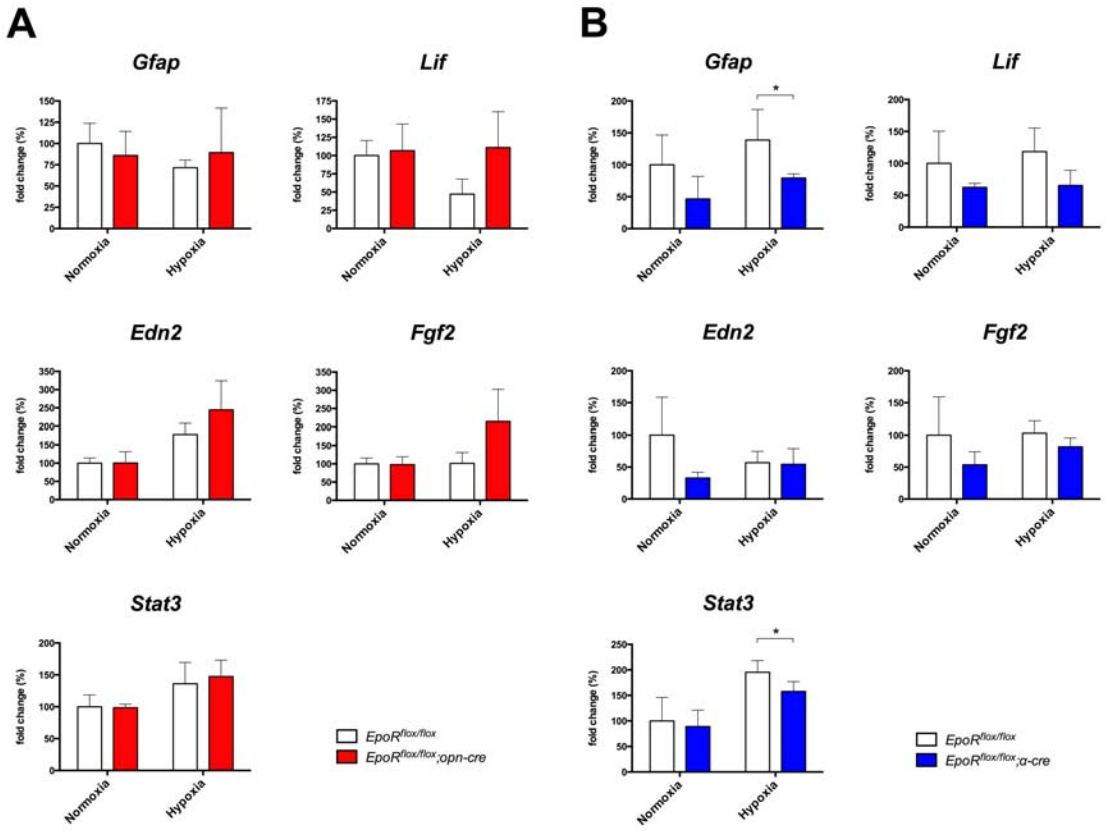

Figure 56 Expression of a selection of stress-related genes in retinas of *EpoR* knockdown mice. Relative quantification of *Gfap* (glial fibrillary acidic protein), *Lif* (leukemia inhibitory factor), *Edn2* (endothelin 2), *Fgf2* (fibroblast growth factor 2), and *Stat3* (signal transducer and activator of transcription 3) gene expression in retinas of *EpoR*$^{flox/flox}$*Opn-Cre* (**A**, red bars), and *EpoR*$^{flox/flox}$*;α-Cre* mice (**B**, blue bars) compared to *EpoR*$^{flox/flox}$ control littermates (white bars) by semi-quantitative real-time PCR. cDNAs were prepared from total retinal RNA isolated at 12 weeks of age. Animals were kept under normoxic or hypoxic (6 Hrs, 7% O_2) conditions and retinas were isolated immediately after the experimental treatment. Given are mean values ± SD of N = 4 retinas, amplified in duplicates. Values were normalized to *Actb* and expressed relatively to *EpoR*$^{flox/flox}$ control littermates under normoxic conditions, which was set to 100%. Differences in gene expression levels between knockdown and control mice at individual time points were tested for significance using a Students t-test *: $P < 0.05$ (Figure: Caprara and Grimm, manuscript in preparation).

Stimulation of the EPOR in neurons leads to the activation of JAK2/STAT3 and STAT5 signalling (Kawakami et al., 2001; Kretz et al., 2005; Zhang et al., 2007; Sola et al., 2005), activation of the PI3K/AKT pathway (Siren et al., 2001a; Digicaylioglu et al., 2004), and increased phosphorylation of extracellular-signal-regulated kinases (ERK)1/2 (Kilic et al., 2005a, b; Shen et al., 2010). In the *EpoR$^{flox/flox}$;Opn-Cre* mouse retina, we found unaltered expression and phosphorylation of AKT and ERK1/2, but a minor and statistically non-significant increase in the phosphorylation of STAT3 in hypoxia. Interestingly, in the hypoxic *EpoR$^{flox/flox}$;Opn-Cre* mouse retina, CASP1 protein expression was significantly ($p<0.05$) reduced by about 40% relatively to control littermates (Fig. 57A). This reduction in CASP1 protein levels was not measured for *Casp1* gene expression (Fig.55A). The expression of AKT was significantly ($p<0.05$) reduced by approximately 40% in the retina of *EpoR$^{flox/flox}$;α-Cre* mice kept in hypoxia compared to control animals (Fig. 57B). However, phosphorylation of AKT and ERK1/2 was not affected by *EpoR* knockdown neither under hypoxia nor under normoxia (Fig. 57). Also, expression of STAT3 was not affected by ablation of *EpoR* in the peripheral retina (Fig. 57B), even though a reduced expression of *Stat3* was found at the mRNA level in hypoxia (Fig. 56B). There was a trend towards increased STAT3 phosphorylation under hypoxic conditions in *EpoR$^{flox/flox}$;α-Cre* retinas, even though the changes were not statistically significant (Fig. 57B). Interestingly, despite statistical significance was not reached, ablation of *EpoR* in the retinal periphery caused a reduction in GFAP protein levels (roughly 50%) under both normoxia and hypoxia (Fig. 57B), confirming the results obtained by gene expression analysis (Fig. 56B). Moreover, expression of CASP1 was slightly, but not significantly, reduced of 25% in *EpoR$^{flox/flox}$;α-Cre* mouse retinas (Fig. 57B), thus confirming the expression of *Casp1* mRNA (Fig. 55B).

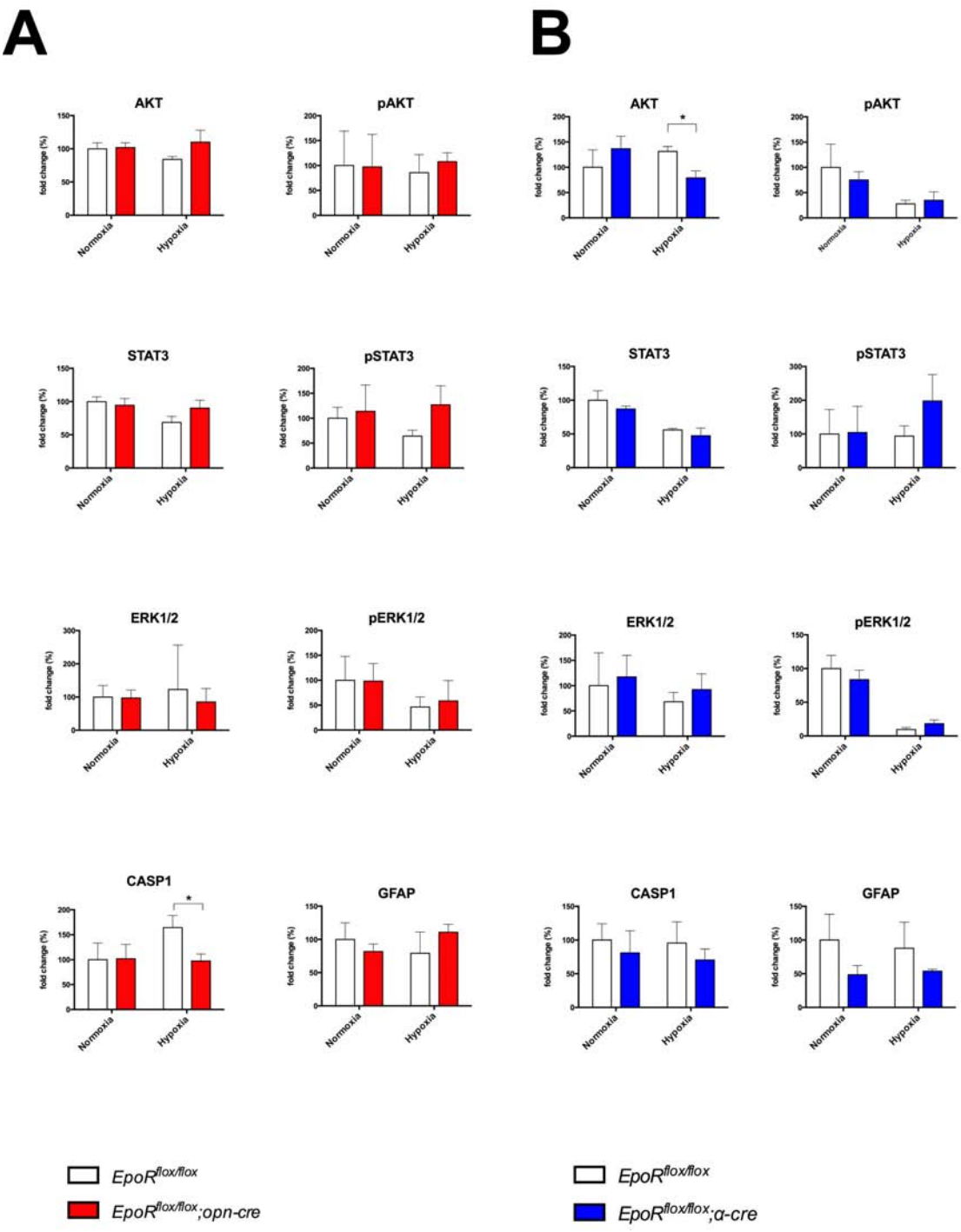

Figure 57 Protein expression and activation of signalling pathways upon ablation of *EpoR* in rod photoreceptors or in the peripheral retina. Western blot analysis of total retinal extracts at PND 84 of *EpoR*$^{flox/flox}$*;Opn-Cre* (red bars) **(A)**, and *EpoR*$^{flox/flox}$*;α-Cre* (blue bars) **(B)** mice compared to *EpoR*$^{flox/flox}$ control littermates (white bars). Animals were kept under normoxic or hypoxic (6 Hrs, 7% O_2) conditions. Shown is relative quantification (mean value ± SD of N = 3 animals per conditions and genotype) of protein expression or phosphorylation levels of different proteins (as indicated, refer to main text for details) that were quantified using BioD1 software (see Methods). Values were normalized to ACTB and are shown relative to normoxic *EpoR*$^{flox/flox}$ control littermates, which were set to 100%. (Figure: Caprara and Grimm, manuscript in preparation)

In conclusion, analysis of gene and protein expression revealed an unexpected increase in the expression of *Bdnf* and a reduced expression of *Apaf1*, a well as *Gfap* transcripts and protein in the retina of hypoxic *EpoR$^{flox/flox}$;α-Cre* mice. Irrespectively of the low expression of *EpoR* in photoreceptors, and the non-statistically significant reduction of expression in the ONL of *EpoR$^{flox/flox}$;Opn-Cre* mice, *Vegfa* and *Nos2(iNos)* transcripts were increased while *Mt2* mRNA and CASP1 protein were reduced in the retina of these mice. The expression of known targets of EPO-EPOR signalling, such as *Bcl2* and *Bcl2l1(Bcl$_{XL}$)*, was not affect in the retina of *EpoR* knockdown mice.

4.12 Ablation of *EpoR* in Rods or the Peripheral Retina Does not Affect Retinal Angiogenesis

In the recent past, the contribution of the EPO/EPOR axis in developmental angiogenesis began to be elucidated (Noguchi et al., 2008). Absence of EPO-EPOR signalling in early post-natal days could impair retinal angiogenesis. Thus, we analyzed the retinal vasculature of *EpoR$^{flox/flox}$;α-Cre* mice because knockdown of *EpoR* is expected to occur already during embryogenesis in these mice. Ablation of *EpoR* in the retinal periphery did not result in overt vascular abnormalities, as the retinal vasculature of *EpoR$^{flox/flox}$;α-Cre* was comparable to control littermates (Fig. 58A). In addition, all three retinal capillary plexi did develop properly and were found at their correct location (Fig. 58B).

On the other hand, knockdown of *EpoR* in the retina of *EpoR$^{flox/flox}$;Opn-Cre* mice is efficient at around 10 weeks of age (Chapter 4.1). Hence, ablation of *EpoR* in rod photoreceptors of these mice is not expected to have consequences on retinal angiogenesis, a process occurring during the first two-three post-natal weeks in mice (Fruttiger, 2007). As expected, the pattern of the retinal vasculature (Fig. 58A), and in particular the location of the retinal capillary plexi of *EpoR$^{flox/flox}$;Opn-Cre* mice was comparable to control littermates (Fig. 58B).

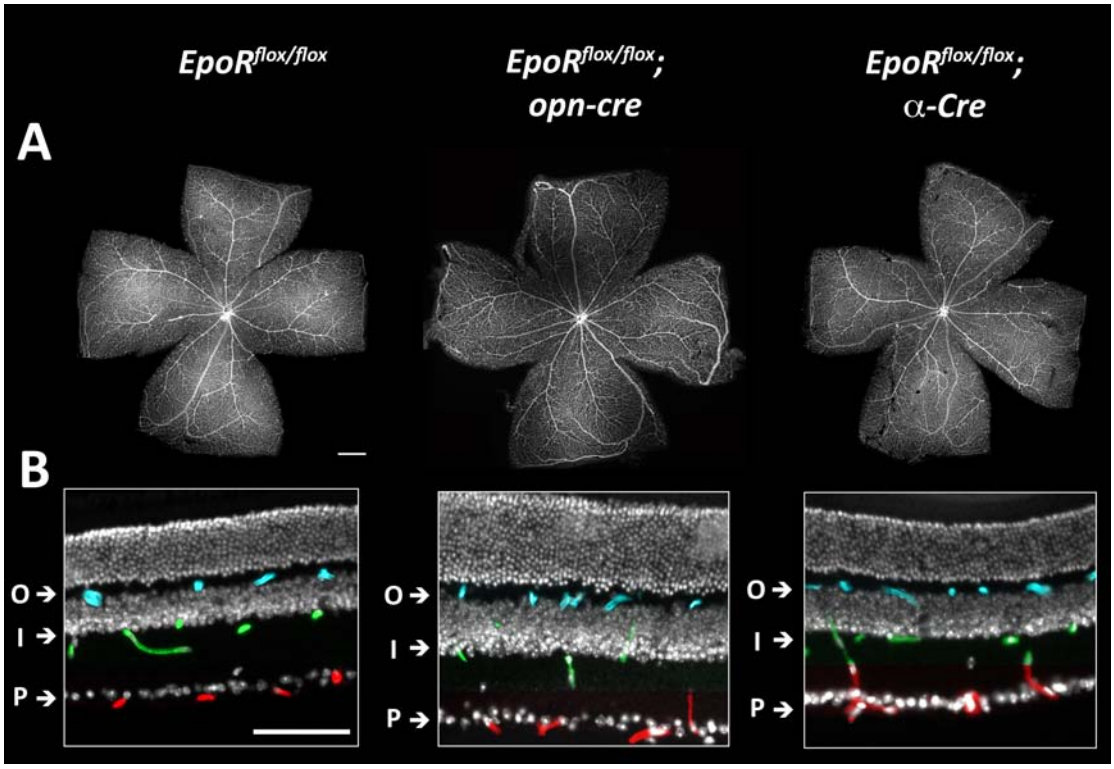

Figure 58 Normal development of the retinal vasculature in *EpoR* knockdown mice. (A) Retinal flatmounts of *EpoR*$^{flox/flox}$;*Opn-Cre* mice (center) at PND 84, *EpoR*$^{flox/flox}$;α-*Cre* mice (right) at PND 30, and *EpoR*$^{flox/flox}$ littermates (left) at PND 84. Vessels were stained with isolectin IB_4 coupled to Alexa594 (white). Shown are representative flatmounts for 3 animals per genotype. Scale bar: 500 µm. **(B)** Staining of blood vessels on retinal cryosections (isolectin IB_4, coupled to Alexa594) in *EpoR*$^{flox/flox}$;*Opn-Cre* mice (center), *EpoR*$^{flox/flox}$;*α-Cre* mice (right), and *EpoR*$^{flox/flox}$ littermates (left) at PND 84. Vessels were highlighted by artificial colouring (primary plexus (P): red; intermediate plexus (I): green; outer plexus (O): blue). Morphology of the retina can be recognized by staining of cell nuclei (DAPI, white). Scale bar: 100µm (Figure: Caprara and Grimm, manuscript in preparation)

In order to determine eventual consequences of *EpoR* knockdown for the perfusion of the retinal vasculature and the stability of the BRB, we performed FL angiography with help of the Micron III ophthalmoscopy-imaging device. By this method, the retinal vasculature of both *EpoR* knockdown lines showed a correct perfusion, as well as the absence of any sign of vascular leakage under normoxic conditions (Fig. 59).

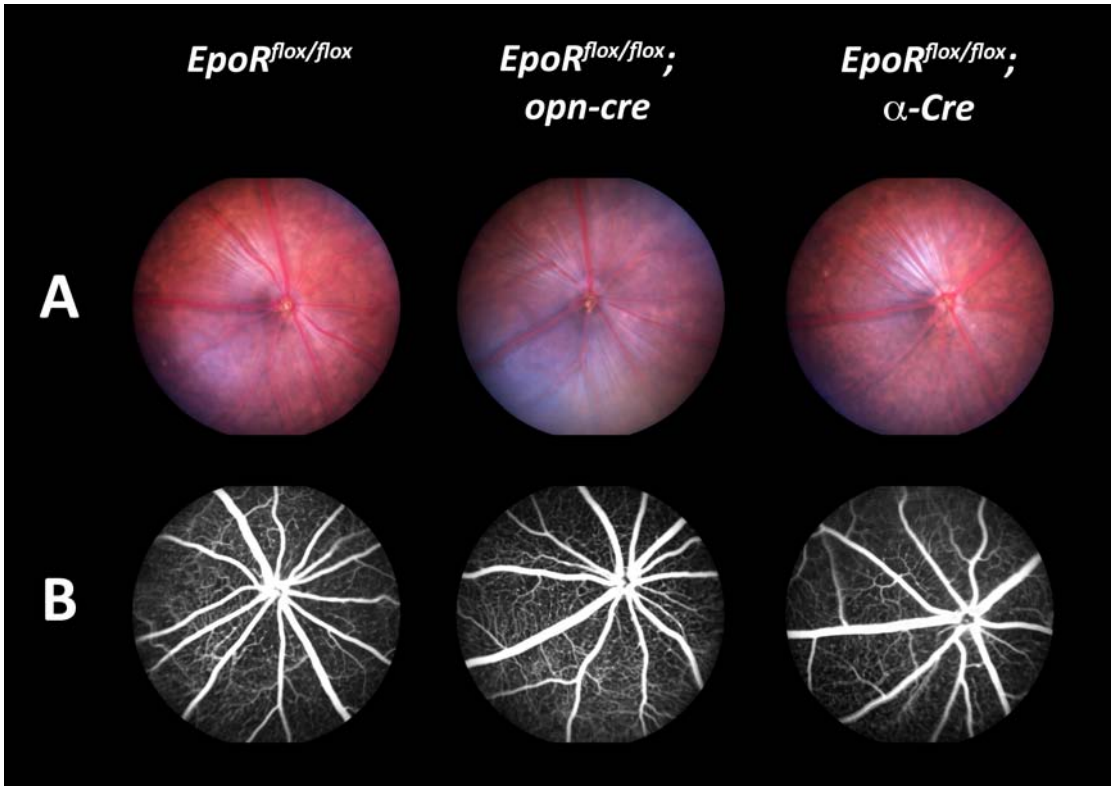

Figure 59 Vascular perfusion of *EpoR* knockdown retinas. Retina fundus imaging **(A)** and fluorescein angiography **(B)** of *EpoR*$^{flox/flox}$;*Opn-Cre* mice (center), *EpoR*$^{flox/flox}$;α-*Cre* mice (right), and *EpoR*$^{flox/flox}$ littermates (left) at PND 84 performed by Micron III imaging. Shown are representative images for 3 animals per genotype. Representative images from A and B are not derived from the same animal.

4.13 *EpoR*$^{flox/flox}$*;Opn-Cre* Retinas Are Constitutively Protected Against Light-induced Photoreceptor Apoptosis

The neuroprotective activities of rhEPO against light-induced photoreceptor degeneration have been proposed to rely on EPOR downstream signalling in photoreceptor cells (Grimm et al., 2002). To test whether the localization of EPOR in the cell surface of rods is necessary for the protective effects of rhEPO, we exposed *EpoR*$^{flox/flox}$*Opn-Cre* mice to toxic levels of light (17000 lux, 2 Hrs). Knockdown mice and control littermates were injected intraperitoneally with rhEPO (5000 IU/Kg) or PBS 1 hour prior to light exposure. Measurements of rhodposin concentration by spectrometry in the retina 12 days after the damaging insult were used to assess the extent of photoreceptor loss. If EPOR on the surface of rod photoreceptors would be necessary for the protective effects of rhEPO, one would expect an increased light damage in *EpoR*$^{flox/flox}$*;Opn-Cre*

retinas, despite rhEPO applications. Surprisingly, and unexpectedly, this was not the case. Measurements of retinal rhodopsin showed that PBS-injected control mice did loose photoreceptors following light damage, while rhEPO-injected animals were partially protected, as reported earlier (Grimm et al., 2002). This confirms the validity of our experimental setup. On the other hand, *EpoR$^{flox/flox}$;Opn-Cre* mice did not show any loss of photoreceptor cells, irrespectively of the treatment prior to light exposure, thereby showing to be basically insensitive to light-induced photoreceptor apoptosis. This was confirmed by the absence of photoreceptor degeneration in *EpoR$^{flox/flox}$;Opn-Cre* mice that did not receive any injection (Fig. 60A). The reason for this observation is unclear and warrants further investigation.

The same experimental setup was also applied to *EpoR$^{flox/flox}$;α-Cre* mice. However, in this case a high variability of the extent of photoreceptor apoptosis was noticed and no definitive conclusion could be drawn from these experiments (Fig. 60B).

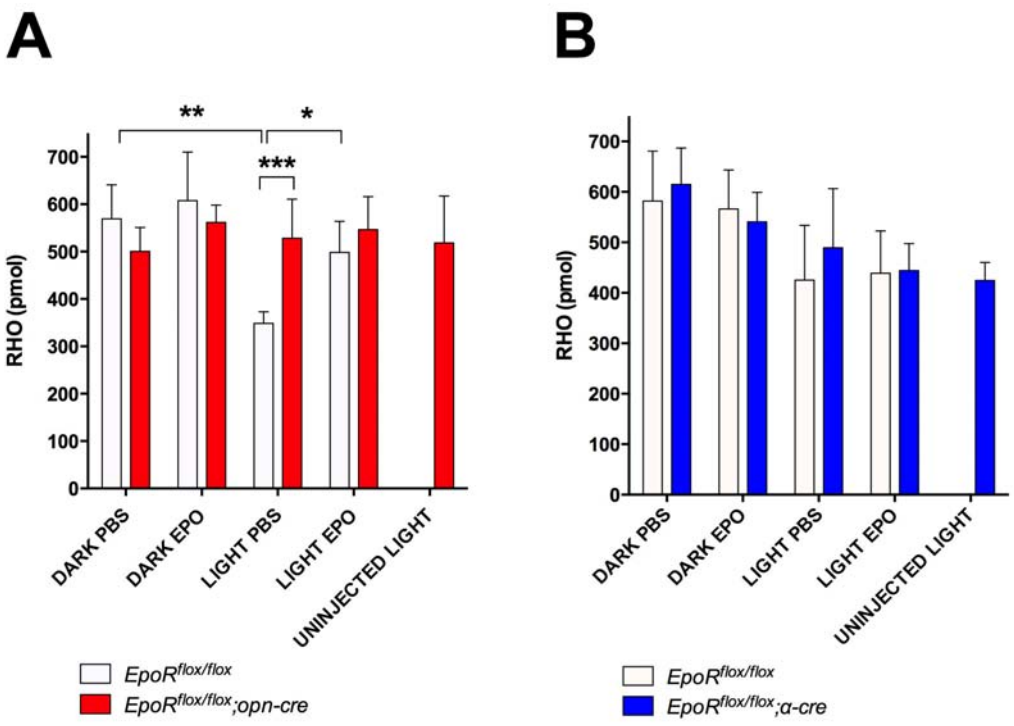

Figure 60 Susceptibility of *EpoR* knockdown mouse retinas to light-induced photoreceptor degeneration upon rhEPO administration. Measurements of rhodopsin (RHO) levels in retinas of *EpoR$^{flox/flox}$;Opn-Cre* mice (red bars) at PND 84 **(A)**, *EpoR$^{flox/flox}$;α-Cre* mice (blue bars) at PND 49 **(B)** and *EpoR$^{flox/flox}$* littermates (white bars). Animals were exposed for 2 Hrs to 17000 lux of light (LIGHT) or kept in darkness (DARK). 1 Hr before light exposure, mice were injected intraperitoneally with 5000 IU/Kg of rhEPO (EPO) or 50 μL PBS (PBS). Retinas were collected 12 days after light exposure for rhodopsin measurements. To test for the effects of the injection procedure, animals were exposed to light without injection (UNINJECTED LIGHT). Shown are mean values ± SD of at least N = 3 animals per genotype and condition. *: p<0.05; **: p<0.01; ***:p<0.001. (Figure: Caprara and Grimm, unpublished)

5 Discussion

5.1 CRE-mediated Recombination in *α-Cre*, *Opn-Cre*, and *Pdgfra-Cre* Mice

In genetics research, Cre-loxP recombination is a site-specific recombinase technology mainly employed to carry out deletions of genomic sequences, i.e. gene knockout strategies. This methodology takes advantage of the ability of an enzyme, CRE recombinase, to catalyze recombination between specific DNA sequences called *loxP* sites (Sternberg and Hamilton, 1981). This technology allows to specifically deleting DNA sequences only in cells expressing *Cre* recombinase, whose expression is spatially and timely regulated by an inducible or constitutive promoter of choice, resulting in the so-called "conditional knockout" technology (Utomo et al., 1999). The conditional knockout technology allows both to investigate the roles of specific genes that would result in an embryonic lethal phenotype if ablated systemically, as well as to define gene function in specific cell types by ablation of the gene of interest at the time and in the cell population of choice. Nevertheless, the pattern and timeframe of *Cre* expression need to be evaluated in order to obtain the highest advantage from this genetic technology. *Cre* reporter strains have been developed to meet these needs. These allow the investigator to assess the time and location of CRE-mediated recombination of an individual *Cre* line. In this thesis, I employed different *Cre* mouse lines to ablate *Hif1a* and/or *EpoR* in different retinal cell populations. However, it is necessary to deeply investigate the expression pattern of *Cre* in each of these strains, in order to validate the specificity of the knockout strategy.

In the α-*Cre* transgenic mouse line, expression of *Cre* is driven by the *Pax6 P0* promoter and the peripheral retina enhancer known as α-element (Marquardt et al., 2001). PAX6 is a highly conserved transcription factor necessary for ocular development (Ton et al., 1991; Hill et al., 1991) and for the proliferation and differentiation of retinal progenitors (Marquardt et al., 2001). The expression of *Cre* in the *α-Cre* mouse has been previously reported to start around E10.5 (Marquardt et al., 2001). As reported by Marquardt *et al*, CRE-mediated recombination occurs in a large and heterogeneous cell population of the peripheral retina (Marquardt et al.,

2001). We confirmed these findings in *Ai6;*α-*Cre* mice and by analyzing the spatial expression pattern of ZSGREEN which reflected *Cre* expression (Madisen et al., 2010). Expression and activity of CRE was detectable in a large cell population of the retinal periphery, and was limited to a subset of amacrine and presumably RGCs in the central retina. In addition, CRE activity was absent in the dorsal retina (Fig. 19)(Marquardt et al., 2001). These results collectively confirm the endogenous expression pattern of *Pax6* during retinal development (Ziman et al., 2003; Reza et al., 2007). Co-localization analysis revealed that cells in the retinal periphery that express *Cre* are photoreceptors, Müller glia, and subsets of amacrine, horizontal and most probably RGCs (Fig. 20). Expression of *Cre* recombinase was also previously reported in amacrine cells in the mature retina of the α-*Cre* mouse line (Marquardt et al., 2001; Duquette et al., 2010). Even though a clear co-localization of ZSGREEN and the ganglion-cell marker POU4F1 (BRN3A) was not found, the different localization of the two proteins - ZSGREEN in the cytoplasm and POU4F1 (BRN3A) in the nucleus – could explain the lack of co-localization (Fig. 21). A confirmation that RGCs express *Cre* recombinase comes from the analysis performed by Nakamura-Ishitzu and colleagues by immunohistochemistry, which identified $PAX6^{+}$ RPCs and neurofilament $(NF)^{+}$ ganglion cells as *Cre*-expressing cells in the α-*Cre* mouse (Nakamura-Ishizu et al., 2012). Also, Badea and co-workers described the expression of *Cre* in a subset of RGCs (Badea et al., 2012). I was not able to detect expression of ZSGREEN in astrocytes of the *Ai6;*α-*Cre* retina by immunohistochemical analysis with anti-GFAP antibody (Fig. 20). This was reported also by Nakamura-Ishizu *et al*, that performed flatmount immunohistochemistry and FACS analysis and excluded the expression of *Cre* in astrocytes and vascular endothelial cells (Nakamura-Ishizu et al., 2012). Expression of *Cre* was also absent from the RPE (Fig. 20), as previously described (Marquardt et al., 2001). Taken together, these observations underline the heterogeneity of the retinal cell types that express *Cre* in the α-*Cre* mouse. This can be of great advantage when aiming to ablate a gene in most cell types of a tissue, but can become problematic in the view of specificity, i.e. when the absence of a particular gene needs to be connected to a particular cell type. Nevertheless, the α-*Cre* mouse has the advantage to provide a knockdown accompanied by an internal negative control, i.e. the central retina where *Cre* is not expressed.

Roesch *et al* reported that expression of *Cre* recombinase in the *Pdgfra-Cre* mouse was restricted to the Müller glia population. Nevertheless, the authors also suggested that CRE

activity might be present in the ONL and GCL (Roesch et al., 2008). Analysis of ZSGREEN co-localization with different retinal cell markers on retinal cryosections of *Ai6;Pdgfra-Cre* mice revealed a clear co-localization of both GLUL (GS) and GFAP with ZSGREEN. This supports the previous findings of the expression of *Cre* recombinase in Müller cells, but also suggests that astrocytes are *Cre*-expressing cells (Fig. 23). A weak co-localization of CALB1 and ZSGREEN was detected in the OPL. This hints that also horizontal cells express *Cre* recombinase in the *Pdgfra-Cre* mouse (Fig. 23). In addition, CRE activity was also observed in the sclera and choroid, as well as extraocular tissues (e.g. skin, data not shown). Altogether, these results point to an elevated percentage of Müller cells expressing *Cre* in the *Pdgfra-Cre* mouse. Yet, CRE activity might be present also in astrocytes and horizontal cells, thus significantly reducing the specificity of this Müller cell *Cre* strain. Furthermore, the expression of *Cre* in extraocular tissues of the *Pdgfra-Cre* mouse points to potentially problematic side effects. In fact, the undesired knockout of a gene of interest in extraocular tissues may cause systemic effects, or may even lead to developmental defects, lethality, or other severe problems. For further use, this strain would need thorough characterization to identify as many extraocular expression sites as possible.

Expression of *Cre* recombinase in rod photoreceptors of the *Opn-Cre* mouse was previously analyzed by immunohistochemistry for CRE, and by the analysis of a *lacZ* reporter mouse. The authors reported that the onset of *Cre* expression was at approximately PND 7 and expression increased up to 6 weeks of age. Furthermore, cone photoreceptors did not express *Cre* (Le et al., 2006). I analyzed the specificity of *Cre* expression in the *Opn-Cre* mouse by breeding it to the *ROSA-flox-RFP* reporter mouse, and detected distribution of RFP in rod photoreceptors in 10-week old *ROSA-flox-RFP;Opn-Cre* mice. CRE-mediated recombination was found in a patchy pattern in roughly 40% of the total rod photoreceptor population (Fig. 24). In conclusion, the *Opn-Cre* mouse has certainly the advantage to provide a rod-specific conditional knockout strategy. However, based on our observation, efficient knockdown is reached only after approximately 10-weeks of age (data not shown), and does not occur in the whole population of rod photoreceptors.

5.2 Transcription of *Hif* Genes May Be Regulated by Hypoxia

To gain first hints on the roles of HIF isoforms in the retina, I analyzed the transcription pattern of *Hif1a*, *Epas1 (Hif2a)*, *Hif3a,* and *Hif1b* in the juvenile and adult retina. In recent years, increasing evidence pointed to the importance of the transcriptional regulation of *Hifa* subunits for the hypoxic response, besides the oxygen-dependent protein stabilization. Transcription of both *Hif1a* and *Epas1 (Hif2a)* in the post-natal retina have very similar kinetics, with low mRNA level detected up to PND 10, when the expression of both genes strongly increased and was maintained over adulthood (Fig. 25). This increase is in partial concomitance with the period of developmental hypoxia of the mouse retina (Chapter 1.3.4), and suggests that expression of these genes may be induced by reduced oxygen tension. Shortly after the discovery of *Hif1a*, it was proposed that transcription of this gene might not be regulated by hypoxia *in vivo*, as was previously observed in cultured cell lines (Wang and Semenza, 1993). However, additional experiments performed *in vivo* with the exposure of animals to intermittent hypoxia demonstrated that increased expression of *Hif1a* mRNA could be measured under these conditions (Semenza, 2000; Lam et al., 2008). Hence, the regulation of *Hif1a* gene expression under hypoxic conditions is still under debate, but it appears that intermittent hypoxia is more prone to induce transcription of *Hif1a* compared to a single hypoxic exposure. Belaiba and co-workers investigated the regulation of *Hif1a* transcription in response to hypoxia in pulmonary artery smooth muscle cells, and concluded that hypoxia induces *Hif1a* mRNA expression via the PI3K/AKT pathway and nuclear translocation of nuclear factor κB (NFκB) (Belaiba et al., 2007). These data support the hypothesis that in the retina *Hif1a* and possibly *Epas1 (Hif2a)* transcription are upregulated by developmental hypoxia. However, increased transcription of *Hi1a* and *Epas1 (Hif2a)* was sustained throughout adulthood, i.e. a time-point when the hypoxic insult is relieved by angiogenesis. This suggests that hypoxia may be the initiator of *Hif1a* and *Epas1 (Hif2a)* transcriptional upregulation, but other mechanisms have to be in place to sustain the increased transcription. One of these mechanisms may involve oxidative stress. Recent advances in the field have demonstrated that *Hif1a* gene expression is controlled by NFκB though NFκB binding sites on the *Hif1a* promoter (Rius et al., 2008; Bonello et al., 2007). In particular, in the absence of NFκB, transcription of the *Hif1a* gene does not occur (van Uden et al., 2008;

Kenneth et al., 2009). In a study performed by Bonello *et al*, ROS were demonstrated to induce *Hif1a* transcription via NFκB (Bonello et al., 2007). The increase in oxidative phosphorylation following the onset of retinal activity (Graymore, 1959) may result in a drastic increase of ROS production. ROS generated by NADPH oxidase, and the ensuing changes in intracellular Ca^{2+} are triggering HIF1A accumulation by both increased transcription and protein stability in conditions of intermittent hypoxia (Yuan et al., 2008). Intriguingly, the end stage of retinal neuronal differentiation and the onset of retinal function timely match the increase in expression of *Hif1a* and *Epas1 (Hif2a)*. Thus, increased oxidative stress could be the inducer of transcription of *Hifa* isoforms via NFκB, and may as well maintain high expression levels through adulthood. Nevertheless this conclusion is highly speculative and additional experiments are needed to test this hypothesis.

The expression profile of *Hif1b* in the post-natal retina showed very similar kinetics as *Hif1a* and *Epas1 (Hif2a)* (Fig. 25). *Hif1b* is constitutively expressed and the regulation of its gene and protein expression has long been considered to be oxygen-independent (Zagórska and Dulak, 2004). In spite of this, evidence shows that in a limited number of cell types, *Hif1b* transcription and protein levels are increased in a HIF1A-dependent manner when cells are exposed to low oxygen tension or treated with the hypoxia-mimetic cobalt chloride ($CoCl_2$) (Chilov et al., 1999b; Wang et al., 1995b; Mandl et al., 2013). Similarly as for *Hif1a*, also *Hif1b* gene expression is regulated by binding of NFκB to its promoter, in particular when cells are stimulated by cytokines such as TNFA (van Uden et al., 2011). In conclusion, *Hif1b* transcription in the post-natal retina might be increased by similar mechanisms regulating *Hifa* gene expression, i.e. hypoxia and / or NFκB nuclear translocation.

In the recent past, different *Hif3a* splice variants were shown to negatively regulate HIF-induced gene expression, a mechanism which may involve a negative dominant effect of HIF3A by competition for binding to HIFB (Makino et al., 2001; Heikkilä et al., 2011). The function of HIF3A splice variants seems to include the inhibition of HIF-induced VEGFA expression, eventually suppressing angiogenesis (Jang et al., 2005; Ando et al., 2013). Interestingly, *Hif3a* mRNA expression is induced by hypoxia in a HIF1-dependent manner (Augstein et al., 2011; Pasanen et al., 2010), and this notion may explain the increased expression of this gene at PND 10 in the mouse retina (Fig. 25). At this post-natal age, HIF1A protein levels are elevated in the

mouse retina (Fig. 16) (Grimm et al., 2005). Hence, the decrease in expression of *Hif3a* starting at PND 15 may be linked to the concomitant decrease of HIF1A protein levels that are observed after the retinal vasculature has completely developed (Ozaki et al., 1999). Thus, it is tempting to hypothesize a possible involvement of *Hif3a* isoforms in the regulation of retinal angiogenesis, for example as terminator of HIF-induced expression of pro-angiogenic genes, such as *Vegfa*. To test this hypothesis, the exact expression profile of different *Hif3a* splice variants should be investigated, as well as the retinal vascular phenotype of *Hif3a*-null mice.

5.3 HIF1A is Essential for the Development of the Retinal Vascular Intermediate Plexus

In rodents, during the first two weeks after birth, the retina has to face a chronic period of physiological hypoxia that ensues as neuronal differentiation terminates and retinal function starts (Chapter 1.3.4). At this time, the embryonic hyaloid vasculature is inadequate in delivering a sufficient amount of metabolites and oxygen to the retina, and the presence of hyaloid vessels in the vitreous is an obstacle for light penetrating the eye. For these reasons, hyaloid vessels progressively regress and are replaced by the retinal vasculature, which develops during the first three post-natal weeks in mice and rats. This angiogenic process is tightly linked to the hypoxia-controlled gene expression, leading to the production of proteins that drive the growth of new blood vessels into the retina ((Fruttiger, 2007), Chapter 1.3.5). The transcription factor HIF1A plays a central role in both the cellular adaptation to hypoxia and angiogenesis (Chapter 1.4). Hence, lack of HIF1A during the aforementioned period of hypoxia might impair retinal cell survival and vascularisation of the retina. To test this hypothesis, we generated mice deficient of *Hif1a* in a heterogeneous population of neurons and glia of the peripheral retina, including photoreceptors, Müller cells, and a subset of horizontal, amacrine and ganglion cells. This was accomplished by generating *Hif1a*$^{flox/flox}$*;α-Cre* mice, which are expected to lead to the ablation of *Hif1a* embryonically (Marquardt et al., 2001), and in our hands show a reduced expression of *Hif1a* in the post-natal retina (Fig. 26). In *Hif1a* knockdown mice, a reduced amount of HIF1A

protein was detected at PND 10, thus validating the knockdown strategy (Fig. 26).

As we expected, the post-natal angiogenic process was impaired in *Hif1a*$^{flox/flox}$*;α-Cre* mice. The development of the intermediate capillary plexus was significantly affected in the retinal periphery in the absence of HIF1A, resulting in a reduction of 75% of vessel coverage when compared to control littermates (Fig. 34). However, the vascular coverage of the primary plexus and of the outer plexus was comparable between *Hif1a* knockdown retinas and controls. Since the intermediate plexus is the last capillary plexus that is established in the mouse retina, we conclude that the angiogenic process in *Hif1a* knockdown retina is not complete. The significance of this remark needs to be established, but may nevertheless suggest that different regulatory mechanisms are present for the formation of each vascular plexus. Despite the reduced vascular coverage, vessels from the primary plexus were interconnected to the capillaries of the outer plexus and the vascular system was fully functional, without any sign of leakage, as demonstrated *in vivo* by FL angiographic analysis (Fig. 35). Nevertheless, by this method, the presence of vascular lesions was revealed. Hence, it would be of particular interest to analyze the retinal vasculature of older *Hif1a* knockdown mice to assess whether the presence of these lesions accumulates over time.

Even though we did not find major alterations in the growth of the primary vascular plexus, Nakamura-Ishizu and co-workers analyzed in detail the development of this vascular plexus in the retina of *Hif1a*$^{flox/flox}$*;a-Cre* mice. In particular, the authors showed that development of the primary plexus was also slightly impaired and was characterized by decreased tip cell filopodia and a reduction in vessel branching, as a result of a hypoplastic astrocyte network. These alterations in the astrocyte network were a result of the downregulation of platelet-derived growth factor A (PDGFA), a mitogen for astrocytes that is secreted by the neuroretina, presumably by RPCs (Nakamura-Ishizu et al., 2012). Also, other studies investigated the contribution of astrocytes and neurons in the establishment of the primary plexus. Astrocyte-specific knockdowns of *Vegfa, Hif1a* or *Epas1 (Hif2a)* did not influence the physiological development of the retinal vasculature (Weidemann et al., 2010). However, a conditional knockdown of *Vhl* in astrocytes caused a normoxic stabilization of HIF transcription factors. This led to an increased expression of *Vegfa* and pathological retinal angiogenesis, resulting into hypervascularity of the primary plexus (Weidemann et al., 2010). Simultaneous ablation of *Vhl*

and *Vegfa* in astrocytes rescued the vascular phenotype (Weidemann et al., 2010). On the other hand, RGC-deficient mice (*Brn3*$^{bZ\text{-}dta/+}$*; Six3-Cre*) show a complete lack of the retinal vasculature, thereby suggesting a central role of RGCs in retinal angiogenesis (Sapieha et al., 2008). Altogether these observations suggest that retinal neurons (e.g. RGCs) rather than astrocytes may act as primary oxygen sensor to control the development of the primary plexus of the retinal vasculature by regulating the growth of the astrocyte template (Nakamura-Ishizu et al., 2012). While astrocyte-derived *Vegfa* might not be fundamental for physiological angiogenesis in the retina, it may yet be able to modulate the process and contribute to pathological neovascularisation (Weidemann et al., 2010).

5.4 Search for the Molecular Basis of the Lack of the Retinal Vascular Intermediate Plexus

The tightly regulated process of retinal angiogenesis involves the production and secretion of a multitude of pro- and anti-angiogenic factors. A strong candidate for the induction and regulation of angiogenesis is VEGFA, a well-known angiogenic and vasopermeability factor, that has shown to contribute to angiogenesis in virtually every tissue, including the retina (Ferrara and Gerber, 2001). The induction of *Vegfa* gene expression is regulated by HIFs, as underlined by the presence of HRE sequences in the *Vegfa* promoter region (Kimura et al., 2001). Hence, an increased expression and secretion of VEGFA occurs under hypoxic conditions (Shweiki et al., 1992). In the retina, secretion origin of VEGFA in hypoxia has been attributed to several cell types, including vascular endothelial cells, pericytes, Müller cells, astrocytes, and RPE cells (Adamis et al., 1993; Aiello et al., 1995). In our mouse model, due to the expression of *Cre* recombinase by Müller glia (among other cells) (Fig. 20), a decreased secretion of VEGFA upon ablation of *Hif1a* would be expected. Surprisingly, no decrease in *Vegfa* expression was detected, in particular during the angiogenic time-window (Fig. 36). This was unexpected, as the development of intraretinal capillaries is preceded by a transient upregulation of *Vegfa* transcripts in the INL, at least in the rat retina (Stone et al., 1995). A possible explanation could

rely on a "dilution effect". In fact, *Vegfa* mRNA levels were quantified in total retinal extracts, and CRE-mediated recombination occurs predominantly in the peripheral retina, thus masking local and transient changes of *Vegfa* expression by such an analysis. Nevertheless, our observation is in line with results obtained by Weidemann *et al*, which reported that ablation of *Hif1a* in Müller cells and astrocytes did not alter *Vegfa* expression (Weidemann et al., 2010). Our observations support the conclusion that other transcription factors may drive *Vegfa* expression during retinal development. A major candidate might be EPAS1 (HIF2A), which was already shown to induce *Vegfa* expression in other cells (Wiesener et al., 1998; Xia et al., 2001; Takeda et al., 2004). Supporting this hypothesis, knockdown of VHL protein during retinal development resulted in a normoxic accumulation of both HIF1 and HIF2, and in an increased *Vegfa* expression (Lange et al., 2011a; Kurihara et al., 2010). While a simultaneous knockdown of *Vhl* and *Hif1a* in retinal glia also resulted into augmented VEGFA levels, simultaneous ablation of *Vhl* and *Epas1* (*Hif2a*) did not (Weidemann et al., 2010). All this suggests that EPAS1 (HIF2A) may regulate *Vegfa* expression, possibly in conjunction with HIF1A, or alone. Thus, the increased expression of EPAS1 (HIF2A) in our model might compensate for the downregulation of HIF1A (Fig. 38), eventually resulting in unaltered expression levels of *Vegfa.*

Not only VEGFA, but also a multitude of other pro- and anti-angiogenic molecules orchestrate retinal angiogenesis. We therefore analyzed the expression pattern of different genes known to be involved in this process. SERPINF1 (PEDF) is among the anti-angiogenic factors known to regulate retinal angiogenesis by counterbalancing high VEGFA levels (Eichler et al., 2004), and long-term overexpression of this protein inhibited retinal neovascularisation (Haurigot et al., 2012). Under hypoxic conditions, HIF1A has been reported to drive SERPINF1 (PEDF) expression and the source of its secretion in the retina is thought to include Müller cells (Yang et al., 2012). Hence, increased secretion of this protein may lead to a reduced vascular growth, as observed in *Hif1a* knockdown retinas. However, *Serpinf1 (Pedf)* mRNA expression profiles were similar in *Hif1a* knockdown and control retinas (Fig. 36). ANG2 is another protein that is involved in retinal angiogenesis and vascular remodelling by acting as an antagonist of TEK (TIE2), a tyrosine kinase receptor expressed on endothelial cells (Maisonpierre et al., 1997). *Ang2* mRNA expression has been shown to be increased in the INL during development of the deep retinal capillaries (Hackett et al., 2000). *Ang2*-deficient retinas show an absence of the

intermediate and outer capillary plexi (Hackett et al., 2002), a phenotype partially matching with what we observed in *Hif1a* knockdown retinas. In our mouse model, *Ang2* mRNA expression was not significantly affected in the time window between PND 5 and 10 when compared to control retinas (Fig. 36). Intriguingly, *Tek (Tie2)* expression at PND 21 in *Hif1a* knockdown retinas was significantly increased by two-fold ($p<0.001$) (Fig. 36), even though the relative number of endothelial cells should be reduced due to the lack of the intermediate vascular plexus. This points to a possible involvement of vascular remodelling in the vascular phenotype of *Hif1a*$^{flox/flox}$*;α-Cre* mice. Netrins are ligands for deleted in colorectal cancer (DCC) receptor and uncoordinated five (UNC5) receptor families (Livesey, 1999). These proteins act as diffusible secreted factors that regulate axon guidance and the development of the ONH (Hackett et al., 2002). NTN1 has recently been implicated as a pro-angiogenic factor in the retina and is upregulated under hypoxic conditions (Tian et al., 2011; Xu et al., 2012). NTN4 is a Müller-cell secreted factor upregulated under hypoxic conditions in a HIF1-dependent manner. This protein has been suggested to promote proliferation and migration of vascular endothelial cells, and therefore to contribute to retinal angiogenesis (Lange et al., 2012). In line with these reports, we would expect a reduction in the expression of netrin family members upon *Hif1a* knockdown, in particular *Ntn4*. Indeed, both *Ntn1* and *Ntn4* gene expression was significantly reduced at PND 10 upon *Hif1a* knockdown (Fig. 36). This observation is highly interesting and points to these axon guidance molecules as potential candidates for the vascular phenotype. However, in a recently published work, Li *et al.* analyzed the retinal vasculature of Ntn4$^{-/-}$ and excluded major phenotypical alterations of retinal vessels due to lack of NTN4 (Li et al., 2012). Norrie disease is a pathological condition characterized by congenital blindness, deafness and mental retardation (Fradkin, 1971). Mutations in the human *NDP* gene, encoding norrin, have been recognized as causative factors in Norrie disease (Chen et al., 1993). In the retina, NDP is produced by Müller cells and acts as a ligand of a receptor complex that includes FZD4, LRP5 and TSPAN12. Upon binding to the receptor complex on vascular endothelial cells, NDP activates the canonical WNT signalling pathway (Xu et al., 2004; Ye et al., 2009; Wang et al., 2012). In the past years, *Ndp* has been implicated in the regression of hyaloid vessels and in retinal angiogenesis, in particular in the development of the deep capillary networks (Ohlmann and Tamm, 2012). In fact, in Ndp$^{y/-}$ mice the deep capillary plexi are not formed, and the outgrowth of the primary vascular plexus is

delayed. It appears that this phenomenon, together with decreased angiogenic sprouting, is a consequence of reduced proliferation of vascular endothelial cells (Rehm et al., 2002; Richter et al., 1998; Zuercher et al., 2012). Moreover, in *Fzd4*$^{-/-}$, *Lrp5*$^{-/-}$ and *Tspan12*$^{-/-}$ retinas, the development of the primary plexus is delayed and incomplete, and the outer and intermediate capillary plexi are lacking, thus essentially phenocopying the vascular phenotype described in Ndp$^{y/-}$ mouse retinas (Xu et al., 2004; Junge et al., 2009; Luhmann et al., 2005; Xia et al., 2010). We did not measure significant modifications in the expression of *Ndp* upon *Hif1a* knockdown. However, significantly reduced expression of the receptor components *Fzd4* and *Tspan12* were measured at PND 10, a time frame conceivable with the development of the intermediate plexus (Fig. 36). It is important to note that a reduced vascular coverage in *Hif1a*$^{flox/flox}$*;α-Cre* mouse retinas might explain the reduced mRNA expression of *Fzd4* and *Tspan12*, which are both expressed on vascular endothelial cells (Ye et al., 2009). In this case, one would expect reduced expression levels of these receptor components even in the retina of adult mice, but this was not confirmed at a statistical significant degree. Alternatively, expression of *Fzd4* and *Tspan12* could be reduced in vascular endothelial cells, thus reducing WNT signalling, and lead to an incomplete retinal angiogenesis. ADM is a peptide that was reported to act as a potent vasodilator on retinal arteries, and was shown to augment choroidal blood flow and flow velocity of the ophthalmic arteries (Kitamura et al., 1993). Expression of *Adm* is induced in hypoxic retina (Thiersch et al., 2008). In addition, a possible involvement of ADM in retinal angiogenesis has been suggested by the embryonically lethal vascular defects described in *Adm* knockout mice (Shindo et al., 2001), and by the observation that ADM enhanced the proliferation and migration of retinal endothelial cells, besides playing a role in pathological angiogenesis in the OIR model (Iesato et al., 2013). Upon ablation of *Hif1a* in the retinal periphery, increased transcripts levels of *Adm* were measured at PND 15 and PND 21 (Fig. 36). The incomplete vascularisation of the inner retina of *Hif1a*$^{flox/flox}$*;α-Cre* mice may result in local hypoxia, and this could explain the increased expression of *Adm*. Increased secretion of the peptide may induce vasodilation of retinal arteries and consequently relief the hypoxic insult. However, the reason for the absence of increased *Adm* expression in the adult retina deserves further investigation, as the vascular phenotype of *Hif1a*$^{flox/flox}$*;α-Cre* retina persisted into adulthood.

In conclusion, changes in the expression of genes involved in retinal angiogenesis were

detected in the timeframe when the intermediate plexus is normally formed, i.e. at around PND 10. These include reduced mRNA levels of netrin family members as well as *Fzd4* and *Tspan12*, which are involved in WNT signalling. Altered expression of these genes may explain the vascular phenotype in *Hif1a*$^{flox/flox}$*;α-Cre* retina, but the definition of the molecular basis of the phenotype clearly needs further investigation. A problem in this perspective might be represented by short-term and gradient-like expression patterns of factors guiding the growth of the intermediate plexus. Detection of such a gradient is not possible by analyzing global transcripts levels in the retina. Other methods would be needed, such as high resolution *in situ* hybridization or the isolation of RNA from different retinal layers by laser capture microdissection.

Beside the identification of proteins involved in retinal angiogenesis, it is crucial to discover the cellular origin of expression of pro- and anti-angiogenic factors. The recognition of the cell population(s) responsible for the vascular phenotype described in *Hif1a* knockdown retinas is rendered difficult by the heterogeneity of the population of retinal cells that expresses *Cre* in the *α-Cre* mouse (Chapter 5.1). Müller cells have long been recognized to express proteins that regulate retinal angiogenesis (Bringmann et al., 2006), and these glia are part of the heterogeneous population of cells were *Hif1a* is ablated in the *Hif1a* knockdown retina. Yet, the more specific ablation of *Hif1a* in astrocytes and Müller cells (in *Hif1a*$^{flox/flox}$*;Pdgfra-Cre* mice) did not lead to a comparable or even appreciable phenotype at the vascular level, as shown here (Fig. 44) and reported by others (Weidemann et al., 2010). Hence, the correct formation of the intermediate plexus of the retinal vasculature may be regulated by a correct HIF1A protein stabilization profile in cells other than Müller cells. Retinal neurons such as RGCs, horizontal and photoreceptor cells are unlikely to be involved in the process since their location in the retina is not in proximity of the intermediate plexus. In this view, possible candidates are bipolar and amacrine cells. Bipolar cells do not express *Cre* in the *Hif1a*$^{flox/flox}$*;α-Cre* retina, and may thus not be directly responsible for the vascular phenotype. On the contrary, *Hif1a* is ablated in amacrine cells in proximity to the site where the intermediate plexus is established. It is thus possible that either diffusible or cell-to-cell contact factors expressed by this cell population are responsible for the development of this vascular plexus. In order to test this hypothesis, the retinal vasculature of conditional knockout mice with deletion of *Hif1a* in amacrine cells should be analyzed. Importantly, only a particular subset of amacrine cells may contribute to retinal

angiogenesis. In fact, in the central retina of *Hif1a*$^{flox/flox}$*;α-Cre* mice, a subset of amacrine cells expresses *Cre* but no vascular phenotype was observed, compared to the retinal periphery. Also, the production of multiple factors produced by a combination of different retinal cell types may regulate the development of the intermediate plexus.

In general, our results establish and support the importance of a correct spatial and temporal expression profile of *Hif1a* for the development of a normal retinal vasculature and especially for the formation of the intermediate plexus. Many events may be involved in the incomplete development of the intermediate plexus resulting from *Hif1a* knockdown in the retinal periphery. These may include a reduced WNT signalling through FZD4 receptor, reduced expression of netrin family members, and/or transient and local changes in the expression of *Vegfa* and *Ang2*. Possible adaptive mechanisms to increase blood flow in the inner retina of *Hif1a*$^{flox/flox}$*;α-Cre* mice may involve vasodilation of arteries. This mechanism may be induced by increased expression of *Adm* driven by reduced oxygenation of the tissue.

Not only HIF1A, but also EPAS1 (HIF2A) was shown to contribute to the process of retinal angiogenesis. In fact, systemic *Epas1 (Hif2a)* knockout mice show significant defects in the development of the retinal vasculature, characterized by a reduced vascular coverage of the peripheral retina, tortuous central vessels, and inhibited regression of the hyaloid artery. Together with these vascular abnormalities, *Epas1 (Hif2a)*-null mice display a strong retinopathy (Ding et al., 2005).

5.5 HIFs as Therapeutic Targets to Inhibit Pathological Retinal Angiogenesis

The use of conditional knockdown strategies to investigate the functions of HIFs in retinal angiogenesis has been accompanied and supported by the analysis of mouse models genetically designed to show a long-lasting stabilization of HIFs under normoxic conditions. These animal models have been particularly useful to elucidate the contribution of HIFs in pathological angiogenesis. A prominent example is represented by the inactivation of the *Vhl* tumour suppressor gene in the autosomal dominant von Hippel-Lindau disease. This results in a constitutive normoxic stabilization of HIFAs, ensuing in a constant expression of pro-angiogenic

growth factors, such as VEGFA, leading to the growth of vascular endothelial tumours (i.e. hemangioblastomas) in the retina and other organs (Chan et al., 2007; Rankin et al., 2005). In a *Vhl* conditional knockdown mouse model, genetically designed to mimic the von Hippel-Lindau disease, a chronic stabilization of HIFA proteins under normoxic conditions was described to occur already in the early post-natal retina (Lange et al., 2010; Kurihara et al., 2010). This persistent hypoxia-like response resulted in a severe retinopathy, glia activation and severely reduced retinal function in the adult mouse. At the vascular level, regression of the hyaloid vasculature was impaired, the density of the retinal vasculature was severely reduced, the capillaries of the deeper plexi did not form, and retinal vessels growing into the photoreceptor layer were observed (Lange et al., 2010). The underlying mechanisms for this aberrant vascular phenotype might rely on the significantly increased ectopic *Vegfa* expression in *Vhl* knockdown mice (Lange et al., 2010; Kurihara et al., 2010). Indeed, the vascular defects in this mouse model could be rescued either by administration of a VEGFA inhibitor, or by a simultaneous ablation of *Hif1a*, but not *Epas1 (Hif2a)* (Kurihara et al., 2010). A supplementary support for a contributory function for HIF1A in proliferative vascular phenotypes as well as developmental angiogenesis comes from observations made in retinas of *Phd2*-null mice. In the retina of these mice, abnormal vessels are formed, characterized by increased arterial branching and mild alterations in the patterning of retinal vessels (Duan et al., 2011).

The biologically relevant implication of HIFs in the induction and regulation of retinal angiogenesis, as well as their contribution in the process of pathological neovascularisation, makes these transcription factors good candidates for pharmacological treatment of proliferative retinopathies. In this prospective, Yoshida *et al.* used a pharmacological approach to reduce HIF1A levels and to study the implications of the transcription factor in retinal neovascularisation. The authors used digoxin, an inhibitor of HIF1-dependent transcriptional activity, and confirmed ensuing reduced levels of HIF1A protein accumulation in the OIR model. As a consequence, a suppression of both retinal and choroidal neovascularisation was observed (Yoshida et al., 2010). Likewise, DeNiro *et al.* reported that YC-1, another inhibitor of HIF1A, decreased accumulation of HIF1A protein in normoxia and inhibited its synthesis, protein stability, and nuclear translocation under hypoxic conditions. Treatment with YC-1 was accompanied by a significant decrease of the expression of HIF1-dependent genes, and a

consequent reduction of retinal vascular density (Deniro et al., 2009). Altogether, our observations and the aforementioned studies confirm that inhibition of HIF1 leads to a reduction of the extent of retinal vascularisation and certify the potential of modulating the *Hif1a* pathway as a therapeutic strategy to inhibit pathological neovascularisation.

5.6 The Viability of the Retina Is Preserved in the Absence of HIF1A

HIF transcription factors are crucial for the adaptation and survival of cells under ischemic / hypoxic conditions (Chapter 1.4). Stabilization of HIF1A in the post-natal retina may be crucial to allow the survival of retinal cells, in particular RPCs, to the period of hypoxia occurring in the post-natal retina (see Chapter 1.3.4). Nakamura-Ishitzu and colleagues demonstrated that at PND 6, HIF1A protein levels are reduced in most RPCs of *Hif1a*$^{flox/flox}$*;α-Cre* mice. In spite of this, the number of RPCs is not diminished, thereby suggesting that the absence of HIF1A does not affect the survival of these cells (Nakamura-Ishizu et al., 2012). We confirmed these observations by analyzing the retina of adult *Hif1a*$^{flox/flox}$*;α-Cre* mice for the presence of developmental defects suggesting for reduced proliferation or increased loss of RPCs. Tissue development, layering, and maturation were not affected despite absence of *Hif1a* in neurons and Müller glia of the peripheral retina of *Hif1a*$^{flox/flox}$*;α-Cre* mice (Fig. 27). The same conclusion can be drawn when *Hif1a* is ablated in Müller cells and astrocytes of *Hif1a*$^{flox/flox}$*;Pdgfra-Cre* mice (Fig. 45). Furthermore, no appreciable signs of tissue degeneration were observed in 1-year old retinas for both *Hif1a* knockdown strains (Fig. 45 and data not shown for *Hif1a*$^{flox/flox}$*;α-Cre* mice). Hence, HIF1A does not appear to be required for the survival of retinal cells in the aging retina. Whether retinal cells not undergoing ablation of *Hif1a* in *Hif1a*$^{flox/flox}$*;α-Cre* mice, in particular in the central retina, would be negatively affected by deletion of the transcription factor is not known. Importantly, also the function of the retina appears not to be significantly impaired by the lack of HIF1A and absence of intermediate capillary plexus in the retinal periphery, even though a minor decrease in the b-wave amplitude was measured (Fig. 37). It is important to remember that ERG measurements give an overall retinal response to flashes of light, with the central retina largely contributing to the recordings. Therefore, due to the peripheral knockdown of our model, conclusive discussions on the effects of *Hif1a* ablation on the ERG are not possible. Nevertheless,

the lack of the intermediate capillary plexus in the retinal periphery, and a possible reduced oxygenation of the inner retina, could explain the minor reduction in b-wave amplitude. Hence, it would be of high interest to obtain measurements of retinal function in the retinal periphery by multi-focal ERG, or alternatively to measure ERG amplitudes in mice lacking HIF1A in the central retina.

In different experimental models, absence of HIFs is shown to increase tissue injury caused by hypoxic/ischemic insults (Baranova et al., 2007; Kojima et al., 2007). Based on these considerations, absence of *Hif1a* in the retina may lead to an increased susceptibility of the tissue to hypoxic stress. We tested this hypothesis by exposing *Hif1a*$^{flox/flox}$*;Pdgfra-Cre* mice to a prolonged period of hypoxia (6 Hrs, 7% O_2) and analyzed the morphology of the retina for the presence of signs of degeneration. Absence of HIF1A in retinal glia did not result in retinal damage upon hypoxic exposure (Fig. 47). This suggests that Müller cells and astrocytes can survive a relatively long period of hypoxia without undergoing cell death. This concept can be partially explained by the specialized energy metabolism of glia cells, which use mainly glycolysis for the generation of ATP, even in the presence of sufficient oxygen (Poitry-Yamate et al., 1995; Pellerin et al., 2007). This results in a low rate of oxygen consumption and may explain why these cells are resistant to hypoxia and even long-lasting anoxia (Winkler et al., 2000). A second conclusion that can be drawn is that knockdown of *Hif1a* in retinal glia does not impair the survival of retinal neurons, an event that could result from a reduced release of HIF1A-induced glia-derived survival factors.

Exposure of *Hif1a*$^{flox/flox}$*;α-Cre* mice to hypoxia could potentially give insights on the contribution of HIF1A for the survival of retinal neurons, since different neuronal populations lack HIF1A in the retina of this mouse model. However, the vascular phenotype described in the retina of *Hif1a* knockdown mice is problematic in the view of such an experimental design. In fact, due to the absence of the retinal intermediate plexus, exposure of *Hif1a*$^{flox/flox}$*;α-Cre* mice to hypoxia may result in tissue damage and this event may be independent from the absence of HIF1A in neurons. This would make any inference on the direct role of HIF1A for resistance to hypoxia relatively complicated. For this reasons, *Hif1a*$^{flox/flox}$*;α-Cre* mice were not used in this experimental paradigm.

Altogether, these observations indicate that retinal cells might be able to sustain retinal

hypoxia even in the absence of HIF1A. Our results are supported by other studies that used the Cre-loxP system to delete *Hif1a* in specific retinal cells. When *Hif1a* is ablated in adult rod photoreceptors (Thiersch et al., 2009) or Müller cells (Lin et al., 2011) no obvious histological and visual functional abnormalities were noticed. This knowledge increases the relevance of HIF1A as target for the treatment of retinal neovascular diseases. Inhibition of HIF1-induced gene expression emerges as an attractive possibility, since the absence of this transcription factor does not show detrimental effects for the retina.

A possible mechanism underlying these observations could involve the presence of other factors that have redundant roles with HIF1A. A candidate would be EPAS1 (HIF2A), which has been repeatedly reported to share many target genes with HIF1A and to significantly contribute to the hypoxic response, in particular under chronic episodes (Chapter 1.4). The possibility that EPAS1 (HIF2A) shares redundant roles with HIF1A in retinal development and supports cell survival in the absence of HIF1A may explain the normal retinal morphology observed in *Hif1a*$^{flox/flox}$*;α-Cre* mice. Indeed, protein levels of EPAS1 (HIF2A) were elevated in *Hif1a*$^{flox/flox}$*;α-Cre* mouse retinas when compared to control littermates (Fig. 38). It is important to note that EPAS1 (HIF2A) seems to be particularly important for development and physiology of the retina, in particular during angiogenesis. Support for this note comes from the observation that *Epas1 (Hif2a)* knockout mice displayed a retinopathy, accompanied by abnormalities in retinal vascular development. Retinopathy eventually resulted in a marked thinning of the retinal layers, in particular, a reduction of the photoreceptor layer. This was accompanied by loss of vision by one month of age (Ding et al., 2005; Scortegagna et al., 2003a). Since neuronal and vascular development in the retina is tightly interconnected and interdependent, it is hard to discriminate the precise contribution of EPAS1 (HIF2A) to each of these processes. In other words, the vascular phenotype in *Epas1 (Hif2a)*-null mice may be a direct result of altered vascular development (Gariano and Gardner, 2005) or may be an indirect outcome of photoreceptor loss, eventually reducing retinal oxygen consumption, and thus leading to relatively increased oxygen tension in the developing tissue. Such a relative increased oxygenation may reduce or abrogate the hypoxic stimulus driving angiogenesis, and may even result in vaso-obliteration (Penn et al., 2000; Lahdenranta et al., 2001; Yu and Cringle, 2005). Yet, the direct contribution of EPAS1 (HIF2A) to retinal angiogenesis is supported by the observation that this protein is stabilized and

accumulates mainly in vascular endothelial cells in the post-natal retina (Kurihara et al., 2010). In conclusion, inhibition of HIF-induced production of angiogenic factors is an attractive alternative to specifically targeting VEGFA for the treatment of retinal neovascular diseases. However, caution should be taken when deciding which HIFA isoform to target, as absence of EPAS1 (HIF2A) seems to be more detrimental than HIF1A for retinal tissue survival.

5.7 Double Knockdown of *Hif1a* and *EpoR* in the Peripheral Retina Does not Lead to Retinal Degeneration

EPO is a candidate factor that may contribute to the survival of retinal neurons in *Hif1a* knockdown retinas. In fact, this cytokine has shown to exert many protective effects in the retina on both neuronal and vascular cell types (Chapter 1.6). The increased expression of *Epo* in the retina of *Hif1a*$^{flox/flox}$*;α-Cre* mice could be induced by the accumulation of EPAS1 (HIF2A) upon *Hif1a* ablation (Fig. 38). Indeed, EPAS1 (HIF2A) has been reported to be the main HIF isoform driving expression of *Epo* in the brain and retina (Morita et al., 2003; Yeo et al., 2008). Lack of the development of the intermediate plexus may have led to reduced oxygen tension in the retina and thus to the stabilization of EPAS1 (HIF2A). EPO could therefore be a mediator of the retinal response to improper vascularisation and the consequent altered delivery of oxygen.

To test whether EPO acts as an endogenous pro-survival agent in the retina of *Hif1a*$^{flox/flox}$*;α-Cre* mice, we generated *Hif1a*$^{flox/flox}$*;EpoR*$^{flox/flox}$*; α-Cre* mice and analyzed for the presence of any sign of degeneration, in particular in the senescent retina. In the retina of these mice, *EpoR* is ablated in the same cell populations that lack HIF1A, i.e. photoreceptors, Müller glia, and a subset of horizontal, amacrine and ganglion cells of the retinal periphery. The investigation on the neuroprotective effects of EPO is thus restricted to the aforementioned cell populations, and implies that the cytokine provides its neuroprotective effects through EPOR signalling. At 6 months of age, *Hif1a*$^{flox/flox}$*;EpoR*$^{flox/flox}$*;α-Cre* mice expressed significantly reduced retinal *Hif1a* and *EpoR* mRNA levels when compared to control animals, thus validating the knockdown strategy (Fig. 39). *Hif1a*$^{flox/flox}$*;EpoR*$^{flox/flox}$*;α-Cre* mouse retina showed increased expression of *Epo* (Fig. 39), and presented the same vascular phenotype in the retinal periphery

as described for *Hif1a*$^{flox/flox}$*;α-Cre* mice (Fig. 44). However, regardless of a persistent upregulation of *Epo* and concomitant ablation of *EpoR*, the retinas of *Hif1a*$^{flox/flox}$*;EpoR*$^{flox/flox}$*;α-Cre* mice did not show signs of degeneration even in the aging retina (Fig. 40, 41). The possibility that other receptors, e.g. βCR, may be involved in mediating EPO neuroprotective effects is still unclear. Despite the absence of obvious signs of neuropathy, the expression of *Gfap* was increased by astrocytes in the *Hif1a*$^{flox/flox}$*;EpoR*$^{flox/flox}$*;α-Cre* retina (Fig. 42). Furthermore, the morphology of the stellate glia showed a reduction in astroglial protrusions (Fig. 43). This phenotype is reminiscent of the hypoplastic astroglial network described by Nakamura-Ishizu *et al* in the *Hif1a*$^{flox/flox}$*;α-Cre* mouse retina and may thus not be due to the *EpoR* knockdown (Nakamura-Ishizu et al., 2012).

In conclusion, it appears that the increased mRNA expression of *Epo* measured upon ablation of *Hif1a* in the retinal periphery is most probably not responsible for providing long-standing neuroprotection, at least not by the activation of EPOR downstream signalling pathways.

5.8 *Epo*, *EpoR*, and *Csf2rb (βCR)* Are Expressed in The Retina

Epo has been previously described to be endogenously expressed in the retina (Grimm et al., 2002). *Epo* may be expressed by Müller cells (Fu et al., 2008) and/or cells found in the GCL (Scheerer et al., 2010). Data obtained from mice lacking *Hif1a* or V*hl* in rod photoreceptors indirectly support such a conclusion, and rule out photoreceptors as main source of EPO secretion (Thiersch et al., 2009; Lange et al., 2011b). The expression profile of *Epo* in the post-natal mouse retina shows a modest increase of expression at around two weeks after birth (Fig. 48). Since *Epo* is induced by HIFs (Fandrey, 2004), the hypoxic episode occurring in the post-natal mouse retina may explain this observation (Chapter 1.3.4). The extent of *Epo* induction at PND 15 (2.5 fold) is not comparable to the increase in expression when animals are exposed to hypoxia (roughly 6-fold for 7% O_2) (compare Fig. 48 and 54). However, the extent of *Epo* induction is proportional to the severity of hypoxia: a strong expression is measured at 10% O_2, intermediate induction was observed at 14% O_2 while *Epo* was not upregulated at 18% O_2

(Grimm et al., 2002). Thus, the mechanism of *Epo* induction in the post-natal mouse retina may be controlled by the presence of a relatively mild hypoxic event in the post-natal retina. It is also important to note that *Epo* transcripts are not present at high levels in the normoxic retina (Chapter 4.9). This conclusion is based on measurement of gene expression by semi-quantitative real-time PCR and suggests that EPO may exert its neuroprotective activities only when its secretion is augmented, e.g. under hypoxic conditions or upon exogenous applications.

EpoR transcripts accumulate at elevated levels in the INL and GCL (Colella et al., 2011). Our data on the expression of *EpoR* in retinal nuclear layers confirm this observation, and most importantly rule out photoreceptors as neurons expressing high levels of *EpoR* (Fig. 50). Based on these considerations, we conclude that the *EpoR* is transcribed predominantly in neurons and presumably Müller cells of the inner retina. The strong increase in expression of *EpoR* measured at PND 10 could be related to retinal hypoxia (Fig. 48). Neural cells lacking *EpoR* showed increased sensitivity to hypoxia *in vitro* (Chen et al., 2007). Similarly, retinal cells may induce *EpoR* transcription to survive the period of hypoxia occurring in the post-natal retina. Numerous studies suggest that EPOR protein expression can be induced by hypoxia or ischemia, as has been demonstrated for example in the ischemic brain (Li et al., 2007), carotid bodies (Lam et al., 2009), HMVEC-L cells (Beleslin-Cokic et al., 2011), or in the retina (Junk et al., 2002). But, it is important to mention that most of the aforementioned studies investigate EPOR protein levels but did not analyze expression at the transcriptional level, which may differ and not show the same degree of upregulation. The commercially available anti-EPOR antibodies have been suggested to give unreliable results (Elliott et al., 2006; Kirkeby et al., 2007), and therefore caution should be taken when interpreting these studies. Our observations suggest that exposure of mice to hypoxia does not cause increased expression of *EpoR* (Fig. 49). Alternatively, the strong induction of *EpoR* expression in the post-natal retina could rely on an upregulation of *EpoR* expression in specific retinal cells upon differentiation of RPCs. Chen and co-workers reported that neural progenitors express higher levels of EPOR than mature neurons (Chen et al., 2007). However, this may not be the case for the retina, where RPCs may express low levels of EPOR. Bipolar and Müller cells are among the last retinal cell populations to differentiate during post-natal development (Levine and Green, 2004). Increased levels of *EpoR* transcripts are found in the INL of the adult mouse retina (Colella et al., 2011), the nuclear layer where somata of

Müller and bipolar cells are found. These evidences suggest that the increase in *EpoR* expression could be related to the generation of Müller glia and/or bipolar cells. But, elevated levels of *EpoR* transcripts have been found also in RGCs (Colella et al., 2011), and these retinal neurons differentiate early during embryogenesis (Levine and Green, 2004). Hence, additional mechanisms beside hypoxia or cell differentiation may induce *EpoR* expression in the retina.

Expression of *Csf2rb (βCR)* has been previously described in the mouse retina, in particular in the INL and GCL (Colella et al., 2011). We also detected expression of the cytokine co-receptor in the post-natal mouse retina. In contrast to *EpoR*, the profile of *Csf2rb (βCR)* expression did not show particular trends during development or in the adult retina (Fig. 48). The proposed role for EPOR/βCR heterodimers in mediating tissue protective effects of EPO implies that both heteroreceptor subunits are expressed in the same cell population (Brines et al., 2004). The observations made by Colella *et al* about the localization of *EpoR* and *Csf2rb* transcripts in the INL and GCL support this hypothesis (Colella et al., 2011).

5.9 Absence of *EpoR* Does not Affect Retinal Development, Function and Tissue Survival

To examine the function of endogenous EPO in the retina, I generated and analyzed *Epo* conditional knockdown mice (data not presented). Knockdown of *Epo* in the retinal periphery, rod photoreceptors, and retinal glia was carried out by generating $Epo^{flox/flox}$*;α-Cre,* $Epo^{flox/flox}$*;Opn-Cre,* and $Epo^{flox/flox}$*;Pdgfra-Cre* mice, respectively. However, analysis of gene expression in these mice showed elevated basal expression levels of *Epo* in $Epo^{flox/flox}$ mice as compared to BL6/JFue and 129S6 wild-type mice (data not shown). These results, together with data obtained by Zeigler *et al*, suggest that regulation of *Epo* expression in $Epo^{flox/flox}$ mice is compromised, most probably due to insertion of *loxP* sites in the *Epo* locus (Zeigler et al., 2010).

Based on these observations, we decided to terminate the analysis of *Epo* knockdown mice, and concentrated on the examination of *EpoR* knockdown mice. To investigate the roles of *EpoR* in the retina during post-natal development and in the adult tissue, we ablated *EpoR* either

in rod photoreceptors *(EpoR$^{flox/flox}$;Opn-Cre),* or in a heterogeneous population of cells in the retinal periphery *(EpoR$^{flox/flox}$;α-Cre)*.

Knockdown in the retinal periphery showed a significant decrease of *EpoR* mRNA levels, confirming the validity of the knockdown strategy (Fig. 49B2). On the other hand, *EpoR* expression in the total retina of *EpoR$^{flox/flox}$;Opn-Cre* mice was not measurably decreased as we expected (Fig. 49A2). Nonetheless, *EpoR* transcripts were reduced in the ONL of *EpoR$^{flox/flox}$;Opn-Cre* mice, even though the knockdown did not reach statistical significance. Importantly, the comparison of *EpoR* mRNA levels in retinal layers revealed that this gene in expressed at very low levels in the ONL when compared to the INL and GCL (Fig. 50). It is thus not surprising that a decrease in *EpoR* expression in photoreceptors is hardly detectable when expression is measured in total retinal extracts. In addition, detection of the knockdown of *EpoR* is complicated by the transcription of *Cre* only in a fraction of rod photoreceptors in the *Opn-Cre* mouse (Fig. 24).

Chen and co-workers showed that *EpoR*-null mice have less neural progenitor cells. This suggests that endogenous EPO-EPOR signalling supports cell viability in the embryonic brain (Chen et al., 2007). In the *α-Cre* mouse, expression of *Cre* recombinase has been reported to start at embryonic stages (Marquardt et al., 2001), and therefore ablation of *EpoR* is expected to occur in RPCs. Unexpectedly, no morphological or functional defect was observed that could hint towards increased apoptosis of progenitor cells in the retina of *EpoR$^{flox/flox}$;α-Cre* mice (Fig. 51, 53). A detailed analysis of apoptotic cells in the embryonic and post-natal retina of *EpoR$^{flox/flox}$;α-Cre* mice would give more insights on this issue. These observations altogether strongly hint towards the absence of a crucial role for endogenous EPO-EPOR signalling in the mouse embryonic retina. In a similar manner, the absence of any developmental and functional consequences of *EpoR* knockdown in rod photoreceptors (Fig. 51, 53) could be explained by the low levels of expression of *EpoR* in the ONL. This insinuates that this protein does not have fundamental direct roles for photoreceptor physiology and survival. This is confirmed by the integrity of the retinal tissue in aging mice, which do not show signs of photoreceptor degeneration in the senescent retina (Fig. 51).

5.10 Increased EPOR Signalling May Be Present in the Retina of *EpoR$^{flox/flox}$;α-Cre* Mice

Beside the membrane-bound isoform, we also detected expression of *sEpoR,* as has been previously reported for the brain (Soliz et al., 2007) (Fig. 49). Based on a study published by Soliz *et al*, the soluble isoform of EPOR is thought to act as a negative regulator of EPO signalling. The soluble isoform consists of the extracellular domain and binds EPO, thereby sequestering the cytokine, preventing it from binding to the membrane-bound EPOR, and thus from activating intracellular signalling cascades (Soliz et al., 2007; Khankin et al., 2010). It is well established that soluble receptors frequently modulate cytokine signalling by stabilizing the cytokine, changing its concentrations, or modifying its interaction with the membrane bound receptor (Maynard et al., 2003; Venkatesha et al., 2006). For example, intravitreal injection of sEPOR in a rat model of retinal detachment led to increased photoreceptor apoptosis (Chen et al., 2012), and co-application of EPO and sEPOR blocked the protective effects of EPO in an *in vitro* model of cerebral ischemia (Ruscher et al., 2002). The soluble form of EPOR could have a similar function in the retina and abrogate EPO-EPOR signalling by sequestering endogenous EPO. As a consequence, EPO-EPOR signalling in the retina may only occur under conditions where EPO protein levels are elevated, such as under hypoxia or upon exogenous applications. Intriguingly, the expression of *sEpoR* is reduced in hypoxia (Soliz et al., 2007; Brugniaux et al., 2011), thus allowing an advanced modulation of the EPO response under these conditions.

Which *EpoR* splice variant does each retinal cell population express? Ablation of *EpoR* in the retinal periphery caused a strong and significant decrease in *sEpoR* transcript levels (Fig. 49B3), relatively stronger than the reduction in *mEpoR* expression (Fig. 49B3). Based on this observation, we can deduce that the cellular subpopulation that is CRE-positive in the *EpoR$^{flox/flox}$;α-Cre* retina is expressing elevated levels of *sEpoR* expression under normal (CRE-negative) conditions. Unfortunately, it is hard to make any assumption about the identity of the retinal cell types that express *sEpoR*, due to the heterogeneous population of cells undergoing CRE-mediated recombination in the *α-Cre* mouse retina. Nevertheless, based on the unaltered expression of *sEpoR* in the retina of *EpoR$^{flox/flox}$;Opn-Cre* mice, we suggest that rod photoreceptors do not participate in the secretion of sEPOR (Fig. 49A3).

Cells not affected by *EpoR* ablation (cells that do not express *Cre*) could show increased EPO-EPOR signalling due to decreased expression of the *sEpoR* in the *EpoR$^{flox/flox}$;α-Cre* mouse retina. In fact, a diminished secretion of sEPOR would result in reduced sequestration of EPO, thus allowing augmented binding to the membrane-bound EPOR. On the other hand, reduced EPO-EPOR signalling would be expected for retinal cells affected by *EpoR* ablation (cells that do express *Cre*), in particular when the transcription of an EPOR-signalling target gene expressed by these cells is analyzed. This hypothesis is highly speculative and needs additional support by experimental data. Nevertheless, it could partially explain some of the results obtained by gene expression analysis (see below).

In order to gain knowledge on the signalling pathways activated or deactivated in the absence of EPOR, as well as the resulting changes in gene expression, we exposed *EpoR* knockdown mice to hypoxia and isolated retinas immediately after the hypoxic exposure for analysis. This experimental procedure results in an increased expression of *Epo* in the retina (Fig. 54), and is thus expected to show activation of EPO-EPOR signalling. Different intracellular pathways are modulated by EPO-EPOR signalling in neuronal cells. These include phosphorylation of JAK2/STAT3/5 (Kretz et al., 2005; Zhang et al., 2007), activation of the PI3K/AKT pathway (Siren et al., 2001a; Digicaylioglu et al., 2004), phosphorylation of MAPKs such as ERK1/2 (Kilic et al., 2005a), and NFκB nuclear translocation (Digicaylioglu and Lipton, 2001). In *EpoR* knockdown retinas we detected only minor changes in the phosphorylation or expression of protein members of the aforementioned signalling pathways. Ablation of *EpoR* in rod photoreceptors, or in the peripheral retina, resulted in a minor increase in phosphorylation of STAT3 in hypoxia, even though this was not statistically significant. In addition, decreased AKT protein levels were measured under hypoxic conditions upon ablation of *EpoR* in the retinal periphery (Fig. 57). The absence of major modifications in intracellular signalling under hypoxic conditions in *EpoR* knockdown retinas is surprising. Exposure of mice to hypoxia was expected to increase EPO-EPOR signalling due to the increased secretion of the cytokine. A possible explanation for the absence of major effects could rely on the timing chosen for tissue isolation after the hypoxic exposure (immediate, without reoxygenation). In order to observe significant changes in intracellular signalling, a longer interval of reoxygenation could be required.

The gene expression profile in *EpoR* knockdown mice gave unexpected and contradictory

results. In the retina of *EpoR$^{flox/flox}$;Opn-Cre* mice exposed to hypoxia, *Vegfa, Nos2(iNos),* and *Mt2* were differentially regulated when compared to controls. However, *EpoR* expression is relatively low in the ONL and the knockdown did not reach statistical significance in the ONL of *EpoR$^{flox/flox}$;Opn-Cre* mice. This suggests that rod photoreceptors may not require EPO-EPOR signalling for their physiology and function. Considering that no morphological defects were observed, the relatively minor chnges in the expression of *Vegfa, Nos2(iNos),* and *Mt2* may not be biologically relevant. Similarly, the changes in gene / protein in the retina of *EpoR$^{flox/flox}$;α-Cre* mice did not show elevated alterations when compared to control littermates. However, it is interesting to note that for those genes that were expected to show decreased expression in the absence of EPOR, an increase in expression was measured, and the opposite was true for those genes that were expected to be upregulated in *EpoR$^{flox/flox}$;α-Cre* mice. Modulation of EPOR downstream signalling has been shown to alter the expression of a plethora of genes, that may eventually contribute to the effects of EPO for cell survival (Chateauvieux et al., 2011; Singh et al., 2012). For example, intracellular signalling events elicited by EPOR activation also include the upregulation of anti-apoptotic proteins such as BCL2L1(BCL-X_L) (Wen et al., 2002; Renzi et al., 2002) and BCL2 (Yamasaki et al., 2005), together with the downregulation of pro-apoptotic proteins such as CASP1 (Grimm et al., 2002). We did not detect changes in the expression of *Bcl2* and *Bcl2l1(Bcl$_{XL}$)* in the retina of *EpoR* knockdown mice (Fig. 55). Ablation of *EpoR* in the peripheral retina led to a reduced *Casp1* expression under hypoxic conditions (Fig. 55B). The reduced expression of *Casp1* could be related to a reduced secretion of sEPOR and the resulting increase in "free" EPO in the retinal milieu. This event would result in increased EPO-EPOR signalling in cells not affected by *EpoR* ablation, for example cells in the central retina of *EpoR$^{flox/flox}$;α-Cre* mice. Assembly of the APAF1 oligomer known as "apoptosome", a caspase-activating complex, is the central point in the mitochondrial pathway of apoptosis. Mitochondrial release of cytochrome c is a key mechanism in the apoptotic cascade that can result in activation of caspases (Reubold and Eschenburg, 2012). Formation of the apoptosome is driven by binding of cytochrome c to APAF1 in the presence of ATP (Cain et al., 2002). EPO has shown to prevent apoptosis by reducing the expression of *Apaf1* (Chong et al., 2003a; Shang et al., 2011a). We expected to observe increased expression of *Apaf1* as a consequence of knockdown of *EpoR*. In spite of this, ablation of *EpoR* in the retinal periphery resulted in a decrease in expression of

Apaf1 (Fig. 55B). As in the case of *Casp1* (se above), the decreased expression of *Apaf1* might be explained by increased EPO-EPOR signalling in cells of the central retina of *EpoR$^{flox/flox}$;α-Cre* mice due to reduced *sEpoR* expression and, probably, secretion. The tissue protective effects of EPO are also related to the production of neurotrophic factors, such as BDNF. This neurotrophic factor is induced by treatments with rhEPO (Viviani et al., 2005). We observed increased expression of *Bdnf* in the retina of *EpoR$^{flox/flox}$;α-Cre* mice kept under hypoxic conditions (Fig. 55B). Müller cells and RGCs have been identified as source of *Bdnf* expression under different experimental conditions (Perez and Caminos, 1995; Vecino et al., 1998; Seki et al., 2005; Hu et al., 2011). Based on our data, we suggest that Müller cells or RGCs in the central retina of *EpoR$^{flox/flox}$;α-Cre* mice may express higher levels of *Bdnf* due to increased EPO-EPOR signalling. Retinal stress and/or injury induce a gliotic response that is characterized by increased expression of *Gfap* in activated Müller cells (Bringmann and Wiedemann, 2011). Exogenous applications of rhEPO have the ability to lessen the gliotic response, an effect that has been demonstrated by reduced *Gfap* expression and immunoreactivity of Müller cells in various disease models (Hu et al., 2011). We detected a reduction in *Gfap* gene and protein expression in the retina of *EpoR$^{flox/flox}$;α-Cre* mice (Fig. 56B, 57B), a result that is in line with the aforementioned observations that suggest for the presence of augmented EPO-EPOR signalling in these mice.

Taken together, the data obtained from the analysis of gene / protein expression in the retina of *EpoR$^{flox/flox}$;α-Cre* mice are controversial and need further investigation. Different factors may explain these observations. The strong reduction in expression (and presumably secretion) of *sEpoR* in the peripheral retina of *EpoR$^{flox/flox}$;α-Cre* mice may result in an increased availability of "free" EPO. This may eventually lead to increased EPO-EPOR signalling under hypoxic conditions in the peripheral and especially central retina of *EpoR$^{flox/flox}$;α-Cre* mice. An additional component could rely on the identity of the cell populations affected by *EpoR* knockdown. Signs of increased EPO-EPOR signalling may be measured in cells where *Cre* is not expressed (and EPOR is present). This phenomenon is revealed when the analysis of expression is performed for a particular gene or protein of interest that is expressed in these retinal cells. For example, the unexpected increase in expression of *Casp1*, *Apaf1*, and *Bdnf* in the retina of *EpoR$^{flox/flox}$;α-Cre* mice may be a result of increased availability of EPO in the central retina due to reduced secretion of sEPOR. On the other side, retinal cell populations undergoing CRE-mediated ablation

of *EpoR* would show a reduction in EPO-EPOR signalling, independently of the concentration of sEPOR in the retinal milieu. Nevertheless, further investigation is required to deeply study the influences of reduced *sEpoR* expression in the retina of *EpoR$^{flox/flox}$;α-Cre* mice. For example, sEPOR protein levels should be measured to confirm the downregulation of *sEpoR* transcripts. Also, intravitreal injections of sEPOR, in concomitance with rhEPO or under hypoxic conditions, could give more insights on EPO-EPOR signalling in the retina.

In conclusion, it is relatively difficult to make any inference about EPO-EPOR signalling in the retina based on data obtained from the *EpoR* knockdown lines described in this study. Analysis of gene and protein expression in mice with an efficient knockdown of *EpoR* in a single retinal cell type would be of great interest. Alternatively, the consequences of the absence of EPOR in the retina could be studied in EPOR-null mice rescued with selective *EpoR* expression driven by the endogenous *EpoR* promoter in hematopoietic tissue, but not in the neural cells (Chen et al., 2007).

5.11 Lack of *EpoR* in Retinal Glia and Neurons Does not Affect Retinal Angiogenesis

The angiogenic potential of EPO in different tissues has been revealed over the past years. Targeted deletion of *Epo* or *EpoR* in mice severely affected angiogenesis and resulted in a reduced complexity of the vessel networks, a phenotype characterized by narrower vessel diameter and reduced vascular branching (Kertesz et al., 2004). The angiogenic activity of EPO during development may be related to the stimulation of endothelial progenitor cell mobilisation or proliferation (Ribatti et al., 1999). Expression of *EpoR* has been detected in various types of vascular endothelial cells (Anagnostou et al., 1990b). It is therefore assumed that the angiogenic activities of EPO are directly mediated through binding on EPOR expressed on the surface of vascular endothelial cells. In the *α-Cre* mouse, *Cre* recombinase is not expressed in vascular endothelial cells (Chapter 5.1). As a consequence, it is not surprising that the retinal vasculature does not show any sign of developmental defect in *EpoR$^{flox/flox}$;α-Cre* mice. In this mouse model, the retinal capillary plexi did develop correctly, blood perfusion appeared as normal, and no

sings of leakage were observed (Fig. 58, 59). It would be of great interest to specifically ablate *EpoR* in vascular cells and analyze the retinal vasculature under these conditions.

We did not expect to observe an effect on post-natal retinal angiogenesis in *EpoR$^{flox/flox}$;Opn-Cre* mouse retinas, since in this model the ablation of *EpoR* is not considered to be efficient up to 10 weeks of age (Chapter 5.1). Therefore, *EpoR$^{flox/flox}$;Opn-Cre* retinas could be considered as additional control animals. Indeed, a correctly developed and fully functional vasculature was observed in these mice (Fig. 58, 59).

5.12 *EpoR$^{flox/flox}$;Opn-Cre* Mice Are Not Susceptible to Light-induced Retinal Degeneration

EPO has been implicated as modulator of the protective effects mediated by hypoxic preconditioning (Grimm et al., 2002). Applications of rhEPO partially mimicked neuroprotection obtained with the preconditioning protocol (Grimm et al., 2002). Also, other studies reported on the beneficial effects of rhEPO on the survival of stressed photoreceptors (Grimm et al., 2004; Rex et al., 2004, 2009). An important question that has not yet been answered asks for the nature of the intra- and intercellular signalling events elicited by this cytokine in the retina that result in neuroprotection. Are the survival effects of EPO mediated by signalling through binding to the EPOR expressed by the protected cell? Does the effect involve additional cells types stimulated by EPO to secrete additional factors that ultimately provide the protective effects and/or the modulation of the tissue milieu? To answer the first question, we tested for the presence of neuroprotection upon rhEPO administrations by exposing *EpoR$^{flox/flox}$;Opn-Cre* mice to cytotoxic levels of light to induce photoreceptor apoptosis. If expression of *EpoR* by photoreceptors would be a prerequisite for neuroprotection, absence of the receptor would aggravate the damage. However, we found a constitutive protection against photoreceptor apoptosis in *EpoR$^{flox/flox}$;Opn-Cre* mice, irrespective of the treatment preceding light exposure (Fig. 60A). This phenomenon is difficult to explain, as it does not seem plausible that the absence of *EpoR* in rods could result in a direct protective effect. It seems more likely that the constitutive resistance to light damage could

result from an indirect effect of the knockdown or it may be possible that factors associated with the genetic background of *Opn-Cre* mice may lead to insensitivity against light damage.

In the recent past, different studies have suggested that the cytoprotective effects of EPO may be mediated through a receptor complex that is pharmacologically different from the classical hematopoietic EPOR homodimer (Leist et al., 2004). Brines and colleagues suggested that a heteroreceptor complex formed by EPOR and βCR mediates these protective effects (Brines et al., 2004). In this sense, the importance of the activation of βCR has been demonstrated by the absence of EPO-mediated protective effects in βCR-knockout mice in different experimental models (Brines et al., 2004; Coldewey et al., 2013). Increased activation of βCR may result in augmented production of NO, a molecule that has demonstrated its involvement in tissue protection (Chen et al., 2010b). For this reason it would be important to investigate the activation of βCR in the retina of *EpoR$^{flox/flox}$;Opn-Cre* mice.

The contribution of retinal cells other than photoreceptors could be crucial for the protective mechanisms induced by EPO. The low expression of *EpoR* in the ONL compared to the relatively higher expression in the inner retina (Fig. 50) points towards an involvement of paracrine mechanisms for protection of photoreceptors. Other retinal cells, such as Müller cells, may be stimulated by EPO and release cell supportive factors to reduce photoreceptor apoptosis. To investigate this possibility, we exposed *EpoR$^{flox/flox}$;α-Cre* mice to light and tested for the ability of EPO to mediate neuroprotective effects. Unfortunately, we obtained variable results in the extent of photoreceptor degeneration in *EpoR$^{flox/flox}$;α-Cre* mice. This variability was not linked to the experimental treatment. In addition, the absence of CRE recombination in the central retina of *EpoR$^{flox/flox}$;α-Cre* mice poses some questions on the validity of these mice in the light-damage setup. In fact, light exposure has damaging effects predominantly in the central (ventral) retina. This area is not expected to present a knockdown of *EpoR* in *EpoR$^{flox/flox}$;α-Cre* mice. Hence, it is difficult to draw conclusions on such experiments. As alternative, retinal degeneration could be induced by other experimental setups, such as MNU injections or ischemia-reperfusion.

In conclusion, based on the data obtained from light exposure of *EpoR* knockdown mice does not allow to make assumptions on the contribution of EPO-EPOR signalling for neuroprotection upon injections of rhEPO. Whether the insensitivity of *EpoR$^{flox/flox}$;Opn-Cre* mice to light-induced photoreceptor apoptosis is a direct or indirect effect of *EpoR* knockdown is

difficult to conclude based on our data. In spite of this, the lower expression of *EpoR* in the ONL compared to the inner retina (Fig. 50) hints towards an action of EPO on retinal cells other than photoreceptors. In this sense, activation of EPOR on Müller cells may ameliorate the tissue milieu and provide neuroprotection of photoreceptors by a paracrine mechanism (Hu et al., 2011; Lei et al., 2011). To verify this hypothesis, a mouse strain with a specific deletion of *EpoR* in Müller cells should be tested for light-induced photoreceptor apoptosis in the presence or absence of rhEPO injections. This would give more insights on a putative paracrine nature of the tissue-protective effects mediated by EPO, and allow to investigate the identity of the factors released by Müller cells that eventually support photoreceptor viability.

6 Concluding Remarks and Outlook

In this thesis, I aimed to unravel/determine the contribution of HIF1A in the response to hypoxic episodes occurring in the retina. Since the mouse retina is avascular at the time when retinal activity begins and oxygen consumption increases (Fruttiger, 2007), hypoxic areas may develop during post-natal maturation of the retina (Chan-Ling et al., 1995). The accumulation of HIF1A in the post-natal mouse retina was an important hint towards a central role for this transcription factor in counteracting tissue hypoxia in this period (Grimm et al., 2005). I show that HIF1A is required for the development of the retinal vasculature. In the absence of HIF1A, retinal angiogenesis is incomplete, as the intermediate plexus does not develop correctly. The link between hypoxia, HIF1A, and angiogenesis has been long recognized in many tissues (Fraisl et al., 2009). In the retina, a role for HIF1A in developmental angiogenesis was not clearly established, while more effort was put on the elucidation of the contribution of this transcription factor to pathological neovascularisation (Caprara and Grimm, 2012). Our results also suggest that initiation of the angiogenic process does not require HIF1A, while the completion of the process may require this transcription factor. Factors such as EPAS1 (HIF2A) share redundant roles with HIF1A and may be more important in the initiation of retinal angiogenesis. Based on our observations, absence of HIF1A is well tolerated by the majority of neuronal and glial cells of the retina. Here again, EPAS1 (HIF2A) may compensate for the absence of HIF1A by sharing redundant roles on the hypoxic response.

These observations are highly attractive in the perspective of targeting HIF1A for the clinical treatment of retinal neovascular diseases. In fact, inhibition of HIF1A-induced gene expression appears to affect angiogenesis without influencing cell survival. Nevertheless, many questions need to be answered. For example, which factors regulate the development of the intermediate plexus? How is retinal angiogenesis initiated in the absence of HIF1A? Is the survival of retinal cells affected by concomitant ablation of *Hif1a* and *Epas1 (Hif2a)*?

EPO is a tissue-protective cytokine endogenously secreted by retinal cells into the tissue milieu (Grimm et al., 2002). Another aim of this thesis was to investigate EPO-EPOR signalling in the retina, as well as decipher its roles in development and physiology of the tissue. Our results

strongly suggest that EPOR downstream signalling is dispensable for a correct maturation and survival of the retina. Rod photoreceptor express low levels of *EpoR*, in contrast to the higher expression in cells of the inner retina. Also, we demonstrate the expression of the *sEpoR* splice variant in the retina. The analysis of *EpoR* knockdown mice hints towards a possible role of sEPOR in counteracting endogenous EPO-EPOR signalling in the retina. This issue needs further investigation, in particular to identify retinal cells responsible for the secretion of sEPOR.

7 References

Abdel-Mageed, A.B., Zhao, F., Rider, B.J., Agrawal, K.C. 2003. Erythropoietin-induced metallothionein gene expression: role in proliferation of K562 cells. Exp Biol Med (Maywood) 228, 1033-1039

Adamis, A.P., Shima, D.T., Yeo, K.T., Yeo, T.K., Brown, L.F., Berse, B., D'Amore, P.A., Folkman, J. 1993. Synthesis and secretion of vascular permeability factor/vascular endothelial growth factor by human retinal pigment epithelial cells. Biochem Biophys Res Commun 193, 631-638

Adams, M.K., Simpson, J.A., Aung, K.Z., Makeyeva, G.A., Giles, G.G., English, D.R., Hopper, J., Guymer, R.H., Baird, P.N., Robman, L.D. 2011. Abdominal Obesity and Age-related Macular Degeneration. Am J Epidemiol 173, 1246-1255

Ahmed, J., Braun, R.D., Dunn, R.J., Linsenmeier, R.A. 1993. Oxygen distribution in the macaque retina. Invest Ophthalmol Vis Sci 34, 516-521

Aiello, L.P., Avery, R.L., Arrigg, P.G., Keyt, B.A., Jampel, H.D., Shah, S.T., Pasquale, L.R., Thieme, H., Iwamoto, M.A., Park, J.E., et, a. 1994. Vascular endothelial growth factor in ocular fluid of patients with diabetic retinopathy and other retinal disorders. N Engl J Med 331, 1480-1487

Aiello, L.P., Northrup, J.M., Keyt, B.A., Takagi, H., Iwamoto, M.A. 1995. Hypoxic regulation of vascular endothelial growth factor in retinal cells. Arch Ophthalmol 113, 1538-1544

Aitola, M.H., Pelto-Huikko, M.T. 2003. Expression of Arnt and Arnt2 mRNA in developing murine tissues. J Histochem Cytochem 51, 41-54

Alder, V.A., Cringle, S.J., Constable, I.J. 1983. The retinal oxygen profile in cats. Invest Ophthalmol Vis Sci 24, 30-36

Ames, A.r. 1992. Energy requirements of CNS cells as related to their function and to their vulnerability to ischemia: a commentary based on studies on retina. Can J Physiol Pharmacol 70 Suppl, S158-64

Ames, A.r., Li, Y.Y., Heher, E.C., Kimble, C.R. 1992. Energy metabolism of rabbit retina as related to function: high cost of Na+ transport. J Neurosci 12, 840-853

Anagnostou, A., Lee, E.S., Kessimian, N., Levinson, R., Steiner, M. 1990a. Erythropoietin has a mitogenic and positive chemotactic effect on endothelial cells. Proc Natl Acad Sci U S A 87, 5978-5982

Anagnostou, A., Lee, E.S., Kessimian, N., Levinson, R., Steiner, M. 1990b. Erythropoietin has a mitogenic and positive chemotactic effect on endothelial cells. Proceedings of the National Academy of Sciences 87, 5978-5982

Anderson, B.J., Saltzman, H.A. 1964. Retinal oxygen utilization measured by hyperbaric blackout. Arch Ophthalmol 72, 792-795

Anderson, G.R., Posokhova, E., Martemyanov, K.A. 2009. The R7 RGS protein family: multi-subunit regulators of neuronal G protein signaling. Cell Biochem Biophys 54, 33-46

Ando, H., Natsume, A., Iwami, K., Ohka, F., Kuchimaru, T., Kizaka-Kondoh, S., Ito, K., Saito, K., Wakabayashi, T. 2013. A hypoxia-inducible factor (HIF)-3α splicing variant, HIF-3α4 impairs angiogenesis in hypervasucular malignant meningiomas with epigenetically silenced HIF-3α4. Biochemical and Biophysical Research Communications

Arany, Z., Huang, L.E., Eckner, R., Bhattacharya, S., Jiang, C., Goldberg, M.A., Bunn, H.F., Livingston, D.M. 1996. An essential role for p300/CBP in the cellular response to hypoxia. Proc Natl Acad Sci U S A 93, 12969-12973

Artemyev, N.O. 2008. Light-dependent compartmentalization of transducin in rod photoreceptors. Mol Neurobiol 37, 44-51

Ashery-Padan, R., Marquardt, T., Zhou, X., Gruss, P. 2000. Pax6 activity in the lens primordium is required for lens formation and for correct placement of a single retina in the eye. Genes Dev 14, 2701-2711

Ashton, N. 1965. Bowman lecture. The blood-retinal barrier and vaso-glial relationships in retinal disease. Trans Ophthalmol Soc U K 85, 199-230

Augstein, A., Poitz, D.M., Braun-Dullaeus, R.C., Strasser, R.H., Schmeisser, A. 2011. Cell-specific and hypoxia-dependent regulation of human HIF-3α: inhibition of the expression of HIF target genes in vascular cells. Cellular and Molecular Life Sciences 68, 2627-2642

Azad, M.B., Chen, Y., Henson, E.S., Cizeau, J., McMillan-Ward, E., Israels, S.J., Gibson, S.B. 2008. Hypoxia induces autophagic cell death in apoptosis-competent cells through a mechanism involving BNIP3. Autophagy 4, 195-204

Badea, T.C., Williams, J., Smallwood, P., Shi, M., Motajo, O., Nathans, J. 2012. Combinatorial expression of Brn3 transcription factors in somatosensory neurons: genetic and morphologic analysis. J Neurosci 32, 995-1007

Baehr, W., Wu, S.M., Bird, A.C., Palczewski, K. 2003. The retinoid cycle and retina disease. Vision Res 43, 2957-2958

Balabanov, R., Dore-Duffy, P. 1998. Role of the CNS microvascular pericyte in the blood-brain barrier. J Neurosci Res 53, 637-644

Balasubramanian, V., Sterling, P. 2009. Receptive fields and functional architecture in the retina. J Physiol 587, 2753-2767

Ban, Y., Rizzolo, L.J. 2000. Regulation of glucose transporters during development of the retinal pigment epithelium. Brain Res Dev Brain Res 121, 89-95

Bandopadhyay, R., Orte, C., Lawrenson, J.G., Reid, A.R., De Silva, S., Allt, G. 2001. Contractile proteins in pericytes at the blood-brain and blood-retinal barriers. J Neurocytol 30, 35-44

Baranova, O., Miranda, L.F., Pichiule, P., Dragatsis, I., Johnson, R.S., Chavez, J.C. 2007. Neuron-specific inactivation of the hypoxia inducible factor 1α increases brain injury in a mouse model of transient focal cerebral ischemia. The Journal of neuroscience 27, 6320-6332

Bardos, J.I., Ashcroft, M. 2005. Negative and positive regulation of HIF-1: a complex network. Biochim Biophys Acta 1755, 107-120

Barron, K.D. 1995. The microglial cell. A historical review. J Neurol Sci 134 Suppl, 57-68

Bay, V., Butt, A.M. 2012. Relationship between glial potassium regulation and axon excitability: a role for glial Kir4.1 channels. Glia 60, 651-660

Baylor, D.A., Lamb, T.D., Yau, K.W. 1979. Responses of retinal rods to single photons. J Physiol 288, 613-634

Bazan, J.F. 1990. Structural design and molecular evolution of a cytokine receptor superfamily. Proc Natl Acad Sci U S A 87, 6934-6938

Beatty, S., Koh, H., Phil, M., Henson, D., Boulton, M. 2000. The role of oxidative stress in the pathogenesis of age-related macular degeneration. Surv Ophthalmol 45, 115-134

Belaiba, R.S., Bonello, S., Zahringer, C., Schmidt, S., Hess, J., Kietzmann, T., Gorlach, A. 2007. Hypoxia up-regulates hypoxia-inducible factor-1alpha transcription by involving phosphatidylinositol 3-kinase and nuclear factor kappaB in pulmonary artery smooth muscle cells. Mol Biol Cell 18, 4691-4697

Beleslin-Cokic, B.B., Cokic, V.P., Wang, L., Piknova, B., Teng, R., Schechter, A.N., Noguchi, C.T. 2011. Erythropoietin and hypoxia increase erythropoietin receptor and nitric oxide levels in lung microvascular endothelial cells. Cytokine 54, 129-135

Benhar, I., London, A., Schwartz, M. 2012. The privileged immunity of immune privileged organs: the case of the eye. Front Immunol 3, 296

Bernaudin, M., Marti, H.H., Roussel, S., Divoux, D., Nouvelot, A., MacKenzie, E.T., Petit, E. 1999. A potential role for erythropoietin in focal permanent cerebral ischemia in mice. J Cereb Blood Flow Metab 19, 643-651

Berntson, A., Taylor, W.R. 2000. Response characteristics and receptive field widths of on-bipolar cells in the mouse retina. The Journal of physiology 524, 879-889

Berson, E.L., Rosner, B., Sandberg, M.A., Hayes, K.C., Nicholson, B.W., Weigel-DiFranco, C., Willett, W. 1993. A randomized trial of vitamin A and vitamin E supplementation for retinitis pigmentosa. Archives of ophthalmology 111, 761-772

Birch, D.G., Anderson, J.L., Fish, G.E. 1999. Yearly rates of rod and cone functional loss in retinitis pigmentosa and cone-rod dystrophy. Ophthalmology 106, 258-268

Blake, T.J., Jenkins, B.J., D'Andrea, R.J., Gonda, T.J. 2002. Functional cross-talk between cytokine receptors revealed by activating mutations in the extracellular domain of the beta-subunit of the GM-CSF receptor. J Leukoc Biol 72, 1246-1255

Bloomfield, S.A., Dacheux, R.F. 2001. Rod vision: pathways and processing in the mammalian retina. Prog Retin Eye Res 20, 351-384

Bocker-Meffert, S., Rosenstiel, P., Rohl, C., Warneke, N., Held-Feindt, J., Sievers, J., Lucius, R. 2002. Erythropoietin and VEGF promote neural outgrowth from retinal explants in postnatal rats. Invest Ophthalmol Vis Sci 43, 2021-2026

Bondurant, M.C., Koury, M.J. 1986. Anemia induces accumulation of erythropoietin mRNA in the kidney and liver. Mol Cell Biol 6, 2731-2733

Bonello, S., Zähringer, C., BelAiba, R.S., Djordjevic, T., Hess, J., Michiels, C., Kietzmann, T., Görlach, A. 2007. Reactive oxygen species activate the HIF-1α promoter via a functional NFκB site. Arteriosclerosis, thrombosis, and vascular biology 27, 755-761

Bonora, M., Patergnani, S., Rimessi, A., De Marchi, E., Suski, J.M., Bononi, A., Giorgi, C., Marchi, S., Missiroli, S., Poletti, F., Wieckowski, M.R., Pinton, P. 2012. ATP synthesis and storage. Purinergic Signal 8, 343-357

Bornancin, F., Pfister, C., Chabre, M. 1989. The transitory complex between photoexcited rhodopsin and transducin. Reciprocal interaction between the retinal site in rhodopsin and the nucleotide site in transducin. Eur J Biochem 184, 687-698

Boulton, M., Dontsov, A., Jarvis-Evans, J., Ostrovsky, M., Svistunenko, D. 1993. Lipofuscin is a photoinducible free radical generator. J Photochem Photobiol B 19, 201-204

Bowes, C., Li, T., Danciger, M., Baxter, L.C., Applebury, M.L., Farber, D.B. 1990. Retinal degeneration in the rd mouse is caused by a defect in the beta subunit of rod cGMP-phosphodiesterase. Nature 347, 677-680

Bracken, C.P., Fedele, A.O., Linke, S., Balrak, W., Lisy, K., Whitelaw, M.L., Peet, D.J. 2006. Cell-specific regulation of hypoxia-inducible factor (HIF)-1alpha and HIF-2alpha stabilization and transactivation in a graded oxygen environment. J Biol Chem 281, 22575-22585

Braekevelt, C.R. 1983. Photoreceptor fine structure in the domestic ferret. Anat Anz 153, 33-44

Bratton, S.B., Salvesen, G.S. 2010. Regulation of the Apaf-1-caspase-9 apoptosome. J Cell Sci 123, 3209-3214

Bressler, N.M., Bressler, S.B., Fine, S.L. 1988. Age-related macular degeneration. Surv Ophthalmol 32, 375-413

Brines, M., Grasso, G., Fiordaliso, F., Sfacteria, A., Ghezzi, P., Fratelli, M., Latini, R., Xie, Q.W., Smart, J., Su-Rick, C.J., Pobre, E., Diaz, D., Gomez, D., Hand, C., Coleman, T., Cerami, A. 2004. Erythropoietin mediates tissue protection through an erythropoietin and common beta-subunit heteroreceptor. Proc Natl Acad Sci U S A 101, 14907-14912

Brines, M.L., Ghezzi, P., Keenan, S., Agnello, D., de Lanerolle, N.C., Cerami, C., Itri, L.M., Cerami, A. 2000. Erythropoietin crosses the blood-brain barrier to protect against experimental brain injury. Proc Natl Acad Sci U S A 97, 10526-10531

Bringmann, A., Faude, F., Reichenbach, A. 1997. Mammalian retinal glial (Muller) cells express large-conductance Ca(2+)-activated K+ channels that are modulated by Mg2+ and pH and activated by protein kinase A. Glia 19, 311-323

Bringmann, A., Pannicke, T., Biedermann, B., Francke, M., Iandiev, I., Grosche, J., Wiedemann, P., Albrecht, J., Reichenbach, A. 2009. Role of retinal glial cells in neurotransmitter uptake and metabolism. Neurochem Int 54, 143-160

Bringmann, A., Pannicke, T., Grosche, J., Francke, M., Wiedemann, P., Skatchkov, S.N., Osborne, N.N., Reichenbach, A. 2006. Muller cells in the healthy and diseased retina. Prog Retin Eye Res 25, 397-424

Bringmann, A., Reichenbach, A., Wiedemann, P. 2004. Pathomechanisms of cystoid macular edema. Ophthalmic Res 36, 241-249

Bringmann, A., Uckermann, O., Pannicke, T., Iandiev, I., Reichenbach, A., Wiedemann, P. 2005. Neuronal versus glial cell swelling in the ischaemic retina. Acta Ophthalmol Scand 83, 528-538

Bringmann, A., Wiedemann, P. 2011. Müller glial cells in retinal disease. Ophthalmologica 227, 1-19

Brown, J.L., Hill, J.H., Burke, R.E. 1957. The effect of hypoxia on the human electroretinogram. Am J Ophthalmol 44, 57-67

Brugniaux, J.V., Pialoux, V., Foster, G.E., Duggan, C.T.C., Eliasziw, M., Hanly, P.J., Poulin, M.J. 2011. Effects of intermittent hypoxia on erythropoietin, soluble erythropoietin receptor and ventilation in humans. European Respiratory Journal 37, 880-887

Burgi, S., Samardzija, M., Grimm, C. 2009. Endogenous leukemia inhibitory factor protects photoreceptor cells against light-induced degeneration. Mol Vis 15, 1631-1637

Burstedt, M.S., Ristoff, E., Larsson, A., Wachtmeister, L. 2009. Rod-cone dystrophy with maculopathy in genetic glutathione synthetase deficiency: a morphologic and electrophysiologic study. Ophthalmology 116, 324-331

Burton, G.J., Jaunaiux, E. 2001. Maternal vascularisation of the human placenta: does the embryo develop in a hypoxic environment? Gynecol Obstet Fertil 29, 503-508

Cai, Z., Manalo, D.J., Wei, G., Rodriguez, E.R., Fox-Talbot, K., Lu, H., Zweier, J.L., Semenza, G.L. 2003. Hearts from rodents exposed to intermittent hypoxia or erythropoietin are protected against ischemia-reperfusion injury. Circulation 108, 79-85

Cain, K., Bratton, S.B., Cohen, G.M. 2002. The Apaf-1 apoptosome: a large caspase-activating complex. Biochimie 84, 203-214

Calderone, J.B., Jacobs, G.H. 1995. Regional variations in the relative sensitivity to UV light in the mouse retina. Vis Neurosci 12, 463-468

Caprara, C., Grimm, C. 2012. From oxygen to erythropoietin: relevance of hypoxia for retinal development, health and disease. Prog Retin Eye Res 31, 89-119

Caprara, C., Thiersch, M., Lange, C., Joly, S., Samardzija, M., Grimm, C. 2011. HIF1A is essential for the development of the intermediate plexus of the retinal vasculature. Invest Ophthalmol Vis Sci

Carter-Dawson, L.D., LaVail, M.M. 1979. Rods and cones in the mouse retina. I. Structural analysis using light and electron microscopy. J Comp Neurol 188, 245-262

Cash, T.P., Pan, Y., Simon, M.C. 2007. Reactive oxygen species and cellular oxygen sensing. Free Radic Biol Med 43, 1219-1225

Caspi, R.R., Roberge, F.G. 1989. Glial cells as suppressor cells: characterization of the inhibitory function. J Autoimmun 2, 709-722

Casson, R.J., Wood, J.P., Melena, J., Chidlow, G., Osborne, N.N. 2003. The effect of ischemic preconditioning on light-induced photoreceptor injury. Invest Ophthalmol Vis Sci 44, 1348-1354

Celik, M., Gokmen, N., Erbayraktar, S., Akhisaroglu, M., Konakc, S., Ulukus, C., Genc, S., Genc, K., Sagiroglu, E., Cerami, A., Brines, M. 2002. Erythropoietin prevents motor neuron apoptosis and neurologic disability in experimental spinal cord ischemic injury. Proc Natl Acad Sci U S A 99, 2258-2263

Chan-Ling, T., Gock, B., Stone, J. 1995. The effect of oxygen on vasoformative cell division. Evidence that 'physiological hypoxia' is the stimulus for normal retinal vasculogenesis. Invest Ophthalmol Vis Sci 36, 1201-1214

Chan, C.C., Collins, A.B., Chew, E.Y. 2007. Molecular pathology of eyes with von Hippel-Lindau (VHL) Disease: a review. Retina 27, 1-7

Chang, B., Hawes, N.L., Pardue, M.T., German, A.M., Hurd, R.E., Davisson, M.T., Nusinowitz, S., Rengarajan, K., Boyd, A.P., Sidney, S.S., Phillips, M.J., Stewart, R.E., Chaudhury, R., Nickerson, J.M., Heckenlively, J.R., Boatright, J.H. 2007. Two mouse retinal degenerations caused by missense mutations in the beta-subunit of rod cGMP phosphodiesterase gene. Vision Res 47, 624-633

Chateauvieux, S., Grigorakaki, C., Morceau, F., Dicato, M., Diederich, M. 2011. Erythropoietin, erythropoiesis and beyond. Biochem Pharmacol

Chavez, J.C., Baranova, O., Lin, J., Pichiule, P. 2006. The transcriptional activator hypoxia inducible factor 2 (HIF-2/EPAS-1) regulates the oxygen-dependent expression of erythropoietin in cortical astrocytes. J Neurosci 26, 9471-9481

Chen, C.K. 2005. The vertebrate phototransduction cascade: amplification and termination mechanisms. Rev Physiol Biochem Pharmacol 154, 101-121

Chen, C.K., Inglese, J., Lefkowitz, R.J., Hurley, J.B. 1995. Ca(2+)-dependent interaction of recoverin with rhodopsin kinase. J Biol Chem 270, 18060-18066

Chen, F., Xie, Z., Wu, X., Du, W., Wang, J., Zhu, J., Ji, H., Wang, Y. 2012. Intravitreal Injection of Soluble Erythropoietin Receptor Exacerbates Photoreceptor Cell Apoptosis in a Rat Model of Retinal Detachment. Current Eye Research 37, 1156-1164

Chen, J., Connor, K.M., Aderman, C.M., Smith, L.E. 2008. Erythropoietin deficiency decreases vascular stability in mice. J Clin Invest 118, 526-533

Chen, J., Connor, K.M., Aderman, C.M., Willett, K.L., Aspegren, O.P., Smith, L.E. 2009. Suppression of retinal neovascularization by erythropoietin siRNA in a mouse model of proliferative retinopathy. Invest Ophthalmol Vis Sci 50, 1329-1335

Chen, J., Woodruff, M.L., Wang, T., Concepcion, F.A., Tranchina, D., Fain, G.L. 2010a. Channel modulation and the mechanism of light adaptation in mouse rods. J Neurosci 30, 16232-16240

Chen, M., Curtis, T.M., Stitt, A.W. 2013. Advanced Glycation End Products and Diabetic Retinopathy. Curr Med Chem

Chen, Z., Wang, L., Asavaritkrai, P., Noguchi, C.T. 2010b. Up-regulation of erythropoietin receptor by nitric oxide mediates hypoxia preconditioning. Journal of neuroscience research 88, 3180-3188

Chen, Z.Y., Asavaritikrai, P., Prchal, J.T., Noguchi, C.T. 2007. Endogenous erythropoietin signaling is required for normal neural progenitor cell proliferation. J Biol Chem 282, 25875-25883

Chen, Z.Y., Battinelli, E.M., Hendriks, R.W., Powell, J.F., Middleton-Price, H., Sims, K.B., Breakefield, X.O., Craig, I.W. 1993. Norrie disease gene: characterization of deletions and possible function. Genomics 16, 533-535

Chilov, D., Camenisch, G., Kvietikova, I., Ziegler, U., Gassmann, M., Wenger, R.H. 1999a. Induction and nuclear translocation of hypoxia-inducible factor-1 (HIF-1): heterodimerization with ARNT is not necessary for nuclear accumulation of HIF-1alpha. J Cell Sci 112, 1203-1212

Chilov, D., Camenisch, G., Kvietikova, I., Ziegler, U., Gassmann, M., Wenger, R.H. 1999b. Induction and nuclear translocation of hypoxia-inducible factor-1 (HIF-1): heterodimerization with ARNT is not necessary for nuclear accumulation of HIF-1alpha. Journal of cell science 112, 1203-1212

Chong, Z.Z., Kang, J.-Q., Maiese, K. 2003a. Apaf-1, Bcl-xL, cytochrome c, and caspase-9 form the critical elements for cerebral vascular protection by erythropoietin. Journal of Cerebral Blood Flow & Metabolism 23, 320-330

Chong, Z.Z., Kang, J.Q., Maiese, K. 2003b. Apaf-1, Bcl-xL, cytochrome c, and caspase-9 form the critical elements for cerebral vascular protection by erythropoietin. J Cereb Blood Flow Metab 23, 320-330

Chung, R.S., Penkowa, M., Dittmann, J., King, C.E., Bartlett, C., Asmussen, J.W., Hidalgo, J., Carrasco, J., Leung, Y.K., Walker, A.K., Fung, S.J., Dunlop, S.A., Fitzgerald, M., Beazley, L.D., Chuah, M.I., Vickers, J.C., West, A.K. 2008. Redefining the role of metallothionein within the injured brain: extracellular metallothioneins play an important role in the astrocyte-neuron response to injury. J Biol Chem 283, 15349-15358

Cideciyan, A.V., Aleman, T.S., Boye, S.L., Schwartz, S.B., Kaushal, S., Roman, A.J., Pang, J.J., Sumaroka, A., Windsor, E.A., Wilson, J.M., Flotte, T.R., Fishman, G.A., Heon, E., Stone, E.M., Byrne, B.J., Jacobson, S.G., Hauswirth, W.W. 2008. Human gene therapy for RPE65 isomerase deficiency activates the retinoid cycle of vision but with slow rod kinetics. Proc Natl Acad Sci U S A 105, 15112-15117

Coldewey, S.M., Khan, A.I., Kapoor, A., Collino, M., Rogazzo, M., Brines, M., Cerami, A., Hall, P., Sheaff, M., Kieswich, J.E., Yaqoob, M.M., Patel, N.S., Thiemermann, C. 2013. Erythropoietin attenuates acute kidney dysfunction in murine experimental sepsis by activation of the beta-common receptor. Kidney Int

Colella, P., Iodice, C., Di Vicino, U., Annunziata, I., Surace, E.M., Auricchio, A. 2011. Non-erythropoietic erythropoietin derivatives protect from light-induced and genetic photoreceptor degeneration. Hum Mol Genet 20, 2251-2262

Coleman, K., Fitzgerald, D., Eustace, P., Bouchier-Hayes, D. 1990. Electroretinography, retinal ischaemia and carotid artery disease. Eur J Vasc Surg 4, 569-573

Compernolle, V., Brusselmans, K., Acker, T., Hoet, P., Tjwa, M., Beck, H., Plaisance, S., Dor, Y., Keshet, E., Lupu, F., Nemery, B., Dewerchin, M., Van Veldhoven, P., Plate, K., Moons, L., Collen, D., Carmeliet, P. 2002. Loss of HIF-2alpha and inhibition of VEGF impair fetal lung maturation, whereas treatment with VEGF prevents fatal respiratory distress in premature mice. Nat Med 8, 702-710

Connolly, S.E., Hores, T.A., Smith, L.E., D'Amore, P.A. 1988. Characterization of vascular development in the mouse retina. Microvasc Res 36, 275-290

Constantinescu, S.N., Ghaffari, S., Lodish, H.F. 1999. The Erythropoietin Receptor: Structure, Activation and Intracellular Signal Transduction. Trends Endocrinol Metab 10, 18-23

Cowden, K.D., Simon, M.C. 2002. The bHLH/PAS factor MOP3 does not participate in hypoxia responses. Biochem Biophys Res Commun 290, 1228-1236

Cringle, S.J., Yu, D.Y., Alder, V.A. 1991. Intraretinal oxygen tension in the rat eye. Graefes Arch Clin Exp Ophthalmol 229, 574-577

Cringle, S.J., Yu, D.Y., Yu, P.K., Su, E.N. 2002. Intraretinal oxygen consumption in the rat in vivo. Invest Ophthalmol Vis Sci 43, 1922-1927

Cruickshanks, K.J., Klein, R., Klein, B.E. 1993. Sunlight and age-related macular degeneration. The Beaver Dam Eye Study. Arch Ophthalmol 111, 514-518

Cunha-Vaz, J. 1979. The blood-ocular barriers. Surv Ophthalmol 23, 279-296

Cunha-Vaz, J.G. 1978. The blood-ocular barriers. Invest Ophthalmol Vis Sci 17, 1037-1039

Curcio, C.A., Sloan, K.R., Kalina, R.E., Hendrickson, A.E. 1990. Human photoreceptor topography. J Comp Neurol 292, 497-523

Dacey, D.M. 1993. The mosaic of midget ganglion cells in the human retina. J Neurosci 13, 5334-5355

Dayan, F., Roux, D., Brahimi-Horn, M.C., Pouyssegur, J., Mazure, N.M. 2006. The oxygen sensor factor-inhibiting hypoxia-inducible factor-1 controls expression of distinct genes through the bifunctional transcriptional character of hypoxia-inducible factor-1alpha. Cancer Res 66, 3688-3698

de Vries, C., Escobedo, J.A., Ueno, H., Houck, K., Ferrara, N., Williams, L.T. 1992. The fms-like tyrosine kinase, a receptor for vascular endothelial growth factor. Science 255, 989-991

Deitmer, J.W. 2002. A role for CO(2) and bicarbonate transporters in metabolic exchanges in the brain. J Neurochem 80, 721-726

Deniro, M., Al-Halafi, A., Al-Mohanna, F.H., Alsmadi, O., Al-Mohanna, F.A. 2009. Pleiotropic Effects of YC-1 Selectively Inhibits Pathological Retinal Neovascularization and Promotes Physiological Revascularization in a Mouse Model of Oxygen-Induced Retinopathy. Mol Pharmacol

DeVries, S.H., Baylor, D.A. 1995. An alternative pathway for signal flow from rod photoreceptors to ganglion cells in mammalian retina. Proc Natl Acad Sci U S A 92, 10658-10662

Dick, A.D., Carter, D., Robertson, M., Broderick, C., Hughes, E., Forrester, J.V., Liversidge, J. 2003. Control of myeloid activity during retinal inflammation. J Leukoc Biol 74, 161-166

Digicaylioglu, M., Garden, G., Timberlake, S., Fletcher, L., Lipton, S.A. 2004. Acute neuroprotective synergy of erythropoietin and insulin-like growth factor I. Proc Natl Acad Sci U S A 101, 9855-9860

Digicaylioglu, M., Lipton, S.A. 2001. Erythropoietin-mediated neuroprotection involves cross-talk between Jak2 and NF-kappaB signalling cascades. Nature 412, 641-647

Dinculescu, A., Glushakova, L., Min, S.H., Hauswirth, W.W. 2005. Adeno-associated virus-vectored gene therapy for retinal disease. Hum Gene Ther 16, 649-663

Ding, K., Scortegagna, M., Seaman, R., Birch, D.G., Garcia, J.A. 2005. Retinal disease in mice lacking hypoxia-inducible transcription factor-2alpha. Invest Ophthalmol Vis Sci 46, 1010-1016

Dorrell, M.I., Aguilar, E., Friedlander, M. 2002. Retinal vascular development is mediated by endothelial filopodia, a preexisting astrocytic template and specific R-cadherin adhesion. Invest Ophthalmol Vis Sci 43, 3500-3510

Drescher, K.M., Whittum-Hudson, J.A. 1996. Herpes simplex virus type 1 alters transcript levels of tumor necrosis factor-alpha and interleukin-6 in retinal glial cells. Invest Ophthalmol Vis Sci 37, 2302-2312

Duan, L.J., Takeda, K., Fong, G.H. 2011. Prolyl Hydroxylase Domain Protein 2 (PHD2) Mediates Oxygen-Induced Retinopathy in Neonatal Mice. Am J Pathol 178, 1881-1890

Duh, E.J., Yang, H.S., Suzuma, I., Miyagi, M., Youngman, E., Mori, K., Katai, M., Yan, L., Suzuma, K., West, K., Davarya, S., Tong, P., Gehlbach, P., Pearlman, J., Crabb, J.W., Aiello, L.P., Campochiaro, P.A., Zack, D.J. 2002. Pigment epithelium-derived factor suppresses ischemia-induced retinal neovascularization and VEGF-induced migration and growth. Invest Ophthalmol Vis Sci 43, 821-829

Dumont, D.J., Gradwohl, G., Fong, G.H., Puri, M.C., Gertsenstein, M., Auerbach, A., Breitman, M.L. 1994. Dominant-negative and targeted null mutations in the endothelial receptor tyrosine kinase, tek, reveal a critical role in vasculogenesis of the embryo. Genes Dev 8, 1897-1909

Duquette, P.M., Zhou, X., Yap, N.L., MacLaren, E.J., Lu, J.J., Wallace, V.A., Chen, H.H. 2010. Loss of LMO4 in the retina leads to reduction of GABAergic amacrine cells and functional deficits. PLoS One 5, e13232

Edwards, A.O., Ritter, R.r., Abel, K.J., Manning, A., Panhuysen, C., Farrer, L.A. 2005. Complement factor H polymorphism and age-related macular degeneration. Science 308, 421-424

Eichler, W., Kuhrt, H., Hoffmann, S., Wiedemann, P., Reichenbach, A. 2000. VEGF release by retinal glia depends on both oxygen and glucose supply. Neuroreport 11, 3533-3537

Eichler, W., Yafai, Y., Keller, T., Wiedemann, P., Reichenbach, A. 2004. PEDF derived from glial Muller cells: a possible regulator of retinal angiogenesis. Exp Cell Res 299, 68-78

Ejaz, S., Chekarova, I., Ejaz, A., Sohail, A., Lim, C.W. 2008. Importance of pericytes and mechanisms of pericyte loss during diabetes retinopathy. Diabetes Obes Metab 10, 53-63

El-Remessy, A.B., Behzadian, M.A., Abou-Mohamed, G., Franklin, T., Caldwell, R.W., Caldwell, R.B. 2003. Experimental diabetes causes breakdown of the blood-retina barrier by a mechanism involving tyrosine nitration and increases in expression of vascular endothelial growth factor and urokinase plasminogen activator receptor. Am J Pathol 162, 1995-2004

Elliott, S., Busse, L., Bass, M.B., Lu, H., Sarosi, I., Sinclair, A.M., Spahr, C., Um, M., Van, G., Begley, C.G. 2006. Anti-Epo receptor antibodies do not predict Epo receptor expression. Blood 107, 1892-1895

Ema, M., Taya, S., Yokotani, N., Sogawa, K., Matsuda, Y., Fujii-Kuriyama, Y. 1997. A novel bHLH-PAS factor with close sequence similarity to hypoxia-inducible factor 1alpha regulates the VEGF expression and is potentially involved in lung and vascular development. Proc Natl Acad Sci U S A 94, 4273-4278

Engerman, R.L., Meyer, R.K. 1965. Development of retinal vasculature in rats. Am J Ophthalmol 60, 628-641

Enroth-Cugell, C., Hertz, B.G., Lennie, P. 1974. Proceedings: Convergence of rod and cone signals on retinal ganglion cells of the cat. J Physiol 242, 126P-127P

Enroth-Cugell, C., Hertz, B.G., Lennie, P. 1977. Convergence of rod and cone signals in the cat's retina. J Physiol 269, 297-318

Epstein, A.C., Gleadle, J.M., McNeill, L.A., Hewitson, K.S., O'Rourke, J., Mole, D.R., Mukherji, M., Metzen, E., Wilson, M.I., Dhanda, A., Tian, Y.M., Masson, N., Hamilton, D.L., Jaakkola, P., Barstead, R., Hodgkin, J., Maxwell, P.H., Pugh, C.W., Schofield, C.J., Ratcliffe, P.J. 2001. C. elegans EGL-9 and mammalian homologs define a family of dioxygenases that regulate HIF by prolyl hydroxylation. Cell 107, 43-54

Erickson, P.A., Feinstein, S.C., Lewis, G.P., Fisher, S.K. 1992. Glial fibrillary acidic protein and its mRNA: ultrastructural detection and determination of changes after CNS injury. J Struct Biol 108, 148-161

Euler, T., Masland, R.H. 2000. Light-evoked responses of bipolar cells in a mammalian retina. J Neurophysiol 83, 1817-1829

Fandrey, J. 2004. Oxygen-dependent and tissue-specific regulation of erythropoietin gene expression. Am J Physiol Regul Integr Comp Physiol 286, R977-88

Farrell, F., Lee, A. 2004. The erythropoietin receptor and its expression in tumor cells and other tissues. Oncologist 9 Suppl 5, 18-30

Feeney, S.A., Simpson, D.A., Gardiner, T.A., Boyle, C., Jamison, P., Stitt, A.W. 2003. Role of vascular endothelial growth factor and placental growth factors during retinal vascular development and hyaloid regression. Invest Ophthalmol Vis Sci 44, 839-847

Feke, G.T., Zuckerman, R., Green, G.J., Weiter, J.J. 1983. Response of human retinal blood flow to light and dark. Invest Ophthalmol Vis Sci 24, 136-141

Ferrara, N., Gerber, H.P. 2001. The role of vascular endothelial growth factor in angiogenesis. Acta Haematol 106, 148-156

Ferreira, I.L., Duarte, C.B., Carvalho, A.P. 1996. Ca2+ influx through glutamate receptor-associated channels in retina cells correlates with neuronal cell death. Eur J Pharmacol 302, 153-162

Fesenko, E.E., Kolesnikov, S.S., Lyubarsky, A.L. 1985. Induction by cyclic GMP of cationic conductance in plasma membrane of retinal rod outer segment. Nature 313, 310-313

Filipek, S., Stenkamp, R.E., Teller, D.C., Palczewski, K. 2003. G protein-coupled receptor rhodopsin: a prospectus. Annu Rev Physiol 65, 851-879

Finkelstein, M.A., Hood, D.C. 1981. Cone system saturation: more than one stage of sensitivity loss. Vision Res 21, 319-328

Fischer, B., Bavister, B.D. 1993. Oxygen tension in the oviduct and uterus of rhesus monkeys, hamsters and rabbits. J Reprod Fertil 99, 673-679

Fischer, M.D., Huber, G., Beck, S.C., Tanimoto, N., Muehlfriedel, R., Fahl, E., Grimm, C., Wenzel, A., Reme, C.E., van de Pavert, S.A., Wijnholds, J., Pacal, M., Bremner, R., Seeliger, M.W. 2009. Noninvasive, in vivo assessment of mouse retinal structure using optical coherence tomography. PLoS One 4, e7507

Flamme, I., Frohlich, T., von Reutern, M., Kappel, A., Damert, A., Risau, W. 1997. HRF, a putative basic helix-loop-helix-PAS-domain transcription factor is closely related to hypoxia-inducible factor-1 alpha and developmentally expressed in blood vessels. Mech Dev 63, 51-60

Flammer, J., Mozaffarieh, M. 2008. Autoregulation, a balancing act between supply and demand. Can J Ophthalmol 43, 317-321

Foster, A., Resnikoff, S. 2005. The impact of Vision 2020 on global blindness. Eye 19, 1133-1135

Foster, A., Johnson, G.J. 1990. Magnitude and causes of blindness in the developing world. International ophthalmology 14, 135-140

Fradkin, A.H. 1971. Norrie's disease. Congenital progressive oculo-acoustico-cerebral degeneration. Am J Ophthalmol 72, 947-948

Fraisl, P., Mazzone, M., Schmidt, T., Carmeliet, P. 2009. Regulation of angiogenesis by oxygen and metabolism. Developmental cell 16, 167-179

Francke, M., Makarov, F., Kacza, J., Seeger, J., Wendt, S., Gartner, U., Faude, F., Wiedemann, P., Reichenbach, A. 2001. Retinal pigment epithelium melanin granules are phagocytozed by Muller glial cells in experimental retinal detachment. J Neurocytol 30, 131-136

Frank, R.N., Turczyn, T.J., Das, A. 1990. Pericyte coverage of retinal and cerebral capillaries. Invest Ophthalmol Vis Sci 31, 999-1007

Frasson, M., Picaud, S., Leveillard, T., Simonutti, M., Mohand-Said, S., Dreyfus, H., Hicks, D., Sabel, J. 1999. Glial cell line-derived neurotrophic factor induces histologic and functional protection of rod photoreceptors in the rd/rd mouse. Invest Ophthalmol Vis Sci 40, 2724-2734

Frede, S., Stockmann, C., Winning, S., Freitag, P., Fandrey, J. 2009. Hypoxia-inducible factor (HIF) 1alpha accumulation and HIF target gene expression are impaired after induction of endotoxin tolerance. J Immunol 182, 6470-6476

Fried, W., Kilbridge, T., Krantz, S., McDonald, T.P., Lange, R.D. 1969. Studies on extrarenal erythropoietin. J Lab Clin Med 73, 244-248

Friedlander, M., Brooks, P.C., Shaffer, R.W., Kincaid, C.M., Varner, J.A., Cheresh, D.A. 1995. Definition of two angiogenic pathways by distinct alpha v integrins. Science 270, 1500-1502

Friedman, E., Krupsky, S., Lane, A.M., Oak, S.S., Friedman, E.S., Egan, K., Gragoudas, E.S. 1995. Ocular blood flow velocity in age-related macular degeneration. Ophthalmology 102, 640-646

Fruttiger, M. 2007. Development of the retinal vasculature. Angiogenesis 10, 77-88

Fruttiger, M., Calver, A.R., Kruger, W.H., Mudhar, H.S., Michalovich, D., Takakura, N., Nishikawa, S., Richardson, W.D. 1996. PDGF mediates a neuron-astrocyte interaction in the developing retina. Neuron 17, 1117-1131

Fu, Q.L., Wu, W., Wang, H., Li, X., Lee, V.W., So, K.F. 2008. Up-regulated endogenous erythropoietin/erythropoietin receptor system and exogenous erythropoietin rescue retinal ganglion cells after chronic ocular hypertension. Cell Mol Neurobiol 28, 317-329

Fung, B.K., Hurley, J.B., Stryer, L. 1981. Flow of information in the light-triggered cyclic nucleotide cascade of vision. Proc Natl Acad Sci U S A 78, 152-156

Gardner, T.W., Lieth, E., Khin, S.A., Barber, A.J., Bonsall, D.J., Lesher, T., Rice, K., Brennan, W.A.J. 1997. Astrocytes increase barrier properties and ZO-1 expression in retinal vascular endothelial cells. Invest Ophthalmol Vis Sci 38, 2423-2427

Gariano, R.F. 2010. Special features of human retinal angiogenesis. Eye (Lond) 24, 401-407

Gariano, R.F., Gardner, T.W. 2005. Retinal angiogenesis in development and disease. Nature 438, 960-966

Gariano, R.F., Iruela-Arispe, M.L., Hendrickson, A.E. 1994. Vascular development in primate retina: comparison of laminar plexus formation in monkey and human. Invest Ophthalmol Vis Sci 35, 3442-3455

Gariano, R.F., Sage, E.H., Kaplan, H.J., Hendrickson, A.E. 1996. Development of astrocytes and their relation to blood vessels in fetal monkey retina. Invest Ophthalmol Vis Sci 37, 2367-2375

Gaunt, P. 1968. The saturation of rod receptors. Opt Acta (Lond) 15, 287-293

Gehrs, K.M., Anderson, D.H., Johnson, L.V., Hageman, G.S. 2006. Age-related macular degeneration--emerging pathogenetic and therapeutic concepts. Ann Med 38, 450-471

Genc, S., Kuralay, F., Genc, K., Akhisaroglu, M., Fadiloglu, S., Yorukoglu, K., Fadiloglu, M., Gure, A. 2001. Erythropoietin exerts neuroprotection in 1-methyl-4-phenyl-1,2,3,6-tetrahydropyridine-treated C57/BL mice via increasing nitric oxide production. Neurosci Lett 298, 139-141

Gerhardt, H., Golding, M., Fruttiger, M., Ruhrberg, C., Lundkvist, A., Abramsson, A., Jeltsch, M., Mitchell, C., Alitalo, K., Shima, D., Betsholtz, C. 2003. VEGF guides angiogenic sprouting utilizing endothelial tip cell filopodia. J Cell Biol 161, 1163-1177

Gorio, A., Gokmen, N., Erbayraktar, S., Yilmaz, O., Madaschi, L., Cichetti, C., Di Giulio, A.M., Vardar, E., Cerami, A., Brines, M. 2002. Recombinant human erythropoietin counteracts secondary injury and markedly enhances neurological recovery from experimental spinal cord trauma. Proc Natl Acad Sci U S A 99, 9450-9455

Goureau, O., Régnier-Ricard, F., Courtois, Y. 1999. Requirement for nitric oxide in retinal neuronal cell death induced by activated Müller glial cells. Journal of neurochemistry 72, 2506-2515

Govardovskii, V.I., Fyhrquist, N., Reuter, T., Kuzmin, D.G., Donner, K. 2000. In search of the visual pigment template. Vis Neurosci 17, 509-528

Gradin, K., McGuire, J., Wenger, R.H., Kvietikova, I., fhitelaw, M.L., Toftgard, R., Tora, L., Gassmann, M., Poellinger, L. 1996. Functional interference between hypoxia and dioxin signal transduction pathways: competition for recruitment of the Arnt transcription factor. Mol Cell Biol 16, 5221-5231

Graymore, C. 1959. Metabolism of the developing retina. I. Aerobic and anaerobic glycolysis in the developing rat retina. Br J Ophthalmol 43, 34-39

Green, B.H., Monger, T.G., Alfano, R.R., Aton, B., Callender, R.H. 1977. Cis-trans isomerisation in rhodopsin occurs in picoseconds. Nature 269, 179-180

Grimm, C., Hermann, D.M., Bogdanova, A., Hotop, S., Kilic, U., Wenzel, A., Kilic, E., Gassmann, M. 2005. Neuroprotection by hypoxic preconditioning: HIF-1 and erythropoietin protect from retinal degeneration. Semin Cell Dev Biol 16, 531-538

Grimm, C., Wenzel, A., Acar, N., Keller, S., Seeliger, M., Gassmann, M. 2006. Hypoxic preconditioning and erythropoietin protect retinal neurons from degeneration. Adv Exp Med Biol 588, 119-131

Grimm, C., Wenzel, A., Groszer, M., Mayser, H., Seeliger, M., Samardzija, M., Bauer, C., Gassmann, M., Reme, C.E. 2002. HIF-1-induced erythropoietin in the hypoxic retina protects against light-induced retinal degeneration. Nat Med 8, 718-724

Grimm, C., Wenzel, A., Stanescu, D., Samardzija, M., Hotop, S., Groszer, M., Naash, M., Gassmann, M., Reme, C. 2004. Constitutive overexpression of human erythropoietin protects the mouse retina against induced but not inherited retinal degeneration. J Neurosci 24, 5651-5658

Grimm, C., Willmann, G. 2012. Hypoxia in the eye: a two-sided coin. High Alt Med Biol 13, 169-175

Grimm, C., Wenzel, A., Hafezi, F., Yu, S., Redmond, T.M., Remé, C.E. 2000. Protection of Rpe65-deficient mice identifies rhodopsin as a mediator of light-induced retinal degeneration. Nature genetics 25, 63-66

Grosche, J., Grimm, D., Clemens, N., Reichenbach, A. 1997. Retinal light damage vs. normal aging of rats: altered morphology, intermediate filament expression, and nuclear organization of Muller (glial) cells. J Hirnforsch 38, 459-470

Gruber, M., Hu, C.J., Johnson, R.S., Brown, E.J., Keith, B., Simon, M.C. 2007. Acute postnatal ablation of Hif-2 results in anemia. Proceedings of the National Academy of Sciences 104, 2301

Grunwald, J.E., Hariprasad, S.M., DuPont, J., Maguire, M.G., Fine, S.L., Brucker, A.J., Maguire, A.M., Ho, A.C. 1998. Foveolar choroidal blood flow in age-related macular degeneration. Invest Ophthalmol Vis Sci 39, 385-390

Grunwald, J.E., Metelitsina, T.I., Dupont, J.C., Ying, G.S., Maguire, M.G. 2005. Reduced foveolar choroidal blood flow in eyes with increasing AMD severity. Invest Ophthalmol Vis Sci 46, 1033-1038

Gu, Y.Z., Moran, S.M., Hogenesch, J.B., Wartman, L., Bradfield, C.A. 1998. Molecular characterization and chromosomal localization of a third alpha-class hypoxia inducible factor subunit, HIF3alpha. Gene Expr 7, 205-213

Guerin, C.J., Anderson, D.H., Fisher, S.K. 1990. Changes in intermediate filament immunolabeling occur in response to retinal detachment and reattachment in primates. Invest Ophthalmol Vis Sci 31, 1474-1482

Guo, M.-F., Yu, J.-Z., Ma, C.-G. 2011. Mechanisms related to neuron injury and death in cerebral hypoxic ischaemia. Folia Neuropathol 49, 78-87

Hackett, S.F., Ozaki, H., Strauss, R.W., Wahlin, K., Suri, C., Maisonpierre, P., Yancopoulos, G., Campochiaro, P.A. 2000. Angiopoietin 2 expression in the retina: upregulation during physiologic and pathologic neovascularization. J Cell Physiol 184, 275-284

Hackett, S.F., Wiegand, S., Yancopoulos, G., Campochiaro, P.A. 2002. Angiopoietin-2 plays an important role in retinal angiogenesis. J Cell Physiol 192, 182-187

Hagins, W.A., Penn, R.D., Yoshikami, S. 1970. Dark current and photocurrent in retinal rods. Biophys J 10, 380-412

Hamann, S. 2002. Molecular mechanisms of water transport in the eye. Int Rev Cytol 215, 395-431

Hamel, C. 2006. Retinitis pigmentosa. Orphanet J Rare Dis 1, 40

Hamel, C.P. 2007. Cone rod dystrophies. Orphanet J Rare Dis 2, 7

Hanisch, U.K. 2002. Microglia as a source and target of cytokines. Glia 40, 140-155

Hanisch, U.K., Kettenmann, H. 2007. Microglia: active sensor and versatile effector cells in the normal and pathologic brain. Nat Neurosci 10, 1387-1394

Hara, S., Hamada, J., Kobayashi, C., Kondo, Y., Imura, N. 2001. Expression and characterization of hypoxia-inducible factor (HIF)-3alpha in human kidney: suppression of HIF-mediated gene expression by HIF-3alpha. Biochem Biophys Res Commun 287, 808-813

Harris, A., Chung, H.S., Ciulla, T.A., Kagemann, L. 1999. Progress in measurement of ocular blood flow and relevance to our understanding of glaucoma and age-related macular degeneration. Prog Retin Eye Res 18, 669-687

Harris, A.L. 2002. Hypoxia--a key regulatory factor in tumour growth. Nat Rev Cancer 2, 38-47

Harris, K.W., Winkelmann, J.C. 1996. Enzyme-linked immunosorbent assay detects a potential soluble form of the erythropoietin receptor in human plasma. Am J Hematol 52, 8-13

Hartong, D.T., Berson, E.L., Dryja, T.P. 2006. Retinitis pigmentosa. Lancet 368, 1795-1809

Haugh, L.M., Linsenmeier, R.A., Goldstick, T.K. 1990. Mathematical models of the spatial distribution of retinal oxygen tension and consumption, including changes upon illumination. Ann Biomed Eng 18, 19-36

Haurigot, V., Villacampa, P., Ribera, A., Bosch, A., Ramos, D., Ruberte, J., Bosch, F. 2012. Long-term retinal PEDF overexpression prevents neovascularization in a murine adult model of retinopathy. PLoS One 7, e41511

He, W., Cowan, C.W., Wensel, T.G. 1998. RGS9, a GTPase accelerator for phototransduction. Neuron 20, 95-102

Heeschen, C., Aicher, A., Lehmann, R., Fichtlscherer, S., Vasa, M., Urbich, C., Mildner-Rihm, C., Martin, H., Zeiher, A.M., Dimmeler, S. 2003. Erythropoietin is a potent physiologic stimulus for endothelial progenitor cell mobilization. Blood 102, 1340-1346

Heid, C.A., Stevens, J., Livak, K.J., Williams, P.M. 1996. Real time quantitative PCR. Genome research 6, 986-994

Heidbreder, M., Frohlich, F., Johren, O., Dendorfer, A., Qadri, F., Dominiak, P. 2003. Hypoxia rapidly activates HIF-3alpha mRNA expression. FASEB J 17, 1541-1543

Heikkilä, M., Pasanen, A., Kivirikko, K.I., Myllyharju, J. 2011. Roles of the human hypoxia-inducible factor (HIF)-3α variants in the hypoxia response. Cellular and Molecular Life Sciences 68, 3885-3901

Hellstrom, A., Perruzzi, C., Ju, M., Engstrom, E., Hard, A.L., Liu, J.L., Albertsson-Wikland, K., Carlsson, B., Niklasson, A., Sjodell, L., LeRoith, D., Senger, D.R., Smith, L.E. 2001. Low IGF-I suppresses VEGF-survival signaling in retinal endothelial cells: direct correlation with clinical retinopathy of prematurity. Proc Natl Acad Sci U S A 98, 5804-5808

Hestrin, S. 1987. The properties and function of inward rectification in rod photoreceptors of the tiger salamander. J Physiol 390, 319-333

Hewitson, K.S., McNeill, L.A., Elkins, J.M., Schofield, C.J. 2003. The role of iron and 2-oxoglutarate oxygenases in signalling. Biochem Soc Trans 31, 510-515

Hicks, T.P., Lee, B.B., Vidyasagar, T.R. 1983. The responses of cells in macaque lateral geniculate nucleus to sinusoidal gratings. J Physiol 337, 183-200

Higuchi, R., Fockler, C., Dollinger, G., Watson, R. 1993. Kinetic PCR analysis: real-time monitoring of DNA amplification reactions. Biotechnology 11, 1026-1030

Hill, R.E., Favor, J., Hogan, B.L., Ton, C.C., Saunders, G.F., Hanson, I.M., Prosser, J., Jordan, T., Hastie, N.D., van Heyningen, V. 1991. Mouse small eye results from mutations in a paired-like homeobox-containing gene. Nature 354, 522-525

Hirose, K., Morita, M., Ema, M., Mimura, J., Hamada, H., Fujii, H., Saijo, Y., Gotoh, O., Sogawa, K., Fujii-Kuriyama, Y. 1996. cDNA cloning and tissue-specific expression of a novel basic helix-loop-helix/PAS factor (Arnt2) with close sequence similarity to the aryl hydrocarbon receptor nuclear translocator (Arnt). Mol Cell Biol 16, 1706-1713

Hogenesch, J.B., Gu, Y.Z., Jain, S., Bradfield, C.A. 1998. The basic-helix-loop-helix-PAS orphan MOP3 forms transcriptionally active complexes with circadian and hypoxia factors. Proc Natl Acad Sci U S A 95, 5474-5479

Hogenesch, J.B., Gu, Y.Z., Moran, S.M., Shimomura, K., Radcliffe, L.A., Takahashi, J.S., Bradfield, C.A. 2000. The basic helix-loop-helix-PAS protein MOP9 is a brain-specific heterodimeric partner of circadian and hypoxia factors. J Neurosci 20, RC83

Holmes, D.I., Zachary, I. 2005. The vascular endothelial growth factor (VEGF) family: angiogenic factors in health and disease. Genome Biol 6, 209

Holmquist-Mengelbier, L., Fredlund, E., Lofstedt, T., Noguera, R., Navarro, S., Nilsson, H., Pietras, A., Vallon-Christersson, J., Borg, A., Gradin, K., Poellinger, L., Pahlman, S. 2006. Recruitment of HIF-1alpha and HIF-2alpha to common target genes is differentially regulated in neuroblastoma: HIF-2alpha promotes an aggressive phenotype. Cancer Cell 10, 413-423

Hsu, Y.T., Molday, R.S. 1993. Modulation of the cGMP-gated channel of rod photoreceptor cells by calmodulin. Nature 361, 76-79

Hu, C.J., Sataur, A., Wang, L., Chen, H., Simon, M.C. 2007. The N-terminal transactivation domain confers target gene specificity of hypoxia-inducible factors HIF-1alpha and HIF-2alpha. Mol Biol Cell 18, 4528-4542

Hu, L.M., Luo, Y., Zhang, J., Lei, X., Shen, J., Wu, Y., Qin, M., Unver, Y.B., Zhong, Y., Xu, G.T., Li, W. 2011. EPO reduces reactive gliosis and stimulates neurotrophin expression in Muller cells. Front Biosci (Elite Ed) 3, 1541-1555

Huang, L.E., Arany, Z., Livingston, D.M., Bunn, H.F. 1996. Activation of hypoxia-inducible transcription factor depends primarily upon redox-sensitive stabilization of its alpha subunit. J Biol Chem 271, 32253-32259

Huang, Q., Wang, S., Sorenson, C.M., Sheibani, N. 2008. PEDF-deficient mice exhibit an enhanced rate of retinal vascular expansion and are more sensitive to hyperoxia-mediated vessel obliteration. Exp Eye Res 87, 226-241

Huber, G., Beck, S.C., Grimm, C., Sahaboglu-Tekgoz, A., Paquet-Durand, F., Wenzel, A., Humphries, P., Redmond, T.M., Seeliger, M.W., Fischer, M.D. 2009. Spectral domain optical coherence tomography in mouse models of retinal degeneration. Invest Ophthalmol Vis Sci 50, 5888-5895

Hughes, S.M., Brand, M.D. 1985. Light changes the membrane potential and ion balances of retinal rod disks. FEBS Lett 182, 380-384

Hume, D.A., Perry, V.H., Gordon, S. 1983. Immunohistochemical localization of a macrophage-specific antigen in developing mouse retina: phagocytosis of dying neurons and differentiation of microglial cells to form a regular array in the plexiform layers. J Cell Biol 97, 253-257

Huster, D., Reichenbach, A., Reichelt, W. 2000. The glutathione content of retinal Muller (glial) cells: effect of pathological conditions. Neurochem Int 36, 461-469

Iesato, Y., Toriyama, Y., Sakurai, T., Kamiyoshi, A., Ichikawa-Shindo, Y., Kawate, H., Yoshizawa, T., Koyama, T., Uetake, R., Yang, L., Yamauchi, A., Tanaka, M., Igarashi, K., Murata, T., Shindo, T. 2013. Adrenomedullin-RAMP2 System Is Crucially Involved in Retinal Angiogenesis. Am J Pathol

Ikeda, M., Nomura, M. 1997. cDNA cloning and tissue-specific expression of a novel basic helix-loop-helix/PAS protein (BMAL1) and identification of alternatively spliced variants with alternative translation initiation site usage. Biochem Biophys Res Commun 233, 258-264

Izumi, Y., Shimamoto, K., Benz, A.M., Hammerman, S.B., Olney, J.W., Zorumski, C.F. 2002. Glutamate transporters and retinal excitotoxicity. Glia 39, 58-68

Jaakkola, P., Mole, D.R., Tian, Y.M., Wilson, M.I., Gielbert, J., Gaskell, S.J., Kriegsheim, A., Hebestreit, H.F., Mukherji, M., Schofield, C.J., Maxwell, P.H., Pugh, C.W., Ratcliffe, P.J. 2001. Targeting of HIF-alpha to the von Hippel-Lindau ubiquitylation complex by O2-regulated prolyl hydroxylation. Science 292, 468-472

Jacobs, G.H. 1993. The distribution and nature of colour vision among the mammals. Biol Rev Camb Philos Soc 68, 413-471

Jager, R.D., Mieler, W.F., Miller, J.W. 2008. Age-related macular degeneration. N Engl J Med 358, 2606-2617

Jain, S., Maltepe, E., Lu, M.M., Simon, C., Bradfield, C.A. 1998. Expression of ARNT, ARNT2, HIF1 alpha, HIF2 alpha and Ah receptor mRNAs in the developing mouse. Mech Dev 73, 117-123

Jang, M.S., Park, J.E., Lee, J.A., Park, S.G., Myung, P.K., Lee, D.H., Park, B.C., Cho, S. 2005. Binding and regulation of hypoxia-inducible factor-1 by the inhibitory PAS proteins. Biochemical and biophysical research communications 337, 209-215

Jelkmann, W. 2004. Molecular biology of erythropoietin. Intern Med 43, 649-659

Jiang, B., Bezhadian, M.A., Caldwell, R.B. 1995. Astrocytes modulate retinal vasculogenesis: effects on endothelial cell differentiation. Glia 15, 1-10

Jiang, B.H., Rue, E., Wang, G.L., Roe, R., Semenza, G.L. 1996. Dimerization, DNA binding, and transactivation properties of hypoxia-inducible factor 1. J Biol Chem 271, 17771-17778

Jiang, S., Wu, M.W., Sternberg, P., Jones, D.P. 2000. Fas mediates apoptosis and oxidant-induced cell death in cultured hRPE cells. Invest Ophthalmol Vis Sci 41, 645-655

Johnson, N.F., Foulds, W.S. 1978. The effects of total acute ischaemia on the structure of the rabbit retina. Exp Eye Res 27, 45-59

Joly, S., Lange, C., Thiersch, M., Samardzija, M., Grimm, C. 2008. Leukemia inhibitory factor extends the lifespan of injured photoreceptors in vivo. J Neurosci 28, 13765-13774

Joly, S., Francke, M., Ulbricht, E., Beck, S., Seeliger, M., Hirrlinger, P., Hirrlinger, J., Lang, K.S., Zinkernagel, M., Odermatt, B. 2009. Cooperative phagocytes: resident microglia and bone marrow immigrants remove dead photoreceptors in retinal lesions. The American journal of pathology 174, 2310-2323

Josko, J., Knefel, K. 2003. The role of vascular endothelial growth factor in cerebral oedema formation. Folia Neuropathol 41, 161-166

Jubinsky, P.T., Krijanovski, O.I., Nathan, D.G., Tavernier, J., Sieff, C.A. 1997. The beta chain of the interleukin-3 receptor functionally associates with the erythropoietin receptor. Blood 90, 1867-1873

Junge, H.J., Yang, S., Burton, J.B., Paes, K., Shu, X., French, D.M., Costa, M., Rice, D.S., Ye, W. 2009. TSPAN12 regulates retinal vascular development by promoting Norrin- but not Wnt-induced FZD4/beta-catenin signaling. Cell 139, 299-311

Junk, A.K., Mammis, A., Savitz, S.I., Singh, M., Roth, S., Malhotra, S., Rosenbaum, P.S., Cerami, A., Brines, M., Rosenbaum, D.M. 2002. Erythropoietin administration protects retinal neurons from acute ischemia-reperfusion injury. Proc Natl Acad Sci U S A 99, 10659-10664

Juul, S.E., Yachnis, A.T., Christensen, R.D. 1998. Tissue distribution of erythropoietin and erythropoietin receptor in the developing human fetus. Early Hum Dev 52, 235-249

Kallio, P.J., Pongratz, I., Gradin, K., McGuire, J., Poellinger, L. 1997. Activation of hypoxia-inducible factor 1alpha: posttranscriptional regulation and conformational change by recruitment of the Arnt transcription factor. Proc Natl Acad Sci U S A 94, 5667-5672

Kaplan, E., Shapley, R.M. 1986. The primate retina contains two types of ganglion cells, with high and low contrast sensitivity. Proc Natl Acad Sci U S A 83, 2755-2757

Karan, G., Lillo, C., Yang, Z., Cameron, D.J., Locke, K.G., Zhao, Y., Thirumalaichary, S., Li, C., Birch, D.G., Vollmer-Snarr, H.R. 2005. Lipofuscin accumulation, abnormal electrophysiology, and photoreceptor degeneration in mutant ELOVL4 transgenic mice: a model for macular degeneration. Proceedings of the National Academy of Sciences of the United States of America 102, 4164-4169

Karschin, A., Wassle, H., Schnitzer, J. 1986. Shape and distribution of astrocytes in the cat retina. Invest Ophthalmol Vis Sci 27, 828-831

Kaur, C., Foulds, W.S., Ling, E.A. 2008. Blood-retinal barrier in hypoxic ischaemic conditions: basic concepts, clinical features and management. Prog Retin Eye Res 27, 622-647

Kaur, C., Sivakumar, V., Foulds, W.S. 2006. Early response of neurons and glial cells to hypoxia in the retina. Invest Ophthalmol Vis Sci 47, 1126-1141

Kaur, C., Sivakumar, V., Yong, Z., Lu, J., Foulds, W.S., Ling, E.A. 2007. Blood-retinal barrier disruption and ultrastructural changes in the hypoxic retina in adult rats: the beneficial effect of melatonin administration. J Pathol 212, 429-439

Kawakami, M., Sekiguchi, M., Sato, K., Kozaki, S., Takahashi, M. 2001. Erythropoietin receptor-mediated inhibition of exocytotic glutamate release confers neuroprotection during chemical ischemia. J Biol Chem 276, 39469-39475

Kawamura, S., Murakami, M. 1989. Regulation of cGMP levels by guanylate cyclase in truncated frog rod outer segments. J Gen Physiol 94, 649-668

Keith, B., Adelman, D.M., Simon, M.C. 2001. Targeted mutation of the murine arylhydrocarbon receptor nuclear translocator 2 (Arnt2) gene reveals partial redundancy with Arnt. Proc Natl Acad Sci U S A 98, 6692-6697

Keller, C., Grimm, C., Wenzel, A., Hafezi, F., Remé, C.E. 2001. Protective effect of halothane anesthesia on retinal light damage: inhibition of metabolic rhodopsin regeneration. Investigative ophthalmology & visual science 42, 476-480

Kenneth, N.S., Mudie, S., van Uden, P., Rocha, S. 2009. SWI/SNF regulates the cellular response to hypoxia. Journal of Biological Chemistry 284, 4123-4131

Kertesz, N., Wu, J., Chen, T.H., Sucov, H.M., Wu, H. 2004. The role of erythropoietin in regulating angiogenesis. Dev Biol 276, 101-110

Khandhadia, S., Lotery, A. 2010. Oxidation and age-related macular degeneration: insights from molecular biology. Expert Rev Mol Med 12, e34

Khankin, E.V., Mutter, W.P., Tamez, H., Yuan, H.-T., Karumanchi, S.A., Thadhani, R. 2010. Soluble erythropoietin receptor contributes to erythropoietin resistance in end-stage renal disease. PloS one 5, e9246

Kilic, E., Kilic, U., Soliz, J., Bassetti, C.L., Gassmann, M., Hermann, D.M. 2005a. Brain-derived erythropoietin protects from focal cerebral ischemia by dual activation of ERK-1/-2 and Akt pathways. FASEB J 19, 2026-2028

Kilic, U., Kilic, E., Soliz, J., Bassetti, C.I., Gassmann, M., Hermann, D.M. 2005b. Erythropoietin protects from axotomy-induced degeneration of retinal ganglion cells by activating ERK-1/-2. FASEB J 19, 249-251

Kim, J.H., Yu, Y.S., Kim, K.W., Kim, J.H. 2010. Impaired retinal vascular development in anencephalic human fetus. Histochem Cell Biol 134, 277-284

Kimble, E.A., Svoboda, R.A., Ostroy, S.E. 1980. Oxygen consumption and ATP changes of the vertebrate photoreceptor. Exp Eye Res 31, 271-288

Kimura, H., Weisz, A., Ogura, T., Hitomi, Y., Kurashima, Y., Hashimoto, K., D'Acquisto, F., Makuuchi, M., Esumi, H. 2001. Identification of hypoxia-inducible factor 1 ancillary sequence and its function in vascular endothelial growth factor gene induction by hypoxia and nitric oxide. J Biol Chem 276, 2292-2298

King, C.E., Rodger, J., Bartlett, C., Esmaili, T., Dunlop, S.A., Beazley, L.D. 2007. Erythropoietin is both neuroprotective and neuroregenerative following optic nerve transection. Exp Neurol 205, 48-55

Kirino, T., Tsujita, Y., Tamura, A. 1991. Induced tolerance to ischemia in gerbil hippocampal neurons. J Cereb Blood Flow Metab 11, 299-307

Kirkeby, A., van Beek, J., Nielsen, J., Leist, M., Helboe, L. 2007. Functional and immunochemical characterisation of different antibodies against the erythropoietin receptor. J Neurosci Methods 164, 50-58

Kitamura, K., Kangawa, K., Kawamoto, M., Ichiki, Y., Nakamura, S., Matsuo, H., Eto, T. 1993. Adrenomedullin: a novel hypotensive peptide isolated from human pheochromocytoma. Biochem Biophys Res Commun 192, 553-560

Klein, R., Cruickshanks, K.J., Nash, S.D., Krantz, E.M., Javier Nieto, F., Huang, G.H., Pankow, J.S., Klein, B.E. 2010. The prevalence of age-related macular degeneration and associated risk factors. Arch Ophthalmol 128, 750-758

Klenchin, V.A., Calvert, P.D., Bownds, M.D. 1995. Inhibition of rhodopsin kinase by recoverin. Further evidence for a negative feedback system in phototransduction. J Biol Chem 270, 16147-16152

Kodjikian, L., Souied, E.H., Mimoun, G., Mauget-Faysse, M., Behar-Cohen, F., Decullier, E., Huot, L., Aulagner, G. 2013. Ranibizumab versus Bevacizumab for Neovascular Age-related Macular Degeneration: Results from the GEFAL Noninferiority Randomized Trial. Ophthalmology

Kofuji, P., Biedermann, B., Siddharthan, V., Raap, M., Iandiev, I., Milenkovic, I., Thomzig, A., Veh, R.W., Bringmann, A., Reichenbach, A. 2002. Kir potassium channel subunit expression in retinal glial cells: implications for spatial potassium buffering. Glia 39, 292-303

Kohno, T., Inomata, H., Taniguchi, Y. 1982. Identification of microglia cell of the rat retina by light and electron microscopy. Jpn J Ophthalmol 26, 53-68

Kojima, I., Tanaka, T., Inagi, R., Kato, H., Yamashita, T., Sakiyama, A., Ohneda, O., Takeda, N., Sata, M., Miyata, T. 2007. Protective role of hypoxia-inducible factor-2α against ischemic damage and oxidative stress in the kidney. Journal of the American Society of Nephrology 18, 1218-1226

Kotch, L.E., Iyer, N.V., Laughner, E., Semenza, G.L. 1999. Defective vascularization of HIF-1alpha-null embryos is not associated with VEGF deficiency but with mesenchymal cell death. Dev Biol 209, 254-267

Koury, M.J., Bondurant, M.C. 1988. Maintenance by erythropoietin of viability and maturation of murine erythroid precursor cells. J Cell Physiol 137, 65-74

Koury, S.T., Bondurant, M.C., Semenza, G.L., Koury, M.J. 1993. The use of in situ hybridization to study erythropoietin gene expression in murine kidney and liver. Microsc Res Tech 25, 29-39

Kraft, T.W., Schneeweis, D.M., Schnapf, J.L. 1993. Visual transduction in human rod photoreceptors. J Physiol 464, 747-765

Kretz, A., Happold, C.J., Marticke, J.K., Isenmann, S. 2005. Erythropoietin promotes regeneration of adult CNS neurons via Jak2/Stat3 and PI3K/AKT pathway activation. Mol Cell Neurosci 29, 569-579

Kretz, A., Kugler, S., Happold, C., Bahr, M., Isenmann, S. 2004. Excess Bcl-XL increases the intrinsic growth potential of adult CNS neurons in vitro. Mol Cell Neurosci 26, 63-74

Krugel, K., Wurm, A., Linnertz, R., Pannicke, T., Wiedemann, P., Reichenbach, A., Bringmann, A. 2010. Erythropoietin inhibits osmotic swelling of retinal glial cells by Janus kinase- and extracellular signal-regulated kinases1/2-mediated release of vascular endothelial growth factor. Neuroscience 165, 1147-1158

Kubota, Y., Hirashima, M., Kishi, K., Stewart, C.L., Suda, T. 2008. Leukemia inhibitory factor regulates microvessel density by modulating oxygen-dependent VEGF expression in mice. J Clin Invest 118, 2393-2403

Kuhn, H., Wilden, U. 1987. Deactivation of photoactivated rhodopsin by rhodopsin-kinase and arrestin. J Recept Res 7, 283-298

Kur, J., Newman, E.A., Chan-Ling, T. 2012. Cellular and physiological mechanisms underlying blood flow regulation in the retina and choroid in health and disease. Prog Retin Eye Res 31, 377-406

Kurihara, T., Kubota, Y., Ozawa, Y., Takubo, K., Noda, K., Simon, M.C., Johnson, R.S., Suematsu, M., Tsubota, K., Ishida, S., Goda, N., Suda, T., Okano, H. 2010. von Hippel-Lindau protein regulates transition from the fetal to the adult circulatory system in retina. Development 137, 1563-1571

Kurz, T., Terman, A., Gustafsson, B., Brunk, U.T. 2008. Lysosomes and oxidative stress in aging and apoptosis. Biochim Biophys Acta 1780, 1291-1303

Lagali, P.S., Balya, D., Awatramani, G.B., Munch, T.A., Kim, D.S., Busskamp, V., Cepko, C.L., Roska, B. 2008. Light-activated channels targeted to ON bipolar cells restore visual function in retinal degeneration. Nat Neurosci 11, 667-675

Lahdenranta, J., Pasqualini, R., Schlingemann, R.O., Hagedorn, M., Stallcup, W.B., Bucana, C.D., Sidman, R.L., Arap, W. 2001. An anti-angiogenic state in mice and humans with retinal photoreceptor cell degeneration. Proc Natl Acad Sci U S A 98, 10368-10373

Lam, S.Y., Tipoe, G.L., Fung, M.L. 2009. Upregulation of erythropoietin and its receptor expression in the rat carotid body during chronic and intermittent hypoxia. Adv Exp Med Biol 648, 207-214

Lam, S.Y., Tipoe, G.L., Liong, E.C., Fung, M.L. 2008. Differential expressions and roles of hypoxia-inducible factor-1alpha, -2alpha and -3alpha in the rat carotid body during chronic and intermittent hypoxia. Histol Histopathol 23, 271-280

Lamb, T.D., Pugh, E.N.J. 2004. Dark adaptation and the retinoid cycle of vision. Prog Retin Eye Res 23, 307-380

Lando, D., Peet, D.J., Gorman, J.J., Whelan, D.A., Whitelaw, M.L., Bruick, R.K. 2002a. FIH-1 is an asparaginyl hydroxylase enzyme that regulates the transcriptional activity of hypoxia-inducible factor. Genes Dev 16, 1466-1471

Lando, D., Peet, D.J., Whelan, D.A., Gorman, J.J., Whitelaw, M.L. 2002b. Asparagine hydroxylation of the HIF transactivation domain a hypoxic switch. Science 295, 858-861

Lange, C., Caprara, C., Tanimoto, N., Beck, S., Huber, G., Samardzija, M., Seeliger, M., Grimm, C. 2010. Retina specific activation of a sustained hypoxia-like response leads to severe retinal degeneration and loss of vision. Neurobiol Dis

Lange, C., Caprara, C., Tanimoto, N., Beck, S., Huber, G., Samardzija, M., Seeliger, M., Grimm, C. 2011a. Retina-specific activation of a sustained hypoxia-like response leads to severe retinal degeneration and loss of vision. Neurobiol Dis 41, 119-130

Lange, C., Heynen, S.R., Tanimoto, N., Thiersch, M., Le, Y.Z., Meneau, I., Seeliger, M.W., Samardzija, M., Caprara, C., Grimm, C. 2011b. Normoxic activation of hypoxia inducible factors in photoreceptors provides transient protection against light induced retinal degeneration. Invest Ophthalmol Vis Sci

Lange, J., Yafai, Y., Noack, A., Yang, X.M., Munk, A.B., Krohn, S., Iandiev, I., Wiedemann, P., Reichenbach, A., Eichler, W. 2012. The axon guidance molecule Netrin-4 is expressed by Muller cells and contributes to angiogenesis in the retina. Glia 60, 1567-1578

LaVail, M.M. 1976. Rod outer segment disc shedding in relation to cyclic lighting. Exp Eye Res 23, 277-280

LaVail, M.M. 1983. Outer segment disc shedding and phagocytosis in the outer retina. Trans Ophthalmol Soc U K 103, 397-404

Le, Y.Z., Zheng, L., Zheng, W., Ash, J.D., Agbaga, M.P., Zhu, M., Anderson, R.E. 2006. Mouse opsin promoter-directed Cre recombinase expression in transgenic mice. Mol Vis 12, 389-398

Lei, X., Zhang, J., Shen, J., Hu, L.M., Wu, Y., Mou, L., Xu, G., Li, W., Xu, G.T. 2011. EPO attenuates inflammatory cytokines by Muller cells in diabetic retinopathy. Front Biosci (Elite Ed) 3, 201-211

Leibovic, K.N., Pan, K.Y. 1994. The saturated response of vertebrate rods and its relation to cGMP metabolism. Brain Res 653, 325-329

Leist, M., Ghezzi, P., Grasso, G., Bianchi, R., Villa, P., Fratelli, M., Savino, C., Bianchi, M., Nielsen, J., Gerwien, J., Kallunki, P., Larsen, A.K., Helboe, L., Christensen, S., Pedersen, L.O., Nielsen, M., Torup, L., Sager, T., Sfacteria, A., Erbayraktar, S., Erbayraktar, Z., Gokmen, N., Yilmaz, O., Cerami-Hand, C., Xie, Q.W., Coleman, T., Cerami, A., Brines, M. 2004. Derivatives of erythropoietin that are tissue protective but not erythropoietic. Science 305, 239-242

Leskov, I.B., Klenchin, V.A., Handy, J.W., Whitlock, G.G., Govardovskii, V.I., Bownds, M.D., Lamb, T.D., Pugh, E.N.J., Arshavsky, V.Y. 2000. The gain of rod phototransduction: reconciliation of biochemical and electrophysiological measurements. Neuron 27, 525-537

Levine, E.M., Green, E.S. 2004. Cell-intrinsic regulators of proliferation in vertebrate retinal progenitors. Seminars in cell & developmental biology 15(1), 63-74

Lewczuk, P., Hasselblatt, M., Kamrowski-Kruck, H., Heyer, A., Unzicker, C., Siren, A.L., Ehrenreich, H. 2000. Survival of hippocampal neurons in culture upon hypoxia: effect of erythropoietin. Neuroreport 11, 3485-3488

Li, Y., Lu, Z., Keogh, C.L., Yu, S.P., Wei, L. 2007. Erythropoietin-induced neurovascular protection, angiogenesis, and cerebral blood flow restoration after focal ischemia in mice. J Cereb Blood Flow Metab 27, 1043-1054

Li, Y.N., Pinzon-Duarte, G., Dattilo, M., Claudepierre, T., Koch, M., Brunken, W.J. 2012. The expression and function of netrin-4 in murine ocular tissues. Exp Eye Res 96, 24-35

Lin, M., Chen, Y., Jin, J., Hu, Y., Zhou, K.K., Zhu, M., Le, Y.Z., Ge, J., Johnson, R.S., Ma, J.X. 2011. Ischaemia-induced retinal neovascularisation and diabetic retinopathy in mice with conditional knockout of hypoxia-inducible factor-1 in retinal Muller cells. Diabetologia

Lindblom, P., Gerhardt, H., Liebner, S., Abramsson, A., Enge, M., Hellstrom, M., Backstrom, G., Fredriksson, S., Landegren, U., Nystrom, H.C., Bergstrom, G., Dejana, E., Ostman, A., Lindahl, P., Betsholtz, C. 2003. Endothelial PDGF-B retention is required for proper investment of pericytes in the microvessel wall. Genes Dev 17, 1835-1840

Ling, T.L., Mitrofanis, J., Stone, J. 1989. Origin of retinal astrocytes in the rat: evidence of migration from the optic nerve. J Comp Neurol 286, 345-352

Linsenmeier, R.A. 1986. Effects of light and darkness on oxygen distribution and consumption in the cat retina. J Gen Physiol 88, 521-542

Livesey, F.J. 1999. Netrins and netrin receptors. Cell Mol Life Sci 56, 62-68

Livnah, O., Stura, E.A., Middleton, S.A., Johnson, D.L., Jolliffe, L.K., Wilson, I.A. 1999. Crystallographic evidence for preformed dimers of erythropoietin receptor before ligand activation. Science 283, 987-990

Loboda, A., Jozkowicz, A., Dulak, J. 2010. HIF-1 and HIF-2 transcription factors--similar but not identical. Mol Cells 29, 435-442

Loos, B., Engelbrecht, A.M. 2009. Cell death: a dynamic response concept. Autophagy 5, 590-603

Luche, H., Weber, O., Nageswara Rao, T., Blum, C., Fehling, H.J. 2007. Faithful activation of an extra-bright red fluorescent protein in "knock-in" Cre-reporter mice ideally suited for lineage tracing studies. Eur J Immunol 37, 43-53

Luhmann, U.F., Lin, J., Acar, N., Lammel, S., Feil, S., Grimm, C., Seeliger, M.W., Hammes, H.P., Berger, W. 2005. Role of the Norrie disease pseudoglioma gene in sprouting angiogenesis during development of the retinal vasculature. Invest Ophthalmol Vis Sci 46, 3372-3382

Lund, R.D., Ono, S.J., Keegan, D.J., Lawrence, J.M. 2003. Retinal transplantation: progress and problems in clinical application. J Leukoc Biol 74, 151-160

Ma, J., Norton, J.C., Allen, A.C., Burns, J.B., Hasel, K.W., Burns, J.L., Sutcliffe, J.G., Travis, G.H. 1995. Retinal degeneration slow (rds) in mouse results from simple insertion of at haplotype-specific element into protein-coding exon II. Genomics 28, 212-219

Madisen, L., Zwingman, T.A., Sunkin, S.M., Oh, S.W., Zariwala, H.A., Gu, H., Ng, L.L., Palmiter, R.D., Hawrylycz, M.J., Jones, A.R., Lein, E.S., Zeng, H. 2010. A robust and high-throughput Cre reporting and characterization system for the whole mouse brain. Nat Neurosci 13, 133-140

Maeda, T., Imanishi, Y., Palczewski, K. 2003. Rhodopsin phosphorylation: 30 years later. Prog Retin Eye Res 22, 417-434

Magalhaes, M.M., Coimbra, A. 1970. Electron microscope radioautographic study of glycogen synthesis in the rabbit retina. J Cell Biol 47, 263-275

Magistretti, P.J., Pellerin, L. 1999. Cellular mechanisms of brain energy metabolism and their relevance to functional brain imaging. Philos Trans R Soc Lond B Biol Sci 354, 1155-1163

Mahon, P.C., Hirota, K., Semenza, G.L. 2001. FIH-1: a novel protein that interacts with HIF-1alpha and VHL to mediate repression of HIF-1 transcriptional activity. Genes Dev 15, 2675-2686

Maisonpierre, P.C., Suri, C., Jones, P.F., Bartunkova, S., Wiegand, S.J., Radziejewski, C., Compton, D., McClain, J., Aldrich, T.H., Papadopoulos, N., Daly, T.J., Davis, S., Sato, T.N., Yancopoulos, G.D. 1997. Angiopoietin-2, a natural antagonist for Tie2 that disrupts in vivo angiogenesis. Science 277, 55-60

Majmundar, A.J., Wong, W.J., Simon, M.C. 2010. Hypoxia-inducible factors and the response to hypoxic stress. Mol Cell 40, 294-309

Makarov, F.N., Hollender, H., Stone, J. 2000. The structure of interrelationships between neuroglial and ganglion cells in the retina. Neurosci Behav Physiol 30, 707-711

Makino, Y., Cao, R., Svensson, K., Bertilsson, G., Asman, M., Tanaka, H., Cao, Y., Berkenstam, A., Poellinger, L. 2001. Inhibitory PAS domain protein is a negative regulator of hypoxia-inducible gene expression. Nature 414, 550-554

Makino, Y., Kanopka, A., Wilson, W.J., Tanaka, H., Poellinger, L. 2002. Inhibitory PAS domain protein (IPAS) is a hypoxia-inducible splicing variant of the hypoxia-inducible factor-3alpha locus. J Biol Chem 277, 32405-32408

Maltepe, E., Keith, B., Arsham, A.M., Brorson, J.R., Simon, M.C. 2000. The role of ARNT2 in tumor angiogenesis and the neural response to hypoxia. Biochem Biophys Res Commun 273, 231-238

Maltepe, E., Schmidt, J.V., Baunoch, D., Bradfield, C.A., Simon, M.C. 1997. Abnormal angiogenesis and responses to glucose and oxygen deprivation in mice lacking the protein ARNT. Nature 386, 403-407

Mandl, M., Kapeller, B., Lieber, R., Macfelda, K. 2013. Hypoxia-inducible factor-1β (HIF-1β) is upregulated in a HIF-1α-dependent manner in 518A2 human melanoma cells under hypoxic conditions. Biochemical and biophysical …

Marcaggi, P., Coles, J.A. 2001. Ammonium in nervous tissue: transport across cell membranes, fluxes from neurons to glial cells, and role in signalling. Prog Neurobiol 64, 157-183

Maricq, A.V., Korenbrot, J.I. 1990. Potassium currents in the inner segment of single retinal cone photoreceptors. J Neurophysiol 64, 1929-1940

Marquardt, T., Ashery-Padan, R., Andrejewski, N., Scardigli, R., Guillemot, F., Gruss, P. 2001. Pax6 is required for the multipotent state of retinal progenitor cells. Cell 105, 43-55

Marzo, F., Lavorgna, A., Coluzzi, G., Santucci, E., Tarantino, F., Rio, T., Conti, E., Autore, C., Agati, L., Andreotti, F. 2008. Erythropoietin in heart and vessels: focus on transcription and signalling pathways. J Thromb Thrombolysis 26, 183-187

Masland, R.H. 2001. The fundamental plan of the retina. Nat Neurosci 4, 877-886

Masland, R.H. 2012. The neuronal organization of the retina. Neuron 76, 266-280

Masuda, S., Nagao, M., Takahata, K., Konishi, Y., Gallyas, F.J., Tabira, T., Sasaki, R. 1993. Functional erythropoietin receptor of the cells with neural characteristics. Comparison with receptor properties of erythroid cells. J Biol Chem 268, 11208-11216

Maxwell, P.H., Pugh, C.W., Ratcliffe, P.J. 2001. Activation of the HIF pathway in cancer. Curr Opin Genet Dev 11, 293-299

Maxwell, P.H., Wiesener, M.S., Chang, G.W., Clifford, S.C., Vaux, E.C., Cockman, M.E., Wykoff, C.C., Pugh, C.W., Maher, E.R., Ratcliffe, P.J. 1999. The tumour suppressor protein VHL targets hypoxia-inducible factors for oxygen-dependent proteolysis. Nature 399, 271-275

Mayhew, T.M., Astle, D. 1997. Photoreceptor number and outer segment disk membrane surface area in the retina of the rat: stereological data for whole organ and average photoreceptor cell. J Neurocytol 26, 53-61

Maynard, S.E., Min, J.-Y., Merchan, J., Lim, K.-H., Li, J., Mondal, S., Libermann, T.A., Morgan, J.P., Sellke, F.W., Stillman, I.E. 2003. Excess placental soluble fms-like tyrosine kinase 1 (sFlt1) may contribute to endothelial dysfunction, hypertension, and proteinuria in preeclampsia. Journal of Clinical Investigation 111, 649-658

McNeill, L.A., Hewitson, K.S., Claridge, T.D., Seibel, J.F., Horsfall, L.E., Schofield, C.J. 2002a. Hypoxia-inducible factor asparaginyl hydroxylase (FIH-1) catalyses hydroxylation at the beta-carbon of asparagine-803. Biochem J 367, 571-575

McNeill, L.A., Hewitson, K.S., Gleadle, J.M., Horsfall, L.E., Oldham, N.J., Maxwell, P.H., Pugh, C.W., Ratcliffe, P.J., Schofield, C.J. 2002b. The use of dioxygen by HIF prolyl hydroxylase (PHD1). Bioorg Med Chem Lett 12, 1547-1550

Menger, N.I.C.O.L.E., Wassle, H. 2000. Morphological and physiological properties of the A17 amacrine cell of the rat retina. Visual neuroscience 17, 769-780

Merigan, W.H. 1989. Chromatic and achromatic vision of macaques: role of the P pathway. J Neurosci 9, 776-783

Merigan, W.H., Katz, L.M., Maunsell, J.H. 1991. The effects of parvocellular lateral geniculate lesions on the acuity and contrast sensitivity of macaque monkeys. J Neurosci 11, 994-1001

Metelitsina, T.I., Grunwald, J.E., DuPont, J.C., Ying, G.S., Brucker, A.J., Dunaief, J.L. 2008. Foveolar choroidal circulation and choroidal neovascularization in age-related macular degeneration. Invest Ophthalmol Vis Sci 49, 358-363

Millauer, B., Wizigmann-Voos, S., Schnurch, H., Martinez, R., Moller, N.P., Risau, W., Ullrich, A. 1993. High affinity VEGF binding and developmental expression suggest Flk-1 as a major regulator of vasculogenesis and angiogenesis. Cell 72, 835-846

Miller, J.W., Adamis, A.P., Shima, D.T., D'Amore, P.A., Moulton, R.S., O'Reilly, M.S., Folkman, J., Dvorak, H.F., Brown, L.F., Berse, B., et, a. 1994. Vascular endothelial growth factor/vascular permeability factor is temporally and spatially correlated with ocular angiogenesis in a primate model. Am J Pathol 145, 574-584

Min, Y., Ghose, S., Boelte, K., Li, J., Yang, L., Lin, P.C. 2011. C/EBP-δ regulates VEGF-C autocrine signaling in lymphangiogenesis and metastasis of lung cancer through HIF-1α. Oncogene 30, 4901-4909

Mink, J.W., Blumenschine, R.J., Adams, D.B. 1981. Ratio of central nervous system to body metabolism in vertebrates: its constancy and functional basis. Am J Physiol 241, R203-12

Morishita, E., Masuda, S., Nagao, M., Yasuda, Y., Sasaki, R. 1997. Erythropoietin receptor is expressed in rat hippocampal and cerebral cortical neurons, and erythropoietin prevents in vitro glutamate-induced neuronal death. Neuroscience 76, 105-116

Morita, M., Ohneda, O., Yamashita, T., Takahashi, S., Suzuki, N., Nakajima, O., Kawauchi, S., Ema, M., Shibahara, S., Udono, T., Tomita, K., Tamai, M., Sogawa, K., Yamamoto, M., Fujii-Kuriyama, Y. 2003. HLF/HIF-2alpha is a key factor in retinopathy of prematurity in association with erythropoietin. EMBO J 22, 1134-1146

Mowat, F.M., Luhmann, U.F., Smith, A.J., Lange, C., Duran, Y., Harten, S., Shukla, D., Maxwell, P.H., Ali, R.R., Bainbridge, J.W. 2010. HIF-1alpha and HIF-2alpha are differentially activated in distinct cell populations in retinal ischaemia. PLoS One 5, e11103

Munch, M., Kawasaki, A. 2013. Intrinsically photosensitive retinal ganglion cells: classification, function and clinical implications. Curr Opin Neurol 26, 45-51

Mustafi, D., Engel, A.H., Palczewski, K. 2009. Structure of cone photoreceptors. Prog Retin Eye Res 28, 289-302

Muzumdar, M.D., Tasic, B., Miyamichi, K., Li, L., Luo, L. 2007. A global double-fluorescent Cre reporter mouse. Genesis 45, 593-605

Naarendorp, F., Esdaille, T.M., Banden, S.M., Andrews-Labenski, J., Gross, O.P., Pugh, E.N.J. 2010. Dark light, rod saturation, and the absolute and incremental sensitivity of mouse cone vision. J Neurosci 30, 12495-12507

Naash, M.I., Hollyfield, J.G., al-Ubaidi, M.R., Baehr, W. 1993. Simulation of human autosomal dominant retinitis pigmentosa in transgenic mice expressing a mutated murine opsin gene. Proc Natl Acad Sci U S A 90, 5499-5503

Nadam, J., Navarro, F., Sanchez, P., Moulin, C., Georges, B., Laglaine, A., Pequignot, J.M., Morales, A., Ryvlin, P., Bezin, L. 2007. Neuroprotective effects of erythropoietin in the rat hippocampus after pilocarpine-induced status epilepticus. Neurobiol Dis 25, 412-426

Nagao, M., Masuda, S., Abe, S., Ueda, M., Sasaki, R. 1992. Production and ligand-binding characteristics of the soluble form of murine erythropoietin receptor. Biochem Biophys Res Commun 188, 888-897

Nakamura-Ishizu, A., Kurihara, T., Okuno, Y., Ozawa, Y., Kishi, K., Goda, N., Tsubota, K., Okano, H., Suda, T., Kubota, Y. 2012. The formation of an angiogenic astrocyte template is regulated by the neuroretina in a HIF-1-dependent manner. Dev Biol 363, 106-114

Nawy, S., Jahr, C.E. 1991. cGMP-gated conductance in retinal bipolar cells is suppressed by the photoreceptor transmitter. Neuron 7, 677-683

Neckers, L., Ivy, S.P. 2003. Heat shock protein 90. Curr Opin Oncol 15, 419-424

Neubauer, H., Cumano, A., Muller, M., Wu, H., Huffstadt, U., Pfeffer, K. 1998. Jak2 deficiency defines an essential developmental checkpoint in definitive hematopoiesis. Cell 93, 397-409

Neumann, C.J., Nuesslein-Volhard, C. 2000. Patterning of the zebrafish retina by a wave of sonic hedgehog activity. Science 289, 2137-2139

Newman, E.A. 1994. A physiological measure of carbonic anhydrase in Muller cells. Glia 11, 291-299

Nimmerjahn, A., Kirchhoff, F., Helmchen, F. 2005. Resting microglial cells are highly dynamic surveillants of brain parenchyma in vivo. Science 308, 1314-1318

Noguchi, C.T., Wang, L., Rogers, H.M., Teng, R., Jia, Y. 2008. Survival and proliferative roles of erythropoietin beyond the erythroid lineage. Expert Rev Mol Med 10, e36

Nomura, A., Shigemoto, R., Nakamura, Y., Okamoto, N., Mizuno, N., Nakanishi, S. 1994. Developmentally regulated postsynaptic localization of a metabotropic glutamate receptor in rat rod bipolar cells. Cell 77, 361-369

Novak, A., Guo, C., Yang, W., Nagy, A., Lobe, C.G. 2000. Z/EG, a double reporter mouse line that expresses enhanced green fluorescent protein upon Cre-mediated excision. Genesis 28, 147-155

Obara, N., Suzuki, N., Kim, K., Nagasawa, T., Imagawa, S., Yamamoto, M. 2008. Repression via the GATA box is essential for tissue-specific erythropoietin gene expression. Blood 111, 5223-5232

Oehmichen, M. 1982. Are resting and/or reactive microglia macrophages? Immunobiology 161, 246-254

Ohlmann, A., Tamm, E.R. 2012. Norrin: molecular and functional properties of an angiogenic and neuroprotective growth factor. Prog Retin Eye Res 31, 243-257

Okawa, H., Sampath, A.P., Laughlin, S.B., Fain, G.L. 2008. ATP consumption by mammalian rod photoreceptors in darkness and in light. Curr Biol 18, 1917-1921

Ozaki, H., Yu, A.Y., Della, N., Ozaki, K., Luna, J.D., Yamada, H., Hackett, S.F., Okamoto, N., Zack, D.J., Semenza, G.L., Campochiaro, P.A. 1999. Hypoxia inducible factor-1alpha is increased in ischemic retina: temporal and spatial correlation with VEGF expression. Invest Ophthalmol Vis Sci 40, 182-189

Parsa, C.J., Matsumoto, A., Kim, J., Riel, R.U., Pascal, L.S., Walton, G.B., Thompson, R.B., Petrofski, J.A., Annex, B.H., Stamler, J.S., Koch, W.J. 2003. A novel protective effect of erythropoietin in the infarcted heart. J Clin Invest 112, 999-1007

Pasanen, A., Heikkila, M., Rautavuoma, K., Hirsila, M., Kivirikko, K.I., Myllyharju, J. 2010. Hypoxia-inducible factor (HIF)-3alpha is subject to extensive alternative splicing in human tissues and cancer cells and is regulated by HIF-1 but not HIF-2. Int J Biochem Cell Biol 42, 1189-1200

Patel, N.S., Sharples, E.J., Cuzzocrea, S., Chatterjee, P.K., Britti, D., Yaqoob, M.M., Thiemermann, C. 2004. Pretreatment with EPO reduces the injury and dysfunction caused by ischemia/reperfusion in the mouse kidney in vivo. Kidney Int 66, 983-989

Patnaik, M.M., Tefferi, A. 2009. The complete evaluation of erythrocytosis: congenital and acquired. Leukemia 23, 834-844

Peichl, L. 2005. Diversity of mammalian photoreceptor properties: adaptations to habitat and lifestyle? Anat Rec A Discov Mol Cell Evol Biol 287, 1001-1012

Pellerin, L., Bouzier-Sore, A.K., Aubert, A., Serres, S., Merle, M., Costalat, R., Magistretti, P.J. 2007. Activity-dependent regulation of energy metabolism by astrocytes: an update. Glia 55, 1251-1262

Peng, J., Zhang, L., Drysdale, L., Fong, G.H. 2000. The transcription factor EPAS-1/hypoxia-inducible factor 2alpha plays an important role in vascular remodeling. Proc Natl Acad Sci U S A 97, 8386-8391

Peng, Y.W., Blackstone, C.D., Huganir, R.L., Yau, K.W. 1995. Distribution of glutamate receptor subtypes in the vertebrate retina. Neuroscience 66, 483-497

Penn, J.S., Li, S., Naash, M.I. 2000. Ambient hypoxia reverses retinal vascular attenuation in a transgenic mouse model of autosomal dominant retinitis pigmentosa. Invest Ophthalmol Vis Sci 41, 4007-4013

Pepperberg, D.R., Lurie, M., Brown, P.K., Dowling, J.E. 1976. Visual adaptation: effects of externally applied retinal on the light-adapted, isolated skate retina. Science 191, 394-396

Perez, M.-T.R., Caminos, E. 1995. Expression of brain-derived neurotrophic factor and of its functional receptor in neonatal and adult rat retina. Neuroscience letters 183, 96-99

Pfeiffer-Guglielmi, B., Francke, M., Reichenbach, A., Fleckenstein, B., Jung, G., Hamprecht, B. 2005. Glycogen phosphorylase isozyme pattern in mammalian retinal Muller (glial) cells and in astrocytes of retina and optic nerve. Glia 49, 84-95

Pierce, E.A., Avery, R.L., Foley, E.D., Aiello, L.P., Smith, L.E. 1995. Vascular endothelial growth factor/vascular permeability factor expression in a mouse model of retinal neovascularization. Proc Natl Acad Sci U S A 92, 905-909

Pierce, E.A., Foley, E.D., Smith, L.E. 1996. Regulation of vascular endothelial growth factor by oxygen in a model of retinopathy of prematurity. Arch Ophthalmol 114, 1219-1228

Poitry-Yamate, C.L., Poitry, S., Tsacopoulos, M. 1995. Lactate released by Muller glial cells is metabolized by photoreceptors from mammalian retina. J Neurosci 15, 5179-5191

Portera-Cailliau, C., Sung, C.H., Nathans, J., Adler, R. 1994. Apoptotic photoreceptor cell death in mouse models of retinitis pigmentosa. Proc Natl Acad Sci U S A 91, 974-978

Pournaras, C.J., Riva, C.E., Tsacopoulos, M., Strommer, K. 1989. Diffusion of O2 in the retina of anesthetized miniature pigs in normoxia and hyperoxia. Exp Eye Res 49, 347-360

Pournaras, C.J., Rungger-Brandle, E., Riva, C.E., Hardarson, S.H., Stefansson, E. 2008. Regulation of retinal blood flow in health and disease. Prog Retin Eye Res 27, 284-330

Pow, D.V., Crook, D.K. 1995. Immunocytochemical evidence for the presence of high levels of reduced glutathione in radial glial cells and horizontal cells in the rabbit retina. Neurosci Lett 193, 25-28

Powell, W.H., Hahn, M.E. 2002. Identification and functional characterization of hypoxia-inducible factor 2alpha from the estuarine teleost, Fundulus heteroclitus: interaction of HIF-2alpha with two ARNT2 splice variants. J Exp Zool 294, 17-29

Provis, J.M. 2001. Development of the primate retinal vasculature. Prog Retin Eye Res 20, 799-821

Puri, M.C., Rossant, J., Alitalo, K., Bernstein, A., Partanen, J. 1995. The receptor tyrosine kinase TIE is required for integrity and survival of vascular endothelial cells. EMBO J 14, 5884-5891

Quigley, H.A., Broman, A.T. 2006. The number of people with glaucoma worldwide in 2010 and 2020. Br J Ophthalmol 90, 262-267

Quillen, D.A. 1999. Common causes of vision loss in elderly patients. American Family Physician 60, 99

Rafferty, C.N. 1977. Spectral studies on the conformation of rhodopsin. Biophys Struct Mech 3, 123-126

Ranchon Cole, I., Bonhomme, B., Doly, M. 2007. Pre-treatment of adult rats with high doses of erythropoietin induces caspase-9 but prevents light-induced retinal injury. Exp Eye Res 85, 782-789

Rankin, E.B., Biju, M.P., Liu, Q., Unger, T.L., Rha, J., Johnson, R.S., Simon, M.C., Keith, B., Haase, V.H. 2007. Hypoxia-inducible factor-2 (HIF-2) regulates hepatic erythropoietin in vivo. J Clin Invest 117, 1068-1077

Rankin, E.B., Higgins, D.F., Walisser, J.A., Johnson, R.S., Bradfield, C.A., Haase, V.H. 2005. Inactivation of the arylhydrocarbon receptor nuclear translocator (Arnt) suppresses von Hippel-Lindau disease-associated vascular tumors in mice. Mol Cell Biol 25, 3163-3172

Reese, B.E. 2011. Development of the retina and optic pathway. Vision Res 51, 613-632

Rehm, H.L., Zhang, D.S., Brown, M.C., Burgess, B., Halpin, C., Berger, W., Morton, C.C., Corey, D.P., Chen, Z.Y. 2002. Vascular defects and sensorineural deafness in a mouse model of Norrie disease. J Neurosci 22, 4286-4292

Reichelt, W., Stabel-Burow, J., Pannicke, T., Weichert, H., Heinemann, U. 1997. The glutathione level of retinal Muller glial cells is dependent on the high-affinity sodium-dependent uptake of glutamate. Neuroscience 77, 1213-1224

Reichenbach, A., Stolzenburg, J.U., Eberhardt, W., Chao, T.I., Dettmer, D., Hertz, L. 1993. What do retinal muller (glial) cells do for their neuronal 'small siblings'? J Chem Neuroanat 6, 201-213

Reichenbach, A., Wurm, A., Pannicke, T., Iandiev, I., Wiedemann, P., Bringmann, A. 2007. Muller cells as players in retinal degeneration and edema. Graefes Arch Clin Exp Ophthalmol 245, 627-636

Renzi, M.J., Farrell, F.X., Bittner, A., Galindo, J.E., Morton, M., Trinh, H., Jolliffe, L.K. 2002. Erythropoietin induces changes in gene expression in PC-12 cells. Brain Res Mol Brain Res 104, 86-95

Reubold, T.F., Eschenburg, S. 2012. A molecular view on signal transduction by the apoptosome. Cellular signalling 24, 1420-1425

Rex, T.S., Allocca, M., Domenici, L., Surace, E.M., Maguire, A.M., Lyubarsky, A., Cellerino, A., Bennett, J., Auricchio, A. 2004. Systemic but not intraocular Epo gene transfer protects the retina from light-and genetic-induced degeneration. Mol Ther 10, 855-861

Rex, T.S., Wong, Y., Kodali, K., Merry, S. 2009. Neuroprotection of photoreceptors by direct delivery of erythropoietin to the retina of the retinal degeneration slow mouse. Exp Eye Res 89, 735-740

Reynolds, R., Rosner, B., Seddon, J.M. 2010. Serum lipid biomarkers and hepatic lipase gene associations with age-related macular degeneration. Ophthalmology 117, 1989-1995

Reza, H.M., Takahashi, Y., Yasuda, K. 2007. Stage-dependent expression of Pax6 in optic vesicle/cup regulates patterning genes through signaling molecules. Differentiation 75, 726-736

Ribatti, D., Vacca, A., Roccaro, A.M., Crivellato, E., Presta, M. 2003. Erythropoietin as an angiogenic factor. Eur J Clin Invest 33, 891-896

Ribatti, D., Presta, M., Vacca, A., Ria, R., Giuliani, R., Dell'Era, P., Nico, B., Roncali, L., Dammacco, F. 1999. Human erythropoietin induces a pro-angiogenic phenotype in cultured endothelial cells and stimulates neovascularization in vivo. Blood 93, 2627-2636

Richter, M., Gottanka, J., May, C.A., Welge-Lussen, U., Berger, W., Lutjen-Drecoll, E. 1998. Retinal vasculature changes in Norrie disease mice. Invest Ophthalmol Vis Sci 39, 2450-2457

Riepe, R.E., Norenburg, M.D. 1977. Muller cell localisation of glutamine synthetase in rat retina. Nature 268, 654-655

Rius, J., Guma, M., Schachtrup, C., Akassoglou, K., Zinkernagel, A.S., Nizet, V., Johnson, R.S., Haddad, G.G., Karin, M. 2008. NF-&kgr; B links innate immunity to the hypoxic response through transcriptional regulation of HIF-1&agr. Nature 453, 807-811

Roesch, K., Jadhav, A.P., Trimarchi, J.M., Stadler, M.B., Roska, B., Sun, B.B., Cepko, C.L. 2008. The transcriptome of retinal Muller glial cells. J Comp Neurol 509, 225-238

Rosenberg, E.A., Sperazza, L.A.U.R.A.C. 2008. The visually impaired patient. Am Fam Physician 77, 1431-1436

Roth, S., Li, B., Rosenbaum, P.S., Gupta, H., Goldstein, I.M., Maxwell, K.M., Gidday, J.M. 1998. Preconditioning provides complete protection against retinal ischemic injury in rats. Invest Ophthalmol Vis Sci 39, 777-785

Rousseau, B., Dubayle, D., Sennlaub, F., Jeanny, J.C., Costet, P., Bikfalvi, A., Javerzat, S. 2000. Neural and angiogenic defects in eyes of transgenic mice expressing a dominant-negative FGF receptor in the pigmented cells. Exp Eye Res 71, 395-404

Ruscher, K., Freyer, D., Karsch, M., Isaev, N., Megow, D., Sawitzki, B., Priller, J., Dirnagl, U., Meisel, A. 2002. Erythropoietin is a paracrine mediator of ischemic tolerance in the brain: evidence from an in vitro model. The Journal of neuroscience 22, 10291-10301

Ruschitzka, F.T., Wenger, R.H., Stallmach, T., Quaschning, T., de Wit, C., Wagner, K., Labugger, R., Kelm, M., Noll, G., Rulicke, T., Shaw, S., Lindberg, R.L., Rodenwaldt, B., Lutz, H., Bauer, C., Luscher, T.F., Gassmann, M. 2000. Nitric oxide prevents cardiovascular disease and determines survival in polyglobulic mice overexpressing erythropoietin. Proc Natl Acad Sci U S A 97, 11609-11613

Ryan, H.E., Lo, J., Johnson, R.S. 1998. HIF-1 alpha is required for solid tumor formation and embryonic vascularization. EMBO J 17, 3005-3015

Ryan, H.E., Poloni, M., McNulty, W., Elson, D., Gassmann, M., Arbeit, J.M., Johnson, R.S. 2000. Hypoxia-inducible factor-1alpha is a positive factor in solid tumor growth. Cancer Res 60, 4010-4015

Saari, J.C. 2012. Vitamin A metabolism in rod and cone visual cycles. Annu Rev Nutr 32, 125-145

Saint-Geniez, M., D'Amore, P.A. 2004. Development and pathology of the hyaloid, choroidal and retinal vasculature. Int J Dev Biol 48, 1045-1058

Sakanaka, M., Wen, T.C., Matsuda, S., Masuda, S., Morishita, E., Nagao, M., Sasaki, R. 1998. In vivo evidence that erythropoietin protects neurons from ischemic damage. Proc Natl Acad Sci U S A 95, 4635-4640

Samardzija, M., Neuhauss, S.C.F., Joly, S., Kurz-Levin, M., Grimm, C. 2010. Animal models for retinal degeneration. Animal Models for Retinal Diseases 46, 51-79

Samardzija, M., Wariwoda, H., Imsand, C., Huber, P., Heynen, S.R., Gubler, A., Grimm, C. 2012. Activation of survival pathways in the degenerating retina of rd10 mice. Exp Eye Res 99, 17-26

Samardzija, M., Wenzel, A., Aufenberg, S., Thiersch, M., Reme, C., Grimm, C. 2006. Differential role of Jak-STAT signaling in retinal degenerations. FASEB J 20, 2411-2413

Sandercoe, T.M., Geller, S.F., Hendrickson, A.E., Stone, J., Provis, J.M. 2003. VEGF expression by ganglion cells in central retina before formation of the foveal depression in monkey retina: evidence of developmental hypoxia. J Comp Neurol 462, 42-54

Santos, C.R.A., Martinho, A., Quintela, T., Gonçalves, I. 2012. Neuroprotective and neuroregenerative properties of metallothioneins. IUBMB life 64, 126-135

Sapieha, P., Sirinyan, M., Hamel, D., Zaniolo, K., Joyal, J.S., Cho, J.H., Honore, J.C., Kermorvant-Duchemin, E., Varma, D.R., Tremblay, S., Leduc, M., Rihakova, L., Hardy, P., Klein, W.H., Mu, X., Mamer, O., Lachapelle, P., Di Polo, A., Beausejour, C., Andelfinger, G., Mitchell, G., Sennlaub, F., Chemtob, S. 2008. The succinate receptor GPR91 in neurons has a major role in retinal angiogenesis. Nat Med 14, 1067-1076

Sarna, T. 1992. Properties and function of the ocular melanin--a photobiophysical view. J Photochem Photobiol B 12, 215-258

Sarthy, P.V. 1982. The uptake of [3H]gamma-aminobutyric acid by isolated glial (Muller) cells from the mouse retina. J Neurosci Methods 5, 77-82

Sarthy, P.V., Lam, D.M. 1978. Biochemical studies of isolated glial (Muller) cells from the turtle retina. J Cell Biol 78, 675-684

Sattler, M.B., Merkler, D., Maier, K., Stadelmann, C., Ehrenreich, H., Bahr, M., Diem, R. 2004. Neuroprotective effects and intracellular signaling pathways of erythropoietin in a rat model of multiple sclerosis. Cell Death Differ 11 Suppl 2, S181-92

Scheerer, N., Dunker, N., Imagawa, S., Yamamoto, M., Suzuki, N., Fandrey, J. 2010. The anemia of the newborn induces erythropoietin expression in the developing mouse retina. Am J Physiol Regul Integr Comp Physiol 299, R111-8

Schiller, P.H. 2010. Parallel information processing channels created in the retina. Proc Natl Acad Sci U S A 107, 17087-17094

Schiller, P.H., Logothetis, N.K., Charles, E.R. 1990. Functions of the colour-opponent and broad-band channels of the visual system. Nature 343, 68-70

Schnitzer, J. 1988a. Astrocytes in the guinea pig, horse, and monkey retina: their occurrence coincides with the presence of blood vessels. Glia 1, 74-89

Schnitzer, J. 1988b. Immunocytochemical studies on the development of astrocytes, Muller (glial) cells, and oligodendrocytes in the rabbit retina. Brain Res Dev Brain Res 44, 59-72

Schnitzer, J., Karschin, A. 1986. The shape and distribution of astrocytes in the retina of the adult rabbit. Cell Tissue Res 246, 91-102

Schonthaler, H.B., Lampert, J.M., Isken, A., Rinner, O., Mader, A., Gesemann, M., Oberhauser, V., Golczak, M., Biehlmaier, O., Palczewski, K., Neuhauss, S.C., von Lintig, J. 2007. Evidence for RPE65-independent vision in the cone-dominated zebrafish retina. Eur J Neurosci 26, 1940-1949

Schuetz, E., Thanos, S. 2004. Microglia-targeted pharmacotherapy in retinal neurodegenerative diseases. Curr Drug Targets 5, 619-627

Schutte, M., Werner, P. 1998. Redistribution of glutathione in the ischemic rat retina. Neurosci Lett 246, 53-56

Scortegagna, M., Ding, K., Oktay, Y., Gaur, A., Thurmond, F., Yan, L.J., Marck, B.T., Matsumoto, A.M., Shelton, J.M., Richardson, J.A., Bennett, M.J., Garcia, J.A. 2003a. Multiple organ pathology, metabolic abnormalities and impaired homeostasis of reactive oxygen species in Epas1-/- mice. Nat Genet 35, 331-340

Scortegagna, M., Ding, K., Zhang, Q., Oktay, Y., Bennett, M.J., Bennett, M., Shelton, J.M., Richardson, J.A., Moe, O., Garcia, J.A. 2005. HIF-2alpha regulates murine hematopoietic development in an erythropoietin-dependent manner. Blood 105, 3133-3140

Scortegagna, M., Morris, M.A., Oktay, Y., Bennett, M., Garcia, J.A. 2003b. The HIF family member EPAS1/HIF-2alpha is required for normal hematopoiesis in mice. Blood 102, 1634-1640

Seeliger, M.W., Beck, S.C., Pereyra-Munoz, N., Dangel, S., Tsai, J.Y., Luhmann, U.F., van de Pavert, S.A., Wijnholds, J., Samardzija, M., Wenzel, A., Zrenner, E., Narfstrom, K., Fahl, E., Tanimoto, N., Acar, N., Tonagel, F. 2005. In vivo confocal imaging of the retina in animal models using scanning laser ophthalmoscopy. Vision Res 45, 3512-3519

Seeliger, M.W., Grimm, C., Stahlberg, F., Friedburg, C., Jaissle, G., Zrenner, E., Guo, H., Reme, C.E., Humphries, P., Hofmann, F., Biel, M., Fariss, R.N., Redmond, T.M., Wenzel, A. 2001. New views on RPE65 deficiency: the rod system is the source of vision in a mouse model of Leber congenital amaurosis. Nat Genet 29, 70-74

Seki, M., Tanaka, T., Sakai, Y., Fukuchi, T., Abe, H., Nawa, H., Takei, N. 2005. Müller cells as a source of brain-derived neurotrophic factor in the retina: noradrenaline upregulates brain-derived neurotrophic factor levels in cultured rat Müller cells. Neurochemical research 30, 1163-1170

Semenza, G.L. 2000. Surviving ischemia: adaptive responses mediated by hypoxia-inducible factor 1. J Clin Invest 106, 809-812

Semenza, G.L. 2001. HIF-1 and mechanisms of hypoxia sensing. Curr Opin Cell Biol 13, 167-171

Semenza, G.L., Koury, S.T., Nejfelt, M.K., Gearhart, J.D., Antonarakis, S.E. 1991. Cell-type-specific and hypoxia-inducible expression of the human erythropoietin gene in transgenic mice. Proc Natl Acad Sci U S A 88, 8725-8729

Semenza, G.L., Wang, G.L. 1992. A nuclear factor induced by hypoxia via de novo protein synthesis binds to the human erythropoietin gene enhancer at a site required for transcriptional activation. Mol Cell Biol 12, 5447-5454

Sennlaub, F., Courtois, Y., Goureau, O. 2001. Inducible nitric oxide synthase mediates the change from retinal to vitreal neovascularization in ischemic retinopathy. Journal of Clinical Investigation 107, 717-725

Shakib, M., Cunha-Vaz, J.G. 1966. Studies on the permeability of the blood-retinal barrier. IV. Junctional complexes of the retinal vessels and their role in the permeability of the blood-retinal barrier. Exp Eye Res 5, 229-234

Shang, Y.C., Chong, Z.Z., Wang, S., Maiese, K. 2011a. Erythropoietin and Wnt1 govern pathways of mTOR, Apaf-1, and XIAP in inflammatory microglia. Current neurovascular research 8, 270

Shang, Y.C., Chong, Z.Z., Wang, S., Maiese, K. 2011b. Erythropoietin and Wnt1 govern pathways of mTOR, Apaf-1, and XIAP in inflammatory microglia. Curr Neurovasc Res 8, 270-285

Sharma, R.K., Ehinger, B.E.J. 2003. Development and structure of the retina. Kaufman, P.L., Alm, A., Adler's Physiology of the Eye. Mosby, St. Louis, 319-347

Shen, J., Wu, Y., Xu, J.Y., Zhang, J., Sinclair, S.H., Yanoff, M., Xu, G., Li, W., Xu, G.T. 2010. ERK- and Akt-dependent neuroprotection by erythropoietin (EPO) against glyoxal-AGEs via modulation of Bcl-xL, Bax, and BAD. Invest Ophthalmol Vis Sci 51, 35-46

Shimizu, S., Eguchi, Y., Kamiike, W., Itoh, Y., Hasegawa, J.-, Yamabe, K., Otsuki, Y., Matsuda, H., Tsujimoto, Y. 1996. Induction of apoptosis as well as necrosis by hypoxia and predominant prevention of apoptosis by Bcl-2 and Bcl-XL. Cancer research 56, 2161-2166

Shindo, T., Kurihara, Y., Nishimatsu, H., Moriyama, N., Kakoki, M., Wang, Y., Imai, Y., Ebihara, A., Kuwaki, T., Ju, K.H., Minamino, N., Kangawa, K., Ishikawa, T., Fukuda, M., Akimoto, Y., Kawakami, H., Imai, T., Morita, H., Yazaki, Y., Nagai, R., Hirata, Y., Kurihara, H. 2001. Vascular abnormalities and elevated blood pressure in mice lacking adrenomedullin gene. Circulation 104, 1964-1971

Shweiki, D., Itin, A., Soffer, D., Keshet, E. 1992. Vascular endothelial growth factor induced by hypoxia may mediate hypoxia-initiated angiogenesis. Nature 359, 843-845

Silveira, L.C., Saito, C.A., Lee, B.B., Kremers, J., da Silva Filho, M., Kilavik, B.E., Yamada, E.S., Perry, V.H. 2004. Morphology and physiology of primate M- and P-cells. Prog Brain Res 144, 21-46

Sims, D.E. 1991. Recent advances in pericyte biology--implications for health and disease. Can J Cardiol 7, 431-443

Singh, S., Dev, A., Verma, R., Pradeep, A., Sathyanarayana, P., Green, J.M., Narayanan, A., Wojchowski, D.M. 2012. Defining an EPOR-regulated transcriptome for primary progenitors, including Tnfr-sf13c as a novel mediator of EPO-dependent erythroblast formation. PloS one 7, e38530

Siren, A.L., Fratelli, M., Brines, M., Goemans, C., Casagrande, S., Lewczuk, P., Keenan, S., Gleiter, C., Pasquali, C., Capobianco, A., Mennini, T., Heumann, R., Cerami, A., Ehrenreich, H., Ghezzi, P. 2001a. Erythropoietin prevents neuronal apoptosis after cerebral ischemia and metabolic stress. Proc Natl Acad Sci U S A 98, 4044-4049

Siren, A.L., Knerlich, F., Poser, W., Gleiter, C.H., Bruck, W., Ehrenreich, H. 2001b. Erythropoietin and erythropoietin receptor in human ischemic/hypoxic brain. Acta Neuropathol 101, 271-276

Skatchkov, S.N., Eaton, M.J., Shuba, Y.M., Kucheryavykh, Y.V., Derst, C., Veh, R.W., Wurm, A., Iandiev, I., Pannicke, T., Bringmann, A., Reichenbach, A. 2006. Tandem-pore domain potassium channels are functionally expressed in retinal (Muller) glial cells. Glia 53, 266-276

Slepak, V.Z., Hurley, J.B. 2008. Mechanism of light-induced translocation of arrestin and transducin in photoreceptors: interaction-restricted diffusion. IUBMB Life 60, 2-9

Smith, W., Mitchell, P., Leeder, S.R. 1996. Smoking and age-related maculopathy. The Blue Mountains Eye Study. Arch Ophthalmol 114, 1518-1523

Sola, A., Wen, T.C., Hamrick, S.E., Ferriero, D.M. 2005. Potential for protection and repair following injury to the developing brain: a role for erythropoietin? Pediatr Res 57, 110R-117R

Soliz, J., Gassmann, M., Joseph, V. 2007. Soluble erythropoietin receptor is present in the mouse brain and is required for the ventilatory acclimatization to hypoxia. J Physiol 583, 329-336

Sparrow, J.R., Cai, B., Fishkin, N., Jang, Y.P., Krane, S., Vollmer, H.R., Zhou, J., Nakanishi, K. 2003. A2E, a fluorophore of RPE lipofuscin: can it cause RPE degeneration? Adv Exp Med Biol 533, 205-211

Stahl, A., Connor, K.M., Sapieha, P., Chen, J., Dennison, R.J., Krah, N.M., Seaward, M.R., Willett, K.L., Aderman, C.M., Guerin, K.I., Hua, J., Lofqvist, C., Hellstrom, A., Smith, L.E. 2010. The mouse retina as an angiogenesis model. Invest Ophthalmol Vis Sci 51, 2813-2826

Stalmans, I., Ng, Y.S., Rohan, R., Fruttiger, M., Bouche, A., Yuce, A., Fujisawa, H., Hermans, B., Shani, M., Jansen, S., Hicklin, D., Anderson, D.J., Gardiner, T., Hammes, H.P., Moons, L., Dewerchin, M., Collen, D., Carmeliet, P., D'Amore, P.A. 2002. Arteriolar and venular patterning in retinas of mice selectively expressing VEGF isoforms. J Clin Invest 109, 327-336

Stefansson, E., Geirsdottir, A., Sigurdsson, H. 2011. Metabolic physiology in age related macular degeneration. Prog Retin Eye Res 30, 72-80

Stefansson, E., Wolbarsht, M.L., Landers, M.B.r. 1983. In vivo O2 consumption in rhesus monkeys in light and dark. Exp Eye Res 37, 251-256

Stephen, R., Filipek, S., Palczewski, K., Sousa, M.C. 2008. Ca2+ -dependent regulation of phototransduction. Photochem Photobiol 84, 903-910

Stepinac, T.K., Chamot, S.R., Rungger-Brandle, E., Ferrez, P., Munoz, J.L., van den Bergh, H., Riva, C.E., Pournaras, C.J., Wagnieres, G.A. 2005. Light-induced retinal vascular damage by Pd-porphyrin luminescent oxygen probes. Invest Ophthalmol Vis Sci 46, 956-966

Sterling, P., Freed, M.A., Smith, R.G. 1988. Architecture of rod and cone circuits to the on-beta ganglion cell. J Neurosci 8, 623-642

Sternberg, N., Hamilton, D. 1981. Bacteriophage P1 site-specific recombination. I. Recombination between loxP sites. J Mol Biol 150, 467-486

Stone, J., Chan-Ling, T., Pe'er, J., Itin, A., Gnessin, H., Keshet, E. 1996. Roles of vascular endothelial growth factor and astrocyte degeneration in the genesis of retinopathy of prematurity. Invest Ophthalmol Vis Sci 37, 290-299

Stone, J., Dreher, Z. 1987. Relationship between astrocytes, ganglion cells and vasculature of the retina. J Comp Neurol 255, 35-49

Stone, J., Itin, A., Alon, T., Pe'er, J., Gnessin, H., Chan-Ling, T., Keshet, E. 1995. Development of retinal vasculature is mediated by hypoxia-induced vascular endothelial growth factor (VEGF) expression by neuroglia. J Neurosci 15, 4738-4747

Streit, W.J. 2002. Microglia as neuroprotective, immunocompetent cells of the CNS. Glia 40, 133-139

Stryer, L. 1983. Transducin and the cyclic GMP phosphodiesterase: amplifier proteins in vision. Cold Spring Harb Symp Quant Biol 48 Pt 2, 841-852

Sung, C.H., Chuang, J.Z. 2010. The cell biology of vision. J Cell Biol 190, 953-963

Suri, C., Jones, P.F., Patan, S., Bartunkova, S., Maisonpierre, P.C., Davis, S., Sato, T.N., Yancopoulos, G.D. 1996. Requisite role of angiopoietin-1, a ligand for the TIE2 receptor, during embryonic angiogenesis. Cell 87, 1171-1180

Takeda, N., Maemura, K., Imai, Y., Harada, T., Kawanami, D., Nojiri, T., Manabe, I., Nagai, R. 2004. Endothelial PAS domain protein 1 gene promotes angiogenesis through the transactivation of both vascular endothelial growth factor and its receptor, Flt-1. Circ Res 95, 146-153

Tang, P.H., Kono, M., Koutalos, Y., Ablonczy, Z., Crouch, R.K. 2013. New insights into retinoid metabolism and cycling within the retina. Prog Retin Eye Res 32, 48-63

Tanimoto, N., Muehlfriedel, R.L., Fischer, M.D., Fahl, E., Humphries, P., Biel, M., Seeliger, M.W. 2009. Vision tests in the mouse: Functional phenotyping with electroretinography. Front Biosci 14, 2730-2737

Terman, A., Brunk, U.T. 2004. Lipofuscin. Int J Biochem Cell Biol 36, 1400-1404

Thiersch, M., Lange, C., Joly, S., Heynen, S., Le, Y.Z., Samardzija, M., Grimm, C. 2009. Retinal neuroprotection by hypoxic preconditioning is independent of hypoxia-inducible factor-1 alpha expression in photoreceptors. Eur J Neurosci 29, 2291-2302

Thiersch, M., Raffelsberger, W., Frigg, R., Samardzija, M., Wenzel, A., Poch, O., Grimm, C. 2008. Analysis of the retinal gene expression profile after hypoxic preconditioning identifies candidate genes for neuroprotection. BMC Genomics 9, 73

Thoreson, W.B., Mangel, S.C. 2012. Lateral interactions in the outer retina. Prog Retin Eye Res 31, 407-441

Tian, H., Hammer, R.E., Matsumoto, A.M., Russell, D.W., McKnight, S.L. 1998. The hypoxia-responsive transcription factor EPAS1 is essential for catecholamine homeostasis and protection against heart failure during embryonic development. Genes Dev 12, 3320-3324

Tian, H., McKnight, S.L., Russell, D.W. 1997. Endothelial PAS domain protein 1 (EPAS1), a transcription factor selectively expressed in endothelial cells. Genes Dev 11, 72-82

Tian, X.F., Xia, X.B., Xiong, S.Q., Jiang, J., Liu, D., Liu, J.L. 2011. Netrin-1 overexpression in oxygen-induced retinopathy correlates with breakdown of the blood-retina barrier and retinal neovascularization. Ophthalmologica 226, 37-44

Tinjust, D., Kergoat, H., Lovasik, J.V. 2002. Neuroretinal function during mild systemic hypoxia. Aviat Space Environ Med 73, 1189-1194

Tolppanen, A.M., Nevalainen, T., Kolehmainen, M., Seitsonen, S., Immonen, I., Uusitupa, M., Kaarniranta, K., Pulkkinen, L. 2009. Single nucleotide polymorphisms of the tenomodulin gene (TNMD) in age-related macular degeneration. Mol Vis 15, 762-770

Ton, C.C., Hirvonen, H., Miwa, H., Weil, M.M., Monaghan, P., Jordan, T., van Heyningen, V., Hastie, N.D., Meijers-Heijboer, H., Drechsler, M., et, a. 1991. Positional cloning and characterization of a paired box- and homeobox-containing gene from the aniridia region. Cell 67, 1059-1074

Travis, G.H., Brennan, M.B., Danielson, P.E., Kozak, C.A., Sutcliffe, J.G. 1989. Identification of a photoreceptor-specific mRNA encoded by the gene responsible for retinal degeneration slow (rds). Nature 338, 70-73

Tretiach, M., Madigan, M.C., Wen, L., Gillies, M.C. 2005. Effect of Muller cell co-culture on in vitro permeability of bovine retinal vascular endothelium in normoxic and hypoxic conditions. Neurosci Lett 378, 160-165

Tsacopoulos, M., Poitry-Yamate, C.L., MacLeish, P.R., Poitry, S. 1998. Trafficking of molecules and metabolic signals in the retina. Prog Retin Eye Res 17, 429-442

Tsai, J.C., Wu, L., Worgul, B., Forbes, M., Cao, J. 2005. Intravitreal administration of erythropoietin and preservation of retinal ganglion cells in an experimental rat model of glaucoma. Curr Eye Res 30, 1025-1031

Tsai, P.T., Ohab, J.J., Kertesz, N., Groszer, M., Matter, C., Gao, J., Liu, X., Wu, H., Carmichael, S.T. 2006. A critical role of erythropoietin receptor in neurogenesis and post-stroke recovery. J Neurosci 26, 1269-1274

Um, M., Gross, A.W., Lodish, H.F. 2007. A "classical" homodimeric erythropoietin receptor is essential for the antiapoptotic effects of erythropoietin on differentiated neuroblastoma SH-SY5Y and pheochromocytoma PC-12 cells. Cell Signal 19, 634-645

Utomo, A.R., Nikitin, A.Y., Lee, W.H. 1999. Temporal, spatial, and cell type-specific control of Cre-mediated DNA recombination in transgenic mice. Nat Biotechnol 17, 1091-1096

Valente, T., Straccia, M., Gresa-Arribas, N., Dentesano, G., Tusell, J.M., Serratosa, J., Mancera, P., Sola, C., Saura, J. 2013. CCAAT/enhancer binding protein delta regulates glial proinflammatory gene expression. Neurobiol Aging 34, 2110-2124

van Leeuwen, R., Ikram, M.K., Vingerling, J.R., Witteman, J.C., Hofman, A., de Jong, P.T. 2003. Blood pressure, atherosclerosis, and the incidence of age-related maculopathy: the Rotterdam Study. Invest Ophthalmol Vis Sci 44, 3771-3777

van Rossum, D., Hanisch, U.K. 2004. Microglia. Metab Brain Dis 19, 393-411

van Rossum, M.C., Smith, R.G. 1998. Noise removal at the rod synapse of mammalian retina. Vis Neurosci 15, 809-821

van Uden, P., Kenneth, N., Rocha, S. 2008. Regulation of hypoxia-inducible factor-1alpha by NF-kappaB. Biochem. J 412, 477-484

van Uden, P., Kenneth, N.S., Webster, R., Müller, H.A., Mudie, S., Rocha, S. 2011. Evolutionary conserved regulation of HIF-1β by NF-κB. PLoS genetics 7, e1001285

Vardi, N., Duvoisin, R., Wu, G., Sterling, P. 2000. Localization of mGluR6 to dendrites of ON bipolar cells in primate retina. J Comp Neurol 423, 402-412

Vardi, N., Morigiwa, K. 1997. ON cone bipolar cells in rat express the metabotropic receptor mGluR6. Vis Neurosci 14, 789-794

Vardi, N., Smith, R.G. 1996. The AII amacrine network: coupling can increase correlated activity. Vision Res 36, 3743-3757

Vecino, E., Caminos, E., Ugarte, M., Osborne, N.N. 1998. Immunohistochemical Distribution of Neurotrophins and their Receptors in the Rat Retina and the Effects of Ischemia and Reperfusion*. General Pharmacology: The Vascular System 30, 305-314

Venkatesha, S., Toporsian, M., Lam, C., Hanai, J.-, Mammoto, T., Kim, Y.M., Bdolah, Y., Lim, K.-H., Yuan, H.-T., Libermann, T.A. 2006. Soluble endoglin contributes to the pathogenesis of preeclampsia. Nature medicine 12, 642-649

Vinores, S.A., Derevjanik, N.L., Ozaki, H., Okamoto, N., Campochiaro, P.A. 1999. Cellular mechanisms of blood-retinal barrier dysfunction in macular edema. Doc Ophthalmol 97, 217-228

Viviani, B., Bartesaghi, S., Corsini, E., Villa, P., Ghezzi, P., Garau, A., Galli, C.L., Marinovich, M. 2005. Erythropoietin protects primary hippocampal neurons increasing the expression of brain-derived neurotrophic factor. J Neurochem 93, 412-421

Vu, T.Q., McCarthy, S.T., Owen, W.G. 1997. Linear transduction of natural stimuli by dark-adapted and light-adapted rods of the salamander, Ambystoma tigrinum. J Physiol 505, 193-204

Wakida, K., Shimazawa, M., Hozumi, I., Satoh, M., Nagase, H., Inuzuka, T., Hara, H. 2007. Neuroprotective effect of erythropoietin, and role of metallothionein-1 and -2, in permanent focal cerebral ischemia. Neuroscience 148, 105-114

Wang, G.L., Jiang, B.H., Rue, E.A., Semenza, G.L. 1995a. Hypoxia-inducible factor 1 is a basic-helix-loop-helix-PAS heterodimer regulated by cellular O2 tension. Proc Natl Acad Sci U S A 92, 5510-5514

Wang, G.L., Semenza, G.L. 1993. General involvement of hypoxia-inducible factor 1 in transcriptional response to hypoxia. Proc Natl Acad Sci U S A 90, 4304-4308

Wang, G.L., Semenza, G.L. 1996. Molecular basis of hypoxia-induced erythropoietin expression. Curr Opin Hematol 3, 156-162

Wang, G.L., Jiang, B.-H., Rue, E.A., Semenza, G.L. 1995b. Hypoxia-inducible factor 1 is a basic-helix-loop-helix-PAS heterodimer regulated by cellular O2 tension. Proceedings of the national academy of sciences 92, 5510-5514

Wang, L., Chopp, M., Gregg, S.R., Zhang, R.L., Teng, H., Jiang, A., Feng, Y., Zhang, Z.G. 2008. Neural progenitor cells treated with EPO induce angiogenesis through the production of VEGF. J Cereb Blood Flow Metab 28, 1361-1368

Wang, M., Ma, W., Zhao, L., Fariss, R.N., Wong, W.T. 2011a. Adaptive Muller cell responses to microglial activation mediate neuroprotection and coordinate inflammation in the retina. J Neuroinflammation 8, 173

Wang, Q., Gorbey, S., Pfister, F., Hoger, S., Dorn-Beineke, A., Krugel, K., Berrone, E., Wu, L., Korff, T., Lin, J., Busch, S., Reichenbach, A., Feng, Y., Hammes, H.P. 2011b. Long-term Treatment with Suberythropoietic Epo is Vaso- and Neuroprotective in Experimental Diabetic Retinopathy. Cell Physiol Biochem 27, 769-782

Wang, Q., Pfister, F., Dorn-Beineke, A., vom Hagen, F., Lin, J., Feng, Y., Hammes, H.P. 2010. Low-dose erythropoietin inhibits oxidative stress and early vascular changes in the experimental diabetic retina. Diabetologia 53, 1227-1238

Wang, Y., Rattner, A., Zhou, Y., Williams, J., Smallwood, P.M., Nathans, J. 2012. Norrin/Frizzled4 signaling in retinal vascular development and blood brain barrier plasticity. Cell 151, 1332-1344

Warnecke, C., Zaborowska, Z., Kurreck, J., Erdmann, V.A., Frei, U., Wiesener, M., Eckardt, K.U. 2004. Differentiating the functional role of hypoxia-inducible factor (HIF)-1alpha and HIF-2alpha (EPAS-1) by the use of RNA interference: erythropoietin is a HIF-2alpha target gene in Hep3B and Kelly cells. FASEB J 18, 1462-1464

Watanabe, T., Raff, M.C. 1988. Retinal astrocytes are immigrants from the optic nerve. Nature 332, 834-837

Weidemann, A., Johnson, R.S. 2009. Nonrenal regulation of EPO synthesis. Kidney Int 75, 682-688

Weidemann, A., Krohne, T.U., Aguilar, E., Kurihara, T., Takeda, N., Dorrell, M.I., Simon, M.C., Haase, V.H., Friedlander, M., Johnson, R.S. 2010. Astrocyte hypoxic response is essential for pathological but not developmental angiogenesis of the retina. Glia 58, 1177-1185

Weiland, J.D., Cho, A.K., Humayun, M.S. 2011. Retinal prostheses: current clinical results and future needs. Ophthalmology 118, 2227-2237

Weiter, J.J., Zuckerman, R. 1980. The influence of the photoreceptor-RPE complex on the inner retina. An explanation for the beneficial effects of photocoagulation. Ophthalmology 87, 1133-1139

Wen, T.C., Sadamoto, Y., Tanaka, J., Zhu, P.X., Nakata, K., Ma, Y.J., Hata, R., Sakanaka, M. 2002. Erythropoietin protects neurons against chemical hypoxia and cerebral ischemic injury by up-regulating Bcl-xL expression. J Neurosci Res 67, 795-803

Wenger, R.H., Stiehl, D.P., Camenisch, G. 2005. Integration of oxygen signaling at the consensus HRE. Sci STKE 2005, re12

Wenzel, A., Grimm, C., Samardzija, M., Reme, C.E. 2003. The genetic modifier Rpe65Leu(450): effect on light damage susceptibility in c-Fos-deficient mice. Invest Ophthalmol Vis Sci 44, 2798-2802

Wenzel, A., Grimm, C., Samardzija, M., Reme, C.E. 2005. Molecular mechanisms of light-induced photoreceptor apoptosis and neuroprotection for retinal degeneration. Prog Retin Eye Res 24, 275-306

Wenzel, A., Remé, C.E., Williams, T.P., Hafezi, F., Grimm, C. 2001. The Rpe65 Leu450Met variation increases retinal resistance against light-induced degeneration by slowing rhodopsin regeneration. The Journal of Neuroscience 21, 53-58

West, H., Richardson, W.D., Fruttiger, M. 2005. Stabilization of the retinal vascular network by reciprocal feedback between blood vessels and astrocytes. Development 132, 1855-1862

Westenbrink, B.D., Ruifrok, W.P., Voors, A.A., Tilton, R.G., van Veldhuisen, D.J., Schoemaker, R.G., van Gilst, W.H., de Boer, R.A. 2010. Vascular endothelial growth factor is crucial for erythropoietin-induced improvement of cardiac function in heart failure. Cardiovasc Res 87, 30-39

Westheimer, G. 2007. The ON-OFF dichotomy in visual processing: from receptors to perception. Prog Retin Eye Res 26, 636-648

Westphal, G., Braun, K., Debus, J. 2002. Detection and quantification of the soluble form of the human erythropoietin receptor (sEpoR) in the growth medium of tumor cell lines and in the plasma of blood samples. Clin Exp Med 2, 45-52

White, R.D., Neal, M.J. 1976. The uptake of L-glutamate by the retina. Brain Res 111, 79-93

Wiesener, M.S., Jurgensen, J.S., Rosenberger, C., Scholze, C.K., Horstrup, J.H., Warnecke, C., Mandriota, S., Bechmann, I., Frei, U.A., Pugh, C.W., Ratcliffe, P.J., Bachmann, S., Maxwell, P.H., Eckardt, K.U. 2003. Widespread hypoxia-inducible expression of HIF-2alpha in distinct cell populations of different organs. FASEB J 17, 271-273

Wiesener, M.S., Turley, H., Allen, W.E., Willam, C., Eckardt, K.U., Talks, K.L., Wood, S.M., Gatter, K.C., Harris, A.L., Pugh, C.W., Ratcliffe, P.J., Maxwell, P.H. 1998. Induction of endothelial PAS domain protein-1 by hypoxia: characterization and comparison with hypoxia-inducible factor-1alpha. Blood 92, 2260-2268

Wikler, K.C., Rakic, P. 1990. Distribution of photoreceptor subtypes in the retina of diurnal and nocturnal primates. J Neurosci 10, 3390-3401

Wimmers, S., Karl, M.O., Strauss, O. 2007. Ion channels in the RPE. Prog Retin Eye Res 26, 263-301

Winkler, B.S., Arnold, M.J., Brassell, M.A., Puro, D.G. 2000. Energy metabolism in human retinal Muller cells. Invest Ophthalmol Vis Sci 41, 3183-3190

Winkler, B.S., Boulton, M.E., Gottsch, J.D., Sternberg, P. 1999. Oxidative damage and age-related macular degeneration. Mol Vis 5, 32

Witthuhn, B.A., Quelle, F.W., Silvennoinen, O., Yi, T., Tang, B., Miura, O., Ihle, J.N. 1993. JAK2 associates with the erythropoietin receptor and is tyrosine phosphorylated and activated following stimulation with erythropoietin. Cell 74, 227-236

Wright, A.F., Chakarova, C.F., Abd El-Aziz, M.M., Bhattacharya, S.S. 2010. Photoreceptor degeneration: genetic and mechanistic dissection of a complex trait. Nat Rev Genet 11, 273-284

Wunderlich, K.A., Leveillard, T., Penkowa, M., Zrenner, E., Perez, M.T. 2010. Altered expression of metallothionein-I and -II and their receptor megalin in inherited photoreceptor degeneration. Invest Ophthalmol Vis Sci 51, 4809-4820

Xia, C.H., Yablonka-Reuveni, Z., Gong, X. 2010. LRP5 is required for vascular development in deeper layers of the retina. PLoS One 5, e11676

Xia, G., Kageyama, Y., Hayashi, T., Kawakami, S., Yoshida, M., Kihara, K. 2001. Regulation of vascular endothelial growth factor transcription by endothelial PAS domain protein 1 (EPAS1) and possible involvement of EPAS1 in the angiogenesis of renal cell carcinoma. Cancer 91, 1429-1436

Xie, Z., Wu, X., Qiu, Q., Gong, Y., Song, Y., Gu, Q., Li, C. 2007. Expression pattern of erythropoietin and erythropoietin receptor in experimental model of retinal detachment. Curr Eye Res 32, 757-764

Xu, H., Liu, J., Xiong, S., Le, Y.Z., Xia, X. 2012. Suppression of retinal neovascularization by lentivirus-mediated netrin-1 small hairpin RNA. Ophthalmic Res 47, 163-169

Xu, Q., Wang, Y., Dabdoub, A., Smallwood, P.M., Williams, J., Woods, C., Kelley, M.W., Jiang, L., Tasman, W., Zhang, K., Nathans, J. 2004. Vascular development in the retina and inner ear: control by Norrin and Frizzled-4, a high-affinity ligand-receptor pair. Cell 116, 883-895

Yamasaki, M., Mishima, H.K., Yamashita, H., Kashiwagi, K., Murata, K., Minamoto, A., Inaba, T. 2005. Neuroprotective effects of erythropoietin on glutamate and nitric oxide toxicity in primary cultured retinal ganglion cells. Brain Res 1050, 15-26

Yancopoulos, G.D., Davis, S., Gale, N.W., Rudge, J.S., Wiegand, S.J., Holash, J. 2000. Vascular-specific growth factors and blood vessel formation. Nature 407, 242-248

Yang, X.M., Yafai, Y., Wiedemann, P., Kuhrt, H., Wang, Y.S., Reichenbach, A., Eichler, W. 2012. Hypoxia-induced upregulation of pigment epithelium-derived factor by retinal glial (Muller) cells. J Neurosci Res 90, 257-266

Yatsiv, I., Grigoriadis, N., Simeonidou, C., Stahel, P.F., Schmidt, O.I., Alexandrovitch, A.G., Tsenter, J., Shohami, E. 2005. Erythropoietin is neuroprotective, improves functional recovery, and reduces neuronal apoptosis and inflammation in a rodent model of experimental closed head injury. FASEB J 19, 1701-1703

Yau, K.W. 1994. Phototransduction mechanism in retinal rods and cones. The Friedenwald Lecture. Invest Ophthalmol Vis Sci 35, 9-32

Ye, X., Wang, Y., Cahill, H., Yu, M., Badea, T.C., Smallwood, P.M., Peachey, N.S., Nathans, J. 2009. Norrin, frizzled-4, and Lrp5 signaling in endothelial cells controls a genetic program for retinal vascularization. Cell 139, 285-298

Yeo, E.J., Cho, Y.S., Kim, M.S., Park, J.W. 2008. Contribution of HIF-1alpha or HIF-2alpha to erythropoietin expression: in vivo evidence based on chromatin immunoprecipitation. Ann Hematol 87, 11-17

Yoshida, T., Zhang, H., Iwase, T., Shen, J., Semenza, G.L., Campochiaro, P.A. 2010. Digoxin inhibits retinal ischemia-induced HIF-1{alpha} expression and ocular neovascularization. FASEB J

Yu, D.Y., Cringle, S.J. 2001. Oxygen distribution and consumption within the retina in vascularised and avascular retinas and in animal models of retinal disease. Prog Retin Eye Res 20, 175-208

Yu, D.Y., Cringle, S.J. 2005. Retinal degeneration and local oxygen metabolism. Exp Eye Res 80, 745-751

Yu, D.Y., Cringle, S.J., Alder, V.A., Su, E.N. 1994. Intraretinal oxygen distribution in rats as a function of systemic blood pressure. Am J Physiol 267, H2498-507

Yu, D.Y., Cringle, S.J., Su, E.N. 2005. Intraretinal oxygen distribution in the monkey retina and the response to systemic hyperoxia. Invest Ophthalmol Vis Sci 46, 4728-4733

Yu, D.Y., Cringle, S.J., Yu, P.K., Su, E.N. 2007. Intraretinal oxygen distribution and consumption during retinal artery occlusion and graded hyperoxic ventilation in the rat. Invest Ophthalmol Vis Sci 48, 2290-2296

Yu, X., Shacka, J.J., Eells, J.B., Suarez-Quian, C., Przygodzki, R.M., Beleslin-Cokic, B., Lin, C.S., Nikodem, V.M., Hempstead, B., Flanders, K.C., Costantini, F., Noguchi, C.T. 2002. Erythropoietin receptor signalling is required for normal brain development. Development 129, 505-516

Yu, X., Si, J., Zhang, Y., DeWille, J.W. 2010. CCAAT/Enhancer Binding Protein-delta (C/EBP-delta) regulates cell growth, migration and differentiation. Cancer cell international 10, 48

Yuan, G., Nanduri, J., Khan, S., Semenza, G.L., Prabhakar, N.R. 2008. Induction of HIF-1alpha expression by intermittent hypoxia: involvement of NADPH oxidase, Ca2+ signaling, prolyl hydroxylases, and mTOR. J Cell Physiol 217, 674-685

Zagórska, A., Dulak, J. 2004. HIF-1: the knowns and unknowns of hypoxia sensing. ACTA BIOCHIMICA POLONICA-ENGLISH EDITION- 563-586

Zeigler, B.M., Vajdos, J., Qin, W., Loverro, L., Niss, K. 2010. A mouse model for an erythropoietin-deficiency anemia. Disease Models & Mechanisms 3, 763-772

Zeng, H.Y., Zhu, X.A., Zhang, C., Yang, L.P., Wu, L.M., Tso, M.O. 2005. Identification of sequential events and factors associated with microglial activation, migration, and cytotoxicity in retinal degeneration in rd mice. Invest Ophthalmol Vis Sci 46, 2992-2999

Zhang, C., Rosenbaum, D.M., Shaikh, A.R., Li, Q., Rosenbaum, P.S., Pelham, D.J., Roth, S. 2002. Ischemic preconditioning attenuates apoptotic cell death in the rat retina. Invest Ophthalmol Vis Sci 43, 3059-3066

Zhang, F., Wang, S., Cao, G., Gao, Y., Chen, J. 2007. Signal transducers and activators of transcription 5 contributes to erythropoietin-mediated neuroprotection against hippocampal neuronal death after transient global cerebral ischemia. Neurobiol Dis 25, 45-53

Zhang, J., Hu, L.M., Xu, G., Wu, Y., Shen, J., Luo, Y., Zhong, Y., Sinclair, S.H., Yanoff, M., Li, W., Xu, G.T. 2010. Anti-VEGF effects of intravitreal erythropoietin in early diabetic retinopathy. Front Biosci (Elite Ed) 2, 912-927

Zhang, J., Wu, Y., Jin, Y., Ji, F., Sinclair, S.H., Luo, Y., Xu, G., Lu, L., Dai, W., Yanoff, M., Li, W., Xu, G.T. 2008. Intravitreal injection of erythropoietin protects both retinal vascular and neuronal cells in early diabetes. Invest Ophthalmol Vis Sci 49, 732-742

Zhang, W., Tsuchiya, T., Yasukochi, Y. 1999. Transitional change in interaction between HIF-1 and HNF-4 in response to hypoxia. J Hum Genet 44, 293-299

Zhang, Y., Stone, J. 1997. Role of astrocytes in the control of developing retinal vessels. Invest Ophthalmol Vis Sci 38, 1653-1666

Zheng, X., Wang, X., Ma, Z., Sunkari, V.G., Botusan, I., Takeda, T., Björklund, A., Inoue, M., Catrina, S.B., Brismar, K. 2012. Acute hypoxia induces apoptosis of pancreatic β-cell by activation of the unfolded protein response and upregulation of CHOP. Cell death & disease 3, e322

Zhong, L., Bradley, J., Schubert, W., Ahmed, E., Adamis, A.P., Shima, D.T., Robinson, G.S., Ng, Y.S. 2007. Erythropoietin promotes survival of retinal ganglion cells in DBA/2J glaucoma mice. Invest Ophthalmol Vis Sci 48, 1212-1218

Zhu, B., Wang, W., Gu, Q., Xu, X. 2008. Erythropoietin protects retinal neurons and glial cells in early-stage streptozotocin-induced diabetic rats. Exp Eye Res 86, 375-382

Zhu, Y., Ohlemiller, K.K., McMahan, B.K., Gidday, J.M. 2002. Mouse models of retinal ischemic tolerance. Invest Ophthalmol Vis Sci 43, 1903-1911

Ziman, M., Rodger, J., Lukehurst, S., Hancock, D., Dunlop, S., Beazley, L. 2003. A dorso-ventral gradient of Pax6 in the developing retina suggests a role in topographic map formation. Brain Res Dev Brain Res 140, 299-302

Zuercher, J., Fritzsche, M., Feil, S., Mohn, L., Berger, W. 2012. Norrin stimulates cell proliferation in the superficial retinal vascular plexus and is pivotal for the recruitment of mural cells. Hum Mol Genet 21, 2619-2630

8 List of Abbreviations

βCR: β common receptor

ACTB: actin beta

ADM: adrenomedullin

adRP: autosomal dominant RP

AKT: ak thymoma/protein kinase B

AMD: age-related macular degeneration

AMPA: α-amino-3-hydroxy-5-methyl-4-isoxazolepropionic acid

ANG1: angiopoietin 1

ANG: angiopoietin

APAF1: apoptotic peptidase activating factor 1

ARNT: aryl hydrocarbon receptor nuclear translocator

ASN: asparagine

ATP: adenosine triphosphate

BBB: blood-brain barrier

BCL2: B cell leukemia/lymphoma 2

BCL2L1: BCL2-like 1/ BCLXL

BDNF: brain-derived neurotrophic factor

bHLH: basic helix-loop-helix

BRAO: branch retinal artery occlusion

BRB: blood-retina barrier

BRN3A: brain-specific homeobox/POU domain protein 3A

CALB1: calbindin 1

CALB2: calbindin 2 (calretinin)

CASP1: caspase 1

CBP: CREB binding protein

CDC42: cell division cycle 42

CEBP/D: CCAAT/enhancer binding protein delta

cGMP: cyclic guanosine monophosphate

CHX10: ceh-10 homeo domain containing homolog

CNS: central nervous system

CNV: choroidal neovascularisation

CRAO: central retinal artery occlusion

cSLO: confocal scanning laser ophthalmoscopy

DAPI: 4',6-diamidino-2-phenylindole

DCC: deleted in colorectal carcinoma

DR: diabetic retinopathy

E: embryonic day

EDN2: endothelin 2

ELOVL4: elongation of very long chain fatty acids protein 4

eNOS: endothelial nitric oxide synthase

EPAS1: endothelial PAS domain protein 1

EPO: erythropoietin

EPOR: erythropoietin receptor

ERG: electroretinogram

ERK1/2: extracellular signal-regulated kinase ½

FGF2: fibroblast growth factor 2

FIH: factor inhibiting HIF

FL: fluorescein

FZD4: frizzled 4

Gαt: transducin α subunit

GATA2: GATA-binding protein 2

GC: guanylyl cyclase

GCAP: guanylyl cyclase activating protein

GCL: ganglion cell layer

GFAP: glial fibrillary acidic protein

GFP: green fluorescent protein

GLUL: glutamate-ammonia ligase

GNAT1: guanine nucleotide binding protein, alpha transducing 1

GNAT2: guanine nucleotide binding protein, alpha transducing 2

GS: glutamine synthetase

HGF: hepatocyte growth factor

HIF1A: HIF 1 alpha

HIF3A: HIF 3 alpha

HIF: hypoxia-inducible factor

HNF4: hepatocyte nuclear factor 4

HP: hypoxic preconditioning

HRE: hypoxia responsive element

HS: horse serum

HSP90: heat shock protein 90

IBA1: induction of brown adipocytes 1

iBRB: inner BRB

IGC: indocyanine green

IGF1: insulin-like growth factor 1

IL1B: interleukin 1B

IL6: interleukin 6

ILM: inner limiting membrane

INL: inner nuclear layer

iNOS: inducible nitric oxide synthase

IOP: intraocular pressure

IPAS: inhibitory PAS domain protein

IPC: ischemic preconditioning

IPL: inner plexiform layer

ipRGC: intrinsically photosensitive RGC

IS: inner segment

JAK2: janus kinase 2

LGN: lateral geniculate nucleus

LIF: leukemia inhibitory factor

LRP5: low density lipoprotein receptor-related protein 5

MAPK: mitogen-activated protein kinase

mEPOR: membrane EPOR

MMP: matrix metalloproteinase

MNU: *N*-methyl-*N*-nitrosourea

MT1: metallothionein 1

MT2: metallothionein 2

NDP: Norrie disease (pseudoglioma)

NF: neurofilament

NFkB: nuclear factor kappa B

NFL: nerve fibre layer

NMDAR1: NMDA receptor 1

NO: nitric oxide

NTN1: netrin 1

NTN4: netrin 4

oBRB: outer BRB

ODDD: oxygen-dependant degradation domain

OIR: oxygen-induced retinopathy

OLM: outer limiting membrane

ONH: optic nerve head

ONL: outer nuclear layer

OPL: outer plexiform layer

OS: outer segment

PAX6: paired box gene 6

PB: phosphate buffer

PBS: phosphate buffer saline

PDE: phosphodiesterase

PDGF: platelet-derived growth factor

PDGFA: platelet-derived growth factor alpha

PDGFB: platelet-derived growth factor B

PDGFRA: platelet-derived growth factor receptor alpha

PDR: proliferative diabetic retinopathy

PEDF: pigment epithelium-derived factor

PFA: paraformaldehyde

PHD: prolyl hydroxylase

PI3K: phosphatidylinositol 3-kinase

PIGF: phosphatidylinositol glycan anchor biosynthesis F

PKCA: protein kinase C alpha

PND: post-natal day

POU4F1: POU domain 4, transcription factor 1

PRO: proline

RCS: Royal College of Surgeons

rd1: retinal degeneration 1

rd10: retinal degeneration 10

RFP: red fluorescent protein

RGC: retinal ganglion cell

RPGR: retinitis pigmentosa GTPase regulator

rhEPO: recombinant human EPO

RHO: rhodopsin

ROP: retinopathy of prematurity

ROS: reactive oxygen species

RP: retinitis pigmentosa

RPC: retinal progenitor cell

RPE65: retinal pigment epithelium 65

RPE: retinal pigment epithelium

SD-OCT: spectral domain optical coherence tomography

SD: standard deviation

SDS: sodium dodecyl sulphate

sEPOR: soluble EPOR

SERPINF1: serpin peptidase inhibitor F1

STAT3/5: signal-transducer and activator of transcription protein 3/5

SYP: synaptophysin

TAD: transactivation domain

TBS: tris buffer saline

TCA: tricarboxylic acid

TEK: endothelial-specific receptor tyrosine kinase

THB: tissue homogenization buffer

TIE2: tunica internal endothelial cell kinase 2

TNFA: tumour necrosis factor A

TSP1: thrombospondin 1

TSPAN12: tetraspanin 12

UNC5: unc-5 homolog

USH2A: Usher syndrome 2A

VEGFA: vascular endothelial growth factor A

VHL: von Hippel Lindau

VSX2: visual system homeobox 2

9 Rights and Permissions

Elsevier License Number for reproduction of figures:

Figure 2: 3204640166050

Figure 4: 3204620270467

Figure 11: 3205210709010

Figure 13: 3198120896280

Figure 14: 3198120896280

Figure 15: 3198120896280

Figure 16: 3217640609292

Figure 18: 3204691322201

10 First Author Publications

10.1 HIF1A Is Essential for the Development of the Intermediate Plexus of the Retinal Vasculature

Christian Caprara[1], Markus Thiersch[1], Christina Lange[1], Sandrine Joly[1], Marijana Samardzija[1] and Christian Grimm[1,2,3]

[1]Lab for Retinal Cell Biology, Department of Ophthalmology, University of Zurich, Zurich, Switzerland.

[2]Zurich Center for Integrative Human Physiology (ZIHP), University of Zurich, Zurich, Switzerland.

[3]Neuroscience Center (ZNZ), University of Zurich, Zurich, Switzerland.

Published in Investigative Ophthalmology and Visual Science, 2011, **52** (5): 2109-2117

Personal Contribution

Performed project design, breeding of mouse model, experiments (Fig. 1-7), interpretation of results, and manuscript writing/editing.

Key Findings

HIF1A is a transcription factors that regulates tissue response to hypoxia. It controls the expression of genes involved in different cellular processes, including cell survival, proliferation, and angiogenesis. In the early post-natal retina, HIF1A is found at increased levels. In this study, we analyzed its potential function during post-natal development of the mouse retina and retinal vasculature by generating a mouse line lacking HIF1A in a heterogeneous population of cells in the retinal periphery.

Here are some of the key findings of the study:

- Ablation of *Hif1a* caused a significant reduction in *Hif1a* gene expression and HIF1A protein levels in the early post-natal retina.
- Retinal morphology was normal but the *Hif1a* knockdown prevented the formation of the intermediate vascular plexus in the peripheral retina.
- *Hif1a* knockdown did not affect expression of angiogenesis-related genes as *Vegfa* but strongly induced expression of *Epo*. At the protein level, EPAS1 (HIF2A) was stabilized in the *Hif1a* knockdown mice

Retinal Cell Biology

HIF1A Is Essential for the Development of the Intermediate Plexus of the Retinal Vasculature

Christian Caprara,[1] *Markus Thiersch,*[1,2] *Christina Lange,*[1] *Sandrine Joly,*[1,3] *Marijana Samardzija,*[1] *and Christian Grimm*[1,4,5]

Purpose. HIF1A is one of the major transcription factors that regulate tissue response to low oxygen tension. It controls expression of a large number of genes involved in cell survival, proliferation, angiogenesis, and other cellular processes. HIF1A is present at increased levels in the early postnatal retina. In this study its potential function during postnatal development of the mouse retina and retinal vasculature was analyzed.

Methods. A mouse line was generated with a Cre-mediated *Hif1a* knockdown in the peripheral retina. Retinal morphology and vasculature were analyzed in sections and flat mount preparations. Gene and protein expression were determined by real-time PCR and Western blot analysis.

Results. The Cre-mediated knockdown caused a significant reduction in *Hif1a* gene expression and HIF1A protein levels in the early postnatal retina. Retinal morphology was normal but the *Hif1a* knockdown prevented the formation of the intermediate vascular plexus in the peripheral retina. The primary plexus and the outer plexus were less affected. The *Hif1a* knockdown did not affect expression of such angiogenesis-related genes as vascular endothelial growth factor (*Vegf*) but strongly induced expression of erythropoietin (*Epo*). At the protein level, EPAS1 (HIF2A) was stabilized in the *Hif1a* knockdown mice.

Conclusions. The results suggest that HIF1A may be directly or indirectly required for normal development of the retinal vasculature, especially of the intermediate plexus. EPO but not VEGF may play a significant role in the development of this phenotype. HIF1A may not be the main factor that regulates *Vegf* expression during retinal development in the mouse. (*Invest Ophthalmol Vis Sci.* 2011;52:2109–2117) DOI:10.1167/iovs.10-6222

The retina is one of the most metabolically active tissues in the body and is therefore highly sensitive to alterations in oxygen tension. Hypoxia is defined as a state in which oxygen tension is below the normal limits in tissue beds. Systemic hypoxemia caused by lung or cardiac disease or occlusive vascular diseases in the eye may result in retinal hypoxia,[1] with negative effects on retinal cell viability and function.

Hypoxia-inducible factors (HIFs) are the primary signaling proteins responsible for driving the cellular response to hypoxia. They regulate the transcription of more than 70 genes that encode proteins with a wide array of actions.[2] HIF1, the most-studied example of the HIF protein family, is a heterodimeric transcription factor consisting of a constitutively expressed subunit ARNT (aryl hydrocarbon receptor nuclear translocator) and an oxygen-regulated α-subunit (HIF1A). In the presence of normal oxygen levels, the HIF1A subunit is hydroxylated by proline-hydroxylase-2 (PHD-2/EGLN1), polyubiquitinated by the von-Hippel-Lindau (VHL) ubiquitin ligase complex, and subsequently degraded by proteasomes. Therefore, HIF-1 does not normally activate transcription of target genes in the presence of sufficient oxygen.[3] However, in hypoxic conditions, HIF1A is stable and active, as hydroxylases and VHL proteins are inhibited by the lack of oxygen. In these conditions, HIF1A is able to interact with its co-activators and to dimerize with the constitutively expressed β-subunit. Once stabilized and assembled, the HIF1 complex can regulate the transcription of its target genes involved in cell survival, adaptation, anaerobic metabolism, immune reaction, cytokine production, vascularization, and general tissue homeostasis.[4]

The vasculature is of primary importance for tissue oxygenation. The vascular network that supplies the inner portion of the retina with oxygen and nutrients undergoes dramatic changes and reorganization during development. Initially, the hyaloid vasculature metabolically supports the inner part of the eye. In the later stages of development, the hyaloid vessels are replaced by the retinal vasculature. This switch occurs in humans at midgestation and in mice at birth. During the regression of the hyaloid vasculature, a vascular plexus emerges from the optic nerve head and spreads in the nerve fiber layer across the inner surface of the retina. In mice, the primary plexus reaches the periphery of the retina within 8 to 10 days after birth.[5] This primary plexus eventually remodels into three parallel but interconnected networks located in the nerve fiber layer and the two plexiform layers. The deeper plexi of the retinal vasculature develop by sprouting from the primary plexus. Angiogenic sprouts start to penetrate the retina along the Müller cells, perpendicular to the primary plexus. They turn at the outer (forming the outer plexus) and inner (forming the intermediate plexus) boundaries of the inner nuclear layer (INL), to establish two additional capillary networks parallel to the primary plexus. This process is preceded by a transient expression of VEGF in cells of the INL. In contrast to the formation of the primary plexus, the deeper plexi develop independently of retinal astrocytes.[6] Vascular differentiation occurs in a central-to-peripheral gradient, with vessels at the growing edge of the vascular network being less mature than the more central vessels.[5] However, the mechanisms that in-

From the [1]Lab for Retinal Cell Biology, Department of Ophthalmology, the [4]Zurich Center for Integrative Human Physiology (ZIHP), and the [5]Neuroscience Center (ZNZ), University of Zurich, Zurich, Switzerland.

Present affiliation: [2]Department of Materials, ETH (Eidgenössische Technische Hochschule) Zurich, Zurich, Switzerland; and the [3]Brain Research Institute, University of Zurich, Zurich, Switzerland.

Supported by Grant 3100A0-117760 from the Swiss National Science Foundation).

Submitted for publication July 15, 2010; revised September 21, 2010; accepted October 21, 2010.

Disclosure: **C. Caprara**, None; **M. Thiersch**, None; **C. Lange**, None; **S. Joly**, None; **M. Samardzija**, None; **C. Grimm**, None

Corresponding author: Christian Caprara, Lab for Retinal Cell Biology, Department Ophthalmology, University Hospital Zurich, CH 8091 Zurich, Switzerland; christian.caprara@usz.ch.

TABLE 1. Primers and Conditions for Real-time PCR

Gene	Upstream (5′–3′)	Downstream (5′–3′)	Product Size (bp)
β-Actin	CAACGGCTCCGGCATGTGC	CTCTTGCTCTGGGCCTCG	153
Hif1a	TCATCAGTTGCCACTTCCCCAC	CCGTCATCTGTTAGCACCATCAC	198
Epas 1 (Hif2a)	GGAGCTCAAAAGGTGTCAGG	CAGGTAAGGCTCGAACGATG	61
Vegf	ACTTGTGTTGGGAGGAGGATGTC	AATGGGTTTGTCGTGTTTCTGG	171
Serpin 1f (Pedf)	TCCACAGCACCTACAAGGAG	TAAGCCACGCCAAGGAGAAG	280
Epo	GCCCTGCTAGCCAATTCC	GGCGACATCAATTCCTTCTG	128
Gfap	CTACATCGAGAAGGTCCGCT	CGGATCTGGAGGTTGGAGAA	850
Tie2	CCATCACCATAGGAAGGGACTTTG	TAGGAAGGACGCTTGTTGACGCATC	215
Lif	AATGCCACCTGTGCCATACG	CAACTTGGTCTTCTCTGTCCCG	216
Vsx2 (Chx10)	CCAGAAGACAGGATACAGGTG	GGCTCCATAGAGACCATACT	111
Rho	CTTCACCTGGATCATGGCGTT	TTCGTTGTTGACCTCAGGCTTG	130
Cntf	AGCCTTGACTCAGTGGATGGTG	ATCAGCCTCTTTTTCAGGGACC	276
Nos2 (iNos)	ATGTGCTGCCTCTGGTCTT	CCTGGAACCACTCGTACTTG	114
Mmp2	TCATCGCAGACTCCTGGAATGC	AACTTCACGCTCTTGAGACTTTGG	280
Edn1	TCCCGTGATCTTCTCTCTGC	AGTTCGGCTCCCAAGACAG	72
Edn2	AGACCTCCTCCGAAAGCTG	CTGGCTGTAGCTGGCAAAG	64
Bdnf	CACTGAGTCTCCAGGACAGC	GTCAGACCTCTCGAACCTGC	223
Fgf2	TGTGTCTATCAAGGGAGTGTGTGC	ACCAACTGGAGTATTTCCGTGACCG	158
Gnat1	GAGGATGCTGAGAAGGATGC	TGAATGTTGAGCGTGGTCAT	209
Gnat2	GCATCAGTGCTGAGGACAAA	CTAGGCACTCTTCGGGTGAG	192

duce and guide deeper plexus angiogenesis are still largely unknown.

Because the retina of the newborn mouse is virtually avascular, lacking especially the two inner vascular plexi that do not form until the first 2 weeks after birth, reduced tissue oxygenation is expected to trigger an appropriate molecular response. Indeed, HIF1A levels are high in the young mouse retina and decrease as the retinal vasculature develops.[7] In the present study, we used a conditional knockdown mouse with a selective downregulation of *Hif1a* in the retinal periphery to study the role of *Hif1a* for retinal development and specifically for the formation of the vascular network in the retina.

METHODS

Animals

All animal experiments were conducted in accordance with the regulations of the Cantonal Veterinary Authority of Zurich and with the ARVO Statement for the Use of Animals in Ophthalmic and Vision Research. Conditional *Hif1a* knockdowns were generated by breeding $Hif1a^{flox/flox}$ mice[8] to mice expressing Cre recombinase under control of the α-element of the *Pax6* promoter (α-Cre),[9] resulting in $Hif1a^{flox/flox}$;α-Cre double-mutant animals. $Hif1a^{flox/flox}$ littermates were used as wild-type controls.

For study of the spatial expression of the Cre recombinase in α-Cre mice, a ROSA-flox-RFP reporter line[10] was crossed to $Hif1a^{flox/flox}$;α-Cre animals. Retinas were cryosectioned and analyzed for red fluorescence protein (RFP) expression by fluorescence microscopy. Mice were raised in standard conditions in a regular light–dark cycle (12 hour–12 hour) with 60 lux at cage level. Retinas for gene and protein expression analysis and for immunohistologic and morphologic examinations were collected at various postnatal days (PNDs), as indicated in the text and figure legends.

RNA Isolation, cDNA Synthesis, and Real-Time PCR

Retinas were isolated through a slit in the cornea, immediately frozen in liquid nitrogen, and stored at −80°C. Total retinal RNA was extracted with a kit (RNeasy isolation kit; Qiagen, Hilden, Germany), including a DNase treatment to digest residual genomic DNA. cDNA was prepared from equal amounts of total retinal RNA with oligo(dT) primers and M-MLV reverse transcriptase (Promega, Madison, WI). Ten nanograms of cDNA were amplified in a thermocycler (LightCycler 480; Roche Diagnostics AG, Rotkreuz, Switzerland) with a master mix (SYBR Green I; Roche Diagnostics AG) and the appropriate primer pairs (Table 1). cDNA levels were normalized to β-actin, and relative values were calculated with a respective calibrator sample.

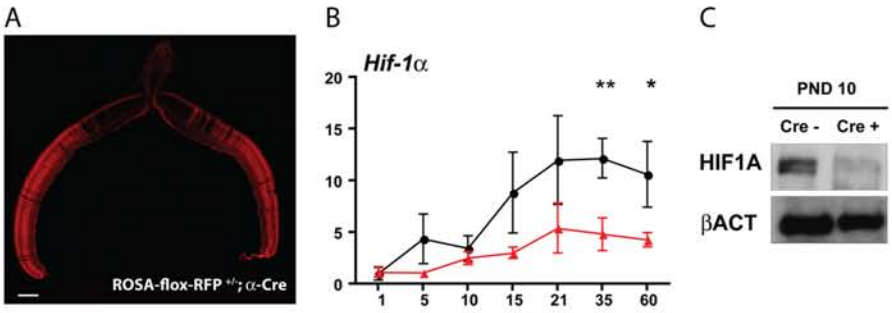

FIGURE 1. Knockdown of *Hif1a* in retinas of $Hif1a^{flox/flox}$;a-Cre mice. (**A**) Detection of the Cre expression pattern as indicated by the expression of RFP in ROSA-flox-RFP;α-Cre mice at PND21. Shown is a nasotemporal section through the optic nerve head. (**B**) Relative quantification of *Hif1a* gene expression in retinas of $Hif1a^{flox/flox}$ mice that served as wild-type controls (*black filled circles*) and of *Hif1a* knockdown (*red filled triangles*) mice by real-time PCR. cDNAs were prepared from total retinal RNA isolated at the PNDs indicated on the *x*-axis. Given are the mean values ± SD of three retinas per time point and genotype, amplified in duplicate. Values were normalized to β-actin and are expressed relative to that at PND1 in the $Hif1a^{flox/flox}$ mice, which was set to 1. Differences in gene expression levels between the knockdown and control mice at individual time points were tested for significance with Student's *t*-test; $^{*}P < 0.05$; $^{**}P < 0.01$. (**C**) Western blot showing retinal HIF1A protein levels at PND10 in $Hif1a^{flox/flox}$ mice without (Cre –) or with (Cre +) α-Cre. β-Actin served as loading control. Scale bar, 200 μm.

Western Blot Analysis

For protein extraction, isolated retinas were sonified in 0.1 M Tris-HCl (pH 8.0) at 4°C, and protein content was determined with a Bradford assay. Protein extracts were mixed with sodium dodecylsulfate (SDS) sample buffer and incubated for 10 minutes at 95°C. Proteins were separated by SDS polyacrylamide gel electrophoresis and blotted onto a nitrocellulose membrane. After the membranes were blocked with 5% nonfat dry milk (Bio-Rad, Munich, Germany) in 10 mM Tris-HCl (pH 8), 150 mM NaCl, and 0.05% Tween-20, they were incubated with primary antibodies at 4°C overnight. The primary antibodies used were as follows: rabbit anti-HIF1A (1:1000; cat no. 100-479; Novus Biologicals, Littleton, CO); rabbit anti-EPAS1 (HIF2A, 1:500; cat. no. 100-480; Novus Biologicals); and mouse anti-β-actin (sc1616, 1:1000; Santa Cruz Biotechnology, Santa Cruz, CA). After the membranes were incubated with horseradish peroxidase–labeled secondary antibodies for 1 hour at room temperature, the protein bands were visualized by the application of a chemiluminescent substrate (PerkinElmer, Boston, MA) and exposure to autoradiograph film (Super RX; Fujifilm, Dielsdorf, Switzerland).

Morphology and Retinal Thickness

Eyes were enucleated, fixed in glutaraldehyde, embedded in Epon, and processed for light microscopy, as previously described.[11] A digitalized microscope (Axiovision; Carl Zeiss Meditec, Jena, Germany) was used to examine the slides. Retinal thickness was measured on 0.5-μm-thick nasotemporal sections at fixed distances (0, 150, 500, 1000, 1500, 1750, 2000, and 2250 μm) from the optic nerve head using ImageJ (ver. 1.43; developed by Wayne Rasband, National Institutes of Health, Bethesda, MD; available at http://rsb.info.nih.gov/ij/index.html) for both *Hif1a*$^{flox/flox}$;α-Cre mice and control littermates (n = 3).

Immunofluorescence

Eyes were isolated and incubated for 10 minutes in phosphate-buffered saline (PBS) containing 4% paraformaldehyde. Cornea and lens were removed, and the remaining tissue, including the retina, was incubated for another 15 minutes in 4% paraformaldehyde. The eye cups were then immersed in 30% sucrose, kept at 4°C overnight, and embedded in cryoprotective medium (Jung, Nussloch, Germany). Twelve-micrometer sections were cut (nasotemporal orientation), and the cryoslides

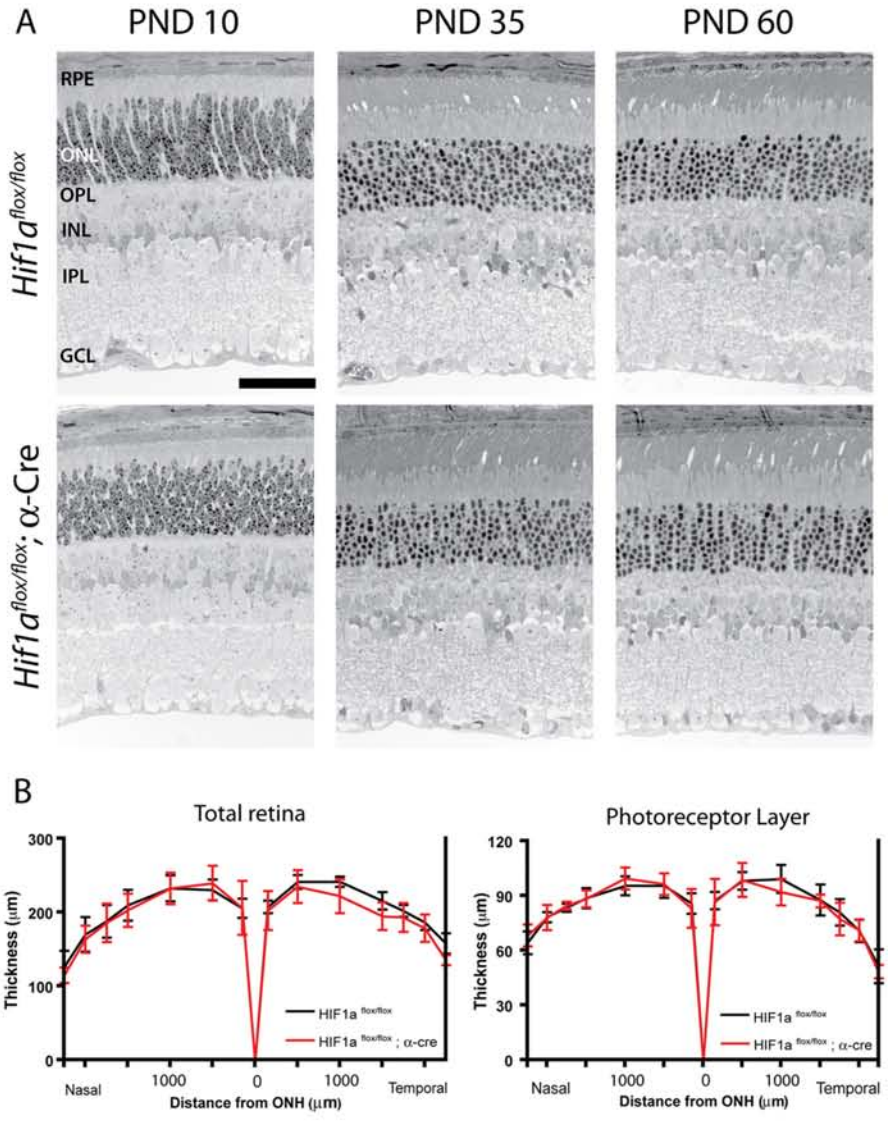

Figure 2. Normal retinal morphology in *Hif1a* knockdown mice. (**A**) Retinal morphology of *Hif1a*$^{flox/flox}$;α-Cre mice, and *Hif1a*$^{flox/flox}$ littermates at PND10, -35, and -60 were analyzed. Shown are representative sections of the retinal periphery of at least three animals per time point. RPE, retinal pigment epithelium; ONL, outer nuclear layer; OPL, outer plexiform layer; INL, inner nuclear layer; IPL, inner plexiform layer; GCL, ganglion cell layer. Scale bar, 100 μm. (**B**) The thickness of the retina and of the photoreceptor layer (ONL plus photoreceptor segments) in *Hif1a*$^{flox/flox}$;α-Cre mice and control littermates. Thickness was measured at 0, 150, 500, 1000, 1500, 1750, 2000, and 2250 μm from the optic nerve head (ONH) in both nasal and temporal hemispheres, as indicated. Mean ± SD; n = 3. Ticks on the x-axis correspond to 500 μm.

were blocked in a humid chamber with PBS containing 3% normal goat serum and 0.3% Triton X-100. The slides were incubated with rabbit anti-VSX2 (CHX10; 1:500) antibody (the generous gift of Connie Cepko, Harvard University, Boston, MA;), rabbit anti-GNAT1 (sc-389, 1:500; Santa Cruz Biotechnology), rabbit anti-GNAT2 (sc-390, 1:500; Santa Cruz Biotechnology), mouse anti-BRN3A (MAB1585, 1:100; Chemicon, Billerica, MA), mouse anti-GS (B302, 1:500; Millipore, Billerica, MA), mouse anti-GFAP (G-3893, 1:500; Sigma-Aldrich, St. Louis, MO), mouse anti-SYP (synaptophysin, NCL-L-SYNAP-299, 1:100; Novocastra, Newcastle, UK,), *Griffonia simplicifolia* isolectin IB_4-Alexa594 (I21413, 1:50; Invitrogen, Basel, Switzerland,), and rabbit anti-CALB1 (calbindin, AB1778, 1:500; Chemicon). After being washed with PBS, the slides were incubated with Cy3-labeled secondary antibodies (Jackson ImmunoResearch Europe, Newmarket, UK), for 1 hour at room temperature, washed with PBS, counterstained with 4,6-diamidino-2-phenylindole dilactate (Molecular Probes, Invitrogen, Carlsbad, CA) and mounted with polyvinyl alcohol (Mowiol 4-88 Reagent; VWR International AG, Lucerna, Switzerland). Immunofluorescent stainings were analyzed with the digitalized microscope (Axiovision; Carl Zeiss Meditec).

Flat Mount Immunofluorescence and Quantification of Vasculature

Eyes were isolated and incubated for 3 to 5 minutes in phosphate-buffered saline (PBS) containing 2% paraformaldehyde. The cornea and lens were removed, and the retina was dissected from the sclera and flat mounted in PBS. The retina was then stored in methanol at −20°C. Before immunofluorescence analysis, retinal flat mounts were incubated another 10 minutes in 4% paraformaldehyde in PBS and blocked with PBS containing 3% normal goat serum and 0.3% Triton X-100. Flat mounts were incubated with the vascular-specific *G. simplicifolia* isolectin IB_4-Alexa594 (I21413, 1:500; Invitrogen) overnight. After they were washed with PBS, the flat mounts were mounted with polyvinyl alcohol (Mowiol 4-88 Reagent; VWR International AG). Immunofluorescent staining was analyzed with the digitalized microscope (Axiovision; Carl Zeiss Meditec) or with a laser scanning confocal microscope (model SP5; Leica, Wetzlar, Germany). Image-analysis software (Imaris; Bitplane AG, Zurich, Switzerland) was used to analyze confocal microscope *z*-stacks and to generate *x*-*z* projections.

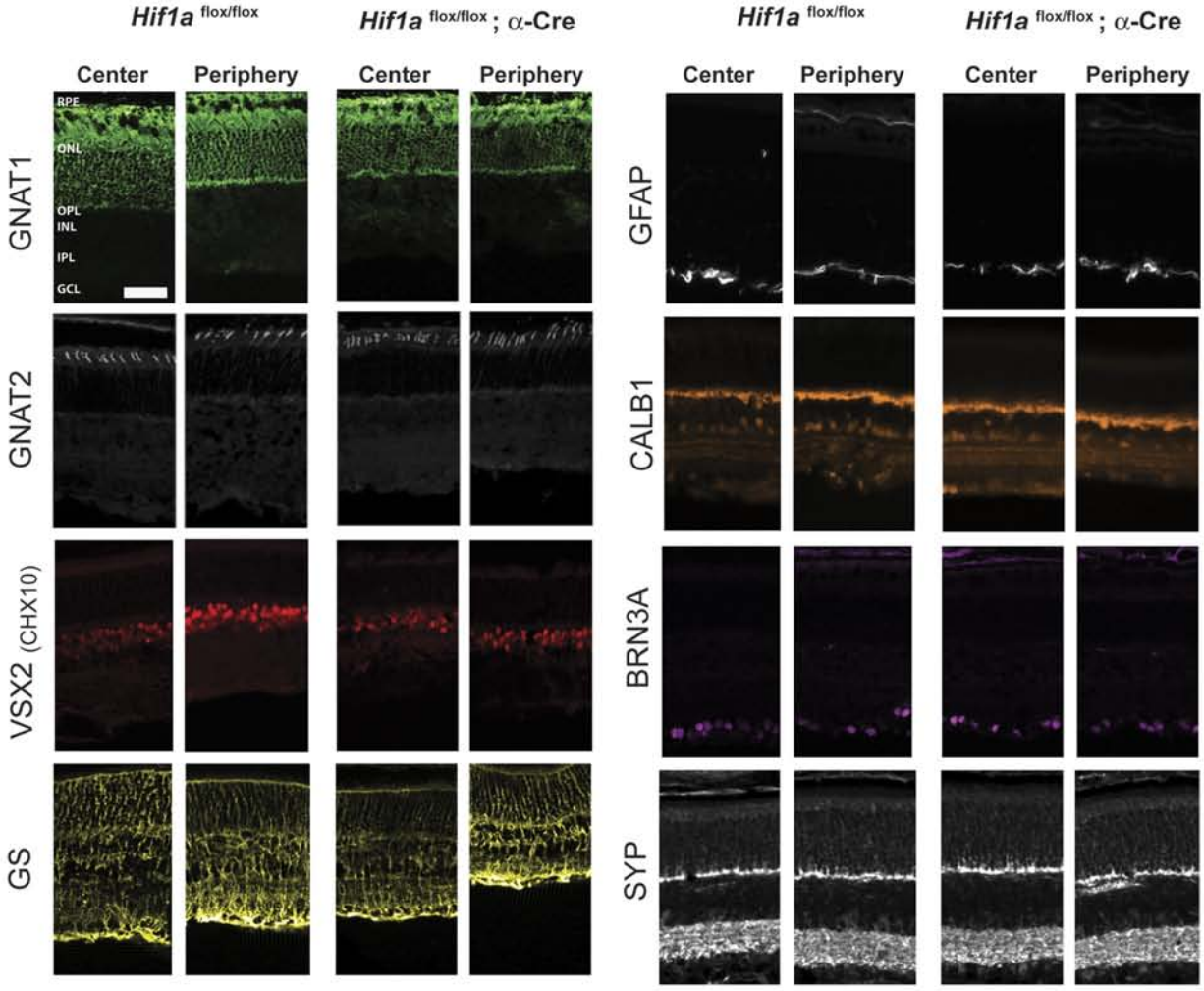

Figure 3. Normal distribution of major retinal cell types in *Hif1a* knockdown mice. Immunostaining of rods (rod transducin, GNAT1, *green*), cones (cone transducin, GNAT2, *white*), bipolar cells (VSX2 [CHX10], *red*), Müller cells (glutamine synthase [GS] *yellow*), astrocytes and Müller cell endfeet (glial fibrillary acid protein [GFAP] *white*), horizontal cells (calbindin [CALB1] *orange*), ganglion cells (BRN3A, *purple*), and synapses in the inner plexiform and outer plexiform layers (synaptophysin, SYP, *white*) in $Hif1a^{flox/flox}$;α-Cre mice, and $Hif1a^{flox/flox}$ littermates at PND90. Note that the mice used in the study were light-adapted, which caused the redistribution of rod transducin to rod inner segments and cell bodies. Shown are stainings for the central and the peripheral retina. Scale bar, 50 μm.

For quantification of vascular coverage, three regions (770 μm^2) at a distance of 2000 μm from the optic nerve head were analyzed for each flat-mounted retina (PND60) by laser scanning confocal microscopy ($n = 3$ for both the *Hif1a*$^{flox/flox}$;α-Cre mice and the control littermates). The image-analysis software (Imaris; Bitplane AG) was used to analyze confocal microscope *z*-stacks and to generate *x*–*y*-sections for each vascular layer. The sections layer were then postprocessed (thresholded and binarized), with ImageJ used to obtain binary data from which vascular coverage was determined (ratio of black pixels to total pixels).

Results

Peripheral *Hif1a* Knockdown Does Not Lead to Abnormal Retinal Architecture

Cre recombinase in the α-Cre mouse is expressed starting around E10.5 and leads to deletion of floxed sequences in most cells of the peripheral but not of the central retina.[9] Visualization of expressed RFP protein after Cre-mediated deletion of a floxed STOP sequence in 21-day-old ROSA-flox-RFP;α-Cre mice confirmed the spatial distribution of Cre activity and revealed that virtually every cell type in the peripheral retina expressed Cre recombinase (Fig. 1A). In contrast, the central retina in proximity to the optic nerve head did not show RFP protein, indicating that Cre recombinase was not expressed in this region (Fig. 1A). The *Hif1a*$^{flox/flox}$;α-Cre knockdown mice showed a reduced retinal expression of *Hif1a* mRNA as early as PND5 (Fig. 1B). Similarly, HIF1A protein levels were severely downregulated in the knockdown retina (Fig. 1C). The strong downregulation of HIF1A protein at PND10 suggests that in the early postnatal retina, HIF-1A is normally stabilized mainly in the periphery, the region of Cre recombinase activity in knockdown mice. This possibility is conceivable because the central retina is already fully vascularized at PND10, whereas the outer and intermediate plexi are not yet formed in the peripheral retina,[12] which may lead to hypoxic stabilization of HIF1A in wild-type retinas.

Analysis of the retinal morphology by light microscopy revealed no abnormalities or degeneration in the *Hif1a*$^{flox/flox}$;α-Cre mice (Fig. 2A). The architecture of the *Hif1a* knockdown retina at PND10 appeared normal in the center (not shown) as well as in the periphery, where Cre-mediated deletion of *Hif1a* genomic DNA led to a knockdown of HIF1A protein. Maturation of the retina also proceeded normally, resulting in a retinal morphology indistinguishable from that of the control mice, at least up to PND60, the latest time point analyzed (Fig. 2A). Normal retinal morphology was further supported by a similar thickness of the retina and of the photoreceptor layer in the knockdown and wild-type mice at PND60 (Fig. 2B).

In line with normal retinal morphology, no appreciable differences in localization and spatial arrangement of the main neuronal and glial cells were observed between the knockdown and control retinas (Fig. 3). It is important to note that expression of GFAP was not upregulated in Müller cells of the *Hif1a*$^{flox/flox}$;α-Cre mice. This finding suggests that the *Hif1a* knockdown retinas were not gliotic and indicates that the absence of *Hif1a* did not lead to retinal stress or injury.

Hif1a Knockdown Results in a Reduced Peripheral Vascular Density

Since HIF1A levels are high in the early postnatal retina of wild-type mice and are reduced concomitantly with the development of the retinal vasculature,[7] we analyzed the vessel network in retinal flat mounts of the *Hif1a* knockdown and wild-type mice. At PND5, vessels of the primary plexus covered about two thirds of the retinal surface in both the control and knockdown mice (Fig. 4). The superficial capillary network of the primary plexus

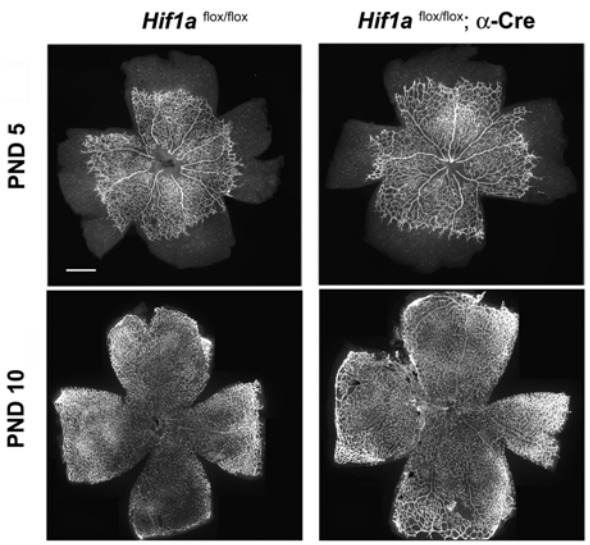

Figure 4. The development of the primary plexus in *Hif1a* knockdown mice. Retinal flat mounts of the *Hif1a*$^{flox/flox}$;α-Cre mice (*right*) and the *Hif1a*$^{flox/flox}$ littermates (*left*) at PND5 (*top*) and PND10 (*bottom*). Vessels were stained with isolectin IB_4 coupled to Alexa594. Shown are representative images. Scale bar, 500 μm.

extended toward the periphery with approximately the same kinetics and reached the periphery at ~PND10 in both the *Hif1a* knockdown and control mice. Thus, the lack of HIF1A in the peripheral retina did not affect the correct timing of the development of the postnatal retinal vasculature.

When we analyzed the vasculature in more detail, the *Hif1a*$^{flox/flox}$;α-Cre mice showed an incomplete development of the intermediate plexus in the peripheral retina at PND21 (Fig. 5). In contrast, the primary plexus and the outer plexus were well established. In the central retina of the *Hif1a*$^{flox/flox}$;α-Cre mice (where Cre recombinase is not expressed and floxed gene sequences are not deleted[9]), both deeper plexi were present and showed a pattern comparable to that in the control mice (Fig. 5A). The incomplete vasculature in the periphery persisted at least until PND60 (the last time point observed). Confocal imaging of flat-mounted retinas of the wild-type controls at PND60 showed the dense capillary network of the intermediate plexus (Fig. 5B). In the *Hif1a* knockdown mice, however, horizontally extending vessels were largely absent in the intermediate plexus and only individual spots were visible in the peripheral retina. The *x*–*z*-stacks of the area shown in the flat mounts revealed that these spots were most likely vessels connecting the primary plexus with the outer plexus without establishing the intermediate plexus (Fig. 5B). The area shown for the *Hif1a* knockdown retina in Figure 5B shows the transition zone from the central to the peripheral retina. The asterisk denominates the more central area where the vascular network of the intermediate plexus was still visible. In contrast, horizontally extending capillaries were missing in the adjacent peripheral retina, resulting in an *x*–*z*-stack with no horizontal intermediate plexus visible in the more peripheral region of the retina (left side on *x*–*z* stack) but with an intermediate plexus formed in the region of the more central retina (right side on the *x*–*z* stack). The two yellow lines in each *x*–*z* stack show the focal plane of the flat mounts above the stacks. In contrast to the intermediate plexus, vessel density in the primary and outer plexi was less affected in the knockdown retinas. When the extent of vascular coverage in 21-day-old retinas was quantified for each individual plexus, the knockdown mice showed a reduction of 75% ± 0.06% SD ($P < 0.01$) in the extent of vascularization of the intermediate plexus compared with the controls.

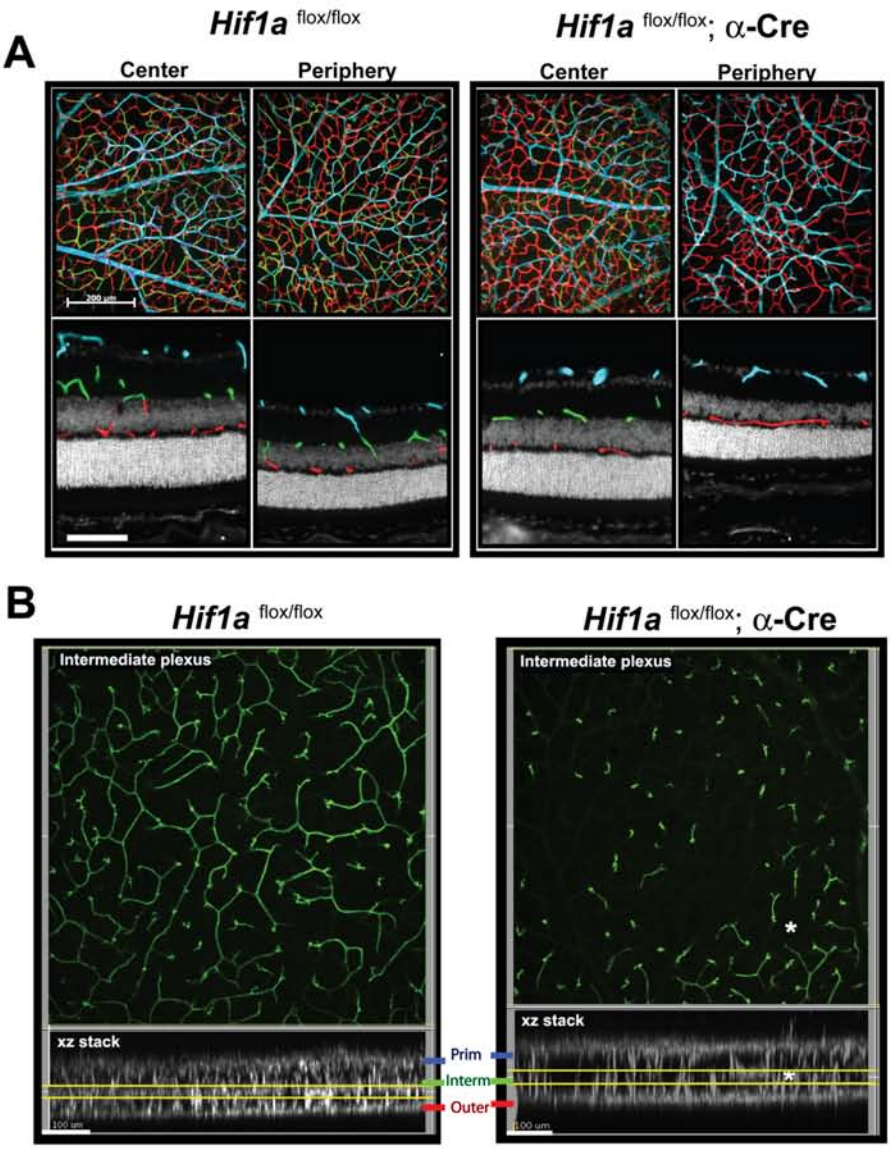

FIGURE 5. Lack of the intermediate plexus in the peripheral retina of *Hif1a* knockdown mice. (**A**) Immunostaining of blood vessels (isolectin IB_4, coupled to Alexa594) in $Hif1a^{flox/flox}$ littermates (*left*) and $Hif1a^{flox/flox}$;α-Cre mice (*right*). Shown are flat mounts (*top*) and retinal cryosections (*bottom*) at PND21. Images of the vascular layers in flat mounts were taken by adjusting the focal plane of the confocal microscope accordingly. Vessels were highlighted by artificial coloring (primary plexus: *blue*; intermediate plexus: *green*; outer plexus: *red*). Note that the density of the vessels in the intermediate plexus was strongly reduced in the peripheral retina of the *Hif1a* knockdown mice. (**B**) Representative images of the intermediate plexus in flat mounts of $Hif1a^{flox/flox}$ littermates (*left*), and $Hif1a^{flox/flox}$;α-Cre mice (*right*) at PND60. The focal plane was adjusted to visualize exclusively the intermediate plexus (*top*). The *x*–*z*-stacks (*bottom*) are artificial sections and show the sum of all signals (including signals in the primary, the intermediate, and the outer plexi) of the area shown in the flat mount panels above the stacks. For better recognition of the different plexi, the *z*-value of the *z*-stacks was increased five times ($x = 1$; $y = 1$; $z = 5$). *Yellow* lanes depict the focal planes used for the flat mount pictures. Note the absence of a continuous capillary network in the intermediate plexus of $Hif1a^{lox/flox}$;α-Cre mice. In these mice, such a network is only formed in the lower right corner of the flat-mounted retina, which is the more central area of the retina and presumably the region where *Hif1a* was not knocked down. (✱) The more central retina. Scale bar: (**A**) 200 μm (flat mounts); 100 μm (sections); (**B**) 100 μm.

A mildly increased vascular density of 130% ± 0.11% SD ($P < 0.05$) of that of the control littermates was observed for the primary plexus in the $Hif1a^{flox/flox}$;α-Cre mice. At the level of the outer plexus, no significant differences were detected. This result suggests that HIF1A has a direct or indirect role in the development of a correct retinal vasculature and especially of the intermediate plexus.

Erythropoietin (*Epo*) Is Upregulated in *Hif1a* Knockdown Mice

Even though HIF1A protein levels (Fig. 1B) and vessel density (Fig. 5) were reduced in the *Hif1a*-knockdown mice, no significant differences in the expression levels of the proangiogenic *Vegf* (pan-*Vegf*) and antiangiogenic *Serpinf1 (Pedf)* genes were observed between the knockdown and control mice (Fig. 6). However, the *Hif1a* knockdown mice showed a strong upregulation of *Epo* expression starting at PND15. This upregulation was sustained up to PND60 (Fig. 6). Interestingly, *Epas1* (*Hif2a*) mRNA levels appeared upregulated at PND21 as a consequence of the *Hif1a* knockdown. No significant differences were found in the expression levels of *Edn1*, *Edn2*, *Mmp2*, *Nos2* (*iNos*), *Ffg2*, *Bdnf*, *Cntf*, and *Gfap*. At the same time, *Tie2* and *Lif* expression levels were also transiently elevated. The significance of this observation and whether expression of the three upregulated genes is connected needs to be determined. The unaltered expression of the bipolar cell marker *Vsx2* (*Chx10*), of the rod markers *Rho* and *Gnat1*, and of the cone marker *Gnat2* confirmed that the knockdown retinas did not undergo degeneration, despite the lack of vessels in the intermediate plexus.

The strong induction of *Epo* gene expression in retinas of the $Hif1a^{flox/flox}$;α-Cre mice may have been regulated by EPAS1 (HIF2A). EPAS1 was present at increased levels in the *Hif1a* knockdown mice at the same time (PND15) as increased *Epo* expression was observed (Fig. 7). EPAS1 continued to be present at elevated levels at least until PND75 in $Hif1a^{flox/flox}$;α-Cre mice. In contrast, EPAS1 levels were very low in both the

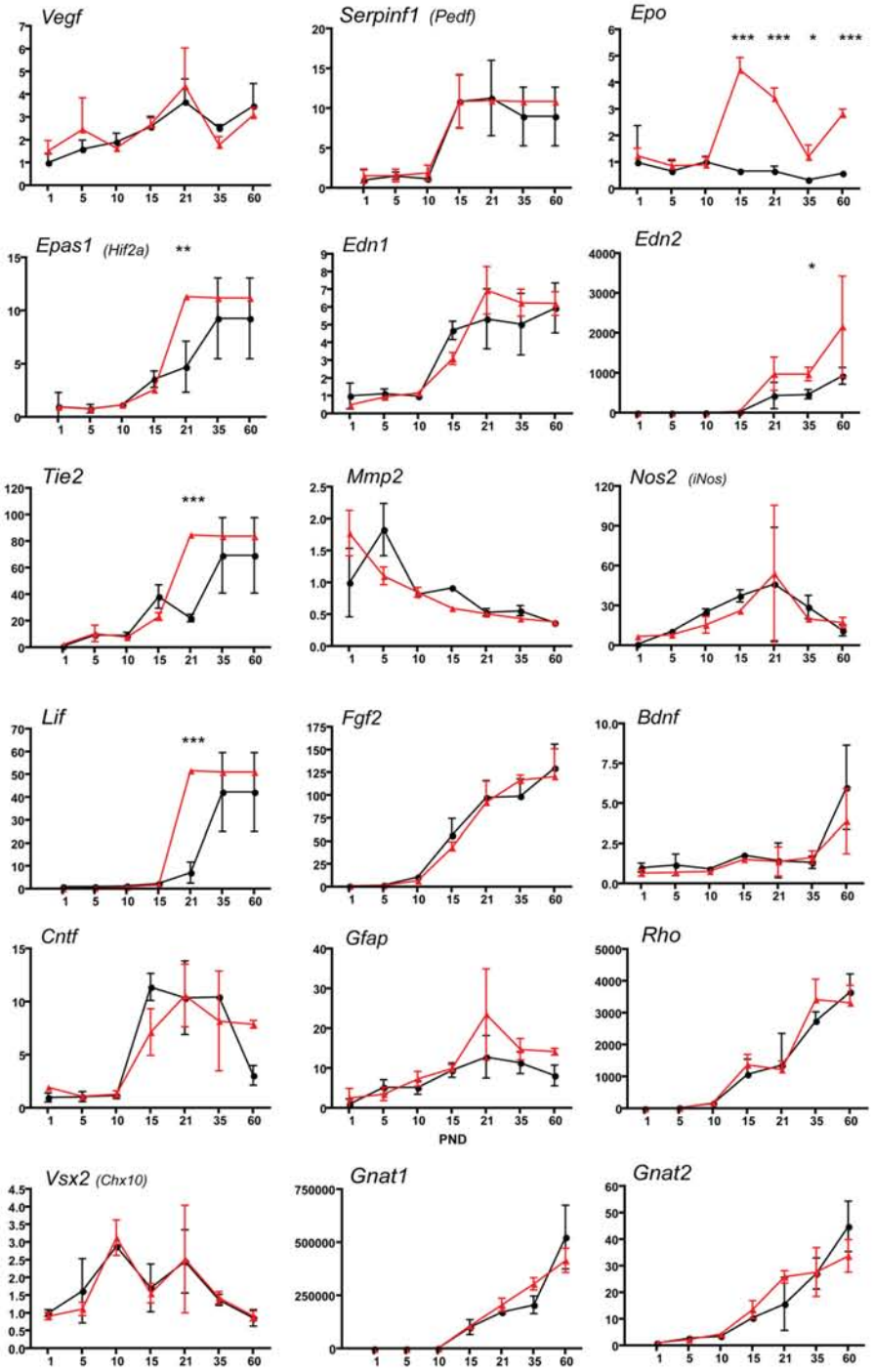

FIGURE 6. Induced expression of *Epo* in retinas of *Hif1a* knockdown mice. Relative quantification of gene expression in retinas of the wild-type (*black filled circles*) and the *Hif1a* knockdown (*red filled triangles*) mice by real-time PCR. cDNAs were prepared from total retinal RNA isolated at the PNDs indicated on the *x*-axis. Given are mean values ± SD of three retinas per time point and genotype, amplified in duplicate. Values were normalized to β-actin and are expressed relative to that at PND1 in the $Hif1a^{flox/flox}$ mice, which was set to 1. Differences in gene expression levels between knockdown and control mice at individual time points were tested for significance by using a Student's *t*-test; $^{*}P < 0.05$; $^{**}P < 0.025$; $^{***}P < 0.01$.

Hif1a knockdown and control mice at PND10. At this time point, also *Epo* was expressed at similar low levels in the two mice (Fig. 6).

DISCUSSION

The development of the retinal vasculature in mice starts shortly after birth at the optic nerve head in the center of the retina and expands toward the periphery. First, the primary plexus develops and reaches the retinal periphery after 8 to 10 days. Vessel growth is guided by a preestablished network formed by astrocytes. From the primary plexus, angiogenic sprouts emerge, and vessels start to penetrate the retina, perpendicular to the primary plexus. Transient expression of VEGF precedes formation of the intermediate and outer plexi, which develop from the center toward the periphery, independent of the retinal astrocytes.[6] This process was obviously disturbed in mice lacking

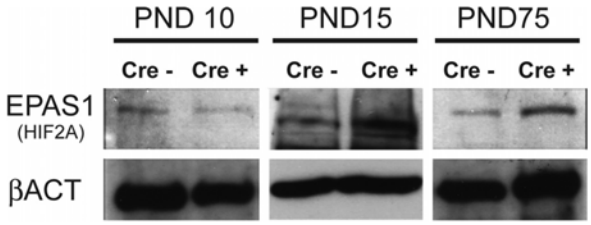

FIGURE 7. Elevated protein levels of EPAS1 in retinas of *Hif1a* knockdown mice. Western blot analysis of total retinal extracts at PND10, -15, and -75 of the *Hif1a*$^{flox/flox}$ mice, without (Cre−) or with α-Cre (Cre+), as indicated. β-Actin served as the loading control. Shown are representative blots of three mice per time point and genotype.

HIF1A in the peripheral retina. Whereas vessels of the primary plexus and of the outer plexus developed similarly in the knockdown and control mice, the capillaries of the intermediate plexus were significantly reduced in the retinal periphery of the *Hif1a* knockdowns. It is interesting to note that the intermediate plexus, which is incompletely formed in the knockdown retina, is the last vascular plexus to develop in the normal postnatal mouse retina. The significance of this observation must be established, but it may suggest regulatory mechanisms specific for each vascular plexus.

The most prominent candidate for involvement in vessel formation is VEGF, a potent angiogenic and vasopermeability factor, whose contribution to general and ocular angiogenesis has been extensively studied.[13,14] The gene for VEGF is strongly regulated by HIFs, which leads to increased production and secretion of VEGF under hypoxic conditions.[15] Several retinal cell types, including endothelial cells, astrocytes, pericytes, Müller cells, and retinal pigment epithelial cells, upregulate VEGF expression under conditions of low oxygen tension.[16,17] Although the *Hif1a*$^{flox/flox}$;α-Cre mice had severely reduced levels of HIF1A in the developing retina (Fig. 1) and a pronounced vessel phenotype, no reduction in *Vegf* expression was detected. This surprising observation is in line with recent results of Weidemann et al.,[18] who showed that astrocyte- and Müller cell–specific *Hif1a* knockdown also did not influence *Vegf* expression in the retina. Given the strong knockdown of HIF1A and the unaltered *Vegf* expression levels in the *Hif1a*$^{flox/flox}$;α-Cre mice, our results support the conclusion that transcription factors other than HIF1 are the main regulators of *Vegf* expression during retinal development. Although the identity of these factors has yet to be established, recent results suggest a prominent role of EPAS1 in the regulation of *Vegf* expression. Knockdown of the von Hippel-Lindau (VHL) protein during retinal development led to the activation of HIF1 and -2 and to increased *Vegf* expression.[19,20] Whereas the simultaneous knockdown of *Vhl* and *Hif1a* also led to increased VEGF levels, simultaneous ablation of *Vhl* and *Epas1* (*Hif2a*) did not.[18] Furthermore, functional studies in a mutant cell line expressing neither HIF1A nor EPAS1 showed stronger transactivation of the VEGF promoter by EPAS1.[21] In addition, the introduction of *Epas1* cDNA into 293 fetal kidney cells[22] or an adenovirus-mediated delivery of the *Epas1* gene in mouse wound-healing models significantly induced the expression of VEGF.[23] These data suggest that EPAS1 may be able to regulate *Vegf* expression, either alone or in conjunction with HIF1A. Therefore, the increased expression of EPAS1 in our model may compensate for the downregulation of HIF1A, resulting in unaltered expression levels of *Vegf*. However, despite normal *Vegf* expression, the intermediate plexus did not develop, suggesting an essential role for other, HIF1A-controlled factors in this process. Importantly, knocking down *Hif1a* in astrocytes and Müller cells did not lead to alterations in the vascular organization.[18] This result is in contrast to the reduced vessel density and the lack of the peripheral intermediate plexus in our pan-*Hif1a* knockdown mouse line, suggesting that the correct formation of the retinal vasculature, or at least of the intermediate plexus, may be regulated by a correct *Hif1a*-expressing profile in cells other than Müller cells or astrocytes.

Our results are also in line with those in recent studies that elucidated the role of *Hif1a* in the postnatal vascular development and/or oxygen-induced neovascularization by pharmacologic approaches. Yoshida et al.[24] showed that digoxin reduces HIF1A levels in ischemic tissues in vivo and suppresses retinal and choroidal neovascularization. Similarly, DeNiro et al.[25] reported that another inhibitor of HIF1A, YC-1, decreases basal expression levels of HIF1A protein in normoxia and inhibits HIF1A protein synthesis, stability, and nuclear translocation in hypoxia. This effect was accompanied by a significant influence on HIF1 target gene expression that finally resulted in a reduction of vascular density in the retina.[25] Both of these studies confirm that inhibition of HIF1 results in a reduction of retinal vascularization. These results, along with our data and the availability of HIF1A inhibitors, validate the potential of modulating the *Hif1a* signaling pathway as a therapeutic strategy to inhibit vessel growth.

Although the lack of the capillaries in the intermediate plexus most likely affects delivery of nutrients and oxygen to cells especially of the INL, retinal architecture, and the number and distribution of cells were not affected by the *Hif1a* knockdown. Compensatory mechanisms may thus be in place, allowing the cells to cope with this special situation. A possible candidate for involvement in such an adaptational response is EPO, which was shown to be neuroprotective of retinal cells.[26,27] *Epo* expression was upregulated in the knockdown retinas (Fig. 6) around the time when the retinal vasculature should be mature. EPO may thus be part of the retinal response to improper vascularization. Interestingly, EPO was not only shown to be neuroprotective, but it was also suggested to be involved in angiogenesis and thus in the regulation of the growth of blood vessels.[28,29] It was also suggested that EPO is a main factor in the development of retinopathy of prematurity (ROP)[30–32] and is involved in vessel stability.[33] The upregulation of *Epo* expression in the *Hif1a* knockdown mice may thus protect cells from damage but may correct the vascular abnormalities. Increased expression of *Epo* was probably caused by the increased presence of EPAS1 in the knockdown retinas. EPAS1 has been shown to be the main regulator of *Epo* expression in other organs,[34,35] and EPAS1, like HIF1A, is regulated through stabilization in hypoxic conditions. Lack of the development of the intermediate plexus may have led to reduced oxygen tension in the retina and thus to the stabilization of EPAS1.

In general, our results establish and support the importance of a correct spatial and temporal expression profile of *Hif1a* for the development of a normal retinal vasculature and especially for the formation of the intermediate plexus.

Acknowledgments

The authors thank Coni Imsand for excellent technical assistance with retinal morphology and genotyping, the Center for Microscopy and Image Analysis of the University of Zurich for assistance with confocal microscopy analysis, and Hans Joerg Fehling (University Clinics Ulm, Germany) for providing us the ROSA-flox-RFP reporter mice.

References

1. Arjamaa O, Nikinmaa M. Oxygen-dependent diseases in the retina: role of hypoxia-inducible factors. *Exp Eye Res.* 2006;83:473–483.
2. Semenza GL. Hydroxylation of HIF-1: oxygen sensing at the molecular level. *Physiology (Bethesda).* 2004;19:176–182.
3. Huang LE, Gu J, Schau M, Bunn HF. Regulation of hypoxia-inducible factor 1alpha is mediated by an O2-dependent degradation domain via the ubiquitin-proteasome pathway. *Proc Natl Acad Sci U S A.* 1998;95:7987–7992.
4. Ziello JE, Jovin IS, Huang Y. Hypoxia-inducible factor (HIF)-1 regulatory pathway and its potential for therapeutic intervention in malignancy and ischemia. *Yale J Biol Med.* 2007;80:51–60.
5. Fruttiger M. Development of the retinal vasculature. *Angiogenesis.* 2007;10:77–88.
6. Stone J, Itin A, Alon T, et al. Development of retinal vasculature is mediated by hypoxia-induced vascular endothelial growth factor (VEGF) expression by neuroglia. *J Neurosci.* 1995;15:4738–4747.
7. Grimm C, Hermann DM, Bogdanova A, et al. Neuroprotection by hypoxic preconditioning: HIF-1 and erythropoietin protect from retinal degeneration. *Semin Cell Dev Biol.* 2005;16:531–538.
8. Ryan HE, Poloni M, McNulty W, et al. Hypoxia-inducible factor-1alpha is a positive factor in solid tumor growth. *Cancer Res.* 2000;60:4010–4015.
9. Marquardt T, Ashery-Padan R, Andrejewski N, Scardigli R, Guillemot F, Gruss P. Pax6 is required for the multipotent state of retinal progenitor cells. *Cell.* 2001;105:43–55.
10. Luche H, Weber O, Nageswara Rao T, Blum C, Fehling HJ. Faithful activation of an extra-bright red fluorescent protein in "knock-in" Cre-reporter mice ideally suited for lineage tracing studies. *Eur J Immunol.* 2007;37:43–53.
11. Samardzija M, Wenzel A, Thiersch M, Frigg R, Reme C, Grimm C. Caspase-1 ablation protects photoreceptors in a model of autosomal dominant retinitis pigmentosa. *Invest Ophthalmol Vis Sci.* 2006;47:5181–5190.
12. Stahl A, Connor KM, Sapieha P, et al. The mouse retina as an angiogenesis model. *Invest Ophthalmol Vis Sci.* 2010;51:2813–2826.
13. Senger DR, Perruzzi CA, Feder J, Dvorak HF. A highly conserved vascular permeability factor secreted by a variety of human and rodent tumor cell lines. *Cancer Res.* 1986;46:5629–5632.
14. Leung DW, Cachianes G, Kuang WJ, Goeddel DV, Ferrara N. Vascular endothelial growth factor is a secreted angiogenic mitogen. *Science.* 1989;246:1306–1309.
15. Shweiki D, Itin A, Soffer D, Keshet E. Vascular endothelial growth factor induced by hypoxia may mediate hypoxia-initiated angiogenesis. *Nature.* 1992;359:843–845.
16. Adamis AP, Shima DT, Yeo KT, et al. Synthesis and secretion of vascular permeability factor/vascular endothelial growth factor by human retinal pigment epithelial cells. *Biochem Biophys Res Commun.* 1993;193:631–638.
17. Aiello LP, Northrup JM, Keyt BA, Takagi H, Iwamoto MA. Hypoxic regulation of vascular endothelial growth factor in retinal cells. *Arch Ophthalmol.* 1995;113:1538–1544.
18. Weidemann A, Krohne TU, Aguilar E, et al. Astrocyte hypoxic response is essential for pathological but not developmental angiogenesis of the retina. *Glia.* 2010;58:1177–1185.
19. Lange C, Caprara C, Tanimoto N, et al. Retina specific activation of a sustained hypoxia-like response leads to severe retinal degeneration and loss of vision. *Neurobiol Dis.* 2010.
20. Kurihara T, Kubota Y, Ozawa Y, et al. von Hippel-Lindau protein regulates transition from the fetal to the adult circulatory system in retina. *Development.* 2010;137:1563–1571.
21. Wiesener MS, Turley H, Allen WE, et al. Induction of endothelial PAS domain protein-1 by hypoxia: characterization and comparison with hypoxia-inducible factor-1alpha. *Blood.* 1998;92:2260–2268.
22. Xia G, Kageyama Y, Hayashi T, Kawakami S, Yoshida M, Kihara K. Regulation of vascular endothelial growth factor transcription by endothelial PAS domain protein 1 (EPAS1) and possible involvement of EPAS1 in the angiogenesis of renal cell carcinoma. *Cancer.* 2001;91:1429–1436.
23. Takeda N, Maemura K, Imai Y, et al. Endothelial PAS domain protein 1 gene promotes angiogenesis through the transactivation of both vascular endothelial growth factor and its receptor, Flt-1. *Circ Res.* 2004;95:146–153.
24. Yoshida T, Zhang H, Iwase T, Shen J, Semenza GL, Campochiaro PA. Digoxin inhibits retinal ischemia-induced HIF-1α expression and ocular neovascularization. *FASEB J.* 2010;24:1759–1767.
25. DeNiro M, Alsmadi O, Al-Mohanna F. Modulating the hypoxia-inducible factor signaling pathway as a therapeutic modality to regulate retinal angiogenesis. *Exp Eye Res.* 2009;89:700–717.
26. Grimm C, Wenzel A, Groszer M, et al. HIF-1-induced erythropoietin in the hypoxic retina protects against light-induced retinal degeneration. *Nat Med.* 2002;8:718–724.
27. Becerra SP, Amaral J. Erythropoietin–an endogenous retinal survival factor. *N Engl J Med.* 2002;347:1968–1970.
28. Ribatti D. Erythropoietin and tumor angiogenesis. *Stem Cells Dev.* 2010;19:1–4.
29. Heeschen C, Aicher A, Lehmann R, et al. Erythropoietin is a potent physiologic stimulus for endothelial progenitor cell mobilization. *Blood.* 2003;102:1340–1346.
30. Watanabe D, Suzuma K, Matsui S, et al. Erythropoietin as a retinal angiogenic factor in proliferative diabetic retinopathy. *N Engl J Med.* 2005;353:782–792.
31. Morita M, Ohneda O, Yamashita T, et al. HLF/HIF-2alpha is a key factor in retinopathy of prematurity in association with erythropoietin. *EMBO J.* 2003;22:1134–1146.
32. Chen J, Connor KM, Aderman CM, Willett KL, Aspegren OP, Smith LE. Suppression of retinal neovascularization by erythropoietin siRNA in a mouse model of proliferative retinopathy. *Invest Ophthalmol Vis Sci.* 2009;50:1329–1335.
33. Chen J, Connor KM, Aderman CM, Smith LE. Erythropoietin deficiency decreases vascular stability in mice. *J Clin Invest.* 2008;118:526–533.
34. Rankin EB, Biju MP, Liu Q, et al. Hypoxia-inducible factor-2 (HIF-2) regulates hepatic erythropoietin in vivo. *J Clin Invest.* 2007;117:1068–1077.
35. Chavez JC, Baranova O, Lin J, Pichiule P. The transcriptional activator hypoxia inducible factor 2 (HIF-2/EPAS-1) regulates the oxygen-dependent expression of erythropoietin in cortical astrocytes. *J Neurosci.* 2006;26:9471–9481.

10.2 From Oxygen to Erythropoietin: Relevance of Hypoxia for Retinal Development, Health and Disease

Christian Caprara[1], Christian Grimm[1, 2]

[1] Lab for Retinal Cell Biology, Department Ophthalmology, University of Zurich, Zurich, Switzerland

[2] Zurich Center for Integrative Human Physiology (ZIHP), University of Zurich, Zurich, Switzerland

[3] Neuroscience Centre (ZNZ), University of Zurich, Zurich, Switzerland

Published in Progress in Retinal and Eye Research, 2012, **31**(1):89-119

Personal Contribution

Performed literature search, manuscript writing/editing.

Progress in Retinal and Eye Research 31 (2012) 89–119

Contents lists available at SciVerse ScienceDirect

Progress in Retinal and Eye Research

journal homepage: www.elsevier.com/locate/prer

From oxygen to erythropoietin: Relevance of hypoxia for retinal development, health and disease

Christian Caprara [a], Christian Grimm [a,b,*]

[a] Lab for Retinal Cell Biology, Department of Ophthalmology, University of Zurich, Zurich, Switzerland
[b] Zurich Center for Integrative Human Physiology (ZIHP), and Neuroscience Center (ZNZ), University of Zurich, Zurich, Switzerland

ARTICLE INFO

Article history:
Available online 16 November 2011

Keywords:
Oxygen
Hypoxia
Retina
HIF
Retinal vasculature
Preconditioning
EPO
Retinal development
Degeneration
Neuroprotection
VEGF
Angiogenesis
Neovascularization

ABSTRACT

Photoreceptors and other cells of the retina consume large quantities of energy to efficiently convert light information into a neuronal signal understandable by the brain. The necessary energy is mainly provided by the oxygen-dependent generation of ATP in the numerous mitochondria of retinal cells. To secure the availability of sufficient oxygen for this process, the retina requires constant blood flow through the vasculature of the retina and the choroid. Inefficient supply of oxygen and nutrients, as it may occur in conditions of disturbed hemodynamics or vascular defects, results in tissue ischemia or hypoxia. This has profound consequences on retinal function and cell survival, requiring an adaptational response by cells to cope with the reduced oxygen tension. Central to this response are hypoxia inducible factors, transcription factors that accumulate under hypoxic conditions and drive the expression of a large variety of target genes involved in angiogenesis, cell survival and metabolism. Prominent among these factors are vascular endothelial growth factor and erythropoietin, which may contribute to normal angiogenesis during development, but may also cause neovascularization and vascular leakage under pathologically reduced oxygen levels. Since ischemia and hypoxia may have a role in various retinal diseases such as diabetic retinopathy and retinopathy of prematurity, studying the cellular and molecular response to reduced tissue oxygenation is of high relevance. In addition, the concept of preconditioning with ischemia or hypoxia demonstrates the capacity of the retina to activate endogenous survival mechanisms, which may protect cells against a following noxious insult. Part of these mechanisms is the local production of protective factors such as erythropoietin. Due to its plethora of effects in the retina including neuro- and vaso-protective activities, erythropoietin has gained strong interest as potential therapeutic factor for retinal degenerative diseases.

Abbreviations: A(2A)R, adenosine A(2A) receptor; AAV, adeno-associated virus; Adm, adrenomedullin; AGE, advanced glycation end product; AMD, age-related macular degeneration; Angpt2, angiopoietin 2; AP1, activator protein 1; ARNT, aryl hydrocarbon receptor nuclear translocator; Ars, aminoacyl-tRNA synthetase; ATP, adenosine-5′-triphosphate; BBB, blood–brain barrier; Bcl-X_L, B-cell lymphoma extra large; Bcl2, B-cell lymphoma 2; Bcl2l10, Bcl2-like 10; Bdnf, brain-derived neurotrophic factor; bFgf, basic fibroblast growth factor; bHLH, basic helix-loop-helix; BRAO, branch retinal artery occlusion; BRB, blood–retinal barrier; C/ebpd, CCAAT/enhancer binding protein delta; CA, carbonic anhydrase; CBP, CREB binding protein; CEPO, carbamylated EPO; CNS, central nervous system; Cntf, ciliary neurotrophic factor; CNV, choroidal neovascularization; CRAO, central retinal artery occlusion; Cre, cyclic recombinase; DOR, δ-opioid receptor; DR, diabetic retinopathy; ECM, extracellular matrix; Egln, Egl nine homolog; Epas1, endothelial PAS protein 1; EPO, erythropoietin; Epor, erythropoietin receptor; ERG, electroretinogram; Erk, extracellular-signal-regulated kinase; FIH, factor inhibiting HIF; GABA, γ-aminobutyric acid; GCL, ganglion cell layer; Gfap, glial fibrillary acidic protein; Glut1, glucose transporter 1; Gp130, glycoprotein 130; Gpr91, G-protein coupled receptor 91; HBP, helix B peptide; HBPSP, HBP surface peptide; HGF, hepatocyte growth factor; HIF, hypoxia-inducible factor; HNF4, hepatocyte nuclear factor 4; Ho1, heme oxygenase 1; HP, hypoxic preconditioning; Hph, HIF prolyl hydroxylase; HRE, hypoxia response element; Hsp, heath shock protein; Igf1, insulin-like growth factor 1; Il1b, interleukin 1 beta; Il6, interleukin 6; INL, inner nuclear layer; IOP, intraocular pressure; IPAS, inhibitory PAS-domain protein; IPC, ischemic preconditioning; IPL, inner plexiform layer; ipRGC, intrinsically photosensitive retinal ganglion cell; Jak2, Janus kinase 2; Lif, leukemia inhibitory factor; Mapk, mitogen-activated protein kinase; mKATP, mitochondrial potassium ATP channels; Mt, metallothionein; NFL, nerve fiber layer; Nfκb, nuclear factor κB; NO, nitric oxide; Nos, nitric oxide synthase; NR, Norrie disease; ODDD, oxygen-dependent degradation domain; OIR, oxygen-induced retinopathy; ONL, outer nuclear layer; OPL, outer plexiform layer; PAS, PER-ARNT-SIM Motif; Pdgf, platelet-derived growth factor; Pdgfb, platelet-derived growth factor beta; PDR, proliferative diabetic retinopathy; Phd, prolyl-4-hydroxylase; Pi3k, phosphatidylinositol 3-kinase; Pigf, placenta growth factor; Pkc, protein kinase C; Plcγ, phospholipase C-γ; PND, postnatal day; Ptdsr, phosphatidylserine receptor; RGC, retinal ganglion cell; rhEPO, recombinant human EPO; RHP, repetitive hypoxic preconditioning; ROP, retinopathy of prematurity; ROS, reactive oxygen species; RP, retinitis pigmentosa; RPE, retinal pigment epithelium; Scf, stem cell factor; Sdf1, stromal-cell derived factor 1; shRNA, short hairpin RNA; siRNA, short interfering RNA; Stat, signal transducer and activator of transcription; TAD, transactivation domain; TCA, tricarboxylic acid; Tie2, endothelium-specific receptor tyrosine kinase 2; Tnfa, tumor necrosis factor alpha; Tsp1, thrombospondin 1; Ttr, transthyretin; Vdm2, vitelliform macular dystrophy 2; Vegf, vascular endothelial growth factor; VHL, von Hippel–Lindau protein; βcR, common β receptor.

* Corresponding author. Lab for Retinal Cell Biology, Department of Ophthalmology, USZ, University of Zurich, Wagistrasse 14, 8952 Schlieren, Switzerland. Tel.: +41 44 556 3001.
E-mail address: cgrimm@opht.uzh.ch (C. Grimm).

1350-9462/$ – see front matter © 2011 Elsevier Ltd. All rights reserved.
doi:10.1016/j.preteyeres.2011.11.003

Contents

1. Introduction 90
2. Retinal oxygen distribution and consumption 91
3. Hypoxic events in retinal development 92
   3.1. Hypoxia and retinal angiogenesis 92
4. Hypoxia inducible factors 94
   4.1. HIFs in the developing retina 96
   4.2. HIFs in retinal angiogenesis 96
5. Retinal ischemia and hypoxia 97
   5.1. Effects of ischemia and hypoxia on retinal function 97
   5.2. Retinal ischemic damage 98
6. Impact of hypoxia on retinal pathologies 98
   6.1. Diabetic retinopathy 98
   6.2. Retinopathy of prematurity 99
   6.3. The model of oxygen-induced retinopathy 100
   6.4. Age-related macular degeneration 101
      6.4.1. Choroidal neovascularization 101
   6.5. Glaucoma 101
7. Ischemic and hypoxic preconditioning 102
   7.1. Ischemic tolerance 102
      7.1.1. Signal transduction and second messengers 102
      7.1.2. Transcriptomics 102
      7.1.3. Protective factors and epigenetics 103
   7.2. Protection against light-induced photoreceptor degeneration 103
8. Erythropoietin 104
   8.1. Intracellular signaling 104
   8.2. Neuroprotection in the retina 105
      8.2.1. Protection of retinal ganglion cells 105
      8.2.2. Protection of photoreceptors 105
   8.3. Pleiotropic effects in the diabetic retina 106
      8.3.1. Effects on blood–retinal barrier integrity and cell survival 106
      8.3.2. Effects on Müller cell physiology 106
   8.4. EPO as angiogenic factor 107
   8.5. EPO dosage and non-hematopoietic variants 107
9. Conclusions and future directions 108
   Acknowledgments 108
   References 109

1. Introduction

Metazoan life evolved on the utilization of oxygen for vital metabolic processes. Besides the crucial roles in energy production by oxidative phosphorylation, oxygen has also a profound influence on many other processes such as intracellular signaling, regulation of gene expression and cell survival (Carmeliet et al., 1998; Lopez-Barneo et al., 2001; Semenza, 2001). Consequently, even small changes in oxygen tension may have severe effects on cellular metabolism, cell viability and eventually tissue function (Banasiak et al., 2000). Thus, it seems not surprising that most cells of the human body possess an elaborate molecular system to sense and respond to changes in oxygen concentrations in order to adapt to a given condition (Cherniack, 2004). Central to this system are the transcription factors of the family of hypoxia inducible factors (HIFs) which regulate the expression of a vast number of genes involved in the cellular response to altered tissue oxygenation (see chapter 4).

The retina is one of the most metabolically active tissues in the body (Ames, 1992). It consumes oxygen more rapidly than other tissues due to the high-energy demanding task of providing and sustaining a highly sensitive and efficient system for the conversion of light energy into a neuronal signal 'readable' by the brain (Kimble et al., 1980; Weiter and Zuckerman, 1980; Anderson and Saltzman, 1964). It has been calculated that a single rod consumes up to 10^8 ATP s^{-1} under dark conditions (Okawa et al., 2008), mostly to maintain ion gradients by extrusion of Na^+ ions in outer segments, and Na^+ and Ca^{2+} in the inner segments. Compared to the energy needed for ion pumping, the energy expenditure of the signal transduction machinery, protein synthesis and trafficking, as well as synthesis of glutamate and synaptic vesicular turnover is relatively small (Ames et al., 1992; Okawa et al., 2008). Since rods normally rely on oxidative phosphorylation for ATP production (Ames et al., 1992), the retina requires a high oxygenation level to generate sufficient ATP for proper photoreceptor function, especially under dark conditions (Stefansson et al., 1983; Haugh et al., 1990). Light causes photoreceptors to hyperpolarize which leads to the closure of cGMP-gated channels and to a decreased ion influx (Sung and Chuang, 2010). As a consequence, cells can reduce their ion pumping and require much less ATP to maintain intracellular ion homeostasis. This leads to a reduction in total energy consumption by more than 75% of the energy expenditure required under dark conditions (Okawa et al., 2008).

Thus, in times of increased energy demand, oxygen becomes one of the most limited metabolites in the retina (Anderson and Saltzman, 1964). This makes the retina, and especially photoreceptor cells, highly sensitive to alterations in oxygen tension, and in particular to hypoxia (see chapter 5), a state defined by an oxygen tension below the level normally found in a specific cell, tissue, or organism. This sensitivity may be reflected by the large number of blinding diseases that are at least partially characterized by

perturbations in retinal oxygenation (see chapter 6). Such diseases include proliferative diabetic retinopathy (PDR), retinopathy of prematurity (ROP), age-related macular degeneration (AMD), glaucoma, von Hippel–Lindau disease and Norrie disease (ND) to name a few.

The aim of this review is to summarize and analyze the current knowledge about the retinal response to hypoxia at the molecular level and to discuss the influence of tissue oxygenation on retinal physiology, development and disease. Individual chapters will address the role of HIF transcription factors during retinal development and their contribution to oxygen-dependent retinal diseases, the consequences of unbalanced oxygenation for retinal function and cell survival, and the experimental manipulation of the oxygen tension in therapeutic paradigms. Finally, the plethora of biological effects of hypoxia-induced erythropoietin (EPO) in the retina will be presented and discussed.

2. Retinal oxygen distribution and consumption

Proper function of many metabolic processes depends on the constant availability of oxygen, which normally is supplied by a steady blood flow through the vascular system. In mammals, the extent of retinal vascularization varies among species and reaches from richly vascularized (e.g. rodents, primates, cats, pigs, and others) to partially vascularized (e.g. rabbits) and to avascular retinas (e.g. guinea pig). In vascularized retinas, oxygen is delivered through two distinct and separate systems: the choroidal and the retinal vasculature. The choroidal system provides oxygen mainly to the outer retina, i.e. photoreceptors, and the retinal vasculature nourishes the inner retinal layers.

These two vascular systems have remarkably different circulation properties. The retinal vasculature is relatively sparse, has well-developed autoregulatory mechanisms (Flammer and Mozaffarieh, 2008), and a high arteriovenous oxygen gradient. In contrast, the choroid is highly vascularized, has little autoregulatory response to oxygen fluctuations, and has only a small difference in the arteriovenous oxygen concentration (Pournaras et al., 2008).

Avascular retinas rely on oxygen supplied solely by the choroidal system. The existence of the intraretinal vasculature may be justified by the difficulty to supply the retinal synaptic layers with sufficient oxygen by diffusion from the choroidal vessels alone. A positive correlation between retinal thickness and the presence of a retinal vasculature in different mammals has been noticed and led to the hypothesis that the thickness of an avascular retina is limited by the maximal diffusion capacity of choroidal-derived oxygen. Indeed, vascularized retinas are about 60% thicker than those without retinal vessels (Chase, 1982; Buttery et al., 1991; Dreher et al., 1992).

Nonetheless, the presence of a vasculature in the inner retina has the potential disadvantage of blocking or scattering the incoming light, which might impair photoreception and visual acuity. Thus, the retinal vascular system may have been minimized during evolution, balancing the need of the retina for sufficient metabolic support with the demand for high acuity and efficiency of the visual system. The avascularity of the fovea in primates for example allows the undisturbed penetration of light to the photoreceptors underlining the specialization of this retinal region for high acuity vision. In contrast, up to 40% of incident photons may be absorbed by hemoglobin in red blood cells circulating in vessels of the extrafoveal region. This absorption not only casts shadows on photoreceptors, but may eventually even lead to angioscotomas in the striate cortex (Gariano, 2010; Adams and Horton, 2003; Song et al., 2008b). The delicate balance between optimal visual acuity and sufficient oxygen and nutrient delivery to retinal cells does not leave room for the generation of new vessels to increase blood supply in situations of higher energy needs as neovascularization would increase light scattering and interfere with the vision process (Friedman et al., 1964).

Retinal oxygen profiles of mammalian species with vascularized retinas, such as pigs (Pournaras et al., 1989), cats (Alder et al., 1983), rats (Cringle et al., 1991; Yu et al., 1994), and monkeys (Ahmed et al., 1993; Yu et al., 2005) are similar and reflect both the spatial arrangement of the oxygen source (vessels) and the oxygen consumption rates of the different retinal cell classes. In the rat eye, for instance, the oxygen distribution across the various retinal layers and the choroid is heterogeneous, with the highest oxygen levels found in the choroid (Fig. 1). Levels fall dramatically across the outer retina with a steep gradient towards the inner segments of photoreceptors, reflecting the high oxygen consumption rate of these cells and the localization of mitochondria in photoreceptor inner segments (Linsenmeier, 1986; Yu et al., 1994; Cringle et al., 2002). In the inner retina, the two plexiform layers are the dominant oxygen consuming layers, as they contain large numbers of mitochondria and high levels of neuroglobin, a hemoprotein suggested to be involved in oxygen homeostasis (Yu et al., 2007; Yu and Cringle, 2001; Bentmann et al., 2005). Though this consumption is counterbalanced by oxygen delivery through the vessels of the deep capillary network, the high-energy demand in these layers nonetheless causes its oxygen concentration to drop. In the innermost retina, oxygen levels rise again due to the presence of the primary vascular plexus (Yu et al., 1994). Despite the elevated oxygen tension in the choroid, the extraordinarily high oxygen consumption of photoreceptors together with the avascular nature of the outer retina substantially increases the risk for these cells to experience hypoxic episodes. This risk of insufficient oxygen supply even further increases under dark conditions when ATP (see chapter 1) and oxygen consumption in photoreceptor inner segments are highest (Linsenmeier, 1986). In an attempt to nevertheless maintain sufficient tissue oxygenation, the outer retina may increase oxygen utilization from the deep retinal capillaries. This suggests a dynamic regulation of the oxygen supply to the outer retina and a profound role of the deep retinal capillaries in the maintenance of the oxygen homeostasis under conditions of increased physiological demand (Yu and Cringle, 2002). Furthermore, the autoregulatory abilities of the retinal vasculature might compensate for increased oxygen demand under dark and scotopic conditions. In fact, laser Doppler based measurements revealed a 40% to 70% increased retinal blood flow in human subjects after the transition from light to dark (Feke et al., 1983).

The dependency on high levels of energy for function may explain the presence of a strong Pasteur effect (ratio of anaerobic to aerobic glycolysis) in most retinas. The frog retina presents the highest Pasteur effect and is able to keep the same ATP levels under both aerobic and anaerobic conditions (Fliesler et al., 1997), while the rat retina maintains 50–70% anaerobic ATP levels compared to conditions of normal oxygen availability (Winkler, 1981). The capacity of cells to switch to anaerobic glycolysis in order to efficiently produce ATP will eventually allow adequate tissue function under challenging conditions. This suggests that a switch to anaerobic glycolysis during acute hypoxia contributes to the maintenance of retinal integrity (Bui et al., 2003). Indeed, several *in vitro* and *ex vivo* experiments with retinal preparations performed in the presence of glucose with or without short-term inhibition of mitochondrial function, suggested that the Pasteur effect adequately supports the maintenance of ATP levels in such conditions (Winkler, 1981; Winkler et al., 1997, 2000, 2003; Fliesler et al., 1997).

Nevertheless, pathological hypoxia may still develop in retinal vascular diseases with impaired blood supply leading to severe consequences for tissue function and cell viability.

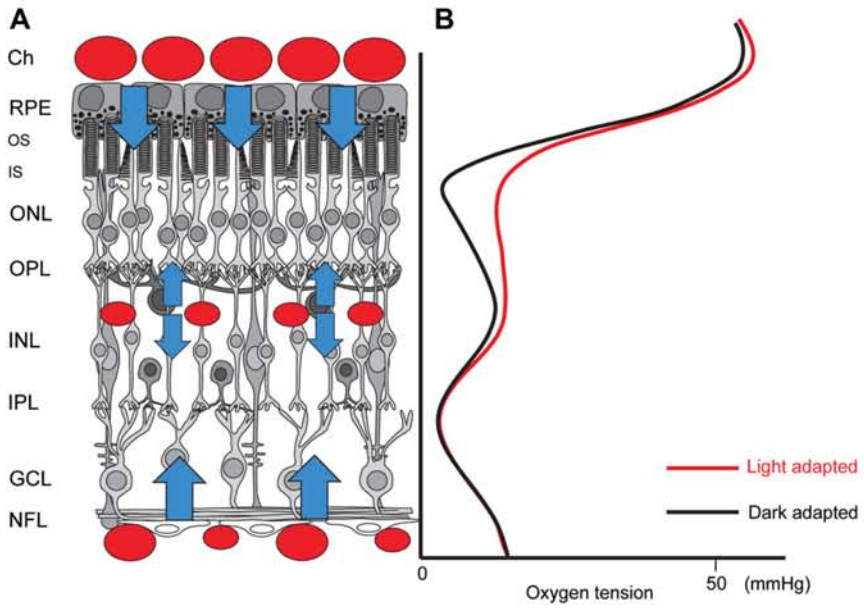

Fig. 1. Oxygen distribution in the retina. (A) Schematic representation of a rat retina.The choroid (Ch) is located on the basolateral side of the retinal pigment epithelium (RPE). The neural retina is composed of several defined layers: photoreceptor outer (OS) and inner (IS) segments, outer nuclear layer (ONL), outer plexiform layer (OPL), inner nuclear layer (INL), inner plexiform layer (IPL), ganglion cell layer (GCL), and nerve fiber layer (NFL). In the rat retina only two distinct vascular plexi are found: the superficial plexus (located in the NFL) and the deeper capillary plexus (found at the outer boundary of the INL) (Cairns, 1959). In addition, the choroidal vasculature provides nutrients and oxygen to the outer retina. Red circles represent vessels; blue arrows show the directions of oxygen diffusion from the corresponding vascular plexus. (B) Intraretinal oxygen distribution profile of a rat retina. The oxygen distribution profiles of a light-adapted (red line) and a dark-adapted (black line) rat retina are shown. The *y*-axis follows the section through the retina shown in A). Oxygen tension is highest near the choroidal vasculature and falls dramatically towards the inner segments of photoreceptors. In the inner retina, oxygen tension is lower in the plexiform layers, whereas higher oxygen tension is measured in the region where the retinal vasculature is found. Note that oxygen levels are reduced in the dark-adapted retina, especially in the ONL (adapted from Yu and Cringle, 2002; Bentmann et al., 2005).

3. Hypoxic events in retinal development

The balance between oxygen demand and supply during development of the retina differs from the situation in the adult tissue. In rats, retinal oxygen consumption at postnatal day (PND) 15 is about 70% of that of the adult retina, most probably because photoreceptor segments and plexiform layers have not yet fully developed (Graymore, 1959, 1960). However, photoreceptors eventually start to function and to increase their oxidative metabolism before the retinal vasculature has been fully established (Graymore, 1959). Thus, the developing retina may experience a physiological period of reduced oxygen availability (Chan-Ling et al., 1995). It has been suggested that this hypoxic period contributes to the regulation of developmental photoreceptor death and thus may be involved in controlling the number of neuronal cells in the retina (Mervin and Stone, 2002; Maslim et al., 1997).

3.1. Hypoxia and retinal angiogenesis

The vascular network that provides oxygen and nutrients to the inner portion of the retina undergoes dramatic reorganization during development, when the hyaloid vasculature in the vitreous, that supports the inner part of the embryonic eye, is replaced by the retinal vasculature. In humans, this switch occurs at mid-gestation, whereas in mice and other non-primates the retinal vasculature develops postnatally as the hyaloid vasculature regresses. The formation of the retinal vessels is preceded by an invasion of migrating astrocytes, which emerge from the optic nerve head at around birth in rodents. This population of astrocytes proliferates and spreads in a radial fashion across the nerve fiber layer (NFL) towards the retinal periphery (Stone and Dreher, 1987; Watanabe and Raff, 1988; Ling et al., 1989). The resulting astrocytic network acts as a template for the development of the vessels of the primary plexus by providing guidance for the migration of endothelial cells (Stone et al., 1995; Jiang et al., 1995; Zhang and Stone, 1997; Fruttiger et al., 1996; Dorrell et al., 2002). Like the population of guiding astrocytes, the vessels of the primary plexus also grow from the optic nerve head and spread in the NFL across the inner surface of the retina, reaching the periphery within the first postnatal week in mice (Connolly et al., 1988) (Fig. 2A).

The "physiological hypoxia" occurring during this time of retinal development causes increased expression of *vascular endothelial growth factor (Vegf)*, forming a concentration gradient with high levels in the avascular peripheral retina and lower levels towards the already vascularized central region (Stone et al., 1995; Pierce et al., 1996; West et al., 2005). This gradient is assumed to control and guide the growth of the vessels of the primary plexus. Retinal astrocytes have been proposed to be the source of VEGF in the avascular retina (Chan-Ling et al., 1995; Stone et al., 1995; Pierce et al., 1996; Dorrell et al., 2002; Gerhardt et al., 2003; West et al., 2005) but this notion has recently been questioned by the observation that the vasculature apparently develops quite normally in mice with an astrocyte-specific knockdown of *Vegf* (Weidemann et al., 2010). As an alternative, retinal ganglion cells (RGCs) are a possible source of VEGF for regulation of developmental angiogenesis (Stone et al., 1996; Sapieha et al., 2008; Kim et al., 2010). This is supported by the observation that RGC deficiency in *brn3b*$^{Z\text{-}dta/+}$;*six3-cre* mice leads to the complete absence of retinal vasculature, in spite of the presence of an astrocytic network (Sapieha et al., 2008). In addition, RGCs were found to be the main retinal cell population responding to succinate, a Krebs cycle intermediate, which accumulates under

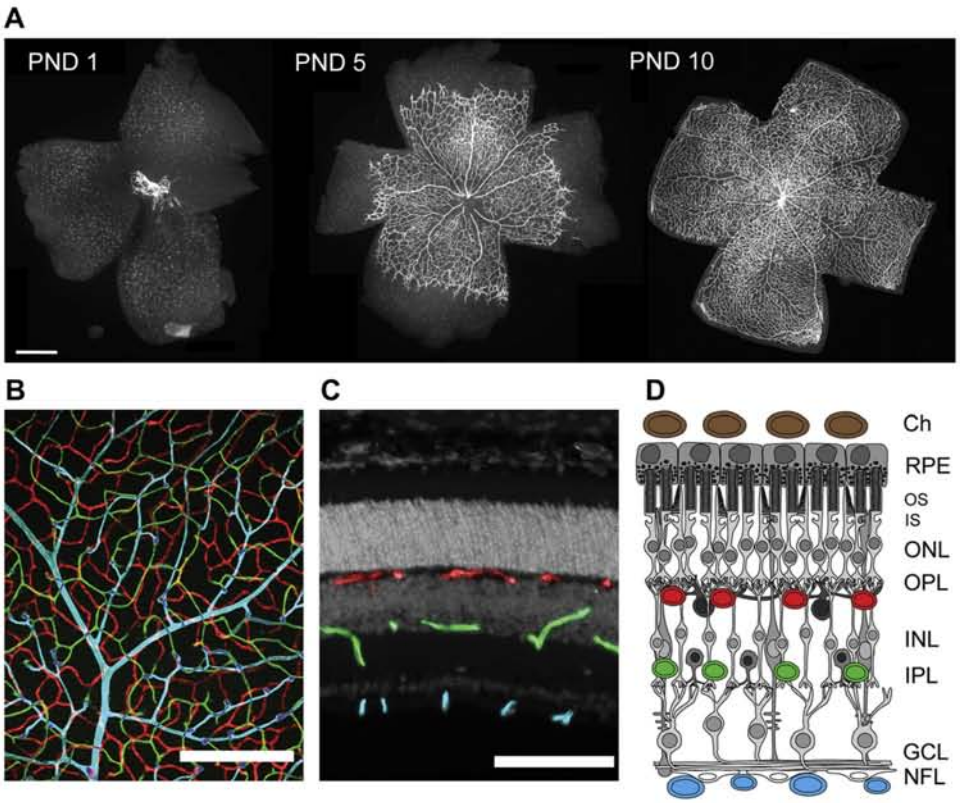

Fig. 2. Development of retinal vasculature in mouse. (A) Retinal flat mounts of the mouse retina at PND1, 5, and 10. Vessels are stained with isolectin IB_4. Note the radial development of the primary plexus from the central to peripheral retina. (B, C) The mouse retinal vascular plexi. Isolectin IB_4 staining of vessels on a retinal flat mount (B) and cryosection (C) of the adult mouse. Vessels are highlighted by artificial coloring (primary plexus: blue; intermediate plexus: green; outer plexus: red). (D) Schematic representation of the location of the mouse retinal vascular plexi. Three vascular plexi are formed in the mouse retina. The primary plexus is located in the nerve fiber layer (NFL), the intermediate plexus at the inner boundary of the inner nuclear layer (INL), and the outer plexus at the outer boundary of the INL. Scale bars: 500 μm (A), 200 μm (B), 100 μm (C).

hypoxic conditions in the retina. Succinate has been reported to have pro-angiogenic properties (Murray and Wilson, 2001; Burns and Wilson, 2003) and to mediate retinal angiogenesis by provoking the release of pro-angiogenic factors from cells via its cognate receptor G-protein coupled receptor 91 (GPR91) (Sapieha et al., 2008). Although these data implicate both RGCs and astrocytes in the regulation of angiogenesis during development, the precise contribution of each cell type to the hypoxia-mediated production and release of pro-angiogenic factors needs to be established. Even though VEGF may be the main regulatory factor, it is important to note that other growth factors including insulin-like growth factor 1 (IGF1) (Hellstrom et al., 2001), placental growth factor (PlGF) (Feeney et al., 2003), platelet-derived growth factor (PDGF) (Fruttiger et al., 1996; Lindblom et al., 2003), basic fibroblast growth factor (bFGF) (Friedlander et al., 1995; Rousseau et al., 2000), and leukemia inhibitory factor (LIF) (Kubota et al., 2008) also influence endothelial cell proliferation and the formation of the primary plexus.

Even before the primary plexus is completed, the deeper plexi start to develop by angiogenic sprouting from the primary plexus, independently of retinal astrocytes (Gariano et al., 1994; Provis, 2001). In rodents, as the primary plexus reaches the retinal periphery, angiogenic sprouts emerge from veins, venules and capillaries near veins, penetrating the retina along Muller cell processes perpendicularly to the primary plexus (Engerman and Meyer, 1965; Stahl et al., 2010). Once the growing sprouts reach the inner and outer boundaries of the inner nuclear layer (INL) they turn "sideways" to form the deep and intermediate plexi of the mouse retina (Stahl et al., 2010) (Fig. 2B–D). This process starts in the center and expands towards the retinal periphery. It is preceded by transient, hypoxia-driven expression of *Vegf* mRNA in cell somatas of the INL (Stone et al., 1995; Sandercoe et al., 2003). The *Vegf* expressing cells are presumably Müller glia, which have also been shown to increase VEGF production upon hypoxia in the adult retina (Pierce et al., 1995). For a detailed description of the mechanisms leading to the formation of the retinal vasculature, we refer to recent excellent reviews by Fruttiger (Fruttiger, 2007) and Stahl and colleagues (Stahl et al., 2010).

In conclusion, regulatory mechanisms react to altered oxygen profiles during retinal development to induce a controlled and organized angiogenic response, re-establishing oxygen homeostasis in the retinal tissue. Reduced oxygen levels are therefore a critical driving force for the development of the retinal vasculature through the regulation of expression of angiogenic factors like VEGF. Small changes in oxygen tension may influence local and/or general activities of molecular oxygen sensors, which then induce an appropriate cellular response. Mis-regulation of this response may have profound consequences for developmental angiogenesis, leading to capillary vaso-obliteration and alterations in the architecture of the retinal vasculature (Phelps, 1988).

Despite the importance of "physiological hypoxia" for the regulation of retinal development, acute or chronic episodes of

disturbed oxygen homeostasis (e.g. under pathological conditions) are no longer beneficial for the mature retina. In contrast to the tightly organized and highly regulated process of developmental angiogenesis, pathological vessel growth as response to non-physiological reduction in oxygenation often leads to uncontrolled neovascularization, including abnormal vascular structures and vessel locations. Pathological neovascularization or impaired retinal angiogenesis during development are hallmarks of several blinding diseases, which are at least partially characterized by perturbations in retinal oxygenation (see chapter 6).

4. Hypoxia inducible factors

Oxygen tension has a profound impact on the regulation of vascular growth and retinal neurogenesis in the developing retina, and the adult retina is continuously at risk for developing tissue ischemia or hypoxia, especially under pathological conditions and during the process of aging. Thus, retinal cell populations must adequately respond to alterations in oxygen tension to maintain tissue integrity and function. Central to this response are the HIFs, heterodimeric transcription factors that have earned the nickname of "master regulators" of hypoxic gene expression. Under hypoxic conditions, HIFs regulate the expression of target genes implicated in a multitude of biochemical events, including erythropoiesis, angiogenesis, adjustment of the vascular tone, metal transport, glycolysis, glucose uptake, growth factor signaling, mitochondrial function, cell growth and survival, invasion and metastasis (Majmundar et al., 2010). Since several excellent recent reviews give detailed information about expression, function, biological role and regulation of the HIF transcription factors in general (Majmundar et al., 2010; Loboda et al., 2010), we will only give a brief overview on some of the important aspects of HIF biology which may help to understand the role of these transcription factors in the retina.

HIF heterodimers are composed of a 120 kDa oxygen-labile alpha subunit (HIFA) and a 91–94 kDa stable beta subunit (HIFB), also known as the aryl hydrocarbon receptor nuclear translocator (ARNT) (Semenza, 2001; Maxwell et al., 2001; Harris, 2002). In mammals, three *Hifa* isoforms have been identified: *Hif1a* (Wang et al., 1995), *Hif2a/Endothelial PAS domain-containing protein 1(Epas1)* (Tian et al., 1997; Ema et al., 1997; Flamme et al., 1997), and *Hif3a* (Hara et al., 2001; Heidbreder et al., 2003; Makino et al., 2001, 2002). In addition, three paralogues of the gene encoding for the HIFB subunit (*Arnt1*, *Arnt2*, and *Arnt3*) have been found at different genetic loci (Hirose et al., 1996; Ikeda and Nomura, 1997; Hogenesch et al., 1998, 2000). *In situ* hybridization studies have shown that *Arnt1* is nearly ubiquitously expressed, *Arnt2* is expressed predominantly in brain and kidney, while *Arnt3* is highly expressed in brain, thymus and muscle (Aitola and Pelto-Huikko, 2003; Hogenesch et al., 1998). HIF1A and HIF2A have been shown to form functional heterodimers with ARNT1 and ARNT2, which seem to have a partial functional redundancy in the hypoxic response *in vivo* (Maltepe et al., 1997, 2000; Keith et al., 2001; Powell and Hahn, 2002). Even though *in vitro* binding data have demonstrated that ARNT3 can also form transcriptionally active heterodimers with HIFAs (Hogenesch et al., 1998; Takahata et al., 1998), *in vivo* observations suggested that ARNT3 is not or at least not strongly implicated in the hypoxic response (Cowden and Simon, 2002).

Both HIFA and HIFB subunits are members of the basic helix-loop-helix (bHLH) family and are PER-ARNT-SIM (PAS) domain-containing transcription factors (Wang et al., 1995). The PAS domain is involved in protein-protein interactions, while the bHLH domain contributes to both HIF heterodimerization and DNA binding (Jiang et al., 1996). Apart from these domains, HIFAs have an oxygen-dependent degradation domain (ODDD), and two transactivation domains (TAD): the N-terminal TAD, essential for target gene specificity, and the C-terminal TAD, which contributes to the regulation of the majority of HIF target genes (Dayan et al., 2006; Hu et al., 2007) (Fig. 3).

Among the HIFA subunits, HIF1A and HIF2A are more structurally related than HIF3A, which lacks a transactivation domain (Gu et al., 1998). HIF3A does not form functional transcription factors but instead is thought to inhibit HIF1- and HIF2-mediated gene regulation (Lisy and Peet, 2008; Gu et al., 1998). In addition, a splice variant of *Hif3a* encodes for the inhibitory PAS domain protein (IPAS), which was suggested to act as a suppressor of HIF1A and HIF2A in a dominant negative manner by capturing HIFB and forming transcriptionally inactive heterodimers (Makino et al., 2001). Whereas *Hif1a* is ubiquitously expressed throughout most if not all organs, *Hif2a* is highly expressed particularly in vascular structures (Jain et al., 1998) and in distinct cell populations of most organs, including brain, heart, lung, kidney, liver, pancreas, and intestine (Wiesener et al., 2003). Expression of both *Hif1a* and *Hif2a* has also been found in the retina (Thiersch et al., 2009; Caprara et al., 2011; Mowat et al., 2010).

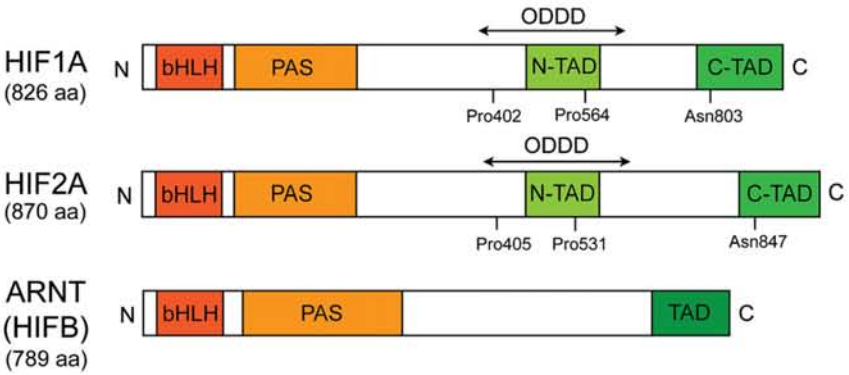

Fig. 3. Structure of human HIF1A, HIF2A and ARNT (HIFB). Shown are the main protein domains, including the PER-ARNT-SIM (PAS) domain (involved in protein–protein interactions), the basic helix-loop-helix (bHLH) domain (responsible for both protein–protein interactions and DNA binding), the oxygen-dependent degradation domain (ODDD) containing proline (Pro) residues that are hydroxylated under normoxic conditions, the N-terminal transactivation domain (N-TAD) (required for target gene specificity), and the C-terminal transactivation domain (C-TAD) (contributes to the regulation of most HIF target genes). Note that ARNT does not contain an ODDD and is stable under normoxic conditions. HIF1A and HIF2A but not ARNT contain also an asparagine (Asn) residue in the C-TAD that is hydroxylated by FIH under normoxic conditions to reduce the transcriptional activity.

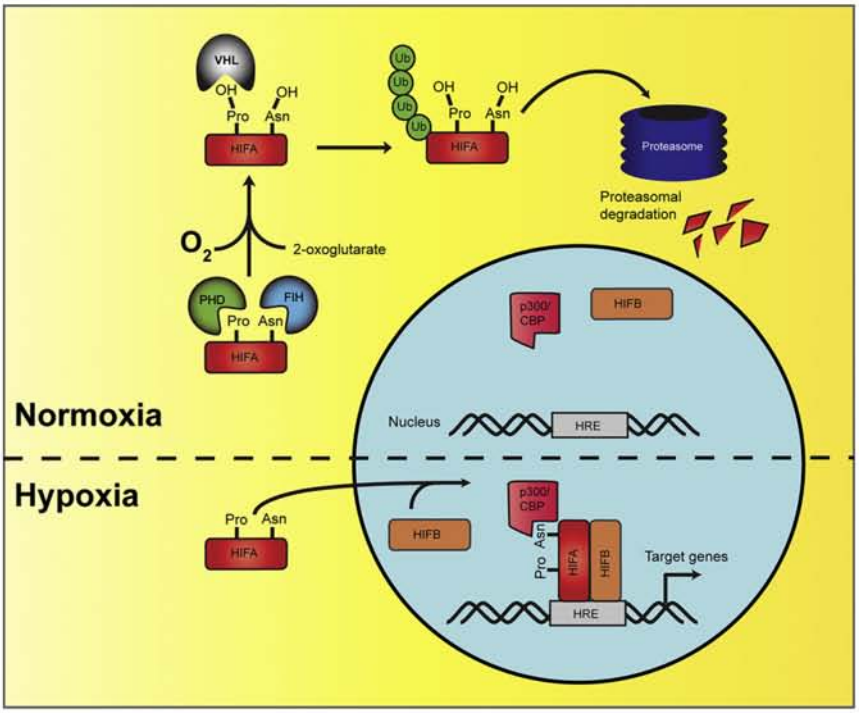

Fig. 4. Schematic representation of the oxygen-dependent regulation of HIF activity. Under normoxic conditions, HIFA subunits undergo proteasomal degradation by a mechanism involving hydroxylation of proline (Pro) residues in the oxygen-dependent degradation domain (ODDD) of HIFA by prolyl-4-hydroxylase (PHD) enzymes and subsequent poly-ubiquitinylation by the Von Hippel Lindau (pVHL) E3 ubiquitin ligase complex. Additional hydroxylation of an asparagine (Asn) residue of HIFA by factor inhibiting HIF (FIH) abrogates HIFA interaction with the p300/CBP transcriptional co-activator. PHD-mediated Pro hydroxylation requires oxygen and 2-oxoglutarate as substrates. Under hypoxic conditions, when oxygen availability is limited, HIFA escapes hydroxylation by PHD and FIH, translocates to the nucleus where it heterodimerizes with HIFB, complexes with p300/CBP and accessory transcriptional co-activators, binds hypoxia response elements (HREs) and drives transcription of target genes.

To prepare the cell for an immediate response to reduced oxygen tension, both HIFA and HIFB proteins are constitutively expressed under normoxic conditions. However, whereas HIFB is stable, HIFA is rapidly degraded with a half-life of less than 5 min in an environment with normal oxygen levels (Huang et al., 1996). The protein levels of the alpha subunits are regulated by several oxygen-dependent and -independent mechanisms, the most important one being a fast oxygen-dependent degradation (Fig. 4). This is achieved by post-translational hydroxylation of proline (Pro) residues 402 and 564 within the ODDD of the HIF1A subunit and Pro405 and Pro531 in the HIF2A subunit by members of the prolyl-4-hydroxylase (PHD) family of proteins. This family consists of several proteins: PHD1 (Egl Nine Homolog (EGLN)2, HIF Prolyl Hydroxylase (HPH)3), PHD2, (EGLN1, HPH2), PHD3 (EGLN3, HPH1) (Epstein et al., 2001), and the collagen prolyl-4-hydroxylases. The latter are responsible for the hydroxylation of collagen to stabilize collagen helices (Saika et al., 1994; Ko and Kay, 2002). Hydroxylated HIFA proteins are then recognized by the von Hippel–Lindau protein (VHL) complex, which contains, among other proteins, an E3 ubiquitin ligase. This leads to the ubiquitinylation of HIFA proteins targeting them for rapid proteasomal degradation (Maxwell et al., 1999; Jaakkola et al., 2001). The hydroxylation status of HIFAs is directly dependent on oxygen availability, since PHDs are Fe(II) dependent dioxygenases that require oxygen and the tricarboxylic acid (TCA) cycle intermediate 2-oxoglutarate as substrates (Hewitson et al., 2003; McNeill et al., 2002b). For this reason, PHDs have been proposed to be the "oxygen sensors" directly linking cellular oxygen concentration to PHD activity, HIFA hydroxylation, and thus HIFA stability. Under hypoxic conditions, PHDs lack oxygen as a cofactor, are thus inactive or only partially active and do not or not efficiently hydroxylate HIFAs. As a consequence, HIFA proteins are stable, accumulate and translocate to the nucleus. There, they heterodimerize with HIFB, recruit transcriptional co-activators such as p300/CREB binding protein (CBP) (Arany et al., 1996) (a description of some co-activators for HIF1A or HIF2A can be found in (Loboda et al., 2010)), and bind to hypoxia response elements (HREs) within promoters of HIF target genes to regulate gene expression (Chilov et al., 1999; Gradin et al., 1996; Kallio et al., 1997; Wenger et al., 2005). An additional step in the regulation of the activity of HIFA proteins is mediated by factor inhibiting HIF (FIH), which hydroxylates HIFAs at an asparagine (Asn) residue (Asn803 for HIF1A and Asn847 for HIF2A) in the C-terminal TAD, thereby preventing its interaction with the transcriptional co-activator p300/CBP (McNeill et al., 2002a; Lando et al., 2002a,b; Mahon et al., 2001).

Besides the oxygen-dependent negative regulation of HIFAs, a number of oxygen-independent mechanisms are known to regulate the stability and activity of HIF1A in normoxia and hypoxia. These include cytokine and growth factor-dependent signaling pathways (reviewed in (Bardos and Ashcroft, 2005; Majmundar et al., 2010)) and the interaction with the chaperone heath shock protein 90 (HSP90) (Neckers and Ivy, 2003). Considerable evidence also suggests that mitochondria-produced reactive oxygen species (ROS) are involved in the regulation of HIF activity, most probably through the inhibition of HIFA hydroxylation by PHDs, resulting in increased HIF transcriptional activity in normoxia (Cash et al., 2007; Yuan et al., 2008; Frede et al., 2009).

Although HIF1 and HIF2 share several common target genes such as *Vegf*, *adrenomedullin (Adm)* and *glucose transporter 1*

(Glut1)(Hu et al., 2003; Wiesener et al., 1998), they also appear to regulate their own specific sets of targets. Activation of *carbonic anhydrase (CA)* and genes involved in the glycolytic pathway, for example, seems specific for HIF1 (Hu et al., 2007; Sowter et al., 2003; Raval et al., 2005), whereas the endothelial-specific receptor tyrosine kinase *Tie2* may be preferentially regulated by HIF2 (Tian et al., 1997). In addition to having their own specific target genes, HIF1A and HIF2A isoforms may also be differentially stabilized depending on the duration and extent of a hypoxic insult. HIF1A appears to be transiently stabilized in acute hypoxia, whereas HIF2A may mediate prolonged gene activation under conditions of relatively moderate and chronic hypoxia (Wiesener et al., 1998; Holmquist-Mengelbier et al., 2006; Bracken et al., 2006).

Lessons obtained from knockout animals show that HIFA subunits mostly play non-redundant and specific roles, particularly during development. Systemic *Hif1a* knockout mice display cardiac and vascular malformations and embryonic lethality at embryonic day 10.5 (Ryan et al., 1998; Kotch et al., 1999). In contrast, various phenotypes have been reported for systemic *Hif2a* knockouts. These include embryonic lethality with vascular defects (Peng et al., 2000), perinatal lethality due to impairment in catecholamine production (Tian et al., 1998) or respiratory distress syndrome (Compernolle et al., 2002), postnatal lethality caused by progressive multiorgan failure (Scortegagna et al., 2003a,b), and viability into adulthood (Ding et al., 2005). The reasons for the different phenotypes are not clear, but may include differences in genetic background and gene targeting strategies.

4.1. HIFs in the developing retina

Due to the low oxygen concentration experienced by embryos inside the maternal body (Rodesch et al., 1992), retinal tissue is exposed to prolonged periods of hypoxia during embryonic development. As a consequence, hypoxic areas are found throughout all retinal layers in the embryonic mouse (Kurihara et al., 2010). Although newborn mice are exposed to atmospheric oxygen levels, considerably reducing the hypoxic stress in the inner retina after birth, hypoxic areas in the ganglion cell layer (GCL) and INL persist up to PND5 (Kurihara et al., 2010).

To understand the regulatory role of hypoxia during retinal development in general, it is essential to determine expression pattern and specific function of individual HIF isoforms during tissue maturation. A preferential expression or stabilization of particular HIF proteins in specific retinal cell types might suggest for example that individual cells in the retina have specific tasks in the tissue response to hypoxia and thus in the maturation process. Others and we began to address this point using different approaches including the elucidation of the spatio-temporal expression pattern of *Hifa* isoforms, the investigation of the hypoxic transcriptome in the retina and the generation of cell- or tissue-specific knockdowns of *Hif1a* and *Vhl* (see below). Although expression of both *Hif1a* and *Hif2a* was detected in all retinal cell layers, at least in the adult retina (Thiersch et al., 2009), the spatio-temporal pattern of HIFA protein stabilization is dynamic and diverges during embryogenesis and postnatal development. As would be expected from the low oxygen tension in the initially avascular retina, total retinal HIF1A protein levels in newborn mice are high and decrease as the retina becomes vascularized. Very low but detectable basal HIF1A levels persist in the retina even after the vasculature has been fully developed (Ozaki et al., 1999; Grimm et al., 2005). Correlating with the broad distribution of hypoxic areas, HIF1A is stabilized ubiquitously in all layers of the embryonic retina. The deep retinal layers considerably downregulate HIF1A soon after birth – as expected given the increased oxygen supply to these layers through diffusion from the choroidal vasculature. In contrast, HIF1A levels persist in the GCL and INL at least until PND5 (Kurihara et al., 2010; Ozaki et al., 1999). HIF2A was detected predominantly in endothelial cells of the hyaloid vessels during embryogenesis and in retinal vessels of the primary plexus at PND5 (Kurihara et al., 2010). In the adult mouse retina, *Hif2a* seems to be expressed by vascular endothelial cells as well as by cells within the GCL, INL, and retinal pigment epithelium (RPE) (Ding et al., 2005). Taken together, these observations highlight the responsiveness of the retinal tissue to hypoxic events during development via stabilization of HIFA proteins. However, each isoform seems to have specific spatio-temporal stabilization and expression patterns, pointing to distinct roles for HIF1A and HIF2A during retinal development and probably adulthood.

Because a systemic knockout of *Hif1a* is embryonically lethal, conditional knockdown strategies have been used to elucidate the function of HIF1A in the developing and adult retina. Knockdown of *Hif1a* in adult rod photoreceptors (Thiersch et al., 2009) and Müller cells (Lin et al., 2011) did not result in any apparent histological and/or visual functional abnormalities. In contrast, when we generated a more general *Hif1a* knockdown in most cells of the developing retinal periphery, we noticed that formation of the intermediary vascular plexus was prevented. Lack of this plexus persisted into adulthood without additional detectable histological abnormalities (Caprara et al., 2011). Aside from this mis-development of the retinal vasculature, the relative lack of a phenotype in the *Hif1a* knockdown suggests that HIF1A plays only a moderate role in the development and survival of retinal cells under physiological conditions. In contrast, HIF2A may have a more prominent function, since *Hif2a* knockout mice display a retinopathy with marked thinning of the retinal layers, especially the photoreceptor layer, and loss of vision by one month of age. In addition, *Hif2a* knockout mice show an abnormal retinal vascular development characterized by a diminished vascular density in the retinal periphery, tortuous vessels in the central retina and a persistent hyaloid artery (Ding et al., 2005; Scortegagna et al., 2003a,b). Because of the strong interdependency between neuronal and vascular development in the retina, it is difficult to discriminate the specific contribution of HIF2A to each of these processes. That is, vascular defects in the retina lacking HIF2A may be a direct result of abnormal vascular development (Gariano and Gardner, 2005) or may be an indirect consequence of photoreceptor death, the resulting reduced oxygen consumption, and thus increased oxygen tension. Such an increased oxygen concentration may present a reduced and thus insufficient hypoxic stimulus for normal angiogenesis and may even lead to vaso-obliteration (Penn et al., 2000; Lahdenranta et al., 2001; Yu and Cringle, 2005). However, the recent observation that HIF2A protein is stabilized mainly in vascular endothelial cells in the postnatal retina (Kurihara et al., 2010) might support the hypothesis that the absence of HIF2A primarily leads to the mis-development of the vasculature, followed by the observed retinopathy. A clear definition of the pathophysiological processes in *Hif2a* knockout retinas is still needed to unambiguously determine the definitive role of HIF2 in retinal development, physiology and pathophysiology.

4.2. HIFs in retinal angiogenesis

As noted above, reduced oxygen tension appears to be a main driving force for normal retinal vascularization during development, but may also cause abnormal neovascularization in disease (see chapter 6) (Ashton, 1966; Provis et al., 1997; Stone et al., 1995). To understand the molecular processes during these events, it is crucial to know how the retina responds to physiological alterations in oxygen tension, to what extent the VHL-HIF signaling

cascade mediates expression of genes involved in the angiogenic response, and how developing vessels are guided by the reactions of different retinal cell populations to an hypoxic insult. Insight into the relevant mechanisms may be obtained by investigating the autosomal dominant von Hippel–Lindau disease, in which vascular endothelial tumors, or hemangioblastomas, arise in the retina and other organs as a consequence of the inactivation of the *Vhl* tumor suppressor gene (Chan et al., 2007). Such an inactivation results in constitutively active HIF signaling and thus sustained production and release of pro-angiogenic growth factors (Rankin et al., 2005). A mouse model designed to mimic the genetics of von Hippel–Lindau disease has been recently described in two independent studies by us and others (Kurihara et al., 2010). In both studies, the conditional knockdown of *Vhl* in the retina led to a long-lasting stabilization of HIF1A and HIF2A during development and in adulthood under normoxic conditions. The persistent hypoxia-like response caused severe retinal degeneration, gliosis and reduction in retinal function in the adult mouse. Additionally, regression of the hyaloid vessels was inhibited, and the retinal vasculature developed to a reduced density (Kurihara et al., 2010). Furthermore, the development of the capillaries of the deeper plexi was incomplete, and retinal vessels penetrating the photoreceptor layer were observed. Both studies point to increased ectopic *Vegf* expression as a crucial factor responsible for vascular defects and incomplete transition from the embryonic to the adult retinal circulatory system in *Vhl* knockdown mice (Kurihara et al., 2010). Importantly, Kurihara and colleagues demonstrated that the vascular defects in *Vhl* knockdown animals could be rescued either by injecting a VEGF inhibitor or by the genetic inactivation of *Hif1a*, but not *Hif2a* (Kurihara et al., 2010). Similar to the phenotype observed in *Vhl* knockdown retinas in mice, genetic inactivation of *Vhl* in the predominantly avascular zebrafish retina caused neovascularization and vascular leakage resulting in the formation of severe edema and retinal detachment. Here again the vascular defects were accompanied by increased expression of *Vegf* (van Rooijen et al., 2010). Observations made in systemic *Phd2* knockout mice further support a causative role for HIF1A in such a vessel phenotype. Lack of PHD2 led to increased HIF1A levels and to abnormal vessel formation characterized by an increase in arterial branching morphogenesis and moderate alterations in retinal vascular patterning (Duan et al., 2011).

Not only increased but also reduced levels of HIF1A can lead to an abnormal phenotype of the retinal vasculature. As mentioned above, Cre-mediated inactivation of *Hif1a* during retinal development led to a marked underdevelopment of the intermediate vascular plexus, the last vascular plexus to develop (Caprara et al., 2011). As the regular development of the intermediate plexus is normally preceded by a transient expression of *Vegf* mRNA in cells of the INL (Pierce et al., 1995; Stone et al., 1995; Sandercoe et al., 2003), the absence of HIF1A may cause reduced local expression of VEGF which may thus be responsible for the development of the observed vascular phenotype. Additional experiments are still required to test this hypothesis, but it seems clear that the spatio-temporal expression and activation of HIF1A needs to be delicately balanced to achieve correct development and maintenance of the retinal vasculature. In addition to HIF1A, HIF2A was also shown to contribute to the development of the retinal vasculature. Besides marked thinning of the retina and the virtual absence of photoreceptor function, *Hif2a* systemic knockout mice also present defects in the development of the retinal vasculature (reduced peripheral vasculature, tortuous central vessels) and impaired regression of the hyaloid artery (Ding et al., 2005).

Taken together, these results point to the crucial role of the VHL-HIF pathway in the regulation of the transition from the fetal to the adult ocular circulatory system and postnatal retinal angiogenesis. To fully understand these processes, it is of fundamental importance to identify and characterize the retinal cell populations that mediate the hypoxic response required for retinal vascular development. The historical role of astrocytes as main source of hypoxia-induced VEGF expression driving the development of the primary plexus has recently become controversial due to the observation that astrocyte-specific knockdowns of *Vegf*, *Hif1a* or *Hif2a* did not influence the normal development of the retinal vasculature (Weidemann et al., 2010). On the other hand, the astrocyte-specific stabilization of HIF transcription factors in a conditional knockdown of *Vhl* caused significant upregulation of HIF2-mediated *Vegf* expression and was accompanied by uncontrolled retinal angiogenesis, eventually leading to extensive hypervascularity of the primary plexus (Weidemann et al., 2010). Knockdown of *Vegf* in astrocytes of these mice rescued the vascular phenotype (Weidemann et al., 2010), suggesting that although astrocyte-derived *Vegf* might not be essential for normal development of the retinal vasculature, it may nevertheless be able to modulate the process (see chapter 3.1).

5. Retinal ischemia and hypoxia

Ischemia develops when the blood supply is inadequate to provide sufficient oxygen and nutrients to cells in a particular tissue. Although both ischemia and hypoxia lead to reduced oxygenation, an ischemic insult may have a more severe effect due to the additional reduction in supply of nutrients and decreased waste removal. Thus, ischemia is generally a severe condition and like in brain and heart, contributes to the pathogenesis of a number of retinal diseases (see chapter 6).

Local or systemic defects of the circulatory system are common causes of retinal ischemia with local impairments, especially occlusion of terminal arteries, contributing more frequently to pathological ischemia. The most frequent arterial ischemic disorders of the retina include central retinal artery occlusion (CRAO), branch retinal artery occlusion (BRAO), and amaurosis fugax (reviewed in Hayreh, 2011). Importantly, impairment of the retinal circulation affects the inner retinal layers but does not usually cause the outer retina to become ischemic as it is metabolically supported by the choriocapillaries. As a consequence, retinal ischemia usually leads to neuronal damage in the inner retina without strongly affecting photoreceptors (Birol et al., 2007). However, failure of the choroidal vascular system or separation of the outer retina from the RPE during retinal detachment, results in outer retinal ischemia. Complete retinal ischemia, affecting both the outer and inner retina, can also occur through occlusion of the ophthalmic artery, which supplies all the structures in the orbit (Hayreh, 2011).

Total occlusion of the arterial blood supply results in ischemic edema in the inner layers, eventually leading to inner retinal atrophy (Hayreh and Zimmerman, 2007). In contrast, a partial arteriolar occlusion may lead to hemorrhages and microaneurysms in affected areas that can also be accompanied by retinal edema (Bek, 2009). In the case of total or partial venous outflow occlusion, microaneurysms, hemorrhages, exudates and edema are often observed (Pournaras et al., 1990; Hayreh, 2005). Chronic retinal ischemia is usually linked to capillary occlusion in the retinal midperiphery to periphery. This is often the result of systemic cardiovascular, metabolic or hematological diseases. Retinal capillary non-perfusion is commonly encountered in different retinopathies and has been particularly studied in retinal vein thrombosis and PDR (Cai and Boulton, 2002).

5.1. Effects of ischemia and hypoxia on retinal function

Disturbance of the delivery of oxygen and metabolites has inevitably negative effects on cellular metabolism and may be

detrimental to neuronal function. Electroretinograms (ERGs) from both humans and animals show that ischemia and hypoxia mainly affect the b-wave, which represents a mixed response of different retinal cell types including bipolar, amacrine, and Müller glia cells (Dick and Miller, 1978; Kline et al., 1978; Gurevich and Slaughter, 1993). The extent of the reduction in b-wave amplitude depends on the duration and severity of the insult and on the degree of recovery (Coleman et al., 1990; Block and Schwarz, 1998; Brown et al., 1957; Janaky et al., 2007; Tinjust et al., 2002). At a cellular level, evidence from functional studies suggests that RGCs may be even more sensitive to experimental transient ischemia or mild systemic hypoxia than cells of the ONL and INL (Siliprandi et al., 1988, 1993; Kergoat et al., 2006).

Despite these consequences of reduced or interrupted retinal blood flow, the inner retinal layers appear to be better protected from ischemic insults than other parts of the central nervous system (CNS), and can functionally recover even after extended periods of acute ischemia. The monkey retina for example is able to recover even after 100 min of acute ischemia (Hayreh and Weingeist, 1980). This relative tolerance may at least partially be explained by the large surface to volume ratio of the retina, which facilitates diffusion of metabolites from the vitreous body to cells of the inner retina (Bek, 2009). However, detailed mechanisms of this tolerance have not been fully clarified.

5.2. Retinal ischemic damage

Chronic retinal hypoxia and especially retinal ischemia may eventually lead to cell death and therefore to visual impairment without potential for recovery. Death of RGCs and thinning of the NFL are hallmarks of retinal diseases in which ischemia is proposed to play an etiological role, such as retinal and choroidal vessel occlusions, PDR, ROP and glaucoma (Osborne et al., 1999b). Similarly, loss of RGCs is a feature shared by all experimentally induced ischemic conditions such as increased intraocular pressure (IOP) (Adachi et al., 1996; Selles-Navarro et al., 1996), or ligation of ophthalmic vessels (Lafuente et al., 2002). Apart from RGCs, which seem to be most sensitive to an ischemic insult, amacrine cells are reported to be vulnerable and may also degenerate under such conditions (Osborne and Herrera, 1994; Wood et al., 2001; Singh et al., 2001). Additional evidence suggests that ischemia may also lead to a gradual loss of photoreceptors (Osborne et al., 1999a). However, whether photoreceptor death is directly caused by the ischemic insult or whether their degeneration is an indirect consequence of the loss of ganglion cells remains to be determined. It has been suggested that the reduced number of ganglion cells after ischemia may lead to a diminished pupillary light reflex due to the loss of intrinsically photosensitive RGCs (ipRGCs). This, in turn, may result in elevated light levels reaching the retina that might eventually be toxic to photoreceptors (Stevens et al., 2002).

The molecular mechanisms impairing neuronal survival after ischemia are complex. A main mechanism appears to be excitotoxicity mediated by glutamate, the principal retinal excitatory neurotransmitter (Louzada-Junior et al., 1992; el-Asrar et al., 1992; Lombardi et al., 1994). Under normal physiological conditions, astrocytes and Müller glia cells remove excessive glutamate from the extracellular space and convert it to glutamine, which, after release, is used by neurons to replenish their pool of the neurotransmitter (Riepe and Norenburg, 1977; Pellerin and Magistretti, 1994). However, this high energy-demanding task can easily be affected by a reduction in intracellular ATP levels as it may occur in conditions of limited oxygen availability such as hypoxia or ischemia. In fact, glutamate (Louzada-Junior et al., 1992; Neal et al., 1994) and other neurotransmitters such as γ-aminobutyric acid (GABA) (Neal et al., 1994; Perlman et al., 1996), glycine, dopamine, and acetylcholine (Neal et al., 1994), and the neuromodulator adenosine (Roth et al., 1997b) accumulate in the extracellular space under hypoxic or ischemic conditions. Since glutamate uptake by glial cells also depends on cellular Na^+ influx, this accumulation is at least partially due to impaired activity of the transmembrane Na^+/K^+ ATPase transporter in conditions of reduced ATP levels (Napper et al., 1999). In addition to glutamate-mediated toxicity, many other events may contribute to the detrimental effects of hypoxic-ischemic insults in the retina. Among them are increased oxidative stress during oxygen deprivation through enhanced free radical production by mitochondria (Muller et al., 1997; Szabo et al., 1997; Harada et al., 2006), increased nitric oxide (NO) (Adachi et al., 1998; Kaur et al., 2009) and VEGF (Kaur et al., 2006) levels, disruption of the blood–retinal barrier (BRB) resulting in retinal edema (Kaur et al., 2008; Abcouwer et al., 2010), enhanced inflammatory cytokine expression (Joussen et al., 2004; Zheng et al., 2007; Husain et al., 2011) and recruitment of leukocytes (Jo et al., 2003). An excellent review discussing many of these aspects has been published recently (Osborne et al., 2004).

6. Impact of hypoxia on retinal pathologies

Apart from their essential role in retinal physiology, blood vessels are a major source of severe alterations that can lead to loss of vision in various retinal pathologies such as PDR, ROP, AMD and glaucoma (Bek, 2009). Although triggering insults may differ among these retinopathies, disturbed retinal hemodynamics, defects in the microcirculation and/or retinal capillary vaso-obliteration may eventually lead to the formation of hypoxic areas with subsequent neovascularization. The importance of reduced oxygen tension as a stimulus for the formation of new blood vessels was emphasized in a paradigm in which chronic systemic hypoxia induced retinal neovascularization in the absence of any pre-existing pathologies (Shortt et al., 2004). Reduced oxygen tension and retinal hypoxia affect the stability and function of HIF transcription factors (see chapter 4). Thus, it is not surprising that various HIF-regulated angiogenic factors such as VEGF (Pierce et al., 1995; Aiello et al., 1995; Robinson et al., 1996; Reich et al., 2003), PlGF (Carmeliet et al., 2001), angiopoietin 2 (ANGPT2) (Hackett et al., 2002), platelet-derived growth factor beta (PDGFB) (Jo et al., 2006), stromal-cell derived factor 1 (SDF1) (Butler et al., 2005), and EPO (Morita et al., 2003) have been implicated in the initiation and progression of retinal diseases involving microvascular changes. To understand the mechanisms behind these diseases, it is thus important to elucidate the reactions of the pathological tissue to ischemic or hypoxic stress and to analyze disease progression on a molecular level.

6.1. Diabetic retinopathy

Diabetic retinopathy (DR), a frequent complication in patients affected by diabetes mellitus, is the most common microangiopathy in the retina and a leading cause of blindness and visual impairment in the industrialized world (Ferris et al., 1999; Kocur and Resnikoff, 2002). However, it has become increasingly clear that DR also affects the survival of non-vascular cells, primarily RGCs, photoreceptors and RPE cells. Loss of synaptic proteins, altered intracellular calcium signaling and functional changes within photoreceptors, may additionally contribute to impairment of visual function (Lieth et al., 2000; Lorenzi and Gerhardinger, 2001; Barber, 2003; Barber et al., 2011) (reviewed in Villarroel et al., 2010). Nearly every patient suffering from diabetes for at least 20 years with disease onset before the age of 30 shows relevant signs of DR. About 50% of these cases are proliferative (Ferris et al., 1999), characterized by bi-phasic progression with an initial

vaso-obliterative phase and a subsequent uncontrolled vaso-proliferative period. The vascular pathogenesis involves thickening of the basement membrane, loss of intramural pericytes, development of microaneurysms, increased vascular leakage, and vessel regression (Addison et al., 1970; Robison, 1988; Stitt et al., 1994; Engerman and Kern, 1995). During the progression of the disease, macular edema, ischemia, retinal and vitreous hemorrhage, and retinal detachment can eventually lead to blindness in patients affected by DR (Morello, 2007).

Although a decrease in retinal blood flow is one of the earliest changes often observed in the diabetic retina (Feke et al., 1994; Bursell et al., 1996), contradictory data exist (Kohner et al., 1975) and the precise contribution of altered hemodynamics in the progression of the disease is still under debate. Nevertheless it has been hypothesized that vascular changes perturb the tightly regulated delivery of oxygen and nutrients to the retina, which may lead to the development of hypoxic areas with reduced tissue oxygenation as the disease progresses. However, direct evidence for the presence of retinal hypoxia in human diabetic patients is still limited.

Some evidence for the presence of hypoxia in the diabetic retina was found in human patients where the oxygen tension in the vitreous was only 5.7 mmHg on average, compared to 8.5 mmHg in healthy patients (Holekamp et al., 2006). In a recent comparative cross-sectional study, Lange and co-workers investigated the pre-retinal oxygen distribution in human patients in the advanced proliferative phase of DR. The authors demonstrated the presence of significant intraocular oxygen gradients in PDR patients, with 46% decreased mean oxygen tension in the mid-vitreous compared to control subjects (Lange et al., 2011c). A significant limitation of these studies, however, is the involvement of patients with advanced PDR, which does not allow drawing conclusions on a potential contribution of hypoxia in the early, non-proliferative stages of DR. Results from animal studies suggest that such retinal hypoxia may only develop at a later stage in experimental diabetes. Indeed, a study in cats with 6–8 years of diabetes found an oxygen tension in the inner retina of only 7.7 mmHg as compared to the 16.4 mmHg in control cats. This correlated with endothelial cell death, the presence of leukocytes plugging vessels, and microaneurysms (Linsenmeier et al., 1998). However, pre-retinal oxygen tension was equivalent in cats and dogs with less than one year of diabetes when compared to control animals (Stefansson et al., 1986, 1989). In the early phase of the disease, reduced oxygen consumption by neuronal cells may paradoxically lead to increased oxygenation of the retina. This might create a relative hyperoxia, resulting in vasoconstriction and reduced blood flow due to autoregulation of retinal hemodynamics (Wright et al., 2010, 2011). As a consequence, mild retinal hypoxia may then develop, as has been detected in mice after 5 months of diabetes (de Gooyer et al., 2006). Recent immunofluorescence studies of the diabetic retina in mice and rats provide somewhat puzzling data which revealed different stabilization patterns for HIF1A and HIF2A already early after the onset of diabetes. HIF1A levels increased after 2 weeks in rats (Poulaki et al., 2004) but not after 3 (Wright et al., 2011), 4 and 12 weeks (Wright et al., 2010), whereas HIF2A was elevated after 3 weeks of diabetes (Wright et al., 2011), but not after 4 or 12 weeks (Wright et al., 2010). However, stabilization of HIFA proteins and the development of retinal hypoxia may not strictly correlate. In fact, evidence linking the stabilization of HIFA transcription factors to conditions independent of hypoxia exists. For instance, common features involved in the etiology of DR such as inflammation and oxidative stress (Gardner et al., 2002; Lopes de Faria et al., 2011), can result in HIFA stabilization (Dehne and Brune, 2009; Yuan et al., 2008). Further investigations are required to define mechanisms of HIF activation and their function in the early diabetic retina as well as to elucidate the precise contribution of retinal hypoxia for the progression of the disease.

It seems clear, however, that HIF1A is a major factor involved in the neovascular process of the proliferative late phase of DR. Elevated HIF1A protein levels were found in fibrovascular epiretinal membranes (Abu El-Asrar et al., 2007) more often in diabetics than in non-diabetics (Lim et al., 2010), and VEGF is increased in patients with DR (Aiello et al., 1994). During the progression of the disease into a proliferative phase, neurons (Sapieha et al., 2008), astrocytes (Dorrell et al., 2002) and other cells react by an over-production of pro-angiogenic factors including VEGF. This may occur in a HIF1A-dependent manner since deletion of *Hif1a* in Müller cells resulted in reduced VEGF protein expression, reduced vascular leakage and reduced leukocyte adherence in a diabetic mouse model (Lin et al., 2011). In addition, intensive insulin therapy in diabetic rats was shown to result in BRB breakdown via a HIF1A-mediated increase in retinal VEGF expression (Poulaki et al., 2002).

Although DR is mainly characterized by alterations in the retinal vasculature and hemodynamics, tissue oxygenation and thus the function of factors regulating the molecular response to hypoxia might be central to development, progression and especially vascular proliferation of DR. Thus, additional information about the role of HIFs in the pathology of this disease, particularly in the control of the proliferative phase is needed. A very useful model to study molecular and cellular processes in the hypoxic retina before and during retinal neovascularization is the model of oxygen-induced retinopathy (OIR), which we describe below (see chapter 6.3).

6.2. Retinopathy of prematurity

ROP, a complication often found in pre-term infants, is associated with fluctuations in oxygen levels during artificial ventilation of the newborns, a link that was recognized more than 50 years ago (Ashton et al., 1954). As more pre-term infants survive, ROP has become a leading cause of visual impairment and blindness in children. An estimated 11% of infants are born pre-term and 6–18% of blindness or visual impairment in children in the industrialized world are caused by ROP (Gilbert et al., 1997).

Infants are born into an environment that is hyperoxic relative to the situation *in utero*, as oxygen tension averages 32 mmHg in the umbilical cord, while room air has an oxygen level of ~150 mmHg, resulting in an arterial pO_2 of close to 100 mmHg in a healthy human (Bell and Klein, 1994). Since development of the human retinal vasculature is complete at term (Roth, 1977) this change in environmental oxygen concentration is usually well tolerated in full-term infants and does not negatively influence their visual system. Infants born prematurely, however, may experience greater relative hyperoxia secondary to mechanical ventilation (Weinberger et al., 2002) already before the retinal vasculature has fully developed. This may prevent stabilization of HIF transcription factors, which would be needed for the production of angiogenic factors required for normal development of the retinal vasculature. Indeed, crucial factors such as VEGF and EPO are reduced in animals exposed to hyperoxia (van Wijngaarden et al., 2007; Chen et al., 2008) and it has been shown that the administration of VEGF (Alon et al., 1995) or EPO (Chen et al., 2008) during the vaso-obliterative phase of the disease can preserve the retinal vasculature and protect vessels from hyperoxia-induced dropout. Increasing the complexity of disease pathology, vaso-obliteration may not only be caused by the lack of angiogenic factors but also by endothelial cell damage due to increased levels of ROS, which are produced during hyperoxia (Niesman et al., 1997; Penn et al., 1997; Raju et al., 1997). The high susceptibility of the developing retina to ROS is further accentuated by compromised autoregulation of the retinal blood flow in

neonates due to high perinatal levels of prostaglandins and NO (Hardy et al., 1994; Dumont et al., 1998, 1999), the high rate of oxidative metabolism, significant stores of free iron that support the catalysis of oxidative reactions (Moncada et al., 1997; Stamler et al., 1992), and reduced levels of antioxidants in the immature retina (Flynn et al., 1991; Nielsen et al., 1988).

In the phase following vaso-obliteration, relative hypoxia develops in the retina of preterm newborns, causing neurons and astrocytes to induce a pro-angiogenic response leading to an over-compensatory vascular proliferation (Sapieha et al., 2008; Dorrell et al., 2002). As in other proliferative retinopathies, this neovascular response differs from the tightly regulated developmental angiogenic wave in that it is exaggerated and uncontrolled, eventually resulting in vascular growth towards the vitreous and lens. A secondary effect of the pathological neovascularization is the formation of fibrous scars, which exert physical force that might result in retinal detachment (Sapieha et al., 2010). Hypoxia appears again to be the main driving force for the progression of ROP into the proliferative phase. The majority of knowledge about the pathogenesis of ROP including the role of hypoxia and HIFs for disease development and progression comes from animal models of OIR (see chapter 6.3), which mimic many aspects of the disease (Smith et al., 1994; Penn et al., 1993).

6.3. The model of oxygen-induced retinopathy

OIR is an *in vivo* model to study pathomechanisms of proliferative retinopathies including ROP and PDR. It has been successfully reproduced in several animal species including rodents, cats and dogs (Penn et al., 1993, 1994; Smith et al., 1994; Chan-Ling et al., 1992; McLeod et al., 1998). Similar to human ischemic retinopathies, OIR presents a biphasic disease progression with vaso-obliteration in the first phase (phase I) and vaso-proliferation in the second phase (phase II). In this model, neonatal animals are exposed to hyperoxia (75% O_2) for several days to cause an arrest in vascular development along with the obliteration of pre-formed blood vessels in the central retina. The vaso-proliferative phase is then induced following the return of the animals to room air, which causes the avascular retina to experience relative hypoxia. This triggers the production and release of compensatory pro-angiogenic factors, including VEGF, IGF1 (Smith et al., 1997, 1999) and EPO (see chapter 8), but also of anti-angiogenic proteins like thrombospondin 1 (TSP1) (Kermorvant-Duchemin et al., 2005). Abnormal production of these proteins leads to chaotic neovascularization, resulting in the formation of neovascular tufts protruding from the inner retinal surface into the vitreous cavity (Smith, 2003; Smith et al., 1994).

Given the regulatory role of oxygen for disease induction and progression, it is not surprising that strong evidence points to a central role of HIF transcription factors in the pathophysiology of OIR. During phase I of the disease, HIFA protein levels decrease as a result of hyperoxia (Duan et al., 2011). This leads to suppression of VEGF expression and to vaso-obliteration (Alon et al., 1995; Pierce et al., 1996). Conversely, early during phase II, HIF1A and HIF2A protein levels increase within 2 h after the onset of relative hypoxia (Ozaki et al., 1999; Mowat et al., 2010). In correlation with HIFA stabilization, *Vegf* gene expression is rapidly upregulated, mainly in glial and Müller cells (Ozaki et al., 1999). Since a Müller cell-specific knockdown of *Vegf* significantly reduced neovascularization and vascular leakage (Bai et al., 2009), VEGF may be the main factor responsible for the vessel phenotype in OIR (Alon et al., 1995; Pierce et al., 1995; Stone et al., 1996). However, the control mechanism for *Vegf* expression in this model remains somewhat controversial. HIF1A was implicated in the process as a conditional knockdown of *Hif1a* in Müller cells resulted in significantly lower expression of *Vegf*, reduced neovascularization, and diminished vascular leakage in OIR (Lin et al., 2011). In addition, intraocular overexpression of a constitutively active form of HIF1A increased levels of VEGF (among other factors) and caused neovascularization even in the absence of hypoxia (Kelly et al., 2003). On the other hand, data from Weidemann and colleagues suggest that rather HIF2A but not HIF1A is required in astrocytes for VEGF-mediated neovascularization in OIR (Weidemann et al., 2010). A direct comparison of these results, however, is difficult since Lin et al. used a *vitelliform macular dystrophy (Vdm2)* and Weidemann et al. a *glial fibrillary acidic protein (Gfap)* promoter to drive *Cre* expression. Thus the mice may not only differ in their respective knockdown efficiencies but also in the pattern of cells affected by the knockdown. It seems clear, however, that HIF2A at least contributes to OIR, since the full knockout (Morita et al., 2003) or a haploinsufficiency (Dioum et al., 2008) of *Hif2a* resulted in a significant reduction of pathological neovascularization.

The strong involvement of VEGF in the pathogenesis of OIR prompted the use of anti-VEGF antibodies or antibody fragments to reduce or prevent hypoxia-driven retinal neovascularization (Aiello et al., 1995). Although this has now become the approach of choice for the treatment of neovascular complications in patients, targeting solely VEGF may not always lead to a significant improvement of disease progression (Brown et al., 2006a,b) because VEGF may not be the only factor contributing to the pathology. Thus, modulation of HIF activity as an upstream element controlling production of several pro-angiogenic factors is considered an option to treat or prevent pathological neovascularization with increased efficiency. Depending on the stage of the disease, however, modulation of HIF activity must be fine-tuned and either be supported or suppressed. Stabilization of HIF1A during phase I of OIR by using PHD inhibitors (Sears et al., 2008) or by a conditional knockout of *Phd2* (Duan et al., 2011) was shown to be beneficial, as it caused upregulation of pro-angiogenic molecules like EPO and VEGF, among others, and reduced vascular loss. This lessened the hypoxic burden in phase II of OIR and prevented the development of hypoxia-induced vaso-proliferative retinopathy. During phase II of OIR, however, modulation of HIF activity must aim at suppression rather than stabilization of these transcription factors. Indeed, intravitreal injections of both *Hif1a* short interfering RNA (siRNA) and *Vegf* siRNA just before onset of phase II were successful in inhibiting the development of retinal neovascularization, with maximal efficacy after co-application (Jiang et al., 2009). Similarly, inhibition of HIF1 transcriptional activity during this phase by digoxin significantly reduced the expression of pro-angiogenic genes including *Vegf*, *Pigf*, *Pdgfb*, *Sdf1*, and *stem cell factor (Scf)* in the model of OIR and led to a strong inhibition of retinal neovascularization (Yoshida et al., 2010).

Despite these studies, the mechanisms underlying OIR are still not completely understood. Other factors in addition to HIFs and HIF-induced angiogenic and endothelial cell survival proteins might contribute to the pathology. Increased ROS production, for example, may lead to oxidative stress-induced apoptosis of endothelial cells and may thus be a possible causative factor for the capillary vaso-obliteration in phase I of OIR (Hardy et al., 2000; Byfield et al., 2009; Uno et al., 2010). Pigment epithelium-derived factor (PEDF), a serine protease inhibitor (Becerra, 1997), was shown to counterbalance VEGF levels and to reduce not only retinal but also choroidal neovascularization (CNV) (Park et al., 2011). Similarly, a fragment of hepatocyte growth factor (HGF) also reduced neovascularization in OIR (Xu et al., 2010) as did a knockout of adenosine A(2A) receptor (A(2A)R) (Liu et al., 2010). Although various pathways may contribute to the development of neovascularization (Recchia et al., 2010), VEGF is clearly central in the pathology of OIR and a main factor involved in the abnormal vessel formation.

6.4. Age-related macular degeneration

AMD is the leading cause of blindness in the elderly: survey studies estimate that 50 million people are affected worldwide by AMD and that one-third of them is visually impaired (Gehrs et al., 2006). Risk factors to develop AMD are difficult to define, but include aging (Klein et al., 2010), smoking (Smith et al., 1996), and genetic predisposition (Edwards et al., 2005; Tolppanen et al., 2009). Other possible factors are obesity (Adams et al., 2011), hypertension (van Leeuwen et al., 2003), hypercholesterolemia (Reynolds et al., 2010), and light exposure (Cruickshanks et al., 1993). The disease is characterized by a progressive loss of central vision attributable to degenerative and neovascular changes in the macula leading to a disturbance of fine and color vision. AMD can be separated into early and late phases, as well as into dry and exudative forms (Bressler et al., 1988). The dry stage of AMD is characterized by the formation of soft and hard drusen and geographic atrophy. These pathological events may lead to the development of the neovascular/exudative form of AMD, which is most devastating for patients (Bressler et al., 1988). The progression from dry to exudative AMD is characterized by the formation of new, leaky vessels that penetrate Bruch's membrane from choroidal capillaries and grow into the RPE and the neural retina (Bressler et al., 1988).

Using different techniques such as fluorescein and indocyanine green angiography, laser Doppler flowmetry, and color Doppler imaging, abnormalities in ocular blood flow and retinal hemodynamics in early and late AMD have been described (Friedman et al., 1995; Ciulla et al., 1999) (reviewed in Harris et al., 1999) and reduced choroidal perfusion has been correlated to increased AMD severity (Grunwald et al., 1998, 2005). Quantification of oxygen tension, blood flow and perfusion pressure in the retina and optic nerve head in AMD patients suggests that the decreased choroidal circulation results in tissue hypoxia and activation of its molecular sensors which then may contribute to disease progression and the development of CNV (Grunwald et al., 2005; Metelitsina et al., 2008; Pournaras et al., 2008). Indeed, HIF1A and HIF2A have been detected in the endothelium and macrophages of human choroidal neovascular membranes associated with AMD (Inoue et al., 2007; Sheridan et al., 2009).

Stabilization and increased activity of HIF transcription factors in AMD may also be stimulated by chronic oxidative stress, which has also been implicated in the pathogenesis of AMD (reviewed in Khandhadia and Lotery, 2010). Oxidative stress, as a result of increased ROS production, may damage lysosomal membranes in RPE cells, impairing their capacity to remove metabolites from phagocytosed material. This may eventually contribute to the accumulation of lipofuscin in senescent RPE cells (Terman and Brunk, 2004; Kurz et al., 2008). Since lipofuscin may generate free radicals on its own, its accumulation may further magnify ROS production (Boulton et al., 1993; Sparrow et al., 2003) leading to a vicious cycle and an accelerated disease progression. A link between ROS and HIF stabilization was established during hypoxia (Cash et al., 2007) and thus, elevated ROS levels may eventually also lead to increased VEGF production via activation of HIF transcription factors. In addition, the thickening of Bruch's membrane and formation of drusen during AMD augment hypoxia by impairing the diffusion of oxygen from the choriocapillaries towards the retina (Schlingemann, 2004). As a result, outer retinal hypoxia ensues and may be an additional driving force for CNV via HIF-mediated over-expression of VEGF by RPE cells.

6.4.1. Choroidal neovascularization

CNV is encountered in many chorioretinal diseases such as ocular histoplasmosis syndrome, pathologic myopia, idiopathic CNV, and in particular AMD (Green and Wilson, 1986). CNV is a dynamic process characterized by an initiation stage, beginning with a break or a defect in Bruch's membrane, a maintenance stage, and an involution stage characterized by a decrease in cytokine production linked to scarring and fibrosis (Grossniklaus et al., 2002). Animal models of CNV are subdivided into three categories, where a break or defect in Bruch's membrane is induced either by laser treatment, mechanically via surgery or upon genetic engineering (reviewed in Grossniklaus et al., 2010). Once a defect in Bruch's membrane is present, choriocapillary endothelial cells proliferate and migrate into the RPE and the subretinal space along with pericytes, fibrocytes and inflammatory cells. Increased production of angiogenic factors like VEGF, bFGF and PDGF (Amin et al., 1994; Kvanta et al., 1996; Lopez et al., 1996) stimulate this process, and extracellular matrix (ECM) components form a provisional fibrin matrix acting as a scaffold for the growing vessels (Schlingemann, 2004).

Many reports point to VEGF as central factor for the development of CNV, as it is strongly expressed in surgically excised CNV membranes from AMD patients (Kvanta et al., 1996; Lopez et al., 1996) and in laser-induced CNV lesions in animal models (Song et al., 2008c). Also, experimental overexpression of VEGF by RPE cells induced CNV (Spilsbury et al., 2000), while inhibition of its expression in the same cells suppressed cellular processes involved in neovascularization *in vitro* (Zhao et al., 2008). Additionally, subretinal (Reich et al., 2003) or intravitreal (Tolentino et al., 2004) delivery of siRNA against VEGF significantly inhibited laser-induced CNV and vascular permeability. These results provided the basis for the successful application of VEGF or VEGF receptor antagonists such as pegaptanib (Macugen), ranibizumab (Lucentis), bevacizumab (Avastin), VEGF-Trap, or siRNA as therapeutic approaches to inhibit CNV progression (Aiello, 2005; Ferrara et al., 2006; Kinose et al., 2005; Check, 2005; Campa and Harding, 2011).

However, as in wet AMD, these approaches target only one of multiple angiogenic factors involved in the process of neovascularization. Manipulating the activity of a master regulator of the angiogenic response appears therefore to be a potential and attractive clinical alternative, which may lead to a more complete effect. One such option is HIF1A, which has been shown to be involved in the pathology of CNV together with VEGF (Song et al., 2008c; Yang et al., 2009). Expression of HIF1A was increased under hypoxic conditions in cultured RPE cells from donor eyes (Yanjun et al., 2007) and in the ARPE-19 cell line (Forooghian et al., 2007). In addition, it has been suggested that HIF1A is the main HIF isoform induced upon hypoxia, regulating VEGF expression in RPE cells (Forooghian et al., 2007; Zhang et al., 2007a,b). siRNA against *Hif1a* dramatically decreased the hypoxia-induced upregulation of *Vegf* transcription in RPE cells (Zhang et al., 2007a,b), and short hairpin RNA (shRNA) targeting *Hif1a* inhibited proliferation, migration and tube formation of choroidal microvascular endothelial cells co-cultured with RPE cells *in vitro* (Zhao et al., 2008). Similarly, intravitreal delivery of nanoparticles loaded with a vector expressing shRNA against *Hif1a* (Zhang et al., 2010a,b), and the systemic application of digoxin (Yoshida et al., 2010) successfully reduced neovascularization in animal models of laser-induced CNV.

6.5. Glaucoma

Glaucoma is a progressive optic neuropathy and the second leading cause of blindness worldwide, affecting 60 million people (Quigley and Broman, 2006). Glaucoma is characterized by degeneration of RGCs and their axons in the optic nerve. Although increased IOP is often found in glaucoma and can cause damage to RGCs, normal-tension glaucoma is also frequently observed, with RGC degeneration despite normal IOP. Clinical observations in

glaucomatous eyes include retinal vascular abnormalities such as vasospasm, alterations in blood flow and defects in angiographic vascular perfusion, suggesting that impaired blood flow at the optic nerve head may result in local tissue hypoxia (Flammer, 1994; Chung et al., 1999; Flammer et al., 2002) which may contribute to RGC death in glaucoma (Osborne et al., 2001). *In vitro* studies investigating the adverse effects of hypoxia on RGC survival (Kitano et al., 1996; Tezel and Wax, 1999; Gross et al., 1999; Morgan et al., 1999) further support the involvement of hypoxia/ischemia in the pathogenesis of glaucoma. In addition, the observation has been made *in vivo* that chronic ischemia in the primate optic nerve head results in degeneration of the NFL similar to that observed in glaucoma patients (Cioffi and Sullivan, 1999). Also, Tezel and Wax analyzed the localization of HIF1A in post mortem donor eyes from patients with glaucoma and showed that HIF1A immunostaining in the retina and optic nerve head was higher in glaucomatous eyes than in control eyes. Moreover, increased HIF1A immunostaining was closely correlated with the location of visual field defects recorded in these eyes (Tezel and Wax, 2004). These findings support, although indirectly, the presence of hypoxic areas in the optic nerve head and retina in glaucoma patients, pointing to the relevance of the HIF signaling system in the pathology of this disease.

7. Ischemic and hypoxic preconditioning

Whereas sustained ischemia or hypoxia may cause retinal damage and eventually loss of vision (see chapters 5 and 6), short and controlled periods of ischemia or hypoxia may protect retinal cells against damage by a subsequent insult. This phenomenon is described by the term preconditioning, which is characterized by the exposure of a cell, tissue, or organism to a brief and non-damaging period of stress - or to a substance - in preparation to cope with a subsequent insult that is normally harmful.

In relation to oxygen, two basic types of preconditioning protocols are frequently used in vision research. Ischemic preconditioning (IPC) was originally developed by Roth and co-workers and involves a brief period of retinal ischemia, produced either by the occlusion of the central retinal artery (Roth et al., 1998) or by an increase of IOP (Zhang et al., 2002). IPC leads to a local and transient reduction of oxygen tension, nutrient availability and clearance of metabolic waste. Hypoxic preconditioning (HP) is induced in cells or tissues by the reduction of environmental oxygen levels in the culture medium, and in animals by the exposure to breathing air with reduced oxygen concentrations. In animals, HP thus induces systemic effects as well as a strong molecular response in the retina. Although IPC was mostly used to study mechanisms of ganglion cell survival and HP primarily provided protection of photoreceptors, both IPC and HP prevented injury of retinal cells due to ischemia-reperfusion (Roth et al., 1998; Zhu et al., 2002) and exposure to bright light (Grimm et al., 2002; Casson et al., 2003). Protection by IPC or HP is thought to result from the differential expression of specific factors, which control and activate endogenous protective mechanisms (Kirino et al., 1991). Elucidating the molecular mechanisms of protection after preconditioning may give much needed insights into potential therapeutic options for the preservation of vision in patients.

7.1. Ischemic tolerance

IPC provides profound but short-lived morphological and functional protection against ischemia-reperfusion injury. This ischemic tolerance is most effective in a time-window of up to 72 h after the preconditioning stimulus (Roth et al., 1998; Sakamoto et al., 2004). From a clinical point of view, however, a long-lasting and general protective effect would be needed to counteract slowly progressing disorders such glaucoma and other retinopathies. In a study designed to extend the protective period of HP in mice, Zhu et al. exposed animals to multiple hypoxic insults over 12 days in a so called repetitive hypoxic preconditioning (RHP) protocol (Zhu et al., 2007). This was successful in extending ischemic tolerance to more than 4 weeks. Compared to a single HP stimulus, RHP was shown to further increase and sustain HIF1A protein stabilization and heme oxygenase 1 (HO1) protein expression over a prolonged time (Zhu et al., 2007). This supports the growing evidence that mechanisms inducing HIF1A protein expression and *Hif1a* transcriptional activation are different after acute, intermittent or continuous hypoxia (Semenza, 2006; Rapino et al., 2005; Nanduri et al., 2008).

The molecular events leading to ischemic tolerance or to protection after preconditioning in general can be divided into three steps. First, activation of signal transduction pathways lead to changes in second messenger levels and to activation or repression of transcription factors. This then leads to the second step, the expression of pro-survival genes or the downregulation of pro-apoptotic genes. The third and final step includes the cytoprotective actions mediated by the induced proteins.

7.1.1. Signal transduction and second messengers

Adenosine is a key mediator of alterations in retinal blood flow under ischemic or hypoxic conditions (Ostwald et al., 1997; Gidday and Park, 1993), and levels of adenosine significantly and rapidly increase after short periods of ischemia (Roth et al., 1997b) or reperfusion (Roth et al., 1997a). Involvement of adenosine in neuroprotection after retinal ischemia (Larsen and Osborne, 1996) is supported by data suggesting that activation of adenosine A1 and A(2A) receptors is a critical early component of ischemic tolerance after preconditioning (Li and Roth, 1999; Sakamoto et al., 2001) (reviewed in Ghiardi et al., 1999). The downstream neuroprotective steps after adenosine receptor activation include the opening of mitochondrial potassium ATP channels (mKATP), eventually resulting in the activation of AKT, protein kinase C (PKC), and the mitogen-activated protein kinase (MAPK) p38 (Li et al., 2000; Ettaiche et al., 2001; Sakamoto et al., 2001; Roth et al., 2006; Ding et al., 2009; Dreixler et al., 2009a,c; Zhang et al., 2002; Roth et al., 2003). In addition to adenosine, NO has also been shown to be rapidly increased in the retina after a brief ischemic insult (Cheon et al., 2002; Hangai et al., 1999; Kobayashi et al., 2000) and to be required for ischemic tolerance after IPC (Zhu et al., 2006). Although the contribution of the different NO synthase (NOS) isoforms to NO production after IPC remains controversial data suggest that endothelial NOS (eNOS) and neuronal NOS (nNOS) are more relevant than inducible NOS (iNOS) in this paradigm (Cheon et al., 2002; Hangai et al., 1999; Kobayashi et al., 2000; Sakamoto et al., 2006; Roth et al., 2006).

7.1.2. Transcriptomics

Studies investigating the mechanisms of HP have demonstrated that a short single hypoxic exposure (Grimm et al., 2002) or a RHP protocol (Peng et al., 2009) dramatically increased protein levels of the HIF1A transcription factor in retinas of mice and rats. This suggested a potential role of HIF1A in HP-mediated neuroprotection, a hypothesis supported by data showing that treatment with $CoCl_2$ (Whitlock et al., 2005) or desferrioxamine (Zhu et al., 2008a,b) stabilized HIF1A and provided protection against an ischemic insult. To address the role of HIF and/or other transcription factors for neuroprotection, several groups, including our own lab, have analyzed transcriptomic changes induced by IPC and HP protocols. IPC in the rat retina reduced expression of genes involved in the regulation of transcription, aminoacyl-tRNA synthetase (ARS)

activity, and amino acid transport in the time window of ischemic tolerance (Kamphuis et al., 2007b). Even though *de novo* protein synthesis seems required for protection provided by IPC (Roth et al., 1998), a generally reduced rate of protein synthesis may contribute to the protective effect, most likely by reducing the amount of ATP required in translational processes. In addition, the significantly different expression patterns of several genes involved in the immune responses of ischemic-tolerant and non-tolerant retinas suggest that ischemia leads to the activation of components of the immune system and to the attraction and adhesion of leukocytes (Kamphuis et al., 2007a). Indeed, IPC reduced leukocyte rolling and leukocyte accumulation during retinal ischemia-reperfusion injury (Nonaka et al., 2001). Genes involved in apoptotic pathways have also been shown to be differentially regulated after IPC, with expression of genes both up- and downregulated (Kamphuis et al., 2007a,b).

Using whole genome microarrays, our lab recently identified 431 genes that were differentially regulated in the mouse retina immediately after HP (Thiersch et al., 2008). Such a large number of differentially regulated genes and their association to different signaling pathways suggests that HP (and IPC) not only modulates expression of genes which are directly involved in the regulation of cell survival or death, but which may function in a multitude of pathways apart from neuroprotection. Nevertheless, several of the upregulated genes such as *Epo, bFgf, Vegf* (Grimm et al., 2002), *metallothionein-1 and -2* (*Mt1* and *Mt2*), *Adm*, *Bcl2-like 10 (Bcl2l10), phosphatidylserine receptor (Ptdsr),* and *transthyretin (Ttr)* (Thiersch et al., 2008) might contribute to the neuroprotective effect of HP. Our lab and others have demonstrated that many of these genes indeed protect retinal cells in various experimental paradigms (Grimm et al., 2002; Suemori et al., 2006; Nishijima et al., 2007; O'Driscoll et al., 2008). Among these factors, EPO is of special interest due to its pleiotropic effects and its long-standing clinical application as a therapeutic agent for patients with anemia. The physiological role of EPO in the retina and the neuroprotective capacity of locally or systemically delivered EPO are currently in the focus of intense research (see chapter 8).

Intriguingly, whereas the retinal transcriptome after HP returned quickly (within 16 h) to the normoxic pattern (Thiersch et al., 2008), the transcriptomic changes induced by IPC were longer lasting and detected until up to 7 days (Kamphuis et al., 2007b). This might explain why protection after IPC is generally observed over a longer period (days; (Roth et al., 1998)) than after HP (4 to 8 h (Grimm et al., 2002)) and suggests differences in the mechanisms underlying IPC and HP-mediated neuroprotection. In addition to the difference in the length of exposure to reduced oxygen tension between IPC and HP, the interrupted supply of nutrients during IPC (but not during HP) might partially explain the low similarity in the retinal transcriptome after IPC and HP. Nevertheless, a few genes have been found to be differently regulated by both types of preconditioning protocols, among them *p21, Mt2*, and *CCAAT/enhancer binding protein delta (C/ebpd)*, a transcription factor related to apoptosis (Thiersch et al., 2008; Kamphuis et al., 2007a,b). Whereas *p21* is not essential for protection observed after HP (Thiersch et al., 2008), it will be important to analyze the other commonly regulated genes in more detail.

7.1.3. Protective factors and epigenetics

Based on the number of differentially regulated genes after IPC or HP, it is not surprising that the majority of factors involved in mediating protection after preconditioning remain to be identified and analyzed. Nevertheless, apart from EPO, which has already been shown to be a central neuroprotective factor in the preconditioning response (see chapter 8), other potentially protective proteins include heat shock protein 27 (HSP27) and HO1. Their upregulation follows the time-course of IPC-mediated protection (Li et al., 2003; Roth, 2004) and $CoCl_2$ – induced stabilization of HIF1A leads to increased expression of HSP27 and to protection of retinal function against ischemic damage (Whitlock et al., 2005). In addition, stabilization of HIF1A after HP also leads to an increased expression of the δ-opioid receptor (DOR) in the rat retina (Peng et al., 2009). Activation of opioid receptors with morphine ameliorated ischemia-induced damage, while pre-treatment with the non-selective opioid receptor antagonist naloxone prevented the functional and morphological protection of IPC (Husain et al., 2009). The molecular events that are involved in opioid-mediated retinal neuroprotection are still largely unknown, but may involve downregulation of *tumor necrosis factor a (Tnfa)* expression (Husain et al., 2011).

It has become increasingly clear that HIFA stabilization and activity may be modulated by epigenetical mechanisms which may also induce longer lasting cellular changes via histone modifications and DNA methylation (Watson et al., 2010). A role for an epigenetic regulation of gene expression in neuroprotection after IPC is supported by a recent proteomic analysis performed by Stowell and co-workers. In ischemia-tolerant retinas, the levels of histone proteins H2B, H3 and H4 were increased while histone H2A was reduced. Immunohistochemical analysis confirmed these observations and demonstrated an increase of trimethylated histone H3, mono-ubiquitinylated histone H2A and polycomb group protein RING2 (Stowell et al., 2010). Histone H2A mono-ubiquitinylation and histone H3 methylation were implicated earlier in epigenetic transcriptional suppression (Bantignies and Cavalli, 2006). Recently, a general approach revealed that HIF-binding sites on genomic DNA were more frequently occupied by HIF in DNAse-1 hypersensitive areas. This led the authors to suggest that epigenetic regulation of the chromatin structure might be important for the regulation of the hypoxic response (Schodel et al., 2011). These data and the widespread involvement of epigenetic mechanisms in the modulation of cellular signaling pathways certainly warrant a detailed study of epigenetics in the control of the cellular reaction to hypoxia. These will be highly important for a more complete understanding of the molecular mechanisms leading to neuroprotection after IPC and HP.

7.2. Protection against light-induced photoreceptor degeneration

HP and IPC not only induced ischemic tolerance, but also effectively rescued photoreceptor cells after excessive light exposure (Grimm et al., 2002; Casson et al., 2003). Light damage is an experimental model for retinal degenerative diseases such as retinitis pigmentosa (RP) (Portera-Cailliau et al., 1994). Although many genetic models mimicking inherited human retinal degenerations are available (Samardzija et al., 2010), the light damage model has the advantage that the timing and intensity of the stimulus triggering degeneration can be adjusted to meet experimental needs. This allows the induction of the degeneration at the age of choice and the control of the extent of photoreceptor death. Furthermore, short pulses of high light levels induce a synchronized burst of photoreceptor apoptosis, facilitating the analysis of the molecular events of the initiation, progression and termination of the degeneration. For this reason, light-induced retinal degeneration is also a useful method to test the capacity of HP to protect photoreceptor cells.

Detailed analysis showed that HP stabilized HIF1A in a dose-dependent manner in the mouse retina, with the highest levels of stabilization after exposure of the animal to 6% and 10% oxygen for 6 h, intermediate stabilization after exposure to 14% oxygen and no stabilization when animals were kept in air with

slightly reduced (18%) or normoxic (21%) levels of O_2. In correlation with oxygen tension and HIF1A stabilization, preconditioning with 6% and 10% oxygen almost completely protected photoreceptors from light-induced degeneration, whereas 14% oxygen resulted in only partial, and 18% oxygen in no protection (Grimm et al., 2002). The direct correlation between neuroprotection and HIF1A protein stabilization suggests that hypoxia-induced HIF1-target genes may contribute to the protective mechanisms induced by HP. To address this question directly, we generated photoreceptor specific knockdowns of *Hif1a* and of *Vhl*. Despite reduced hypoxic expression of several hypoxia-regulated genes, HP still mediated full protection for photoreceptors lacking HIF1A (Thiersch et al., 2008). Similarly, although normoxic retinas of photoreceptor-specific *Vhl* knockdowns had higher basal expression of genes normally induced by hypoxia, photoreceptors were only partially and transiently protected against light damage (Lange et al., 2011b). This suggests that HP-mediated protection might not solely be an intrinsic response of photoreceptors to hypoxia but might rely on paracrine mechanisms involving other retinal cell types, like Müller glia cells. Alternatively, protection may not be mediated by the HIF system at all, but by some other factors regulated by reduced oxygen availability.

EPO is a candidate factor in such a paracrine mechanism, as it has been shown to protect photoreceptors and other cells even when applied exogenously (see chapter 8). Although *Epo* gene expression is controlled by HIF transcription factors, *Epo* was not upregulated in the photoreceptor-specific *Vhl* knockdown and not downregulated in hypoxic retinas lacking HIF1A in photoreceptors. Thus, retinal levels of EPO were largely unaffected in the knockdown mice, which might explain the observed sustained protection, or lack of protection, respectively. This, however, postulates a central role for EPO in the neuroprotection after HP and suggests that EPO may be produced by retinal cells different from photoreceptors, an interpretation supported by our finding that retinal *Epo* expression was strongly elevated in mice lacking VHL in most retinal cell types (Lange et al., 2011a).

It is still largely unknown how factors produced by HP interfere with the apoptotic events after light exposure. Nevertheless, interference is downstream of activator protein 1 (AP1) DNA binding (Grimm et al., 2002), which is induced after light exposure and necessary for the degenerative process (reviewed in Wenzel et al., 2005). Thus, more research is still needed to elucidate the mechanisms of neuroprotection after IPC and HP. In addition to factors controlled by hypoxia, cytokines and growth factors regulated by other mechanisms might also play an important part. For example, it is known that preconditioning by mechanical injury (Faktorovich et al., 1992), bright light (Liu et al., 1998; Ueki et al., 2009) and optic nerve sectioning (Bush and Williams, 1991) triggers retinal endogenous protective response pathways protecting photoreceptors against light damage. These pathways may include gp130 signaling (Ueki et al., 2009) and the upregulation and release of various trophic factors such as bFGF and ciliary neurotrophic factor (CNTF) (Faktorovich et al., 1990; Liu et al., 1998; Wen et al., 1995). It is therefore interesting and of potential relevance that IPC in rats (Casson et al., 2003) and HP in mice (Grimm et al., 2002) induce expression of *bFgf* mRNA.

8. Erythropoietin

EPO, a secreted glycoprotein of the type I cytokine superfamily, plays a central role in tissue oxygenation via regulation of erythrocyte production. By binding to its cognate EPO receptor (EPOR), EPO prevents apoptosis of early erythroid progenitor cells in bone marrow and allows their differentiation. Early findings showed that *Epo* gene expression is strongly oxygen-regulated, as its transcript was induced by orders of magnitude in anemia and subsequent hypoxia (Bondurant and Koury, 1986). This rise in systemic EPO levels under hypoxic conditions eventually results in an increase in hematocrit and thus the oxygen transport capacity of the blood (reviewed in Jelkmann, 2004).

During fetal development, EPO is primarily produced in the liver, the site of definitive erythropoiesis at that time (Dame et al., 1998). At birth, when the site of production of blood cells shifts to the bone marrow, EPO expression switches from the liver to the kidney (Zanjani et al., 1981). However, about 10% of EPO in the circulation of adults originates from non-renal tissues (Fried et al., 1969) such as brain, spleen, lung, placenta, uterus, testis, and retina (reviewed in Fandrey, 2004). The detection of an HRE in the 3′ regulatory region of the *Epo* gene gave insight into its oxygen- and HIF-dependent transcriptional regulation (Semenza and Wang, 1992). HIF1A has initially been purified from Hep3B cells as the HIF isoform binding to the HRE of the *Epo* gene (Semenza et al., 1991; Wang et al., 1995). In spite of this, recent *in vivo* and *in vitro* evidence suggests that HIF2 may be the main regulator of systemic EPO homoeostasis and thus the key mediator of the hypoxic induction of *Epo* gene expression in adult kidney and liver (Tian et al., 1997; Gruber et al., 2007; Morita et al., 2003; Rankin et al., 2007; Scortegagna et al., 2005, 2003a,b; Warnecke et al., 2004; Gruber et al., 2007). Similarly, expression of *Epo* in brain (Chavez et al., 2006; Yeo et al., 2008) and retina (Morita et al., 2003; Ding et al., 2005) under hypoxic conditions has been proposed to be HIF2-dependent. However, tissue-specific *Epo* gene expression may not solely be HIF-driven, but may also involve regulation by other factors such as hepatocyte nuclear factor 4 (HNF4), GATA and other accessory signaling pathways that remain to be discovered (reviewed in Weidemann and Johnson, 2009).

Several reports confirmed the expression of *Epo* and *EpoR* in human and rodent retina (Juul et al., 1998; Xie et al., 2007; Grimm et al., 2002; Chen et al., 2009). However, retinal cell types expressing *Epo* have not yet been clearly defined, and recent reports suggest either Müller cells (Fu et al., 2008) or cells of the GCL (Scheerer et al., 2010) to be the main source of EPO in the retina. Our own data from *Hif1a* and V*hl* knockdown animals indirectly support such a conclusion (see above) (Thiersch et al., 2009; Lange et al., 2011b). Although many different studies describe localization of the EPOR in Müller cells (Zhu et al., 2008a,b; Wang et al., 2011a,b; Hu et al., 2011), RGCs (Kilic et al., 2005b; Zhong et al., 2007a; Fu et al., 2008; Zhu et al., 2008a,b), the inner plexiform layer (IPL) and outer plexiform layer (OPL) (Zhong et al., 2007a; Fu et al., 2008; Zhu et al., 2008a,b), and photoreceptors (Grimm et al., 2002; Zhong et al., 2007a), the spatial expression pattern of EPOR in the retina still needs to be verified, especially since antibodies used for most localization studies give variable if not unreliable results (Elliott et al., 2006; Kirkeby et al., 2007). As in other tissues, increased EPOR protein levels have been found after retinal ischemia (Junk et al., 2002; Dreixler et al., 2009b), hypoxia (Grimm et al., 2002), ocular hypertension (Fu et al., 2008), but not after optic nerve transection (Weishaupt et al., 2004). Therefore, as in other parts of the CNS, regulation of *EpoR* expression in the retina may depend on type and extent of injury, as well as expression of pro-inflammatory cytokines and of EPO itself.

8.1. Intracellular signaling

The pro-survival activity of EPO on erythroid progenitor cells is mediated by binding to the EPOR homodimer, leading to a conformational change of the receptor that results in its trans-phosphorylation and activation of the associated janus kinase 2 (JAK2) (Witthuhn et al., 1993; Livnah et al., 1999). Once activated,

JAK2 phosphorylates EPOR and activates downstream signal transduction pathways that lead to cellular proliferation and inhibition of apoptosis of hematopoietic cells. It was observed that EPO binds to erythrocyte precursors with different affinity than to cells with neuronal characteristics (Masuda et al., 1993) and that non-hematopoietic EPO variants still retain tissue-protective abilities without binding to EPOR homodimers (Leist et al., 2004). Thus the involvement of another receptor in neuronal signaling and neuroprotection has been considered. EPOR has been previously reported to physically (Jubinsky et al., 1997) and functionally (Blake et al., 2002) interact with the common β receptor (βcR), also known as CD131. Since protection by EPO was abolished in mice lacking βcR, Brines and colleagues proposed that neuroprotection might be mediated through an EpoR/βcR heteroreceptor complex (Brines et al., 2004). However, the contribution of βcR to EPO signaling has been contradicted by experiments showing that EPO also protected neuroblastoma cells that do not detectably express βcR (Um et al., 2007), and hippocampus cells which express only very low levels of βcR (Nadam et al., 2007). In the mouse retina, βcR is expressed during postnatal development and in adult tissue (Britschgi and Grimm, unpublished), and *in situ* hybridization analysis revealed its expression in RGCs, in the INL, and to a lower extent in photoreceptors (Colella et al., 2011). Nevertheless its potential contribution to EPO-mediated neuroprotection has not yet been investigated.

The downstream events elicited by EPO in neurons include phosphorylation of signal transducer and activator of transcription (STAT) 3/5 (Kretz et al., 2005; Zhang et al., 2007a,b), phosphatidylinositol 3-kinase (PI3K)-AKT activation (Siren et al., 2001; Digicaylioglu et al., 2004), phosphorylation of MAPKs such as extracellular-signal-regulated kinases (ERK) 1/2 (Kilic et al., 2005a,b; Shen et al., 2010), and nuclear factor (NF)-κB nuclear translocation (Digicaylioglu and Lipton, 2001). These events eventually result in the upregulation of anti-apoptotic proteins such as B-cell lymphoma-extra large (BCL-X_L) (Wen et al., 2002; Renzi et al., 2002) and B-cell lymphoma 2 (BCL2) (Yamasaki et al., 2005), as well as in the inhibition of cytochrome c release and caspase activation (Weishaupt et al., 2004; Chong et al., 2003). Additionally, activation of phospholipase C-γ (PLCγ) results in the regulation of calcium influx, thereby influencing neuronal activity and neurotransmitter release (Koshimura et al., 1999; Morishita et al., 1997; Kawakami et al., 2000; Marrero et al., 1998).

8.2. Neuroprotection in the retina

In addition to a cytoprotective effect of EPO in kidney after ischemia-reperfusion (Patel et al., 2004) and in different models of myocardial ischemia (Cai et al., 2003; Parsa et al., 2003), results supporting a general neuroprotective capacity of EPO have accumulated over the past decade. For example, recombinant human EPO (rhEPO) protected primary neurons from hypoxia (Lewczuk et al., 2000), glutamate toxicity (Morishita et al., 1997), and serum withdrawal (Siren et al., 2001). *In vivo*, systemic delivery of rhEPO provided protection against experimental brain injury (Brines et al., 2000; Yatsiv et al., 2005), ischemic damage and stroke (Sakanaka et al., 1998; Bernaudin et al., 1999), experimental Parkinson's disease (Genc et al., 2001), multiple sclerosis (Sattler et al., 2004), spinal cord injury (Celik et al., 2002; Gorio et al., 2002), and retinal degeneration (see below). In clinical trials, treatment with rhEPO was initially reported to be beneficial for the outcome of stroke (Ehrenreich et al., 2002) but later results from a larger study did not find a similar effect (Ehrenreich et al., 2009). Tissue protection by EPO may not only rely on a direct counteraction of apoptotic processes in cells but also on modifications of the tissue milieu. For example, rhEPO treatment may inhibit NO overproduction (Calapai et al., 2000), modulate antioxidant enzymes (Kumral et al., 2005), reduce neuronal glutamate release (Kawakami et al., 2001), induce stem cells to differentiate into neuronal progenitors (Shingo et al., 2001), and stimulate anti-inflammatory actions (Agnello et al., 2002; Villa et al., 2003).

8.2.1. Protection of retinal ganglion cells

Glaucoma results in RGC death, as does injury or axotomy of the optic nerve. Several recent studies reported significantly increased levels of EPO in the aqueous humor of glaucomatous patients. EPO concentrations in the serum, however, did not differ, suggesting that the increased levels in the eye were derived from locally produced EPO (Cumurcu et al., 2007; Mokbel et al., 2010; Wang et al., 2010a,b). The increased intraocular EPO levels in glaucoma may document an activated endogenous tissue defense mechanism, which may have been initiated to protect RGCs from rapid death in an attempt to preserve vision. Such an interpretation is supported by the observation that neutralization of endogenous EPO by the application of a soluble EPOR aggravated ischemic injury (Junk et al., 2002; Dreixler et al., 2009b). The capacity of rhEPO to protect RGCs *in vitro* is further substantiated by the increased survival of RGCs upon deprivation of neurotrophic factors (Weishaupt et al., 2004), or after a toxic insult with glutamate and NO (Yamasaki et al., 2005). *In vivo*, EPO protected mouse or rat RGCs against optic nerve axotomy-induced apoptosis after a single systemic injection (Fu et al., 2008), after repetitive intravitreal applications (Weishaupt et al., 2004), or after neural specific expression of a transgene encoding for human EPO (Kilic et al., 2005b). While protection in the rat suggested a role for the PI3K/AKT pathway, protection in mouse seemed to depend rather on ERK1/2 signaling. This points to species differences in the protecting mechanisms but this still needs confirmation. EPO protected RGCs also in models of mild (Tsai et al., 2005) and chronic ocular hypertension (Fu et al., 2008).

Other reports have shown that repetitive intraperitoneal injections of rhEPO (Zhong et al., 2007a) or the adeno-associated virus (AAV)-mediated delivery and systemic expression (from skeletal muscle cells) of EPO or of a non-hematopoietic form of EPO (Sullivan et al., 2011b) (see chapter 8.5) rescued RGCs in the DBA/2J mouse, a strain that spontaneously develops increased IOP. In some instances, endogenous EPO was antagonized by the intravitreal delivery of soluble EPOR, which exacerbated the injury and underlined the protective effect of EPO signaling in the retina (Fu et al., 2008).

In addition to stimulating RGC survival, EPO supported axonal regeneration and neurite outgrowth in RGCs as observed *in vivo* in adult rats after axotomy (King et al., 2007), and *in vitro* in rat retinal explants (Bocker-Meffert et al., 2002), primary cultures of adult rat retinas (Kretz et al., 2004, 2005), cultured rat retinal neurocytes (Zhong et al., 2007b), and primary rat retinal neurons (Hu et al., 2011). The molecular mechanisms involved have not been clearly defined but may include BCL-X_L and brain-derived neurotrophic factor (BDNF), as well as JAK2/STAT3 and the PI3K/AKT signaling pathways (Kretz et al., 2004, 2005; Hu et al., 2011).

Altogether, these studies suggest a critical role for the EPO/EPOR system in promoting survival and recovery of RGCs, and encourage the further exploration of EPO as a potential therapeutic cytokine to treat retinal degenerative diseases such as glaucoma involving apoptotic loss of RGCs.

8.2.2. Protection of photoreceptors

Both EPO and EPOR protein expression follow a circadian rhythm in the retina, with increased protein levels anticipating daily light onset (Chung et al., 2009). It is tempting to speculate that this expression pattern prepares the light absorbing cells to cope

with increased phototoxic stress during the day. Support for such a hypothesis comes from *in vivo* studies, which have demonstrated in different models of light-induced retinal degeneration that exogenous application of rhEPO partially prevented photoreceptor apoptosis (Grimm et al., 2002; Ranchon Cole et al., 2007). In line with these data, systemic overexpression of *Epo* following intramuscular AAV-mediated gene transfer resulted in the morphological rescue of photoreceptors from light-induced apoptosis. This was complemented by an improvement of photoreceptor function (Rex et al., 2004). Similarly, systemic overexpression of a human *Epo* transgene (Ruschitzka et al., 2000) resulted in a 20-fold increased level of EPO protein in the retina, and led to photoreceptor protection against light-induced damage (Grimm et al., 2004). It is relevant to note that in most instances, protection of photoreceptors by EPO treatment was not as complete as after HP, thereby suggesting that hypoxia triggers additional protective mechanisms.

Whereas it seems clear that EPO can protect photoreceptor cells against phototoxic stress, protection against inherited photoreceptor degeneration seems to depend on the model and thus on the particular molecular pathway which causes cell death. Transgenic *Epo* overexpression or repetitive intraperitoneal injections of rhEPO in rd1 and VPP mice did not rescue photoreceptor cells (Grimm et al., 2004). Similarly, Rex and co-workers demonstrated that photoreceptors of the rd10 mouse (Chang et al., 2007) were not protected by the expression of an *Epo* transgene in skeletal muscles after AAV-mediated transfer (Rex et al., 2004). However, the same approach significantly prevented degeneration in the rds mouse (Rex et al., 2004), as did the subretinal injection of rhEPO (Rex et al., 2009). Surprisingly, protection in the rds mouse was only achieved after intramuscular but not after intraocular injection of AAV-*Epo* vectors. The observation that EPO isoforms produced in the retina after AAV-mediated gene transfer differed depending on the retinal cell type transduced, and also differed from both physiological EPO and EPO produced by a transgene in skeletal muscle cells (Stieger et al., 2006; Lasne et al., 2004) may help to explain this finding. In addition, large local EPO concentrations achieved through intraocular expression of a transgene may not be optimal to mediate the neuroprotective effect (see chapter 8.5). Alternatively, specific posttranslational modifications other than glycosylation (Rex et al., 2009) might also be important for protection.

The mechanisms leading to photoreceptor protection after intramuscular *Epo* gene transfer are still unclear. However, since expression of non-erythropoietic forms of EPO resulted only in a slight increase of the hematocrit but still protected neuronal cells efficiently (Sullivan et al., 2011a), increased tissue oxygenation through an increase in the erythrocyte population may not be the basis for the protection. The failure of EPO to protect photoreceptors in the rd1, rd10 and VPP models (Rex et al., 2004; Grimm et al., 2004) also suggests that EPO may not be universally neuroprotective, but rather may interfere only with specific apoptotic mechanisms. These mechanisms seem to be activated in the rds mouse but not in other models of retinal degeneration investigated so far. Thus, to define the mechanisms of protection by EPO, it will be important to elucidate the various apoptotic pathways as they occur in the different models of retinal degeneration (Nir et al., 2000; Kim et al., 2002; Doonan et al., 2003; Hao et al., 2002).

8.3. Pleiotropic effects in the diabetic retina

Elevated levels of EPO protein have been detected in the vitreous of eyes with diabetic macular edema (Hernandez et al., 2006) and in post mortem eyes of diabetic patients (Garcia-Ramirez et al., 2008). Accumulation of EPO may have been caused by enhanced local production, as the same post mortem eyes also showed increased levels of *Epo* mRNA in the retina (Garcia-Ramirez et al., 2008). However, since patients suffering from early diabetic nephropathy with low systemic EPO production display a more severe progression of DR, systemic EPO may also contribute to the survival of retinal cells in this condition. To experimentally investigate the intraocular role of EPO in diabetes, injection of streptozotocin in rats is frequently used to induce tissue alterations representing early, non-proliferative, DR (Yu et al., 2001). Although streptozotocin injections in rats results rather in an increased expression of *EpoR* than of *Epo* itself, the data nevertheless suggest an increased endogenous EPO/EPOR signaling to ameliorate the consequences of diabetes in the retina (Zhang et al., 2008a; Hu et al., 2011). Three possible mechanisms may be involved: EPO may influence retinal pericytes and endothelial cells to support integrity of the BRB and prevent vascular leakage; it may target Müller cells to reduce osmotic swelling and support their normal function; and/or may directly or indirectly improve survival of retinal cells.

8.3.1. Effects on blood–retinal barrier integrity and cell survival

A single intravitreal injection of rhEPO at the onset of diabetes significantly reduced BRB breakdown in streptozotocin-treated rats (Zhang et al., 2008a). The mechanism behind this finding may include reduced production of VEGF by a negative feedback loop, which regulates the HIF1A pathway in the presence of high EPO levels at both the transcriptional and the translational level (Zhang et al., 2010a,b). In agreement with these data, retinal VEGF protein expression was reduced in diabetic rats after long-term (3 months) treatment with rhEPO (Wang et al., 2011a,b). In addition, *in vitro* evidence supports the ability of EPO to preserve the integrity of the blood–brain barrier (BBB) against VEGF-induced permeability by restoring tight junction proteins (Martinez-Estrada et al., 2003).

Apart from VEGF, apoptosis or migration of pericytes contributes to vascular pathogenesis in DR (Mizutani et al., 1996; Pfister et al., 2008). Since pericytes are major factors in the maintenance of the BRB and the survival of endothelial cells, preserving normal pericyte function may reduce vessel dropout and be beneficial for BRB integrity in early DR (Wang et al., 2011a,b). Indeed, treatment of diabetic rats with sub-erythropoietic doses of rhEPO over 6 months significantly inhibited loss of pericytes and the formation of acellular capillaries, without affecting leukostasis and endothelial cell proliferation (Wang et al., 2011a,b). In addition to increasing AKT phosphorylation, rhEPO treatment also reduced oxidative and nitrosative stress, HSP27 production, glial activation, formation of advanced glycation end products (AGEs) and the expression of *Angpt2* (Wang et al., 2010a,b). The beneficial effects of rhEPO treatment on the retinal vasculature have also been accompanied by reduced neurodegeneration and functional damage (Wang et al., 2011a,b; Zhu et al., 2008a,b), for example by protecting retinal cells against the toxicity of AGEs (Shen et al., 2010). Thus, the effects of EPO on the survival of vascular cells and the integrity of the BRB in early diabetes could potentially prevent vessel dropout and vascular leakage and thus progression of the disease into a proliferative DR.

8.3.2. Effects on Müller cell physiology

DR involves low-grade inflammation, with inflammatory cytokines such as TNFA, interleukin-6 (IL6) and interleukin 1B (IL1B) playing a role in BRB breakdown and disease progression (Joussen et al., 2002; Carmo et al., 2000; Funatsu et al., 2001). The retinal source of such cytokines may be Müller glia cells which may also contribute to neurodegeneration, vascular changes, and the formation of retinal edema, through reactive gliosis and impaired fluid clearance (osmotic swelling) (Bringmann et al., 2004;

Pannicke et al., 2006; Reichenbach et al., 2007) (reviewed in Fletcher et al., 2007). Thus, modulating Müller cell activity may help to reduce detrimental tissue changes associated with DR. Indeed, rhEPO attenuated the increased production of TNFA and IL1B in diabetic rats (Lei et al., 2011) and inhibited osmotic swelling of retinal glial cells *in vitro*, probably through the activation of a glutamatergic-purinergic signaling cascade involved in ion channel opening and fluid clearance (Krugel et al., 2010). Whether or not such a decrease in Müller cell swelling will be relevant to the protective effects of EPO *in vivo* remains to be investigated. Besides production of pro-inflammatory cytokines (Tezel and Wax, 2000), Müller cells are also an important source for neurotrophic factors in the retina. Reactive gliosis as it occurs during DR may significantly alter the production of neurotrophins and influence disease progression (Aizu et al., 2003; Seki et al., 2004; Hu et al., 2011) (reviewed in Bringmann et al., 2006). A single intravitreal injection of rhEPO ameliorated Müller cell gliosis induced by diabetes, increased *Cntf* mRNA expression, and most prominently increased *Bdnf* mRNA and protein expression in the retina *in vivo* and a Müller cell line *in vitro* (Hu et al., 2011). Similarly, a significant reduction of Müller cell gliosis, characterized by reduced GFAP immunoreactivity upon intraocular delivery of rhEPO, was also demonstrated in the *rds* mouse model of inherited photoreceptor degeneration (Rex et al., 2009). Whether this effect is explained by a direct influence of EPO on Müller cell physiology or whether the effect is caused indirectly through the preservation of photoreceptors remains to be elucidated.

Taken together, growing experimental evidence supports a protective role of EPO in the first pathological stages of DR. Exogenous delivery of rhEPO has demonstrated promise for the protection of retinal neurons and vascular cells (Zhu et al., 2008a,b; Zhang et al., 2008a), inhibition of oxidative stress (Wang et al., 2010a,b), maintenance of BRB integrity (Zhang et al., 2008a, 2010a,b; Wang et al., 2010a,b, 2011a,b), control of excessive Müller cell gliosis with a concomitant promotion of the production of neurotrophic factors (Hu et al., 2011), and reduced secretion of pro-inflammatory cytokines by glial cells (Lei et al., 2011). The first experiments testing EPO in human patients are also encouraging. Intravenous rhEPO injections to treat azotemia-induced anemia in diabetic patients were beneficial for diabetic macular edema and improved visual outcome (Friedman et al., 2003). Also, three intravitreal injections of rhEPO demonstrated a short-term positive response with anatomic and visual improvements in three out of five patients with severe, chronic diabetic macular edema (Li et al., 2010).

8.4. EPO as angiogenic factor

Even though the treatment with EPO might be beneficial in early stages of DR, the timing of a potential treatment must be carefully considered since EPO has long been recognized as a pro-angiogenic factor (Anagnostou et al., 1990; Ribatti et al., 2003) and may therefore become involved in the progression of retinal diseases from a non-proliferative to a proliferative form. For example, using a combination of case-control association and functional studies, Tong and co-workers demonstrated that polymorphisms increasing the activity of the *Epo* gene promoter, and thus increasing *Epo* transcripts, are linked to PDR in patients (Tong et al., 2008). In addition, increased EPO levels have been detected in the vitreous of human eyes with PDR (Inomata et al., 2004; Katsura et al., 2005; Watanabe et al., 2005).

Both beneficial and detrimental effects of EPO treatment have also been experimentally demonstrated in the OIR model (see chapter 6.3). Application of rhEPO during phase I of OIR prevented vessel dropout and reduced the formation of hypoxic areas. This also diminished the neovascular response in the second phase of OIR. In contrast, rhEPO treatment during phase II enhanced the pathological neovascular response (Chen et al., 2008). A role of EPO in neovascular processes is also supported by the observation that siRNA against *Epo*, or blockade of EPO with soluble EPOR, significantly suppressed neovascularization in OIR (Watanabe et al., 2005; Chen et al., 2009). Similarly, reduced intravitreal *Epo* mRNA levels in *Hif2a* knockdown mice correlate with reduced pathogenic neovascularization, an effect partially reversed by the intraperitoneal injection of rhEPO (Morita et al., 2003).

However, further investigations are still needed to clarify some conflicting data and define the individual contributions of VEGF and EPO in the progression of proliferative retinal diseases. For example, Slusarski and co-workers did not observe reduced vaso-obliteration or increased neovascularization, respectively, after the application of rhEPO during the two phases of OIR (Slusarski et al., 2009). Similarly, contradictory data exist in the treatment of ROP, especially with respect to the timing of EPO application. While two reports have shown that early treatment of pre-term infants with rhEPO increased the risk of ROP, and late treatment did not (Ohlsson and Aher, 2006; Aher and Ohlsson, 2006), other reports have associated late treatment with higher risk for ROP (Brown et al., 2006a,b; Suk et al., 2008). Until such discrepancies are resolved, EPO should be used cautiously for the treatment of retinal complications in human patients.

8.5. EPO dosage and non-hematopoietic variants

Despite such conflicting data, EPO is nevertheless an attractive molecule to be considered as a therapeutic agent in ocular disorders: EPO has pleiotropic biological activities which may be beneficial for various conditions and strong clinical experience has already been collected during the treatment of patients suffering from anemic complications. Even though long-term systemic use of rhEPO can be associated with adverse effects such as hypertension, polycythemia vera, and thromboembolism (Buckner et al., 1990; Stohlawetz et al., 2000; Dai et al., 2005), prolonged local application in the eye may prove to be less problematic. Preliminary results suggest for example that constantly elevated intraocular levels of human EPO in a transgenic mouse did not result in any detectable changes in retinal morphology or in severe alterations of the retinal vasculature, apart from a slight vessel tortuosity (unpublished data). Similarly, no adverse effects have been reported after systemic or local delivery of EPO protein or after expression of a virally delivered *Epo* transgene.

For the development of therapeutic strategies, it is important to consider the bell-shaped dose-response curve of EPO that has been reported for the protection of neuronal cells *in vitro* (Siren et al., 2001; Weishaupt et al., 2004; Shen et al., 2010; Wang et al., 2009) and *in vivo* (Sakanaka et al., 1998; King et al., 2007) and for a variety of other biological effects (Beleslin-Cokic et al., 2004; Hu et al., 2011; Zhang et al., 2008a). Such a dose-response effect is characteristic for cytokines (Brines and Cerami, 2005), and implies that rhEPO dosage must be carefully titrated in order to achieve optimal results. In fact, the most effective rhEPO dosage might be much below the dose shown to be safe for intravitreal injections in rat (up to 62.5 U) (Tsai, 2008), rabbit (up to 1000 U) (Zhang et al., 2008b; Song et al., 2008a), and humans (up to 2000 U) (Lagreze et al., 2009).

Of special interest is the difference in the optimal dose required for the neuroprotective (lower dose) and the neuroregenerative (higher dose) actions of rhEPO on axotomized RGCs *in vivo* (King et al., 2007). Such a difference suggests that the two mechanisms may vary in their mode of action and their signaling pathways. It has already been shown that the neuroprotective function of EPO

can be separated from its erythropoietic activity, which prompted the recent development of EPO derivatives that are no longer erythropoietic but still retain their neuroprotective potential. For example, carbamylated EPO (CEPO) does not show hematopoietic activity but has still been cytoprotective in various *in vitro* and *in vivo* approaches, including models of stroke and diabetic neuropathy. Interestingly, CEPO does not bind to the classical EPOR, suggesting that it mediates protection against cell death via other signaling systems (Leist et al., 2004; Coleman et al., 2006). Support for this notion comes also from our own experiments showing that photoreceptors lacking functional EpoR are still fully protected after HP in a light-damage paradigm (unpublished data). Similar to CEPO, carbamylated darbepoietin (Caranesp), a non-erythropoietic form of darbepoietin, also showed neuroprotective abilities in an *in vivo* model of stroke (Villa et al., 2007). AsialoEPO has neuroprotective actions similar to EPO, but the removal of sialic acid results in a significantly shorter plasma half-life of the protein, which obviously allows the initiation of the neuroprotective signaling but not the stimulation of erythropoiesis which may require longer circulating time in the plasma (Leist et al., 2004; Erbayraktar et al., 2003).

Further support of the hypothesis that the individual functions of EPO might be separable and attributable to specific regions of the protein is provided by studies using epopeptide AB, a 17-mer long EPO-derived peptide. This peptide showed neuroprotective and neurotrophic properties *in vivo* without promoting proliferation of erythropoietic cell lines (Campana et al., 1998). In accordance with these findings, Brines and co-workers aimed to define the tissue-protecting domains within the *Epo* sequence by synthesizing a helix B peptide (HBP) based on the tertiary structure of EPO. They demonstrated that HBP bound to the EPOR/βCR heterodimer and was neuroprotective both *in vitro* and *in vivo* in different models including ischemic stroke, diabetes-induced retinal edema, and peripheral nerve trauma. Similar findings were reported for a second peptide, the HBP surface peptide (HBPSP) (Brines et al., 2008).

In addition, several mutant EPO proteins with single amino acid substitutions have been generated which retain their cytoprotective abilities with no or strongly reduced hematopoietic activity. Leist and co-workers generated two mutant forms of EPO with a single amino acid exchange, EPO-R103E and EPO-S100E. Both mutant EPO variants retained high cytoprotective capacity *in vitro* despite significantly reduced affinity for EPOR (Leist et al., 2004). In addition, EPO-S100E protected against ischemic damage and improved neurologic function after experimental focal cerebral ischemia in rats (Villa et al., 2007). Recently, Colella et al. tested the EPO-S100E mutant variant for neuroprotection in three different models of photoreceptor degeneration in mice. Systemic expression EPO-S100E after intramuscular AAV-mediated gene transfer protected photoreceptors from degeneration in the light-damage model as well as in *rds* and *Aipl1*$^{-/-}$ (Dyer et al., 2004) mice, both are models for inherited photoreceptor degeneration. Importantly, expression of EPO-S100E did not result in a significant increase of the hematocrit. Sullivan and co-workers developed and tested the EPO-R76E variant for neuroprotection in an *in vivo* model of retinal degeneration. Here a single intramuscular injection of AAV carrying EPO-R76E protected the photoreceptors of the *rds* mouse, without increasing the hematocrit to dangerous levels (Sullivan et al., 2011a). The neuroprotective capacity of the EPO-R76E variant was also tested in the DBA/2J mouse model of glaucoma. Systemic gene delivery of EPO-R76E protected both RGC somata and axons from degeneration and also resulted in a functional rescue of the visual pathway. Again the hematocrit was maintained within healthy limits (Sullivan et al., 2011b). The successful application of such non-hematopoietic EPO variants in various disease models seems promising for a potential use of these proteins to treat slowly progressing degenerative retinal diseases in human patients in the future.

9. Conclusions and future directions

Proper retinal function requires high levels of energy and a strong metabolic tissue activity. Impaired oxygenation and reduced nutrient supply during retinal pathologies may thus contribute to the progression of many if not the majority of retinal degenerative diseases. While the contribution of reduced oxygen and nutrient levels to pathological vessel growth in PDR and ROP has been long established, it is becoming evident that they are also involved in the etiology of AMD, glaucoma and potentially other retinal diseases. Understanding how ischemia and hypoxia influence disease induction and/or progression, and how retinal cells respond to the stressful condition of reduced oxygen tension and insufficient nourishment is essential for the characterization of disease mechanisms. Knowledge of the cellular and molecular components involved in the tissue response to such conditions provides the basis for the identification of new molecular targets to interfere with disease progression. In recent years it has become increasingly evident that the molecular VHL-HIF axis is central not only to normal retinal development including formation of the vascular plexi but also to irreversible pathological changes such as neovascularization. The latter usually requires prolonged and sustained stimulation of the molecular response to reduced oxygen levels and does normally not occur after a transient short-term activation of the hypoxia response system. Quite the contrary, experimental paradigms using such short-term ischemic or hypoxic exposures can even precondition the tissue and prepare the cells to successfully cope with a subsequent stress. IPC and HP have demonstrated their neuroprotective potential and have led to the identification of molecules that are attractive to be explored from a therapeutic point of view. Among those, locally produced EPO might be one of the most prominent and promising molecules that deserve deeper investigation with respect to both, its physiological role in the retina as well as its therapeutic potential for the treatment of human blinding diseases. It is of relevance that the neuroprotective activity of EPO can be separated from its erythropoietic function making the molecule even more appealing for the exploration of its therapeutical use in neurodegenerative diseases. Since the molecular response to IPC and HP is not restricted to few individual molecules like EPO but involves a multitude of factors, it is expected that a thorough investigation of the respective transcriptomes, proteomes, secretomes and metabolomes may identify additional signaling pathways and molecules which could be targeted by pharmacological approaches to preserve tissue integrity and function, and thus vision for human patients.

Acknowledgments

Research in the area of hypoxia and how it influences the retina is extensive and evolves rapidly. A large number of excellent publications amply documents the vast influence of oxygen, of oxygen-regulated processes and of the molecular mediators of the hypoxic tissue response on retinal development, physiology and pathophysiology. All of these publications strongly contribute to our understanding of the biological relevance of retinal hypoxia in health and disease. Since we probably failed to cite all relevant results and articles, we wish to apologize to all of our colleagues whose contributions we missed during the process of writing this review.

We would like to thank Marijana Samardzija and Sarah Willcox for fruitful discussions and critical comments on the manuscript. Supported by the Swiss National Science Foundation (31003A_133043).

References

Abcouwer, S.F., Lin, C.M., Wolpert, E.B., Shanmugam, S., Schaefer, E.W., Freeman, W.M., Barber, A.J., Antonetti, D.A., 2010. Effects of ischemic preconditioning and bevacizumab on apoptosis and vascular permeability following retinal ischemia-reperfusion injury. Invest. Ophthalmol. Vis. Sci. 51, 5920–5933.

Abu El-Asrar, A.M., Missotten, L., Geboes, K., 2007. Expression of hypoxia-inducible factor-1alpha and the protein products of its target genes in diabetic fibrovascular epiretinal membranes. Br. J. Ophthalmol. 91, 822–826.

Adachi, K., Kashii, S., Masai, H., Ueda, M., Morizane, C., Kaneda, K., Kume, T., Akaike, A., Honda, Y., 1998. Mechanism of the pathogenesis of glutamate neurotoxicity in retinal ischemia. Graefes Arch. Clin. Exp. Ophthalmol. 236, 766–774.

Adachi, M., Takahashi, K., Nishikawa, M., Miki, H., Uyama, M., 1996. High intraocular pressure-induced ischemia and reperfusion injury in the optic nerve and retina in rats. Graefes Arch. Clin. Exp. Ophthalmol. 234, 445–451.

Adams, D.L., Horton, J.C., 2003. The representation of retinal blood vessels in primate striate cortex. J. Neurosci. 23, 5984–5997.

Adams, M.K., Simpson, J.A., Aung, K.Z., Makeyeva, G.A., Giles, G.G., English, D.R., Hopper, J., Guymer, R.H., Baird, P.N., Robman, L.D., 2011. Abdominal obesity and age-related macular degeneration. Am. J. Epidemiol. 173, 1246–1255.

Addison, D.J., Garner, A., Ashton, N., 1970. Degeneration of intramural pericytes in diabetic retinopathy. Br. Med. J. 1, 264–266.

Agnello, D., Bigini, P., Villa, P., Mennini, T., Cerami, A., Brines, M.L., Ghezzi, P., 2002. Erythropoietin exerts an anti-inflammatory effect on the CNS in a model of experimental autoimmune encephalomyelitis. Brain Res. 952, 128–134.

Aher, S., Ohlsson, A., 2006. Late erythropoietin for preventing red blood cell transfusion in preterm and/or low birth weight infants. Cochrane Database Syst. Rev. 3, CD004868.

Ahmed, J., Braun, R.D., Dunn, R.J., Linsenmeier, R.A., 1993. Oxygen distribution in the macaque retina. Invest. Ophthalmol. Vis. Sci. 34, 516–521.

Aiello, L.P., 2005. Angiogenic pathways in diabetic retinopathy. N. Engl. J. Med. 353, 839–841.

Aiello, L.P., Avery, R.L., Arrigg, P.G., Keyt, B.A., Jampel, H.D., Shah, S.T., Pasquale, L.R., Thieme, H., Iwamoto, M.A., Park, J.E., et al., 1994. Vascular endothelial growth factor in ocular fluid of patients with diabetic retinopathy and other retinal disorders. N. Engl. J. Med. 331, 1480–1487.

Aiello, L.P., Pierce, E.A., Foley, E.D., Takagi, H., Chen, H., Riddle, L., Ferrara, N., King, G.L., Smith, L.E., 1995. Suppression of retinal neovascularization in vivo by inhibition of vascular endothelial growth factor (VEGF) using soluble VEGF-receptor chimeric proteins. Proc. Natl. Acad. Sci. U.S.A. 92, 10457–10461.

Aitola, M.H., Pelto-Huikko, M.T., 2003. Expression of Arnt and Arnt2 mRNA in developing murine tissues. J. Histochem. Cytochem. 51, 41–54.

Aizu, Y., Katayama, H., Takahama, S., Hu, J., Nakagawa, H., Oyanagi, K., 2003. Topical instillation of ciliary neurotrophic factor inhibits retinal degeneration in streptozotocin-induced diabetic rats. Neuroreport 14, 2067–2071.

Alder, V.A., Cringle, S.J., Constable, I.J., 1983. The retinal oxygen profile in cats. Invest. Ophthalmol. Vis. Sci. 24, 30–36.

Alon, T., Hemo, I., Itin, A., Pe'er, J., Stone, J., Keshet, E., 1995. Vascular endothelial growth factor acts as a survival factor for newly formed retinal vessels and has implications for retinopathy of prematurity. Nat Med 1, 1024–1028.

Ames, A.R., 1992. Energy requirements of CNS cells as related to their function and to their vulnerability to ischemia: a commentary based on studies on retina. Can. J. Physiol. Pharmacol. 70 (Suppl.), S158–S164.

Ames, A.R., Li, Y.Y., Heher, E.C., Kimble, C.R., 1992. Energy metabolism of rabbit retina as related to function: high cost of Na+ transport. J. Neurosci. 12, 840–853.

Amin, R., Puklin, J.E., Frank, R.N., 1994. Growth factor localization in choroidal neovascular membranes of age-related macular degeneration. Invest. Ophthalmol. Vis. Sci. 35, 3178–3188.

Anagnostou, A., Lee, E.S., Kessimian, N., Levinson, R., Steiner, M., 1990. Erythropoietin has a mitogenic and positive chemotactic effect on endothelial cells. Proc. Natl. Acad. Sci. U.S.A. 87, 5978–5982.

Anderson, B.J., Saltzman, H.A., 1964. Retinal oxygen utilization measured by hyperbaric blackout. Arch. Ophthalmol. 72, 792–795.

Arany, Z., Huang, L.E., Eckner, R., Bhattacharya, S., Jiang, C., Goldberg, M.A., Bunn, H.F., Livingston, D.M., 1996. An essential role for p300/CBP in the cellular response to hypoxia. Proc. Natl. Acad. Sci. U.S.A. 93, 12969–12973.

Ashton, N., 1966. Oxygen and the growth and development of retinal vessels. In vivo and in vitro studies. The XX Francis I. Proctor Lecture. Am. J. Ophthalmol. 62, 412–435.

Ashton, N., Ward, B., Serpell, G., 1954. Effect of oxygen on developing retinal vessels with particular reference to the problem of retrolental fibroplasia. Br. J. Ophthalmol. 38, 397–432.

Bai, Y., Ma, J.X., Guo, J., Wang, J., Zhu, M., Chen, Y., Le, Y.Z., 2009. Muller cell-derived VEGF is a significant contributor to retinal neovascularization. J. Pathol. 219, 446–454.

Banasiak, K.J., Xia, Y., Haddad, G.G., 2000. Mechanisms underlying hypoxia-induced neuronal apoptosis. Prog. Neurobiol. 62, 215–249.

Bantignies, F., Cavalli, G., 2006. Cellular memory and dynamic regulation of polycomb group proteins. Curr. Opin. Cell Biol. 18, 275–283.

Barber, A.J., 2003. A new view of diabetic retinopathy: a neurodegenerative disease of the eye. Prog. Neuropsychopharmacol. Biol. Psychiatry 27, 283–290.

Barber, A.J., Gardner, T.W., Abcouwer, S.F., 2011. The significance of vascular and neural apoptosis to the pathology of diabetic retinopathy. Invest. Ophthalmol. Vis. Sci. 52, 1156–1163.

Bardos, J.I., Ashcroft, M., 2005. Negative and positive regulation of HIF-1: a complex network. Biochim. Biophys. Acta 1755, 107–120.

Becerra, S.P., 1997. Structure-function studies on PEDF. A noninhibitory serpin with neurotrophic activity. Adv. Exp. Med. Biol. 425, 223–237.

Bek, T., 2009. Inner retinal ischaemia: current understanding and needs for further investigations. Acta Ophthalmol. 87, 362–367.

Beleslin-Cokic, B.B., Cokic, V.P., Yu, X., Weksler, B.B., Schechter, A.N., Noguchi, C.T., 2004. Erythropoietin and hypoxia stimulate erythropoietin receptor and nitric oxide production by endothelial cells. Blood 104, 2073–2080.

Bell, E.F., Klein, J.M., 1994. Comments on Oxygen Toxicity and Retinopathy (ROP) in the Premature Infant. Iowa Neonatology Handbook: Pulmonary. University of Iowa, Children's Hospital, Department of Pediatrics.

Bentmann, A., Schmidt, M., Reuss, S., Wolfrum, U., Hankeln, T., Burmester, T., 2005. Divergent distribution in vascular and avascular mammalian retinae links neuroglobin to cellular respiration. J. Biol. Chem. 280, 20660–20665.

Bernaudin, M., Marti, H.H., Roussel, S., Divoux, D., Nouvelot, A., MacKenzie, E.T., Petit, E., 1999. A potential role for erythropoietin in focal permanent cerebral ischemia in mice. J. Cereb. Blood Flow Metab. 19, 643–651.

Birol, G., Wang, S., Budzynski, E., Wangsa-Wirawan, N.D., Linsenmeier, R.A., 2007. Oxygen distribution and consumption in the macaque retina. Am. J. Physiol. Heart Circ. Physiol. 293, H1696–H1704.

Blake, T.J., Jenkins, B.J., D'Andrea, R.J., Gonda, T.J., 2002. Functional cross-talk between cytokine receptors revealed by activating mutations in the extracellular domain of the beta-subunit of the GM-CSF receptor. J. Leukoc. Biol. 72, 1246–1255.

Block, F., Schwarz, M., 1998. The b-wave of the electroretinogram as an index of retinal ischemia. Gen. Pharmacol. 30, 281–287.

Bocker-Meffert, S., Rosenstiel, P., Rohl, C., Warneke, N., Held-Feindt, J., Sievers, J., Lucius, R., 2002. Erythropoietin and VEGF promote neural outgrowth from retinal explants in postnatal rats. Invest. Ophthalmol. Vis. Sci 43, 2021–2026.

Bondurant, M.C., Koury, M.J., 1986. Anemia induces accumulation of erythropoietin mRNA in the kidney and liver. Mol. Cell Biol. 6, 2731–2733.

Boulton, M., Dontsov, A., Jarvis-Evans, J., Ostrovsky, M., Svistunenko, D., 1993. Lipofuscin is a photoinducible free radical generator. J. Photochem. Photobiol. B 19, 201–204.

Bracken, C.P., Fedele, A.O., Linke, S., Balrak, W., Lisy, K., Whitelaw, M.L., Peet, D.J., 2006. Cell-specific regulation of hypoxia-inducible factor (HIF)-1alpha and HIF-2alpha stabilization and transactivation in a graded oxygen environment. J. Biol. Chem. 281, 22575–22585.

Bressler, N.M., Bressler, S.B., Fine, S.L., 1988. Age-related macular degeneration. Surv. Ophthalmol. 32, 375–413.

Brines, M., Cerami, A., 2005. Emerging biological roles for erythropoietin in the nervous system. Nat. Rev. Neurosci. 6, 484–494.

Brines, M., Grasso, G., Fiordaliso, F., Sfacteria, A., Ghezzi, P., Fratelli, M., Latini, R., Xie, Q.W., Smart, J., Su-Rick, C.J., Pobre, E., Diaz, D., Gomez, D., Hand, C., Coleman, T., Cerami, A., 2004. Erythropoietin mediates tissue protection through an erythropoietin and common beta-subunit heteroreceptor. Proc. Natl. Acad. Sci. U.S.A. 101, 14907–14912.

Brines, M., Patel, N.S., Villa, P., Brines, C., Mennini, T., De Paola, M., Erbayraktar, Z., Erbayraktar, S., Sepodes, B., Thiemermann, C., Ghezzi, P., Yamin, M., Hand, C.C., Xie, Q.W., Coleman, T., Cerami, A., 2008. Nonerythropoietic, tissue-protective peptides derived from the tertiary structure of erythropoietin. Proc. Natl. Acad. Sci. U.S.A. 105, 10925–10930.

Brines, M.L., Ghezzi, P., Keenan, S., Agnello, D., de Lanerolle, N.C., Cerami, C., Itri, L.M., Cerami, A., 2000. Erythropoietin crosses the blood–brain barrier to protect against experimental brain injury. Proc. Natl. Acad. Sci. U.S.A. 97, 10526–10531.

Bringmann, A., Pannicke, T., Grosche, J., Francke, M., Wiedemann, P., Skatchkov, S.N., Osborne, N.N., Reichenbach, A., 2006. Muller cells in the healthy and diseased retina. Prog. Retin. Eye Res. 25, 397–424.

Bringmann, A., Reichenbach, A., Wiedemann, P., 2004. Pathomechanisms of cystoid macular edema. Ophthalmic Res. 36, 241–249.

Brown, D.M., Kaiser, P.K., Michels, M., Soubrane, G., Heier, J.S., Kim, R.Y., Sy, J.P., Schneider, S., 2006a. Ranibizumab versus verteporfin for neovascular age-related macular degeneration. N. Engl. J. Med. 355, 1432–1444.

Brown, M.S., Baron, A.E., France, E.K., Hamman, R.F., 2006b. Association between higher cumulative doses of recombinant erythropoietin and risk for retinopathy of prematurity. J. AAPOS 10, 143–149.

Brown, J.L., Hill, J.H., Burke, R.E., 1957. The effect of hypoxia on the human electroretinogram. Am. J. Ophthalmol. 44, 57–67.

Buckner, F.S., Eschbach, J.W., Haley, N.R., Davidson, R.C., Adamson, J.W., 1990. Hypertension following erythropoietin therapy in anemic hemodialysis patients. Am. J. Hypertens. 3, 947–955.

Bui, B.V., Kalloniatis, M., Vingrys, A.J., 2003. The contribution of glycolytic and oxidative pathways to retinal photoreceptor function. Invest. Ophthalmol. Vis. Sci. 44, 2708–2715.

Burns, P.A., Wilson, D.J., 2003. Angiogenesis mediated by metabolites is dependent on vascular endothelial growth factor (VEGF). Angiogenesis 6, 73–77.

Bursell, S.E., Clermont, A.C., Kinsley, B.T., Simonson, D.C., Aiello, L.M., Wolpert, H.A., 1996. Retinal blood flow changes in patients with insulin-dependent diabetes mellitus and no diabetic retinopathy. Invest. Ophthalmol. Vis. Sci. 37, 886–897.

Bush, R.A., Williams, T.P., 1991. The effect of unilateral optic nerve section on retinal light damage in rats. Exp. Eye Res. 52, 139–153.
Butler, J.M., Guthrie, S.M., Koc, M., Afzal, A., Caballero, S., Brooks, H.L., Mames, R.N., Segal, M.S., Grant, M.B., Scott, E.W., 2005. SDF-1 is both necessary and sufficient to promote proliferative retinopathy. J. Clin. Invest. 115, 86–93.
Buttery, R.G., Hinrichsen, C.F., Weller, W.L., Haight, J.R., 1991. How thick should a retina be? A comparative study of mammalian species with and without intraretinal vasculature. Vision Res. 31, 169–187.
Byfield, G., Budd, S., Hartnett, M.E., 2009. The role of supplemental oxygen and JAK/STAT signaling in intravitreous neovascularization in a ROP rat model. Invest. Ophthalmol. Vis. Sci. 50, 3360–3365.
Cai, J., Boulton, M., 2002. The pathogenesis of diabetic retinopathy: old concepts and new questions. Eye (Lond.) 16, 242–260.
Cai, Z., Manalo, D.J., Wei, G., Rodriguez, E.R., Fox-Talbot, K., Lu, H., Zweier, J.L., Semenza, G.L., 2003. Hearts from rodents exposed to intermittent hypoxia or erythropoietin are protected against ischemia-reperfusion injury. Circulation 108, 79–85.
Cairns, J.E., 1959. Normal development of the hyaloid and retinal vessels in the rat. Br. J. Ophthalmol. 43, 385–393.
Calapai, G., Marciano, M.C., Corica, F., Allegra, A., Parisi, A., Frisina, N., Caputi, A.P., Buemi, M., 2000. Erythropoietin protects against brain ischemic injury by inhibition of nitric oxide formation. Eur. J. Pharmacol. 401, 349–356.
Campa, C., Harding, S.P., 2011. Anti-VEGF compounds in the treatment of neovascular age related macular degeneration. Curr. Drug Targets 12, 173–181.
Campana, W.M., Misasi, R., O'Brien, J.S., 1998. Identification of a neurotrophic sequence in erythropoietin. Int. J. Mol. Med. 1, 235–241.
Caprara, C., Thiersch, M., Lange, C., Joly, S., Samardzija, M., Grimm, C., 2011. HIF1A is essential for the development of the intermediate plexus of the retinal vasculature. Invest. Ophthalmol. Vis. Sci. 52, 2109–2117.
Carmeliet, P., Dor, Y., Herbert, J.M., Fukumura, D., Brusselmans, K., Dewerchin, M., Neeman, M., Bono, F., Abramovitch, R., Maxwell, P., Koch, C.J., Ratcliffe, P., Moons, L., Jain, R.K., Collen, D., Keshert, E., 1998. Role of HIF-1alpha in hypoxia-mediated apoptosis, cell proliferation and tumour angiogenesis. Nature 394, 485–490.
Carmeliet, P., Moons, L., Luttun, A., Vincenti, V., Compernolle, V., De Mol, M., Wu, Y., Bono, F., Devy, L., Beck, H., Scholz, D., Acker, T., DiPalma, T., Dewerchin, M., Noel, A., Stalmans, I., Barra, A., Blacher, S., Vandendriessche, T., Ponten, A., Eriksson, U., Plate, K.H., Foidart, J.M., Schaper, W., Charnock-Jones, D.S., Hicklin, D.J., Herbert, J.M., Collen, D., Persico, M.G., 2001. Synergism between vascular endothelial growth factor and placental growth factor contributes to angiogenesis and plasma extravasation in pathological conditions. Nat. Med. 7, 575–583.
Carmo, A., Cunha-Vaz, J.G., Carvalho, A.P., Lopes, M.C., 2000. Effect of cyclosporin-A on the blood–retinal barrier permeability in streptozotocin-induced diabetes. Mediators Inflamm. 9, 243–248.
Cash, T.P., Pan, Y., Simon, M.C., 2007. Reactive oxygen species and cellular oxygen sensing. Free Radic. Biol. Med. 43, 1219–1225.
Casson, R.J., Wood, J.P., Melena, J., Chidlow, G., Osborne, N.N., 2003. The effect of ischemic preconditioning on light-induced photoreceptor injury. Invest. Ophthalmol. Vis. Sci. 44, 1348–1354.
Celik, M., Gokmen, N., Erbayraktar, S., Akhisaroglu, M., Konakc, S., Ulukus, C., Genc, S., Genc, K., Sagiroglu, E., Cerami, A., Brines, M., 2002. Erythropoietin prevents motor neuron apoptosis and neurologic disability in experimental spinal cord ischemic injury. Proc. Natl. Acad. Sci. U.S.A. 99, 2258–2263.
Chan-Ling, T., Gock, B., Stone, J., 1995. The effect of oxygen on vasoformative cell division. Evidence that 'physiological hypoxia' is the stimulus for normal retinal vasculogenesis. Invest. Ophthalmol. Vis. Sci. 36, 1201–1214.
Chan-Ling, T., Tout, S., Hollander, H., Stone, J., 1992. Vascular changes and their mechanisms in the feline model of retinopathy of prematurity. Invest. Ophthalmol. Vis. Sci. 33, 2128–2147.
Chan, C.C., Collins, A.B., Chew, E.Y., 2007. Molecular pathology of eyes with von Hippel–Lindau (VHL) Disease: a review. Retina 27, 1–7.
Chang, B., Hawes, N.L., Pardue, M.T., German, A.M., Hurd, R.E., Davisson, M.T., Nusinowitz, S., Rengarajan, K., Boyd, A.P., Sidney, S.S., Phillips, M.J., Stewart, R.E., Chaudhury, R., Nickerson, J.M., Heckenlively, J.R., Boatright, J.H., 2007. Two mouse retinal degenerations caused by missense mutations in the beta-subunit of rod cGMP phosphodiesterase gene. Vision Res. 47, 624–633.
Chase, J., 1982. The evolution of retinal vascularization in mammals. A comparison of vascular and avascular retinae. Ophthalmology 89, 1518–1525.
Chavez, J.C., Baranova, O., Lin, J., Pichiule, P., 2006. The transcriptional activator hypoxia inducible factor 2 (HIF-2/EPAS-1) regulates the oxygen-dependent expression of erythropoietin in cortical astrocytes. J. Neurosci. 26, 9471–9481.
Check, E., 2005. A crucial test. Nat. Med. 11, 243–244.
Chen, J., Connor, K.M., Aderman, C.M., Smith, L.E., 2008. Erythropoietin deficiency decreases vascular stability in mice. J. Clin. Invest. 118, 526–533.
Chen, J., Connor, K.M., Aderman, C.M., Willett, K.L., Aspegren, O.P., Smith, L.E., 2009. Suppression of retinal neovascularization by erythropoietin siRNA in a mouse model of proliferative retinopathy. Invest. Ophthalmol. Vis. Sci. 50, 1329–1335.
Cheon, E.W., Park, C.H., Kang, S.S., Cho, G.J., Yoo, J.M., Song, J.K., Choi, W.S., 2002. Nitric oxide synthase expression in the transient ischemic rat retina: neuroprotection of betaxolol. Neurosci. Lett. 330, 265–269.
Cherniack, N.S., 2004. Oxygen sensing: applications in humans. J. Appl. Physiol. 96, 352–358.
Chilov, D., Camenisch, G., Kvietikova, I., Ziegler, U., Gassmann, M., Wenger, R.H., 1999. Induction and nuclear translocation of hypoxia-inducible factor-1 (HIF-1): heterodimerization with ARNT is not necessary for nuclear accumulation of HIF-1alpha. J. Cell Sci. 112, 1203–1212.
Chong, Z.Z., Kang, J.Q., Maiese, K., 2003. Apaf-1, Bcl-xL, cytochrome c, and caspase-9 form the critical elements for cerebral vascular protection by erythropoietin. J. Cereb. Blood Flow Metab. 23, 320–330.
Chung, H., Lee, H., Lamoke, F., Hrushesky, W.J., Wood, P.A., Jahng, W.J., 2009. Neuroprotective role of erythropoietin by antiapoptosis in the retina. J. Neurosci. Res. 87, 2365–2374.
Chung, H.S., Harris, A., Evans, D.W., Kagemann, L., Garzozi, H.J., Martin, B., 1999. Vascular aspects in the pathophysiology of glaucomatous optic neuropathy. Surv. Ophthalmol. 43 (Suppl. 1), S43–S50.
Cioffi, G.A., Sullivan, P., 1999. The effect of chronic ischemia on the primate optic nerve. Eur. J. Ophthalmol. 9 (Suppl. 1), S34–S36.
Ciulla, T.A., Harris, A., Chung, H.S., Danis, R.P., Kagemann, L., McNulty, L., Pratt, L.M., Martin, B.J., 1999. Color Doppler imaging discloses reduced ocular blood flow velocities in nonexudative age-related macular degeneration. Am. J. Ophthalmol. 128, 75–80.
Colella, P., Iodice, C., Di Vicino, U., Annunziata, I., Surace, E.M., Auricchio, A., 2011. Non-erythropoietic erythropoietin derivatives protect from light-induced and genetic photoreceptor degeneration. Hum. Mol. Genet. 20, 2251–2262.
Coleman, K., Fitzgerald, D., Eustace, P., Bouchier-Hayes, D., 1990. Electroretinography, retinal ischaemia and carotid artery disease. Eur. J. Vasc. Surg. 4, 569–573.
Coleman, T.R., Westenfelder, C., Togel, F.E., Yang, Y., Hu, Z., Swenson, L., Leuvenink, H.G., Ploeg, R.J., d'Uscio, L.V., Katusic, Z.S., Ghezzi, P., Zanetti, A., Kaushansky, K., Fox, N.E., Cerami, A., Brines, M., 2006. Cytoprotective doses of erythropoietin or carbamylated erythropoietin have markedly different procoagulant and vasoactive activities. Proc. Natl. Acad. Sci. U.S.A. 103, 5965–5970.
Compernolle, V., Brusselmans, K., Acker, T., Hoet, P., Tjwa, M., Beck, H., Plaisance, S., Dor, Y., Keshet, E., Lupu, F., Nemery, B., Dewerchin, M., Van Veldhoven, P., Plate, K., Moons, L., Collen, D., Carmeliet, P., 2002. Loss of HIF-2alpha and inhibition of VEGF impair fetal lung maturation, whereas treatment with VEGF prevents fatal respiratory distress in premature mice. Nat. Med. 8, 702–710.
Connolly, S.E., Hores, T.A., Smith, L.E., D'Amore, P.A., 1988. Characterization of vascular development in the mouse retina. Microvasc. Res. 36, 275–290.
Cowden, K.D., Simon, M.C., 2002. The bHLH/PAS factor MOP3 does not participate in hypoxia responses. Biochem. Biophys. Res. Commun. 290, 1228–1236.
Cringle, S.J., Yu, D.Y., Alder, V.A., 1991. Intraretinal oxygen tension in the rat eye. Graefes Arch. Clin. Exp. Ophthalmol. 229, 574–577.
Cringle, S.J., Yu, D.Y., Yu, P.K., Su, E.N., 2002. Intraretinal oxygen consumption in the rat in vivo. Invest. Ophthalmol. Vis Sci. 43, 1922–1927.
Cruickshanks, K.J., Klein, R., Klein, B.E., 1993. Sunlight and age-related macular degeneration. The Beaver Dam Eye Study. Arch. Ophthalmol. 111, 514–518.
Cumurcu, T., Bulut, Y., Demir, H.D., Yenisehirli, G., 2007. Aqueous humor erythropoietin levels in patients with primary open-angle glaucoma. J. Glaucoma 16, 645–648.
Dai, C., Chung, I.J., Krantz, S.B., 2005. Increased erythropoiesis in polycythemia vera is associated with increased erythroid progenitor proliferation and increased phosphorylation of Akt/PKB. Exp. Hematol. 33, 152–158.
Dame, C., Fahnenstich, H., Freitag, P., Hofmann, D., Abdul-Nour, T., Bartmann, P., Fandrey, J., 1998. Erythropoietin mRNA expression in human fetal and neonatal tissue. Blood 92, 3218–3225.
Dayan, F., Roux, D., Brahimi-Horn, M.C., Pouyssegur, J., Mazure, N.M., 2006. The oxygen sensor factor-inhibiting hypoxia-inducible factor-1 controls expression of distinct genes through the bifunctional transcriptional character of hypoxia-inducible factor-1alpha. Cancer Res. 66, 3688–3698.
de Gooyer, T.E., Stevenson, K.A., Humphries, P., Simpson, D.A., Gardiner, T.A., Stitt, A.W., 2006. Retinopathy is reduced during experimental diabetes in a mouse model of outer retinal degeneration. Invest. Ophthalmol. Vis. Sci. 47, 5561–5568.
Dehne, N., Brune, B., 2009. HIF-1 in the inflammatory microenvironment. Exp. Cell. Res. 315, 1791–1797.
Dick, E., Miller, R.F., 1978. Light-evoked potassium activity in mudpuppy retina: its relationship to the b-wave of the electroretinogram. Brain Res. 154, 388–394.
Digicaylioglu, M., Garden, G., Timberlake, S., Fletcher, L., Lipton, S.A., 2004. Acute neuroprotective synergy of erythropoietin and insulin-like growth factor I. Proc. Natl. Acad. Sci. U.S.A. 101, 9855–9860.
Digicaylioglu, M., Lipton, S.A., 2001. Erythropoietin-mediated neuroprotection involves cross-talk between Jak2 and NF-kappaB signalling cascades. Nature 412, 641–647.
Ding, J., Ding, N., Wang, N., Lu, Q., Lu, N., Yang, D., Bu, X., Han, S., Li, J., 2009. Determination of conventional protein kinase C isoforms involved in high intraocular pressure-induced retinal ischemic preconditioning of rats. Vision Res. 49, 315–321.
Ding, K., Scortegagna, M., Seaman, R., Birch, D.G., Garcia, J.A., 2005. Retinal disease in mice lacking hypoxia-inducible transcription factor-2alpha. Invest. Ophthalmol. Vis. Sci. 46, 1010–1016.
Dioum, E.M., Clarke, S.L., Ding, K., Repa, J.J., Garcia, J.A., 2008. HIF-2alpha-haploinsufficient mice have blunted retinal neovascularization due to impaired expression of a proangiogenic gene battery. Invest. Ophthalmol. Vis. Sci. 49, 2714–2720.
Doonan, F., Donovan, M., Cotter, T.G., 2003. Caspase-independent photoreceptor apoptosis in mouse models of retinal degeneration. J. Neurosci. 23, 5723–5731.
Dorrell, M.I., Aguilar, E., Friedlander, M., 2002. Retinal vascular development is mediated by endothelial filopodia, a preexisting astrocytic template and specific R-cadherin adhesion. Invest. Ophthalmol. Vis. Sci. 43, 3500–3510.

Dreher, Z., Robinson, S.R., Distler, C., 1992. Muller cells in vascular and avascular retinae: a survey of seven mammals. J. Comp. Neurol. 323, 59–80.
Dreixler, J.C., Barone, F.C., Shaikh, A.R., Du, E., Roth, S., 2009a. Mitogen-activated protein kinase p38alpha and retinal ischemic preconditioning. Exp. Eye Res. 89, 782–790.
Dreixler, J.C., Hagevik, S., Hemmert, J.W., Shaikh, A.R., Rosenbaum, D.M., Roth, S., 2009b. Involvement of erythropoietin in retinal ischemic preconditioning. Anesthesiology 110, 774–780.
Dreixler, J.C., Hemmert, J.W., Shenoy, S.K., Shen, Y., Lee, H.T., Shaikh, A.R., Rosenbaum, D.M., Roth, S., 2009c. The role of Akt/protein kinase B subtypes in retinal ischemic preconditioning. Exp. Eye Res. 88, 512–521.
Duan, L.J., Takeda, K., Fong, G.H., 2011. Prolyl hydroxylase domain protein 2 (PHD2) mediates oxygen-induced retinopathy in neonatal mice. Am. J. Pathol. 178, 1881–1890.
Dumont, I., Hou, X., Hardy, P., Peri, K.G., Beauchamp, M., Najarian, T., Molotchnikoff, S., Varma, D.R., Chemtob, S., 1999. Developmental regulation of endothelial nitric oxide synthase in cerebral vessels of newborn pig by prostaglandin E(2). J. Pharmacol. Exp. Ther. 291, 627–633.
Dumont, I., Peri, K.G., Hardy, P., Hou, X., Martinez-Bermudez, A.K., Molotchnikoff, S., Varma, D.R., Chemtob, S., 1998. PGE2, via EP3 receptors, regulates brain nitric oxide synthase in the perinatal period. Am. J. Physiol. 275, R1812–R1821.
Dyer, M.A., Donovan, S.L., Zhang, J., Gray, J., Ortiz, A., Tenney, R., Kong, J., Allikmets, R., Sohocki, M.M., 2004. Retinal degeneration in Aipl1-deficient mice: a new genetic model of Leber congenital amaurosis. Brain Res. Mol. Brain Res. 132, 208–220.
Edwards, A.O., Ritter, R.R., Abel, K.J., Manning, A., Panhuysen, C., Farrer, L.A., 2005. Complement factor H polymorphism and age-related macular degeneration. Science 308, 421–424.
Ehrenreich, H., Hasselblatt, M., Dembowski, C., Cepek, L., Lewczuk, P., Stiefel, M., Rustenbeck, H.H., Breiter, N., Jacob, S., Knerlich, F., Bohn, M., Poser, W., Ruther, E., Kochen, M., Gefeller, O., Gleiter, C., Wessel, T.C., De Ryck, M., Itri, L., Prange, H., Cerami, A., Brines, M., Siren, A.L., 2002. Erythropoietin therapy for acute stroke is both safe and beneficial. Mol. Med. 8, 495–505.
Ehrenreich, H., Weissenborn, K., Prange, H., Schneider, D., Weimar, C., Wartenberg, K., Schellinger, P.D., Bohn, M., Becker, H., Wegrzyn, M., Jahnig, P., Herrmann, M., Knauth, M., Bahr, M., Heide, W., Wagner, A., Schwab, S., Reichmann, H., Schwendemann, G., Dengler, R., Kastrup, A., Bartels, C., 2009. Recombinant human erythropoietin in the treatment of acute ischemic stroke. Stroke 40, e647–e656.
el-Asrar, A.M., Morse, P.H., Maimone, D., Torczynski, E., Reder, A.T., 1992. MK-801 protects retinal neurons from hypoxia and the toxicity of glutamate and aspartate. Invest. Ophthalmol. Vis. Sci. 33, 3463–3468.
Elliott, S., Busse, L., Bass, M.B., Lu, H., Sarosi, I., Sinclair, A.M., Spahr, C., Um, M., Van, G., Begley, C.G., 2006. Anti-Epo receptor antibodies do not predict Epo receptor expression. Blood 107, 1892–1895.
Ema, M., Taya, S., Yokotani, N., Sogawa, K., Matsuda, Y., Fujii-Kuriyama, Y., 1997. A novel bHLH-PAS factor with close sequence similarity to hypoxia-inducible factor 1alpha regulates the VEGF expression and is potentially involved in lung and vascular development. Proc. Natl. Acad. Sci. U.S.A. 94, 4273–4278.
Engerman, R.L., Kern, T.S., 1995. Retinopathy in animal models of diabetes. Diabetes Metab. Rev. 11, 109–120.
Engerman, R.L., Meyer, R.K., 1965. Development of retinal vasculature in rats. Am. J. Ophthalmol. 60, 628–641.
Epstein, A.C., Gleadle, J.M., McNeill, L.A., Hewitson, K.S., O'Rourke, J., Mole, D.R., Mukherji, M., Metzen, E., Wilson, M.I., Dhanda, A., Tian, Y.M., Masson, N., Hamilton, D.L., Jaakkola, P., Barstead, R., Hodgkin, J., Maxwell, P.H., Pugh, C.W., Schofield, C.J., Ratcliffe, P.J., 2001. C. elegans EGL-9 and mammalian homologs define a family of dioxygenases that regulate HIF by prolyl hydroxylation. Cell 107, 43–54.
Erbayraktar, S., Grasso, G., Sfacteria, A., Xie, Q.W., Coleman, T., Kreilgaard, M., Torup, L., Sager, T., Erbayraktar, Z., Gokmen, N., Yilmaz, O., Ghezzi, P., Villa, P., Fratelli, M., Casagrande, S., Leist, M., Helboe, L., Gerwein, J., Christensen, S., Geist, M.A., Pedersen, L.O., Cerami-Hand, C., Wuerth, J.P., Cerami, A., Brines, M., 2003. Asialoerythropoietin is a nonerythropoietic cytokine with broad neuroprotective activity in vivo. Proc. Natl. Acad. Sci. U.S.A. 100, 6741–6746.
Ettaiche, M., Heurteaux, C., Blondeau, N., Borsotto, M., Tinel, N., Lazdunski, M., 2001. ATP-sensitive potassium channels (K(ATP)) in retina: a key role for delayed ischemic tolerance. Brain Res. 890, 118–129.
Faktorovich, E.G., Steinberg, R.H., Yasumura, D., Matthes, M.T., LaVail, M.M., 1990. Photoreceptor degeneration in inherited retinal dystrophy delayed by basic fibroblast growth factor. Nature 347, 83–86.
Faktorovich, E.G., Steinberg, R.H., Yasumura, D., Matthes, M.T., LaVail, M.M., 1992. Basic fibroblast growth factor and local injury protect photoreceptors from light damage in the rat. J. Neurosci. 12, 3554–3567.
Fandrey, J., 2004. Oxygen-dependent and tissue-specific regulation of erythropoietin gene expression. Am. J. Physiol. Regul. Integr. Comp. Physiol. 286, R977–R988.
Feeney, S.A., Simpson, D.A., Gardiner, T.A., Boyle, C., Jamison, P., Stitt, A.W., 2003. Role of vascular endothelial growth factor and placental growth factors during retinal vascular development and hyaloid regression. Invest. Ophthalmol. Vis. Sci. 44, 839–847.
Feke, G.T., Buzney, S.M., Ogasawara, H., Fujio, N., Goger, D.G., Spack, N.P., Gabbay, K.H., 1994. Retinal circulatory abnormalities in type 1 diabetes. Invest. Ophthalmol. Vis. Sci. 35, 2968–2975.
Feke, G.T., Zuckerman, R., Green, G.J., Weiter, J.J., 1983. Response of human retinal blood flow to light and dark. Invest. Ophthalmol. Vis. Sci. 24, 136–141.
Ferrara, N., Damico, L., Shams, N., Lowman, H., Kim, R., 2006. Development of ranibizumab, an anti-vascular endothelial growth factor antigen binding fragment, as therapy for neovascular age-related macular degeneration. Retina 26, 859–870.
Ferris, F.L.r., Davis, M.D., Aiello, L.M., 1999. Treatment of diabetic retinopathy. N. Engl. J. Med. 341, 667–678.
Flamme, I., Frohlich, T., von Reutern, M., Kappel, A., Damert, A., Risau, W., 1997. HRF, a putative basic helix-loop-helix-PAS-domain transcription factor is closely related to hypoxia-inducible factor-1 alpha and developmentally expressed in blood vessels. Mech. Dev. 63, 51–60.
Flammer, J., 1994. The vascular concept of glaucoma. Surv. Ophthalmol. 38 (Suppl.), S3–S6.
Flammer, J., Mozaffarieh, M., 2008. Autoregulation, a balancing act between supply and demand. Can. J. Ophthalmol. 43, 317–321.
Flammer, J., Orgul, S., Costa, V.P., Orzalesi, N., Krieglstein, G.K., Serra, L.M., Renard, J.P., Stefansson, E., 2002. The impact of ocular blood flow in glaucoma. Prog. Retin. Eye Res. 21, 359–393.
Fletcher, E.L., Phipps, J.A., Ward, M.M., Puthussery, T., Wilkinson-Berka, J.L., 2007. Neuronal and glial cell abnormality as predictors of progression of diabetic retinopathy. Curr. Pharm. Des. 13, 2699–2712.
Fliesler, S.J., Richards, M.J., Miller, C.Y., Mckay, S., Winkler, B.S., 1997. In vitro metabolic competence of the frog retina: effects of glucose and oxygen deprivation. Exp. Eye Res. 64, 683–692.
Flynn, J.T., Bancalari, E., Snyder, E.S., Goldberg, R.N., Feuer, W., Cassady, J., Schiffman, J., Feldman, H.I., Bachynski, B., Buckley, E., et al., 1991. A cohort study of transcutaneous oxygen tension and the incidence and severity of retinopathy of prematurity. Trans. Am. Ophthalmol. Soc. 89, 77–92. discussion 92–95.
Forooghian, F., Razavi, R., Timms, L., 2007. Hypoxia-inducible factor expression in human RPE cells. Br. J. Ophthalmol. 91, 1406–1410.
Frede, S., Stockmann, C., Winning, S., Freitag, P., Fandrey, J., 2009. Hypoxia-inducible factor (HIF) 1alpha accumulation and HIF target gene expression are impaired after induction of endotoxin tolerance. J. Immunol. 182, 6470–6476.
Fried, W., Kilbridge, T., Krantz, S., McDonald, T.P., Lange, R.D., 1969. Studies on extrarenal erythropoietin. J. Lab. Clin. Med. 73, 244–248.
Friedlander, M., Brooks, P.C., Shaffer, R.W., Kincaid, C.M., Varner, J.A., Cheresh, D.A., 1995. Definition of two angiogenic pathways by distinct alpha v integrins. Science 270, 1500–1502.
Friedman, E., Krupsky, S., Lane, A.M., Oak, S.S., Friedman, E.S., Egan, K., Gragoudas, E.S., 1995. Ocular blood flow velocity in age-related macular degeneration. Ophthalmology 102, 640–646.
Friedman, E., Smith, T.R., Kuwabara, T., 1964. Retinal microcirculation in vivo. Invest. Ophthalmol. 3, 217–226.
Friedman, E.A., L'Esperance, F.A., Brown, C.D., Berman, D.H., 2003. Treating azotemia-induced anemia with erythropoietin improves diabetic eye disease. Kidney Int. Suppl., S57–S63.
Fruttiger, M., 2007. Development of the retinal vasculature. Angiogenesis 10, 77–88.
Fruttiger, M., Calver, A.R., Kruger, W.H., Mudhar, H.S., Michalovich, D., Takakura, N., Nishikawa, S., Richardson, W.D., 1996. PDGF mediates a neuron-astrocyte interaction in the developing retina. Neuron 17, 1117–1131.
Fu, Q.L., Wu, W., Wang, H., Li, X., Lee, V.W., So, K.F., 2008. Up-regulated endogenous erythropoietin/erythropoietin receptor system and exogenous erythropoietin rescue retinal ganglion cells after chronic ocular hypertension. Cell. Mol. Neurobiol. 28, 317–329.
Funatsu, H., Yamashita, H., Shimizu, E., Kojima, R., Hori, S., 2001. Relationship between vascular endothelial growth factor and interleukin-6 in diabetic retinopathy. Retina 21, 469–477.
Garcia-Ramirez, M., Hernandez, C., Simo, R., 2008. Expression of erythropoietin and its receptor in the human retina: a comparative study of diabetic and nondiabetic subjects. Diabetes Care 31, 1189–1194.
Gardner, T.W., Antonetti, D.A., Barber, A.J., LaNoue, K.F., Levison, S.W., 2002. Diabetic retinopathy: more than meets the eye. Surv. Ophthalmol. 47 (Suppl. 2), S253–S262.
Gariano, R.F., 2010. Special features of human retinal angiogenesis. Eye (Lond.) 24, 401–407.
Gariano, R.F., Gardner, T.W., 2005. Retinal angiogenesis in development and disease. Nature 438, 960–966.
Gariano, R.F., Iruela-Arispe, M.L., Hendrickson, A.E., 1994. Vascular development in primate retina: comparison of laminar plexus formation in monkey and human. Invest. Ophthalmol. Vis. Sci. 35, 3442–3455.
Gehrs, K.M., Anderson, D.H., Johnson, L.V., Hageman, G.S., 2006. Age-related macular degeneration–emerging pathogenetic and therapeutic concepts. Ann. Med. 38, 450–471.
Genc, S., Kuralay, F., Genc, K., Akhisaroglu, M., Fadiloglu, S., Yorukoglu, K., Fadiloglu, M., Gure, A., 2001. Erythropoietin exerts neuroprotection in 1-methyl-4-phenyl-1,2,3,6-tetrahydropyridine-treated C57/BL mice via increasing nitric oxide production. Neurosci. Lett. 298, 139–141.
Gerhardt, H., Golding, M., Fruttiger, M., Ruhrberg, C., Lundkvist, A., Abramsson, A., Jeltsch, M., Mitchell, C., Alitalo, K., Shima, D., Betsholtz, C., 2003. VEGF guides angiogenic sprouting utilizing endothelial tip cell filopodia. J. Cell. Biol. 161, 1163–1177.
Ghiardi, G.J., Gidday, J.M., Roth, S., 1999. The purine nucleoside adenosine in retinal ischemia-reperfusion injury. Vision Res. 39, 2519–2535.
Gidday, J.M., Park, T.S., 1993. Microcirculatory responses to adenosine in the newborn pig retina. Pediatr. Res. 33, 620–627.
Gilbert, C., Rahi, J., Eckstein, M., O'Sullivan, J., Foster, A., 1997. Retinopathy of prematurity in middle-income countries. Lancet 350, 12–14.

Gorio, A., Gokmen, N., Erbayraktar, S., Yilmaz, O., Madaschi, L., Cichetti, C., Di Giulio, A.M., Vardar, E., Cerami, A., Brines, M., 2002. Recombinant human erythropoietin counteracts secondary injury and markedly enhances neurological recovery from experimental spinal cord trauma. Proc. Natl. Acad. Sci. U.S.A. 99, 9450–9455.

Gradin, K., McGuire, J., Wenger, R.H., Kvietikova, I., Fhitelaw, M.L., Toftgard, R., Tora, L., Gassmann, M., Poellinger, L., 1996. Functional interference between hypoxia and dioxin signal transduction pathways: competition for recruitment of the Arnt transcription factor. Mol. Cell. Biol. 16, 5221–5231.

Graymore, C., 1959. Metabolism of the developing retina. I. Aerobic and anaerobic glycolysis in the developing rat retina. Br. J. Ophthalmol. 43, 34–39.

Graymore, C., 1960. Metabolism of the developing retina. III. Respiration in the developing normal rat retina and the effect of an inherited degeneration of the retinal neuroepithelium. Br. J. Ophthalmol. 44, 363–369.

Green, W.R., Wilson, D.J., 1986. Choroidal neovascularization. Ophthalmology 93, 1169–1176.

Grimm, C., Hermann, D.M., Bogdanova, A., Hotop, S., Kilic, U., Wenzel, A., Kilic, E., Gassmann, M., 2005. Neuroprotection by hypoxic preconditioning: HIF-1 and erythropoietin protect from retinal degeneration. Semin. Cell. Dev. Biol. 16, 531–538.

Grimm, C., Wenzel, A., Groszer, M., Mayser, H., Seeliger, M., Samardzija, M., Bauer, C., Gassmann, M., Reme, C.E., 2002. HIF-1-induced erythropoietin in the hypoxic retina protects against light-induced retinal degeneration. Nat. Med. 8, 718–724.

Grimm, C., Wenzel, A., Stanescu, D., Samardzija, M., Hotop, S., Groszer, M., Naash, M., Gassmann, M., Reme, C., 2004. Constitutive overexpression of human erythropoietin protects the mouse retina against induced but not inherited retinal degeneration. J. Neurosci. 24, 5651–5658.

Gross, R.L., Hensley, S.H., Gao, F., Wu, S.M., 1999. Retinal ganglion cell dysfunction induced by hypoxia and glutamate: potential neuroprotective effects of beta-blockers. Surv. Ophthalmol. 43 (Suppl. 1), S162–S170.

Grossniklaus, H.E., Kang, S.J., Berglin, L., 2010. Animal models of choroidal and retinal neovascularization. Prog. Retin. Eye Res. 29, 500–519.

Grossniklaus, H.E., Ling, J.X., Wallace, T.M., Dithmar, S., Lawson, D.H., Cohen, C., Elner, V.M., Elner, S.G., Sternberg, P.J., 2002. Macrophage and retinal pigment epithelium expression of angiogenic cytokines in choroidal neovascularization. Mol. Vis. 8, 119–126.

Gruber, M., Hu, C.J., Johnson, R.S., Brown, E.J., Keith, B., Simon, M.C., 2007. Acute postnatal ablation of Hif-2 results in anemia. Proc. Natl. Acad. Sci. U.S.A. 104, 2301.

Grunwald, J.E., Hariprasad, S.M., DuPont, J., Maguire, M.G., Fine, S.L., Brucker, A.J., Maguire, A.M., Ho, A.C., 1998. Foveolar choroidal blood flow in age-related macular degeneration. Invest. Ophthalmol. Vis. Sci. 39, 385–390.

Grunwald, J.E., Metelitsina, T.I., Dupont, J.C., Ying, G.S., Maguire, M.G., 2005. Reduced foveolar choroidal blood flow in eyes with increasing AMD severity. Invest. Ophthalmol. Vis. Sci. 46, 1033–1038.

Gu, Y.Z., Moran, S.M., Hogenesch, J.B., Wartman, L., Bradfield, C.A., 1998. Molecular characterization and chromosomal localization of a third alpha-class hypoxia inducible factor subunit, HIF3alpha. Gene Exp. 7, 205–213.

Gurevich, L., Slaughter, M.M., 1993. Comparison of the waveforms of the ON bipolar neuron and the b-wave of the electroretinogram. Vision Res. 33, 2431–2435.

Hackett, S.F., Wiegand, S., Yancopoulos, G., Campochiaro, P.A., 2002. Angiopoietin-2 plays an important role in retinal angiogenesis. J. Cell. Physiol. 192, 182–187.

Hangai, M., Miyamoto, K., Hiroi, K., Tujikawa, A., Ogura, Y., Honda, Y., Yoshimura, N., 1999. Roles of constitutive nitric oxide synthase in postischemic rat retina. Invest. Ophthalmol. Vis. Sci. 40, 450–458.

Hao, W., Wenzel, A., Obin, M.S., Chen, C.K., Brill, E., Krasnoperova, N.V., Eversole-Cire, P., Kleyner, Y., Taylor, A., Simon, M.I., Grimm, C., Reme, C.E., Lem, J., 2002. Evidence for two apoptotic pathways in light-induced retinal degeneration. Nat. Genet. 32, 254–260.

Hara, S., Hamada, J., Kobayashi, C., Kondo, Y., Imura, N., 2001. Expression and characterization of hypoxia-inducible factor (HIF)-3alpha in human kidney: suppression of HIF-mediated gene expression by HIF-3alpha. Biochem. Biophys. Res. Commun. 287, 808–813.

Harada, C., Nakamura, K., Namekata, K., Okumura, A., Mitamura, Y., Iizuka, Y., Kashiwagi, K., Yoshida, K., Ohno, S., Matsuzawa, A., Tanaka, K., Ichijo, H., Harada, T., 2006. Role of apoptosis signal-regulating kinase 1 in stress-induced neural cell apoptosis in vivo. Am. J. Pathol. 168, 261–269.

Hardy, P., Abran, D., Li, D.Y., Fernandez, H., Varma, D.R., Chemtob, S., 1994. Free radicals in retinal and choroidal blood flow autoregulation in the piglet: interaction with prostaglandins. Invest. Ophthalmol. Vis. Sci. 35, 580–591.

Hardy, P., Dumont, I., Bhattacharya, M., Hou, X., Lachapelle, P., Varma, D.R., Chemtob, S., 2000. Oxidants, nitric oxide and prostanoids in the developing ocular vasculature: a basis for ischemic retinopathy. Cardiovasc. Res. 47, 489–509.

Harris, A., Chung, H.S., Ciulla, T.A., Kagemann, L., 1999. Progress in measurement of ocular blood flow and relevance to our understanding of glaucoma and age-related macular degeneration. Prog. Retin. Eye Res. 18, 669–687.

Harris, A.L., 2002. Hypoxia—a key regulatory factor in tumour growth. Nat. Rev. Cancer 2, 38–47.

Haugh, L.M., Linsenmeier, R.A., Goldstick, T.K., 1990. Mathematical models of the spatial distribution of retinal oxygen tension and consumption, including changes upon illumination. Ann. Biomed. Eng. 18, 19–36.

Hayreh, S.S., 2005. Prevalent misconceptions about acute retinal vascular occlusive disorders. Prog. Retin. Eye Res. 24, 493–519.

Hayreh, S.S., 2011. Acute retinal arterial occlusive disorders. Prog. Retin. Eye Res. 30, 359–394.

Hayreh, S.S., Weingeist, T.A., 1980. Experimental occlusion of the central artery of the retina. IV: Retinal tolerance time to acute ischaemia. Br. J. Ophthalmol. 64, 818–825.

Hayreh, S.S., Zimmerman, M.B., 2007. Fundus changes in central retinal artery occlusion. Retina 27, 276–289.

Heidbreder, M., Frohlich, F., Johren, O., Dendorfer, A., Qadri, F., Dominiak, P., 2003. Hypoxia rapidly activates HIF-3alpha mRNA expression. FASEB J. 17, 1541–1543.

Hellstrom, A., Perruzzi, C., Ju, M., Engstrom, E., Hard, A.L., Liu, J.L., Albertsson-Wikland, K., Carlsson, B., Niklasson, A., Sjodell, L., LeRoith, D., Senger, D.R., Smith, L.E., 2001. Low IGF-I suppresses VEGF-survival signaling in retinal endothelial cells: direct correlation with clinical retinopathy of prematurity. Proc. Natl. Acad. Sci. U.S.A. 98, 5804–5808.

Hernandez, C., Fonollosa, A., Garcia-Ramirez, M., Higuera, M., Catalan, R., Miralles, A., Garcia-Arumi, J., Simo, R., 2006. Erythropoietin is expressed in the human retina and it is highly elevated in the vitreous fluid of patients with diabetic macular edema. Diabetes Care 29, 2028–2033.

Hewitson, K.S., McNeill, L.A., Elkins, J.M., Schofield, C.J., 2003. The role of iron and 2-oxoglutarate oxygenases in signalling. Biochem. Soc. Trans. 31, 510–515.

Hirose, K., Morita, M., Ema, M., Mimura, J., Hamada, H., Fujii, H., Saijo, Y., Gotoh, O., Sogawa, K., Fujii-Kuriyama, Y., 1996. cDNA cloning and tissue-specific expression of a novel basic helix-loop-helix/PAS factor (Arnt2) with close sequence similarity to the aryl hydrocarbon receptor nuclear translocator (Arnt). Mol. Cell. Biol. 16, 1706–1713.

Hogenesch, J.B., Gu, Y.Z., Jain, S., Bradfield, C.A., 1998. The basic-helix-loop-helix-PAS orphan MOP3 forms transcriptionally active complexes with circadian and hypoxia factors. Proc. Natl. Acad. Sci. U.S.A. 95, 5474–5479.

Hogenesch, J.B., Gu, Y.Z., Moran, S.M., Shimomura, K., Radcliffe, L.A., Takahashi, J.S., Bradfield, C.A., 2000. The basic helix-loop-helix-PAS protein MOP9 is a brain-specific heterodimeric partner of circadian and hypoxia factors. J. Neurosci. 20, RC83.

Holekamp, N.M., Shui, Y.B., Beebe, D., 2006. Lower intraocular oxygen tension in diabetic patients: possible contribution to decreased incidence of nuclear sclerotic cataract. Am. J. Ophthalmol. 141, 1027–1032.

Holmquist-Mengelbier, L., Fredlund, E., Lofstedt, T., Noguera, R., Navarro, S., Nilsson, H., Pietras, A., Vallon-Christersson, J., Borg, A., Gradin, K., Poellinger, L., Pahlman, S., 2006. Recruitment of HIF-1alpha and HIF-2alpha to common target genes is differentially regulated in neuroblastoma: HIF-2alpha promotes an aggressive phenotype. Cancer Cell 10, 413–423.

Hu, C.J., Sataur, A., Wang, L., Chen, H., Simon, M.C., 2007. The N-terminal transactivation domain confers target gene specificity of hypoxia-inducible factors HIF-1alpha and HIF-2alpha. Mol. Biol. Cell. 18, 4528–4542.

Hu, C.J., Wang, L.Y., Chodosh, L.A., Keith, B., Simon, M.C., 2003. Differential roles of hypoxia-inducible factor 1alpha (HIF-1alpha) and HIF-2alpha in hypoxic gene regulation. Mol. Cell. Biol. 23, 9361–9374.

Hu, L.M., Luo, Y., Zhang, J., Lei, X., Shen, J., Wu, Y., Qin, M., Unver, Y.B., Zhong, Y., Xu, G.T., Li, W., 2011. EPO reduces reactive gliosis and stimulates neurotrophin expression in Muller cells. Front. Biosci. (Elite Ed.) 3, 1541–1555.

Huang, L.E., Arany, Z., Livingston, D.M., Bunn, H.F., 1996. Activation of hypoxia-inducible transcription factor depends primarily upon redox-sensitive stabilization of its alpha subunit. J. Biol. Chem. 271, 32253–32259.

Husain, S., Liou, G.I., Crosson, C.E., 2011. Opioid receptor activation: suppression of ischemia/reperfusion-induced production of TNF-{alpha} in the retina. Invest. Ophthalmol. Vis. Sci. 52, 2577–2583.

Husain, S., Potter, D.E., Crosson, C.E., 2009. Opioid receptor-activation: retina protected from ischemic injury. Invest. Ophthalmol. Vis. Sci. 50, 3853–3859.

Ikeda, M., Nomura, M., 1997. cDNA cloning and tissue-specific expression of a novel basic helix-loop-helix/PAS protein (BMAL1) and identification of alternatively spliced variants with alternative translation initiation site usage. Biochem. Biophys. Res. Commun. 233, 258–264.

Inomata, Y., Hirata, A., Takahashi, E., Kawaji, T., Fukushima, M., Tanihara, H., 2004. Elevated erythropoietin in vitreous with ischemic retinal diseases. Neuroreport 15, 877–879.

Inoue, Y., Yanagi, Y., Matsuura, K., Takahashi, H., Tamaki, Y., Araie, M., 2007. Expression of hypoxia-inducible factor 1alpha and 2alpha in choroidal neovascular membranes associated with age-related macular degeneration. Br. J. Ophthalmol. 91, 1720–1721.

Jaakkola, P., Mole, D.R., Tian, Y.M., Wilson, M.I., Gielbert, J., Gaskell, S.J., Kriegsheim, A., Hebestreit, H.F., Mukherji, M., Schofield, C.J., Maxwell, P.H., Pugh, C.W., Ratcliffe, P.J., 2001. Targeting of HIF-alpha to the von Hippel–Lindau ubiquitylation complex by O2-regulated prolyl hydroxylation. Science 292, 468–472.

Jain, S., Maltepe, E., Lu, M.M., Simon, C., Bradfield, C.A., 1998. Expression of ARNT, ARNT2, HIF1 alpha, HIF2 alpha and Ah receptor mRNAs in the developing mouse. Mech. Dev. 73, 117–123.

Janaky, M., Grosz, A., Toth, E., Benedek, K., Benedek, G., 2007. Hypobaric hypoxia reduces the amplitude of oscillatory potentials in the human ERG. Doc. Ophthalmol. 114, 45–51.

Jelkmann, W., 2004. Molecular biology of erythropoietin. Intern. Med. 43, 649–659.

Jiang, B., Bezhadian, M.A., Caldwell, R.B., 1995. Astrocytes modulate retinal vasculogenesis: effects on endothelial cell differentiation. Glia 15, 1–10.

Jiang, B.H., Rue, E., Wang, G.L., Roe, R., Semenza, G.L., 1996. Dimerization, DNA binding, and transactivation properties of hypoxia-inducible factor 1. J. Biol. Chem. 271, 17771–17778.

Jiang, J., Xia, X.B., Xu, H.Z., Xiong, Y., Song, W.T., Xiong, S.Q., Li, Y., 2009. Inhibition of retinal neovascularization by gene transfer of small interfering RNA targeting HIF-1alpha and VEGF. J. Cell. Physiol. 218, 66–74.

Jo, N., Mailhos, C., Ju, M., Cheung, E., Bradley, J., Nishijima, K., Robinson, G.S., Adamis, A.P., Shima, D.T., 2006. Inhibition of platelet-derived growth factor B signaling enhances the efficacy of anti-vascular endothelial growth factor therapy in multiple models of ocular neovascularization. Am. J. Pathol. 168, 2036–2053.

Jo, N., Wu, G.S., Rao, N.A., 2003. Upregulation of chemokine expression in the retinal vasculature in ischemia-reperfusion injury. Invest. Ophthalmol. Vis. Sci. 44, 4054–4060.

Joussen, A.M., Poulaki, V., Le, M.L., Koizumi, K., Esser, C., Janicki, H., Schraermeyer, U., Kociok, N., Fauser, S., Kirchhof, B., Kern, T.S., Adamis, A.P., 2004. A central role for inflammation in the pathogenesis of diabetic retinopathy. FASEB J. 18, 1450–1452.

Joussen, A.M., Poulaki, V., Mitsiades, N., Kirchhof, B., Koizumi, K., Dohmen, S., Adamis, A.P., 2002. Nonsteroidal anti-inflammatory drugs prevent early diabetic retinopathy via TNF-alpha suppression. FASEB J. 16, 438–440.

Jubinsky, P.T., Krijanovski, O.I., Nathan, D.G., Tavernier, J., Sieff, C.A., 1997. The beta chain of the interleukin-3 receptor functionally associates with the erythropoietin receptor. Blood 90, 1867–1873.

Junk, A.K., Mammis, A., Savitz, S.I., Singh, M., Roth, S., Malhotra, S., Rosenbaum, P.S., Cerami, A., Brines, M., Rosenbaum, D.M., 2002. Erythropoietin administration protects retinal neurons from acute ischemia-reperfusion injury. Proc. Natl. Acad. Sci. U.S.A. 99, 10659–10664.

Juul, S.E., Yachnis, A.T., Christensen, R.D., 1998. Tissue distribution of erythropoietin and erythropoietin receptor in the developing human fetus. Early Hum. Dev. 52, 235–249.

Kallio, P.J., Pongratz, I., Gradin, K., McGuire, J., Poellinger, L., 1997. Activation of hypoxia-inducible factor 1alpha: posttranscriptional regulation and conformational change by recruitment of the Arnt transcription factor. Proc. Natl. Acad. Sci. U.S.A. 94, 5667–5672.

Kamphuis, W., Dijk, F., Bergen, A.A., 2007a. Ischemic preconditioning alters the pattern of gene expression changes in response to full retinal ischemia. Mol. Vis. 13, 1892–1901.

Kamphuis, W., Dijk, F., van Soest, S., Bergen, A.A., 2007b. Global gene expression profiling of ischemic preconditioning in the rat retina. Mol. Vis. 13, 1020–1030.

Katsura, Y., Okano, T., Matsuno, K., Osako, M., Kure, M., Watanabe, T., Iwaki, Y., Noritake, M., Kosano, H., Nishigori, H., Matsuoka, T., 2005. Erythropoietin is highly elevated in vitreous fluid of patients with proliferative diabetic retinopathy. Diabetes Care 28, 2252–2254.

Kaur, C., Foulds, W.S., Ling, E.A., 2008. Blood–retinal barrier in hypoxic ischaemic conditions: basic concepts, clinical features and management. Prog. Retin. Eye Res. 27, 622–647.

Kaur, C., Sivakumar, V., Foulds, W.S., 2006. Early response of neurons and glial cells to hypoxia in the retina. Invest. Ophthalmol. Vis. Sci. 47, 1126–1141.

Kaur, C., Sivakumar, V., Foulds, W.S., Luu, C.D., Ling, E.A., 2009. Cellular and vascular changes in the retina of neonatal rats after an acute exposure to hypoxia. Invest. Ophthalmol. Vis. Sci. 50, 5364–5374.

Kawakami, M., Iwasaki, S., Sato, K., Takahashi, M., 2000. Erythropoietin inhibits calcium-induced neurotransmitter release from clonal neuronal cells. Biochem. Biophys. Res. Commun. 279, 293–297.

Kawakami, M., Sekiguchi, M., Sato, K., Kozaki, S., Takahashi, M., 2001. Erythropoietin receptor-mediated inhibition of exocytotic glutamate release confers neuroprotection during chemical ischemia. J. Biol. Chem. 276, 39469–39475.

Keith, B., Adelman, D.M., Simon, M.C., 2001. Targeted mutation of the murine arylhydrocarbon receptor nuclear translocator 2 (Arnt2) gene reveals partial redundancy with Arnt. Proc. Natl. Acad. Sci. U.S.A. 98, 6692–6697.

Kelly, B.D., Hackett, S.F., Hirota, K., Oshima, Y., Cai, Z., Berg-Dixon, S., Rowan, A., Yan, Z., Campochiaro, P.A., Semenza, G.L., 2003. Cell type-specific regulation of angiogenic growth factor gene expression and induction of angiogenesis in nonischemic tissue by a constitutively active form of hypoxia-inducible factor 1. Circ. Res. 93, 1074–1081.

Kergoat, H., Herard, M.E., Lemay, M., 2006. RGC sensitivity to mild systemic hypoxia. Invest. Ophthalmol. Vis. Sci. 47, 5423–5427.

Kermorvant-Duchemin, E., Sennlaub, F., Sirinyan, M., Brault, S., Andelfinger, G., Kooli, A., Germain, S., Ong, H., d'Orleans-Juste, P., Gobeil, F.J., Zhu, T., Boisvert, C., Hardy, P., Jain, K., Falck, J.R., Balazy, M., Chemtob, S., 2005. Trans-arachidonic acids generated during nitrative stress induce a thrombospondin-1-dependent microvascular degeneration. Nat. Med. 11, 1339–1345.

Khandhadia, S., Lotery, A., 2010. Oxidation and age-related macular degeneration: insights from molecular biology. Expert. Rev. Mol. Med. 12, e34.

Kilic, E., Kilic, U., Soliz, J., Bassetti, C.L., Gassmann, M., Hermann, D.M., 2005a. Brain-derived erythropoietin protects from focal cerebral ischemia by dual activation of ERK-1/-2 and Akt pathways. FASEB J. 19, 2026–2028.

Kilic, U., Kilic, E., Soliz, J., Bassetti, C.I., Gassmann, M., Hermann, D.M., 2005b. Erythropoietin protects from axotomy-induced degeneration of retinal ganglion cells by activating ERK-1/-2. FASEB J. 19, 249–251.

Kim, D.H., Kim, J.A., Choi, J.S., Joo, C.K., 2002. Activation of caspase-3 during degeneration of the outer nuclear layer in the rd mouse retina. Ophthalmic. Res. 34, 150–157.

Kim, J.H., Yu, Y.S., Kim, K.W., Kim, J.H., 2010. Impaired retinal vascular development in anencephalic human fetus. Histochem. Cell. Biol. 134, 277–284.

Kimble, E.A., Svoboda, R.A., Ostroy, S.E., 1980. Oxygen consumption and ATP changes of the vertebrate photoreceptor. Exp. Eye Res. 31, 271–288.

King, C.E., Rodger, J., Bartlett, C., Esmaili, T., Dunlop, S.A., Beazley, L.D., 2007. Erythropoietin is both neuroprotective and neuroregenerative following optic nerve transection. Exp. Neurol. 205, 48–55.

Kinose, F., Roscilli, G., Lamartina, S., Anderson, K.D., Bonelli, F., Spence, S.G., Ciliberto, G., Vogt, T.F., Holder, D.J., Toniatti, C., Thut, C.J., 2005. Inhibition of retinal and choroidal neovascularization by a novel KDR kinase inhibitor. Mol. Vis. 11, 366–373.

Kirino, T., Tsujita, Y., Tamura, A., 1991. Induced tolerance to ischemia in gerbil hippocampal neurons. J. Cereb. Blood. Flow. Metab. 11, 299–307.

Kirkeby, A., van Beek, J., Nielsen, J., Leist, M., Helboe, L., 2007. Functional and immunochemical characterisation of different antibodies against the erythropoietin receptor. J. Neurosci. Methods 164, 50–58.

Kitano, S., Morgan, J., Caprioli, J., 1996. Hypoxic and excitotoxic damage to cultured rat retinal ganglion cells. Exp. Eye Res. 63, 105–112.

Klein, R., Cruickshanks, K.J., Nash, S.D., Krantz, E.M., Javier Nieto, F., Huang, G.H., Pankow, J.S., Klein, B.E., 2010. The prevalence of age-related macular degeneration and associated risk factors. Arch. Ophthalmol. 128, 750–758.

Kline, R.P., Ripps, H., Dowling, J.E., 1978. Generation of b-wave currents in the skate retina. Proc. Natl. Acad. Sci. U.S.A. 75, 5727–5731.

Ko, M.K., Kay, E.P., 2002. Differential interaction of molecular chaperones with procollagen I and type IV collagen in corneal endothelial cells. Mol. Vis. 8, 1–9.

Kobayashi, M., Kuroiwa, T., Shimokawa, R., Okeda, R., Tokoro, T., 2000. Nitric oxide synthase expression in ischemic rat retinas. Jpn. J. Ophthalmol. 44, 235–244.

Kocur, I., Resnikoff, S., 2002. Visual impairment and blindness in Europe and their prevention. Br. J. Ophthalmol. 86, 716–722.

Kohner, E.M., Hamilton, A.M., Saunders, S.J., Sutcliffe, B.A., Bulpitt, C.J., 1975. The retinal blood flow in diabetes. Diabetologia 11, 27–33.

Koshimura, K., Murakami, Y., Sohmiya, M., Tanaka, J., Kato, Y., 1999. Effects of erythropoietin on neuronal activity. J. Neurochem. 72, 2565–2572.

Kotch, L.E., Iyer, N.V., Laughner, E., Semenza, G.L., 1999. Defective vascularization of HIF-1alpha-null embryos is not associated with VEGF deficiency but with mesenchymal cell death. Dev. Biol. 209, 254–267.

Kretz, A., Happold, C.J., Marticke, J.K., Isenmann, S., 2005. Erythropoietin promotes regeneration of adult CNS neurons via Jak2/Stat3 and PI3K/AKT pathway activation. Mol. Cell. Neurosci. 29, 569–579.

Kretz, A., Kugler, S., Happold, C., Bahr, M., Isenmann, S., 2004. Excess Bcl-XL increases the intrinsic growth potential of adult CNS neurons in vitro. Mol. Cell. Neurosci. 26, 63–74.

Krugel, K., Wurm, A., Linnertz, R., Pannicke, T., Wiedemann, P., Reichenbach, A., Bringmann, A., 2010. Erythropoietin inhibits osmotic swelling of retinal glial cells by Janus kinase- and extracellular signal-regulated kinases1/2-mediated release of vascular endothelial growth factor. Neuroscience 165, 1147–1158.

Kubota, Y., Hirashima, M., Kishi, K., Stewart, C.L., Suda, T., 2008. Leukemia inhibitory factor regulates microvessel density by modulating oxygen-dependent VEGF expression in mice. J. Clin. Invest. 118, 2393–2403.

Kumral, A., Gonenc, S., Acikgoz, O., Sonmez, A., Genc, K., Yilmaz, O., Gokmen, N., Duman, N., Ozkan, H., 2005. Erythropoietin increases glutathione peroxidase enzyme activity and decreases lipid peroxidation levels in hypoxic-ischemic brain injury in neonatal rats. Biol. Neonate. 87, 15–18.

Kurihara, T., Kubota, Y., Ozawa, Y., Takubo, K., Noda, K., Simon, M.C., Johnson, R.S., Suematsu, M., Tsubota, K., Ishida, S., Goda, N., Suda, T., Okano, H., 2010. von Hippel–Lindau protein regulates transition from the fetal to the adult circulatory system in retina. Development 137, 1563–1571.

Kurz, T., Terman, A., Gustafsson, B., Brunk, U.T., 2008. Lysosomes and oxidative stress in aging and apoptosis. Biochim. Biophys. Acta 1780, 1291–1303.

Kvanta, A., Algvere, P.V., Berglin, L., Seregard, S., 1996. Subfoveal fibrovascular membranes in age-related macular degeneration express vascular endothelial growth factor. Invest. Ophthalmol. Vis. Sci. 37, 1929–1934.

Lafuente, M.P., Villegas-Perez, M.P., Mayor, S., Aguilera, M.E., Miralles de Imperial, J., Vidal-Sanz, M., 2002. Neuroprotective effects of brimonidine against transient ischemia-induced retinal ganglion cell death: a dose response in vivo study. Exp. Eye Res. 74, 181–189.

Lagreze, W.A., Feltgen, N., Bach, M., Jehle, T., 2009. Feasibility of intravitreal erythropoietin injections in humans. Br. J. Ophthalmol. 93, 1667–1671.

Lahdenranta, J., Pasqualini, R., Schlingemann, R.O., Hagedorn, M., Stallcup, W.B., Bucana, C.D., Sidman, R.L., Arap, W., 2001. An anti-angiogenic state in mice and humans with retinal photoreceptor cell degeneration. Proc. Natl. Acad. Sci. U.S.A. 98, 10368–10373.

Lando, D., Peet, D.J., Gorman, J.J., Whelan, D.A., Whitelaw, M.L., Bruick, R.K., 2002a. FIH-1 is an asparaginyl hydroxylase enzyme that regulates the transcriptional activity of hypoxia-inducible factor. Genes Dev. 16, 1466–1471.

Lando, D., Peet, D.J., Whelan, D.A., Gorman, J.J., Whitelaw, M.L., 2002b. Asparagine hydroxylation of the HIF transactivation domain a hypoxic switch. Science 295, 858–861.

Lange, C., Caprara, C., Tanimoto, N., Beck, S., Huber, G., Samardzija, M., Seeliger, M., Grimm, C., 2011a. Retina-specific activation of a sustained hypoxia-like response leads to severe retinal degeneration and loss of vision. Neurobiol. Dis. 41, 119–130.

Lange, C., Heynen, S.R., Tanimoto, N., Thiersch, M., Le, Y.Z., Meneau, I., Seeliger, M.W., Samardzija, M., Caprara, C., Grimm, C., 2011b. Normoxic activation of hypoxia inducible factors in photoreceptors provides transient protection against light induced retinal degeneration. Invest. Ophthalmol. Vis. Sci. 52, 5872–5880.

Lange, C.A., Stavrakas, P., Luhmann, U.F., de Silva, D.J., Ali, R.R., Gregor, Z.J., Bainbridge, J.W., 2011c. Intraocular oxygen distribution in advanced proliferative diabetic retinopathy. Am. J. Ophthalmol. 152, 406–412. e3.

Larsen, A.K., Osborne, N.N., 1996. Involvement of adenosine in retinal ischemia. Studies on the rat. Invest. Ophthalmol. Vis. Sci. 37, 2603–2611.

Lasne, F., Martin, L., de Ceaurriz, J., Larcher, T., Moullier, P., Chenuaud, P., 2004. "Genetic Doping" with erythropoietin cDNA in primate muscle is detectable. Mol. Ther. 10 (3), 409–410.

Lei, X., Zhang, J., Shen, J., Hu, L.M., Wu, Y., Mou, L., Xu, G., Li, W., Xu, G.T., 2011. EPO attenuates inflammatory cytokines by Muller cells in diabetic retinopathy. Front Biosci. (Elite Ed.) 3, 201–211.
Leist, M., Ghezzi, P., Grasso, G., Bianchi, R., Villa, P., Fratelli, M., Savino, C., Bianchi, M., Nielsen, J., Gerwien, J., Kallunki, P., Larsen, A.K., Helboe, L., Christensen, S., Pedersen, L.O., Nielsen, M., Torup, L., Sager, T., Sfacteria, A., Erbayraktar, S., Erbayraktar, Z., Gokmen, N., Yilmaz, O., Cerami-Hand, C., Xie, Q.W., Coleman, T., Cerami, A., Brines, M., 2004. Derivatives of erythropoietin that are tissue protective but not erythropoietic. Science 305, 239–242.
Lewczuk, P., Hasselblatt, M., Kamrowski-Kruck, H., Heyer, A., Unzicker, C., Siren, A.L., Ehrenreich, H., 2000. Survival of hippocampal neurons in culture upon hypoxia: effect of erythropoietin. Neuroreport 11, 3485–3488.
Li, B., Roth, S., 1999. Retinal ischemic preconditioning in the rat: requirement for adenosine and repetitive induction. Invest. Ophthalmol. Vis. Sci. 40, 1200–1216.
Li, B., Yang, C., Rosenbaum, D.M., Roth, S., 2000. Signal transduction mechanisms involved in ischemic preconditioning in the rat retina in vivo. Exp. Eye Res. 70, 755–765.
Li, W., Sinclair, S.H., Xu, G.T., 2010. Effects of intravitreal erythropoietin therapy for patients with chronic and progressive diabetic macular edema. Ophthalmic. Surg. Lasers Imag. 41, 18–25.
Li, Y., Roth, S., Laser, M., Ma, J.X., Crosson, C.E., 2003. Retinal preconditioning and the induction of heat-shock protein 27. Invest. Ophthalmol. Vis. Sci. 44, 1299–1304.
Lieth, E., Gardner, T.W., Barber, A.J., Antonetti, D.A., 2000. Retinal neurodegeneration: early pathology in diabetes. Clin. Exp. Ophthalmol. 28, 3–8.
Lim, J.I., Spee, C., Hinton, D.R., 2010. A comparison of hypoxia-inducible factor-alpha in surgically excised neovascular membranes of patients with diabetes compared with idiopathic epiretinal membranes in nondiabetic patients. Retina 30, 1472–1478.
Lin, M., Chen, Y., Jin, J., Hu, Y., Zhou, K.K., Zhu, M., Le, Y.Z., Ge, J., Johnson, R.S., Ma, J.X., 2011. Ischaemia-induced retinal neovascularisation and diabetic retinopathy in mice with conditional knockout of hypoxia-inducible factor-1 in retinal Muller cells. Diabetologia 54, 1554–1566.
Lindblom, P., Gerhardt, H., Liebner, S., Abramsson, A., Enge, M., Hellstrom, M., Backstrom, G., Fredriksson, S., Landegren, U., Nystrom, H.C., Bergstrom, G., Dejana, E., Ostman, A., Lindahl, P., Betsholtz, C., 2003. Endothelial PDGF-B retention is required for proper investment of pericytes in the microvessel wall. Genes Dev. 17, 1835–1840.
Ling, T.L., Mitrofanis, J., Stone, J., 1989. Origin of retinal astrocytes in the rat: evidence of migration from the optic nerve. J. Comp. Neurol. 286, 345–352.
Linsenmeier, R.A., 1986. Effects of light and darkness on oxygen distribution and consumption in the cat retina. J. Gen. Physiol. 88, 521–542.
Linsenmeier, R.A., Braun, R.D., McRipley, M.A., Padnick, L.B., Ahmed, J., Hatchell, D.L., McLeod, D.S., Lutty, G.A., 1998. Retinal hypoxia in long-term diabetic cats. Invest. Ophthalmol. Vis. Sci. 39, 1647–1657.
Lisy, K., Peet, D.J., 2008. Turn me on: regulating HIF transcriptional activity. Cell Death Differ. 15, 642–649.
Liu, C., Peng, M., Laties, A.M., Wen, R., 1998. Preconditioning with bright light evokes a protective response against light damage in the rat retina. J. Neurosci. 18, 1337–1344.
Liu, X.L., Zhou, R., Pan, Q.Q., Jia, X.L., Gao, W.N., Wu, J., Lin, J., Chen, J.F., 2010. Genetic inactivation of the adenosine A2A receptor attenuates pathologic but not developmental angiogenesis in the mouse retina. Invest. Ophthalmol. Vis. Sci. 51, 6625–6632.
Livnah, O., Stura, E.A., Middleton, S.A., Johnson, D.L., Jolliffe, L.K., Wilson, I.A., 1999. Crystallographic evidence for preformed dimers of erythropoietin receptor before ligand activation. Science 283, 987–990.
Loboda, A., Jozkowicz, A., Dulak, J., 2010. HIF-1 and HIF-2 transcription factors–similar but not identical. Mol. Cells 29, 435–442.
Lombardi, G., Moroni, F., Moroni, F., 1994. Glutamate receptor antagonists protect against ischemia-induced retinal damage. Eur. J. Pharmacol. 271, 489–495.
Lopes de Faria, J.B., Silva, K.C., Lopes de Faria, J.M., 2011. The contribution of hypertension to diabetic nephropathy and retinopathy: the role of inflammation and oxidative stress. Hypertens. Res. 34, 413–422.
Lopez-Barneo, J., Pardal, R., Ortega-Saenz, P., 2001. Cellular mechanism of oxygen sensing. Annu. Rev. Physiol. 63, 259–287.
Lopez, P.F., Sippy, B.D., Lambert, H.M., Thach, A.B., Hinton, D.R., 1996. Transdifferentiated retinal pigment epithelial cells are immunoreactive for vascular endothelial growth factor in surgically excised age-related macular degeneration-related choroidal neovascular membranes. Invest. Ophthalmol. Vis. Sci. 37, 855–868.
Lorenzi, M., Gerhardinger, C., 2001. Early cellular and molecular changes induced by diabetes in the retina. Diabetologia 44, 791–804.
Louzada-Junior, P., Dias, J.J., Santos, W.F., Lachat, J.J., Bradford, H.F., Coutinho-Netto, J., 1992. Glutamate release in experimental ischaemia of the retina: an approach using microdialysis. J. Neurochem. 59, 358–363.
Mahon, P.C., Hirota, K., Semenza, G.L., 2001. FIH-1: a novel protein that interacts with HIF-1alpha and VHL to mediate repression of HIF-1 transcriptional activity. Genes Dev. 15, 2675–2686.
Majmundar, A.J., Wong, W.J., Simon, M.C., 2010. Hypoxia-inducible factors and the response to hypoxic stress. Mol. Cell 40, 294–309.
Makino, Y., Cao, R., Svensson, K., Bertilsson, G., Asman, M., Tanaka, H., Cao, Y., Berkenstam, A., Poellinger, L., 2001. Inhibitory PAS domain protein is a negative regulator of hypoxia-inducible gene expression. Nature 414, 550–554.
Makino, Y., Kanopka, A., Wilson, W.J., Tanaka, H., Poellinger, L., 2002. Inhibitory PAS domain protein (IPAS) is a hypoxia-inducible splicing variant of the hypoxia-inducible factor-3alpha locus. J. Biol. Chem. 277, 32405–32408.
Maltepe, E., Keith, B., Arsham, A.M., Brorson, J.R., Simon, M.C., 2000. The role of ARNT2 in tumor angiogenesis and the neural response to hypoxia. Biochem. Biophys. Res. Commun. 273, 231–238.
Maltepe, E., Schmidt, J.V., Baunoch, D., Bradfield, C.A., Simon, M.C., 1997. Abnormal angiogenesis and responses to glucose and oxygen deprivation in mice lacking the protein ARNT. Nature 386, 403–407.
Marrero, M.B., Venema, R.C., Ma, H., Ling, B.N., Eaton, D.C., 1998. Erythropoietin receptor-operated Ca2+ channels: activation by phospholipase C-gamma 1. Kidney Int. 53, 1259–1268.
Martinez-Estrada, O.M., Rodriguez-Millan, E., Gonzalez-De Vicente, E., Reina, M., Vilaro, S., Fabre, M., 2003. Erythropoietin protects the in vitro blood–brain barrier against VEGF-induced permeability. Eur. J. Neurosci. 18, 2538–2544.
Maslim, J., Valter, K., Egensperger, R., Hollander, H., Stone, J., 1997. Tissue oxygen during a critical developmental period controls the death and survival of photoreceptors. Invest. Ophthalmol. Vis. Sci. 38, 1667–1677.
Masuda, S., Nagao, M., Takahata, K., Konishi, Y., Gallyas, F.J., Tabira, T., Sasaki, R., 1993. Functional erythropoietin receptor of the cells with neural characteristics. Comparison with receptor properties of erythroid cells. J. Biol. Chem. 268, 11208–11216.
Maxwell, P.H., Pugh, C.W., Ratcliffe, P.J., 2001. Activation of the HIF pathway in cancer. Curr. Opin. Genet. Dev. 11, 293–299.
Maxwell, P.H., Wiesener, M.S., Chang, G.W., Clifford, S.C., Vaux, E.C., Cockman, M.E., Wykoff, C.C., Pugh, C.W., Maher, E.R., Ratcliffe, P.J., 1999. The tumour suppressor protein VHL targets hypoxia-inducible factors for oxygen-dependent proteolysis. Nature 399, 271–275.
McLeod, D.S., D'Anna, S.A., Lutty, G.A., 1998. Clinical and histopathologic features of canine oxygen-induced proliferative retinopathy. Invest. Ophthalmol. Vis. Sci. 39, 1918–1932.
McNeill, L.A., Hewitson, K.S., Claridge, T.D., Seibel, J.F., Horsfall, L.E., Schofield, C.J., 2002a. Hypoxia-inducible factor asparaginyl hydroxylase (FIH-1) catalyses hydroxylation at the beta-carbon of asparagine-803. Biochem. J. 367, 571–575.
McNeill, L.A., Hewitson, K.S., Gleadle, J.M., Horsfall, L.E., Oldham, N.J., Maxwell, P.H., Pugh, C.W., Ratcliffe, P.J., Schofield, C.J., 2002b. The use of dioxygen by HIF prolyl hydroxylase (PHD1). Bioorg. Med. Chem. Lett. 12, 1547–1550.
Mervin, K., Stone, J., 2002. Regulation by oxygen of photoreceptor death in the developing and adult C57BL/6J mouse. Exp. Eye Res. 75, 715–722.
Metelitsina, T.I., Grunwald, J.E., DuPont, J.C., Ying, G.S., Brucker, A.J., Dunaief, J.L., 2008. Foveolar choroidal circulation and choroidal neovascularization in age-related macular degeneration. Invest. Ophthalmol. Vis. Sci. 49, 358–363.
Mizutani, M., Kern, T.S., Lorenzi, M., 1996. Accelerated death of retinal microvascular cells in human and experimental diabetic retinopathy. J. Clin. Invest. 97, 2883–2890.
Mokbel, T.H., Ghanem, A.A., Kishk, H., Arafa, L.F., El-Baiomy, A.A., 2010. Erythropoietin and soluble CD44 levels in patients with primary open-angle glaucoma. Clin. Exp. Ophthalmol. 38, 560–565.
Moncada, S., Higgs, A., Furchgott, R., 1997. International Union of Pharmacology Nomenclature in Nitric Oxide Research. Pharmacol. Rev. 49, 137–142.
Morello, C.M., 2007. Etiology and natural history of diabetic retinopathy: an overview. Am. J. Health Syst. Pharm. 64, S3–S7.
Morgan, J., Caprioli, J., Koseki, Y., 1999. Nitric oxide mediates excitotoxic and anoxic damage in rat retinal ganglion cells cocultured with astroglia. Arch. Ophthalmol. 117, 1524–1529.
Morishita, E., Masuda, S., Nagao, M., Yasuda, Y., Sasaki, R., 1997. Erythropoietin receptor is expressed in rat hippocampal and cerebral cortical neurons, and erythropoietin prevents in vitro glutamate-induced neuronal death. Neuroscience 76, 105–116.
Morita, M., Ohneda, O., Yamashita, T., Takahashi, S., Suzuki, N., Nakajima, O., Kawauchi, S., Ema, M., Shibahara, S., Udono, T., Tomita, K., Tamai, M., Sogawa, K., Yamamoto, M., Fujii-Kuriyama, Y., 2003. HLF/HIF-2alpha is a key factor in retinopathy of prematurity in association with erythropoietin. EMBO. J. 22, 1134–1146.
Mowat, F.M., Luhmann, U.F., Smith, A.J., Lange, C., Duran, Y., Harten, S., Shukla, D., Maxwell, P.H., Ali, R.R., Bainbridge, J.W., 2010. HIF-1alpha and HIF-2alpha are differentially activated in distinct cell populations in retinal ischaemia. PLoS One 5, e11103.
Muller, A., Pietri, S., Villain, M., Frejaville, C., Bonne, C., Culcas, M., 1997. Free radicals in rabbit retina under ocular hyperpressure and functional consequences. Exp. Eye Res. 64, 637–643.
Murray, B., Wilson, D.J., 2001. A study of metabolites as intermediate effectors in angiogenesis. Angiogenesis 4, 71–77.
Nadam, J., Navarro, F., Sanchez, P., Moulin, C., Georges, B., Laglaine, A., Pequignot, J.M., Morales, A., Ryvlin, P., Bezin, L., 2007. Neuroprotective effects of erythropoietin in the rat hippocampus after pilocarpine-induced status epilepticus. Neurobiol. Dis. 25, 412–426.
Nanduri, J., Yuan, G., Kumar, G.K., Semenza, G.L., Prabhakar, N.R., 2008. Transcriptional responses to intermittent hypoxia. Respir. Physiol. Neurobiol. 164, 277–281.
Napper, G.A., Pianta, M.J., Kalloniatis, M., 1999. Reduced glutamate uptake by retinal glial cells under ischemic/hypoxic conditions. Vis. Neurosci. 16, 149–158.
Neal, M.J., Cunningham, J.R., Hutson, P.H., Hogg, J., 1994. Effects of ischaemia on neurotransmitter release from the isolated retina. J. Neurochem. 62, 1025–1033.
Neckers, L., Ivy, S.P., 2003. Heat shock protein 90. Curr. Opin. Oncol. 15, 419–424.
Nielsen, J.C., Naash, M.I., Anderson, R.E., 1988. The regional distribution of vitamins E and C in mature and premature human retinas. Invest. Ophthalmol. Vis. Sci. 29, 22–26.

Niesman, M.R., Johnson, K.A., Penn, J.S., 1997. Therapeutic effect of liposomal superoxide dismutase in an animal model of retinopathy of prematurity. Neurochem. Res. 22, 597–605.
Nir, I., Kedzierski, W., Chen, J., Travis, G.H., 2000. Expression of Bcl-2 protects against photoreceptor degeneration in retinal degeneration slow (rds) mice. J. Neurosci. 20, 2150–2154.
Nishijima, K., Ng, Y.S., Zhong, L., Bradley, J., Schubert, W., Jo, N., Akita, J., Samuelsson, S.J., Robinson, G.S., Adamis, A.P., Shima, D.T., 2007. Vascular endothelial growth factor-A is a survival factor for retinal neurons and a critical neuroprotectant during the adaptive response to ischemic injury. Am. J. Pathol. 171, 53–67.
Nonaka, A., Kiryu, J., Tsujikawa, A., Yamashiro, K., Nishijima, K., Miyamoto, K., Nishiwaki, H., Honda, Y., Ogura, Y., 2001. Inhibitory effect of ischemic preconditioning on leukocyte participation in retinal ischemia-reperfusion injury. Invest. Ophthalmol. Vis. Sci. 42, 2380–2385.
O'Driscoll, C., O'Connor, J., O'Brien, C.J., Cotter, T.G., 2008. Basic fibroblast growth factor-induced protection from light damage in the mouse retina in vivo. J. Neurochem. 105, 524–536.
Ohlsson, A., Aher, S.M., 2006. Early erythropoietin for preventing red blood cell transfusion in preterm and/or low birth weight infants. Cochrane Database Syst. Rev. 3, CD004863.
Okawa, H., Sampath, A.P., Laughlin, S.B., Fain, G.L., 2008. ATP consumption by mammalian rod photoreceptors in darkness and in light. Curr. Biol. 18, 1917–1921.
Osborne, N.N., Casson, R.J., Wood, J.P., Chidlow, G., Graham, M., Melena, J., 2004. Retinal ischemia: mechanisms of damage and potential therapeutic strategies. Prog. Retin. Eye Res. 23, 91–147.
Osborne, N.N., Herrera, A.J., 1994. The effect of experimental ischaemia and excitatory amino acid agonists on the GABA and serotonin immunoreactivities in the rabbit retina. Neuroscience 59, 1071–1081.
Osborne, N.N., Melena, J., Chidlow, G., Wood, J.P., 2001. A hypothesis to explain ganglion cell death caused by vascular insults at the optic nerve head: possible implication for the treatment of glaucoma. Br. J. Ophthalmol. 85, 1252–1259.
Osborne, N.N., Safa, R., Nash, M.S., 1999a. Photoreceptors are preferentially affected in the rat retina following permanent occlusion of the carotid arteries. Vision Res. 39, 3995–4002.
Osborne, N.N., Ugarte, M., Chao, M., Chidlow, G., Bae, J.H., Wood, J.P., Nash, M.S., 1999b. Neuroprotection in relation to retinal ischemia and relevance to glaucoma. Surv. Ophthalmol. 43 (Suppl. 1), S102–S128.
Ostwald, P., Park, S.S., Toledano, A.Y., Roth, S., 1997. Adenosine receptor blockade and nitric oxide synthase inhibition in the retina: impact upon post-ischemic hyperemia and the electroretinogram. Vision Res. 37, 3453–3461.
Ozaki, H., Yu, A.Y., Della, N., Ozaki, K., Luna, J.D., Yamada, H., Hackett, S.F., Okamoto, N., Zack, D.J., Semenza, G.L., Campochiaro, P.A., 1999. Hypoxia inducible factor-1alpha is increased in ischemic retina: temporal and spatial correlation with VEGF expression. Invest. Ophthalmol. Vis. Sci. 40, 182–189.
Pannicke, T., Iandiev, I., Wurm, A., Uckermann, O., vom Hagen, F., Reichenbach, A., Wiedemann, P., Hammes, H.P., Bringmann, A., 2006. Diabetes alters osmotic swelling characteristics and membrane conductance of glial cells in rat retina. Diabetes 55, 633–639.
Park, K., Jin, J., Hu, Y., Zhou, K., Ma, J.X., 2011. Overexpression of pigment epithelium-derived factor inhibits retinal inflammation and neovascularization. Am. J. Pathol. 178, 688–698.
Parsa, C.J., Matsumoto, A., Kim, J., Riel, R.U., Pascal, L.S., Walton, G.B., Thompson, R.B., Petrofski, J.A., Annex, B.H., Stamler, J.S., Koch, W.J., 2003. A novel protective effect of erythropoietin in the infarcted heart. J. Clin. Invest. 112, 999–1007.
Patel, N.S., Sharples, E.J., Cuzzocrea, S., Chatterjee, P.K., Britti, D., Yaqoob, M.M., Thiemermann, C., 2004. Pretreatment with EPO reduces the injury and dysfunction caused by ischemia/reperfusion in the mouse kidney in vivo. Kidney Int. 66, 983–989.
Pellerin, L., Magistretti, P.J., 1994. Glutamate uptake into astrocytes stimulates aerobic glycolysis: a mechanism coupling neuronal activity to glucose utilization. Proc. Natl. Acad. Sci. U.S.A. 91, 10625–10629.
Peng, J., Zhang, L., Drysdale, L., Fong, G.H., 2000. The transcription factor EPAS-1/hypoxia-inducible factor 2alpha plays an important role in vascular remodeling. Proc. Natl. Acad. Sci. U.S.A. 97, 8386–8391.
Peng, P.H., Huang, H.S., Lee, Y.J., Chen, Y.S., Ma, M.C., 2009. Novel role for the delta-opioid receptor in hypoxic preconditioning in rat retinas. J. Neurochem. 108, 741–754.
Penn, J.S., Li, S., Naash, M.I., 2000. Ambient hypoxia reverses retinal vascular attenuation in a transgenic mouse model of autosomal dominant retinitis pigmentosa. Invest. Ophthalmol. Vis. Sci. 41, 4007–4013.
Penn, J.S., Tolman, B.L., Bullard, L.E., 1997. Effect of a water-soluble vitamin E analog, trolox C, on retinal vascular development in an animal model of retinopathy of prematurity. Free Radic. Biol. Med. 22, 977–984.
Penn, J.S., Tolman, B.L., Henry, M.M., 1994. Oxygen-induced retinopathy in the rat: relationship of retinal nonperfusion to subsequent neovascularization. Invest. Ophthalmol. Vis. Sci. 35, 3429–3435.
Penn, J.S., Tolman, B.L., Lowery, L.A., 1993. Variable oxygen exposure causes preretinal neovascularization in the newborn rat. Invest. Ophthalmol. Vis. Sci. 34, 576–585.
Perlman, J.I., McCole, S.M., Pulluru, P., Chang, C.J., Lam, T.T., Tso, M.O., 1996. Disturbances in the distribution of neurotransmitters in the rat retina after ischemia. Curr. Eye Res. 15, 589–596.
Pfister, F., Feng, Y., vom Hagen, F., Hoffmann, S., Molema, G., Hillebrands, J.L., Shani, M., Deutsch, U., Hammes, H.P., 2008. Pericyte migration: a novel mechanism of pericyte loss in experimental diabetic retinopathy. Diabetes 57, 2495–2502.
Phelps, D.L., 1988. Reduced severity of oxygen-induced retinopathy in kittens recovered in 28% oxygen. Pediatr. Res. 24, 106–109.
Pierce, E.A., Avery, R.L., Foley, E.D., Aiello, L.P., Smith, L.E., 1995. Vascular endothelial growth factor/vascular permeability factor expression in a mouse model of retinal neovascularization. Proc. Natl. Acad. Sci. U.S.A. 92, 905–909.
Pierce, E.A., Foley, E.D., Smith, L.E., 1996. Regulation of vascular endothelial growth factor by oxygen in a model of retinopathy of prematurity. Arch. Ophthalmol. 114, 1219–1228.
Portera-Cailliau, C., Sung, C.H., Nathans, J., Adler, R., 1994. Apoptotic photoreceptor cell death in mouse models of retinitis pigmentosa. Proc. Natl. Acad. Sci. U.S.A. 91, 974–978.
Poulaki, V., Joussen, A.M., Mitsiades, N., Mitsiades, C.S., Iliaki, E.F., Adamis, A.P., 2004. Insulin-like growth factor-I plays a pathogenetic role in diabetic retinopathy. Am. J. Pathol. 165, 457–469.
Poulaki, V., Qin, W., Joussen, A.M., Hurlbut, P., Wiegand, S.J., Rudge, J., Yancopoulos, G.D., Adamis, A.P., 2002. Acute intensive insulin therapy exacerbates diabetic blood–retinal barrier breakdown via hypoxia-inducible factor-1alpha and VEGF. J. Clin. Invest. 109, 805–815.
Pournaras, C.J., Riva, C.E., Tsacopoulos, M., Strommer, K., 1989. Diffusion of O2 in the retina of anesthetized miniature pigs in normoxia and hyperoxia. Exp. Eye Res. 49, 347–360.
Pournaras, C.J., Rungger-Brandle, E., Riva, C.E., Hardarson, S.H., Stefansson, E., 2008. Regulation of retinal blood flow in health and disease. Prog. Retin. Eye Res. 27, 284–330.
Pournaras, C.J., Tsacopoulos, M., Strommer, K., Gilodi, N., Leuenberger, P.M., 1990. Experimental retinal branch vein occlusion in miniature pigs induces local tissue hypoxia and vasoproliferative microangiopathy. Ophthalmology 97, 1321–1328.
Powell, W.H., Hahn, M.E., 2002. Identification and functional characterization of hypoxia-inducible factor 2alpha from the estuarine teleost, Fundulus heteroclitus: interaction of HIF-2alpha with two ARNT2 splice variants. J. Exp. Zool. 294, 17–29.
Provis, J.M., 2001. Development of the primate retinal vasculature. Prog. Retin. Eye Res. 20, 799–821.
Provis, J.M., Leech, J., Diaz, C.M., Penfold, P.L., Stone, J., Keshet, E., 1997. Development of the human retinal vasculature: cellular relations and VEGF expression. Exp. Eye Res. 65, 555–568.
Quigley, H.A., Broman, A.T., 2006. The number of people with glaucoma worldwide in 2010 and 2020. Br. J. Ophthalmol. 90, 262–267.
Raju, T.N., Langenberg, P., Bhutani, V., Quinn, G.E., 1997. Vitamin E prophylaxis to reduce retinopathy of prematurity: a reappraisal of published trials. J. Pediatr. 131, 844–850.
Ranchon Cole, I., Bonhomme, B., Doly, M., 2007. Pre-treatment of adult rats with high doses of erythropoietin induces caspase-9 but prevents light-induced retinal injury. Exp. Eye Res. 85, 782–789.
Rankin, E.B., Biju, M.P., Liu, Q., Unger, T.L., Rha, J., Johnson, R.S., Simon, M.C., Keith, B., Haase, V.H., 2007. Hypoxia-inducible factor-2 (HIF-2) regulates hepatic erythropoietin in vivo. J. Clin. Invest. 117, 1068–1077.
Rankin, E.B., Higgins, D.F., Walisser, J.A., Johnson, R.S., Bradfield, C.A., Haase, V.H., 2005. Inactivation of the arylhydrocarbon receptor nuclear translocator (Arnt) suppresses von Hippel–Lindau disease-associated vascular tumors in mice. Mol. Cell. Biol. 25, 3163–3172.
Rapino, C., Bianchi, G., Di Giulio, C., Centurione, L., Cacchio, M., Antonucci, A., Cataldi, A., 2005. HIF-1alpha cytoplasmic accumulation is associated with cell death in old rat cerebral cortex exposed to intermittent hypoxia. Aging Cell 4, 177–185.
Raval, R.R., Lau, K.W., Tran, M.G., Sowter, H.M., Mandriota, S.J., Li, J.L., Pugh, C.W., Maxwell, P.H., Harris, A.L., Ratcliffe, P.J., 2005. Contrasting properties of hypoxia-inducible factor 1 (HIF-1) and HIF-2 in von Hippel–Lindau-associated renal cell carcinoma. Mol. Cell. Biol. 25, 5675–5686.
Recchia, F.M., Xu, L., Penn, J.S., Boone, B., Dexheimer, P.J., 2010. Identification of genes and pathways involved in retinal neovascularization by microarray analysis of two animal models of retinal angiogenesis. Invest. Ophthalmol. Vis. Sci. 51, 1098–1105.
Reich, S.J., Fosnot, J., Kuroki, A., Tang, W., Yang, X., Maguire, A.M., Bennett, J., Tolentino, M.J., 2003. Small interfering RNA (siRNA) targeting VEGF effectively inhibits ocular neovascularization in a mouse model. Mol. Vis. 9, 210–216.
Reichenbach, A., Wurm, A., Pannicke, T., Iandiev, I., Wiedemann, P., Bringmann, A., 2007. Muller cells as players in retinal degeneration and edema. Graefes Arch. Clin. Exp. Ophthalmol. 245, 627–636.
Renzi, M.J., Farrell, F.X., Bittner, A., Galindo, J.E., Morton, M., Trinh, H., Jolliffe, L.K., 2002. Erythropoietin induces changes in gene expression in PC-12 cells. Brain Res. Mol. Brain Res. 104, 86–95.
Rex, T.S., Allocca, M., Domenici, L., Surace, E.M., Maguire, A.M., Lyubarsky, A., Cellerino, A., Bennett, J., Auricchio, A., 2004. Systemic but not intraocular Epo gene transfer protects the retina from light-and genetic-induced degeneration. Mol. Ther. 10, 855–861.
Rex, T.S., Wong, Y., Kodali, K., Merry, S., 2009. Neuroprotection of photoreceptors by direct delivery of erythropoietin to the retina of the retinal degeneration slow mouse. Exp. Eye Res. 89, 735–740.

Reynolds, R., Rosner, B., Seddon, J.M., 2010. Serum lipid biomarkers and hepatic lipase gene associations with age-related macular degeneration. Ophthalmology 117, 1989–1995.
Ribatti, D., Vacca, A., Roccaro, A.M., Crivellato, E., Presta, M., 2003. Erythropoietin as an angiogenic factor. Eur. J. Clin. Invest. 33, 891–896.
Riepe, R.E., Norenburg, M.D., 1977. Muller cell localisation of glutamine synthetase in rat retina. Nature 268, 654–655.
Robinson, G.S., Pierce, E.A., Rook, S.L., Foley, E., Webb, R., Smith, L.E., 1996. Oligodeoxynucleotides inhibit retinal neovascularization in a murine model of proliferative retinopathy. Proc. Natl. Acad. Sci. U.S.A. 93, 4851–4856.
Robison, W.G.J., 1988. Prevention of diabetes-related retinal microangiopathy with aldose reductase inhibitors. Adv. Exp. Med. Biol. 246, 365–372.
Rodesch, F., Simon, P., Donner, C., Jauniaux, E., 1992. Oxygen measurements in endometrial and trophoblastic tissues during early pregnancy. Obstet. Gynecol. 80, 283–285.
Roth, A.M., 1977. Retinal vascular development in premature infants. Am. J. Ophthalmol. 84, 636–640.
Roth, S., 2004. Endogenous neuroprotection in the retina. Brain Res. Bull. 62, 461–466.
Roth, S., Dreixler, J.C., Shaikh, A.R., Lee, K.H., Bindokas, V., 2006. Mitochondrial potassium ATP channels and retinal ischemic preconditioning. Invest. Ophthalmol. Vis. Sci. 47, 2114–2124.
Roth, S., Li, B., Rosenbaum, P.S., Gupta, H., Goldstein, I.M., Maxwell, K.M., Gidday, J.M., 1998. Preconditioning provides complete protection against retinal ischemic injury in rats. Invest. Ophthalmol. Vis. Sci. 39, 777–785.
Roth, S., Park, S.S., Sikorski, C.W., Osinski, J., Chan, R., Loomis, K., 1997a. Concentrations of adenosine and its metabolites in the rat retina/choroid during reperfusion after ischemia. Curr. Eye Res. 16, 875–885.
Roth, S., Rosenbaum, P.S., Osinski, J., Park, S.S., Toledano, A.Y., Li, B., Moshfeghi, A.A., 1997b. Ischemia induces significant changes in purine nucleoside concentration in the retina-choroid in rats. Exp. Eye Res. 65, 771–779.
Roth, S., Shaikh, A.R., Hennelly, M.M., Li, Q., Bindokas, V., Graham, C.E., 2003. Mitogen-activated protein kinases and retinal ischemia. Invest. Ophthalmol. Vis. Sci. 44, 5383–5395.
Rousseau, B., Dubayle, D., Sennlaub, F., Jeanny, J.C., Costet, P., Bikfalvi, A., Javerzat, S., 2000. Neural and angiogenic defects in eyes of transgenic mice expressing a dominant-negative FGF receptor in the pigmented cells. Exp. Eye Res. 71, 395–404.
Ruschitzka, F.T., Wenger, R.H., Stallmach, T., Quaschning, T., de Wit, C., Wagner, K., Labugger, R., Kelm, M., Noll, G., Rulicke, T., Shaw, S., Lindberg, R.L., Rodenwaldt, B., Lutz, H., Bauer, C., Luscher, T.F., Gassmann, M., 2000. Nitric oxide prevents cardiovascular disease and determines survival in polyglobulic mice overexpressing erythropoietin. Proc. Natl. Acad. Sci. U.S.A. 97, 11609–11613.
Ryan, H.E., Lo, J., Johnson, R.S., 1998. HIF-1 alpha is required for solid tumor formation and embryonic vascularization. EMBO J. 17, 3005–3015.
Saika, S., Hashizume, N., Okada, Y., Kobata, S., Yamanaka, O., Uenoyama, K., Ooshima, A., 1994. Prolyl hydroxylase inhibitor and lysyl hydroxylase inhibitor inhibit spreading of corneal epithelium. Graefes Arch. Clin. Exp. Ophthalmol. 232, 499–502.
Sakamoto, K., Kuwagata, M., Nakahara, T., Ishii, K., 2001. Late preconditioning in rat retina: involvement of adenosine and ATP-sensitive K(+) channel. Eur. J. Pharmacol. 418, 89–93.
Sakamoto, K., Yonoki, Y., Kubota, Y., Kuwagata, M., Saito, M., Nakahara, T., Ishii, K., 2006. Inducible nitric oxide synthase inhibitors abolished histological protection by late ischemic preconditioning in rat retina. Exp. Eye Res. 82, 512–518.
Sakamoto, K., Yonoki, Y., Kuwagata, M., Saito, M., Nakahara, T., Ishii, K., 2004. Histological protection against ischemia-reperfusion injury by early ischemic preconditioning in rat retina. Brain Res. 1015, 154–160.
Sakanaka, M., Wen, T.C., Matsuda, S., Masuda, S., Morishita, E., Nagao, M., Sasaki, R., 1998. In vivo evidence that erythropoietin protects neurons from ischemic damage. Proc. Natl. Acad. Sci. U.S.A. 95, 4635–4640.
Samardzija, M., Neuhauss, S.C.F., Joly, S., Kurz-Levin, M., Grimm, C., 2010. Animal models for retinal degeneration. Anim. Mod. Retin. Dis. 46, 51–79.
Sandercoe, T.M., Geller, S.F., Hendrickson, A.E., Stone, J., Provis, J.M., 2003. VEGF expression by ganglion cells in central retina before formation of the foveal depression in monkey retina: evidence of developmental hypoxia. J. Comp. Neurol. 462, 42–54.
Sapieha, P., Joyal, J.S., Rivera, J.C., Kermorvant-Duchemin, E., Sennlaub, F., Hardy, P., Lachapelle, P., Chemtob, S., 2010. Retinopathy of prematurity: understanding ischemic retinal vasculopathies at an extreme of life. J. Clin. Invest. 120, 3022–3032.
Sapieha, P., Sirinyan, M., Hamel, D., Zaniolo, K., Joyal, J.S., Cho, J.H., Honore, J.C., Kermorvant-Duchemin, E., Varma, D.R., Tremblay, S., Leduc, M., Rihakova, L., Hardy, P., Klein, W.H., Mu, X., Mamer, O., Lachapelle, P., Di Polo, A., Beausejour, C., Andelfinger, G., Mitchell, G., Sennlaub, F., Chemtob, S., 2008. The succinate receptor GPR91 in neurons has a major role in retinal angiogenesis. Nat. Med. 14, 1067–1076.
Sattler, M.B., Merkler, D., Maier, K., Stadelmann, C., Ehrenreich, H., Bahr, M., Diem, R., 2004. Neuroprotective effects and intracellular signaling pathways of erythropoietin in a rat model of multiple sclerosis. Cell Death Differ. 11 (Suppl. 2), S181–S192.
Scheerer, N., Dunker, N., Imagawa, S., Yamamoto, M., Suzuki, N., Fandrey, J., 2010. The anemia of the newborn induces erythropoietin expression in the developing mouse retina. Am. J. Physiol. Regul. Integr. Comp. Physiol. 299, R111–R118.
Schlingemann, R.O., 2004. Role of growth factors and the wound healing response in age-related macular degeneration. Graefes Arch. Clin. Exp. Ophthalmol. 242, 91–101.
Schodel, J., Oikonomopoulos, S., Ragoussis, J., Pugh, C.W., Ratcliffe, P.J., Mole, D.R., 2011. High-resolution genome-wide mapping of HIF-binding sites by ChIP-seq. Blood 117, e207–e217.
Scortegagna, M., Ding, K., Oktay, Y., Gaur, A., Thurmond, F., Yan, L.J., Marck, B.T., Matsumoto, A.M., Shelton, J.M., Richardson, J.A., Bennett, M.J., Garcia, J.A., 2003a. Multiple organ pathology, metabolic abnormalities and impaired homeostasis of reactive oxygen species in Epas1−/− mice. Nat. Genet. 35, 331–340.
Scortegagna, M., Morris, M.A., Oktay, Y., Bennett, M., Garcia, J.A., 2003b. The HIF family member EPAS1/HIF-2alpha is required for normal hematopoiesis in mice. Blood 102, 1634–1640.
Scortegagna, M., Ding, K., Zhang, Q., Oktay, Y., Bennett, M.J., Bennett, M., Shelton, J.M., Richardson, J.A., Moe, O., Garcia, J.A., 2005. HIF-2alpha regulates murine hematopoietic development in an erythropoietin-dependent manner. Blood 105, 3133–3140.
Sears, J.E., Hoppe, G., Ebrahem, Q., Anand-Apte, B., 2008. Prolyl hydroxylase inhibition during hyperoxia prevents oxygen-induced retinopathy. Proc. Natl. Acad. Sci. U.S.A. 105, 19898–19903.
Seki, M., Tanaka, T., Nawa, H., Usui, T., Fukuchi, T., Ikeda, K., Abe, H., Takei, N., 2004. Involvement of brain-derived neurotrophic factor in early retinal neuropathy of streptozotocin-induced diabetes in rats: therapeutic potential of brain-derived neurotrophic factor for dopaminergic amacrine cells. Diabetes 53, 2412–2419.
Selles-Navarro, I., Villegas-Perez, M.P., Salvador-Silva, M., Ruiz-Gomez, J.M., Vidal-Sanz, M., 1996. Retinal ganglion cell death after different transient periods of pressure-induced ischemia and survival intervals. A quantitative in vivo study. Invest. Ophthalmol. Vis. Sci. 37, 2002–2014.
Semenza, G.L., 2001. HIF-1 and mechanisms of hypoxia sensing. Curr. Opin. Cell. Biol. 13, 167–171.
Semenza, G.L., 2006. Regulation of physiological responses to continuous and intermittent hypoxia by hypoxia-inducible factor 1. Exp. Physiol. 91, 803–806.
Semenza, G.L., Koury, S.T., Nejfelt, M.K., Gearhart, J.D., Antonarakis, S.E., 1991. Cell-type-specific and hypoxia-inducible expression of the human erythropoietin gene in transgenic mice. Proc. Natl. Acad. Sci. U.S.A. 88, 8725–8729.
Semenza, G.L., Wang, G.L., 1992. A nuclear factor induced by hypoxia via de novo protein synthesis binds to the human erythropoietin gene enhancer at a site required for transcriptional activation. Mol. Cell. Biol. 12, 5447–5454.
Shen, J., Wu, Y., Xu, J.Y., Zhang, J., Sinclair, S.H., Yanoff, M., Xu, G., Li, W., Xu, G.T., 2010. ERK- and Akt-dependent neuroprotection by erythropoietin (EPO) against glyoxal-AGEs via modulation of Bcl-xL, Bax, and BAD. Invest. Ophthalmol. Vis. Sci. 51, 35–46.
Sheridan, C.M., Pate, S., Hiscott, P., Wong, D., Pattwell, D.M., Kent, D., 2009. Expression of hypoxia-inducible factor-1alpha and -2alpha in human choroidal neovascular membranes. Graefes Arch. Clin. Exp. Ophthalmol. 247, 1361–1367.
Shingo, T., Sorokan, S.T., Shimazaki, T., Weiss, S., 2001. Erythropoietin regulates the in vitro and in vivo production of neuronal progenitors by mammalian forebrain neural stem cells. J. Neurosci. 21, 9733–9743.
Shortt, A.J., Howell, K., O'Brien, C., McLoughlin, P., 2004. Chronic systemic hypoxia causes intra-retinal angiogenesis. J. Anat. 205, 349–356.
Siliprandi, R., Bucci, M.G., Canella, R., Carmignoto, G., 1988. Flash and pattern electroretinograms during and after acute intraocular pressure elevation in cats. Invest. Ophthalmol. Vis. Sci. 29, 558–565.
Siliprandi, R., Canella, R., Carmignoto, G., 1993. Nerve growth factor promotes functional recovery of retinal ganglion cells after ischemia. Invest. Ophthalmol. Vis. Sci. 34, 3232–3245.
Singh, M., Savitz, S.I., Hoque, R., Gupta, G., Roth, S., Rosenbaum, P.S., Rosenbaum, D.M., 2001. Cell-specific caspase expression by different neuronal phenotypes in transient retinal ischemia. J. Neurochem. 77, 466–475.
Siren, A.L., Fratelli, M., Brines, M., Goemans, C., Casagrande, S., Lewczuk, P., Keenan, S., Gleiter, C., Pasquali, C., Capobianco, A., Mennini, T., Heumann, R., Cerami, A., Ehrenreich, H., Ghezzi, P., 2001. Erythropoietin prevents neuronal apoptosis after cerebral ischemia and metabolic stress. Proc. Natl. Acad. Sci. U.S.A. 98, 4044–4049.
Slusarski, J.D., McPherson, R.J., Wallace, G.N., Juul, S.E., 2009. High-dose erythropoietin does not exacerbate retinopathy of prematurity in rats. Pediatr. Res. 66, 625–630.
Smith, L.E., 2003. Pathogenesis of retinopathy of prematurity. Semin. Neonatol. 8, 469–473.
Smith, L.E., Kopchick, J.J., Chen, W., Knapp, J., Kinose, F., Daley, D., Foley, E., Smith, R.G., Schaeffer, J.M., 1997. Essential role of growth hormone in ischemia-induced retinal neovascularization. Science 276, 1706–1709.
Smith, L.E., Shen, W., Perruzzi, C., Soker, S., Kinose, F., Xu, X., Robinson, G., Driver, S., Bischoff, J., Zhang, B., Schaeffer, J.M., Senger, D.R., 1999. Regulation of vascular endothelial growth factor-dependent retinal neovascularization by insulin-like growth factor-1 receptor. Nat. Med. 5, 1390–1395.
Smith, L.E., Wesolowski, E., McLellan, A., Kostyk, S.K., D'Amato, R., Sullivan, R., D'Amore, P.A., 1994. Oxygen-induced retinopathy in the mouse. Invest. Ophthalmol. Vis. Sci. 35, 101–111.
Smith, W., Mitchell, P., Leeder, S.R., 1996. Smoking and age-related maculopathy. The Blue Mountains Eye Study. Arch. Ophthalmol. 114, 1518–1523.
Song, B.J., Cai, H., Tsai, J.C., Chang, S., Forbes, M., Del Priore, L.V., 2008a. Intravitreal recombinant human erythropoietin: a safety study in rabbits. Curr. Eye Res. 33, 750–760.

Song, H., Zhao, Y., Qi, X., Chui, Y.T., Burns, S.A., 2008b. Stokes vector analysis of adaptive optics images of the retina. Opt. Lett. 33, 137–139.
Song, S.J., Chung, H., Yu, H.G., 2008c. Inhibitory effect of YC-1, 3-(5′-hydroxymethyl-2′-furyl)-1-benzylindazole, on experimental choroidal neovascularization in rat. Ophthalmic Res. 40, 35–40.
Sowter, H.M., Raval, R.R., Moore, J.W., Ratcliffe, P.J., Harris, A.L., 2003. Predominant role of hypoxia-inducible transcription factor (Hif)-1alpha versus Hif-2alpha in regulation of the transcriptional response to hypoxia. Cancer Res. 63, 6130–6134.
Sparrow, J.R., Cai, B., Fishkin, N., Jang, Y.P., Krane, S., Vollmer, H.R., Zhou, J., Nakanishi, K., 2003. A2E, a fluorophore of RPE lipofuscin: can it cause RPE degeneration? Adv. Exp. Med. Biol. 533, 205–211.
Spilsbury, K., Garrett, K.L., Shen, W.Y., Constable, I.J., Rakoczy, P.E., 2000. Over-expression of vascular endothelial growth factor (VEGF) in the retinal pigment epithelium leads to the development of choroidal neovascularization. Am. J. Pathol. 157, 135–144.
Stahl, A., Connor, K.M., Sapieha, P., Chen, J., Dennison, R.J., Krah, N.M., Seaward, M.R., Willett, K.L., Aderman, C.M., Guerin, K.I., Hua, J., Lofqvist, C., Hellstrom, A., Smith, L.E., 2010. The mouse retina as an angiogenesis model. Invest. Ophthalmol. Vis. Sci. 51, 2813–2826.
Stamler, J.S., Singel, D.J., Loscalzo, J., 1992. Biochemistry of nitric oxide and its redox-activated forms. Science 258, 1898–1902.
Stefansson, E., Hatchell, D.L., Fisher, B.L., Sutherland, F.S., Machemer, R., 1986. Panretinal photocoagulation and retinal oxygenation in normal and diabetic cats. Am. J. Ophthalmol. 101, 657–664.
Stefansson, E., Peterson, J.I., Wang, Y.H., 1989. Intraocular oxygen tension measured with a fiber-optic sensor in normal and diabetic dogs. Am. J. Physiol. 256, H1127–H1133.
Stefansson, E., Wolbarsht, M.L., Landers, M.B.R., 1983. In vivo O2 consumption in rhesus monkeys in light and dark. Exp. Eye Res. 37, 251–256.
Stevens, W.D., Fortin, T., Pappas, B.A., 2002. Retinal and optic nerve degeneration after chronic carotid ligation: time course and role of light exposure. Stroke 33, 1107–1112.
Stieger, K., Le Meur, G., Lasne, F., Weber, M., Deschamps, J.Y., Nivard, D., Mendes-Madeira, A., Provost, N., Martin, L., Moullier, P., Rolling, F., 2006. Long-term doxycycline-regulated transgene expression in the retina of nonhuman primates following subretinal injection of recombinant AAV vectors. Mol. Ther. 13, 967–975.
Stitt, A.W., Anderson, H.R., Gardiner, T.A., Archer, D.B., 1994. Diabetic retinopathy: quantitative variation in capillary basement membrane thickening in arterial or venous environments. Br. J. Ophthalmol. 78, 133–137.
Stohlawetz, P.J., Dzirlo, L., Hergovich, N., Lackner, E., Mensik, C., Eichler, H.G., Kabrna, E., Geissler, K., Jilma, B., 2000. Effects of erythropoietin on platelet reactivity and thrombopoiesis in humans. Blood 95, 2983–2989.
Stone, J., Chan-Ling, T., Pe'er, J., Itin, A., Gnessin, H., Keshet, E., 1996. Roles of vascular endothelial growth factor and astrocyte degeneration in the genesis of retinopathy of prematurity. Invest. Ophthalmol. Vis. Sci. 37, 290–299.
Stone, J., Dreher, Z., 1987. Relationship between astrocytes, ganglion cells and vasculature of the retina. J. Comp. Neurol. 255, 35–49.
Stone, J., Itin, A., Alon, T., Pe'er, J., Gnessin, H., Chan-Ling, T., Keshet, E., 1995. Development of retinal vasculature is mediated by hypoxia-induced vascular endothelial growth factor (VEGF) expression by neuroglia. J. Neurosci. 15, 4738–4747.
Stowell, C., Wang, L., Arbogast, B., Lan, J.Q., Cioffi, G.A., Burgoyne, C.F., Zhou, A., 2010. Retinal proteomic changes under different ischemic conditions – implication of an epigenetic regulatory mechanism. Int. J. Physiol. Pathophysiol. Pharmacol. 2, 148–160.
Suemori, S., Shimazawa, M., Kawase, K., Satoh, M., Nagase, H., Yamamoto, T., Hara, H., 2006. Metallothionein, an endogenous antioxidant, protects against retinal neuron damage in mice. Invest. Ophthalmol. Vis. Sci. 47, 3975–3982.
Suk, K.K., Dunbar, J.A., Liu, A., Daher, N.S., Leng, C.K., Leng, J.K., Lim, P., Weller, S., Fayard, E., 2008. Human recombinant erythropoietin and the incidence of retinopathy of prematurity: a multiple regression model. J. AAPOS 12, 233–238.
Sullivan, T., Kodali, K., Rex, T.S., 2011a. Systemic gene delivery protects the photoreceptors in the retinal degeneration slow mouse. Neurochem. Res. 36, 613–618.
Sullivan, T.A., Geisert, E.E., Hines-Beard, J., Rex, T.S., 2011b. Systemic adeno-associated virus-mediated gene therapy preserves retinal ganglion cells and visual function in DBA/2J glaucomatous mice. Hum. Gene Ther..
Sung, C.H., Chuang, J.Z., 2010. The cell biology of vision. J. Cell. Biol. 190, 953–963.
Szabo, M.E., Droy-Lefaix, M.T., Doly, M., 1997. Direct measurement of free radicals in ischemic/reperfused diabetic rat retina. Clin. Neurosci. 4, 240–245.
Takahata, S., Sogawa, K., Kobayashi, A., Ema, M., Mimura, J., Ozaki, N., Fujii-Kuriyama, Y., 1998. Transcriptionally active heterodimer formation of an Arnt-like PAS protein, Arnt3, with HIF-1a, HLF, and clock. Biochem. Biophys. Res. Commun. 248, 789–794.
Terman, A., Brunk, U.T., 2004. Lipofuscin. Int. J. Biochem. Cell. Biol. 36, 1400–1404.
Tezel, G., Wax, M.B., 1999. Inhibition of caspase activity in retinal cell apoptosis induced by various stimuli in vitro. Invest. Ophthalmol. Vis. Sci. 40, 2660–2667.
Tezel, G., Wax, M.B., 2000. Increased production of tumor necrosis factor-alpha by glial cells exposed to simulated ischemia or elevated hydrostatic pressure induces apoptosis in cocultured retinal ganglion cells. J. Neurosci. 20, 8693–8700.
Tezel, G., Wax, M.B., 2004. Hypoxia-inducible factor 1alpha in the glaucomatous retina and optic nerve head. Arch. Ophthalmol. 122, 1348–1356.
Thiersch, M., Lange, C., Joly, S., Heynen, S., Le, Y.Z., Samardzija, M., Grimm, C., 2009. Retinal neuroprotection by hypoxic preconditioning is independent of hypoxia-inducible factor-1 alpha expression in photoreceptors. Eur. J. Neurosci. 29, 2291–2302.
Thiersch, M., Raffelsberger, W., Frigg, R., Samardzija, M., Wenzel, A., Poch, O., Grimm, C., 2008. Analysis of the retinal gene expression profile after hypoxic preconditioning identifies candidate genes for neuroprotection. BMC Genomics 9, 73.
Tian, H., Hammer, R.E., Matsumoto, A.M., Russell, D.W., McKnight, S.L., 1998. The hypoxia-responsive transcription factor EPAS1 is essential for catecholamine homeostasis and protection against heart failure during embryonic development. Genes Dev. 12, 3320–3324.
Tian, H., McKnight, S.L., Russell, D.W., 1997. Endothelial PAS domain protein 1 (EPAS1), a transcription factor selectively expressed in endothelial cells. Genes Dev. 11, 72–82.
Tinjust, D., Kergoat, H., Lovasik, J.V., 2002. Neuroretinal function during mild systemic hypoxia. Aviat. Space Environ. Med. 73, 1189–1194.
Tolentino, M.J., Brucker, A.J., Fosnot, J., Ying, G.S., Wu, I.H., Malik, G., Wan, S., Reich, S.J., 2004. Intravitreal injection of vascular endothelial growth factor small interfering RNA inhibits growth and leakage in a nonhuman primate, laser-induced model of choroidal neovascularization. Retina 24, 132–138.
Tolppanen, A.M., Nevalainen, T., Kolehmainen, M., Seitsonen, S., Immonen, I., Uusitupa, M., Kaarniranta, K., Pulkkinen, L., 2009. Single nucleotide polymorphisms of the tenomodulin gene (TNMD) in age-related macular degeneration. Mol. Vis. 15, 762–770.
Tong, Z., Yang, Z., Patel, S., Chen, H., Gibbs, D., Yang, X., Hau, V.S., Kaminoh, Y., Harmon, J., Pearson, E., Buehler, J., Chen, Y., Yu, B., Tinkham, N.H., Zabriskie, N.A., Zeng, J., Luo, L., Sun, J.K., Prakash, M., Hamam, R.N., Tonna, S., Constantine, R., Ronquillo, C.C., Sadda, S., Avery, R.L., Brand, J.M., London, N., Anduze, A.L., King, G.L., Bernstein, P.S., Watkins, S., Jorde, L.B., Li, D.Y., Aiello, L.P., Pollak, M.R., Zhang, K., 2008. Promoter polymorphism of the erythropoietin gene in severe diabetic eye and kidney complications. Proc. Natl. Acad. Sci. U.S.A. 105, 6998–7003.
Tsai, J.C., 2008. Safety of intravitreally administered recombinant erythropoietin (an AOS thesis). Trans. Am. Ophthalmol. Soc. 106, 459–472.
Tsai, J.C., Wu, L., Worgul, B., Forbes, M., Cao, J., 2005. Intravitreal administration of erythropoietin and preservation of retinal ganglion cells in an experimental rat model of glaucoma. Curr. Eye Res. 30, 1025–1031.
Ueki, Y., Le, Y.Z., Chollangi, S., Muller, W., Ash, J.D., 2009. Preconditioning-induced protection of photoreceptors requires activation of the signal-transducing receptor gp130 in photoreceptors. Proc. Natl. Acad. Sci. U.S.A. 106, 21389–21394.
Um, M., Gross, A.W., Lodish, H.F., 2007. A "classical" homodimeric erythropoietin receptor is essential for the antiapoptotic effects of erythropoietin on differentiated neuroblastoma SH-SY5Y and pheochromocytoma PC-12 cells. Cell Signal 19, 634–645.
Uno, K., Prow, T.W., Bhutto, I.A., Yerrapureddy, A., McLeod, D.S., Yamamoto, M., Reddy, S.P., Lutty, G.A., 2010. Role of Nrf2 in retinal vascular development and the vaso-obliterative phase of oxygen-induced retinopathy. Exp. Eye Res. 90, 493–500.
van Leeuwen, R., Ikram, M.K., Vingerling, J.R., Witteman, J.C., Hofman, A., de Jong, P.T., 2003. Blood pressure, atherosclerosis, and the incidence of age-related maculopathy: the Rotterdam Study. Invest. Ophthalmol. Vis. Sci. 44, 3771–3777.
van Rooijen, E., Voest, E.E., Logister, I., Bussmann, J., Korving, J., van Eeden, F.J., Giles, R.H., Schulte-Merker, S., 2010. von Hippel–Lindau tumor suppressor mutants faithfully model pathological hypoxia-driven angiogenesis and vascular retinopathies in zebrafish. Dis. Model. Mech. 3, 343–353.
van Wijngaarden, P., Brereton, H.M., Gibbins, I.L., Coster, D.J., Williams, K.A., 2007. Kinetics of strain-dependent differential gene expression in oxygen-induced retinopathy in the rat. Exp. Eye Res. 85, 508–517.
Villa, P., Bigini, P., Mennini, T., Agnello, D., Laragione, T., Cagnotto, A., Viviani, B., Marinovich, M., Cerami, A., Coleman, T.R., Brines, M., Ghezzi, P., 2003. Erythropoietin selectively attenuates cytokine production and inflammation in cerebral ischemia by targeting neuronal apoptosis. J. Exp. Med. 198, 971–975.
Villa, P., van Beek, J., Larsen, A.K., Gerwien, J., Christensen, S., Cerami, A., Brines, M., Leist, M., Ghezzi, P., Torup, L., 2007. Reduced functional deficits, neuroinflammation, and secondary tissue damage after treatment of stroke by non-erythropoietic erythropoietin derivatives. J. Cereb. Blood Flow Metab. 27, 552–563.
Villarroel, M., Ciudin, A., Hernandez, C., Simo, R., 2010. Neurodegeneration: an early event of diabetic retinopathy. World J. Diabetes 1, 57–64.
Wang, G.L., Jiang, B.H., Rue, E.A., Semenza, G.L., 1995. Hypoxia-inducible factor 1 is a basic-helix-loop-helix-PAS heterodimer regulated by cellular O2 tension. Proc. Natl. Acad. Sci. U.S.A. 92, 5510–5514.
Wang, Q., Gorbey, S., Pfister, F., Hoger, S., Dorn-Beineke, A., Krugel, K., Berrone, E., Wu, L., Korff, T., Lin, J., Busch, S., Reichenbach, A., Feng, Y., Hammes, H.P., 2011a. Long-term treatment with suberythropoietic Epo is Vaso- and neuroprotective in experimental diabetic retinopathy. Cell. Physiol. Biochem. 27, 769–782.
Wang, Z.Y., Zhao, K.K., Zhao, P.Q., 2011b. Erythropoietin therapy for early diabetic retinopathy through its protective effects on retinal pericytes. Med. Hypotheses 76, 266–268.
Wang, Q., Pfister, F., Dorn-Beineke, A., vom Hagen, F., Lin, J., Feng, Y., Hammes, H.P., 2010a. Low-dose erythropoietin inhibits oxidative stress and early vascular changes in the experimental diabetic retina. Diabetologia 53, 1227–1238.

Wang, Z.Y., Zhao, K.K., Zhao, P.Q., 2010b. Erythropoietin is increased in aqueous humor of glaucomatous eyes. Curr. Eye Res. 35, 680–684.
Wang, Z.Y., Shen, L.J., Tu, L., Hu, D.N., Liu, G.Y., Zhou, Z.L., Lin, Y., Chen, L.H., Qu, J., 2009. Erythropoietin protects retinal pigment epithelial cells from oxidative damage. Free Radic. Biol. Med. 46, 1032–1041.
Warnecke, C., Zaborowska, Z., Kurreck, J., Erdmann, V.A., Frei, U., Wiesener, M., Eckardt, K.U., 2004. Differentiating the functional role of hypoxia-inducible factor (HIF)-1alpha and HIF-2alpha (EPAS-1) by the use of RNA interference: erythropoietin is a HIF-2alpha target gene in Hep3B and Kelly cells. FASEB J. 18, 1462–1464.
Watanabe, D., Suzuma, K., Matsui, S., Kurimoto, M., Kiryu, J., Kita, M., Suzuma, I., Ohashi, H., Ojima, T., Murakami, T., Kobayashi, T., Masuda, S., Nagao, M., Yoshimura, N., Takagi, H., 2005. Erythropoietin as a retinal angiogenic factor in proliferative diabetic retinopathy. N. Engl. J. Med. 353, 782–792.
Watanabe, T., Raff, M.C., 1988. Retinal astrocytes are immigrants from the optic nerve. Nature 332, 834–837.
Watson, J.A., Watson, C.J., McCann, A., Baugh, J., 2010. Epigenetics, the epicenter of the hypoxic response. Epigenetics 5, 293–296.
Weidemann, A., Johnson, R.S., 2009. Nonrenal regulation of EPO synthesis. Kidney Int. 75, 682–688.
Weidemann, A., Krohne, T.U., Aguilar, E., Kurihara, T., Takeda, N., Dorrell, M.I., Simon, M.C., Haase, V.H., Friedlander, M., Johnson, R.S., 2010. Astrocyte hypoxic response is essential for pathological but not developmental angiogenesis of the retina. Glia 58, 1177–1185.
Weinberger, B., Watorek, K., Strauss, R., Witz, G., Hiatt, M., Hegyi, T., 2002. Association of lipid peroxidation with hepatocellular injury in preterm infants. Crit. Care 6, 521–525.
Weishaupt, J.H., Rohde, G., Polking, E., Siren, A.L., Ehrenreich, H., Bahr, M., 2004. Effect of erythropoietin axotomy-induced apoptosis in rat retinal ganglion cells. Invest. Ophthalmol. Vis. Sci. 45, 1514–1522.
Weiter, J.J., Zuckerman, R., 1980. The influence of the photoreceptor-RPE complex on the inner retina. An explanation for the beneficial effects of photocoagulation. Ophthalmology 87, 1133–1139.
Wen, R., Song, Y., Cheng, T., Matthes, M.T., Yasumura, D., LaVail, M.M., Steinberg, R.H., 1995. Injury-induced upregulation of bFGF and CNTF mRNAS in the rat retina. J. Neurosci. 15, 7377–7385.
Wen, T.C., Sadamoto, Y., Tanaka, J., Zhu, P.X., Nakata, K., Ma, Y.J., Hata, R., Sakanaka, M., 2002. Erythropoietin protects neurons against chemical hypoxia and cerebral ischemic injury by up-regulating Bcl-xL expression. J. Neurosci. Res. 67, 795–803.
Wenger, R.H., Stiehl, D.P., Camenisch, G., 2005. Integration of oxygen signaling at the consensus HRE. Sci. STKE re12.
Wenzel, A., Grimm, C., Samardzija, M., Reme, C.E., 2005. Molecular mechanisms of light-induced photoreceptor apoptosis and neuroprotection for retinal degeneration. Prog. Retin. Eye Res. 24, 275–306.
West, H., Richardson, W.D., Fruttiger, M., 2005. Stabilization of the retinal vascular network by reciprocal feedback between blood vessels and astrocytes. Development 132, 1855–1862.
Whitlock, N.A., Agarwal, N., Ma, J.X., Crosson, C.E., 2005. Hsp27 upregulation by HIF-1 signaling offers protection against retinal ischemia in rats. Invest. Ophthalmol. Vis. Sci. 46, 1092–1098.
Wiesener, M.S., Jurgensen, J.S., Rosenberger, C., Scholze, C.K., Horstrup, J.H., Warnecke, C., Mandriota, S., Bechmann, I., Frei, U.A., Pugh, C.W., Ratcliffe, P.J., Bachmann, S., Maxwell, P.H., Eckardt, K.U., 2003. Widespread hypoxia-inducible expression of HIF-2alpha in distinct cell populations of different organs. FASEB J. 17, 271–273.
Wiesener, M.S., Turley, H., Allen, W.E., Willam, C., Eckardt, K.U., Talks, K.L., Wood, S.M., Gatter, K.C., Harris, A.L., Pugh, C.W., Ratcliffe, P.J., Maxwell, P.H., 1998. Induction of endothelial PAS domain protein-1 by hypoxia: characterization and comparison with hypoxia-inducible factor-1alpha. Blood 92, 2260–2268.
Winkler, B.S., 1981. Glycolytic and oxidative metabolism in relation to retinal function. J. Gen. Physiol. 77, 667–692.
Winkler, B.S., Arnold, M.J., Brassell, M.A., Puro, D.G., 2000. Energy metabolism in human retinal Muller cells. Invest. Ophthalmol. Vis. Sci. 41, 3183–3190.
Winkler, B.S., Dang, L., Malinoski, C., Easter, S.S.J., 1997. An assessment of rat photoreceptor sensitivity to mitochondrial blockade. Invest. Ophthalmol. Vis. Sci. 38, 1569–1577.
Winkler, B.S., Sauer, M.W., Starnes, C.A., 2003. Modulation of the Pasteur effect in retinal cells: implications for understanding compensatory metabolic mechanisms. Exp. Eye Res. 76, 715–723.
Witthuhn, B.A., Quelle, F.W., Silvennoinen, O., Yi, T., Tang, B., Miura, O., Ihle, J.N., 1993. JAK2 associates with the erythropoietin receptor and is tyrosine phosphorylated and activated following stimulation with erythropoietin. Cell 74, 227–236.
Wood, J.P., DeSantis, L., Chao, H.M., Osborne, N.N., 2001. Topically applied betaxolol attenuates ischaemia-induced effects to the rat retina and stimulates BDNF mRNA. Exp. Eye Res. 72, 79–86.
Wright, W.S., McElhatten, R.M., Harris, N.R., 2011. Increase in retinal hypoxia-inducible factor-2alpha, but not hypoxia, early in the progression of diabetes in the rat. Exp. Eye Res. 93, 437–441.
Wright, W.S., McElhatten, R.M., Messina, J.E., Harris, N.R., 2010. Hypoxia and the expression of HIF-1alpha and HIF-2alpha in the retina of streptozotocin-injected mice and rats. Exp. Eye Res. 90, 405–412.
Xie, Z., Wu, X., Qiu, Q., Gong, Y., Song, Y., Gu, Q., Li, C., 2007. Expression pattern of erythropoietin and erythropoietin receptor in experimental model of retinal detachment. Curr. Eye Res. 32, 757–764.
Xu, Y., Zhao, H., Zheng, Y., Gu, Q., Ma, J., Xu, X., 2010. A novel antiangiogenic peptide derived from hepatocyte growth factor inhibits neovascularization in vitro and in vivo. Mol. Vis. 16, 1982–1995.
Yamasaki, M., Mishima, H.K., Yamashita, H., Kashiwagi, K., Murata, K., Minamoto, A., Inaba, T., 2005. Neuroprotective effects of erythropoietin on glutamate and nitric oxide toxicity in primary cultured retinal ganglion cells. Brain Res. 1050, 15–26.
Yang, X.M., Wang, Y.S., Zhang, J., Li, Y., Xu, J.F., Zhu, J., Zhao, W., Chu, D.K., Wiedemann, P., 2009. Role of PI3K/Akt and MEK/ERK in mediating hypoxia-induced expression of HIF-1alpha and VEGF in laser-induced rat choroidal neovascularization. Invest. Ophthalmol. Vis. Sci. 50, 1873–1879.
Yanjun, Z., Guangyu, L., Bin, F., Qing, W., Ving, J., Aizhen, L., 2007. Study of hypoxia-induced expression of HIF-1alpha in retina pigment epithelium. Bull. Exp. Biol. Med. 143, 323–327.
Yatsiv, I., Grigoriadis, N., Simeonidou, C., Stahel, P.F., Schmidt, O.I., Alexandrovitch, A.G., Tsenter, J., Shohami, E., 2005. Erythropoietin is neuroprotective, improves functional recovery, and reduces neuronal apoptosis and inflammation in a rodent model of experimental closed head injury. FASEB J. 19, 1701–1703.
Yeo, E.J., Cho, Y.S., Kim, M.S., Park, J.W., 2008. Contribution of HIF-1alpha or HIF-2alpha to erythropoietin expression: in vivo evidence based on chromatin immunoprecipitation. Ann. Hematol. 87, 11–17.
Yoshida, T., Zhang, H., Iwase, T., Shen, J., Semenza, G.L., Campochiaro, P.A., 2010. Digoxin inhibits retinal ischemia-induced HIF-1{alpha} expression and ocular neovascularization. FASEB J. 24, 1759–1767.
Yu, D.Y., Cringle, S.J., 2001. Oxygen distribution and consumption within the retina in vascularised and avascular retinas and in animal models of retinal disease. Prog. Retin. Eye Res. 20, 175–208.
Yu, D.Y., Cringle, S.J., 2002. Outer retinal anoxia during dark adaptation is not a general property of mammalian retinas. Comp. Biochem. Physiol. A. Mol. Integr. Physiol. 132, 47–52.
Yu, D.Y., Cringle, S.J., 2005. Retinal degeneration and local oxygen metabolism. Exp. Eye Res. 80, 745–751.
Yu, D.Y., Cringle, S.J., Alder, V.A., Su, E.N., 1994. Intraretinal oxygen distribution in rats as a function of systemic blood pressure. Am. J. Physiol. 267, H2498–H2507.
Yu, D.Y., Cringle, S.J., Su, E.N., 2005. Intraretinal oxygen distribution in the monkey retina and the response to systemic hyperoxia. Invest. Ophthalmol. Vis. Sci. 46, 4728–4733.
Yu, D.Y., Cringle, S.J., Su, E.N., Yu, P.K., Jerums, G., Cooper, M.E., 2001. Pathogenesis and intervention strategies in diabetic retinopathy. Clin. Exp. Ophthalmol. 29, 164–166.
Yu, D.Y., Cringle, S.J., Yu, P.K., Su, E.N., 2007. Intraretinal oxygen distribution and consumption during retinal artery occlusion and graded hyperoxic ventilation in the rat. Invest. Ophthalmol. Vis. Sci. 48, 2290–2296.
Yuan, G., Nanduri, J., Khan, S., Semenza, G.L., Prabhakar, N.R., 2008. Induction of HIF-1alpha expression by intermittent hypoxia: involvement of NADPH oxidase, Ca2+ signaling, prolyl hydroxylases, and mTOR. J. Cell. Physiol. 217, 674–685.
Zanjani, E.D., Ascensao, J.L., McGlave, P.B., Banisadre, M., Ash, R.C., 1981. Studies on the liver to kidney switch of erythropoietin production. J. Clin. Invest. 67, 1183–1188.
Zhang, C., Rosenbaum, D.M., Shaikh, A.R., Li, Q., Rosenbaum, P.S., Pelham, D.J., Roth, S., 2002. Ischemic preconditioning attenuates apoptotic cell death in the rat retina. Invest. Ophthalmol. Vis. Sci. 43, 3059–3066.
Zhang, C., Wang, Y.S., Wu, H., Zhang, Z.X., Cai, Y., Hou, H.Y., Zhao, W., Yang, X.M., Ma, J.X., 2010a. Inhibitory efficacy of hypoxia-inducible factor 1alpha short hairpin RNA plasmid DNA-loaded poly (D, L-lactide-co-glycolide) nanoparticles on choroidal neovascularization in a laser-induced rat model. Gene Ther. 17, 338–351.
Zhang, J., Hu, L.M., Xu, G., Wu, Y., Shen, J., Luo, Y., Zhong, Y., Sinclair, S.H., Yanoff, M., Li, W., Xu, G.T., 2010b. Anti-VEGF effects of intravitreal erythropoietin in early diabetic retinopathy. Front. Biosci. (Elite Ed.) 2, 912–927.
Zhang, F., Wang, S., Cao, G., Gao, Y., Chen, J., 2007a. Signal transducers and activators of transcription 5 contributes to erythropoietin-mediated neuroprotection against hippocampal neuronal death after transient global cerebral ischemia. Neurobiol. Dis. 25, 45–53.
Zhang, P., Wang, Y., Hui, Y., Hu, D., Wang, H., Zhou, J., Du, H., 2007b. Inhibition of VEGF expression by targeting HIF-1 alpha with small interference RNA in human RPE cells. Ophthalmologica 221, 411–417.
Zhang, J., Wu, Y., Jin, Y., Ji, F., Sinclair, S.H., Luo, Y., Xu, G., Lu, L., Dai, W., Yanoff, M., Li, W., Xu, G.T., 2008a. Intravitreal injection of erythropoietin protects both retinal vascular and neuronal cells in early diabetes. Invest. Ophthalmol. Vis. Sci. 49, 732–742.
Zhang, J.F., Wu, Y.L., Xu, J.Y., Ye, W., Zhang, Y., Weng, H., Shi, W.D., Xu, G.X., Lu, L., Dai, W., Sinclair, S.H., Li, W.Y., Xu, G.T., 2008b. Pharmacokinetic and toxicity study of intravitreal erythropoietin in rabbits. Acta Pharmacol. Sin. 29, 1383–1390.
Zhang, Y., Stone, J., 1997. Role of astrocytes in the control of developing retinal vessels. Invest. Ophthalmol. Vis. Sci. 38, 1653–1666.
Zhao, W., Wang, Y.S., Hui, Y.N., Zhu, J., Zhang, P., Li, X., Dou, G.R., 2008. Inhibition of proliferation, migration and tube formation of choroidal microvascular endothelial cells by targeting HIF-1alpha with short hairpin RNA-expressing plasmid DNA in human RPE cells in a coculture system. Graefes Arch. Clin. Exp. Ophthalmol. 246, 1413–1422.
Zheng, L., Gong, B., Hatala, D.A., Kern, T.S., 2007. Retinal ischemia and reperfusion causes capillary degeneration: similarities to diabetes. Invest. Ophthalmol. Vis. Sci. 48, 361–367.

Zhong, L., Bradley, J., Schubert, W., Ahmed, E., Adamis, A.P., Shima, D.T., Robinson, G.S., Ng, Y.S., 2007a. Erythropoietin promotes survival of retinal ganglion cells in DBA/2J glaucoma mice. Invest. Ophthalmol. Vis. Sci. 48, 1212–1218.

Zhong, Y., Yao, H., Deng, L., Cheng, Y., Zhou, X., 2007b. Promotion of neurite outgrowth and protective effect of erythropoietin on the retinal neurons of rats. Graefes Arch. Clin. Exp. Ophthalmol. 245, 1859–1867.

Zhu, B., Wang, W., Gu, Q., Xu, X., 2008a. Erythropoietin protects retinal neurons and glial cells in early-stage streptozotocin-induced diabetic rats. Exp. Eye Res. 86, 375–382.

Zhu, Y., Zhang, L., Gidday, J.M., 2008b. Deferroxamine preconditioning promotes long-lasting retinal ischemic tolerance. J. Ocul. Pharmacol. Ther. 24, 527–535.

Zhu, Y., Ohlemiller, K.K., McMahan, B.K., Gidday, J.M., 2002. Mouse models of retinal ischemic tolerance. Invest. Ophthalmol. Vis. Sci. 43, 1903–1911.

Zhu, Y., Ohlemiller, K.K., McMahan, B.K., Park, T.S., Gidday, J.M., 2006. Constitutive nitric oxide synthase activity is required to trigger ischemic tolerance in mouse retina. Exp. Eye Res. 82, 153–163.

Zhu, Y., Zhang, Y., Ojwang, B.A., Brantley, M.A.J., Gidday, J.M., 2007. Long-term tolerance to retinal ischemia by repetitive hypoxic preconditioning: role of HIF-1alpha and heme oxygenase-1. Invest. Ophthalmol. Vis. Sci. 48, 1735–1743.

11 Additional Publications

11.1 Retina-specific Activation of a Sustained Hypoxia-like Response Leads to Severe Retinal Degeneration and Loss of Vision

Christina Lange[1], Christian Caprara[1], Naoyuki Tanimoto[3], Susanne Beck[3], Gesine Huber[3], Marijana Samardzija[1], Mathias Seeliger[3], Christian Grimm[1, 2]

[1] Lab for Retinal Cell Biology, Department Ophthalmology, University of Zurich, Zurich, Switzerland

[2] Zurich Center for Integrative Human Physiology (ZIHP), University of Zurich, Zurich, Switzerland

[3] Institute of Ophthalmic Research, Centre of Ophthalmology, Division of Ocular Neurodegeneration, Tübingen, Germany

Published in Neurobiology of Disease, 2011, **41**(1):119-130

Personal Contribution

Performed immunostaining on retinal flatmounts to visualize blood vessels (Fig.3A)

Key Findings

Hypoxic preconditioning has been previously shown to protect photoreceptors from light-induced degeneration. Hypoxic preconditioning stabilizes and activates HIFs, which play a major role in the hypoxic response of tissues including the retina. To investigate the roles of HIFs in retinal development, angiogenesis, and neuroprotection, HIFA proteins were stabilized in normoxia by ablating VHL in a heterogeneous population of cells in the retinal periphery.

Here are some of the key findings of the study:

- a retina-specific knockdown of von Hippel-Lindau protein (VHL) activated HIF transcription factors in normoxic conditions in the retina.
- sustained activation of HIF1 and HIF2 was accompanied by persisting embryonic vasculatures in the posterior eye and the iris
- embryonic vessels persisted into adulthood and led to a severely abnormal mature vessel system with vessels penetrating the photoreceptor layer in adult mice.
- massive cell death accompanied by severe retinal degeneration was observed in all retinal layers of adult mice

Neurobiology of Disease 41 (2011) 119–130

Contents lists available at ScienceDirect

Neurobiology of Disease

journal homepage: www.elsevier.com/locate/ynbdi

Retina-specific activation of a sustained hypoxia-like response leads to severe retinal degeneration and loss of vision

Christina Lange [a,*], Christian Caprara [a], Naoyuki Tanimoto [c], Susanne Beck [c], Gesine Huber [c], Marijana Samardzija [a], Mathias Seeliger [c], Christian Grimm [a,b]

[a] Lab for Retinal Cell Biology, Department Ophthalmology, University of Zurich, Zurich, Switzerland
[b] Zurich Center for Integrative Human Physiology (ZIHP), University of Zurich, Zurich, Switzerland
[c] Institute of Ophthalmic Research, Centre of Ophthalmology, Division of Ocular Neurodegeneration, Tübingen, Germany

ARTICLE INFO

Article history:
Received 18 June 2010
Revised 17 August 2010
Accepted 25 August 2010
Available online 15 September 2010

Keywords:
Von Hippel-Lindau
HIF
Caspase
Retinal degeneration
Vasculature
Retina
Photoreceptor

ABSTRACT

Loss of vision and blindness in human patients is often caused by the degeneration of neuronal cells in the retina. In mouse models, photoreceptors can be protected from death by hypoxic preconditioning. Preconditioning in low oxygen stabilizes and activates hypoxia inducible transcription factors (HIFs), which play a major role in the hypoxic response of tissues including the retina. We show that a tissue-specific knockdown of von Hippel-Lindau protein (VHL) activated HIF transcription factors in normoxic conditions in the retina. Sustained activation of HIF1 and HIF2 was accompanied by persisting embryonic vasculatures in the posterior eye and the iris. Embryonic vessels persisted into adulthood and led to a severely abnormal mature vessel system with vessels penetrating the photoreceptor layer in adult mice. The sustained hypoxia-like response also activated the leukemia inhibitory factor (LIF)-controlled endogenous molecular cell survival pathway. However, this was not sufficient to protect the retina against massive cell death in all retinal layers of adult mice. Caspases 1, 3 and 8 were upregulated during the degeneration as were several VHL target genes connected to the extracellular matrix. Misregulation of these genes may influence retinal structure and may therefore facilitate growth of vessels into the photoreceptor layer. Thus, an early and sustained activation of a hypoxia-like response in retinal cells leads to abnormal vasculature and severe retinal degeneration in the adult mouse retina.

Introduction

Retinitis pigmentosa (RP) is a major cause of severe visual impairment or blindness in humans. It is characterized by an initial loss of photoreceptors in the peripheral retina causing tunnel vision. As photoreceptor degeneration progresses, affected patients loose vision also in the center leading to complete blindness. Although mechanisms of cell death in RP and other degenerative diseases of the retina have been a subject of intense investigations, the exact molecular events leading to loss of photoreceptors have not been defined. As a consequence, only little is known about possible ways to inhibit cell death by neuroprotective approaches. In experimental model systems, preconditioning by hypoxia or light – the pre-exposure of mice to low oxygen concentrations or to non-damaging levels of light, respectively – protects photoreceptors from light induced degeneration (Grimm et al., 2002; Grimm et al., 2006; Chollangi et al., 2009). These systems may thus be valuable tools to study and develop neuroprotective measures to delay photoreceptor apoptosis.

Conditions of low oxygen availability (hypoxia) activate hypoxia inducible transcription factors (HIFs), which may regulate potentially protective genes during hypoxic preconditioning. HIFs are heterodimeric factors consisting of an α- and a β-subunit. Three isoforms of the α-subunit, HIF1A, HIF2A and HIF3A, and one form of the β-subunit, called aryl-hydrocarbon receptor nuclear translocator (ARNT), are known. ARNT is constitutively expressed and located in the nucleus. In conditions of normal oxygen availability (normoxia) HIF-α subunits are constantly degraded through the proteasomal pathway. Prolyl hydroxylases (PHDs or EGLNs) hydroxylate HIF-α subunits turning them into a binding substrate for the von Hippel-Lindau (VHL) protein complex that includes VHL, Cullin-2, Rbx1, the Elongins B and C and an E3-ubiquitinase (Kibel et al., 1995; Iwai et al., 1999; Kamura et al., 1999). Subsequent ubiquitination targets the HIF-α subunits to proteasomal degradation (Huang et al., 1998; Ivan et al., 2001). The function of PHDs depends on oxygen as a substrate. Hence, during hypoxia, hydroxylation does not occur and the VHL complex cannot bind to HIF-α. HIF-α is stabilized, enters the nucleus, binds ARNT and p300 as a transcriptional co-activator and participates in the regulation of gene expression.

* Corresponding author. Lab for Retinal Cell Biology, Department Ophthalmology, University of Zurich, CH 8091 Zurich, Switzerland. Fax: +41 44 255 43 85.
E-mail address: christina.lange@usz.ch (C. Lange).
Available online on ScienceDirect (www.sciencedirect.com).

0969-9961/$ – see front matter © 2010 Elsevier Inc. All rights reserved.
doi:10.1016/j.nbd.2010.08.028

It has been shown that hypoxic exposure of mice stabilizes and activates HIF1A and HIF2A in the retina (Grimm et al., 2002; Thiersch et al., 2009). However, it is unknown whether activation of HIF transcription factors is sufficient to protect photoreceptors from light induced degeneration as observed after hypoxic preconditioning. Inactivation of VHL prevents degradation of HIF-α subunits and leads to constitutively active HIFs even in normoxia (Haase et al., 2001). Long-term stabilization of HIF transcription factors during normoxia in the retina might provide information about the contribution of HIF to neuroprotection by hypoxic preconditioning. However, overactivation of HIFs may lead to excessive blood vessel growth, a phenomenon particularly important in tumor biology (Senger et al., 1983). In addition, a recent report shows that untimely activation of HIFs during retinal development causes a severely disturbed retinal vasculature (Kurihara et al., 2010).

To activate HIFs in normoxia, we generated a *Vhl* knockdown mouse using the Cre-lox system with Cre-recombinase being expressed under the control of the α-element of the Pax6-promotor. This promoter is active as early as E10.5 and leads to the deletion of floxed sequences in the distal retina and in the iris, but not in the lens or the retinal pigment epithelium (Marquardt et al., 2001). In accordance with a recent report, we show that development of the retinal vasculature is severely disturbed early during development in the *vhl* knockdown mouse (Kurihara et al., 2010). In addition we show that embryonic vasculature persists into adulthood and that the *vhl* knockdown also results in severe cell death in the ageing retina with an increase of *Casp-8* and *Casp-1* expression and induction of HIF-independent stress response pathways.

Materials and methods

Mice and genotyping

Mice were treated in accordance with the regulations of the Veterinary Authority of Zurich and with the statement of 'The Association for Research in Vision and Ophthalmology' for the use of animals in research. 129S-Vhlh^{tm1jae}/J-mice (from now on referred to as *vhl*$^{flox/flox}$ mice), which have *lox*P sites flanking exon 1 and part of the promoter of the *Vhl* gene (Haase et al., 2001) were purchased from Jackson Laboratory (Bar Harbor, USA). To generate retina-specific *Vhl* knockdown mice, *vhl*$^{flox/flox}$ mice were crossed with mice expressing Cre-recombinase under the control of the α-element of the Pax6-promotor (α-Cre), which leads to the deletion of floxed sequences in the distal retina and in the iris (Marquardt et al., 2001). Breeding pairs were established to generate *vhl*$^{flox/flox}$;*α-cre* and *vhl*$^{flox/flox}$ control littermates. The following primers were used to detect wild-type (wt) and *Vhl*-flox alleles: forw (5′-TGAGTATGGGATAACGGGTTGAAC-3') and rev (5'-AGAACTGACTGACTTC CACTGATGC-3′). The wt allele was identified as a 125-bp and the *Vhl*-flox allele as a 317-bp long fragment on a 1.5% agarose gel. Presence of the α-Cre transgene was tested by PCR using the following primer pair: forw (5′-AGGTGTAGA-GAAGG CACTTAGC-3′) and rev (5′-CTAATCGCCATCTTCCAGCAGG-3′). Amplification resulted in a 411-bp fragment.

To detect excision of floxed sequences in the *Vhl* gene, genomic DNA from retina was isolated and tested by PCR using the following primers: forw_un-excised (5′-CTGGTACCCACGAAACTGTC-3′), for-w_excised (5′-CTAGGCACCGAGCTTAG AGGTTTGCG-3′) and rev_both (5′-CTGACTTCCACTGATGCTTGTCACAG-3′). The excised allele was identified as a 260-bp and the un-excised allele as a 460-bp fragment.

RNA, DNA and protein preparation

Retinas were removed through a slit in the cornea and immediately frozen in liquid nitrogen. Total RNA was prepared using the RNeasy RNA isolation kit (Qiagen, Hilden, Germany) according to the manufacturer's directions including a DNase treatment to digest residual genomic DNA. Equal amounts of RNA were used for reverse transcription using oligo(dT) primer and M-MLV reverse transcriptase (Promega, Madison, WI, USA).

For retinal genomic DNA isolation, 10 μl of the homogenate prepared for RNA isolation (RNeasy RNA isolation; see above) was processed with the QIAamp DNA Blood Mini Kit (Qiagen) according to the manufacturer's directions but without proteinase K treatment and heating.

For protein isolation retinas were homogenized by sonication in 100 mM Tris/HCl, pH 8.0, and analyzed for protein content using Bradford reagent. The 4× Laemmli buffer was added and samples were heated for 10 min at 75 °C before loading onto an SDS–PAGE gel for Western blotting (see below).

Semi-quantitative real-time polymerase chain reaction (PCR)

Relative quantification of cDNA was done by semi-quantitative real-time PCR using the LightCycler 480 SybrGreen I Master kit, a LightCycler 480 instrument (Roche Diagnostics, Basel, Switzerland) and specific primer pairs (Table 1). Three animals per time point were analyzed in duplicates and normalized to *β-actin* using the Light Cycler 480 software (Roche Diagnostics, Basel, Switzerland). Values of experimental retinas were expressed relative to the first time point tested, which was set to 1. Significance of differences between expression levels at specific time points in wild-type and knockdown mice was tested using an unpaired Student's *t*-test.

Western blotting

Standard SDS–PAGE (10%) and Western blotting of 40 μg of total retinal extracts were performed. For immunodetection, the following antibodies were used: anti-HIF1A (#Nb100-479 Novus Biologicals, Cambridge, United Kingdom, 1:1000), anti-HIF2A (#Nb100-122, Novus Biologicals, 1:1000), anti-pSTAT3 (#9131 Cell Signaling Technology, 1:500), anti-STAT3 (#9132 Cell Signaling Technology, 1: 1000), anti-GFAP (MAB302 Chemicon/Millipore, Billerica, USA, 1:500), CASP1, CASP3, CASP8 (all kindly provided by Peter Vandenabeele, Ghent University, Belgium, all 1:10000), CASP9 (#9504, Cell Signaling Technology, 1:500) and anti-ACTB (#A5441 Sigma, St. Louis, MO, USA, 1:5000). Blots were incubated overnight at 4 °C with primary antibodies followed by a 1-hour incubation at room temperature (22 °C) with HRP-conjugated secondary antibodies. Immunoreactivity was visualized using the Western Lightning Chemiluminescence reagent (Perkin-Elmer, Boston, MA, USA).

Confocal scanning laser ophthalmoscopy (cSLO)

cSLOs were obtained according to previously reported procedures (Seeliger et al., 2005). Briefly, mice were anaesthetized by a subcutaneous injection of ketamine (66.7 mg/kg) and xylazine (11.7 mg/kg). Pupils were dilated with tropicamide eye drops (Mydriaticum Stulln, Pharma Stulln, Stulln, Germany) in anesthesia. cSLO imaging was performed with a Heidelberg Retina Angiograph (HRA I) equipped with an argon laser featuring two wavelengths (488 nm and 514 nm) in the short wavelength range and two infrared diode lasers (795 nm and 830 nm) in the long wavelength range. The 488-nm and the 795-nm lasers were used for fluorescein (FL) and indocyanine green (ICG) angiography, respectively. FL angiography was performed using a subcutaneous injection of 75 mg/kg body weight fluorescein-Na (University pharmacy, University of Tuebingen, Germany), and ICG angiograhy following an s.c. injection of 50 mg/kg body weight ICG (ICG-Pulsion, Pulsion Medical Systems AG, Munich, Germany).

Table 1
Primers used for real-time PCR.

Gene	Upstream (5′–3′)	Downstream (5′–3′)	Annealing	Product
β-actin	cgacatggagaagatctggc	caacggctccggcatgtgc	62	153
Casp1	ggcaggaattctggagcttcaa	gtcagtcctggaaatgtgcc	60	138
Casp3	ctggaatgtcatctcgctct	actgtctgtctcaatgccac	60	353
Casp8	ccacacaagaagcaggagacca	agcaggctcaagtcatcttccag	68	329
Casp9	ccaatgggactcacagcaaagg	ttctcaatggacacggagcatc	62	554
Cntf	agccttgactcagtggatggtg	atcagcctctttttcagggacc	58	276
Edn2	agacctcctccgaaagctg	ctggctgtagctggcaaag	60	64
Egln1	cattgttggcagaaggtgtg	caaaggactacagggtctcca	62	70
Egln2	gaacccacatgaggtgaagc	aacacctttctgtcccgatg	60	124
Egln3	tgtctggtacttcgatgctga	gcaagagcagattcagttttttct	60	84
Epas1	ggagctcaaaaggtgtcagg	caggtaaggctcgaacgatg	60	61
Epo	gccctgctagccaattcc	gccctgctagccaattcc	60	128
Fgf2	ggctgctggcttctaagtgt	tccgtgaccggtaagtgttg	62	87
Fn1	accagtgccaagattcagag	cttggtgatgtgtgaaggct	60	245
Fzd4	ctacaacgtgaccaagatgc	gggaatttgctgcagttcag	57	277
Gfap	ccaccaaactggctgatgtctac	ttctctccaaatccacacgagc	62	240
Gnat1	gaggatgctgagaaggatgc	tgaatgttgagcgtggtcat	58	209
Gnat2	gcatcagtgctgaggacaaa	ctaggcactcttcgggtgag	58	192
Hif1α	tcatcaggttgccacttccccac	ccgtcatctgttagcaccatcac	60	198
Klf10	cgtctagtgtctcagtgctc	gacttccagtcgcagctcat	62	243
Lif	aatgccacctgtgccatacg	caacttggtcttctctgtcccg	60	216
Opn1mw	tgtacatggtcaacaatcgga	acaccatctccagaatgcaag	58	153
Opn1sw	ctctgctacctccaagtgtgg	aagtatagggccccagcaga	58	154
Rho	cttcacctggatcatggcgtt	ttcgttgttgacctcaggcttg	62	130
Tgfbi	tcctcatgcgactgctgacc	cgacttgccgcagatcttcc	64	224
Tie1	tccagacaaggtcacacacacg	tcgcacgatgagccgaaagaag	60	256
Tek	ccatcaccataggaagggactttg	taggaaggacgcttgttgacgcatc	60	215
Tnf	ccacgctcttctgtctactga	ggccatagaactgatgagagg	62	92
Serpinf1	tccacagcacctacaaggag	taagccacgccaaggagaag	62	280
Vegfa	acttgtgttgggaggaggatgtc	aatgggtttgtcgtgtttctgg	60	171
Vhl	gagggacccgttccaataat	ttggcaaaaataggctgtcc	60	364

Spectral domain optical coherence tomography (SD-OCT)

SD-OCT imaging was done in the same session as cSLO, i.e. animals remained anaesthetized using identical preparatory steps. Mouse eyes were subjected to SD-OCT using the commercially available Spectralis™ HRA+SD-OCT device (Heidelberg Engineering, Heidelberg, Germany) featuring a broadband superluminescent diode at $\lambda = 870$ nm as low coherent light source. Each two-dimensional B-Scan recorded at 30° field of view consists of 1536 A-Scans, which are acquired at a speed of 40,000 scans per second. Optical depth resolution is around 7 µm with digital resolution reaching 3.5 µm (Huber et al., 2009). The optical adjustments to permit the use in mice were described previously (Fischer et al., 2009). Imaging was performed using the proprietary software package Eye Explorer version 3.2.1.0. The combination of scanning laser retinal imaging and SD-OCT allows for real-time tracking of eye movements and real-time averaging of SD-OCT scans, reducing speckle noise in the SD-OCT images considerably (Huber et al., 2009).

Retinal flat mounts and immunofluorescence

Eyes were collected and fixed for 3–5 min in 2% (w/v) paraformaldehyde (PFA) in PBS. The sclera was dissected from the eyes in PBS and lens, iris and vitreous were removed. The retina was flattened and stored in methanol at −20 °C. Before use, the retina was post-fixed in 4% (*w/v*) PFA in PBS for 10 min. For immunofluorescence, the flat-mounted retina was washed in PBS and incubated in blocking buffer (1% fetal bovine serum, 0.1% Triton X-100 in PBS) for 1 h at room temperature (22 °C). Flat mounts were incubated with Alexa594-coupled isolectin-A4 (#I21413, Invitrogen, Basel, Switzerland, 1:50) at 4 °C overnight, washed and mounted in MOWIOL anti-fade medium (10% Mowiol 4-88 (*w/v*) (Calbiochem, San Diego, CA, USA), in 100 mM Tris, pH 8.5, 25% glycerol (*w/v*) and 0.1% 1,4-diazabicyclo [2.2.2] octane (DABCO)), Calbiochem, San Diego, CA, USA). Signals on sections were analyzed with a digitalized Axiovision microscope (Carl Zeiss AG, Feldbach, Switzerland).

Retinal sections and immunofluorescence

After enucleation, eyes were fixed for 2 h in 4% PFA (w/v) at 4 °C before cornea and lens were removed. The remaining ocular tissue was post-fixed for an additional 2 h in 4% PFA at 4 °C, followed by cryoprotection in 30% sucrose in PBS, pH 7.4, at 4 °C overnight. Eyecups were embedded in tissue freezing medium (Leica Microsystems Nussloch GmbH, Nussloch, Germany) and frozen in a 2-methylbutane bath cooled by liquid nitrogen. Retinal sections (12 µm) were cut and blocked in 3% normal goat serum, 0.3% Triton X-100 in 0.1 M PBS (pH 7.4) for 1 h at room temperature. Sections were incubated in blocking solution at 4 °C overnight with one of the following primary antibodies: anti-IBA1 (#019-19741, Wako, Richmond, USA, 1:1000), isolectin-A4 (# L1509; Sigma, St. Louis, MO, USA, 1:50, coupled to FITC), anti-rod opsin (kindly provided by David Hicks, 1:100) and anti-swl-cone opsin (#sc-14363, Santa Cruz Biotechnology, Santa Cruz, CA, USA, 1:500). After 3 washes with PBS, slides were incubated with the appropriate secondary antibody coupled to Cy3 for 1 h at room temperature, counterstained with DAPI and mounted with MOWIOL anti-fade medium (10% Mowiol 4-88 (*w/v*)). Signals on sections were analyzed with a digitalized Axiovision microscope (Carl Zeiss AG, Feldbach, Switzerland).

Morphology

For light microscopy, eyes were fixed in 2.5% glutaraldehyde in 0.1 M cacodylate buffer (pH 7.3) at 4 °C overnight. For each eye, the superior and the inferior retina were prepared, washed in cacodylate buffer, incubated in osmium tetroxide for 1 h, dehydrated and embedded in Epon 812. Sections (0.5 µm) were prepared from the lower central retina and counterstained with methylene blue.

Electroretinographic analysis

Electroretinograms (ERGs) were recorded according to previously described procedures (Seeliger et al., 2001; Tanimoto et al., 2009). The ERG equipment consisted of a Ganzfeld bowl, a direct current amplifier, and a PC-based control and recording unit (Multiliner Vision; VIASYS Healthcare GmbH, Hoechberg, Germany). Mice were dark-adapted overnight and anaesthetized with ketamine (66.7 mg/kg body weight) and xylazine (11.7 mg/kg body weight). Pupils were dilated and single flash ERG responses were obtained under dark-adapted (scotopic) and light-adapted (photopic) conditions. Light adaptation was accomplished with a background illumination of 30 candela (cd) per square meter starting 10 min before recording. Single white-flash stimulus intensity ranged from −4 to 1.5 log cd·s/m^2 under scotopic and from −2 to 1.5 log cd·s/m^2 under photopic conditions, divided into 10 and 8 steps, respectively. Ten responses were averaged with an inter-stimulus interval (ISI) of either 5 seconds (for −4, −3, −2, −1.5, −1 and −0.5 log cd·s/m^2) or 17 seconds (for 0, 0.5, 1 and 1.5 log cd·s/m^2).

Results

Tissue-specific knockdown of Vhl leads to HIFα stabilization in the retina

Analysis of genomic DNA from retinal tissue showed that excision of floxed DNA sequences was obvious in mice expressing Cre-recombinase but not in control mice (Fig. 1A). Accordingly, expression of *Vhl* was significantly reduced in retinas of *vhl*$^{flox/flox}$;*α-cre* mice as compared to *vhl*$^{flox/flox}$ littermates. Strongest reduction was observed at 28 days of age ($P = 0.0044$, Fig. 1B). Surprisingly, expression of *Hif1a*, but not of *Hif2a (Epas1)* was also affected by the *Vhl* knockdown. *Hif1a* was significantly down-regulated up to 1.7 fold (at 28 d, $P = 0.0094$) in *vhl*$^{flox/flox}$;*α-cre* mice until 42 days of age (Fig. 1B). In contrast, expression of the prolyl hydroxylases *Phd2* (*Egln1*) and especially of *Phd3* (*Egln3*) was significantly and strongly induced in the *Vhl* knockdown retinas at early time points (*Egln1*) or throughout the analyzed period (*Egln3*). Expression of *Phd1* (*Egln2*) was not affected by the knockdown. Since VHL controls levels of HIF-α transcription factors by regulating protein stability, we tested levels of

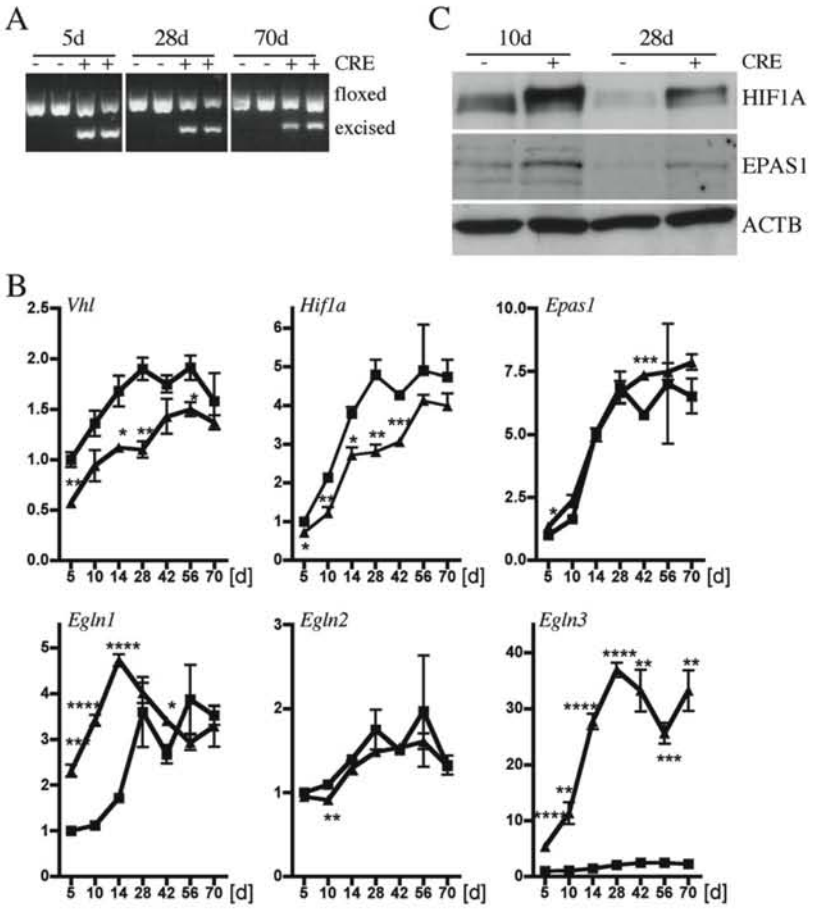

Fig. 1. Hypoxia-like response in *Vhl* knockdown retinas. (A) PCR amplification of genomic DNA isolated from retinal tissue at indicated postnatal days to test Cre-mediated excision of floxed *Vhl* sequences. The un-excised allele (floxed) has a length of 460 bp in both *vhl*$^{flox/flox}$ and *vhl*$^{flox/flox}$;*α-cre* mice. The excised allele (excised) was identified as a 260-bp band in *vhl*$^{flox/flox}$;*α-cre* mice. (B) Semi-quantitative real-time PCR of *Vhl*, *Hif1a*, *Hif2a* (*Epas1*), *Phd2* (*Egln1*), *Phd1* (*Egln2*) and *Phd3* (*Egln3*) in *vhl*$^{flox/flox}$ (squares) and *vhl*$^{flox/flox}$;*α-cre* (triangles) at postnatal days (d) as indicated. Given are mean values ± SD of 3 retinas amplified in duplicates. Values were normalized to *β-actin* and expressed relatively to the first time point (5d) in *vhl*$^{flox/flox}$ mice. (C) Western blot analysis of whole retinal extracts from 10- and 28-day-old *vhl*$^{flox/flox}$;*α-cre* (CRE+) and *vhl*$^{flox/flox}$ (CRE−) mice. β-Actin (ACTB) served as a control for equal loading. *$p<0.05$, **$p<0.01$, ***$p<0.001$, ****$p<0.0001$. Significance between *vhl*$^{flox/flox}$ and *vhl*$^{flox/flox}$;*α-cre* mice was calculated for individual time points by an unpaired *t*-test.

HIF1A and HIF2A (EPAS1) in retinas of 10- and 28-day-old knockdown mice and wild-type littermates. Retinal HIF1A levels are high after birth and decrease with the development of the retinal vasculature (Grimm et al., 2005). In knockdown mice, HIF1A and HIF2A levels were increased at both ages tested (Fig. 1C). Levels of HIF1A decreased with time in retinas of both control and knockdown mice (cross-compare 10d and 28d). Whereas this was expected for wild-type retinas (Grimm et al., 2005), the reduction in HIF1A stability in adult *Vhl* knockdowns probably reflects the restricted loss of VHL activity in the peripheral but not central retina (see below). Thus, in the adult knockdown mice HIF1A is only stabilized in the retinal periphery, in contrast to retinas at 10 days of age where normal development additionally stabilizes HIF1A also in the central retina.

Abnormal vasculature in retina and iris of Vhl knockdown mice

The retinal vasculature of $vhl^{flox/flox}$;*α-cre* mice was assessed with confocal scanning laser ophthalmoscopy (cSLO) in conjunction with fluorescein (FL) and indocyanine green (ICG), which are clinically established dyes to visualize the retinal and choroidal circulation, respectively. ICG angiography depicts both retinal and choroidal structures, whereas FL angiography imaging yields particularly detailed information about retinal capillaries, but not choroidal vessels (Seeliger et al., 2005). We found no indications that either the retinal or the choroidal vascular system of $vhl^{flox/flox}$ mice at the age of 10 weeks was abnormal; they were rather comparable to that of wild-type strains like C57BL/6 (Seeliger et al., 2005). However, in $vhl^{flox/flox}$;*α-cre* mice, abnormal retinal vessels and persistent remnants of the developmental hyaloidal vascular system (Ito and Yoshioka, 1999) were found (Fig. 2A), while choroidal structures appeared unaltered. Retinal vessel density was particularly reduced in the peripheral retina, probably because topographical differences in Cre activity translated into differences in the excision efficiency of floxed sequences (Kurihara et al., 2010; Marquardt et al., 2001). Persistent hyaloidal vessels originating from the optic disc were still present in the vitreous just above the retinal surface at 10 weeks of age. These vessels were functional as they filled with dye in angiography. SD-OCT imaging confirmed the optic disc area as the region of origin of these persisting hyaloidal vessels in $vhl^{flox/flox}$;*α-cre* mice (Fig. 2B). These results extend observations made by Kurihara et al. (2010) who reported persistent hyaloidal vessels only up to postnatal day 6 in the $vhl^{flox/flox}$;*α-cre* mouse (Kurihara et al., 2010). In addition to the abnormal retinal and hyaloidal vessels, 10-week-old $vhl^{flox/flox}$;*α-cre* mice also had an extremely under-developed iris vasculature and a persisting pupillary membrane (Ito and Yoshioka, 1999) (Fig. 2A, white arrow).

Normally, the mature retinal vasculature is fully developed at postnatal day 35 (Fruttiger, 2002) (Fig. 3A). Retinal flatmounts (stained with isolectin-A4) of $vhl^{flox/flox}$ mice showed normal vascular architecture (Fig. 3A upper panels). However, the vasculature of $vhl^{flox/flox}$;*α-cre* mice at 35 days of age was severely under-developed with a strongly reduced density of the capillary network in the retinal periphery. Immunofluorescence stainings of retinal cryosections from $vhl^{flox/flox}$;*α-cre* mice revealed that the capillaries in the deep plexi did not or not completely develop (Fig. 3B, isolectin-A4 staining in green, and data not shown). Instead some retinal vessels in the periphery grew into the outer nuclear layer (ONL; Fig. 3B, arrow). These vessels originated from the retinal vasculature because we did not detect any sprouting vessels in the choroid or vessels penetrating the RPE layer (Fig. 3B and data not shown). This angiogenic vessel-growth activated

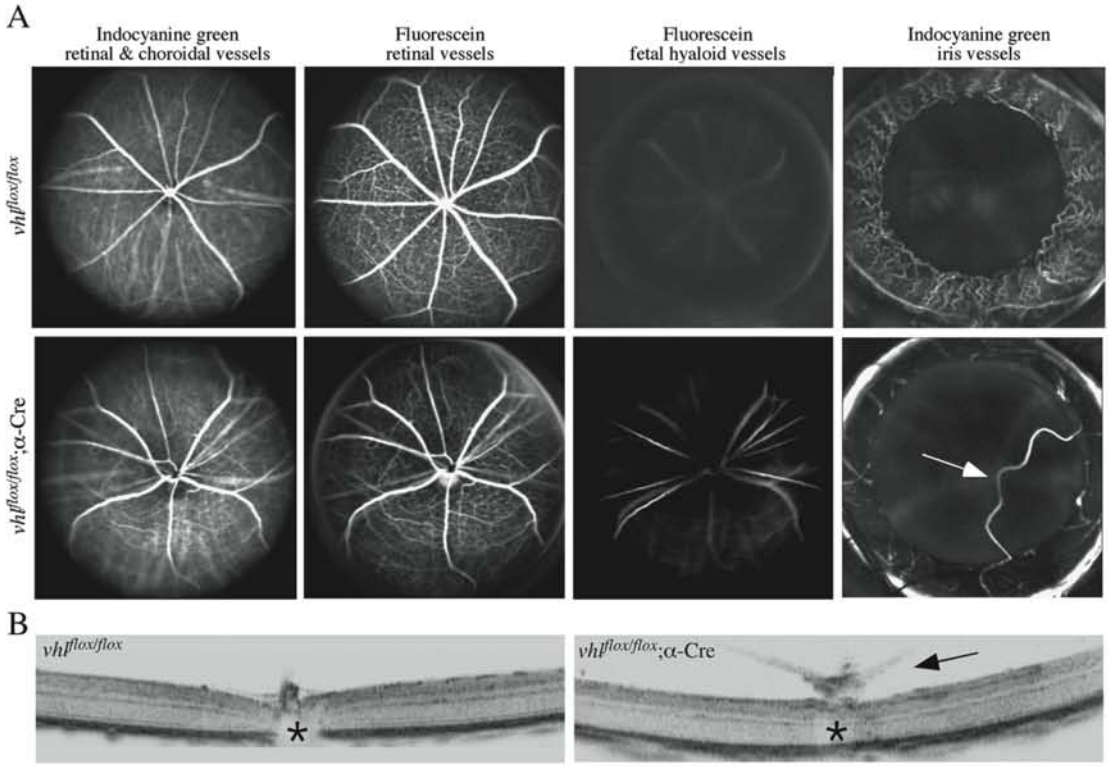

Fig. 2. Abnormal ocular vasculature in $vhl^{flox/flox}$;*α-cre* mice. (A) *In vivo* cSLO imaging of 10–week-old $vhl^{flox/flox}$ and $vhl^{flox/flox}$;*α-cre* mice with ICG (795 nm) and FA (488 nm) angiography to ocular vessels as indicated. Adjustment of the optical plane allowed the visualization of remnant hyaloidal vessels (second from right) and of the abnormal vasculature in the iris (right) in $vhl^{flox/flox}$;*α-cre* mice. White arrow: persistent pupillary membrane. (B) Cross-sectional imaging of $vlh^{flox/flox}$ (left) and $vhl^{flox/flox}$;*α-cre* (right) mice using SD-OCT. *Optic nerve head; black arrow: persistent hyaloidal vessels emerging from optic nerve head.

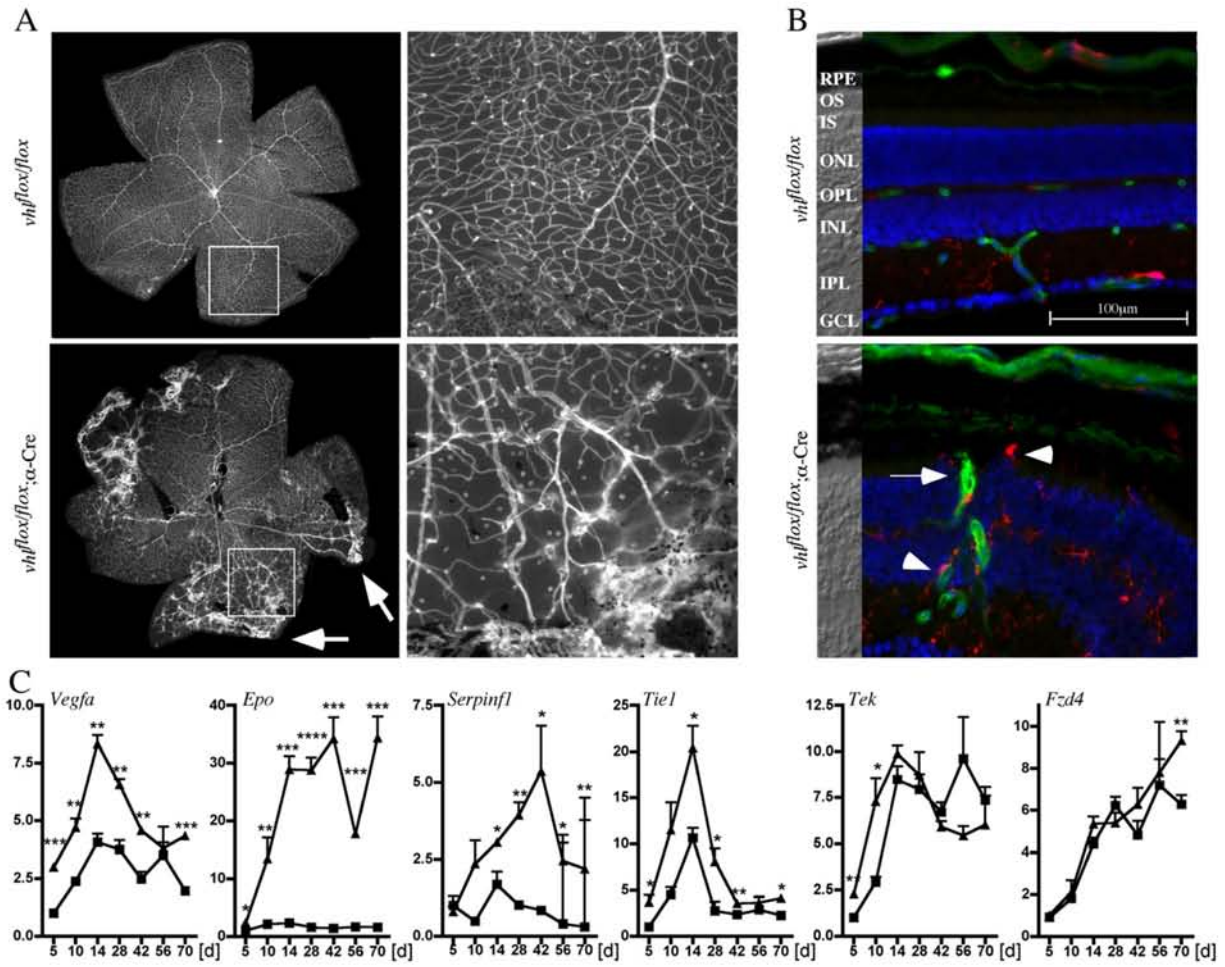

Fig. 3. Abnormal retinal vasculature in $vhl^{flox/flox}$;*α-cre* mice. (A) Retinal flat mounts of 35-day-old $vhl^{flox/flox}$ (top) and $vhl^{flox/flox}$;*α-cre* (bottom) mice stained with isolectin-A4 to visualize blood vessels. Shown are overviews over the whole retinal flat mount and enlarged representative areas (square). Arrows: retinal vessel growth at the retinal periphery. (B) Retinal cross sections of 35-day-old $vhl^{flox/flox}$ (top) and $vhl^{flox/flox}$;*α-cre* (bottom) mice stained for vessels using isolectin-A4 (green) and microglia using anti-IBA1 antibodies (red). DAPI (blue) stained nuclei and nomarski images (gray) are shown for orientation. Shown are representative areas of the peripheral inferior retina. Arrow: abnormal vessel growth into the ONL. Arrowheads: microglia located along ingrown vessels and in the photoreceptor segment layer. (C) Semi-quantitative real-time PCR for expression of *Vegfa*, *Epo*, *Pedf* (*Serpinf1*), *Tie1*, *Tie2* (*Tek*) and *Fzd4* in $vhl^{flox/flox}$ (squares) and $vhl^{flox/flox}$;*α-cre* (triangles) mice at postnatal days (d) as indicated. Given are mean values ± SD of 3 retinas amplified in duplicates. Values were normalized to *β-actin* and expressed relatively to the first time point (5d) in $vhl^{flox/flox}$ mice. RPE: retinal pigment epithelium. OS: photoreceptor outer segments. IS: photoreceptor inner segments. ONL: outer nuclear layer. IPL: inner plexiform layer. INL: inner nuclear layer. GCL: ganglion cell layer. $^{*}p<0.05$, $^{**}p<0.01$, $^{***}p<0.001$, $^{****}p<0.0001$. Significance between $vhl^{flox/flox}$ and $vhl^{flox/flox}$;*α-cre* mice was calculated for individual time points by an unpaired *t*-test.

resident microglia. In wild-type controls, microglia are located mostly to the GCL and IPL (Fig. 3B, IBA1 staining in red). In the *Vhl* knockdown mice, however, many microglia were found in the OPL and along ingrown vessels. Some microglia were even located in the layer of the photoreceptor segments (Fig. 3B, arrowheads). In the central retina, the vasculature of $vhl^{flox/flox}$;*α-cre* mice was comparable to controls (Fig. 3A and data not shown).

The abnormal development of the retinal vasculature may have partly been caused by the increased and sustained expression of the pro-angiogenic genes *Vegfa* and *Epo* (Fig. 3C). Both genes are known to be strongly regulated by HIF transcription factors, which were stabilized in the *Vhl* knockdown retinas (see above). *Serpinf1* encodes pigment epithelium derived factor (PEDF), a neuroprotective and anti-angiogenic protein (Barnstable and Tombran-Tink, 2004). Its increased expression (Fig. 3C) may suggest that the retinal response to the disturbed vascular development involves activation of endogenous protective systems (see also below). Other HIF-inducible and angiogenesis-related genes (*Tie1*, *Tie2* (*Tek*) and *Fzd4*), however, were not or only slightly induced in $vhl^{flox/flox}$;*α-cre* compared to $vhl^{flox/flox}$ mice.

These data show that lack of functional VHL during development and in the mature retina leads to an upregulation of several angiogenic factors, the persistence of the embryonic ocular vasculature (hyaloidal vessels, pupillary membrane) deep into adulthood and to a disturbed and severely under-developed vessel system in the mature retina and iris.

Degeneration of photoreceptors in $vhl^{flox/flox}$;α-cre mice

Ongoing angiogenesis and growth of vessels into the ONL may affect retinal morphology and function, as well as cell physiology and survival. Retinal sections from 2-week-old (Figs. 4A and B) and 10-week-old (Figs. 4C and D) mice were prepared and analyzed by light microscopy. The peripheral retina of 2-week-old $vhl^{flox/flox}$;*α-cre* mice showed structural abnormalities especially in the ONL. Photoreceptor nuclei were not aligned properly affecting also the layering of the cells in the

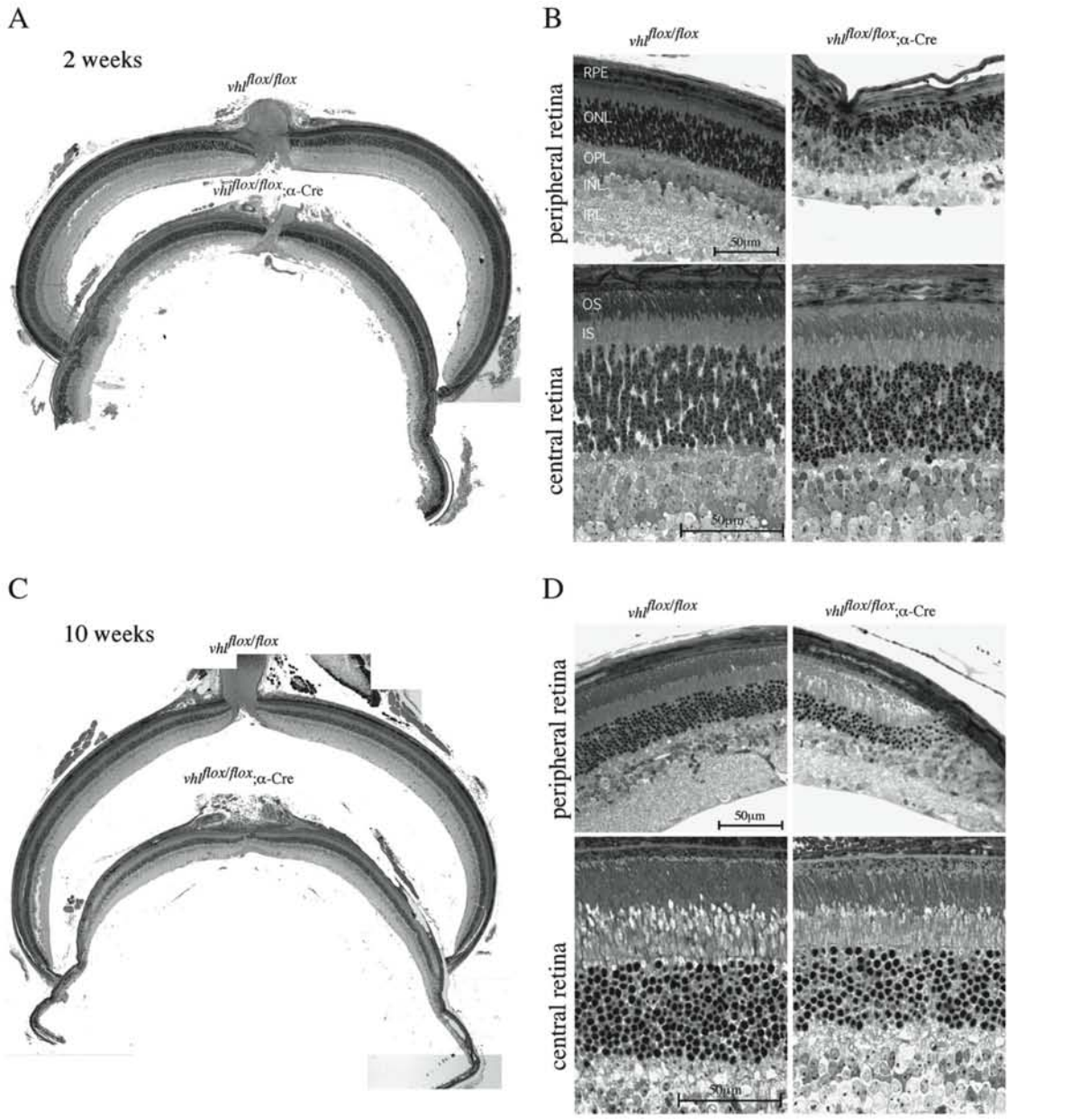

Fig. 4. Retinal degeneration in $vhl^{flox/flox}$;*α-cre* mice. Retinal morphology of 2-week-old (A, B), and 10-week-old (C, D) $vhl^{flox/flox}$ and $vhl^{flox/flox}$;*α-cre* mice as indicated. (A, C) Overviews over the whole retinal morphology. (B, D) Higher magnification pictures of the central and peripheral retina (as indicated). RPE: retinal pigment epithelium. IS: photoreceptor inner segments. OS: photoreceptor outer segments. ONL: outer nuclear layer. IPL: inner plexiform layer. INL: inner nuclear layer. GCL: ganglion cell layer.

INL (Fig. 4B upper right panel). In 10-week-old $vhl^{flox/flox}$;*α-cre* mice, parts of the peripheral retina had completely degenerated and cells of the ONL, the INL and the GCL had been lost (Fig. 4D upper right panel). Degeneration in the retinal periphery of 10-week-old $vhl^{flox/flox}$;*α-cre* mice was not always as severe as shown here but was very pronounced in all animals analyzed. The central retina of 2-week-old *Vhl* knockdowns was comparable to controls, although one or two rows of photoreceptor nuclei were missing (Fig. 4B lower panels). In the central retina of 10-week-old $vhl^{flox/flox}$;*α-cre* mice, however, at least three rows of photoreceptor nuclei were missing and outer and inner segments seemed to be shortened compared to $vhl^{flox/flox}$ controls (Fig. 4D lower panels).

Immunofluorescence analysis of sections prepared from less severely damaged regions in the peripheral ventral retina of 10-week-old animals showed reduced expression of rod opsin and S-cone opsin in knockdown retinas (Fig. 5A). S-cone opsin positive cells were especially sparse, even in the ventral retina, the region of highest S-cone density in mice (Applebury et al., 2000). If all retinal cells were similarly affected by the degeneration, one might expect that expression levels of markers for specific cell types would remain roughly constant when normalized to *β-actin*. This was indeed observed for expression of *Chx10*, a marker for bipolar cells and for *Opn4*, a marker for ganglion cells (data not shown). However, levels of short wave length cone opsin (*Opn1sw*), middle wavelength cone

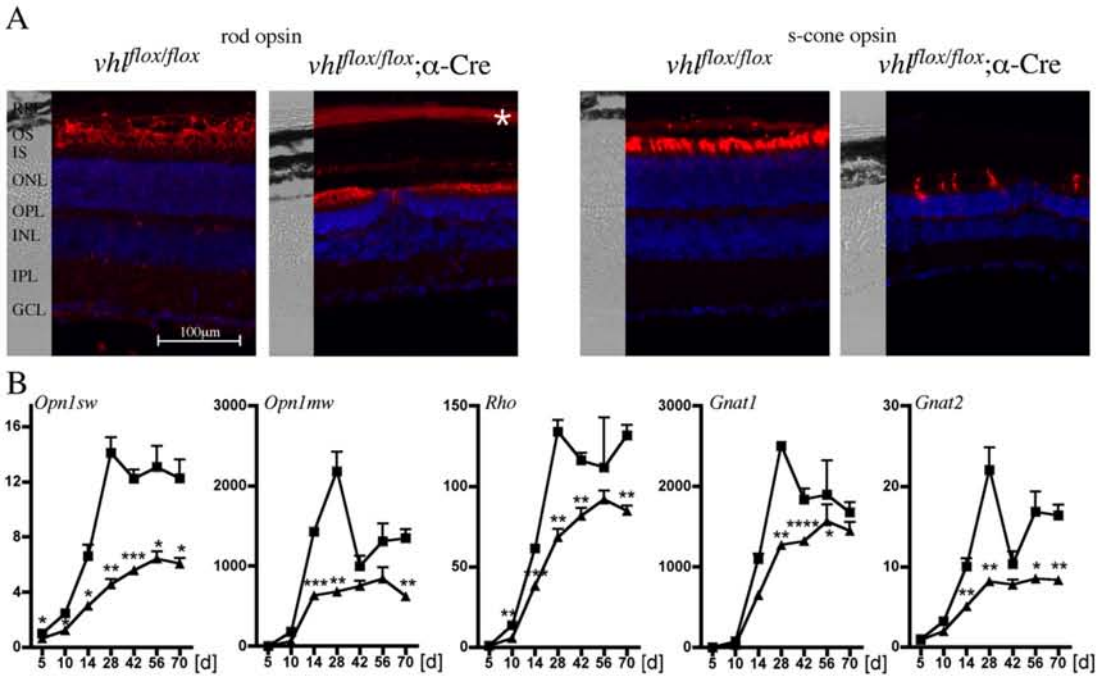

Fig. 5. Rod and cone degeneration in *vhl*$^{flox/flox}$;*α-cre* mice. (A) Immunoflourescence stainings detecting rod opsin (left, red) and S-cone opsin (right, red) in cross sections of 10-week-old *vhl*$^{flox/flox}$ and *vhl*$^{flox/flox}$;*α-cre* mice. DAPI (blue) stained nuclei and nomarski images (gray) are shown for orientation. Shown are representative areas of the peripheral inferior retina. *Unspecific staining in the choroid. (B) Semi-quantitative real-time PCR for expression of s-cone opsin (*Opn1sw*), m-cone opsin (*Opn1mw*), rod opsin (*rho*), rod transducin (*Gnat1*) and cone transducin (*Gnat2*) in *vhl*$^{flox/flox}$ (squares) and *vhl*$^{flox/flox}$;*α-cre* (triangles) mice at postnatal days (d) as indicated. Given are mean values ± SD of 3 retinas amplified in duplicates. Values were normalized to *β-actin* and expressed relatively to the first time point (5d) in *vhl*$^{flox/flox}$ mice. RPE: retinal pigment epithelium. IS: photoreceptor inner segments. OS: photoreceptor outer segments. ONL: outer nuclear layer. IPL: inner plexiform layer. INL: inner nuclear layer. GCL: ganglion cell layer. *$p<0.05$, **$p<0.01$, ***$p<0.001$, ****$p<0.0001$. Significance between *vhl*$^{flox/flox}$ and *vhl*$^{flox/flox}$;*α-cre* mice was calculated for individual time points by an unpaired *t*-test.

opsin (*Opn1mw*), rod opsin (*Rho*), rod transducin (*Gnat1*) and cone transducin (*Gnat2*) were significantly reduced in *vhl*$^{flox/flox}$;*α-cre* mice compared to *vhl*$^{flox/flox}$ littermates (Fig. 5B). This suggests that rod and cone photoreceptors are the most strongly affected cell types by the degeneration and that they may be lost even outside of the severely degenerated peripheral retina (as it is also suggested by the morphology of the central retina, Fig. 4D). Thus, these cells seem to be more sensitive to the abnormal retinal vasculature than cells of the other layers and retinal function may thus be strongly affected.

Reduction of retinal function in vhl$^{flox/flox}$*;α-cre mice*

To investigate functional properties of *vhl*$^{flox/flox}$;*α-cre* mice, flash ERGs were recorded from 10-week-old *vhl*$^{flox/flox}$;*α-cre* and control *vhl*$^{flox/flox}$ mice under scotopic and photopic conditions (Fig. 6). *Vhl*$^{flox/flox}$;*α-cre* mice showed strongly reduced scotopic (Figs. 6A and C) and photopic ERG (Figs. 6B and D) responses, indicating alterations of both rod and cone system components. As the initial portion of the a-wave reflects the primary light response in photoreceptors, the attenuation of the a-wave up to the highest intensity observed in *vhl*$^{flox/flox}$;*α-cre* mice indicates strong photoreceptor dysfunction/degeneration. The b-wave and the oscillatory potentials, generated by downstream retinal circuitry, were also strongly reduced, but this is presumably mainly a consequence of the primary effect on photoreceptors. Rod and cone signaling were about equally affected.

Stress-activated signaling and cell death pathways in vhl$^{flox/flox}$*;α-cre mice*

Degeneration of photoreceptors was shown to activate the JAK/STAT signaling pathway (Samardzija et al., 2006a; Joly et al., 2008; Ueki et al., 2008; Burgi et al., 2009), an endogenous survival system, which is mainly controlled by LIF expression in a subset of Muller glia cells (Joly et al., 2008). So far, however, regulation of this signaling system was only tested in conditions of pure photoreceptor injury. We therefore asked whether the broader retinal degeneration in the Vhl knockdown mice would trigger the same molecular response. Semi-quantitative real-time PCR analysis showed that expression of *Lif*, *Gfap*, *Edn2* and *Fgf2* was strongly induced starting around 10 days of age in *vhl*$^{flox/flox}$;*α-cre* mice. Expression remained high during the degenerative phase and lasted at least until 10 weeks of age (Fig. 7A). In addition, STAT3 was phosphorylated in *vhl*$^{flox/flox}$;*α-cre* but not *vhl*$^{flox/flox}$ control mice (Fig. 7B). This suggests that the same, LIF-dependent signaling system was activated as in models of pure photoreceptor degeneration leading to the hypothesis that the LIF-system may be activated in response to most retinal injuries in a general attempt to protect neurons from degeneration. *Cntf*, another endogenous survival factor was also induced in the *Vhl* knockdown retina. In conditions of pure photoreceptor injury, expression of *Cntf* was not (Joly et al., 2008) or only slightly activated late during the degeneration (Samardzija et al., 2006a). CNTF may thus be a factor, which mainly responds to cellular damage in the INL and/or GCL.

Several pro-apoptotic genes can be regulated in a VHL-dependent manner not involving HIF transcription factors. Among those, expression of Kruppel-like transcription factor 10 (*Klf10*), transforming growth factor β induced (*Tgfbi*) and fibronectin 1 (*Fn1*) was significantly upregulated in *vhl*$^{flox/flox}$;*α-cre* mice (Fig. 8A). In contrast, hepatocyte growth factor (*Hgf*), a VHL-controlled gene related to cancer (Peruzzi et al., 2006) was expressed similarly in *vhl*$^{flox/flox}$;*α-cre* mice and *vhl*$^{flox/flox}$ littermates (data not shown).

Apoptotic cell death is frequently executed through caspase activation. Two general pathways are distinguished. Procaspase-8 is activated through the cell surface death receptor pathway whereas

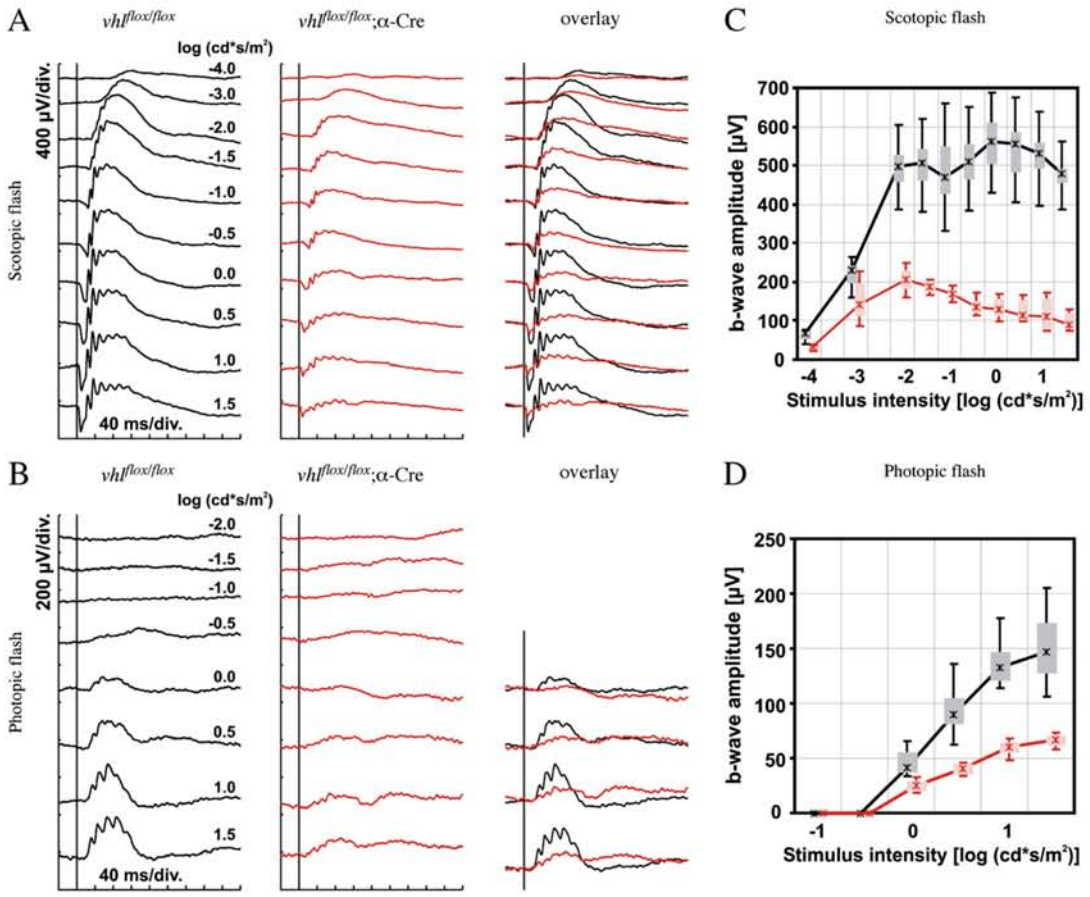

Fig. 6. Reduced retinal function in *vhl*$^{flox/flox}$;*α-cre* mice. Representative scotopic (A, dark-adapted) and photopic (B, light-adapted) single flash ERGs with increasing light intensities were recorded from *vhl*$^{flox/flox}$ control and *vhl*$^{flox/flox}$;*α-cre* mice as indicated. Vertical line crossing each trace shows the timing of the light flash. (C) Scotopic and (D) photopic b-wave amplitudes from control (black, $n=4$) and *vhl*$^{flox/flox}$;*α-cre* mice (red, $n=3$) as a function of the logarithm of the flash intensity. Boxes indicate the 25% and 75% quantile range, whiskers indicate the 5% and 95% quantiles, and the asterisks indicate the median of the data.

activation of procaspase-9 is the first step in the mitochondrial pathway (Budihardjo et al., 1999). Caspase-3 is the main executor caspase of many apoptotic processes and also suspected to be involved in programmed cell death during postnatal development of the mouse retina (Zeiss et al., 2004; O'Driscoll et al., 2006). In the *vhl*$^{flox/flox}$;*α-cre* mouse, expression of *caspase-1* (*Casp1*) and of *caspase-8* (*Casp8*) was significantly upregulated whereas expression of *caspase-3* (*Casp3*) and of *caspase-9* (*Casp9*) was similar to control animals (Fig. 8A). Although expression of tumor necrosis factor α (*Tnf*), which can induce *Casp8* upon binding to death receptors (Guicciardi and Gores, 2009), showed a strong variation between animals, the pattern of expression nevertheless suggested increased levels of *Tnf* in knockdown animals. Western blots detecting the proforms of caspases 1, 3, 8 and 9 indicated increased protein levels of

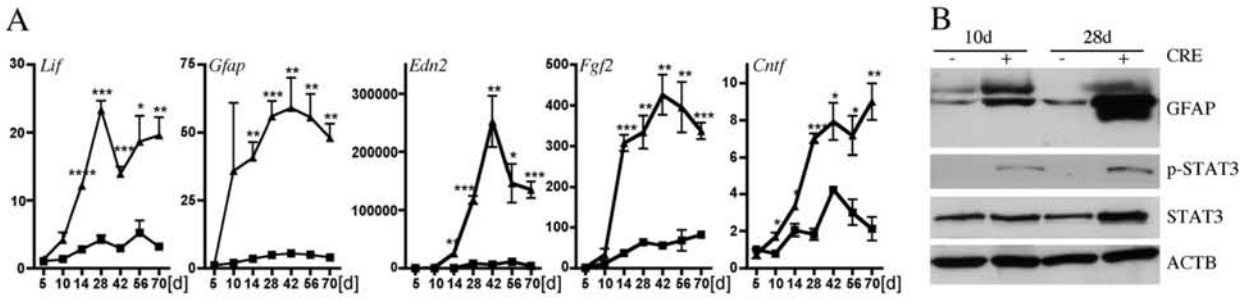

Fig. 7. Activation of LIF response pathway in *vhl*$^{flox/flox}$;*α-cre* mice. (A) Semi-quantitative real-time PCR for expression of *Lif*, *Gfap*, *Edn2*, *Fgf2* and *Cntf* in *vhl*$^{flox/flox}$ (squares) and *vhl*$^{flox/flox}$; *α-cre* (triangles) mice at postnatal days (d) as indicated. Given are mean values ± SD of 3 retinas amplified in duplicates. Values were normalized to *β-actin* and expressed relatively to the first time point (5d) in *vhl*$^{flox/flox}$ mice. (B) Western blot analysis of whole retinal extracts from 10- and 28-day-old *vhl*$^{flox/flox}$;*α-cre* (CRE+) and *vhl*$^{flox/flox}$ (CRE−) mice. Shown are protein levels of GFAP, p-STAT3, STAT3 and ACTB as a control for equal loading. *$p<0.05$, **$p<0.01$, ***$p<0.001$, ****$p<0.0001$. Significance between *vhl*$^{flox/flox}$ and *vhl*$^{flox/flox}$;*α-cre* mice was calculated for individual time points by an unpaired *t*-test.

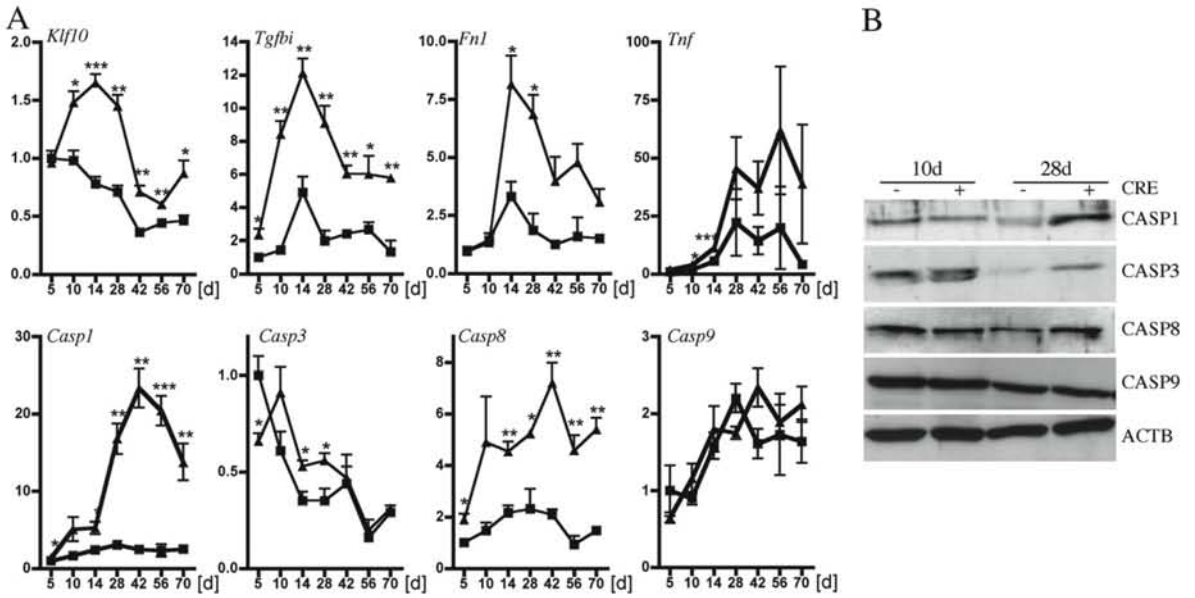

Fig. 8. Activation of apoptosis pathways and pro-caspases in $vhl^{flox/flox}$;α-*cre* mice. (A) Semi-quantitative real-time PCR for expression of *Klf10*, *Tgfbi*, *Fn1*, *Tnf*, *Casp1*, *Casp3*, *Casp8* and *Casp9* in $vhl^{flox/flox}$ (squares) and $vhl^{flox/flox}$;α-*cre* (triangles) mice at postnatal days (d) as indicated. Given are mean values ± SD of 3 retinas amplified in duplicates. Values were normalized to β-*actin* and expressed relatively to the first time point (5d) in $vhl^{flox/flox}$ mice. (B) Western blot analysis of whole retinal extracts from 10- and 28-day-old $vhl^{flox/flox}$;α-*cre* (CRE+) and $vhl^{flox/flox}$ (CRE−) mice. Shown are protein levels of CASP1, CASP3, CASP8, CASP9 and ACTB as a control for equal loading. $^{*}p<0.05$, $^{**}p<0.01$, $^{***}p<0.001$, $^{****}p<0.0001$. Significance between $vhl^{flox/flox}$ and $vhl^{flox/flox}$;α-*cre* mice was calculated for individual time points by an unpaired *t*-test.

CASP1 and CASP3 in 28-day-old knockdown retinas when compared to the wild-type littermates (Fig. 8B). Protein levels of CASP8 were not or only slightly elevated in the knockdown and levels of CASP9 were similar in controls and knockdowns. We did not detect activated (cleaved) forms of the caspases in our blots. The reason why protein levels not always paralleled RNA expression profiles is unclear but may be explained by potential differences in RNA and/or protein stability in young and mature mouse retinas.

Discussion

Hypoxic preconditioning stabilizes HIF transcription factors in the retina of the adult mouse and protects photoreceptors against a subsequent toxic light insult (Grimm et al., 2002). Inactivation of VHL in the peripheral retina by the Cre-mediated deletion of floxed *Vhl* gene sequences led to a normoxic and long-lasting activation of HIF1A and HIF2A during retinal development ((Kurihara et al., 2010); Fig. 1). As a consequence, several pro-angiogenic genes like *Vegfa* and *Epo* but also anti-angiogenic factors like *Pedf* (*Serpinf1*) were upregulated. This misregulated gene expression may have led to the severe abnormalities of the retinal vasculature with persisting hyaloidal vessels (Kurihara et al., 2010; Figs. 2 and 3), reduced density of the capillary network in the peripheral retina and retinal vessels penetrating the photoreceptor layer of the adult mouse (Fig. 3). These ingrown vessels severely disturbed the architecture of the inner and outer nuclear layer and were accompanied by increased numbers of activated microglia, which may migrate along these vessels towards the outer retina (Fig. 3B). Since *Vhl* is also inactivated in iris tissue, iris vasculature was also heavily affected and almost absent in adult knockdown mice (Fig. 2A). Similar to the hyaloidal vessels in the vitreous, the pupillary membrane, which is the embryonic system for nutrient supply to the lens, also persisted. These data support results of a recent publication by Kurihara et al. (2010) which showed in the same *Vhl* knockdown mouse as used here that proper expression of VHL is required for the transition from fetal to adult vasculature in the eye.

Retinal degeneration

Here, we focused on the consequences of *Vhl* knockdown for the retina of the adult mouse. Our data indicate that the lack of VHL not only induced a strong vascular phenotype but also a progressive and severe degeneration of neuronal cells in all peripheral retinal cell layers (Fig. 4). This degeneration might be a direct consequence of the *Vhl* knockdown or, alternatively, might be secondary to the loss of normal retinal vasculature and to the resulting disturbed oxygenation of neuronal cells. In addition, the activation of inflammatory responses – like the microglia activation – might also contribute to the cell death. Since inactivation of VHL in adult rod-photoreceptors did not disturb development of retinal vasculature and only resulted in a late onset and very slow photoreceptor degeneration (Lange C, manuscript in preparation), loss of VHL activity may not, or at least not strongly affect viability of photoreceptor cells directly. We therefore hypothesize that the disturbed vasculogenesis during development, in connection with the upregulation of pro-apoptotic genes and genes connected to the extracellular matrix might be the main factors contributing to the very severe degeneration observed in $Vhl^{flox/flox}$; α-cre mice.

S-cones appeared to be especially affected by the degeneration as shown by the strongly reduced expression of *Opn1sw* and the very low abundance of S-cones in the ventral retina of 10-week-old knockdown mice. The morphological abnormalities were also reflected in the recordings of retinal function. Under all tested conditions, the magnitude of responses to light flashes under both scotopic and photopic conditions was severely reduced in the knockdowns (Fig. 5). Since the sensitivity was roughly regular, it suggests that the reduced retinal function was caused by a severe reduction in the number of cells rather than by a primary photoreceptor defect. However, the functional loss is larger than one would expect based on histological data showing that about 50% of photoreceptors are left (as judged from expression of photoreceptor markers and from retinal morphology). Therefore additional mechanisms might account for the severely reduced function in *Vhl*

knockdown mice. Possible mechanisms include a reduction of tissue oxygenation due to the abnormal vasculature in the *vhl*$^{flox/flox}$;*α-cre* mice, which has been shown to reduce functionality of retinal cells (Braun and Linsenmeier, 1995). Additionally, it has been shown that increased levels of CNTF can negatively influence the ERG in wild-type mice (Schlichtenbrede et al., 2003). Thus, the elevated expression of *Cntf* in *Vhl* knockdown mice (Fig. 7) may also contribute to the reduced retinal function.

Mechanisms of degeneration

Retinal stress imposed by the *Vhl* knockdown strongly activated a neuroprotective response in the retina. In the light-damaged retina as well as during inherited retinal degeneration, a subset of Muller glia cells expresses LIF, which controls an endogenous neuroprotective signaling system. This signaling pathway includes increased expression of *End2*, *Gfap* and p-STAT3, and culminates in the production of the growth and survival factor FGF2 in an attempt to protect cells from death (Samardzija et al., 2006a; Joly et al., 2008; Burgi et al., 2009). The development of an abnormal retinal vasculature and the induction of retinal degeneration strongly induced the same protective system in the *Vhl* knockdown (Fig. 7). However, activation of this pathway was obviously not sufficient to protect retinal cells against execution of cell death and to maintain visual function. In several models of retinal degeneration, caspase-1 was the only caspase associated with the cell death (Doonan et al., 2003; Samardzija et al., 2006b). Here, we observed increased expression of *caspase-8* in addition to *caspase-1*. This suggests a role for the cell surface death receptor pathway in the degenerative process, a hypothesis supported by the increased expression of *Tnf* in the retina of *Vhl* knockdown mice (Fig. 8A). It has already been shown that TNF, produced by glial cells, can be a mediator of cell death in glaucoma through activation of the initiator caspase-8 or through direct neurotoxicity for retinal cells (Tezel, 2008). And an increase in HIF1 transcriptional activity can enhance caspase-8-mediated apoptosis in thymocytes (Biju et al., 2004). Thus, caspase-8 might be a relevant factor in the degenerating retina of the *Vhl* knockdown mouse. Pathways of caspase-mediated apoptosis may converge at the level of the effector caspase-3. In the retina, however, it is still controversially discussed whether caspase-3 is involved in photoreceptor death (Jomary et al., 2001; Doonan et al., 2003). Although gene expression of *caspase-3* was not, or not strongly different between knockdown and control retinas, we detected increased protein expression of pro-caspase-3 in 28-day-old *vhl*$^{flox/flox}$;*α-cre* mice (Fig. 8B) supporting a potential role of caspase-3 in the degeneration observed here. In contrast to the other caspases analyzed, expression of capsase-3 was high early during postnatal development and reduced during maturation. Protein levels of caspase-3 were also high at 10 days of age and almost not detectable at 28 days of age in the wild-type retina. This supports the hypothesis that caspase 3 is involved in programmed cell death during postnatal development of the mouse retina (Zeiss et al., 2004; O'Driscoll et al., 2006).

In addition to caspase-1 and caspase-8, several other genes known to be regulated by VHL and related to cell death were induced in the knockdown retinas. Very strong induction of expression was observed for example for *Phd3* (*Egln3*) (Fig. 1). PHD3 has been connected to apoptosis in neuronal cells (Lee et al., 2005) and tumors (Tennant and Gottlieb, 2010; Schlisio et al., 2008). The transcription factor KLF10 was recently shown to be repressed by wild-type VHL protein (Ivanov et al., 2008). Therefore, increased expression of *Klf10* in the *Vhl* knockdown retina was probably due to the absence of the VHL repressor protein. KLF10 was also reported to be a transactivator of the *Tgfbi* promotor. Increased KLF10 levels caused increased expression of *Tgfbi*, a protein associated with the extracellular matrix. Elevated expression of *Tgfbi* can increase sensitivity of cells to various death inducing agents used in chemotherapy (Irigoyen et al., 2010; Ahmed et al., 2007). It was also shown that elevated levels of TGFBI altered the extracellular matrix facilitating extravasation of metastatic cancer cells (Ma et al., 2008) and that overexpression of a mutant form of TGFBI in the retina caused photoreceptor apoptosis (Bustamante et al., 2008). VHL has been shown before to be involved in the regulation of a proper assembly of the extracellular fibronectin matrix by binding to FN1 (Ohh et al., 1998; Ohh and Kaelin, 1999). Together with increased *Tgfbi* levels, the upregulation of *Fn1* expression in *Vhl* knockdown retinas may point to a problem with extracellular matrix assembly in the absence of VHL. The presence of HIF independent VHL functions in connection to extracellular matrix has already been suggested before (Bishop et al., 2004). Inappropriate formation or destabilization of the extracellular matrix may also facilitate abnormal development of retinal vasculature with vessels penetrating the ONL reaching the photoreceptor segment layer as observed here.

Conclusions

In summary we have shown that downregulation of VHL during development of the retina leads to long-term stabilization of HIF transcription factors and to a strong vascular phenotype with embryonic structures persisting into adulthood. In human patients, mutations in the tumor suppressor gene *Vhl* results in the VHL syndrome, an autosomal dominant disease that manifests itself by hemangioblastomas in the cerebellum, spinal cord and the retina. Tumor development during the disease is thought to be mainly due to overactivation of HIF transcription factors and the subsequent upregulation of angiogenic and growth related genes. Inactivation of *Vhl* in the mouse retina (Kurihara et al., 2010, and this work) and zebrafish (van Rooijen et al., 2010) led to a severe vascular phenotype and may serve as a model to study retinal consequences of VHL syndrome. In addition to the misregulation of vascular development, lack of VHL also caused severe degeneration of all cell types in the mouse retina. Increased levels of caspases as well as induced expression of genes encoding for proteins connected to the regulation of the integrity of the extracellular matrix point to a complex pattern of the molecular mechanisms involved in the degenerative processes. Although such a severe degenerative phenotype has not been reported for patients, the mouse model may be highly useful to investigate the connection between a proper retinal vasculature and the physiology, function and survival of the neuronal retina.

Acknowledgments

The authors thank Coni Imsand and Hedwig Wariwoda for excellent technical assistance. This work was supported by the Swiss National Science Foundation (Grant 3100A0–117760), the Fritz Tobler Foundation and the H. Messerli Foundation. Deutsche Forschungsgemeinschaft (DFG, grants Se837/5-2, Se837/6-1, Se837/7-1), the German Ministry of Education and Research (BMBF, grant 0314106).

References

Ahmed, A.A., Mills, A.D., Ibrahim, A.E., Temple, J., Blenkiron, C., Vias, M., Massie, C.E., Iyer, N.G., McGeoch, A., Crawford, R., Nicke, B., Downward, J., Swanton, C., Bell, S.D., Earl, H.M., Laskey, R.A., Caldas, C., Brenton, J.D., 2007. The extracellular matrix protein TGFBI induces microtubule stabilization and sensitizes ovarian cancers to paclitaxel. Cancer Cell 12, 514–527.

Applebury, M.L., Antoch, M.P., Baxter, L.C., Chun, L.L., Falk, J.D., Farhangfar, F., Kage, K., Krzystolik, M.G., Lyass, L.A., Robbins, J.T., 2000. The murine cone photoreceptor: a single cone type expresses both S and M opsins with retinal spatial patterning. Neuron 27, 513–523.

Barnstable, C.J., Tombran-Tink, J., 2004. Neuroprotective and antiangiogenic actions of PEDF in the eye: molecular targets and therapeutic potential. Prog. Retin. Eye Res. 23, 561–577.

Biju, M.P., Neumann, A.K., Bensinger, S.J., Johnson, R.S., Turka, L.A., Haase, V.H., 2004. Vhlh gene deletion induces Hif-1-mediated cell death in thymocytes. Mol. Cell. Biol. 24, 9038–9047.

Bishop, T., Lau, K.W., Epstein, A.C., Kim, S.K., Jiang, M., O'Rourke, D., Pugh, C.W., Gleadle, J.M., Taylor, M.S., Hodgkin, J., Ratcliffe, P.J., 2004. Genetic analysis of pathways

regulated by the von Hippel-Lindau tumor suppressor in *Caenorhabditis elegans*. PLoS Biol. 2, e289.
Braun, R.D., Linsenmeier, R.A., 1995. Retinal oxygen tension and the electroretinogram during arterial occlusion in the cat. Invest. Ophthalmol. Vis. Sci. 36, 523–541.
Budihardjo, I., Oliver, H., Lutter, M., Luo, X., Wang, X., 1999. Biochemical pathways of caspase activation during apoptosis. Annu. Rev. Cell Dev. Biol. 15, 269–290.
Burgi, S., Samardzija, M., Grimm, C., 2009. Endogenous leukemia inhibitory factor protects photoreceptor cells against light-induced degeneration. Mol. Vis. 15, 1631–1637.
Bustamante, M., Tasinato, A., Maurer, F., Elkochairi, I., Lepore, M.G., Arsenijevic, Y., Pedrazzini, T., Munier, F.L., Schorderet, D.F., 2008. Overexpression of a mutant form of TGFBI/BIGH3 induces retinal degeneration in transgenic mice. Mol. Vis. 14, 1129–1137.
Chollangi, S., Wang, J., Martin, A., Quinn, J., Ash, J.D., 2009. Preconditioning-induced protection from oxidative injury is mediated by leukemia inhibitory factor receptor (LIFR) and its ligands in the retina. Neurobiol. Dis. 34, 535–544.
Doonan, F., Donovan, M., Cotter, T.G., 2003. Caspase-independent photoreceptor apoptosis in mouse models of retinal degeneration. J. Neurosci. 23, 5723–5731.
Fischer, M.D., Huber, G., Beck, S.C., Tanimoto, N., Muehlfriedel, R., Fahl, E., Grimm, C., Wenzel, A., Reme, C.E., van de Pavert, S.A., Wijnholds, J., Pacal, M., Bremner, R., Seeliger, M.W., 2009. Noninvasive, in vivo assessment of mouse retinal structure using optical coherence tomography. PLoS One 4, e7507.
Fruttiger, M., 2002. Development of the mouse retinal vasculature: angiogenesis versus vasculogenesis. Invest. Ophthalmol. Vis. Sci. 43, 522–527.
Grimm, C., Wenzel, A., Groszer, M., Mayser, H., Seeliger, M., Samardzija, M., Bauer, C., Gassmann, M., Reme, C.E., 2002. HIF-1-induced erythropoietin in the hypoxic retina protects against light-induced retinal degeneration. Nat. Med. 8, 718–724.
Grimm, C., Hermann, D.M., Bogdanova, A., Hotop, S., Kilic, U., Wenzel, A., Kilic, E., Gassmann, M., 2005. Neuroprotection by hypoxic preconditioning: HIF-1 and erythropoietin protect from retinal degeneration. Semin. Cell Dev. Biol. 16, 531–538.
Grimm, C., Wenzel, A., Acar, N., Keller, S., Seeliger, M., Gassmann, M., 2006. Hypoxic preconditioning and erythropoietin protect retinal neurons from degeneration. Adv. Exp. Med. Biol. 588, 119–131.
Guicciardi, M.E., Gores, G.J., 2009. Life and death by death receptors. FASEB J. 23, 1625–1637.
Haase, V.H., Glickman, J.N., Socolovsky, M., Jaenisch, R., 2001. Vascular tumors in livers with targeted inactivation of the von Hippel-Lindau tumor suppressor. Proc. Natl. Acad. Sci. U. S. A. 98, 1583–1588.
Huang, L.E., Gu, J., Schau, M., Bunn, H.F., 1998. Regulation of hypoxia-inducible factor 1alpha is mediated by an O_2-dependent degradation domain via the ubiquitin–proteasome pathway. Proc. Natl. Acad. Sci. U. S. A. 95, 7987–7992.
Huber, G., Beck, S.C., Grimm, C., Sahaboglu-Tekgoz, A., Paquet-Durand, F., Wenzel, A., Humphries, P., Redmond, T.M., Seeliger, M.W., Fischer, M.D., 2009. Spectral domain optical coherence tomography in mouse models of retinal degeneration. Invest. Ophthalmol. Vis. Sci. 50, 5888–5895.
Iriyogen, M., Pajares, M.J., Agorreta, J., Ponz-Sarvise, M., Salvo, E., Lozano, M.D., Pio, R., Gil-Bazo, I., Rouzaut, A., 2010. TGFBI expression is associated with a better response to chemotherapy in NSCLC. Mol. Cancer 9, 130.
Ito, M., Yoshioka, M., 1999. Regression of the hyaloid vessels and pupillary membrane of the mouse. Anat. Embryol. (Berl.) 200, 403–411.
Ivan, M., Kondo, K., Yang, H., Kim, W., Valiando, J., Ohh, M., Salic, A., Asara, J.M., Lane, W.S., Kaelin Jr., W.G., 2001. HIFalpha targeted for VHL-mediated destruction by proline hydroxylation: implications for O_2 sensing. Science 292, 464–468.
Ivanov, S.V., Ivanova, A.V., Salnikow, K., Timofeeva, O., Subramaniam, M., Lerman, M.I., 2008. Two novel VHL targets, TGFBI (BIGH3) and its transactivator KLF10, are up-regulated in renal clear cell carcinoma and other tumors. Biochem. Biophys. Res. Commun. 370, 536–540.
Iwai, K., Yamanaka, K., Kamura, T., Minato, N., Conaway, R.C., Conaway, J.W., Klausner, R.D., Pause, A., 1999. Identification of the von Hippel-Lindau tumor-suppressor protein as part of an active E3 ubiquitin ligase complex. Proc. Natl. Acad. Sci. U. S. A. 96, 12436–12441.
Joly, S., Lange, C., Thiersch, M., Samardzija, M., Grimm, C., 2008. Leukemia inhibitory factor extends the lifespan of injured photoreceptors in vivo. J. Neurosci. 28, 13765–13774.
Jomary, C., Neal, M.J., Jones, S.E., 2001. Characterization of cell death pathways in murine retinal neurodegeneration implicates cytochrome *c* release, caspase activation, and bid cleavage. Mol. Cell. Neurosci. 18, 335–346.
Kamura, T., Koepp, D.M., Conrad, M.N., Skowyra, D., Moreland, R.J., Iliopoulos, O., Lane, W.S., Kaelin Jr., W.G., Elledge, S.J., Conaway, R.C., Harper, J.W., Conaway, J.W., 1999. Rbx1, a component of the VHL tumor suppressor complex and SCF ubiquitin ligase. Science 284, 657–661.
Kibel, A., Iliopoulos, O., DeCaprio, J.A., Kaelin Jr., W.G., 1995. Binding of the von Hippel-Lindau tumor suppressor protein to Elongin B and C. Science 269, 1444–1446.
Kurihara, T., Kubota, Y., Ozawa, Y., Takubo, Y., Noda, K., Simon, M.C., Johnson, R.S., Suematsu, M., Tsubota, K., Ishida, K., Goda, N., Suda, T., Okano, H., 2010. von Hippel-Lindau protein regulates transition from the fetal to the adult circulatory system in retina. Development 137, 1563–1571.
Lee, S., Nakamura, E., Yang, H., Wei, W., Linggi, M.S., Sajan, M.P., Farese, R.V., Freeman, R.S., Carter, B.D., Kaelin Jr., W.G., Schlisio, S., 2005. Neuronal apoptosis linked to EglN3 prolyl hydroxylase and familial pheochromocytoma genes: developmental culling and cancer. Cancer Cell 8, 155–167.
Ma, C., Rong, Y., Radiloff, D.R., Datto, M.B., Centeno, B., Bao, S., Cheng, A.W., Lin, F., Jiang, S., Yeatman, T.J., Wang, X.F., 2008. Extracellular matrix protein betaig-h3/TGFBI promotes metastasis of colon cancer by enhancing cell extravasation. Genes Dev. 22, 308–321.
Marquardt, T., Ashery-Padan, R., Andrejewski, N., Scardigli, R., Guillemot, F., Gruss, P., 2001. Pax6 is required for the multipotent state of retinal progenitor cells. Cell 105, 43–55.
O'Driscoll, C., Donovan, M., Cotter, T.G., 2006. Analysis of apoptotic and survival mediators in the early post-natal and mature retina. Exp. Eye Res. 83, 1482–1492.
Ohh, M., Kaelin Jr., W.G., 1999. The von Hippel-Lindau tumour suppressor protein: new perspectives. Mol. Med. Today 5, 257–263.
Ohh, M., Yauch, R.L., Lonergan, K.M., Whaley, J.M., Stemmer-Rachamimov, A.O., Louis, D.N., Gavin, B.J., Kley, N., Kaelin Jr., W.G., Iliopoulos, O., 1998. The von Hippel-Lindau tumor suppressor protein is required for proper assembly of an extracellular fibronectin matrix. Mol. Cell 1, 959–968.
Peruzzi, B., Athauda, G., Bottaro, D.P., 2006. The von Hippel-Lindau tumor suppressor gene product represses oncogenic beta-catenin signaling in renal carcinoma cells. Proc. Natl. Acad. Sci. U. S. A. 103, 14531–14536.
Samardzija, M., Wenzel, A., Aufenberg, S., Thiersch, M., Reme, C., Grimm, C., 2006a. Differential role of Jak-STAT signaling in retinal degenerations. FASEB J. 20, 2411–2413.
Samardzija, M., Wenzel, A., Thiersch, M., Frigg, R., Reme, C., Grimm, C., 2006b. Caspase-1 ablation protects photoreceptors in a model of autosomal dominant retinitis pigmentosa. Invest. Ophthalmol. Vis. Sci. 47, 5181–5190.
Schlichtenbrede, F.C., MacNeil, A., Bainbridge, J.W., Tschernutter, M., Thrasher, A.J., Smith, A.J., Ali, R.R., 2003. Intraocular gene delivery of ciliary neurotrophic factor results in significant loss of retinal function in normal mice and in the Prph2Rd2/Rd2 model of retinal degeneration. Gene Ther. 10, 523–527.
Schlisio, S., Kenchappa, R.S., Vredeveld, L.C., George, R.E., Stewart, R., Greulich, H., Shahriari, K., Nguyen, N.V., Pigny, P., Dahia, P.L., Pomeroy, S.L., Maris, J.M., Look, A.T., Meyerson, M., Peeper, D.S., Carter, B.D., Kaelin Jr., W.G., 2008. The kinesin KIF1Bbeta acts downstream from EglN3 to induce apoptosis and is a potential 1p36 tumor suppressor. Genes Dev. 22, 884–893.
Seeliger, M.W., Grimm, C., Stahlberg, F., Friedburg, C., Jaissle, G., Zrenner, E., Guo, H., Reme, C.E., Humphries, P., Hofmann, F., Biel, M., Fariss, R.N., Redmond, T.M., Wenzel, A., 2001. New views on RPE65 deficiency: the rod system is the source of vision in a mouse model of Leber congenital amaurosis. Nat. Genet. 29, 70–74.
Seeliger, M.W., Beck, S.C., Pereyra-Munoz, N., Dangel, S., Tsai, J.Y., Luhmann, U.F., van de Pavert, S.A., Wijnholds, J., Samardzija, M., Wenzel, A., Zrenner, E., Narfstrom, K., Fahl, E., Tanimoto, N., Acar, N., Tonagel, F., 2005. In vivo confocal imaging of the retina in animal models using scanning laser ophthalmoscopy. Vis. Res. 45, 3512–3519.
Senger, D.R., Galli, S.J., Dvorak, A.M., Perruzzi, C.A., Harvey, V.S., Dvorak, H.F., 1983. Tumor cells secrete a vascular permeability factor that promotes accumulation of ascites fluid. Science 219, 983–985.
Tanimoto, N., Muehlfriedel, R.L., Fischer, M.D., Fahl, E., Humphries, P., Biel, M., Seeliger, M.W., 2009. Vision tests in the mouse: functional phenotyping with electroretinography. Front. Biosci. 14, 2730–2737.
Tennant, D.A., Gottlieb, E., 2010. HIF prolyl hydroxylase-3 mediates alpha-ketoglutarate-induced apoptosis and tumor suppression. J. Mol. Med. 88, 839–849.
Tezel, G., 2008. TNF-alpha signaling in glaucomatous neurodegeneration. Prog. Brain Res. 173, 409–421.
Thiersch, M., Lange, C., Joly, S., Heynen, S., Le, Y.Z., Samardzija, M., Grimm, C., 2009. Retinal neuroprotection by hypoxic preconditioning is independent of hypoxia-inducible factor-1 alpha expression in photoreceptors. Eur. J. Neurosci. 29, 2291–2302.
Ueki, Y., Wang, J., Chollangi, S., Ash, J.D., 2008. STAT3 activation in photoreceptors by leukemia inhibitory factor is associated with protection from light damage. J. Neurochem. 105, 784–796.
van Rooijen, E., Voest, E.E., Logister, I., Bussmann, J., Korving, J., van Eeden, F.J., Giles, R.H., Schulte-Merker, S., 2010. von Hippel-Lindau tumor suppressor mutants faithfully model pathological hypoxia-driven angiogenesis and vascular retinopathies in zebrafish. Model Mech. 3, 343–353.
Zeiss, C.J., Neal, J., Johnson, E.A., 2004. Caspase-3 in postnatal retinal development and degeneration. Invest. Ophthalmol. Vis. Sci. 45, 964–970.

11.2 Normoxic Activation of Hypoxia-inducible Factors in Photoreceptors Provides Transient Protection Against Light-induced Retinal Degeneration

Christina Lange[1], Severin R. Heynen[1], Naoyuki Tanimoto[2], Markus Thiersch[1], Yun-Zheng Le[3], Isabelle Meneau[1], Mathias W. Seeliger[2], Marijana Samardzija[1], Christian Caprara[1] and Christian Grimm[1,4]

[1]Lab for Retinal Cell Biology, Department of Ophthalmology, University of Zurich, Zurich, Switzerland;

[2]Institute of Ophthalmic Research, Center of Ophthalmology, Division of Ocular Neurodegeneration, Tubingen, Germany;

[3]Department of Cell Biology and Dean A. McGee Eye Institute, Oklahoma City, Oklahoma

[4]Zurich Center for Integrative Human Physiology (ZIHP), Zurich, Switzerland

Published in Investigative Ophthalmology & Visual Sciences (IOVS) 2011, **52**(8):5872-5880

Personal Contribution

Contributed to the identification of *Cre*-expressing cells in the *Opn-Cre* mouse by generating *ROSA-flox-RFP;Opn-Cre* mice and analyzing RFP distribution on retinal cryosections (Fig.1A, 1B)

Key Findings

Hypoxic preconditioning provides protection against light-induced photoreceptor degeneration. HIFs are stabilized during the preconditioning period and are thought to contribute to neuroprotection. To investigate whether HIFs are responsible for protection against light-induced photoreceptor death in the retina, HIFA proteins were stabilized under normoxic conditions by ablating VHL in rod photoreceptors.

Here are some of the key findings of the study:

- knockdown of *Vhl* in rod photoreceptor cells led to a normoxic stabilization of HIFA proteins
- histology of young *Vhl* knockdown retinas was comparable to control littermates
- in older animals, progressive retinal degeneration and loss of vision was observed
- *Vhl* knockdown transiently protected photoreceptors against light-induced cell death
- the transient protection may be a result of a significantly increased expression of *Fgf2*

Retinal Cell Biology

Normoxic Activation of Hypoxia-Inducible Factors in Photoreceptors Provides Transient Protection against Light-Induced Retinal Degeneration

Christina Lange,[1] *Severin R. Heynen,*[1] *Naoyuki Tanimoto,*[2] *Markus Thiersch,*[1] *Yun-Zheng Le,*[3] *Isabelle Meneau,*[1] *Mathias W. Seeliger,*[2] *Marijana Samardzija,*[1] *Christian Caprara,*[1] *and Christian Grimm*[1,4]

Purpose. Hypoxic preconditioning activates hypoxia-inducible transcription factors (HIFs) in the retina and protects photoreceptors from light-induced retinal degeneration. The authors tested whether photoreceptor-specific activation of HIFs in normoxia is sufficient for protection.

Methods. Rod-specific *Vhl* knockdown mice were generated using the *Cre-lox* system with the rod opsin promoter controlling expression of CRE recombinase to stabilize HIF transcription factors in normoxic rods. Cell death was induced by light exposure and quantified by ELISA. Rhodopsin was quantified by spectrophotometry. Gene expression was analyzed by real-time PCR, and levels of proteins were determined by Western blotting. Morphology was investigated by light microscopy and retinal function tested by ERG.

Results. The rod-specific *Vhl* knockdown stabilized HIF-α proteins and induced expression of HIF target genes in retinas of 10-week-old mice under normoxic conditions. Retinal morphology and function were normal. At 36 hours after exposure to excessive light, *Vhl* knockdowns showed significantly less photoreceptor cell death than did wild-type controls. Ten days after light exposure, however, photoreceptor degeneration in *Vhl* knockdowns was similar to that of control animals. *Vhl* knockdowns expressed *Fgf2* at higher basal levels before light exposure. After light exposure, however, expression of *Fgf2* was not significantly different from that of wild-type controls.

Conclusions. Artificial activation of HIF transcription factors in normoxic photoreceptors results in an increased basal expression of *Fgf2* that may contribute to a transient protection of rods against light damage. Full photoreceptor protection may require a hypoxia-like response in additional retinal cell types and/or the differential regulation of additional mechanisms. (*Invest Ophthalmol Vis Sci.* 2011;52:5872–5880) DOI: 10.1167/iovs.11-7204

From the [1]Lab for Retinal Cell Biology, Department of Ophthalmology, University of Zurich, Zurich, Switzerland; [2]Institute of Ophthalmic Research, Center of Ophthalmology, Division of Ocular Neurodegeneration, Tubingen, Germany; [3]Department of Cell Biology and Dean A. McGee Eye Institute, Oklahoma City, Oklahoma; and [4]Zurich Center for Integrative Human Physiology (ZIHP), Zurich, Switzerland.

Supported by Swiss National Science Foundation (Grant 3100A0-117760), Deutsche Forschungsgemeinschaft (DFG, Grants Se837/5-2, Se837/6-1, Se837/7-1), German Ministry of Education and Research (BMBF, Grant 0314106), Fritz Tobler Foundation, and H. Messerli Foundation.

Submitted for publication January 11, 2011; revised March 10, 2011; accepted March 17, 2011.

Disclosure: **C. Lange**, None; **S.R. Heynen**, None; **N. Tanimoto**, None; **M. Thiersch**, None; **Y.-Z. Le**, None; **I. Meneau**, None; **M.W. Seeliger**, None; **M. Samardzija**, None; **C. Caprara**, None; **C. Grimm**, None

Corresponding author: Christian Grimm, Lab for Retinal Cell Biology, Department Ophthalmology, USZ, University of Zurich, Wagistrasse 14, CH 8952 Schlieren, Switzerland; cgrimm@opht.uzh.ch.

Retinitis pigmentosa (RP) is characterized by the progressive loss of photoreceptors causing severe visual disturbances and blindness in humans. To investigate molecular mechanisms of photoreceptor degeneration, different mouse models have been developed. The model of light-induced photoreceptor cell death is widely used to analyze immediate changes in gene expression during degeneration or to test the efficacy of neuroprotective strategies[1] such as hypoxic preconditioning. It has been shown that a short pre-exposure of mice to reduced levels of oxygen completely protects photoreceptors from light-induced degeneration.[2]

To cope with the stress imposed by reduced oxygen availability during hypoxia, cells regulate expression of genes for survival, growth, or metabolism.[3] This regulation is achieved mainly by special transcription factors called hypoxia inducible factors (HIFs). HIFs consist of two subunits, α and β. The HIF β-subunit (aryl-hydrocarbon receptor nuclear translocator [ARNT]) is constitutively expressed and located in the nucleus. HIF1A, HIF2A, and HIF3A, the three known isoforms of the HIF α-subunit, are expressed but quickly degraded in conditions of normal oxygen availability (normoxia). Hydroxylation of HIF α-subunits by prolyl hydroxylases (egl nine [EGLN] family) leads to their recognition by the von Hippel-Lindau (VHL) protein. VHL forms a multimeric protein complex together with Cullin-2, RBX1, and the elongins B and C,[4–6] and acts as a E3-ubiquitinase targeting HIF α proteins to proteasomal degradation.[7] Another hydroxylase, the factor inhibiting HIF (FIH), hydroxylates HIF-α at an asparagine residue, inhibiting p300 coactivator recruitment and thus transcriptional activity.[8] Hydroxylation of HIF-α proteins by EGLNs and FIH depends on the availability of oxygen.[8,9] Hence, hydroxylation is strongly reduced during hypoxia and HIF α-subunits are not recognized by VHL. Thus HIF α proteins are stabilized, enter the nucleus, bind HIF-β and p300, and participate in the regulation of gene expression.

It has been shown that during hypoxic preconditioning, HIF1A and HIF2A are stabilized and that HIF target genes are differentially regulated in the retina.[2,10,11] Erythropoietin (*Epo*) was shown to be strongly induced after hypoxic exposure, and injection of recombinant EPO was protective against light-induced retinal degeneration.[2] Using a genetic approach, we recently showed that HIF1A is not essential in rods for protection by hypoxic preconditioning.[10] However, this does not exclude that rod-specific activation of HIF1A contributes to neuroprotection after hypoxic preconditioning. In addition,

Investigative Ophthalmology & Visual Science, July 2011, Vol. 52, No. 8

HIF2A and/or other factors that are expressed in rods and regulated by hypoxia might be involved in neuroprotection by hypoxic preconditioning. Alternatively, hypoxia might regulate factors in other cell types in the retina. Such factors might act in *trans* to protect rods. To address these questions, we investigated whether a hypoxia-like response in rod photoreceptors is sufficient to prevent retinal degeneration in normoxia. To achieve normoxic induction of a hypoxia-like response, we generated photoreceptor-specific *Vhl* knockdown mice using the Cre-lox system. Because the absence of VHL leads to increased stability of HIF α-subunits in normoxia, *Vhl* knockdowns may mimic the hypoxic response at normal oxygen levels. In case of protection, VHL protein may provide a target for tissue-specific pharmacological interventions in the future.

Materials and Methods

Mice and Genotyping

Mice were treated in accordance with the regulations of the Veterinary Authority of Zurich and with the statement of The Association for Research in Vision and Ophthalmology for the use of animals in research. All mice were maintained as breeding colonies at the University of Zurich in a 12-hour/12-hour light/dark cycle (60 lux).

Wild-type BALB/c mice were from a breeding colony at the University Hospital Zurich. 129S-Vhlh^{tm1jae}/J-mice (hereafter *Vhl$^{flox/flox}$* mice), which have *lox*P sites flanking exon 1 and part of the promoter of the *Vhl* gene,[12] were purchased from Jackson Laboratory (Bar Harbor, ME). To generate rod photoreceptor-specific *Vhl* knockdowns, *Vhl$^{flox/flox}$* mice were crossed with mice expressing Cre recombinase under the control of the opsin promoter (LMOPC1, hereafter opsin-Cre mice). In these mice, *Cre* expression in rods starts at approximately postnatal day 7 and increases up to 6 weeks of age.[13] The breeding colonies were kept on the light-sensitive *Rpe65$_{450Leu}$* background.[14] A red fluorescence protein (RFP) reporter strain (ROSA-flox-RFP; kindly provided by Wolf-Dietrich Hardt, ETH, Zurich, Switzerland) was crossed with opsin-Cre mice to assay the expression pattern of Cre recombinase.

The following primers were used to detect wild-type (wt) and *Vhl*-flox alleles: forward (forw) (5′-TGAGTATGGGATAACGGGTTGAAC-3′) and reverse (rev) (5′-AGAACTGACTGACTTCCACTGATGC-3′). The wt allele was identified as a 125-basepair (bp) PCR fragment and the *Vhl*-flox as a 317-bp fragment after gel electrophoresis. Presence of the opsin-cre transgene was tested by PCR using the following primer pair: forw (5′-AGGTGTAGAGAAGGCACTTAGC-3′) and rev (5′-CTAATCGCCATCTTCCAGCAGG-3′). In the presence of the transgene, the amplification reaction resulted in the production of a 411-bp fragment. To detect excision of floxed sequences in the *Vhl* gene, genomic DNA was isolated from retinal tissue and tested by PCR using the following primers: forw_un-excised (5′-CTGGTACCCACGAAACTGTC-3′), forw_excised (5′-CTAGGCACCGAGCTTAGAGGTTTGCG-3′) and rev_both (5′-CTGACTTCCACTGATGCTTGTCACAG-3′). The excised allele was identified as a 260-bp and the unexcised allele as a 460-bp fragment. Presence or absence of the RFP transgene was tested using the ROSA-tg forward primer: 5′-GCGAAGAGTTTGTCCTCAACC-3′ or the ROSA-wt forward primer: 5′-GGAGCGGGAGAAATGGATATG-3′, respectively, together with the ROSA-common reverse primer: 5′-AAAGTCGCTCTGAGTTGTTAT-3′. An amplification product of 300 bp or of 500 bp indicated the presence or absence, respectively, of the RFP locus.

Laser Capture Microdissection

After mice were killed, their eyes were enucleated, immediately embedded in tissue freezing medium (Leica Microsystems Nussloch GmbH, Nussloch, Germany), and frozen in a 2-methylbutane bath cooled with liquid nitrogen. Retinal sections (20 μm) were fixed (5 minutes in acetone), air dried (5 minutes), and dehydrated (30 seconds in 100% ethanol, 5 minutes in xylene). Microdissection was performed using an Arcturus XT Laser capture device (Molecular Devices, Sunnyvale, CA). RNA was isolated using the Arcturus kit for RNA isolation (Molecular Devices) according to the manufacturer's directions including a DNase treatment to digest residual genomic DNA. Equal amounts of RNA were used for reverse transcription using oligo(dT) and M-MLV reverse transcriptase (Promega, Madison, WI).

Semiquantitative Real-Time PCR

Retinas were removed through a slit in the cornea and immediately frozen in liquid nitrogen. Total RNA was prepared using a kit (RNeasy RNA isolation kit; Qiagen, Hilden, Germany) according to the manufacturer's directions including a DNase treatment to digest residual genomic DNA. Equal amounts of RNA were used for reverse transcription using oligo(dT) and M-MLV reverse transcriptase (Promega). Relative quantification of cDNA was conducted via real-time PCR using a kit (LightCycler 480 Sybr Green I Master kit; Roche Diagnostics, Basel, Switzerland), a LightCycler 480 instrument (Roche Diagnostics) and specific primer pairs (Table 1). Expression was normalized to *Actb* (*β-actin*) and relative quantification was calculated using the comparative threshold method ($\Delta\Delta$CT) and commercial software (Light Cycler 480 software; Roche).

Western Blotting Analysis

Retinas were homogenized in 0.1 M Tris–HCl (pH 8) at 4°C and protein content was determined using Bradford reagent. Standard SDS-PAGE and Western blotting were performed. For immunodetection, the following antibodies were used: anti-HIF1A (no. Nb100–479; Novus Biologicals, Cambridge, UK, 1:1000), anti-HIF2A (no. Nb100–122, Novus Biologicals; 1:1000), anti-pSTAT3 (no. 9131; Cell Signaling Technology, Danvers, MA; 1:500) and anti-ACTB (no. A5441; Sigma-Aldrich, St. Louis, MO; 1:5000). Blots were incubated overnight at 4°C with primary antibodies followed by a 1-hour incubation with HRP-conjugated secondary antibodies. Immunoreactivity was visualized using the Renaissance-Western blot detection kit (PerkinElmer Life Sciences, Emeryville, CA).

Electroretinography

ERGs were recorded according to previously described procedures.[15,16] The ERG equipment consisted of a Ganzfeld bowl, a direct current amplifier, and a PC-based control and recording unit (Multiliner Vision; VIASYS Health Care GmbH, Hoechberg, Germany). Mice were dark adapted overnight and anesthetized with ketamine (66.7 mg/kg body weight) and xylazine (11.7 mg/kg body weight). Pupils were dilated and single-flash ERG responses were obtained under dark-adapted (scotopic) and light-adapted (photopic) conditions. Light adaptation was accomplished with a background illumination of 30 cd/m^2 starting 10 minutes before recording. Single white-flash stimulus intensity ranged from −4 to 1.5 log cd · s/m^2 under scotopic and from −2 to 1.5 log cd · s/m^2 under photopic conditions, divided into 10 and 8 steps, respectively. Ten responses were averaged with an interstimulus interval (ISI) of either 5 seconds (for −4, −3, −2, −1.5, −1, and −0.5 log cd · s/m^2) or 17 seconds (for 0, 0.5, 1, and 1.5 log cd · s/m^2).

Light Exposure, Cell Death Detection, and Morphology

Mice were dark adapted overnight and pupils dilated with 1% ophthalmic solution (Cyclogyl; Alcon, Cham, Switzerland) and 5% phenylephrine (Ciba Vision, Niederwangen, Switzerland) 1 hour before exposure to white fluorescent light (13′000 lux) for 1 hour.

After light exposure, mice were placed in darkness overnight. Thereafter, mice were kept in normal cyclic light until they were killed. To quantify apoptosis, mice were killed 36 hours after light exposure. Nucleosomal release was determined using a cell death detection (CDD) kit (Roche Diagnostics) according to the manufacturer's recommendations.

TABLE 1. Primers Used for Real-Time PCR

Gene	Upstream (5′–3′)	Downstream (5′–3′)	Annealing Temperature (°C)	Product (bp)
Adm	ttcgcagttccgaaagaagt	ggtagctgctggatgcttgta	62	77
Actb	cgacatggagaagatctggc	caacggctccggcatgtgc	62	153
Bnip3	cctgtcgcagttgggttc	gaagtgcagttctacccaggag	60	93
Egln1	cattgttggcagaaggtgtg	caaaggactacagggtctcca	62	70
Epo	gccctgctagccaattcc	gccctgctagccaattcc	60	128
Gnat1	gaggatgctgagaaggatgc	tgaatgttgagcgtggtcat	58	209
Gnat2	gcatcagtgctgaggacaaa	ctaggcactcttcgggtgag	58	192
Mt1	gaatggaccccaactgctc	gcagcagctcttcttgcag	62	104
Mt2	tgtacttcctgcaagaaaagctg	acttgtcggaagcctctttg	62	94
Sag	ttacaagccttccaacctctgac	accagcacaacaccatctacag	64	189
Scl2a1	cagtgtatcctgttgcccttctg	gccgaccctcttctttcatctc	62	151
Rho	cttcacctggatcatggcgtt	ttcgttgttgacctcaggcttg	62	130
Vegfa	acttgtgttgggaggaggatgtc	aatgggtttgtcgtgtttctgg	60	171
Vhl	gagggacccgttccaataat	ttggcaaaaataggctgtcc	60	364
Fgf2	tgtgtctatcaagggagtgtgtgc	accaactggagtatttccgtgaccg	62	158
Edn2	agacctcctccgaaagctg	ctggctgtagctggcaaag	60	64
Stat3	caaaaccctcaagagccaagg	tcactcacaatgcttctccgc	62	133
Gfap	ccaccaaactggctgatgtctac	ttctctccaaatccacacgagc	62	240
Socs3	atttcgcttcgggactagc	aacttgctgtgggtgaccat	58	126
Lif	aatgccacctgtgccatacg	caacttggtcttctctgtcccg	60	216
Cntf	ctctgtagccgctctatctg	ggtacaccatccactgagtc	58	125

For light microscopy, eyes were fixed in 2.5% glutaraldehyde in 0.1 M cacodylate buffer (pH 7.3) at 4°C overnight. For each eye, the superior and the inferior retinas were prepared, washed in cacodylate buffer, incubated in osmium tetroxide for 1 hour, dehydrated, and embedded in resin Epon 812. Sections (0.5 μm) were prepared from the lower central retina and counterstained with methylene blue.

Hypoxic Preconditioning

Adult (8–10 weeks of age) BALB/c mice were exposed to reduced oxygen concentrations in a hypoxic chamber with food and water ad libitum. O_2 levels were reduced in steps of 2% by changing the O_2/N_2 ratio to reach a final O_2 concentration of 7% within 90 minutes. After 6 hours of hypoxia, mice were killed immediately to isolate retinal tissue for gene expression analysis.

Rhodopsin Measurements

Mice were dark adapted overnight. Retinas were removed through a slit in the cornea under dim red light and placed in 1 mL of distilled H_2O for 1 minute. After 3 minutes of centrifugation at 15,000*g*, the supernatant was discarded and 700 μL of 1% hexadecyltrimethylammonium bromide (Fluka Chemie, Buchs, Switzerland) in H_2O was added to the pellet. Retinas were mechanically homogenized with a polytron (20 seconds, 3000 rpm), centrifuged for 3 minutes at 15,000*g*, and the supernatant was collected. The absorption at 500 nm was measured before and after exposure to bright white light (20,000 lux for 1 minute). The amount of rhodopsin present per retina was calculated using the following formula derived from the Lambert-Beer equation: $\rho = \text{vol} \times c = \text{vol} \times \Delta\text{abs}500/(\text{E}500 \times l \times n)$. ρ is the amount of rhodopsin per retina (in moles); vol is the volume of the sample (in liters); c is the concentration of rhodopsin per retina (M); Δabs500 is the difference between absorption of the sample at 500 nm before and after bleaching; E500 is the extinction coefficient of rhodopsin at 500 nm (4.2×10^4 cm × M); l is the path length of the cuvette (in cm); and n is the number of retinas.

RESULTS

Successful Knockdown of *Vhl* in Photoreceptors

Expression of Cre recombinase in our line of LMOPC1 mice was specific to the photoreceptor layer but showed a patchy pattern (Figs. 1A, 1B). Analysis of genomic DNA from retinal tissue of 10-week-old $Vhl^{flox/flox}$ and $Vhl^{flox/flox}$;opsin-cre mice showed excision of floxed DNA sequences in mice expressing CRE recombinase but not in control mice (Fig. 1C). Because excision is specific for rod photoreceptors,[13] whole retinal samples contain both the floxed (unexcised; from retinal cells without CRE expression) and the excised allele. Semiquantita-

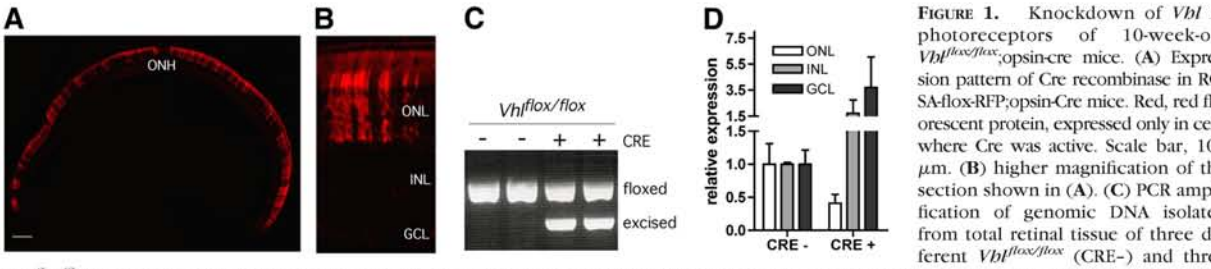

FIGURE 1. Knockdown of *Vhl* in photoreceptors of 10-week-old $Vhl^{flox/flox}$;opsin-cre mice. (**A**) Expression pattern of Cre recombinase in ROSA-flox-RFP;opsin-Cre mice. Red, red fluorescent protein, expressed only in cells where Cre was active. Scale bar, 100 μm. (**B**) higher magnification of the section shown in (**A**). (**C**) PCR amplification of genomic DNA isolated from total retinal tissue of three different $Vhl^{flox/flox}$ (CRE–) and three $Vhl^{flox/flox}$;opsin-cre (CRE+) mice at 10 weeks of age. The amplified fragment from the floxed gene (floxed) has a length of 460 bp. CRE-mediated excision of the floxed sequence (excised) resulted in a 260-bp fragment. (**D**) Semiquantitative real-time PCR after laser capture microdissection showing relative *Vhl* mRNA levels in the different retinal layers (as indicated) of $Vhl^{flox/flox}$ (CRE–) and $Vhl^{flox/flox}$;opsin-cre (CRE+) mice. Values were normalized to *Actb* and expressed relatively to the respective values for each layer in $Vhl^{flox/flox}$ mice, which were set to 1. Shown are mean values ± SD of three different mice amplified in duplicates. ONH, optic nerve head; ONL, outer nuclear layer; INL, inner nuclear layer; GCL, ganglion cell layer.

tive real-time PCR on samples obtained by laser capture microdissection revealed lower expression levels of *Vhl* mRNA in the ONL of $Vhl^{flox/flox}$;opsin-cre mice (CRE+) compared to their control ($Vhl^{flox/flox}$;CRE−) littermates (Fig. 1D). The reason for the upregulation of *Vhl* expression in the other cell layers is unclear, but might involve compensatory effects.

Stabilization of HIF-α Proteins Leads to Increased Expression of HIF Target Genes in 10-Week-Old $Vhl^{flox/flox}$;opsin-cre Mice

Downregulation of *Vhl* in photoreceptors led to a stabilization of HIF-α proteins in normoxic retinas. Increased levels of both HIF1A and HIF2A were detected in retinas of 10-week-old $Vhl^{flox/flox}$;opsin-cre mice (CRE+; Fig. 2A). In addition to HIF-α stabilization, we noticed strong phosphorylation of STAT3. Expression levels of total STAT3 protein was also slightly elevated in *Vhl* knockdown retinas. Although STAT3 is reported to be part of the HIF-pathway,[17] it is unclear whether the increased phosphorylation of STAT3 is a consequence of the stabilized HIF-α proteins or whether it is due to other mechanisms in the *Vhl* knockdown retinas. Importantly, however, stabilization of HIF-α proteins and phosphorylation of STAT3 are features also found in the hypoxic retina. Therefore, the molecular response in the *Vhl* knockdowns may resemble the response in retinas of mice preconditioned by hypoxia. To determine whether the stabilized HIFs are transcriptionally active in normoxia, we analyzed expression of several hypoxia-responsive genes[11] in retinas of 10-week-old $Vhl^{flox/flox}$;opsin-cre mice (Fig. 2B) and in wild-type mice after hypoxic preconditioning (Fig. 2C). Expression of adrenomedullin (*Adm*), prolyl hydroxylase 2 (*Egln1*), solute carrier family 2 (facilitated glucose transporter) member 1 (*Slc2a1*, also called *Glut1*), and vascular endothelial growth factor (*Vegf*) was induced to a similar extent in normoxic $Vhl^{flox/flox}$;opsin-cre mice and in hypoxic wild-type mice (after exposure to 7% oxygen for 6 hours). Regulation of these hypoxia response genes is largely attributed to HIF1.[18–20] Expression of BCL2/adenovirus E1B 19-kDa interacting protein 3 (*Bnip3*), metallothionein 1 (*Mt1*), and metallothionein 2 (*Mt2*) was also upregulated in $Vhl^{flox/flox}$;opsin-cre mice but not to the same extent as in hypoxic wild-type mice. Expression of erythropoietin *Epo*, which is reported to be activated by HIF2,[21] was induced in hypoxic but not in $Vhl^{flox/flox}$;opsin-cre mice. This suggests that the stabilized HIF2 was not transcriptionally active, that induction of *Epo* during hypoxia is regulated by cells other than rod photoreceptors, or that *Epo* expression in photoreceptors is not controlled by HIF2.

Knockdown of *Vhl* in Rod Photoreceptors Does Not Affect Morphology and Function in Young Mice but Leads to Retinal Degeneration in Old Mice

To assess a potential spontaneous degeneration of photoreceptor cells in *Vhl* knockdown mice, we analyzed ERG responses (Figs. 3A–D) in young $Vhl^{flox/flox}$;opsin-cre and $Vhl^{flox/flox}$ littermates. ERG traces and scotopic and photopic b-wave amplitudes in 17-week-old *Vhl* knockdown mice did not differ from those in control $Vhl^{flox/flox}$ littermates and were similar to those in wild-type mice.[16] Normal retinal structure in young *Vhl* knockdown animals was further supported by comparable retinal morphologies (see below) and by similar expression levels of the photoreceptor marker genes rod transducin (*Gnat1*), cone transducin (*Gnat2*), S-antigen (*Sag*), and rod opsin (*Rho*) in 10-week old $Vhl^{flox/flox}$;opsin-cre and $Vhl^{flox/flox}$ littermates (Fig. 3E).

ERG recordings from 1-year-old $Vhl^{flox/flox}$;opsin-cre mice, however, revealed a reduction of a- and b-wave amplitudes under both scotopic and photopic conditions (Figs. 4A–D). The strong reduction in the a-wave amplitude suggested that photoreceptors might be injured or lost. This was confirmed by the morphologic analysis of 1-year-old retinas (Fig. 4E). Compared with the ONL of age-matched $Vhl^{flox/flox}$ and opsin-cre control mice, the ONL of $Vhl^{flox/flox}$;opsin-cre mice was thinned, with only three to four rows of photoreceptor nuclei remaining. In addition, the structure of inner and outer segments appeared severely disintegrated. Thus, knockdown of *Vhl* did not affect retinal function and morphology in mice up to 17 weeks of age but caused retinal degeneration in old mice.

Knockdown of *Vhl* in Rod Photoreceptors Delays Light-Induced Photoreceptor Degeneration in Young Mice

To test whether the activation of the hypoxia-like response in photoreceptors during normoxic conditions is similarly neuroprotective to light exposure as hypoxic preconditioning, we used 10-week-old $Vhl^{flox/flox}$;opsin-cre mice. At this age, retinal morphology (Fig. 5) and expression of photoreceptor-specific genes (Fig. 3) were still similar to controls. In addition, scotopic and photopic b-wave amplitudes in 17-week-old knockdowns were indistinguishable from controls, suggesting that also at 10 weeks, retinal function was comparable. Mice were exposed to 13′000 lux of white light for 1 hour and retinal morphology was analyzed and cell death quantified at 36 hours thereafter (Figs. 5A, 5B). At this time point, photoreceptor outer segments were better preserved (Fig. 5A, middle panels,

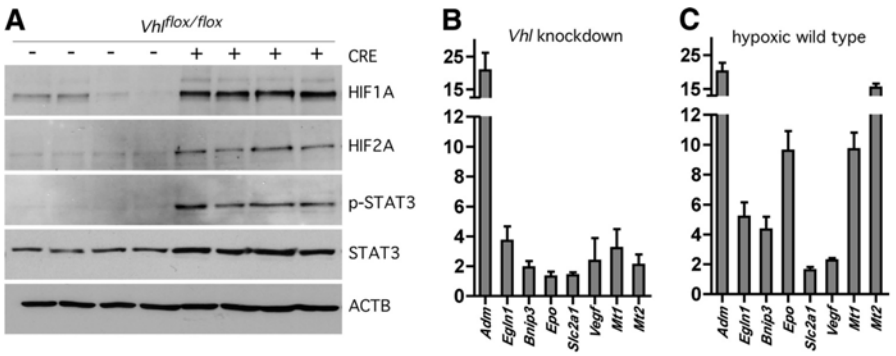

FIGURE 2. Stabilization and activation of transcription factors in 10-week-old $Vhl^{flox/flox}$;opsin-cre mice. (**A**) Western blot analysis showing protein expression of HIF1A, HIF2A, phosphorylated STAT3 (p-STAT3), and STAT3 in four different $Vhl^{flox/flox}$ (CRE−) and $Vhl^{flox/flox}$;opsin-cre (CRE+) mice at 10 weeks of age. ACTB served as a control for equal loading. (**B**) Total retinal RNA was prepared from 10-week-old $Vhl^{flox/flox}$;opsin-cre mice and expression levels of individual genes (as indicated) were determined by semiquantitative real-time PCR. Levels were normalized to *Actb* and expressed relatively to the expression in $Vhl^{flox/flox}$ control mice (set to 1). (**C**) Total retinal RNA was prepared from wild-type mice after hypoxic preconditioning. Expression levels were normalized to *Actb* and expressed relatively to expression in normoxic control mice (set to 1). Shown are mean values ± SD of four retinas amplified in duplicates.

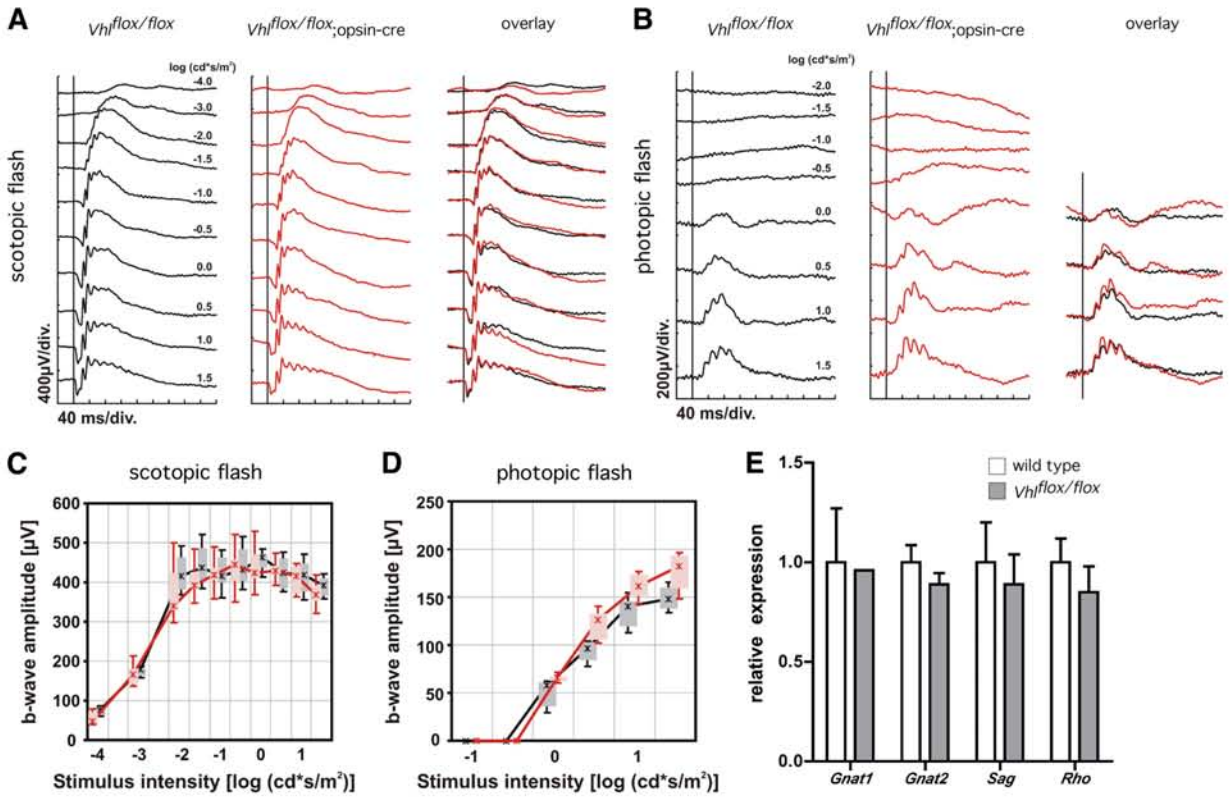

FIGURE 3. Normal retinal function in 17-week-old $Vhl^{flox/flox}$;opsin-cre mice. (**A**) Representative scotopic (dark-adapted) and (**B**) photopic (light-adapted) single-flash ERGs with increasing light intensities recorded from 17-week-old $Vhl^{flox/flox}$ control and $Vhl^{flox/flox}$;opsin-cre mice as indicated. The vertical line crossing each trace shows the time point of the light flash. (**C**) Scotopic and (**D**) photopic b-wave amplitudes from control (black, $n = 3$) and $Vhl^{flox/flox}$;opsin-cre mice (red, $n = 3$) as a function of the logarithm of the flash intensity. Boxes indicate the 25% and 75% quartile range, whiskers indicate the 5% and 95% quantiles, and the asterisks indicate the median of the data. (**E**) Semiquantitative real-time PCR for photoreceptor-specific genes (as indicated) in 10-week-old $Vhl^{flox/flox}$ (white bars) and $Vhl^{flox/flox}$;opsin-cre (gray bars). Values were normalized to *Actb* and expressed relatively to the value of $Vhl^{flox/flox}$ mice, which was set to 1. Shown are mean values ± SD of four animals amplified in duplicates.

black arrows) and fewer pyknotic nuclei (Fig. 5A, white arrows) were found in the ONL of $Vhl^{flox/flox}$;opsin-cre mice. Reduced cell death was confirmed by the ELISA-based quantification of free nucleosomes generated by internucleosomal DNA cleavage during apoptotic cell death. Although variable within groups, light-exposed $Vhl^{flox/flox}$;opsin-cre mice showed significantly less cell death compared to their control littermates and to mice expressing solely opsin-cre (Fig. 5B).

At 10 days after light exposure, however, photoreceptors in $Vhl^{flox/flox}$;opsin-cre mice had degenerated to a similar extent as in $Vhl^{flox/flox}$ controls (Fig. 5A, bottom panels). Accordingly, both genotypes showed a comparable reduction in rhodopsin levels (as a measure for surviving photoreceptors) to 58% ($Vhl^{flox/flox}$) and 52% ($Vhl^{flox/flox}$;opsin-cre) of their respective dark control levels, which were set to 100% (Fig. 5C). This suggests that the knockdown of *Vhl* delayed but did not prevent photoreceptor degeneration after light exposure. We noted that basal levels of dark-adapted rhodopsin levels (before light exposure) were reduced in untreated *Vhl* knockdown animals to 76% of the levels found in control $Vhl^{flox/flox}$ or opsin-cre mice (Fig. 5D). Rhodopsin regeneration, however, was comparable to that in wild-type and reached 8 pmol/min (data not shown). This value is relevant for light damage susceptibility and close to data published for pigmented wild-type animals expressing the RPE65-450Leu variant.[14] Similarly, expression of *Rho* RNA was not affected (Fig. 3E), and intracellular localization of rod opsin was normal (determined by immunofluorescence according to[22]; data not shown) in the knockdown. Thus, the reason for the reduced basal levels of rhodopsin in *Vhl* knockdown retinas is unclear.

Because protection was only transient and not permanent, as observed after hypoxic preconditioning, mechanisms of protection might be different in *Vhl* knockdowns and the hypoxic wild-type retina. To address potential mechanisms for the transient protection against degeneration, we analyzed expression levels of several genes known to be involved in the retinal response to injury or stress. Of particular interest were genes implicated in the protective pathway controlled by leukemia inhibitory factor (LIF) after light exposure.[23,24] Basal expression of several genes downstream of LIF (*Fgf2*, *Edn2*, *Stat3*, *Socs3*, and *Gfap*) was higher in knockdown animals (Fig. 6, triangles) than in controls (Fig. 6, squares). Basal expression of *Cntf* and *Lif* itself was not affected. After light exposure, however, expression levels of all these genes converged in the two strains and already at 12 hours after exposure, levels were no longer significantly different. The expression pattern of the individual genes after light exposure in wild-type mice is in accordance with data published previously.[24,25]

DISCUSSION

Hypoxic preconditioning protects photoreceptors against light-induced degeneration.[2] The exact mechanisms are not

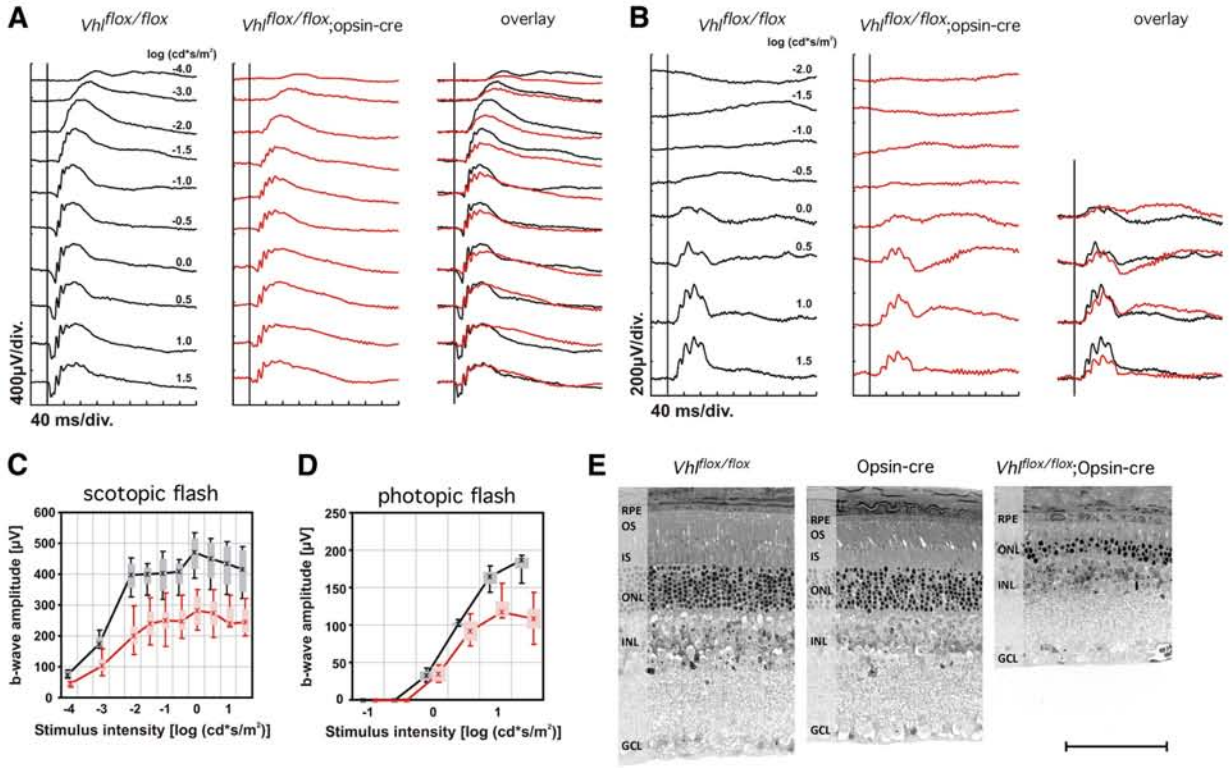

Figure 4. Retinal degeneration in 1-year-old *Vhl*$^{flox/flox}$;opsin-cre mice. (**A**) Representative scotopic (dark-adapted) and (**B**) photopic (light-adapted) single-flash ERGs with increasing light intensities recorded from 1-year-old *Vhl*$^{flox/flox}$ control and *Vhl*$^{flox/flox}$;opsin-cre mice as indicated. The vertical line crossing each trace shows the timing of the light flash. (**C**) Scotopic and (**D**) photopic b-wave amplitudes from control (black, $n = 3$) and *Vhl*$^{flox/flox}$;opsin-cre mice (red, $n = 3$) as a function of the logarithm of the flash intensity. Boxes indicate the 25% and 75% quartile range, whiskers indicate the 5% and 95% quantiles, and the asterisks indicate the median of the data. (**E**) Representative morphologic sections from the lower central retina of 1-year-old *Vhl*$^{flox/flox}$, of opsin-cre and of *Vhl*$^{flox/flox}$;opsin-cre mice. RPE, retinal pigment epithelium; OS, photoreceptor outer segments; IS, photoreceptor inner segments; ONL, outer nuclear layer; INL, inner nuclear layer; GCL, ganglion cell layer. Scale bar, 100 µm.

known but may include differential regulation of neuroprotective genes. Hypoxia-inducible transcription factors such as HIF1 and HIF2 are activated during hypoxic preconditioning in the whole retina[10] and the product of at least one of their target genes, EPO, has been shown to protect photoreceptors.[2,26] Here we show that lack of VHL induced a sustained activation of HIF transcription factors in normoxic photoreceptors that led to a hypoxia-like response and provided protection against light-induced cell death. However, this protection was only transient and did not reach the level observed after hypoxic preconditioning.

Knockdown of *Vhl* in rod photoreceptors stabilized HIF1A and HIF2A and induced phosphorylation of STAT3, leading to the increased expression of a set of target genes that were also activated in the wild-type retina after exposure to hypoxia (Fig. 2). Because the knockdown of *Vhl* was specific to rod photoreceptors, our data suggest that expression of these genes was regulated in rods by HIFs and/or pSTAT3. *Epo* was the only tested gene that was not induced in *Vhl*$^{flox/flox}$;opsin-cre mice. Because lack of VHL is sufficient to induce *Epo* expression in the retina, as shown in *Vhl*$^{flox/flox}$;α-cre mice,[22] our results suggest that upregulation of *Epo* in hypoxic wild-type mice may not occur in rods but in other cell types of the retina. Alternative explanations include the possibility that *Epo* expression in rods is not regulated by one of the factors activated here.

Although retinas of *Vhl*$^{flox/flox}$;opsin-cre mice had a normal retinal morphology and function, levels of rhodopsin were reduced. This cannot be explained by a reduced number of photoreceptor cells because expression of rod and cone marker genes were normal in 10-week-old *Vhl*$^{flox/flox}$;opsin-cre mice. Rhodopsin regeneration was also not affected and reached similar kinetics as in wild-type control mice. In addition, we did not detect mislocalization of rod opsin in retinas of *Vhl*$^{flox/flox}$;opsin-cre mice (data not shown). Thus, the reason for the reduced rhodopsin levels remains unclear and warrants further investigation.

Transient Protection against Light Damage

Knockdown of *Vhl* in rods resulted in a transient protection (or delayed degeneration) of photoreceptor cells against light damage. Although light damage depends on light absorption by the visual pigment,[27–29] light damage susceptibility is determined by rhodopsin regeneration kinetics rather than by the absolute levels of dark-adapted rhodopsin.[14,30] Because regeneration rates were identical in both wild-type and *Vhl* knockdown mice, protection was thus not mediated by differences in photon absorption.

The delayed degeneration suggests that rods lacking VHL have activated some mechanisms that can postpone but not prevent the death of injured photoreceptors. A potential factor involved in this process may be FGF2, which was shown previously to be neuroprotective for photoreceptors.[31,32] The increased basal expression of *Fgf2* in *Vhl*$^{flox/flox}$;opsin-cre mice before light exposure (Fig. 6) may support survival of photo-

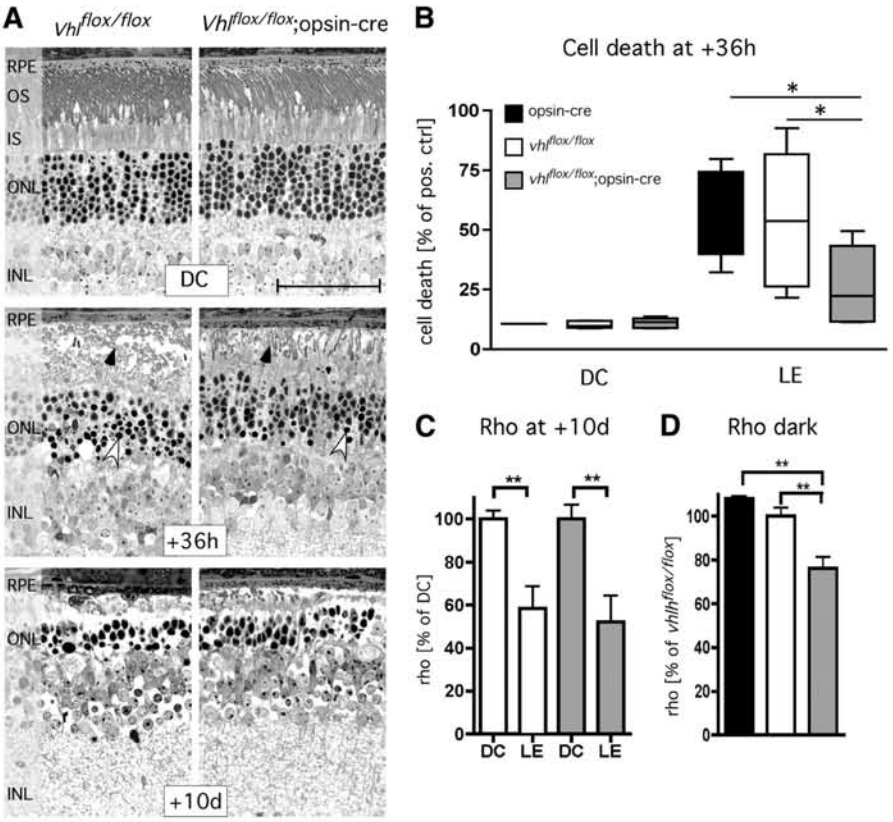

FIGURE 5. Transient photoreceptor protection in *Vhl*$^{flox/flox}$;opsin-cre mice. (**A**) Morphologic sections of dark controls (DC), and at 36 hours (+36h) and 10 days (+10d) after light exposure from retinas of 10-week-old *Vhl*$^{flox/flox}$ and *Vhl*$^{flox/flox}$; opsin-cre mice. Shown are representative sections of the lower central retina, the most affected region in our light damage setup. Arrows indicate the layer of photoreceptor segments; arrowheads show examples of pyknotic nuclei. (**B**) Quantification of retinal cell death at 36 hours after light exposure of opsin-cre (black bars), *Vhl*$^{flox/flox}$ (white bars) and *Vhl*$^{flox/flox}$;opsin-cre mice (gray bars). Values are presented as box blots representing the median and the lower and upper quartiles. Whiskers show the complete range of all data points. Values were calculated relative to the value of a positive control (provided by the kit), which was set to 100%. $n = 1$ (DC, opsin-cre); $n = 7$ (DC, *Vhl*$^{flox/flox}$); $n = 5$ (DC, *Vhl*$^{flox/flox}$;opsin-cre); $n = 4$ (+36h, opsin-cre); $n = 9$ (+36h, *Vhl*$^{flox/flox}$); $n = 6$ (+36h, *Vhl*$^{flox/flox}$;opsin-cre). (**C**) Relative rhodopsin levels of retinas at 10 days after light exposure (LE) in *Vhl*$^{flox/flox}$ (white bars) and *Vhl*$^{flox/flox}$;opsin-cre mice (gray bars). Values are expressed relative to the corresponding dark controls (DC), which were set to 100%. Shown are mean values ± SD of six retinas. (**D**) Basal rhodopsin levels in retinas of dark-adapted and not light-exposed opsin-cre (black bar), *Vhl*$^{flox/flox}$ (white bar) and *Vhl*$^{flox/flox}$; opsin-cre (gray bar) mice. Values are expressed relative to the values of *Vhl*$^{flox/flox}$ mice, which were set to 100%. Shown are mean values ± SD of six retinas. $^{*}P < 0.05$; $^{**}P < 0.01$. Significance was calculated using an unpaired *t*-test. RPE, retinal pigment epithelium; OS, photoreceptor outer segments; IS, photoreceptor inner segments; ONL, outer nuclear layer; INL, inner nuclear layer. Scale bar, 50 μm.

receptors initially. After light exposure, however, expression levels were similar to levels in light-exposed control mice. Because photoreceptors in control mice degenerate, such levels are obviously not sufficient for a long-term rescue of injured photoreceptors. Interestingly, *Lif* knockout and wild- type mice have similar *Fgf2* expression levels before light exposure,

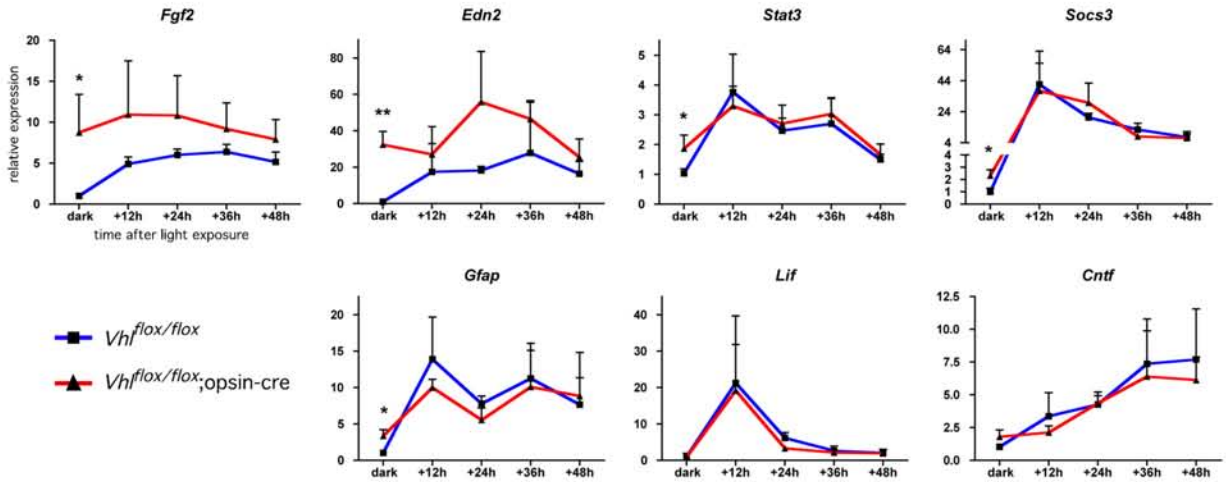

FIGURE 6. Gene expression after light exposure. Relative gene expression levels in retinas of 10-week-old *Vhl*$^{flox/flox}$ (squares, blue) and *Vhl*$^{flox/flox}$;opsin-cre (triangles, red) mice before (dark) or at 12, 24, 36, and 48 hours after exposure to 13′000 lux of white light for 1 hour. Values are expressed relative to values of dark-adapted *Vhl*$^{flox/flox}$ mice which were set to 1. Shown are mean ± SD values of three mice. Expression in the two strains were compared at individual time points using a Student's *t*-test. $^{*}P < 0.05$; $^{**}P < 0.01$.

but whereas wild-type mice upregulate *Fgf2* expression in response to photoreceptor injury, *Lif* knockouts do not.[25] As a consequence, *Lif* knockouts show a light damage severity similar to that of wild-type mice early (unpublished data) but a stronger degeneration late (10 days) after exposure.[25] Therefore, the expression profile of *Fgf2* correlates with degeneration severity early or late after photoreceptor injury.

The mechanism leading to increased expression of *Fgf2* in the absence of VHL needs to be determined. However, *Vhl* knockdown mice also have increased basal levels of *Edn2* (Fig. 6), and we recently showed that activation of the receptor for *Edn2* (EDNRB) induces *Fgf2* expression.[23] Thus, it might be that the increased levels of HIF1 in the *Vhl* knockdown retinas upregulate expression of *Edn2* in photoreceptors, as shown in other systems.[33] EDN2 may then cause induction of *Fgf2* via activation of EDNRB. Thus, increased expression of *Fgf2* may be a consequence of the increased *Edn2* expression through HIF1A stabilization in rods of the *Vhl* knockdown mice. Alternatively, lack of VHL might also directly regulate *Edn2*, as suggested for *Edn1*.[34]

The restriction of the hypoxia-like response to rod photoreceptors might be another reason for the lack of full protection in the $Vhl^{flox/flox}$;opsin-cre mice. In contrast to the knockdown mice, hypoxic preconditioning induces a systemic response and may thus involve factors induced in other cell types of the retina. *Epo*, for example, is strongly upregulated in the hypoxic retina and can protect photoreceptors against light damage[2] and in the rds mouse.[26] *Epo*, however, was not upregulated in the $Vhl^{flox/flox}$;opsin-cre knockdown mice. Thus, at least one neuroprotective factor contributing to protection after hypoxic preconditioning was missing. The complete protection of photoreceptors in *Vhl* knockdown mice after hypoxic exposure (data not shown) suggests that retinas lacking VHL in rods were still able to react to acute hypoxia and further supports the conclusion that mechanisms in addition to rod-specific activation of HIF and STAT3 transcription factors are required for full protection.

Thus, the rod-specific knockdown of *Vhl* mimics the response of the retina to hypoxic preconditioning only partially. Whether or not a more complete retinal knockdown of *Vhl* would result in increased protection cannot be tested because generation of such mice would require an inactivation of *Vhl* in all cells of the adult retina. Inactivation of *Vhl* already during retinal development (e.g., by using the α-cre mouse) results in severe abnormalities of the retinal vasculature and strong retinal degeneration.[22,35] Because long-term lack of VHL and/or activation of HIF transcription factors leads to retinal degeneration (Fig. 4), the *Vhl* knockdown may not only trigger a protective reaction but simultaneously may also alter the physiology of rods and/or of the cellular environment, leading to a retinal stress counteracting the protection. Hence, only a short hypoxic period may be tolerated by the retina and be protective. Long-term hypoxia[36] or a long-term hypoxia-like response (this work) may lead to degeneration.

In summary, we show that a photoreceptor-specific *Vhl* knockdown induced a hypoxia-like response that protected photoreceptors against light-induced cell death in 10-week-old mice. However, protection was only transient and did not reach the level detected after hypoxic preconditioning. We hypothesize that the full and sustained protection of photoreceptors after hypoxic exposure requires regulation of factors in addition to the ones observed here, and/or that hypoxia-mediated protection of photoreceptors is controlled mainly by other retinal cells in a paracrine fashion.

Acknowledgments

The authors thank Coni Imsand and Hedwig Wariwoda for excellent technical assistance.

References

1. Wenzel A, Grimm C, Samardzija M, Reme CE. Molecular mechanisms of light-induced photoreceptor apoptosis and neuroprotection for retinal degeneration. *Prog Retin Eye Res.* 2005;24(2):275–306.
2. Grimm C, Wenzel A, Groszer M, et al. HIF-1-induced erythropoietin in the hypoxic retina protects against light-induced retinal degeneration. *Nat Med.* 2002;8(7):718–724.
3. Webb JD, Coleman ML, Pugh CW. Hypoxia, hypoxia-inducible factors (HIF), HIF hydroxylases and oxygen sensing. *Cell Mol Life Sci.* 2009;66(22):3539–3554.
4. Iwai K, Yamanaka K, Kamura T, et al. Identification of the von Hippel-lindau tumor-suppressor protein as part of an active E3 ubiquitin ligase complex. *Proc Natl Acad Sci USA.* 1999;96(22):12436–12441.
5. Kamura T, Koepp DM, Conrad MN, et al. Rbx1, a component of the VHL tumor suppressor complex and SCF ubiquitin ligase. *Science.* 1999;284(5414):657–661.
6. Kibel A, Iliopoulos O, DeCaprio JA, Kaelin WG Jr. Binding of the von Hippel-Lindau tumor suppressor protein to Elongin B and C. *Science.* 1995;269(5229):1444–1446.
7. Ohh M, Park CW, Ivan M, et al. Ubiquitination of hypoxia-inducible factor requires direct binding to the beta-domain of the von Hippel-Lindau protein. *Nat Cell Biol.* 2000;2(7):423–427.
8. Mahon PC, Hirota K, Semenza GL. FIH-1: a novel protein that interacts with HIF-1alpha and VHL to mediate repression of HIF-1 transcriptional activity. *Genes Dev.* 2001;15(20):2675–2686.
9. Jaakkola P, Mole DR, Tian YM, et al. Targeting of HIF-alpha to the von Hippel-Lindau ubiquitylation complex by O_2-regulated prolyl hydroxylation. *Science.* 2001;292(5516):468–472.
10. Thiersch M, Lange C, Joly S, Heynen S, Le YZ, Samardzija M, Grimm C. Retinal neuroprotection by hypoxic preconditioning is independent of hypoxia-inducible factor-1 alpha expression in photoreceptors. *Eur J Neurosci.* 2009;29(12):2291–2302.
11. Thiersch M, Raffelsberger W, Frigg R, Samardzija M, Wenzel A, Poch O, Grimm C. Analysis of the retinal gene expression profile after hypoxic preconditioning identifies candidate genes for neuroprotection. *BMC Genomics.* 2008;9:73.
12. Haase VH, Glickman JN, Socolovsky M, Jaenisch R. Vascular tumors in livers with targeted inactivation of the von Hippel-Lindau tumor suppressor. *Proc Natl Acad Sci USA.* 2001;98(4):1583–1588.
13. Le YZ, Zheng L, Zheng W, Ash JD, Agbaga MP, Zhu M, Anderson RE. Mouse opsin promoter-directed Cre recombinase expression in transgenic mice. *Mol Vis.* 2006;12:389–398.
14. Wenzel A, Reme CE, Williams TP, Hafezi F, Grimm C. The Rpe65 Leu450Met variation increases retinal resistance against light-induced degeneration by slowing rhodopsin regeneration. *J Neurosci.* 2001;21(1):53–58.
15. Seeliger MW, Grimm C, Stahlberg F, et al. New views on RPE65 deficiency: the rod system is the source of vision in a mouse model of Leber congenital amaurosis. *Nat Genet.* 2001;29(1):70–74.
16. Tanimoto N, Muehlfriedel RL, Fischer MD, Fahl E, Humphries P, Biel M, Seeliger MW. Vision tests in the mouse: functional phenotyping with electroretinography. *Front Biosci.* 2009;14:2730–2737.
17. Jung JE, Lee HG, Cho IH, et al. STAT3 is a potential modulator of HIF-1-mediated VEGF expression in human renal carcinoma cells. *FASEB J.* 2005;19(10):1296–1298.
18. Garayoa M, Martinez A, Lee S, et al. Hypoxia-inducible factor-1 (HIF-1) up-regulates adrenomedullin expression in human tumor cell lines during oxygen deprivation: a possible promotion mechanism of carcinogenesis. *Mol Endocrinol.* 2000;14(6):848–862.
19. Warnecke C, Weidemann A, Volke M, et al. The specific contribution of hypoxia-inducible factor-2alpha to hypoxic gene expression in vitro is limited and modulated by cell type-specific and exogenous factors. *Exp Cell Res.* 2008;314(10):2016–2027.

20. Zhang H, Bosch-Marce M, Shimoda LA, et al. Mitochondrial autophagy is an HIF-1-dependent adaptive metabolic response to hypoxia. *J Biol Chem.* 2008;283(16):10892–10903.
21. Haase VH. Hypoxic regulation of erythropoiesis and iron metabolism. *Am J Physiol Renal Physiol.* 2010;299(1):F1–13.
22. Lange C, Caprara C, Tanimoto N, et al. Retina-specific activation of a sustained hypoxia-like response leads to severe retinal degeneration and loss of vision. *Neurobiol Dis.* 2011;41(1):119–130.
23. Joly S, Lange C, Thiersch M, Samardzija M, Grimm C. Leukemia inhibitory factor extends the lifespan of injured photoreceptors in vivo. *J Neurosci.* 2008;28(51):13765–13774.
24. Samardzija M, Wenzel A, Aufenberg S, Thiersch M, Reme C, Grimm C. Differential role of Jak-STAT signaling in retinal degenerations. *FASEB J.* 2006;20(13):2411–2413.
25. Burgi S, Samardzija M, Grimm C. Endogenous leukemia inhibitory factor protects photoreceptor cells against light-induced degeneration. *Mol Vis.* 2009;15:1631–1637.
26. Rex TS, Wong Y, Kodali K, Merry S. Neuroprotection of photoreceptors by direct delivery of erythropoietin to the retina of the retinal degeneration slow mouse. *Exp Eye Res.* 2009;89(5):735–740.
27. Grimm C, Wenzel A, Hafezi F, Yu S, Redmond TM, Reme CE. Protection of Rpe65-deficient mice identifies rhodopsin as a mediator of light-induced retinal degeneration. *Nat Genet.* 2000; 25(1):63–66.
28. Noell WK, Albrecht R. Irreversible effects on visible light on the retina: role of vitamin A. *Science.* 1971;172(978):76–79.
29. Williams TP, Howell WL. Action spectrum of retinal light-damage in albino rats. *Invest Ophthalmol Vis Sci.* 1983;24(3):285–287.
30. Keller C, Grimm C, Wenzel A, Hafezi F, Reme C. Protective effect of halothane anesthesia on retinal light damage: inhibition of metabolic rhodopsin regeneration. *Invest Ophthalmol Vis Sci.* 2001;42(2):476–480.
31. O'Driscoll C, O'Connor J, O'Brien CJ, Cotter TG. Basic fibroblast growth factor-induced protection from light damage in the mouse retina in vivo. *J Neurochem.* 2008;105(2):524–536.
32. Faktorovich EG, Steinberg RH, Yasumura D, Matthes MT, LaVail MM. Basic fibroblast growth factor and local injury protect photoreceptors from light damage in the rat. *J Neurosci.* 1992;12(9): 3554–3567.
33. Na G, Bridges PJ, Koo Y, Ko C. Role of hypoxia in the regulation of periovulatory EDN2 expression in the mouse. *Can J Physiol Pharmacol.* 2008;86(6):310–319.
34. Wykoff CC, Pugh CW, Maxwell PH, Harris AL, Ratcliffe PJ. Identification of novel hypoxia dependent and independent target genes of the von Hippel-Lindau (VHL) tumour suppressor by mRNA differential expression profiling. *Oncogene.* 2000;19(54):6297–6305.
35. Kurihara T, Kubota Y, Ozawa Y, et al. von Hippel-Lindau protein regulates transition from the fetal to the adult circulatory system in retina. *Development.* 2010;137(9):1563–1571.
36. Neubauer JA. Invited review: physiological and pathophysiological responses to intermittent hypoxia. *J Appl Physiol.* 2001;90(4): 1593–1599.

11.3 Intrinsically Photosensitive Retinal Ganglion Cells Are Resistant to N-methyl-D-aspartic Acid Excitotoxicity

Sarah DeParis[1], Christian Caprara[1], and Christian Grimm[1,2,3]

[1]Lab of Retinal Cell Biology, Dept Ophthalmology, University of Zurich, Switzerland

[2]Zurich Center for Integrative Human Physiology, University of Zurich, Switzerland

[3]Neuroscience Center Zurich, University of Zurich and ETH Zurich, Switzerland

Published in Molecular Vision, 2012, **18**: 2814-2827

Personal Contribution

Performed analysis of BRN3A- and OPN4-positive RGCs by immunofluorescence on retinal flatmounts (Fig.3). Performed co-localization analysis of NMDAR1 and OPN4 by immunofluorescence on retinal flatmounts (Fig.7).

Key Findings

ipRGCs are mainly responsible for non-image-forming visual tasks such as circadian photoentrainment and the pupillary light reflex. Compared to other classes of RGCs, ipRGCs are more resistant to cell death in several experimental models such as ocular hypertension, optic nerve transection, and others. In this study, we tested whether ipRGCs are also resistant to NMDA-induced excitotoxicity.

Here are some of the key findings of the study:

- in contrast to retinal *Brn3a* expression and BRN3A-containing cells, levels of *Opn4* mRNA and the number of OPN4-expressing cells were not reduced after NMDA injection
- survival of ipRGCs after NMDA injection was not strain specific, did not require the presence of photoreceptor cells, and did not depend on PI3K/AKT or JAK/STAT signalling, although both signalling pathways were activated after NMDA treatment

Molecular Vision 2012; 18:2814-2827 <http://www.molvis.org/molvis/v18/a288>
Received 3 May 2012 | Accepted 27 November 2012 | Published 29 November 2012

Intrinsically photosensitive retinal ganglion cells are resistant to N-methyl-D-aspartic acid excitotoxicity

SW DeParis,[1] C Caprara,[1] C Grimm[1,2,3]

[1]Lab of Retinal Cell Biology, Dept Ophthalmology, University of Zurich, Switzerland; [2]Zurich Center for Integrative Human Physiology, University of Zurich, Switzerland; [3]Neuroscience Center Zurich, University of Zurich and ETH Zurich, Switzerland

Purpose: Intrinsically photosensitive retinal ganglion cells (ipRGCs) express the photopigment melanopsin (OPN4) and are mainly responsible for non-image-forming visual tasks such as circadian photoentrainment and the pupillary light reflex. Compared to other classes of RGCs, ipRGCs are more resistant to cell death in several experimental models such as ocular hypertension, optic nerve transection, and others. Here, we tested whether ipRGCs are also resistant to N-methyl-D-aspartic acid (NMDA)-induced excitotoxicity.

Methods: Mice were injected intravitreally with NMDA, and subsequent expression levels of *Opn4* and *Brn3a* mRNA were analyzed with semiquantitative real-time PCR. Cells immunopositive for BRN3A and OPN4 were quantified in retinal flat mounts of NMDA- and PBS-injected eyes. The molecular response of the retina to NMDA treatment was analyzed with real-time PCR and western blotting. Intravitreal injections of wortmannin and AG-490 were used to inhibit phosphatidylinositol 3-kinase (PI3K)/AKT and Janus kinase/signal transducers and activators of transcription (JAK/STAT) signaling, respectively.

Results: In contrast to retinal *Brn3a* expression and BRN3A-containing cells, levels of *Opn4* mRNA and the number of OPN4-expressing cells were not reduced after NMDA injection. Survival of ipRGCs after NMDA injection was not strain specific, did not require the presence of photoreceptor cells, and did not depend on PI3K/AKT or JAK/STAT signaling, although both signaling pathways were activated after NMDA treatment.

Conclusions: Our data support the existence of an efficient survival system for ipRGCs. This system does not depend on PI3K/AKT or JAK/STAT signaling. Identification of the responsible molecular survival mechanisms may provide clues to protect "traditional" ganglion cells in diseases such as glaucoma.

Intrinsically photosensitive retinal ganglion cells (ipRGCs) express the photopigment melanopsin (also known as opsin 4, or OPN4) and make up about 1%–3% of the total ganglion cell population in the mammalian retina [1]. ipRGCs are morphologically diverse with several distinct functions [2]. They are primarily responsible for non-image-forming tasks such as circadian photoentrainment and the pupillary light reflex via projection to the suprachiasmatic nucleus (SCN) and olivary pretectal nucleus, respectively [1-3]. Nevertheless, some ipRGCs project to the dorsal lateral geniculate nucleus (dLGN) and superior colliculus and may be involved in low-acuity pattern vision [2]. Interestingly, ipRGCs have been found to be resistant to cell death in various experimental models such as intraocular hypertension [4,5], optic nerve transection [5,6], and kainic acid treatment [7]. ipRGCs are also less prone to death in the DBA/2J mouse, a model for glaucoma [8], and in advanced stages of human neurodegenerative ocular diseases due to mitochondrial dysfunction [9]. It remains to be investigated whether ipRGCs also survive after N-methyl-D-aspartic acid (NMDA)-induced excitotoxicity, the main experimental approach to induce and study ganglion cell death.

NMDA is an agonist at the NMDA receptor, one of three ionotropic glutamate receptors [10]. NMDA induces degeneration of ganglion and amacrine cells in the ganglion cell layer (GCL) and inner nuclear layer (INL) of the retina [11,12], and is often used to study molecular mechanisms of ganglion cell death and neuroprotection [13]. Since NMDA injury activates not only proapoptotic but also antiapoptotic signaling [14], this model is also suitable for studying survival mechanisms. Detailed characterization of the molecular response after NMDA application may thus allow an understanding of why some cells die and some cells survive in response to a particular stimulus. This seems crucial for comprehending the mechanisms of ganglion cell death and eventually treating diseases such as glaucoma, the second leading cause of blindness worldwide [15].

The molecular basis for protecting ipRGCs has not been identified, but may involve phosphatidylinositol 3-kinase (PI3K)/AKT signaling, at least after optic nerve transection and ocular hypertension [5]. Another endogenous survival signaling pathway that may increase the resistance of ipRGCs

Correspondence to: C Grimm, University of Zurich, Ophthalmology, Laboratory for Retinal Cell Biology, Wagistrasse 14, Schlieren, 8952, Switzerland; Phone: +41 44 556 3001; FAX: +41 44 556 3999; email: cgrimm@opht.uzh.ch

Molecular Vision 2012; 18:2814-2827 <http://www.molvis.org/molvis/v18/a288>

may involve Janus kinase/signal transducer and activator of transcription (JAK/STAT) signaling, which has been shown to support the survival of various retinal cells against cell death. JAK/STAT signaling is activated in response to various inner and outer retinal insults such as photoreceptor injury [16], increased intraocular pressure [17], and NMDA excitotoxicity [18,19]. This signaling is initiated by the binding of cytokines of the interleukin-6 (IL-6) family of proteins to their respective transmembrane receptors. Within the IL-6 family, leukemia inhibitory factor (LIF) in particular has been found to be critical for survival of retinal cells under stress. Photoreceptor injury induces *Lif* expression in a subset of Müller glial cells, which controls a downstream signaling cascade culminating in the increased expression of neuroprotective factors such as fibroblast growth factor (FGF2) [16,20-22]. In addition, *Lif* expression is induced after intravitreal injection of NMDA in mice [18], and STAT3 activation is protective for retinal ganglion cells after glutamate injury in vitro and ischemia-reperfusion in vivo [19]. However, whether these pathways are involved in protecting ipRGCs is not known.

In this study, we show that ipRGCs are also resistant to cell death after intravitreal injection of NMDA in mice and present data suggesting that the PI3K/AKT and JAK/STAT pathways are not major contributing factors in the enhanced survival of ipRGCs in this model.

METHODS

Animals: Animals were treated in accordance with the regulations of the Cantonal Veterinary Authority of Zürich and with the Association for Research in Vision and Ophthalmology Statement for the Use of Animals in Ophthalmic and Vision Research. The 129S6/SvEvTac (129S6) mice (Taconic, Hudson, NY), rd10 mice (Jackson Laboratory, Bar Harbor, ME), and CD1 mice (Charles River Laboratories, Wilmington, MA) were housed in a 12 h:12 h light-dark cycle with access to food and water ad libitum. During the light cycle, the light level was maintained at 60 lux.

Intravitreal injections: Injections were always performed between 9 and 11 AM to control for circadian variations in gene expression levels. Mice were anesthetized with a subcutaneous injection (2 µl per gram bodyweight) of a mixture of 510 µl ketamine and 60 µl xylazine. Withdrawal response to paw pinch was tested after 10 min, and when sufficiently immobilized, the animals were prepared for surgery. A surgical needle was used to create a sling for the upper eyelid, and the cornea and conjunctiva were anesthetized locally with oxybuprocaine 0.4% eye drops (Théa Pharma, Schaffhausen, Switzerland). A small area of conjunctiva 1 mm distal to the limbus was dissected away to reveal the sclera, and a sclerostomy was made with a 30-gauge needle. A 30-gauge blunt-end needle on a 10 µl Hamilton syringe was then used to inject 1 µl of 40 mM NMDA (Sigma-Aldrich, St. Louis, MO) in 0.1 M phosphate buffered saline (PBS: 2.622 g of $NaH_2PO_4xH_2O$; 11.5 g Na_2HPO_4; 8 g NaCl; 0.2 g KCl per 1000 ml H_2O) under light microscopy visualization through the pupil. The fellow eye was injected with PBS alone. Alternately, 1 µl of a mixture of 40 mM NMDA / 1 mM wortmannin (Sigma-Aldrich) in 10% dimethyl sulfoxide (DMSO, Sigma-Aldrich) and PBS or 1 µl of a mixture of 40 mM NMDA / 10 mg/ml AG-490 (LC Laboratories, Woburn, MA) in 50% DMSO and PBS were coinjected. Here, the fellow eye was injected with 40 mM NMDA in 10% DMSO and PBS, with 1 mM wortmannin in 10% DMSO and PBS or with 10 mg/ml AG-490 in 50% DMSO and PBS, respectively. The injection needle was left in place for 20 s before being slowly withdrawn. Care was taken to avoid injury to the lens or retina. After injection, the cornea was dabbed with a cotton swab and coated with a lubricating eye gel (Lacrinorm, Bausch and Lomb, Schenkon, Switzerland). Mice recovered from anesthesia on a heating pad in dimmed light conditions with frequent monitoring and were assessed daily after injection for signs of infection.

Morphology and quantification of retinal ganglion cells: At 6 days post injection, the eyes were enucleated and fixed overnight in 4% (w/v) paraformaldehyde in PBS. After a washing step with PBS, the eyes were dehydrated in a series of increasing ethanol concentrations, washed in xylene, and fixed in paraffin. Semithin sagittal sections (500 nm) bisecting the optic nerve were prepared and stained with hematoxylin and eosin. Sections were analyzed with light microscopy, and cell bodies in the ganglion cell layer were counted from periphery to periphery in two sections per eye and averaged. A total of three eyes (n=3) were analyzed per condition. Erythrocytes and endothelial cells were excluded from counting.

RNA isolation and semiquantitative real time–polymerase chain reaction: Mice were sacrificed at 6 h, 24 h, 48 h, or 6 days post injection. Retinas were isolated through a corneal incision and immediately frozen in liquid nitrogen. Total RNA was extracted using an RNA isolation kit (RNeasy; Qiagen, Hilden, Germany) including a DNase treatment step. Retinas from eyes injected with AG-490 were isolated, and RNA and protein were simultaneously prepared from the same retina: Retinas were homogenized in 200 µl H_2O by sonication (10 cycles; 0.3 s ON (30% output) and 0.7 s OFF) at 4 °C. Immediately after homogenization, 50 µl were added to 450 µl lysis/binding buffer from the High Pure RNA Isolation Kit (Roche Diagnostics, Mannheim, Germany). RNA

Molecular Vision 2012; 18:2814-2827 <http://www.molvis.org/molvis/v18/a288>

isolation was performed using the same kit according to the manufacturer's recommendations. 140 µl of the homogenate were added to 16 µl of 1M Tris-HCl (pH 7.6), and protein concentrations were determined using Bradford reagent and a bovine serum albumin standard. Proteins were used for western blotting as described below.

Reverse transcription was performed using oligo(dT) and M-MLV reverse transcriptase (Promega, Madison, WI). Semiquantitative real-time PCR was used to analyze gene expression of samples in duplicate or triplicate. This was performed with specific primer pairs (Table 1) spanning an exon-exon junction in the RNA of the gene in question, a polymerase ready mix (LightCycler 480 SYBR Green I Master Mix; Roche Diagnostics, Indianapolis, IN), and a thermocycler (LightCycler; Roche Diagnostics). Signals were normalized to *β-actin* (*Actb*) and relative expression was calculated with the comparative threshold cycle (ΔΔCT) method using a control sample for calibration [23].

Immunofluorescence on sagittal sections: Treated 129S6 wild-type mice were sacrificed 6 days following injection. Eyes were enucleated and fixed overnight in 4% (w/v) paraformaldehyde in PBS. After the cornea and lens were removed, eyecups were postfixed in 4% paraformaldehyde for an additional 2 h before being transferred to 30% sucrose in 0.1 M PBS at 4 °C for 4–12 h. The eyes were then embedded in tissue-freezing medium (Leica Microsystems Nussloch GmbH, Nussloch, Germany) and frozen in a 2-methylbutane bath cooled by liquid nitrogen. Retinal sagittal sections (12 µm) were cut, placed on slides, and incubated with a blocking solution (3% normal goat serum, 0.3% Triton X-100 in 0.1 M PBS) for 1 h at room temperature (RT). For protein detection, sections were incubated at 4 °C overnight with mouse anti-BRN3A (1:100, cat no. MAB1585, Millipore, Billerica, MA) diluted in blocking solution. After three washes with PBS, slides were incubated with a secondary antibody coupled to Cy3 for 1 h at room temperature, washed, counterstained with 4',6-diamidino-2-phenylindole (DAPI), and mounted with antifade medium (10% (v/v) Mowiol 4–88; Calbiochem, San Diego, CA), in 100 mM Tris (pH 8.5), 25% glycerol (w/v), and 0.1% 1,4-diazabicyclo (2.2.2) octane. Immunofluorescent staining was analyzed with a digitalized microscope (AxioVision; Carl Zeiss Meditec, Dublin, CA).

Western blots: Wild-type 129S6 mice were sacrificed at 6 h or 24 h following injection and the retinas isolated and snap frozen as described above. Retinas were sonified in 0.1 M Tris/HCl (pH 8.0) and analyzed for protein content using Bradford reagent. Protein extracts were mixed with sodium dodecylsulfate sample buffer and incubated for 10 min at 75 °C. Equivalent amounts of proteins were separated with sodium dodecylsulfate–polyacrylamide gel electrophoresis and transferred to nitrocellulose membranes. Membranes were blocked in 5% milk (Bio-Rad, Hercules, CA) in TBST (10 mM Tris/HCl [pH 8.0], 150 mM NaCl, and 0.05% Tween-20) for 1 h at room temperature before being incubated overnight at 4 °C in the same 5% milk solution containing the respective primary antibody. The primary antibodies used were as follows: rabbit anti-STAT3 (1:1000, no. 9132, Cell Signaling Technology, Beverly, MA), rabbit anti-pSTAT3 (1:500, no. 9131, Cell Signaling Technology), rabbit anti-STAT1 (1:1000, no. 9172, Cell Signaling Technology), rabbit anti-pSTAT1 (1:1000, no. 9171, Cell Signaling Technology), rabbit anti-caspase 1 (1:10,000, generous gift from Peter Vandenabeele, Ghent University, Belgium),

Table 1. Primer pairs used for semiquantitative real time PCR

Gene	Upstream	Downstream	Product
Actb	CAACGGCTCCGGCATGTGC	CTCTTGCTCTGGGCCTCG	153 bp
Brn3a	CGCCGCTGCAGAGCAACCTCTT	TGGTACGTGGCGTCCGGCTT	130 bp
Casp1	GGCAGGAATTCTGGAGCTTCAA	GTCAGTCCTGGAAATGTGCC	138 bp
Clc	GCATCAACTCCGCAGCTTAG	CTGAACGCCATAGCCAGGTCT	443 bp
Edn2	AGACCTCCTCCGAAAGCTG	CTGGCTGTAGCTGGCAAAG	64 bp
Fgf2	TGTGTCTATCAAGGGAGTGTGTGC	ACCAACTGGAGTATTTCCGTGACCG	158 bp
Gfap	CCACCAAACTGGCTGATGTCTAC	TTCTCTCCAAATCCACACGAGC	240 bp
Gnat1	GAGGATGCTGAGAAGGATGC	TGAATGTTGAGCGTGGTCAT	209 bp
Gnat2	GCATCAGTGCTGAGGACAAA	CTAGGCACTCTTCGGGTGAG	192 bp
Lif	AATGCCACCTGTGCCATACG	CAACTTGGTCTTCTCTGTCCCG	216 bp
Mcp-1	GGCTCAGCCAGATGCAGTTA	CTGCTGCTGGTGATCCTCTT	108 bp
Opn4	CCAGCTTCACAACCAGTCCT	CAGCCTGATGTGCAGATGTC	111 bp
Stat3	CAAAACCCTCAAGAGCCAAGG	TCACTCACAATGCTTCTCCGC	139 bp

Molecular Vision 2012; 18:2814-2827 <http://www.molvis.org/molvis/v18/a288>

mouse anti-glial fibrillary acidic protein (1:500, no. G-3893, Sigma-Aldrich), rabbit anti-pAKT$_{Ser473}$ (1:2500, no. 9271, Cell Signaling Technology), rabbit anti-AKT (1:2500, no. 9272, Cell Signaling Technology), and mouse anti-β-actin (1:5000, no. A5441, Sigma-Aldrich). Detection was with horseradish peroxidase–conjugated secondary antibodies, and proteins were visualized using a detection kit (Western Lightning Plus-ECL, PerkinElmer Life Sciences, Boston, MA).

Immunofluorescence and quantification of cells in retinal flat mounts: Six days after intravitreal injection, 129S6 wild-type mice were deeply anesthetized with 200 µl ketamine / 60 µl xylazine administered intraperitoneally before being perfused with 10 ml of PBS followed by 20 ml of 4% paraformaldehyde in PBS. Eyes were enucleated, incubated for 5 min in 2% paraformaldehyde in PBS, and transferred to PBS. The eyes were cut along the ora serrata and the cornea and lens were removed. The retina was then dissected from the sclera and flattened by making four radial cuts yielding a cloverleaf shape [24]. Before immunofluorescence analysis, retinal flat mounts were incubated for 1 h (at RT) in 4% paraformaldehyde in PBS and blocked with PBS containing 3% fetal bovine serum and 0.3% Triton X-100 for 1 h (at RT). They were then incubated with the appropriate primary antibodies for 48 h: mouse anti-BRN3A (1:100, cat no. MAB1585, Millipore), rabbit anti-OPN4 (1:500, generous gift from Dr. Ignacio Provencio, Charlottesville, VA), and mouse anti-NR1 (1:500, clone N308/48, NeuroMab c/o Antibodies Inc., Davis, CA). Flat mounts were washed 3 times for 10 min each in PBS and then incubated for 2 h with the respective secondary antibody (anti-mouse-Cy2, anti-rabbit-Cy3, 1:500). They were washed again with PBS before being mounted with antifade medium (Mowiol 4-88 Reagent, Sigma-Aldrich). Immunofluorescent staining was analyzed with a digitalized microscope (AxioVision, Carl Zeiss Meditec).

Quantification of BRN3A-positive cells was performed by counting labeled cells in eight 380 by 610 µm microscopic fields per retina. Fields were located at 700 µm and 1700 µm from the optic nerve head in each retinal quadrant. The cell counts of all eight fields were averaged and extrapolated to the number of cells per mm^2 using the measured total retina area. As there are far fewer OPN4-positive cells in the retina, these were quantified by counting the total number of labeled cells per whole retina and then converting to cells per mm^2 as above.

Statistical analyses: Statistical analyses were performed using Prism4 software. Statistical differences of means were calculated using one-way (if three or more experimental groups and one variable) or two-way (if two or more variables) analysis of variance (ANOVA) followed by Bonferroni post-hoc testing. A two-tailed unpaired Student *t* test was used only when only two experimental groups and one variable were present. P values less than 0.05 were considered significant.

RESULTS

Ganglion cell death after intravitreal injection of N-methyl-D-aspartic acid: We confirmed loss of cells in the ganglion cell layer with light microscopy of sagittal retinal sections at 6 days after intravitreal injection of NMDA (Figure 1A-C), and with immunofluorescence staining for BRN3A (Figure 1D-F). BRN3A is a POU-domain transcription factor expressed in thalamocortical and collicular projecting RGCs. BRN3A is frequently used as an RGC marker, as a decrease in *Brn3a* mRNA levels correlates with loss of ganglion cells [25-27]. NMDA-treated retinas showed reduced cell density in the GCL (Figure 1G) and probably the INL (not quantified). No difference was observed between PBS-treated and uninjected retinas; they appeared essentially normal. As in previously published studies [11,28-30], we observed a loss of about two-thirds of cells in the ganglion cell layer after NMDA was injected compared to PBS ($p<0.001$). As already shown by others, this effect was dose dependent [11] (data not shown). Although we did not differentiate between ganglion cells and displaced amacrine cells in the ganglion cell layer, NMDA treatment leads to significant loss of both types of cells in the inner retina, and a loss of cells in the ganglion cell layer strongly correlates with axonal loss in the optic nerve [18].

Expression of Opn4 is not affected by N-methyl-D-aspartic acid injection: To test the sensitivity of the melanopsin-expressing subset of ganglion cells to NMDA toxicity, we analyzed expression of *Brn3a* and *Opn4* mRNA via semi-quantitative real-time PCR in wild-type mice at 6 h, 24 h, 48 h, and 6 days after intravitreal injection of NMDA (Figure 2). As expected, expression of *Brn3a* was strongly reduced starting at 24 h after treatment. Although apoptosis starts as early as 6 h after NMDA injection [28], the decrease in *Brn3a* mRNA expression at this early time point was not yet statistically significant. In contrast to *Brn3a*, levels of *Opn4* mRNA were unchanged at all four time points after NMDA injection, suggesting either that *Opn4*-expressing RGCs were resistant against NMDA toxicity or that the surviving cells increased expression as a compensatory reaction. Since *Opn4* is expressed in a circadian pattern [31,32], NMDA-treated and control mice of a particular time group were always treated in parallel and analyzed at the same time of day.

OPN4-positive ganglion cells are resistant to N-methyl-D-aspartic acid–induced excitotoxic cell death: To distinguish

Molecular Vision 2012; 18:2814-2827 <http://www.molvis.org/molvis/v18/a288>

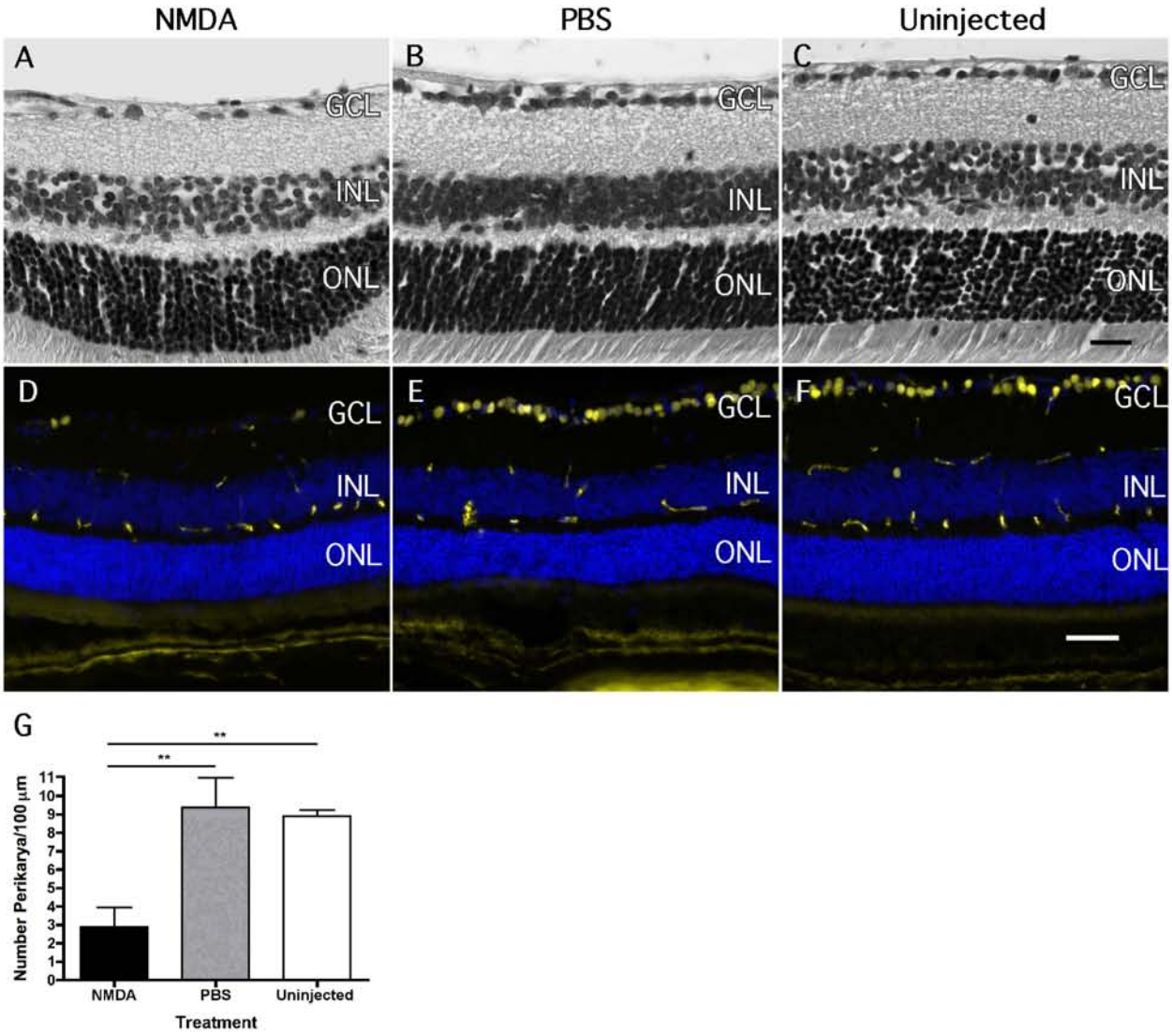

Figure 1. Cells in the ganglion cell layer are lost after intravitreal injection of N-methyl-D-aspartic acid. **A-C**: Shown are representative photomicrographs of retinal sections from wild type mice 6 days after intravitreal injection of **A**: N-methyl-D-aspartic acid (NMDA) or **B**: phosphate buffered saline (PBS). **C**: Untreated retinas served as controls. **D-F**: Shown are representative photomicrographs of immunfluorescent stainings for BRN3A (yellow) and DAPI (blue) in semithin sagittal sections through retinas 6 days after injection of **D**: NMDA or **E**: PBS. **F**: Uninjected eyes served as controls. Note the non-specific staining of blood vessels by the secondary antibody, especially in the outer plexiform layer (OPL), inner nuclear layer (INL), and inner plexiform layer (IPL). **G**: Cell bodies in the ganglion cell layer (GCL) were quantified at 6 days after intravitreal injection of NMDA (black bar) or PBS (grey bar), and in untreated eyes (white bar). Shown are means±SD (n=3) for all treatments and analyses. Scale bars were **A-C**: 20 µm, **D-F**: 50 µm. **: $p<0.01$. A one-way ANOVA with Bonferroni post hoc test was used to test statistical significance.

between resistance against NMDA toxicity and a compensatory upregulation of *Opn4* in surviving RGCs, we costained flat mounted retinas of NMDA- and PBS-injected mice for BRN3A and OPN4 (Figure 3A-H). We observed markedly fewer BRN3A-positive cells in NMDA-treated retinas (Figure 3A,C,G) compared to the control retinas (Figure 3B,D,H), but no obvious difference in the number of OPN4-positive cells between the two treatment groups (Figure 3A,E,G,B,F,H). Quantification of BRN3A- and OPN4-positive cells confirmed the mRNA expression data, showing a significantly reduced number of BRN3A-positive cells in the retinas of the NMDA-treated mice (1188±834.6 cells/mm^2

Molecular Vision 2012; 18:2814-2827 <http://www.molvis.org/molvis/v18/a288>

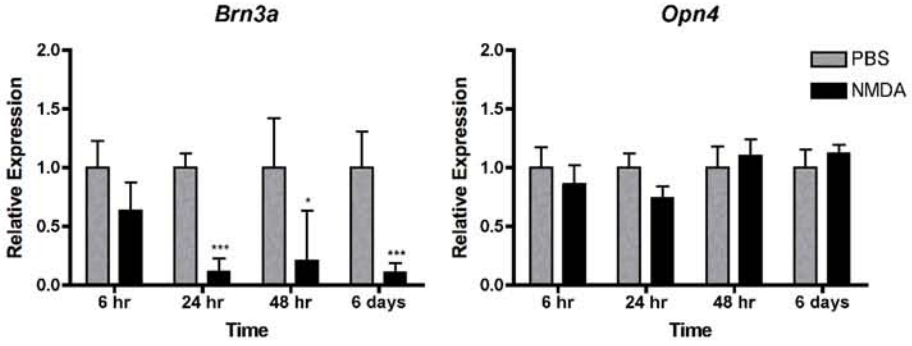

Figure 2. Expression of *Opn4* is not affected by N-methyl-D-aspartic acid injection. Shown are the relative expression levels of *Brn3a* and *Opn4* in retinas of wild type mice at 6 h, 24 h, 48 h, and 6 days after injection of N-methyl-D-aspartic acid (NMDA, black bars) or phosphate buffered saline (PBS, grey bars). Expression after NMDA injection was expressed relative to expression after PBS injection, which was set to 1 for each time point. Shown are means±SD of n=4-6. *; p<0.05; ***; p<0.001. A two-way ANOVA with Bonferroni post hoc test was used to test statistical significance.

for NMDA versus 2567±306 cells/mm² for PBS; mean±SD; Figure 3I) while the number of OPN4-positive cells did not change (37.1±2.3 cells/mm² for NMDA versus 35.5±3.3 cells/mm² for PBS; Figure 3J). Thus, *Opn4* RNA levels were maintained after NMDA treatment not because of a compensatory upregulation of gene expression but because of the resistance of OPN4-positive ipRGCs to NMDA excitotoxicity.

Intrinsically photosensitive retinal ganglion cell resistance to N-methyl-D-aspartic acid toxicity is independent of genetic background, pigmentation, and the presence of photoreceptor cells: To determine whether the survival of OPN4-positive ipRGCs after NMDA treatment was a phenomenon isolated to the particular strain of wild-type mice used (129S6), we also analyzed *Brn3a* and *Opn4* expression in NMDA-treated albino CD1 mice. Again, NMDA treatment significantly reduced *Brn3a* but not *Opn4* expression (Figure 4A). This observation suggests that the survival of ipRGCs after NMDA is a general phenomenon and is not due to differences in pigmentation or genetic background.

To determine whether ipRGC resistance to NMDA toxicity depended on the presence of regulated glutamate release from bipolar cells and thus on phototransduction-initiated signaling from photoreceptor cells, we injected NMDA in rd10 mice. The rd10 mouse carries a missense mutation in exon 13 of the β-subunit of cyclic guanosine monophosphate phosphodiesterase, and exhibits degeneration of rod and cone photoreceptors beginning at PND16 with almost complete degeneration by PND60 [33]. We injected the eyes of rd10 mice at PND20 when the retinas contained functional photoreceptors and at 6 months of age, when the rd10 mice had virtually no photoreceptor function left. We confirmed degeneration of photoreceptors with semiquantitative real-time PCR for rod (*Gnat1*) and cone (*Gnat2*) transducin, which were expressed at the expected levels [34] in each age group (data not shown). Six days after injection, we compared *Brn3a* and *Opn4* expression in young and old rd10 mice. As in the wild-type mice, we observed a significant reduction in *Brn3a* but not *Opn4* mRNA expression in both age groups (Figure 4B,C). This suggests that neither NMDA-induced toxicity to "traditional" ganglion cells nor survival of ipRGCs depended on signaling from photoreceptor cells.

Endogenous rescue and stress pathways are activated after intravitreal N-methyl-D-aspartic acid injection: The JAK/STAT pathway is an endogenous survival signaling pathway activated in response to various inner and outer retinal insults such as photoreceptor injury [16,35] and ganglion cell death after intraocular hypertension [17]. To test a potential role of this signaling mechanism in NMDA-induced excitotoxicity, we analyzed the mRNA levels of several members of the JAK/STAT pathway at various time points after intravitreal NMDA injection (Figure 5A). We found that the *Lif* and *Clc* mRNA levels were significantly increased by a factor of 5 and 3.5, respectively, at 6 h after injection. *Edn2* and *Fgf2* mRNA expression peaked at 24 h, with approximately ten- and threefold greater expression levels compared to the PBS-injected retinas. This was followed by an increase in *Stat3* and *Gfap* expression, which peaked at 48 h. STAT3 is known to have antiapoptotic effects via activation of the suppressor of cytokine signaling (SOCS) family of proteins and the Bcl-2 family [19]. Glial fibrillary acidic protein (*Gfap*) is a marker for activated Müller glial cells. Several genes encoding proapoptotic proteins also increased expression after NMDA injection: Levels of *Stat1* mRNA were significantly increased at 24 h, and caspase-1 (*Casp-1*) mRNA was threefold and fourfold elevated compared to controls at 24 h and 48 h, respectively. In contrast, monocyte chemotactic protein-1 (*Mcp-1*), a cytokine involved in recruiting white blood cells to sites of infection or inflammation [36], was

Molecular Vision 2012; 18:2814-2827 <http://www.molvis.org/molvis/v18/a288>

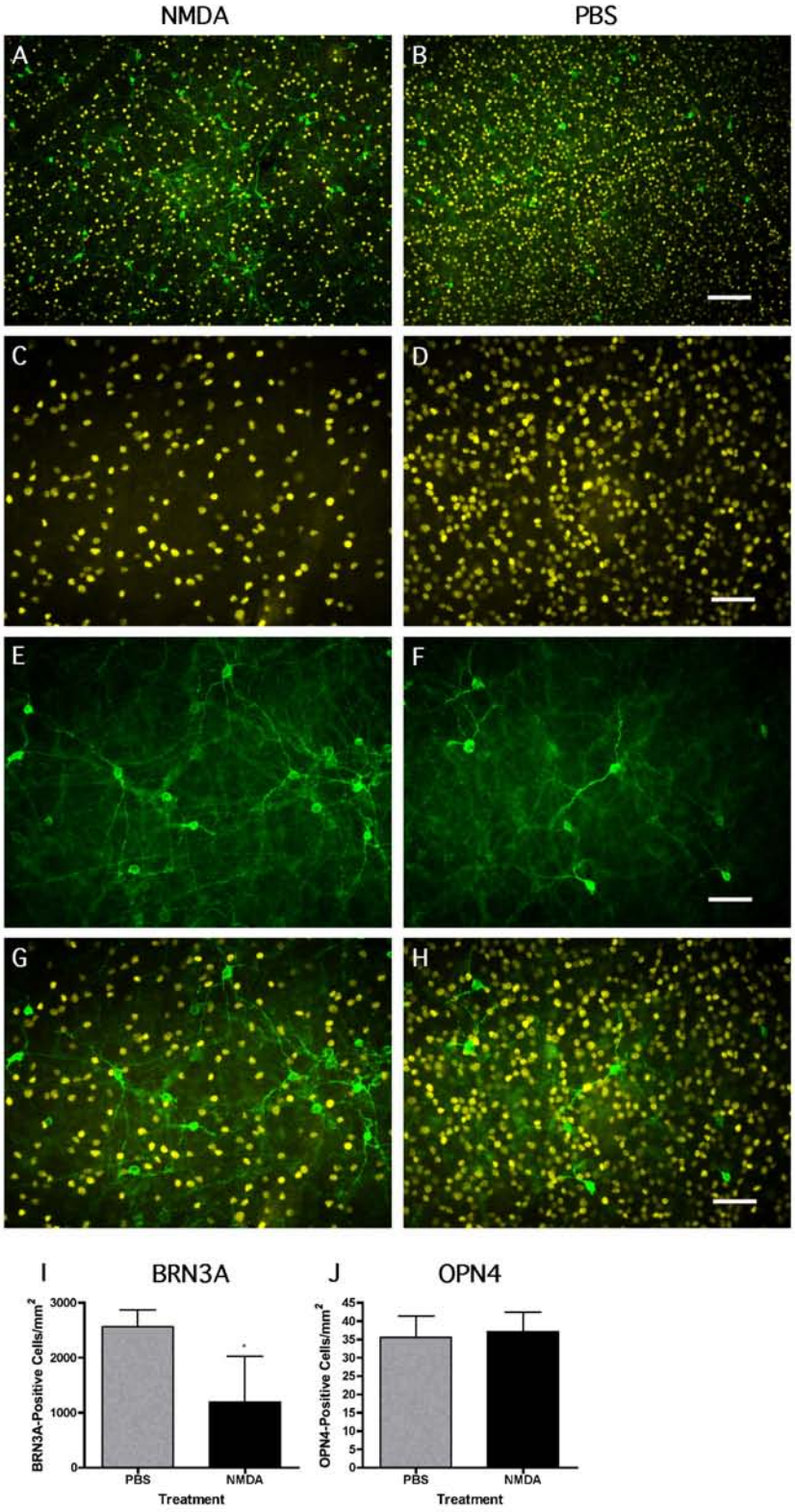

Figure 3. N-methyl-D-aspartic acid treatment does not reduce survival of OPN4-positive ganglion cells. Shown are representative photomicrographs taken from retinal flat mounts stained for BRNA3A (yellow) and OPN4 (green) at 6 days after **A**, **C**, **E**, **G**: N-methyl-D-aspartic acid (NMDA) injection or **B**, **D**, **F**, **H**: phosphate buffered saline (PBS) injection. **A**, **B**: Shown is double labeling for BRN3A and OPN4. **C**, **D**: Shown is BRN3A staining. **E**, **F**: Shown is OPN4 staining. **G**, **H**: Shown are merges of panels **C** and **E**, or **D** and **F**, respectively, n=3-4. Scale bars are **A**, **B**: 100 µm; **C-H**: 50 µm. **I-J**: Shown is quantification of I: BRN3A- positive cells and **J**: OPN4-positive cells in retinal flat mounts at 6 days after NMDA (black bars) or PBS (grey bars) treatment. Shown are means±SD of n=3-4. *; $p<0.05$. An unpaired two-tailed Student t test was used to test statistical significance.

Molecular Vision 2012; 18:2814-2827 <http://www.molvis.org/molvis/v18/a288>

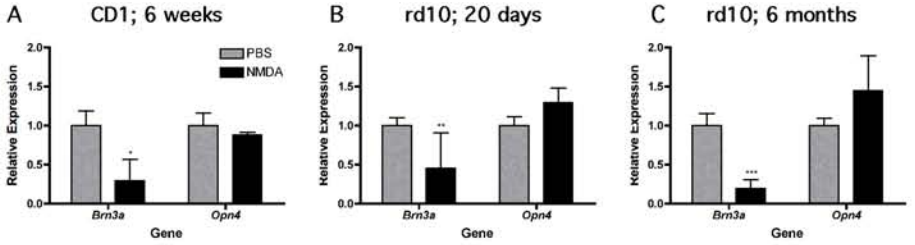

Figure 4. Resistance of OPN4-positive cells against N-methyl-D-aspartic acid toxicity does not depend on genetic background, pigmentation or presence of photoreceptor cells. **A**: Shown is the relative expression of *Brn3a* and *Opn4* mRNAs in retinas of 6 week old albinotic CD1 wild type mice at 6 days after injection of N-methyl-D-aspartic acid (NMDA, black bars) or phosphate buffered saline (PBS, grey bars). **B**: Shown is the relative expression of *Brn3a* and *Opn4* at 6 days after injection of NMDA (black bars) or PBS (grey bars) in rd10 mice at 20 days of age. **C**: Shown is the relative expression of *Brn3a* and *Opn4* at 6 days after injection of NMDA (black bars) or PBS (grey bars) in rd10 mice at 6 months of age. Gene expression after NMDA injection was expressed relative to expression after PBS injection, which was set to 1. Shown are means±SD of n=4-10. *: p<0.05; **: p<0.01; ***: p<0.001. Statistical tests used were **A**: unpaired two-tailed Student t test, and **B-C**: two-way ANOVA with Bonferroni post hoc test.

similarly expressed in the NMDA- and PBS-treated retinas, even though a tendency for increased expression was detected in NMDA retinas at 24 h after injection.

Activation of some of these molecules after NMDA injection was also detectable at the protein level with western blotting (Figure 5B). At 24 h after injection, we found strongly elevated levels of phospho-STAT3, STAT3, phospho-STAT1, and STAT1 in the NMDA-treated retinas compared to the PBS-injected controls. In addition, expression of glial fibrillary acidic protein and the proform of CASP1 was also increased, although somewhat less robustly than the proteins mentioned above.

Intrinsically photosensitive retinal ganglion cell survival after N-methyl-D-aspartic acid injection is independent of phosphatidylinositol 3-kinase/AKT or STAT3 signaling: In models of optic nerve transection and ocular hypertension, the PI3K/AKT pathway was implicated in enhanced survival of ipRGCs [5]. To test whether this pathway may also contribute to the resistance of ipRGCs against NMDA toxicity, we coinjected NMDA with wortmannin (WM), an inhibitor of PI3Ks, and compared the mRNA levels of *Brn3a* and *Opn4* to retinas treated with NMDA or WM alone (Figure 6A). Although *Brn3a* levels were decreased with NMDA and NMDA plus WM injections as expected, *Opn4* remained at control levels even in the presence of the inhibitor. To confirm the inhibitory action of WM on AKT activation, we tested levels of p-AKT_{Ser473} with western blotting. At 6 h after injection, p-AKT_{Ser473} levels were high in NMDA (as previously established [14]), but not in NMDA plus WM injected retinas, indicating that the inhibitor did indeed function as expected (Figure 6B).

Injection of NMDA activated JAK/STAT signaling in the retina (Figure 5), and expression of a constitutively active form of STAT3 protected retinal ganglion cells against ischemia reperfusion in vivo and glutamate toxicity in vitro [19]. We coinjected eyes with NMDA and AG-490, an inhibitor of JAK2, to test whether activation of the JAK/STAT pathway is essential for ipRGC survival in vivo. Coinjection of NMDA with AG-490 reduced phosphorylation of STAT3 compared to injection of NMDA alone suggesting that AG-490 inhibited JAK2 signaling (Figure 6D). However, inhibition of JAK2 did not influence expression of *Brn3a* and *Opn4* after NMDA injection as indicated by the respective RNA levels at 48 h after injection (Figure 6C).

In summary, these results suggest that PI3K/AKT and STAT3 signaling may not be crucial factors in the survival of ipRGCs after NMDA injection.

To verify expression of NMDA receptors on ipRGCs, we treated retinal flat mounts of wild-type mice with anti-NMDAR1 and anti-OPN4 antibodies and analyzed the resulting staining in the GCL. NMDAR1 was widely expressed in cell bodies but not the nuclei of the cells in the GCL (Figure 7A,D). As shown before (Figure 3), OPN4-positive cells were rare but easily detectable (Figure 7B,E). Merged images suggest that OPN4-positive cells also express NMDAR1 subunits (Figure 7C,F).

DISCUSSION

A growing body of evidence suggests that ipRGCs have a generally increased survival rate in various experimental models of ganglion cell death [4-8,37], as well as in human mitochondrial optic neuropathies [9]. Here we demonstrate that ipRGCs are also resistant to NMDA-induced excitotoxicity, and that their resistance does not depend on PI3K/AKT or JAK/STAT signaling. The survival of ipRGCs after various insults is intriguing, and identifying the molecular mechanism(s) responsible for their protection might provide

Molecular Vision 2012; 18:2814-2827 <http://www.molvis.org/molvis/v18/a288>

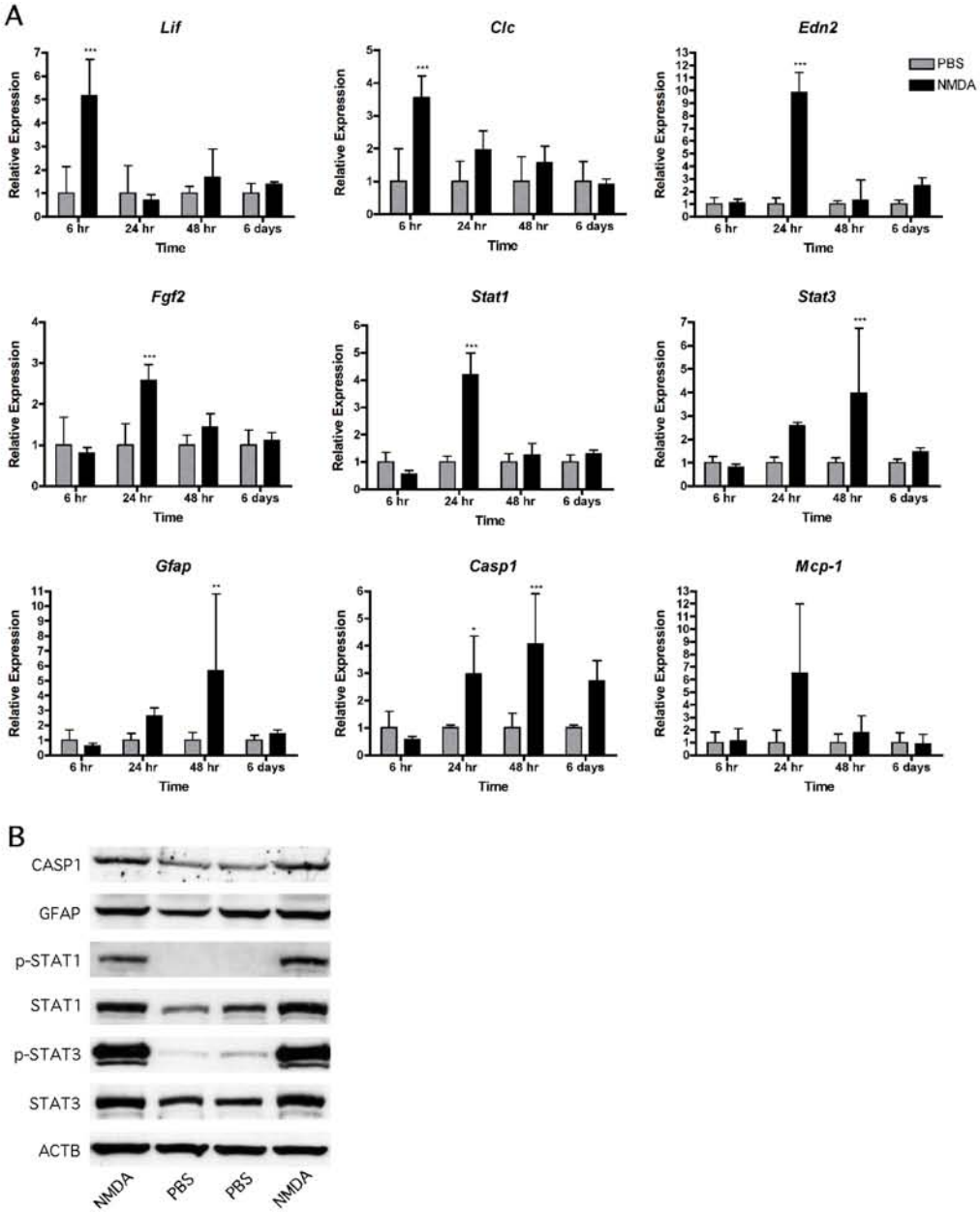

Figure 5. Intravitreal N-methyl-D-aspartic acid injection activates endogenous rescue and stress pathways. **A**: Shown is the relative expression *of Lif, Clc, Edn2, Fgf2, Stat1, Stat3, Gfap, Casp1,* and *Mcp-1* in retinas of 129S6 wild type mice at 6 h, 24 h, 48 h, and 6 days after injection of N-methyl-D-aspartic acid (NMDA, black bars) or phosphate buffered saline (PBS, grey bars). Expression after NMDA injection was expressed relative to expression after PBS injection, which was set to 1 for each time point. Shown are means±SD of n=4-6. *: $p<0.05$; **: $p<0.01$; ***: $p<0.001$. Two-way ANOVA with Bonferroni post hoc test was used to test statistical significance. **B**: Levels of proteins and phosphoproteins in total retinal extracts from 129S6 wild type mice were tested by Western Blotting at 24 h after injection of NMDA or PBS. Shown are protein levels in extracts of two retinas after NMDA and two retinas after PBS injection as indicated, n=3.

the knowledge necessary to preserve ganglion cells in human diseases such as glaucoma.

The mechanism for NMDA excitotoxicity involves activating the NMDA receptor, which results in an influx of

Molecular Vision 2012; 18:2814-2827 <http://www.molvis.org/molvis/v18/a288>

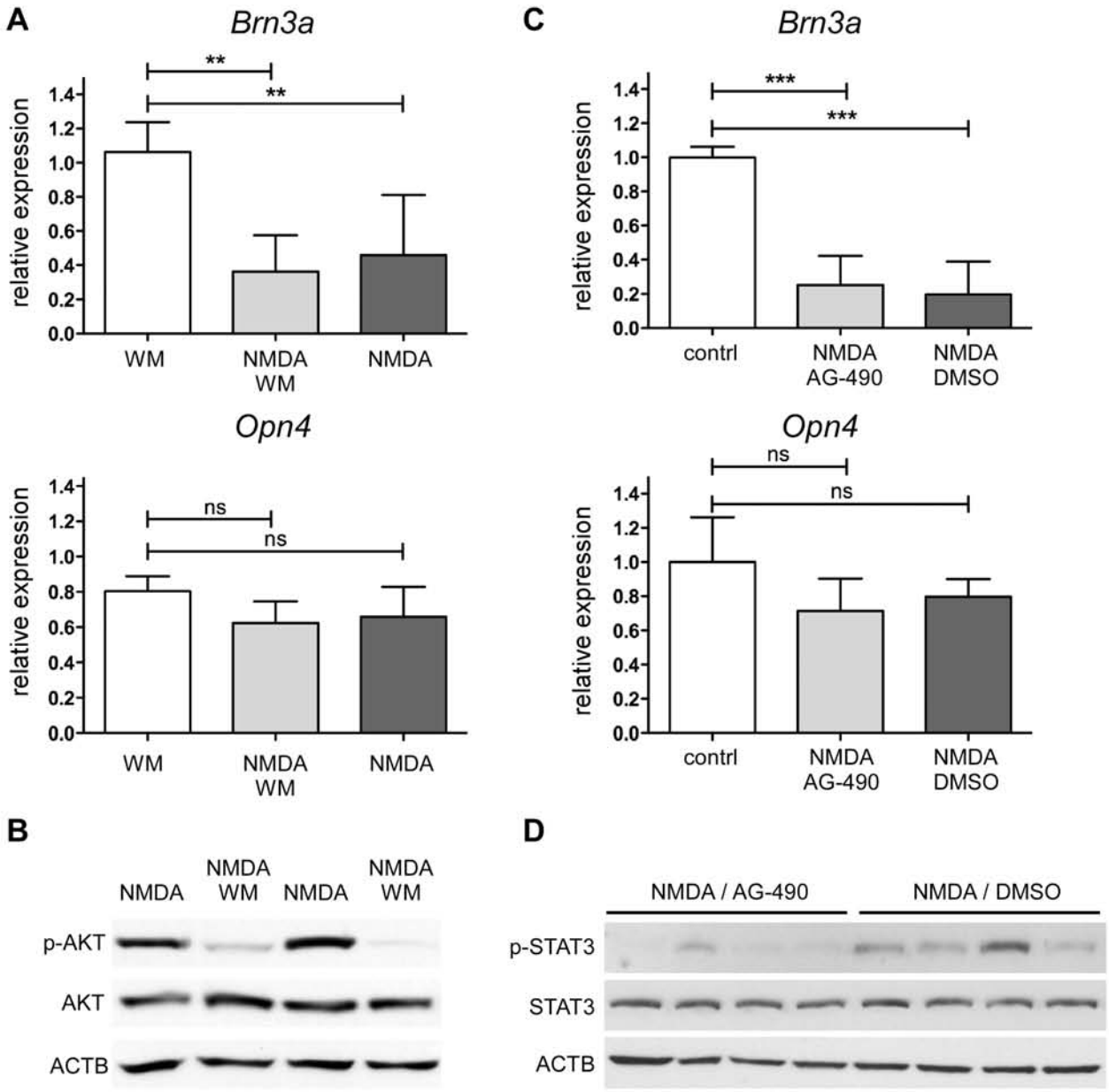

Figure 6. Survival of OPN4-expressing intrinsically photosensitive retinal ganglion cells does not depend on phosphatidylinositol 3-kinase/AKT and Janus kinase/signal transducer and activator of transcription signaling. **A**: Shown is the relative expression of *Brn3a* and *Opn4* in retinas of 129S6 wild type mice at 24 h after injection of N-methyl-D-aspartic acid (NMDA, black bars), NMDA plus wortmannin (WM, grey bars), or WM (white bars). Shown are means±SD of n=4-8. **: $p<0.01$. One-way ANOVA with Bonferroni post hoc test was used to test statistical significance. **B**: Shown are levels of proteins and phosphoproteins in total retinal extracts from 129S6 wild type mice at 6 h after injection of NMDA or NMDA plus WM as indicated, n=3. **C**: Shown is the relative expression of *Brn3a* and *Opn4* in retinas of 129S6 wild type mice at 48 h after injection of NMDA in 50% DMSO (black bars), NMDA plus AG-490 in 50% DMSO (grey bars), or non-injected controls (white bars). Shown are means±SD of n=4. ***: $p<0.001$. One-way ANOVA with Bonferroni post hoc test was used to test statistical significance. **D**: Shown are levels of STAT3 and pSTAT3 in total retinal extracts from 129S6 wild type mice at 48 h after injection of NMDA or NMDA plus AG-490 as indicated. **C**: RNA and **D**: proteins were simultaneously isolated from the same retinas for analysis, n=4.

calcium into the cell, triggering various signaling cascades resulting in apoptotic cell death [30,38,39]. Lack of the

Molecular Vision 2012; 18:2814-2827 <http://www.molvis.org/molvis/v18/a288>

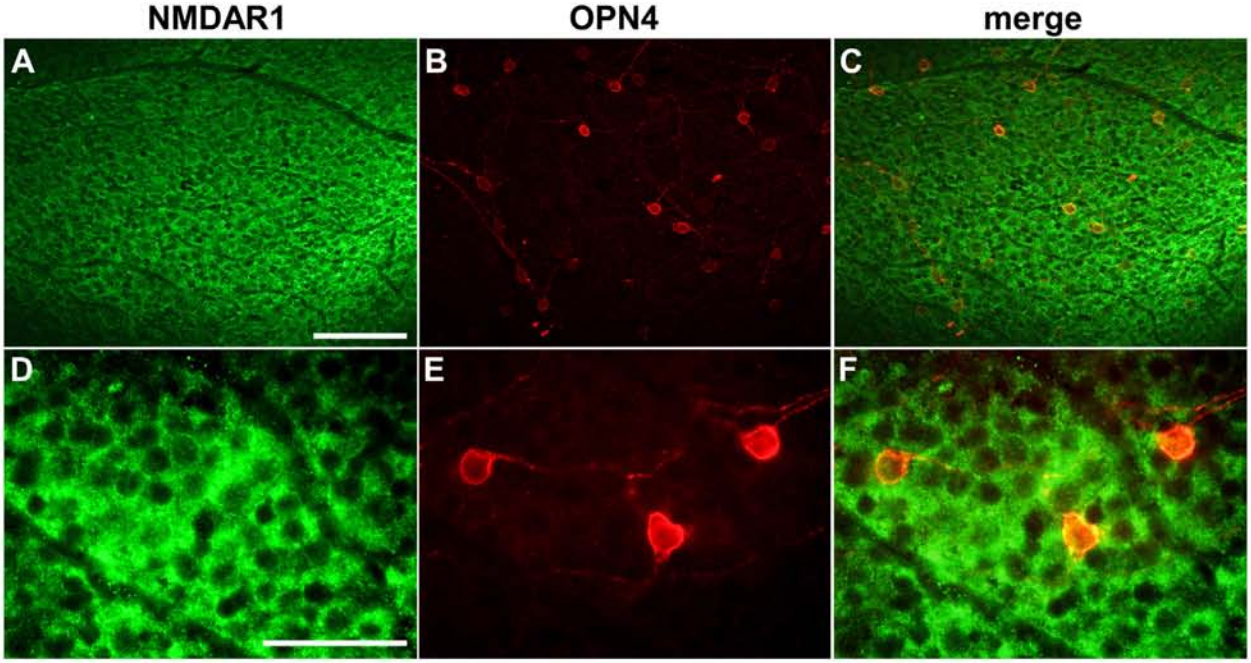

Figure 7. NMDAR1 colocalizes with OPN4 in retinal ganglion cells. Shown are representative photomicrographs taken from retinal flat mounts of untreated wild type mice stained for **A**, **D**: NMDAR1 (green) and **B**, **E**: OPN4 (red) at **A-C**: lower and **D-F**: higher magnification. **C**, **F**: Images shown in panels **A** and **B**, and in panels **D** and **E**, respectively, are merged. Focal plane was at the ganglion cell layer. Scale bars are **A-C**: 100 µm and **D-F**: 50 µm.

NMDA receptor might therefore be a possible explanation for the resistance of ipRGCs to NMDA toxicity. However, several studies including this one (Figure 7) have shown that ipRGCs express glutamate receptors, and single cell PCR data specifically indicates expression of NMDA receptors by ipRGCs [3,40,41]. This suggests that the observed resistance of ipRGCs is based on another mechanism. The calcium permeability of NMDA receptors is reduced when the tripartite receptor complex interacts with NR3A, a subtype of the NR3 component of the receptor [10,42]. Accordingly, lack of NR3A increased susceptibility of RGCs to NMDA toxicity at lower NMDA concentrations of up to 2 nmol [42]. Although the effect was lost at higher NMDA levels [42], it would be interesting to analyze ipRGC survival in NR3A knockouts, especially since Jakobs and coworkers reported expression of NR3A by ipRGCs [41]. Whether increased expression of NR3A and/or reduced expression of other NMDA receptor subunits contributes to protecting ipRGCs against NMDA toxicity must be conclusively shown. However, since such a mechanism may not explain the increased resistance of ipRGCs across the many other models of ganglion cell death (see above), it seems more likely that ipRGCs have developed other mechanisms for their protection against degeneration.

Several such mechanisms have been suggested to explain the greater robustness of ipRGCs. Li and coworkers, for example, implicated the PI3K/AKT pathway in ipRGC survival after optic nerve transection and in a model of intraocular hypertension [5]. However, injection of wortmannin strongly reduced AKT phosphorylation after NMDA application but did not reduce survival of ipRGCs (Figure 6) suggesting that AKT signaling is not the main component of ipRGC resistance against NMDA toxicity.

Other published data point to an involvement of pituitary adenylate cyclase activating polypeptide (PACAP), a peptide found specifically in ipRGCs of the retinohypothalamic tract [37,43]. Exogenous administration of PACAP has been shown to be neuroprotective for "traditional" ganglion cells after optic nerve transection [44], intraocular hypertension [45], kainic acid treatment [46], and NMDA application [28]. Interestingly, exogenous administration of PACAP stimulates IL-6 production by Müller cells in the retina in vitro and in vivo [47]. IL-6 is a known activator of the JAK/STAT pathway, which may confer protection for photoreceptors and ganglion cells [16,17,21]. Several members of this endogenous rescue pathway were activated in response to NMDA injection. As reported by others [19], we observed strongly increased

Molecular Vision 2012; 18:2814-2827 <http://www.molvis.org/molvis/v18/a288>

phosphorylation of STAT3 after NMDA application. In addition, *Lif* was expressed very early, followed by *Edn2* and *Fgf2* (Figure 5), which is similar to models of photoreceptor injury [16,35]. Thus, a signaling mechanism involving Müller glial cells may be activated not only by photoreceptor degeneration but also after NMDA injection. However, blocking JAK/STAT signaling by the application of AG-490 did not reduce survival of ipRGCs after NMDA treatment. Since we also observed elevated levels of proapoptotic proteins such as pSTAT1 and CASP1, NMDA administration activated pro- and antiapoptotic signaling [14]. The nature of the cells that activated the individual signaling pathways still need to be determined in future experiments.

Although RGCs and ipRGCs receive signaling input from rods and cones via synaptic contacts with bipolar and amacrine cells [1,48], survival of ganglion cells is mostly not affected in models of photoreceptor degeneration. However, some species differences seem to exist regarding *Opn4* expression in the absence of photoreceptors. Studies in RCS rats suggest reduced *Opn4* levels despite constant numbers of ipRGCs in the degenerated retina [32]. In addition, N-methyl-N-nitrosourea (MNU) treatment reduced expression of *Opn4* by 83%, whereas only about one-third of melanopsin-expressing cells were lost after MNU injection [49]. Although MNU primarily induces degeneration of photoreceptors, whether this loss of ipRGCs was a direct consequence of MNU or was indirectly caused by photoreceptor degeneration remains to be shown. In contrast, retinas of rod- and cone-less [50,51] as well as of rd10 mice (data not shown) show expression of *Opn4* similar to wild-type mice. Thus, ipRGCs in mice may not be directly influenced by phototransduction-related signaling from photoreceptors and/or regulated glutamate release from second-order neurons. Our data from old rd10 mice support this conclusion and show that survival of ipRGCs after NMDA treatment does not depend on normal retinal physiology and photoreceptor function.

In conclusion, ipRGCs are functionally and morphologically different from "traditional" ganglion cells in that ipRGCs survive high concentrations of intravitreal NMDA. This survival does not depend on PI3K/AKT or JAK/STAT signaling. Clearly, ipRGCs have an intrinsic strength to survive various insults toxic to "traditional" RGCs. Identifying the mechanisms conferring this increased survival competence may prove highly valuable to define strategies for protecting ganglion cells by exogenous approaches.

ACKNOWLEDGMENTS

We thank Cornelia Imsand and Andrea Gubler for excellent technical assistance, Zoltan Nusser (Hungarian Academy of Science, Budapest) for suggesting NMDAR antibodies, and members of the laboratory for their continuous support. This work was funded by the Swiss National Science Foundation (SNF #31003A-133043).

REFERENCES

1. Do MT, Yau KW. Intrinsically photosensitive retinal ganglion cells Physiol Rev 2010; 90:1547-81. [PMID: 20959623].
2. Ecker JL, Dumitrescu ON, Wong KY, Alam NM, Chen SK, LeGates T, Renna JM, Prusky GT, Berson DM, Hattar S. Melanopsin-expressing retinal ganglion-cell photoreceptors: cellular diversity and role in pattern vision Neuron 2010; 67:49-60. [PMID: 20624591].
3. Perez-Leon JA, Warren EJ, Allen CN, Robinson DW, Brown RL. Synaptic inputs to retinal ganglion cells that set the circadian clock Eur J Neurosci 2006; 24:1117-23. [PMID: 16930437].
4. Li RS, Chen BY, Tay DK, Chan HH, Pu ML, So KF. Melanopsin-expressing retinal ganglion cells are more injury-resistant in a chronic ocular hypertension model Invest Ophthalmol Vis Sci 2006; 47:2951-8. [PMID: 16799038].
5. Li SY, Yau SY, Chen BY, Tay DK, Lee VW, Pu ML, Chan HH, So KF. Enhanced survival of melanopsin-expressing retinal ganglion cells after injury is associated with the PI3 K/Akt pathway Cell Mol Neurobiol 2008; 28:1095-107. [PMID: 18512147].
6. Robinson GA, Madison RD. Axotomized mouse retinal ganglion cells containing melanopsin show enhanced survival, but not enhanced axon regrowth into a peripheral nerve graft Vision Res 2004; 44:2667-74. [PMID: 15358062].
7. Sakamoto K, Liu C, Kasamatsu M, Pozdeyev NV, Iuvone PM, Tosini G. Dopamine regulates melanopsin mRNA expression in intrinsically photosensitive retinal ganglion cells Eur J Neurosci 2005; 22:3129-36. [PMID: 16367779].
8. Jakobs TC, Libby RT, Ben Y, John SW, Masland RH. Retinal ganglion cell degeneration is topological but not cell type specific in DBA/2J mice J Cell Biol 2005; 171:313-25. [PMID: 16247030].
9. La Morgia C, Ross-Cisneros FN, Sadun AA, Hannibal J, Munarini A, Mantovani V, Barboni P, Cantalupo G, Tozer KR, Sancisi E, Salomao SR, Moraes MN, Moraes-Filho MN, Heegaard S, Milea D, Kjer P, Montagna P, Carelli V. Melanopsin retinal ganglion cells are resistant to neurodegeneration in mitochondrial optic neuropathies Brain 2010; 133:2426-38. [PMID: 20659957].
10. Low CM, Wee KS. New insights into the not-so-new NR3 subunits of N-methyl-D-aspartate receptor: localization, structure, and function Mol Pharmacol 2010; 78:1-11. [PMID: 20363861].

Molecular Vision 2012; 18:2814-2827 <http://www.molvis.org/molvis/v18/a288>

11. Lam TT, Abler AS, Kwong JM, Tso MO. N-methyl-D-aspartate (NMDA)–induced apoptosis in rat retina Invest Ophthalmol Vis Sci 1999; 40:2391-7. [PMID: 10476807].
12. Li Y, Schlamp CL, Nickells RW. Experimental induction of retinal ganglion cell death in adult mice Invest Ophthalmol Vis Sci 1999; 40:1004-8. [PMID: 10102300].
13. Siliprandi R, Canella R, Carmignoto G, Schiavo N, Zanellato A, Zanoni R, Vantini G. N-methyl-D-aspartate-induced neurotoxicity in the adult rat retina Vis Neurosci 1992; 8:567-73. [PMID: 1586655].
14. Manabe S, Lipton SA. Divergent NMDA signals leading to proapoptotic and antiapoptotic pathways in the rat retina Invest Ophthalmol Vis Sci 2003; 44:385-92. [PMID: 12506100].
15. Quigley HA, Broman AT. The number of people with glaucoma worldwide in 2010 and 2020 Br J Ophthalmol 2006; 90:262-7. [PMID: 16488940].
16. Joly S, Lange C, Thiersch M, Samardzija M, Grimm C. Leukemia inhibitory factor extends the lifespan of injured photoreceptors in vivo J Neurosci 2008; 28:13765-74. [PMID: 19091967].
17. Huang Y, Cen LP, Choy KW, van Rooijen N, Wang N, Pang CP, Cui Q. JAK/STAT pathway mediates retinal ganglion cell survival after acute ocular hypertension but not under normal conditions Exp Eye Res 2007; 85:684-95. [PMID: 17869246].
18. Seitz R, Hackl S, Seibuchner T, Tamm ER, Ohlmann A. Norrin mediates neuroprotective effects on retinal ganglion cells via activation of the Wnt/beta-catenin signaling pathway and the induction of neuroprotective growth factors in Muller cells J Neurosci 2010; 30:5998-6010. [PMID: 20427659].
19. Zhang C, Li H, Liu MG, Kawasaki A, Fu XY, Barnstable CJ, Shao-Min Zhang S. STAT3 activation protects retinal ganglion cell layer neurons in response to stress Exp Eye Res 2008; 86:991-7. [PMID: 18471811].
20. Chollangi S, Wang J, Martin A, Quinn J, Ash JD. Preconditioning-induced protection from oxidative injury is mediated by leukemia inhibitory factor receptor (LIFR) and its ligands in the retina Neurobiol Dis 2009; 34:535-44. [PMID: 19344761].
21. Samardzija M, Wenzel A, Aufenberg S, Thiersch M, Reme C, Grimm C. Differential role of Jak-STAT signaling in retinal degenerations FASEB J 2006; 20:2411-3. [PMID: 16966486].
22. Ueki Y, Wang J, Chollangi S, Ash JD. STAT3 activation in photoreceptors by leukemia inhibitory factor is associated with protection from light damage J Neurochem 2008; 105:784-96. [PMID: 18088375].
23. Joly S, Samardzija M, Wenzel A, Thiersch M, Grimm C. Nonessential role of beta3 and beta5 integrin subunits for efficient clearance of cellular debris after light-induced photoreceptor degeneration Invest Ophthalmol Vis Sci 2009; 50:1423-32. [PMID: 18997092].
24. Caprara C, Thiersch M, Lange C, Joly S, Samardzija M, Grimm C. HIF1A is essential for the development of the intermediate plexus of the retinal vasculature Invest Ophthalmol Vis Sci 2011; 52:2109-17. [PMID: 21212189].
25. Nadal-Nicolás FM, Jimenez-Lopez M, Sobrado-Calvo P, Nieto-Lopez L, Canovas-Martinez I, Salinas-Navarro M, Vidal-Sanz M, Agudo M. Brn3a as a marker of retinal ganglion cells: qualitative and quantitative time course studies in naive and optic nerve-injured retinas Invest Ophthalmol Vis Sci 2009; 50:3860-8. [PMID: 19264888].
26. Quina LA, Pak W, Lanier J, Banwait P, Gratwick K, Liu Y, Velasquez T, O'Leary DD, Goulding M, Turner EE. Brn3a-expressing retinal ganglion cells project specifically to thalamocortical and collicular visual pathways J Neurosci 2005; 25:11595-604. [PMID: 16354917].
27. Torero Ibad R, Rheey J, Mrejen S, Forster V, Picaud S, Prochiantz A, Moya KL. Otx2 promotes the survival of damaged adult retinal ganglion cells and protects against excitotoxic loss of visual acuity in vivo J Neurosci 2011; 31:5495-503. [PMID: 21471386].
28. Endo K, Nakamachi T, Seki T, Kagami N, Wada Y, Nakamura K, Kishimoto K, Hori M, Tsuchikawa D, Shinntani N, Hashimoto H, Baba A, Koide R, Shioda S. Neuroprotective effect of PACAP against NMDA-induced retinal damage in the mouse J Mol Neurosci 2011; 43:22-9. [PMID: 20703829].
29. Ito Y, Shimazawa M, Inokuchi Y, Fukumitsu H, Furukawa S, Araie M, Hara H. Degenerative alterations in the visual pathway after NMDA-induced retinal damage in mice Brain Res 2008; 1212:89-101. [PMID: 18440495].
30. Lebrun-Julien F, Duplan L, Pernet V, Osswald I, Sapieha P, Bourgeois P, Dickson K, Bowie D, Barker PA, Di Polo A. Excitotoxic death of retinal neurons in vivo occurs via a non-cell-autonomous mechanism J Neurosci 2009; 29:5536-45. [PMID: 19403821].
31. Hannibal J. Regulation of melanopsin expression Chronobiol Int 2006; 23:159-66. [PMID: 16687290].
32. Sakamoto K, Liu C, Tosini G. Classical photoreceptors regulate melanopsin mRNA levels in the rat retina J Neurosci 2004; 24:9693-7. [PMID: 15509757].
33. Chang B, Hawes NL, Pardue MT, German AM, Hurd RE, Davisson MT, Nusinowitz S, Rengarajan K, Boyd AP, Sidney SS, Phillips MJ, Stewart RE, Chaudhury R, Nickerson JM, Heckenlively JR, Boatright JH. Two mouse retinal degenerations caused by missense mutations in the beta-subunit of rod cGMP phosphodiesterase gene Vision Res 2007; 47:624-33. [PMID: 17267005].
34. Samardzija M, Wariwoda H, Imsand C, Huber P, Heynen SR, Gubler A, Grimm C. Activation of survival pathways in the degenerating retina of rd10 mice Exp Eye Res 2012; [PMID: 22546314].
35. Bürgi S, Samardzija M, Grimm C. Endogenous leukemia inhibitory factor protects photoreceptor cells against light-induced degeneration Mol Vis 2009; 15:1631-7. [PMID: 19693290].
36. Kolattukudy PE, Niu J. Inflammation, endoplasmic reticulum stress, autophagy, and the monocyte chemoattractant

Molecular Vision 2012; 18:2814-2827 <http://www.molvis.org/molvis/v18/a288>

protein-1/CCR2 pathway Circ Res 2012; 110:174-89. [PMID: 22223213].

37. La Morgia C, Ross-Cisneros FN, Hannibal J, Montagna P, Sadun AA, Carelli V. Melanopsin-expressing retinal ganglion cells: implications for human diseases Vision Res 2011; 51:296-302. [PMID: 20691201].

38. Nakazawa T, Shimura M, Ryu M, Nishida K, Pages G, Pouyssegur J, Endo S. ERK1 plays a critical protective role against N-methyl-D-aspartate-induced retinal injury J Neurosci Res 2008; 86:136-44. [PMID: 17722069].

39. Vorwerk CK, Lipton SA, Zurakowski D, Hyman BT, Sabel BA, Dreyer EB. Chronic low-dose glutamate is toxic to retinal ganglion cells. Toxicity blocked by memantine. Invest Ophthalmol Vis Sci 1996; 37:1618-24. [PMID: 8675405].

40. Hartwick AT, Bramley JR, Yu J, Stevens KT, Allen CN, Baldridge WH, Sollars PJ, Pickard GE. Light-evoked calcium responses of isolated melanopsin-expressing retinal ganglion cells J Neurosci 2007; 27:13468-80. [PMID: 18057205].

41. Jakobs TC, Ben Y, Masland RH. Expression of mRNA for glutamate receptor subunits distinguishes the major classes of retinal neurons, but is less specific for individual cell types Mol Vis 2007; 13:933-48. [PMID: 17653033].

42. Nakanishi N, Tu S, Shin Y, Cui J, Kurokawa T, Zhang D, Chen HS, Tong G, Lipton SA. Neuroprotection by the NR3A subunit of the NMDA receptor J Neurosci 2009; 29:5260-5. [PMID: 19386922].

43. Hannibal J, Hindersson P, Knudsen SM, Georg B, Fahrenkrug J. The photopigment melanopsin is exclusively present in pituitary adenylate cyclase-activating polypeptide-containing retinal ganglion cells of the retinohypothalamic tract J Neurosci 2002; 22:RC191-[PMID: 11756521].

44. Seki T, Itoh H, Nakamachi T, Shioda S. Suppression of ganglion cell death by PACAP following optic nerve transection in the rat J Mol Neurosci 2008; 36:57-60. [PMID: 18642101].

45. Seki T, Itoh H, Nakamachi T, Endo K, Wada Y, Nakamura K, Shioda S. Suppression of rat retinal ganglion cell death by PACAP following transient ischemia induced by high intraocular pressure J Mol Neurosci 2011; 43:30-4. [PMID: 20585899].

46. Seki T, Nakatani M, Taki C, Shinohara Y, Ozawa M, Nishimura S, Ito H, Shioda S. Neuroprotective effect of PACAP against kainic acid-induced neurotoxicity in rat retina Ann N Y Acad Sci 2006; 1070:531-4. [PMID: 16888220].

47. Nakatani M, Seki T, Shinohara Y, Taki C, Nishimura S, Takaki A, Shioda S. Pituitary adenylate cyclase-activating peptide (PACAP) stimulates production of interleukin-6 in rat Muller cells Peptides 2006; 27:1871-6. [PMID: 16427158].

48. Belenky MA, Smeraski CA, Provencio I, Sollars PJ, Pickard GE. Melanopsin retinal ganglion cells receive bipolar and amacrine cell synapses J Comp Neurol 2003; 460:380-93. [PMID: 12692856].

49. Boudard DL, Mendoza J, Hicks D. Loss of photic entrainment at low illuminances in rats with acute photoreceptor degeneration Eur J Neurosci 2009; 30:1527-36. [PMID: 19821841].

50. Semo M, Lupi D, Peirson SN, Butler JN, Foster RG. Light-induced c-fos in melanopsin retinal ganglion cells of young and aged rodless/coneless (rd/rd cl) mice Eur J Neurosci 2003; 18:3007-17. [PMID: 14656296].

51. Semo M, Peirson S, Lupi D, Lucas RJ, Jeffery G, Foster RG. Melanopsin retinal ganglion cells and the maintenance of circadian and pupillary responses to light in aged rodless/coneless (rd/rd cl) mice Eur J Neurosci 2003; 17:1793-801. [PMID: 12752778].

11.4 CDC42 Is Required for Tissue Lamination and Cell Survival in the Mouse Retina

Severin Heynen[1,2], Isabelle Meneau[1], Christian Caprara[1,2], Marijana Samardzija[1], Cornelia Imsand[1], Edward M. Levine[3], Christian Grimm[1,2,4]

[1]Laboratory of Retinal Cell Biology, Ophthalmology Department, University of Zurich, Switzerland

[2]Zurich Center for Integrative Human Physiology, University of Zurich, Switzerland

[3]Department of Ophthalmology and Visual Sciences, John A. Moran Eye Center, University of Utah, Salt Lake City, Utah, United States of America

[4]Center for Neuroscience, University of Zurich, Switzerland

Published in Public Library of Science ONE, 2013, **8** (1): e53806

Personal Contribution

Contributed to breeding of *Ai6;α-Cre* mice, and analysis of ZSGREEN expression in *Ai6;α-Cre* mouse retinal flatmounts (Fig.1A).

Key Findings

The small GTPase CDC42 has various functions during development and in the adult. These functions include intra- as well as intercellular tasks such as organization of the cytoskeleton and, at least in epithelial cells, formation of adherens junctions. To investigate CDC42 in the neuronal retina, we generated retina-specific *Cdc42*-knockdown mice and analyzed the consequences for the developing and post-natal retina.

Here are some of the key findings of the study:

- lack of CDC42 affected organization of the developing retina as early as E17.5, prevented correct tissue lamination, and resulted in progressive retinal degeneration and severely reduced retinal function of the post-natal retina
- despite the disorganization of the retina, formation of the primary vascular plexus was not strongly affected. However, both deeper vascular plexi developed abnormally with no clear layering of the vessels
- retinas of *Cdc42*-knockdown mice showed increased expression of pro-survival, but also of pro-apoptotic and pro-inflammatory genes and exhibited prolonged Müller glia hypertrophy

OPEN ACCESS Freely available online

PLOS ONE

CDC42 Is Required for Tissue Lamination and Cell Survival in the Mouse Retina

Severin Reinhard Heynen[1,2], Isabelle Meneau[1], Christian Caprara[1,2], Marijana Samardzija[1], Cornelia Imsand[1], Edward M. Levine[3], Christian Grimm[1,2,4]*

1 Laboratory of Retinal Cell Biology, Ophthalmology Department, University of Zurich, Switzerland, **2** Zurich Center for Integrative Human Physiology, University of Zurich, Switzerland, **3** Department of Ophthalmology and Visual Sciences, John A. Moran Eye Center, University of Utah, Salt Lake City, Utah, United States of America, **4** Center for Neuroscience, University of Zurich, Switzerland

Abstract

The small GTPase CDC42 has pleiotropic functions during development and in the adult. These functions include intra- as well as intercellular tasks such as organization of the cytoskeleton and, at least in epithelial cells, formation of adherens junctions. To investigate CDC42 in the neuronal retina, we generated retina-specific *Cdc42*-knockdown mice (*Cdc42-KD*) and analyzed the ensuing consequences for the developing and postnatal retina. Lack of CDC42 affected organization of the developing retina as early as E17.5, prevented correct tissue lamination, and resulted in progressive retinal degeneration and severely reduced retinal function of the postnatal retina. Despite the disorganization of the retina, formation of the primary vascular plexus was not strongly affected. However, both deeper vascular plexi developed abnormally with no clear layering of the vessels. Retinas of *Cdc42-KD* mice showed increased expression of pro-survival, but also of pro-apoptotic and pro-inflammatory genes and exhibited prolonged Müller glia hypertrophy. Thus, functional CDC42 is important for correct tissue organization already during retinal development. Its absence leads to severe destabilization of the postnatal retina with strong degeneration and loss of retinal function.

Citation: Heynen SR, Meneau I, Caprara C, Samardzija M, Imsand C, et al. (2013) CDC42 Is Required for Tissue Lamination and Cell Survival in the Mouse Retina. PLoS ONE 8(1): e53806. doi:10.1371/journal.pone.0053806

Editor: Mike O. Karl, Center for Regenerative Therapies Dresden, Germany

Received May 24, 2012; **Accepted** December 5, 2012; **Published** January 23, 2013

Funding: This work was funded by a cooperative ZIHP project (University of Zurich) and the Swiss National Science Foundation (SNF #3100A0-117760). The funders had no role in study design, data collection and analysis, decision to publish, or preparation of the manuscript.

Competing Interests: The authors have declared that no competing interests exist.

* E-mail: cgrimm@opht.uzh.ch

Introduction

The sensory retina contains six neuronal cell classes and one glial cell type (Müller glia), which originate from retinal progenitors during retinal development. Although astrocytes and microglia are additional cells important for retinal physiology, they arise from other progenitor populations, as do the cells that make up the retinal vasculature [1–3]. All cells are arranged in a highly organized, multi-laminar tissue structure positioning individual cell types at specific, stereotypical locations in the mature retina. Cone and rod photoreceptor cell bodies are found in the outer nuclear layer (ONL), nuclei of horizontal, bipolar, amacrine and Müller glia cells reside in the inner nuclear layer (INL), and ganglion and displaced amacrine cells occupy the ganglion cell layer (GCL). Astrocytes and microglia are found mainly in the vicinity of vessels in the primary plexus and in the plexiform layers, respectively. Correct localization of cells in the mature retina involves movement of retinal progenitor cells through the neuroepithelium during development, interkinetic nuclear migration and cell fate decision processes [4]. Anchoring cell processes by junction and adhesion proteins during these processes is important for accurate development and cell placement. In the adult retina, adherens junctions in the outer limiting membrane (OLM) connect the actin cytoskeleton of photoreceptors and neighboring Müller glia cells, which improves tissue stability and organization of the ONL [5]. In addition, adherens junctions were shown to be important for establishing cell polarity [6], a feature especially important for photoreceptors and other cells in the retina [7]. Mutations in adherens junction proteins like crumbs 1 (CRB1) are associated with blinding diseases such as retinitis pigmentosa (RP) and Leber congenital amaurosis (LCA) [8], and ablation of proteins involved in the formation of adherens junctions like N-cadherin or catenins lead to severe retinal disorganization [8–11]. Although it is known that Rho GTPases are involved in the formation of adherens junctions in epithelial cells, no data are available that describe the role of Rho GTPases in the cytoarchitecture of the retina.

Rho GTPases are a group of small molecular weight GTPases that are part of the larger Ras superfamily. Of the 25 members currently identified, Ras-related C3 botulinum substrate 1 (RAC1), cell division cycle 42 homolog (CDC42) and ras homolog gene family member A (RHOA) are the classical and most well studied proteins [12]. Rho GTPases switch from their active, guanosine triphosphate (GTP) bound conformation to their inactive, guanosine diphosphate (GDP) form [13]. In the active conformation, GTPases interact with numerous effector proteins such as p21 activated kinases (PAK) and PAR proteins [14–17], which initiate intracellular signaling cascades for a variety of processes ranging from cellular migration to differentiation and development [18,19].

While the role of CDC42 in epithelial cell biology is well known, its potential functions in neuronal tissues are still under investigation. Nevertheless, CDC42 has been linked to neuronal diseases

Table 1. Primers and conditions for real-time PCR.

Gene	Oligonucleotide Primers		Annealing temp. (°C)	Product (bp)
	Forward 5′-3′	Reverse 5′-3′		
Actb	caacggctccggcatgtgc	ctcttgctctgggcctcg	62	153
Gapdh	agcaatgcatcctgcacc	tggactgtggtcatgagccc	58	96
Pou4f1	cctccctgagcacaagtacc	cacgctattcatcgtgtggt	60	212
Casp1	ggcaggaattctggagcttcaa	gtcagtcctggaaatgtgcc	60	138
Cdc42	ggcggagaagctgaggacaag	agcggtcgtagtctgtcataatcctc	60	275
Vsx2	ccagaagacaggatacaggtg	ggctccatagagaccatact	60	111
Edn2	agacctcctccgaaagctg	ctggctgtagctggcaaag	60	64
Fgf2	tgtgtctatcaagggagtgtgtgc	accaactggagtatttccgtgaccg	62	158
Gfap	ccaccaaactggctgatgtctac	ttctctccaaatccacacgagc	62	240
Gnat1	gaggatgctgagaaggatgc	tgaatgttgagcgtggtcat	58	209
Lif	aatgccacctgtgccatacg	caacttggtcttctctgtcccg	60	216
Ccl2	ggctcagccagatgcagtta	ctgctgctggtgatcctctt	60	108
Csf1	gctccaggaactctccaata	tcttgatcttctccagcagc	62	119
Rlbp1	cctttccagtcgggacaagtatg	gggtttcctcattttccagcag	60	140
Tnfa	ccacgctcttctgtctactga	ggccatagaactgatgagagg	62	92

doi:10.1371/journal.pone.0053806.t001

like Alzheimer and Parkinson's disease through its role in cytoskeletal organization or its connection to alpha-synuclein, respectively [20,21]. In the retina, analyses of Rho GTPases revealed their spatio-temporal expression patterns [22,23], and the involvement of CDC42 in growth cone regulation [24]. In addition, RAC1 and CDC42 have been associated with photoreceptor degeneration and protection [25–28]. Here, we report on the consequences of a conditional knockdown of CDC42 for the postnatal retina. We show that absence of CDC42 during development caused improper retinal lamination, and resulted in progressive retinal degeneration, loss of function and vascular disorganization.

Materials and Methods

Animals and genotyping

All procedures were performed in accordance with the regulations of the Veterinary Authority of Zurich and the statement of 'The Association for Research in Vision and Ophthalmology' for the use of animals in research. Knockdown of *Cdc42* in the developing retina was achieved by crossing *Cdc42* floxed mice [29] with mice expressing cre recombinase under the control of the α element of the *Pax6* promoter [30]. The *Cdc42*$^{flox/flox}$;*α-Cre* (from now on named *Cdc42*-knockdown, *Cdc42-KD*) and *Cdc42*$^{flox/flox}$ (from now on named control) littermates were analyzed at different embryonic and postnatal days as indicated. To study the spatial expression pattern of Cre, *α-cre* mice were crossed with the Ai6 reporter mouse [31] (a gift from Dr. Botond Roska, FMI, Basel, Switzerland) that expresses a green fluorescent protein (Zsgreen) following Cre mediated deletion of a floxed STOP cassette. *Rlbp1-GFP* mice express GFP under control of the retinaldehyde binding protein 1 (RLBP1) promoter in Müller cells and were described before [32]. *Rlbp1-GFP* mice were interbred with *Cdc42*$^{flox/flox}$;*α-cre* mice to generate *Cdc42-KD;Rlbp1-GFP* mice. All mice were kept at the animal facility of the University Hospital Zurich in a dark-light cycle (12 h : 12 h) with 60 lux of light at cage level with food and water *ad libitum*.

Mice were genotyped using genomic DNA isolated from ear biopsies and the following conventional PCR conditions: initial denaturation (95°C, 5 min); 35 cycles of denaturation (95°C, 45 s), annealing (60°C, 45 s) and elongation (72°C, 45 s); final extension (72°C, 10 min). The following primers (Microsynth, Balgach, Switzerland) were used: *Cdc42* floxed (forward: 5′-ttcttcctccaacctcctgatggg-3′, reverse 5′-tgctgtgtgtggcatttgctgc-3′), cre recombinase (forward: 5′-aggtgtagagaaggcacttagc-3′, reverse 5′-ctaatcgccatcttccagcagg-3′), *Ai6* (forward: 5′-aagggagctgcagtg-gagta-3′, reverse 5′-ccgaaaatctgtgggaagtc-3′) and *Rlbp1-GFP* (5′-caagtgtgagagacagcattgc-3′, reverse 5′-gttgcagatatagtaccggctg-3′). PCR products were run on a 1% agarose gel for size detection.

RNA isolation, cDNA synthesis and semi-quantitative real-time PCR

Retinas were isolated through a slit in the cornea and immediately frozen in liquid nitrogen. Total RNA was isolated using the RNeasy isolation kit (RNeasy; Qiagen, Hilden, Germany) and residual genomic DNA was removed by an additional DNase treatment. Identical amounts of RNA were reverse transcribed using oligo(dT) and M-MLV reverse transcriptase (Promega, Madison, WI, USA). Real-time PCR with specific primer pairs (Table 1), a polymerase ready mix (LightCycler 480 SYBR Green I Master Mix; Roche Diagnostics, Indianapolis, IN, USA), and a thermocycler (LightCycler, Roche Diagnostics) were used to analyze gene expression. Signals were normalized to beta-actin (*Actb*) as well as to glyceraldehyde-3-phosphate dehydrogenase (*Gapdh*), and relative expression was calculated using the comparative threshold cycle (ΔΔCT) method.

Western blotting

Proteins from isolated retinas were extracted in 0.1 M Tris-HCL (pH 8.0) by sonication at 4°C. Protein content was determined using the Bradford assay and homogenates were mixed with sodium dodecylsulfate (SDS) buffer. Proteins were resolved by electrophoresis on 10% SDS–polyacrylamide gels and transferred to nitrocellulose membranes. Membranes were

blocked in 5% nonfat dry milk (Bio-Rad, Hercules, CA, USA) in TBST (10 mM Tris/HCl [pH 8.0], 150 mM NaCl, and 0.05% Tween-20) for 1 hour at room temperature. Membranes were incubated overnight at 4°C in 5% milk (in TBST) containing a respective primary antibody (Table 2). Immunolabeled proteins were detected using HRP-conjugated secondary antibodies and visualized using the Renaissance Western Blot Detection Kit (PerkinElmer Life Sciences, Boston, MA, USA).

Light and transmission electron microscopy

Eyes of postnatal mice were enucleated and fixed overnight at 4°C in 2.5% glutaraldehyde in 0.1 M cacodylate buffer (pH 7.3). Cornea and lens were removed and eyecups cut dorso-ventrally through the optic nerve head. Trimmed tissue was washed in cacodylate buffer, incubated in osmium tetroxide for 1 hour, dehydrated in a series of increasing ethanol concentrations, and embedded in Epon 812. For light microscopy (Axioplan, Zeiss, Feldbach, Switzerland) semi-thin cross sections (500 nm) were cut and counterstained with toluidine blue. For transmission electron microscopy (TEM), ultrathin sections (50 nm) were stained with uranyl acetate and lead citrate and analyzed using a Philips CM100 transmission electron microscope. Heads of embryos were isolated at E14.5 and E17.5 and fixed in 2.5% glutaraldehyde in 0.1 M cacodylate buffer (pH 7.3) for at least 24 h. Further preparation and sectioning was as described above for postnatal eyes.

Immunofluorescence

Eyes were enucleated and fixed in 4% (wt/vol) paraformaldehyde (PFA) in 0.1 M phosphate buffered saline (PBS; pH 7.4) overnight. Cornea and lens were removed and eyecups were post-fixed in 4% PFA for an additional 2 hours before being immersed in 30% sucrose in PBS at 4°C overnight. Eyes were embedded in tissue freezing medium (Leica Microsystems Nussloch GmbH, Nussloch, Germany) and slowly frozen in a liquid nitrogen cooled 2-methylbutane bath. Retinal cryosections (12 µm) were cut dorso-ventrally, placed on slides and immersed in blocking solution (3% horse serum, 0.3% Triton X-100, 0.1 M PBS) for 1 hour at room temperature. Sections were incubated overnight at 4°C in a humidity chamber with respective primary antibodies diluted in blocking solution (Table 2). After three washing steps with PBS, the secondary antibody (coupled to Cy2, Cy3 or Cy5; Jackson immunoresearch, Suffolk, UK) was added and incubation continued at room temperature for 1 hour. After washing, cell nuclei were stained with DAPI and slides were mounted with anti-fade medium (10% Mowiol 4–88; vol/vol; Calbiochem, San Diego, CA, USA), in 100 mM Tris (pH 8.5), 25% glycerol (wt/vol), 0.1% 1,4-diazabicyclo [2.2.2] octane (DABCO)). Immunofluorescently labeled proteins were visualized using a fluorescent microscope (Axioplan, Zeiss, Switzerland).

Retinal whole mounts

Eyes were enucleated and incubated in 2% PFA in PBS for 5 minutes. Thereafter, cornea and lens were removed and the retina carefully separated from the eyecup. The retina was cut into a "clover-leaf" shape and post-fixed in 4% PFA in PBS for 10 minutes. Whole mounted retinas were washed briefly with PBS and placed in blocking solution (3% horse serum, 0.3% Triton X-100 in PBS) for 1 hour. Retinas were incubated overnight at 4°C with either *G. simplicifolia* isolectin IB_4-Alexa594 (Invitrogen, Basel, Switzerland) or anti-mouse glial fibrillary acidic protein (GFAP) (see Table 2 for antibody details) in blocking solution. Retinal whole mounts were washed with PBS and either directly mounted using Mowiol or further incubated for 1 hour with a secondary antibody conjugated to fluorescent dye in blocking solution. Immunolabeled proteins were visualized using a digitalized light microscope (Axiovision, Zeiss, Switzerland) or a confocal microscope (Leica SP5 Confocal Microscope). The Imaris software (Bitplane AG, Zurich, Switzerland) was used to analyze z-stacks and to generate xz-projections.

Table 2. Antibodies.

Antigen	Host	Dilution	Catalog number	Source
ACTB	Mouse	1:1000	#5441	Sigma, St. Louis, MO, USA
AKT	Rabbit	1:2500	#9272	Cell signaling technology, Beverly, MA, USA
p-AKT	Rabbit	1:1000	#9271	Cell signaling technology, Beverly, MA, USA
POU4F1	Mouse	1:100	MAB1585	Chemicon, Billerica, MA, USA
CATB	Mouse	1:1000	610153	BD transduction laboratories, Lexington, KY
CRALBP	Rabbit	1:500	-	John C. Saari, Univ. of Washington, USA
ERK1/2	Rabbit	1:1000	9102	Cell signaling technology, Beverly, MA, USA
p-ERK1/2	Rabbit	1:1000	9101	Cell signaling technology, Beverly, MA, USA
GFAP	Mouse	1:500	G3893	Sigma, St. Louis, MO, USA
GNAT1	Rabbit	1:1000	Sc-389	Santa Cruz Biotechnology, USA
GLUL	Mouse	1:500	MAB302	Millipore, Billerica, MA, USA
IBA1	Rabbit	1:500	019-19741	Wako, Neuss, Germany
JAK2	Rabbit	1:500	#44-406	Invitrogen corporation, Camarillo, USA
p-JAK2	Rabbit	1:250	#44-426	Invitrogen corporation, Camarillo, USA
PRKCA	Rabbit	1:1000	P4334	Sigma Aldrich, Missouri, USA
STAT3	Rabbit	1:1000	#9132	Cell signaling technology, Beverly, MA, USA
p-STAT3	Rabbit	1:500	#9131	Cell signaling technology, Beverly, MA, USA

doi:10.1371/journal.pone.0053806.t002

Electroretinogram (ERG) recordings

Electroretinograms were recorded from both eyes simultaneously following published protocols [33,34]. Briefly, mice were dark-adapted overnight and anesthetized the next day with ketamine (66.7 mg/kg) and xylazine (11.7 mg/kg). Pupils were dilated with 1% Cyclogyl (Alcon, Cham, Switzerland) and 5% phenylephrine (Ciba vision, Niederwangen, Switzerland) 30 minutes before performing single flash ERG recordings under dark-adapted (scotopic) and light adapted (photopic) conditions. Light adaptation was accomplished with low background illumination starting 5 minutes before photopic recording. Single white-flash stimulus intensities ranged from −3.7 to 1.9 log cd*s/m^2 under scotopic and from −0.6 to 2.9 log cd*s/m^2 under photopic conditions, divided into 12 and 8 steps, respectively. Ten responses per flash intensity were averaged with an interstimulus interval of either 4.95 seconds or 16.95 seconds (for 1.4, 1.9, 2.4, and 2.9 log cd*s/m^2).

Statistical analysis

Statistical analysis was performed using Prism4 software (GraphPad Inc., San Diego, USA. All data are presented as mean values ± standard deviations (SD). The number of samples (N) used for individual experiments is given in figure legends. Unless stated otherwise, statistical differences of means were calculated using two-way ANOVA followed by a Bonferroni post hoc test. Differences with P-values below 0.05 were considered significant.

Results

Retinal disorganization in the absence of CDC42

To delete CDC42 specifically in the retina we crossed *Cdc42$^{flox/flox}$* (control) mice [29] with α-Cre deleter mice [30] and selected for *Cdc42$^{flox/flox}$;α-Cre* (*Cdc42-KD*). α-Cre mice start to express Cre recombinase at E10.5 in retinal progenitors leading to the deletion of floxed sequences in progenitor-derived cells that localize to the periphery of the postnatal retina [30]. Cells of the retinal pigment epithelium were not affected (not shown and as reported before [30,35]. This spatial distribution of Cre-activity was confirmed by retinal whole mounts from *Ai6;α-cre* reporter mice. Large peripheral areas were positive for Zsgreen1 already at PND1. The central retina as well as a dorso-ventral "streak", however, were negative for fluorescence and thus lacked active Cre protein. The Cre-negative area in the ventral periphery was much narrower than the corresponding dorsal area (Fig. 1A).

Cre-activity resulted in reduced expression levels of *Cdc42* mRNA in retinas of young and adult *Cdc42-KD* mice. Analysis by real-time PCR showed that *Cdc42* levels were reduced by 35% already at PND5, the earliest time point analyzed. This reduction remained roughly constant at all ages tested (Fig. 1B). Morphological analysis of control and *Cdc42-KD* retinas showed minimal differences, if any, at E14.5 (Fig. 1C). By E17.5, however, the retinal neuroepithelium of *Cdc42-KD* mice was severely disorganized, showing disruptions in lamination (Fig. 1D). Consistent with region of Cre activity, the phenotype was most pronounced in the peripheral retina. At PND1, the phenotype in the ventral, peripheral retina persisted and revealed severe disorganization whereas the dorsal retina, which corresponds to the region with the least Cre activity, was comparable to controls (Fig. 1E).

Loss of apically localized adherens junctions

The disorganization of the young retina in *Cdc42-KD* mice (Fig. 1) resulted in an almost complete absence of lamination of the older peripheral retina at PND5, 15 and 35 (Fig. 2A). Central retinal regions of *Cdc42-KD* mice, however, had preserved a tissue layering that was comparable to control retinas (Fig. 2A). Loss of tissue lamination was also observed in the absence of *β-catenin* (CATB) in mouse or of *N-cadherin* in zebrafish [9,10]. Both proteins are part of adherens junctions at the outer limiting membrane (OLM) [36,37], which is located at the apical side of the ONL and connects photoreceptors with processes of Müller glia cells. Since CDC42 is involved in initiation of adherens junction formation in epithelial cells [6], we investigated tissue distribution of CATB and β-Actin (ACTB) in retinas of *Cdc42-KD* mice. In control mice ACTB localized mainly to a narrow band in the apical retina, to the forming inner plexiform layer (IPL) and to the basal side of to the forming GCL at PND5 (Fig. 2B). A faint staining was also observed in the region of the forming outer plexiform layer (OPL). This staining pattern was maintained at PND15 with a more intense labeling of the OPL and in the region of the OLM and photoreceptor segments (arrowheads). In 5-day old *Cdc42-KD* mice, however, staining of the narrow band in the apical region of the peripheral retina was discontinuous (Fig. 2B: arrows), and the signal in the IPL was more diffuse and irregular. At PND15, the irregular pattern of ACTB staining was even more pronounced with the presence of ACTB-positive structures throughout the retina (Fig. 2B). Similar results were obtained for CATB. While CATB localized to different layers in control retinas with a distinct labeling in the region of the OLM at PND15 (arrowheads), staining was much more diffuse in the absence of CDC42. Notably, a distinct and continuous staining in the region of the OLM was missing in *Cdc42-KD* at PND15 (Fig. 2B). Central retinal regions of *Cdc42-KD* mice were not affected and showed ACTB and CATB stainings similar to controls (not shown).

Such unstructured signals for CATB and ACTB in *Cdc42-KD* retinas support the morphological findings that show severe disorganization of the retinal tissue (Fig. 2A). In addition, disruption or lack of staining in the region of the OLM in the apical retina suggested that the OLM and adherens junctions might be affected. Using transmission electron microscopy, adherens junctions were recognized as electron dense structures located apically to the ONL in control retinas (Fig. 2C, top panel). In *Cdc42-KD* retinas, however, adherens junctions were found only in the more central retina (Fig. 2C, left part of bottom panel). In the periphery and thus in the retinal region with Cre activity, retinal organization was lost, adherens junction structures disappeared and the OLM was discontinuous (Fig. 2C, right part of bottom panel). The disruption of the OLM can be recognized especially in the 'transition zone' between the central (unaffected) and the affected peripheral retina (Fig. 2C, bottom panel).

Overall, this suggests that CDC42 is vital for correct lamination of the retina and that this GTPase may be directly or indirectly required for in the formation of adherens junctions between photoreceptors and Müller glia cells. Absence of these junctions may weaken cell-cell contacts and thus contribute to the severe disorganization of the retina.

Lack of CDC42 causes mislocalization and activation of Müller glia cells

Müller cells are radial glial cells that fulfill many functions in the retina including stabilization of the tissue. Disruption of Müller cells in the postnatal retina leads to severe retinal degeneration and retinal dysplasia [38]. Since lack of CDC42 affects radial glia morphology in the cortex and leads to abnormal positioning of cortical neurons [39], we tested whether lack of CDC42 influences Müller cells in the retina. For this purpose, we crossed *Cdc42-KD* with *Rlbp1-GFP* mice, which express green fluorescent protein (GFP) specifically in Müller glia cells [32]. Sections from the central and peripheral retina of 35 days old *Cdc42-KD;Rlbp1-GFP*

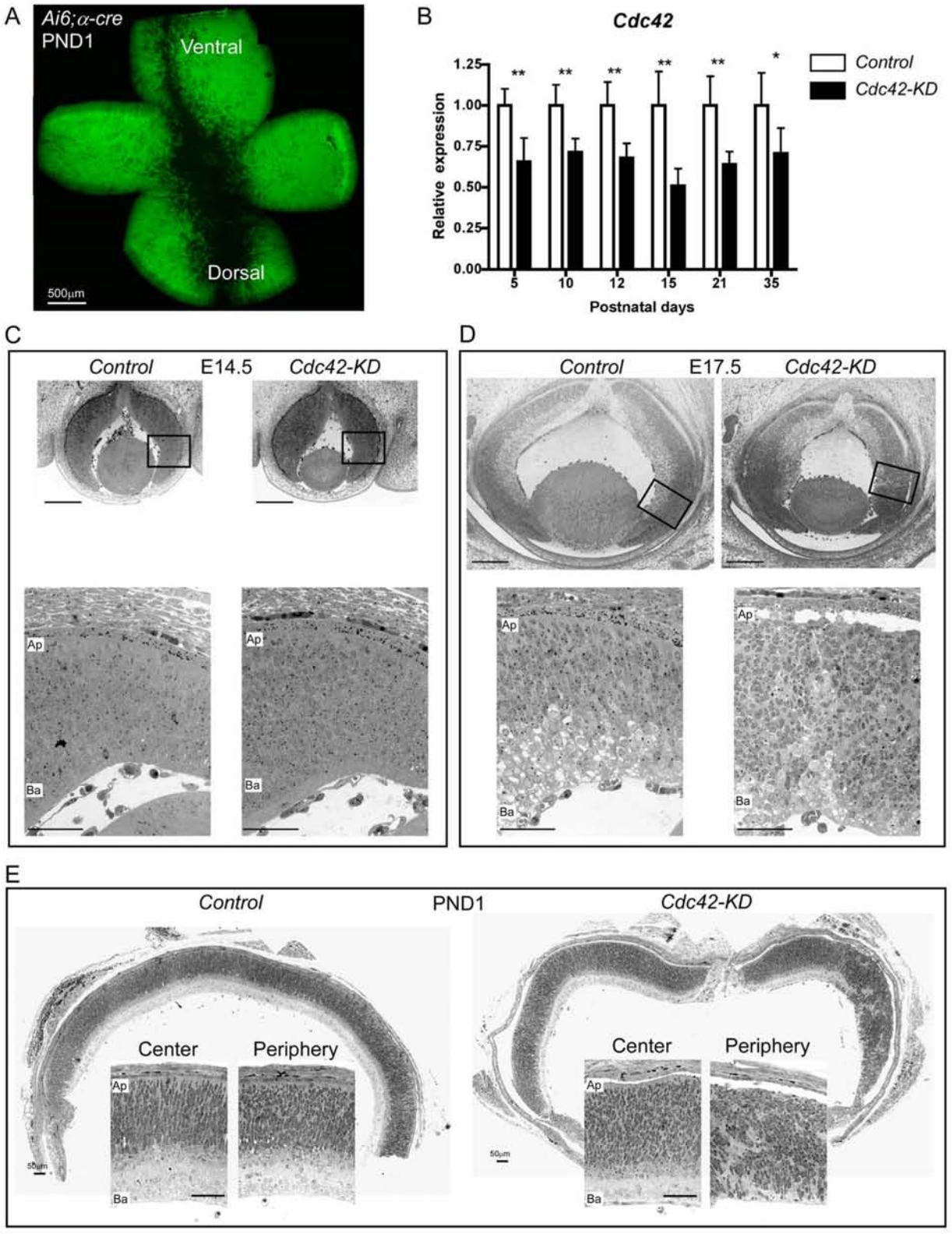

Figure 1. Early retinal disorganization in *Cdc42-KD* mice. (A) Retinal whole mount of a *Ai6;α-cre reporter* mouse at postnatal day (PND) 1. Cells with Cre activity express a bright green fluorescent protein (Zsgreen1). Scale bar: 500 μm. (B) Relative *Cdc42* mRNA levels in retinas of control and *Cdc42-KD* mice at indicated postnatal days. Values were normalized to *β-actin* and expressed relatively to control at each time point tested. Shown

are mean values ± SD of $N=5$ retinas. Statistical significance was calculated using one tailed t tests for each individual time point. *$p<0.05$, **$p<0.01$. (C;D) Retinal morphology of control and *Cdc42-KD* eyes at E14.5 (C) and 17.5 (D), respectively. Top panels: overview, scale bars: 200 μm. Bottom panels: magnifications of boxed areas in top panels, scale bars: 50 μm. (E) Morphology of representative retinal panoramas and sections of central and peripheral retinal regions of control and *Cdc42-KD* mice at PND1. $N=3$ per genotype. Ap: apical, Ba: basal. Scale bars: 50 μm.
doi:10.1371/journal.pone.0053806.g001

mice were stained with antibodies for three glial markers (cellular retinaldehyde binding protein (CRALBP), glial fibrillary acidic protein (GFAP), and glutamine synthetase (GLUL)) (Fig. 3A). The central retina showed the expected staining pattern with localization of CRALBP in the RPE, and in Müller cells stretching from the GCL to the apical side of the ONL. GFAP was only expressed in Müller cell endfeet and in astrocytes residing in the GCL. GLUL showed a similar expression pattern as CRALBP, except

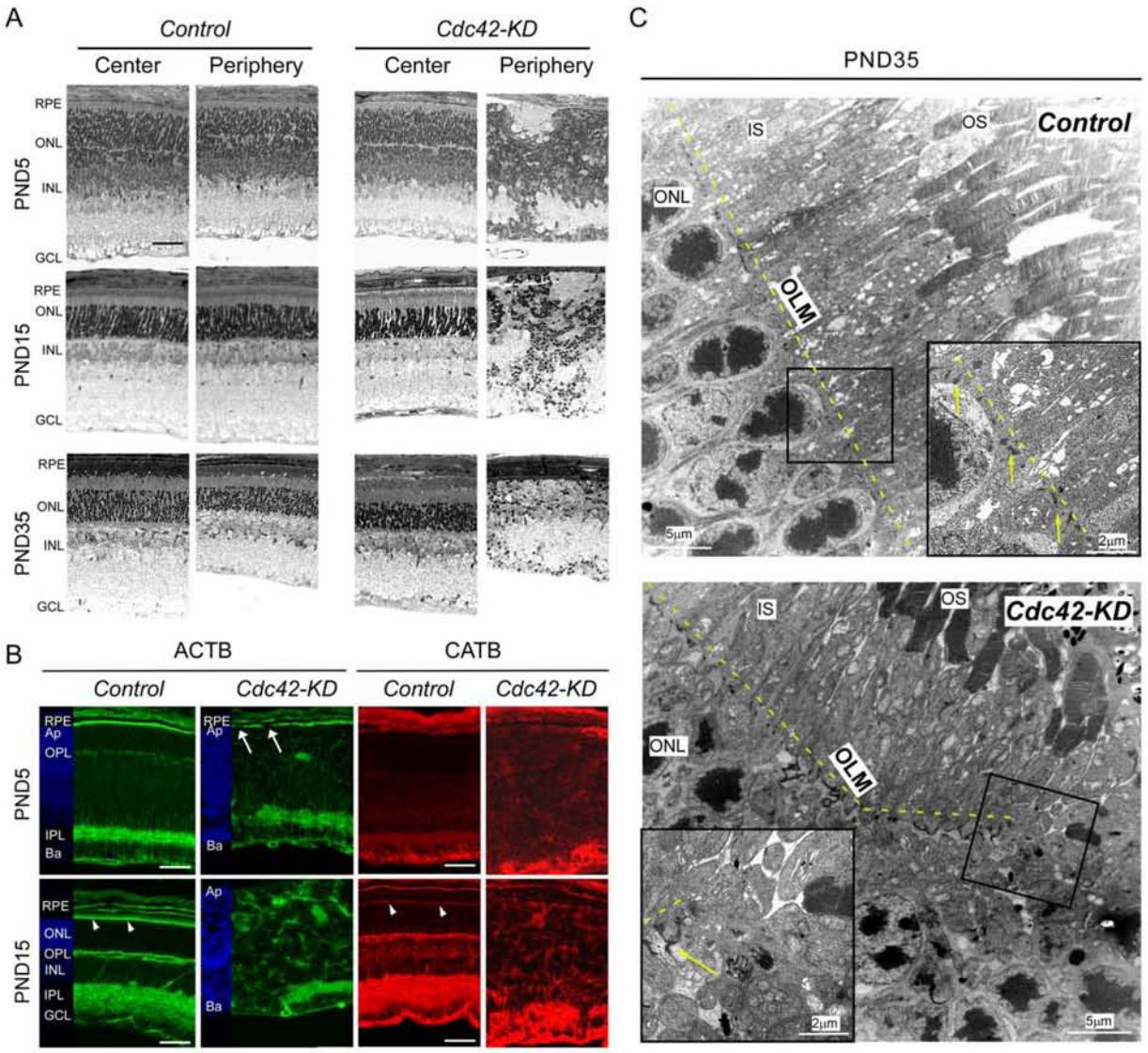

Figure 2. Loss of the outer limiting membrane (OLM) in the retinal periphery of *Cdc42-KD* mice. (A) Retinal morphology of central and peripheral regions of control and *Cdc42-KD* mice at indicated postnatal days (PND). (B) Immunolabeling of β-Actin (ACTB) and β-Catenin (CATB) in peripheral regions of control and *Cdc42-KD* retinas at PND5 and 15. Arrowheads point to the staining in the region of the OLM. Arrows indicate discontinuous ACTB labeling in the region of the OLM in *Cdc42-KD* retinas. DAPI image insets are used for orientation. (C) Transmission electron microscopy pictures of adherens junctions at the OLM in the retinal periphery of control and *Cdc42-KD* retinas at PND35. Insets show magnifications of boxed areas and dashed yellow lines and yellow arrows indicate the location of the OLM. Shown are representative samples of $N=3$ for each panel. RPE: retinal pigment epithelium, ONL: outer nuclear layer, INL: inner nuclear layer, GCL: ganglion cell layer, OS: photoreceptor outer segments, IS: photoreceptor inner segments, OPL: outer plexiform layer, IPL: inner plexiform layer, Ap: apical, Ba: basal. Scale bars: 50 μm or as indicated.
doi:10.1371/journal.pone.0053806.g002

that no signal was present in the RPE. In the peripheral *Cdc42-KD;Rlbp1-GFP* retina, CRALBP staining also colocalized with the transgenic GFP signal from Müller glia cells (Fig. 3A: arrows), but Müller cell bodies were not correctly localized and cellular processes were not detectable. This suggests that Müller cells were present in the retina even in the absence of CDC42 but that they were mislocalized and not radially aligned in the tissue. In contrast to the central retina, GFAP was upregulated in the periphery and also colocalized with transgenic GFP protein in Müller cells (Fig. 3A). Glutamine synthetase, however, was downregulated in the peripheral retina and almost no GLUL protein was detectable in cells expressing GFP (Fig. 3A: arrowheads). Since downregulation of *Glul* expression is known to occur in activated Müller cells [40], this suggests that the peripheral retina of *Cdc42-KD* mice may contain strongly stimulated Müller glia. This is further supported by the GFAP staining pattern in retinal whole mounts of 2-month-old mice (Fig. 3B). In control retinas GFAP was mainly localized in astrocytes, which delineate vessels in the primary plexus (Fig. 3A and B). Thus, GFAP staining in whole-mounted wild type retinas results in a pattern resembling the retinal vasculature of the primary plexus as suggested by others [41]. The specificity of the GFAP staining in Fig. 1B is confirmed by higher magnifications which show that GFAP antibodies recognize radial processes of astrocytes that contact vessels (Fig. 3C). In contrast, isolectin IB4 staining only labels vascular endothelial cells resulting in a immunolabeling pattern different from GFAP-stained whole mounts when viewed at high magnification (Fig. 3C). In *Cdc42-KD* retinas, however, GFAP expression was upregulated in Müller cells of the retinal periphery (Fig. 3A) corresponding to a staining pattern in whole mounts, which may point to the formation of a gliotic scar (Fig. 3B).

Immunofluorescent labeling using specific markers for rods (rod transducin, GNAT1), rod bipolar cells (protein kinase C α, PRKCA), ganglion cells (POU domain class 4 transcription factor 1, POU4F1), and microglia (ionized calcium binding adaptor molecule 1, IBA1) showed the presence of these proteins in both the central and peripheral retina of *Cdc42-KD* mice (Fig. 4). The GNAT1 signal corresponded to the location of photoreceptor outer segments, the PRKCA signal to the position of synaptic endings of rod bipolar cells and to bipolar cell bodies, the POU4F1 signal to the GCL and the IBA1 signal mainly to the plexiform layers in central retinas. In the periphery, however, signals showed an irregular pattern suggesting a severe disorganization of retinal cells expressing these markers (Fig. 4). Also, some microglia seemed to have adopted an amoeboid-like shape (Fig. 4, arrows), which is indicative of an activated state of these cells [42]. Activation of resident microglia is a common phenomenon in degenerating retinas of mice [43].

Disorganization of the retinal vasculature in the absence of CDC42

Glia cells are important for the development of the retinal vasculature. Astrocytes provide a cellular network for growth of the primary vascular plexus, and Müller glia processes may act as guides for endothelial cell sprouting in the process of formation of the deeper vascular plexi [1,44]. Since Müller cells were not correctly localized and processes were not aligned in a radial fashion, we expected retinal vasculature aberrations in the periphery of *Cdc42-KD* mice. To test this, retinal whole mounts were stained for isolectin IB_4 at PND12, 15, 21 and 35, and xz-stack projections of central and peripheral retinal regions of *Cdc42-KD* and control mice were compiled (Fig. 5). Whereas all vascular plexi in central retinal regions were comparable in both mouse strains, the intermediate and deep plexi of the peripheral vasculature in retinas of *Cdc42-KD* mice were severely disturbed. Although the primary plexus apparently has formed, no discernable intermediary and deeper plexi were evident and vessels were disorganized at all ages tested. Note that in 12 day old control mice, the deep plexus had already formed but the intermediate plexus has not yet reached the far periphery, as expected (Fig. 5).

Severe loss of retinal cells and function in the absence of CDC42

To analyze long-term consequences of the severe retinal disorganization observed in young *Cdc42-KD* mice, we analyzed retinal morphology and expression of retinal marker genes in 2, 3 and 5-month-old mice. Whereas the RPE appeared unaffected, progressive and severe reduction of retinal thickness was observed in the periphery of *Cdc42-KD* mice (Fig. 6A). This suggested substantial loss of cells in *Cdc42-KD* mice but not in controls. To identify the cell classes that degenerated in *Cdc42-KD* retinas we tested RNA expression levels of markers for specific cell populations. Levels of *Gnat1* and *Pou4f1* were significantly reduced whereas levels of *Vsx2* and *Rlbp1* were comparable to controls (Fig. 6B). This suggests that lack of CDC42 during retinal development primarily affected survival of photoreceptor and ganglion cells, but not of bipolar and Müller glia cells, respectively.

The consequences of cell loss for overall retinal function was tested using full field electroretinography (ERG). Recordings of single flash light intensity series in 2-month-old control and *Cdc42-KD* mice showed a significant reduction of scotopic and photopic b-wave amplitudes (around 40% at highest flash intensities) in mice lacking CDC42 in the retinal periphery (Fig. 6C). This reduction in function suggests that both the rod and the cone system were affected in *Cdc42-KD* mice.

Together, these results show that the peripheral retina of *Cdc42-KD* mice exhibited progressive retinal degeneration that was also reflected by a significant loss of function.

Activation of endogenous stress response systems in the absence of CDC42

The severe retinal disorganization in retinas of *Cdc42-KD* mice may induce endogenous response systems as seen in degenerating retinas [45]. Such a response may include both pro- and anti-survival signaling pathways. A prominent survival pathway activated in the mouse retina, is regulated by leukemia inhibitory factor (LIF) and involves endothelin 2 (EDN2) and fibroblast growth factor 2 (FGF2) [45–48]. To test whether this system would also be activated in the disorganized and degenerative *Cdc42-KD* retina, we used semi-quantitative real-time PCR to analyze retinal gene expression levels in mice up to 150 days of age (Fig. 7A). All expression data were normalized to *Actb*. Although ACTB has a direct role in the organization of the cytoskeleton, very similar data were obtained after normalization to expression of *Gapdh* (data not shown).

Expression of *Lif*, *Edn2*, and *Fgf2* was strongly induced in *Cdc42-KD* mice with a peak around PND35 (Fig. 7A). It is interesting to note that expression of *Fgf2* increased in *Cdc42-KD* retinas before *Lif* was induced. Since activation of *Fgf2* depends on LIF in models of photoreceptor degeneration [45,46], this may indicate that the disorganized retina, where cells in addition to photoreceptors are affected, uses other or additional mechanisms to activate *Fgf2*. It is also interesting that *Lif* expression was at basal levels until PND21 although retinal organization was severely affected already before that time point (Fig. 2A). Whether this indicates that photoreceptor cells are not recognized as 'injured' in the young dysmorphic *Cdc42-KD* retina needs further exploration. Similar to *Fgf2*,

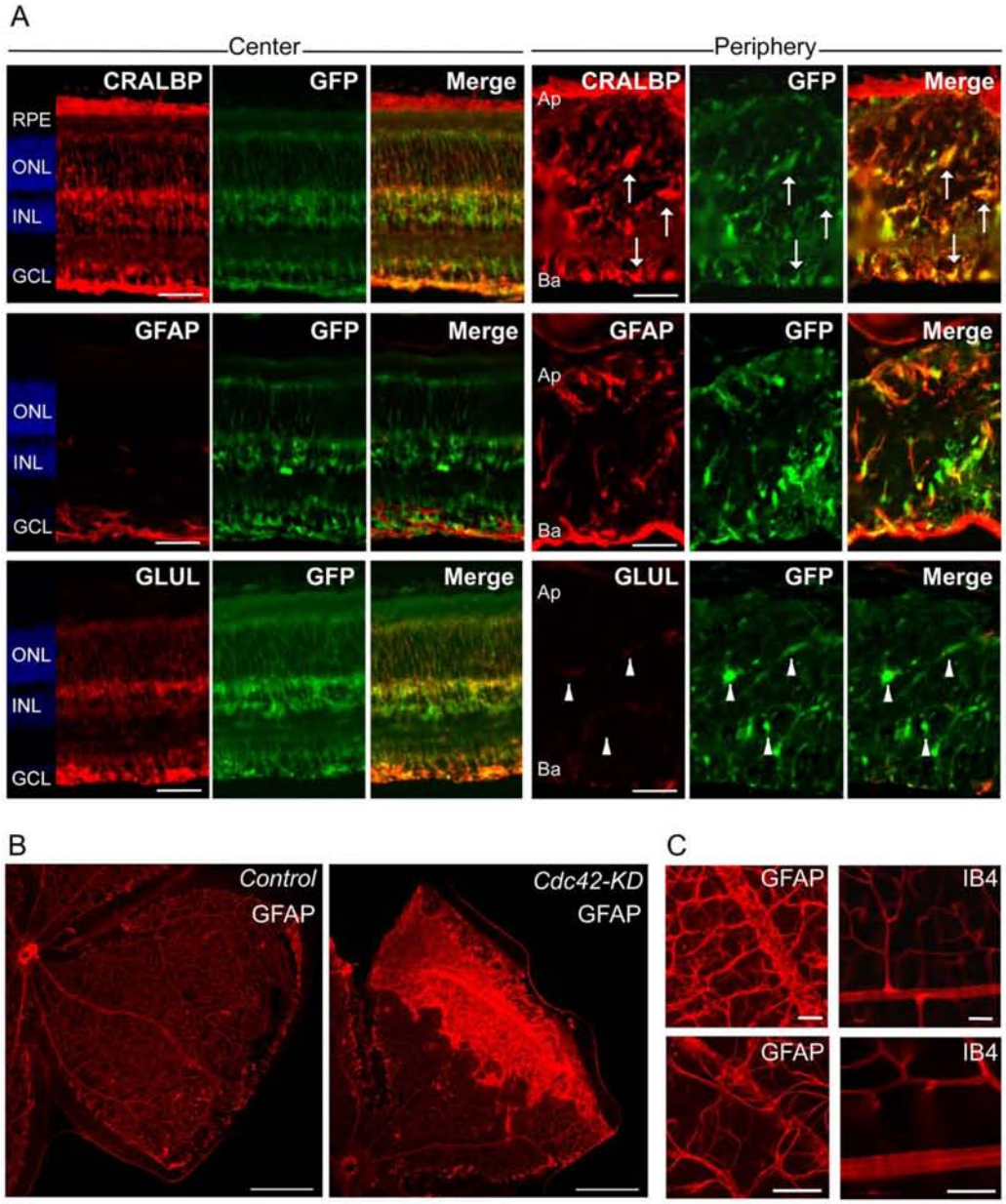

Figure 3. Mislocalization, misalignment and activation of Müller glia cells in Cdc42-KD retinas. (A) Retinal cryosections of central and peripheral regions of 35 days old *Cdc42-KD;Rlbp1-GFP* mice stained for cellular retinaldehyde binding protein (CRALBP), glial fibrillary acidic protein (GFAP) and glutamine synthetase (GLUL) to label Müller glia cells. Arrows indicate colocalization of CRALBP with green fluorescent protein (GFP). Arrowheads indicate minimal colocalization of GLUL with GFP. Scale bar: 50 μm. (B) Retinal whole mounts of 2-month-old control and *Cdc42-KD* mice stained for GFAP. (C) High magnifications of GFAP and isolectin IB4 stainings in whole mounts of retinas from control mice. Scale bars: 50 μm. Shown are representative samples of $N = 3$ for each panel. RPE: retinal pigment epithelium, ONL: outer nuclear layer, INL: inner nuclear layer, GCL: ganglion cell layer, GFP: green fluorescent protein, Ap: apical, Ba: Basal. Scale bar: 500 μm.
doi:10.1371/journal.pone.0053806.g003

expression of *Gfap* was induced early (PND15) and remained significantly elevated throughout the time period analyzed. Pro-apoptotic factors (Caspase1 (*Casp1*), tumor necrosis factor α (*Tnfa*)) and pro-inflammatory chemokines (Chemokine (C-C motif) ligand 2 (*Ccl2*), macrophage colony stimulating factor 1 (*Csf1*)) were expressed at significantly higher levels in *Cdc42-KD* retinas from PND35 or PND90, respectively, onwards (Fig. 7A).

LIF signaling during retinal degeneration is thought to act through the JAK/STAT pathway including activation of Janus activated kinase 2 (JAK2), JAK3 and signal transducers and activators of transcription 3 (STAT3) [45,48–50]. Here we tested activation of STAT3, JAK2, AKT and ERK1,2, the two latter being frequently implicated in degenerative and protective processes in the retina. From these proteins only STAT3 showed

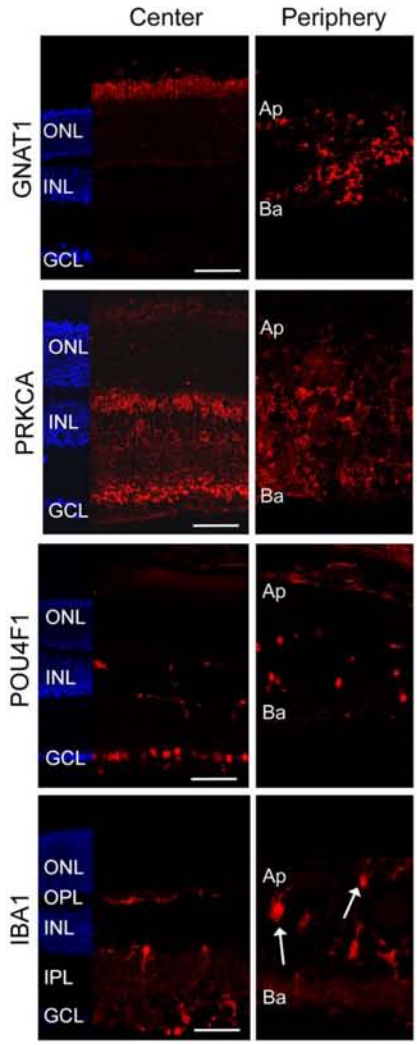

Figure 4. Detection of neuronal and microglial cells in adult *Cdc42-KD* retinas. Retinal cryosections of central and peripheral regions of *Cdc42-KD* mice were stained for rod photoreceptors (GNAT1), rod bipolar cells (PRKCA), ganglion cells (POU4F1), and microglia (IBA1). Shown are representative images of $N = 3$. Arrows point to amoeboid shape microglia in the periphery. ONL: outer nuclear layer, OPL: outer plexiform layer, INL: inner nuclear layer, IPL: inner plexiform layer, GCL: ganglion cell layer, Ap: apical, Ba: basal. Scale bars: 50 μm.
doi:10.1371/journal.pone.0053806.g004

clear and sustained activation through phosphorylation, with a peak at PND35 (Fig. 7B). JAK2 and ERK were not or only slightly phosphorylated at the last time point analyzed. Thus, signaling in the degenerative *Cdc42-KD* retina may not involve AKT or ERK1/2 proteins, and regulation of STAT3 phosphorylation in the *Cdc42-KD* retina may involve JAK2-independent pathways.

Discussion

Positioning of retinal cells during development and establishment of adherens junctions are important to generate a multilayered and correctly organized adult retina [9,10,51]. While it is well known that CDC42 plays a pivotal role in the formation of adherens junctions in epithelial cells [6], little was known about its functions in the developing retina. Our results show that tissue-specific inactivation of *Cdc42* leads to a dysmorphic retina characterized by a strong disorganization of the retinal architecture and the absence of obvious adherens junctions between photoreceptors and Müller glia cells, an abnormal stratification of the retinal vasculature, a loss of retinal function and an activation of endogenous signaling pathways in response to progressive retinal degeneration.

Loss of retinal lamination in the absence of CDC42

Retinal lamination is controlled by several mechanisms including cell migration during development and the formation of adherens junctions [51]. Whether the absence of CDC42 disrupts tissue lamination because it influences migration and spatial placement of cells during retinal development, or because it is required for the generation and/or maintenance of protein junctions for cell adhesion during development and in the adult, is not yet known. Nevertheless, since the phenotype of *Cdc42-KD* mice is similar to the phenotype of retinas lacking the adherens junction protein β-catenin, CDC42 may have an important role for cell adhesion as suggested for β-catenin [10]. Furthermore, since inactivation of *Cdc42* in mature rod photoreceptors does not lead to retinal disorganization and degeneration [28], CDC42 may be particularly important during development and/or in cells different from rods. Among other cells, lack of CDC42 caused Müller glia cells to be mislocalized and misaligned. It has been shown that radial glial cells are important for migration of neurons in the developing cerebral cortex [39] and that movements of progenitor cells are involved in cell fate decision in the mouse telencephalon [52]. Therefore, mislocalization of Müller cells may have impaired movement of retinal progenitors in the developing neuroepithelium, thereby contributing to the lack of retinal lamination observed in *Cdc42-KD* mice. A developmental role of CDC42 is also supported by the observation that ablation of CDC42 in progenitor cells of the developing mouse cortex results

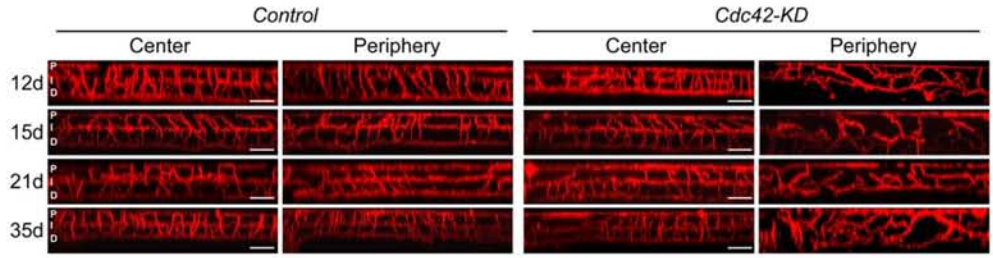

Figure 5. Disorganized retinal vasculature in the retinal periphery of *Cdc42-KD* mice. XZ-projection images of Isolectin IB4 labeled retinal whole mounts from control and *Cdc42-KD* mice at indicated postnatal days (d). Shown are representative samples of $N = 3$ for each genotype and time point. Scale bar: 100 μm. P: primary plexus, I: intermediate plexus, D: deep plexus.
doi:10.1371/journal.pone.0053806.g005

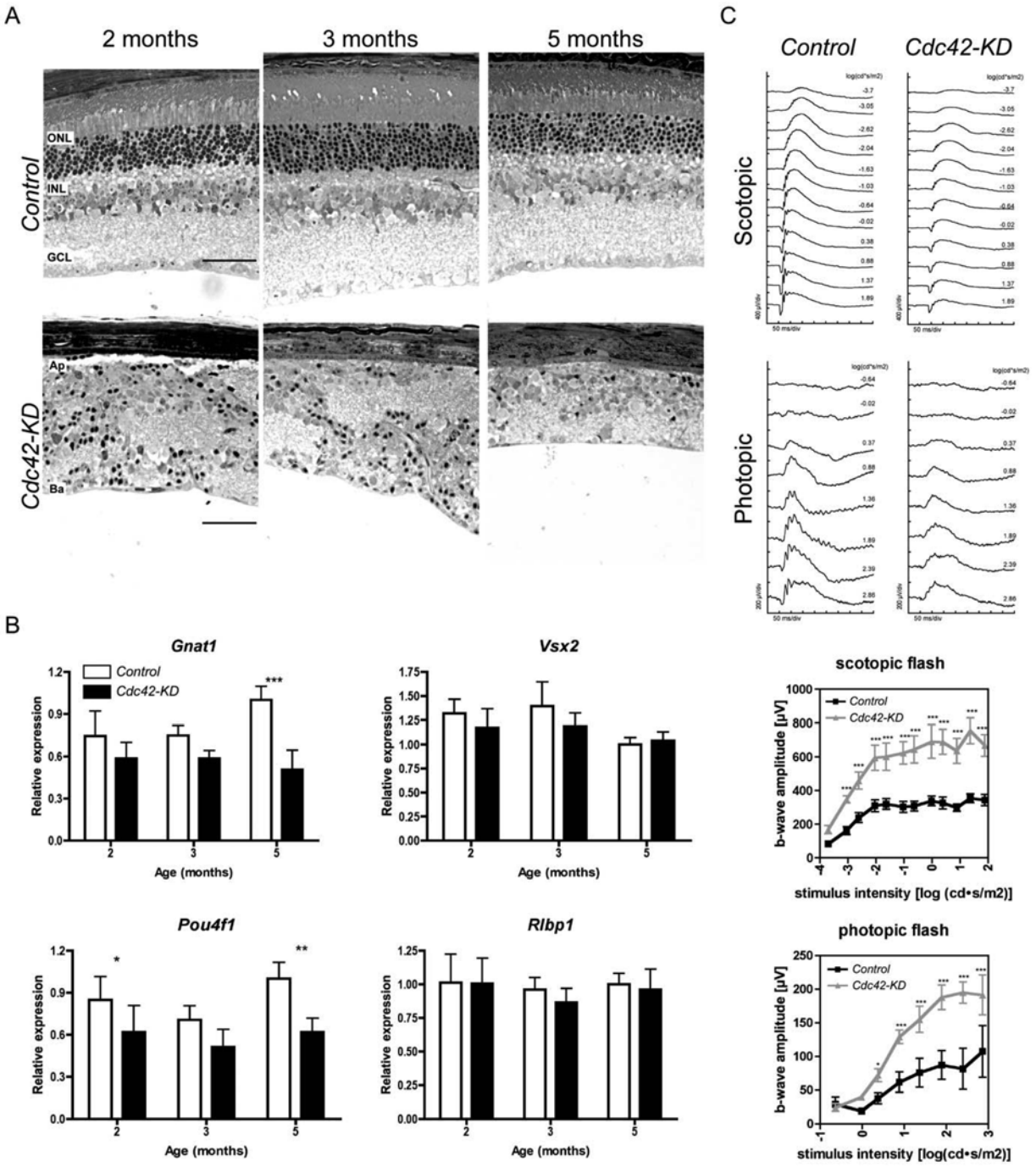

Figure 6. Progressive retinal degeneration and reduced retinal function in *Cdc42-KD* mice. (A) Morphology of the peripheral retina from control and Cdc42-KD mice at indicated ages. Shown are representative samples of $N = 3$. (B) Gene expression of retinal markers in retinas of control (white bars) and *Cdc42-KD* (black bars) mice at indicated ages. Expression was normalized to *Actb* and expressed relatively to control values at 5 months of age, which were set to ''1''. Shown are mean values ± SD of $N = 5$ retinas. Statistical significance was calculated using two-way ANOVA with a Bonferroni post hoc test. *$p<0.05$, **$p<0.01$, ***$p<0.001$. (C) Scotopic (dark adapted) and photopic (light adapted) electroretinogram recordings from control and *Cdc42-KD* mice at 2 months of age. Representative original traces from individual mice are presented (top panels). Scotopic and photopic b-wave amplitudes of control and *Cdc42-KD* mice are calculated as a function of light intensity (bottom panels). $N = 3$ for each genotype. Two-way ANOVA with Bonferroni post hoc tests was used to test statistical significance. *$p<0.05$, ***$p<0.001$. ONL: outer nuclear layer, INL: inner nuclear layer, GCL: ganglion cell layer, Ap: Apical, Ba: Basal. Scale bar 50 µm.
doi:10.1371/journal.pone.0053806.g006

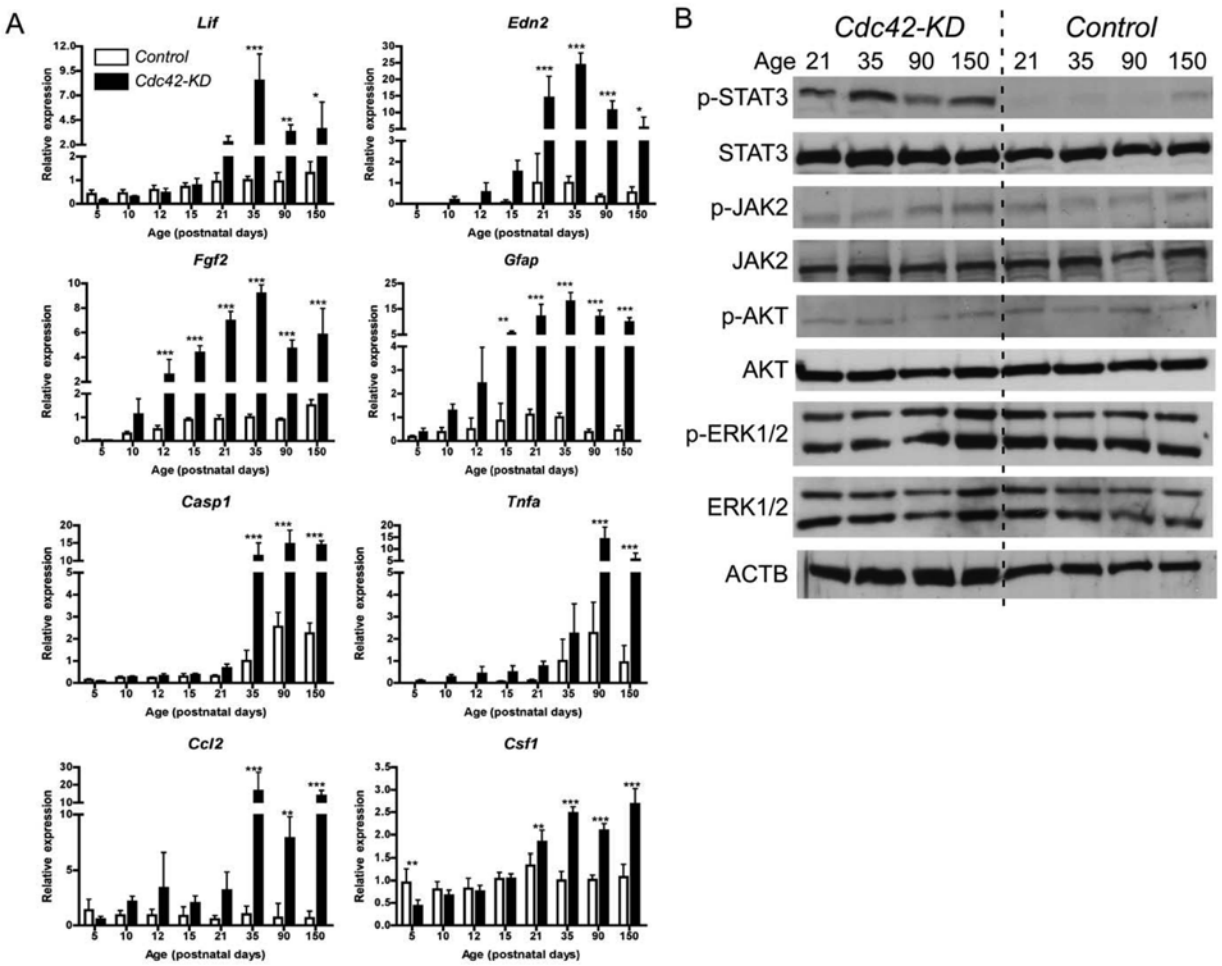

Figure 7. Molecular signaling in retinas of *Cdc42-KD* mice. (A) Semi-quantitative real-time PCR analysis of retinal RNA levels of control (white bars) and *Cdc42-KD* (black bars) mice at postnatal days (PND) as indicated. Gene expression was normalized to *Actb* and expressed relatively to control levels at PND35, which were set to "1". Mean values ± SD of $N = 5$ mice are shown. If no bar is visible: expression below detection limits. Statistical significance was determined by two-way ANOVA with Bonferroni post hoc tests. *$p<0.05$, **$p<0.01$, ***$p<0.001$. (B) Representative Western blots of whole retinal extracts from control and *Cdc42-KD* mice ($N = 3$) at postnatal days (age) as indicated. ACTB was used as loading control.
doi:10.1371/journal.pone.0053806.g007

in a gradual loss of apically localized PAR complex proteins and adherens junctions, as well as in a disturbed interkinetic nuclear migration [52]. The α-Cre driven inactivation of *Cdc42* in retinal progenitor cells already during early embryonic development may have similarly complex consequences leading to the observed phenotype. Identifying the molecular mechanisms downstream of CDC42 that lead to the proper lamination of the developing and mature retina will be important future studies.

In addition to disorganization of the retinal morphology, lack of CDC42 also affects the formation of the vascular plexi in the postnatal retina. In the normal retina, Müller cell processes span almost the entire tissue radially from the inner to the outer limiting membrane. These processes stabilize retinal structure but are also guides for the developing retinal vasculature. Angiogenic sprouts are formed from vessels of the primary plexus and growing vessels penetrate the retina along Müller cell processes to initiate development of the deeper vascular plexi [1]. The mislocalization and non-radial alignment of Müller cells in *Cdc42-KD* mice may have prevented proper guidance of growing vessels and thus correct organization of the intermediate and deep vascular plexi. In contrast, vessels of the primary plexus were less affected. Growing vessels of this plexus reached the retinal periphery around PND10 and the capillary network was similar in both control and *Cdc42-KD* retinas (data not shown). This suggests that the astrocytic network, which provides the scaffold and signals for growing vessels of the primary plexus was not strongly affected in the Cdc42-KD retina, an interpretation supported by the astrocytic GFAP labeling at the basal side of the *Cdc42-KD* retina (Fig. 3A).

Retinal degeneration and loss of function in the absence of CDC42

Lack of CDC42 resulted not only in a disorganized retina but also in severe and progressive degeneration of retinal cells, especially of photoreceptors and ganglion cells. Since ablation of CDC42 in adult rods does not induce degeneration [28], cell death might be caused by defects in other cells or by the dysmorphic tissue environment that might not be able to sufficiently support

survival of delicate cells like photoreceptors and ganglion cells. It has been proposed for example that interactions between microglia and Müller cells modulate expression of factors for photoreceptor survival [53]. In the disorganized *Cdc42-KD* retina, however, cell-cell interactions are altered, which thus may reduce trophic support and allow degeneration. Furthermore, the persistent gliosis and gliotic scar formation in *Cdc42-KD* mice may also be detrimental and contribute to retinal degeneration [54] through the secretion of pro-inflammatory cytokines such as TNFα and CCL2 [55,56]. Expression of both of these factors was highly elevated in *Cdc42-KD* retinas.

Lack of CDC42 also resulted in strongly reduced retinal function. Since both scotopic and photopic b-wave amplitudes were similarly reduced, both the rod and the cone system were affected. Although we cannot conclusively determine from our data whether CDC42 is directly needed for function or whether the reduction in wave amplitudes is a result of retinal disorganization and cell loss. However, since rod photoreceptors do not need intracellular CDC42 for normal function [28], we hypothesize that the reduced ERG in *Cdc42-KD* is likely the consequence of the dysmorphic and degenerative retina.

Molecular signaling in Cdc42-KD retinas

Lack of CDC42 caused cell death in the retinal periphery. It has been shown that the retina possesses endogenous mechanisms, which provide support for neuronal cells in unfavorable situations. One of these mechanisms is controlled by LIF and includes EDN2, FGF2 and members of the JAK/STAT family of proteins [45]. Members of this pathway were also induced in *Cdc42-KD* retinas. However, whereas expression of *Fgf2* may depend on LIF in models of photoreceptor degeneration [45,46], and may be influenced by photoreceptor-derived EDN2 [47], *Fgf2* and *Edn2* expression in *Cdc42-KD* was already upregulated before *Lif* was induced. This suggests that the highly dysmorphic retina of the *Cdc42-KD* mouse activates additional signaling pathways that may culminate in the expression of survival factors independently of LIF. Such pathways may rely on STAT3, which has been shown to be neuroprotective in other systems [48,50], but may not include AKT and ERK signaling (Fig. 7).

Interestingly, upregulation of *Tnfa*, *Casp1*, *Ccl2* and *Csf1*, genes implicated in pro-inflammatory pathways and neurodegeneration [57–59], followed the upregulation of protective genes with a delay. This may suggest that survival mechanisms attempted, but were not capable to provide prolonged protection for neuronal cells and to prevent retinal degeneration in *Cdc42-KD* mice.

Conclusions

We have shown that CDC42 ablated retinas are not properly laminated, lack obvious adherens junctions between photoreceptors and Müller glia cells, and undergo severe retinal degeneration. As a consequence, retinal function is reduced, and pro- as well as anti-survival signaling pathways are activated. Since morphological alterations were obvious as early as at E17.5, CDC42 may be important already early during retinal development for establishing a proper retinal architecture. CDC42 may possibly influence migration of cells to their correct spatial location in the developing retina, and may be required for the generation of adherens junctions between photoreceptors and Müller cells in the OLM to stabilize the retinal tissue. Investigating the CDC42 interaction partners involved in these processes may not only contribute to our understanding of developmental processes in the retina but may also help to unravel mechanisms of retinal pathologies affecting tissue integrity.

Acknowledgments

We thank Christel Beck for excellent technical assistance and members of the lab for their continuous support.

Author Contributions

Conceived and designed the experiments: SRH CG. Performed the experiments: SRH IM CC CI CG. Analyzed the data: SRH MS EML CG. Contributed reagents/materials/analysis tools: EML. Wrote the paper: SRH CG. Significantly contributed to the editing of the manuscript: MS EML.

References

1. Fruttiger M (2007) Development of the retinal vasculature. Angiogenesis 10: 77–88.
2. Santos AM, Calvente R, Tassi M, Carrasco MC, Martin-Oliva D, et al. (2008) Embryonic and postnatal development of microglial cells in the mouse retina. J Comp Neurol 506: 224–239.
3. Watanabe T, Raff MC (1988) Retinal astrocytes are immigrants from the optic nerve. Nature 332: 834–837.
4. Baye LM, Link BA (2008) Nuclear migration during retinal development. Brain Res 1192: 29–36.
5. Rich KA, Figueroa SL, Zhan Y, Blanks JC (1995) Effects of Muller cell disruption on mouse photoreceptor cell development. Exp Eye Res 61: 235–248.
6. Baum B, Georgiou M (2011) Dynamics of adherens junctions in epithelial establishment, maintenance, and remodeling. J Cell Biol 192: 907–917.
7. Koike C, Nishida A, Akimoto K, Nakaya MA, Noda Tm, et al. (2005) Function of atypical protein kinase C lambda in differentiating photoreceptors is required for proper lamination of mouse retina. J Neurosci 25: 10290–10298.
8. Gosens I, den Hollander AI, Cremers FP, Roepman R (2008) Composition and function of the Crumbs protein complex in the mammalian retina. Exp Eye Res 86: 713–726.
9. Erdmann B, Kirsch FP, Rathjen FG, More MI (2003) N-cadherin is essential for retinal lamination in the zebrafish. Dev Dyn 226: 570–577.
10. Fu X, Sun H, Klein WH, Mu X (2006) Beta-catenin is essential for lamination but not neurogenesis in mouse retinal development. Dev Biol 299: 424–437.
11. Mehalow AK, Kameya S, Smith RS, Hawes NL, Denegre JM, et al. (2003) CRB1 is essential for external limiting membrane integrity and photoreceptor morphogenesis in the mammalian retina. Hum Mol Genet 12: 2179–2189.
12. Wennerberg K, Der CJ (2004) Rho-family GTPases: it's not only Rac and Rho (and I like it). J Cell Sci 117: 1301–1312.
13. Paduch M, Jelen F, Otlewski J (2001) Structure of small G proteins and their regulators. Acta Biochim Pol 48: 829–850.
14. Arimura N, Kaibuchi K (2005) Key regulators in neuronal polarity. Neuron 48: 881–884.
15. Jaffer ZM, Chernoff J (2002) p21-activated kinases: three more join the Pak. Int J Biochem Cell Biol 34: 713–717.
16. Wells CM, Jones GE (2010) The emerging importance of group II PAKs. Biochem J 425: 465–473.
17. Zhao ZS, Manser E (2005) PAK and other Rho-associated kinases–effectors with surprisingly diverse mechanisms of regulation. Biochem J 386: 201–214.
18. Govek EE, Newey SE, Van Aelst L (2005) The role of the Rho GTPases in neuronal development. Genes Dev 19: 1–49.
19. Hall A, Nobes CD (2000) Rho GTPases: molecular switches that control the organization and dynamics of the actin cytoskeleton. Philos Trans R Soc Lond B Biol Sci 355: 965–970.
20. Schnack C, Danzer KM, Hengerer B, Gillardon F (2008) Protein array analysis of oligomerization-induced changes in alpha-synuclein protein-protein interactions points to an interference with Cdc42 effector proteins. Neuroscience 154: 1450–1457.
21. Zhu X, Raina AK, Boux H, Simmons ZL, Takeda A, et al. (2000) Activation of oncogenic pathways in degenerating neurons in Alzheimer disease. Int J Dev Neurosci 18: 433–437.
22. Mitchell DC, Bryan BA, Liu JP, Liu WB, Zhang L, et al. (2007) Developmental expression of three small GTPases in the mouse eye. Mol Vis 13: 1144–1153.
23. Santos-Bredariol AS, Santos MF, Hamassaki-Britto DE (2002) Distribution of the small molecular weight GTP-binding proteins Rac1, Cdc42, RhoA and RhoB in the developing chick retina. J Neurocytol 31: 149–159.

24. Chen TJ, Gehler S, Shaw AE, Bamburg JR, Letourneau PC (2006) Cdc42 participates in the regulation of ADF/cofilin and retinal growth cone filopodia by brain derived neurotrophic factor. J Neurobiol 66: 103–114.
25. Belmonte MA, Santos MF, Kihara AH, Yan CY, Hamassaki DE (2006) Light-Induced photoreceptor degeneration in the mouse involves activation of the small GTPase Rac1. Invest Ophthalmol Vis Sci 47: 1193–1200.
26. Chang HY, Ready DF (2000) Rescue of photoreceptor degeneration in rhodopsin-null Drosophila mutants by activated Rac1. Science 290: 1978–1980.
27. Haruta M, Bush RA, Kjellstrom S, Vijayasarathy C, Zeng Y, et al. (2009) Depleting Rac1 in mouse rod photoreceptors protects them from photo-oxidative stress without affecting their structure or function. Proc Natl Acad Sci U S A 106: 9397–9402.
28. Heynen SR, Tanimoto N, Joly S, Seeliger MW, Samardzija M, et al. (2011) Retinal degeneration modulates intracellular localization of CDC42 in photoreceptors. Mol Vis 17: 2934–2946.
29. Wu X, Quondamatteo F, Lefever T, Czuchra A, Meyer H, et al. (2006) Cdc42 controls progenitor cell differentiation and beta-catenin turnover in skin. Genes Dev 20: 571–585.
30. Marquardt T, Ashery-Padan R, Andrejewski N, Scardigli R, Guillemot F, et al. (2001) Pax6 is required for the multipotent state of retinal progenitor cells. Cell 105: 43–55.
31. Madisen L, Zwingman TA, Sunkin SM, Oh SW, Zariwala HA, et al. (2010) A robust and high-throughput Cre reporting and characterization system for the whole mouse brain. Nat Neurosci 13: 133–140.
32. Vazquez-Chona FR, Clark AM, Levine EM (2009) Rlbp1 promoter drives robust Muller glial GFP expression in transgenic mice. Invest Ophthalmol Vis Sci 50: 3996–4003.
33. Seeliger MW, Grimm C, Stahlberg F, Friedburg C, Jaissle G, et al. (2001) New views on RPE65 deficiency: the rod system is the source of vision in a mouse model of Leber congenital amaurosis. Nat Genet 29: 70–74.
34. Tanimoto N, Muehlfriedel RL, Fischer MD, Fahl E, Humphries P, et al. (2009) Vision tests in the mouse: Functional phenotyping with electroretinography. Front Biosci 14: 2730–2737.
35. Caprara C, Thiersch M, Lange C, Joly S, Samardzija M, et al. (2011) HIF1A is essential for the development of the intermediate plexus of the retinal vasculature. Invest Ophthalmol Vis Sci 52: 2109–2117.
36. Matsunaga M, Hatta K, Takeichi M (1988) Role of N-cadherin cell adhesion molecules in the histogenesis of neural retina. Neuron 1: 289–295.
37. Paffenholz R, Kuhn C, Grund C, Stehr S, Franke WW (1999) The arm-repeat protein NPRAP (neurojungin) is a constituent of the plaques of the outer limiting zone in the retina, defining a novel type of adhering junction. Exp Cell Res 250: 452–464.
38. Dubois-Dauphin M, Poitry-Yamate C, de Bilbao F, Julliard AK, Jourdan F, et al. (2000) Early postnatal Muller cell death leads to retinal but not optic nerve degeneration in NSE-Hu-Bcl-2 transgenic mice. Neuroscience 95: 9–21.
39. Yokota Y, Eom TY, Stanco A, Kim WY, Rao S, et al. (2010) Cdc42 and Gsk3 modulate the dynamics of radial glial growth, inter-radial glial interactions and polarity in the developing cerebral cortex. Development 137: 4101–4110.
40. Grosche J, Hartig W, Reichenbach A (1995) Expression of glial fibrillary acidic protein (GFAP), glutamine synthetase (GS), and Bcl-2 protooncogene protein by Muller (glial) cells in retinal light damage of rats. Neurosci Lett 185: 119–122.
41. Hirota S, Liu Q, Lee HS, Hossain MG, Lacy-Hulbert A, et al. (2011) The astrocyte-expressed integrin alphavbeta8 governs blood vessel sprouting in the developing retina. Development 138: 5157–5166.
42. Davis EJ, Foster TD, Thomas WE (1994) Cellular forms and functions of brain microglia. Brain Res Bull 34: 73–78.
43. Joly S, Francke M, Ulbricht E, Beck S, Seeliger M, et al. (2009) Cooperative phagocytes: resident microglia and bone marrow immigrants remove dead photoreceptors in retinal lesions. Am J Pathol 174: 2310–2323.
44. Stone J, Itin A, Alon T, Pe'er J, Gnessin H, et al. (1995) Development of retinal vasculature is mediated by hypoxia-induced vascular endothelial growth factor (VEGF) expression by neuroglia. J Neurosci 15: 4738–4747.
45. Joly S, Lange C, Thiersch M, Samardzija M, Grimm C (2008) Leukemia inhibitory factor extends the lifespan of injured photoreceptors in vivo. J Neurosci 28: 13765–13774.
46. Burgi S, Samardzija M, Grimm C (2009) Endogenous leukemia inhibitory factor protects photoreceptor cells against light-induced degeneration. Mol Vis 15: 1631–1637.
47. Rattner A, Nathans J (2005) The genomic response to retinal disease and injury: evidence for endothelin signaling from photoreceptors to glia. J Neurosci 25: 4540–4549.
48. Samardzija M, Wenzel A, Aufenberg S, Thiersch M, Reme C, et al. (2006) Differential role of Jak-STAT signaling in retinal degenerations. FASEB J 20: 2411–2413.
49. Lange C, Thiersch M, Samardzija M, Burgi S, Joly S, et al. (2010) LIF-dependent JAK3 activation is not essential for retinal degeneration. J Neurochem 113: 1210–1220.
50. Ueki Y, Wang J, Chollangi S, Ash JD (2008) STAT3 activation in photoreceptors by leukemia inhibitory factor is associated with protection from light damage. J Neurochem 105: 784–796.
51. Randlett O, Norden C, Harris WA (2011) The vertebrate retina: A model for neuronal polarization in vivo. Dev Neurobiol 71: 567–583.
52. Cappello S, Attardo A, Wu X, Iwasato T, Itohara S, et al. (2006) The Rho-GTPase cdc42 regulates neural progenitor fate at the apical surface. Nat Neurosci 9: 1099–1107.
53. Harada T, Harada C, Kohsaka S, Wada E, Yoshida K, et al. (2002) Microglia-Muller glia cell interactions control neurotrophic factor production during light-induced retinal degeneration. J Neurosci 22: 9228–9236.
54. Bringmann A, Iandiev I, Pannicke T, Wurm A, Hollborn M, et al. (2009) Cellular signaling and factors involved in Muller cell gliosis: neuroprotective and detrimental effects. Prog Retin Eye Res 28: 423–451.
55. Nakazawa T, Hisatomi T, Nakazawa C, Noda K, Maruyama K, et al. (2007) Monocyte chemoattractant protein 1 mediates retinal detachment-induced photoreceptor apoptosis. Proc Natl Acad Sci U S A 104: 2425–2430.
56. Yuan L, Neufeld AH (2000) Tumor necrosis factor-alpha: a potentially neurodestructive cytokine produced by glia in the human glaucomatous optic nerve head. Glia 32: 42–50.
57. Jacobson SG, Cideciyan AV, Aleman TS, Pianta MJ, Sumaroka A, et al. (2003) Crumbs homolog 1 (CRB1) mutations result in a thick human retina with abnormal lamination. Hum Mol Genet 12: 1073–1078.
58. Murphy GM, Jr., Zhao F, Yang L, Cordell B (2000) Expression of macrophage colony-stimulating factor receptor is increased in the AbetaPP(V717F) transgenic mouse model of Alzheimer's disease. Am J Pathol 157: 895–904.
59. Tezel G, Li LY, Patil RV, Wax MB (2001) TNF-alpha and TNF-alpha receptor-1 in the retina of normal and glaucomatous eyes. Invest Ophthalmol Vis Sci 42: 1787–1794.

11.5 p38 MAPK Signalling Acts Upstream of LIF-dependent Neuroprotection During Photoreceptor Degeneration

Cavit Agca[1], Andrea Gubler [1], Ghislaine Traber[1], Christel Beck[1], Cornelia Imsand[1], Divya Ail[1,3], Christian Caprara[1,2] and Christian Grimm[1,2,3*]

[1] Lab for Retinal Cell Biology, Department of Ophthalmology, University of Zurich, Zurich, 8091, Switzerland

[2] Zurich Center for Integrative Human Physiology (ZIHP), University of Zurich, Zurich, 8091, Switzerland

[3] Neuroscience Center (ZNZ), University of Zurich, Zurich, 8091, Switzerland

Accepted for publication in Cell Death and Disease, 2013 Sep 5;**4**:e785

Personal Contribution

Design of luciferase reporter vector containing NFκB binding sites and preliminary experiments with luciferase assay.

Key Findings

In many blinding diseases of the retina, loss of function and thus severe visual impairment results from apoptotic cell death of damaged photoreceptors. In an attempt to survive, injured photoreceptors generate survival signals to induce intercellular protective mechanisms that eventually may rescue photoreceptors from entering an apoptotic death pathway. One such endogenous survival pathway is controlled by LIF, which is produced by a subset of Muller glia cells in response to photoreceptor injury. In the absence of LIF, survival components are not activated and photoreceptor degeneration is accelerated. Although LIF is a crucial factor for photoreceptor survival, the detailed mechanism of its induction in the retina has not been elucidated.

Here are some of the key findings of the study:

- administration of TNFA was sufficient to fully upregulate *Lif* expression in Muller cells *in vitro* and the retina *in vivo*
- increased *Lif* expression depended on p38 MAPK since inhibition of its activity abolished *Lif* expression *in vitro* and *in vivo*
- inhibition of p38 MAPK activity reduced *Lif* expression also in the model of light-induced retinal degeneration and resulted in increased cell death in the light-exposed retina

OPEN

Citation: Cell Death and Disease (2013) 4, e785; doi:10.1038/cddis.2013.323

www.nature.com/cddis

p38 MAPK signaling acts upstream of LIF-dependent neuroprotection during photoreceptor degeneration

C Agca[1], A Gubler[1], G Traber[1], C Beck[1], C Imsand[1], D Ail[1,2], C Caprara[1,3] and C Grimm*[,1,2,3]

In many blinding diseases of the retina, loss of function and thus severe visual impairment results from apoptotic cell death of damaged photoreceptors. In an attempt to survive, injured photoreceptors generate survival signals to induce intercellular protective mechanisms that eventually may rescue photoreceptors from entering an apoptotic death pathway. One such endogenous survival pathway is controlled by leukemia inhibitory factor (LIF), which is produced by a subset of Muller glia cells in response to photoreceptor injury. In the absence of LIF, survival components are not activated and photoreceptor degeneration is accelerated. Although LIF is a crucial factor for photoreceptor survival, the detailed mechanism of its induction in the retina has not been elucidated. Here, we show that administration of tumor necrosis factor-alpha (TNF) was sufficient to fully upregulate *Lif* expression in Muller cells *in vitro* and the retina *in vivo*. Increased *Lif* expression depended on p38 mitogen-activated protein kinase (MAPK) since inhibition of its activity abolished *Lif* expression *in vitro* and *in vivo*. Inhibition of p38 MAPK activity reduced the *Lif* expression also in the model of light-induced retinal degeneration and resulted in increased cell death in the light-exposed retina. Thus, expression of *Lif* in the injured retina and activation of the endogenous survival pathway involve signaling through p38 MAPK.

Cell Death and Disease (2013) **4**, e785; doi:10.1038/cddis.2013.323; published online 5 September 2013
Subject Category: Neuroscience

Throughout our life span, cells have to be repaired or regenerated in order to maintain tissue function. Whereas this happens frequently in most parts of the body, the regeneration capacity of the nervous system is generally very limited in mammals, and the consequences of neuronal disease or injury are mostly irreversible. Therefore, it is crucial to rescue neurons from devastating insults, a task that requires activation of endogenous neuroprotective systems. In the retina, several pathways exist to support the survival of neurons.[1–7] Leukemia inhibitory factor (LIF) controls one of these pathways and is one of the most important endogenous factors for neuroprotection in the retina.[1,2] Photoreceptor injury or degeneration activates a subset of Muller glia cells to express *Lif*, which controls a cascade of neuroprotective signaling between photoreceptors and Muller cells.[1,8] These signaling events include activation of the Janus kinase/signal transducer and activator of transcription (JAK/STAT) pathway,[9–11] and result in the upregulation of several genes important for neuroprotection, including signal transducer and activator of transcription-3 (*Stat3*), endothelin-2 (*End2*) and fibroblast growth factor-2 (*Fgf2*), and for gliosis (glial fibrillary acidic protein, *Gfap*).[1,12] In the absence of LIF, none of these factors is induced, and photoreceptor cell death is accelerated.[1,12]

Although downstream events of LIF signaling have been studied in the retina,[1,12–14] the signal that initiates *Lif* expression has not been elucidated. One of the hypotheses for the initiation of survival pathways is based on the generation of reactive oxygen species (ROS) in stressed photoreceptors.[15–17] Subtoxic levels of ROS have been shown to be neuroprotective for photoreceptors and ROS may act as signaling molecules for survival pathways in the retina.[15–18] Another hypothesis especially with respect to the involvement of Muller cells includes tumor necrosis factor-alpha (TNF) signaling, as TNF has been recently shown to be the key signaling molecule for Muller cell proliferation and differentiation into a photoreceptor fate in the degenerating zebrafish retina.[19] However, its role during photoreceptor degeneration in the mammalian retina has not been identified in detail.

TNF was shown to regulate expression of several important factors that mediate a proinflammatory response. Likewise, TNF treatment upregulates several cytokines including *Lif* in various cell types.[20,21] The reported neuroprotective effect of TNF is mostly attributed to nuclear factor kappa-light-chain-enhancer of activated B cells (NFκB) activation and the resulting differential regulation of gene expression.[22–27]

[1]Lab for Retinal Cell Biology, Department of Ophthalmology, University of Zurich, Zurich 8091, Switzerland; [2]Neuroscience Center (ZNZ), University of Zurich, Zurich 8091, Switzerland and [3]Zurich Center for Integrative Human Physiology (ZIHP), University of Zurich, Zurich 8091, Switzerland
*Corresponding author: C Grimm, Department of Ophthalmology, University of Zurich, Lab for Retinal Cell Biology, Wagistrasse 14, Schlieren 8952, Switzerland. Tel: +41 44 556 3001; Fax: +41 44 556 3999; E-mail: cgrimm@opht.uzh.ch
Keywords: leukemia inhibitory factor (LIF); p38 MAPK; TNF; Muller glia cell; photoreceptor; neuroprotection
Abbreviations: BSA, bovine serum albumin; Clc, cardiotrophin-like cytokine; Cntf, ciliary neurotrophic factor; End2, endothelin-2; Fgf2, fibroblast growth factor-2; Gfap, glial fibrillary acidic protein; IL-6, interleukin-6; JAK/STAT, Janus kinase/signal transducer and activator of transcription; Lif, leukemia inhibitory factor; Lifr, leukemia inhibitory factor receptor; LIRD, light-induced retinal degeneration; MAPK, mitogen-activated protein kinase; NFκB, nuclear factor kappa-light-chain-enhancer of activated B cells; Pax6, paired box protein-6; RGC, retinal ganglion cell; rMC-1, rat Muller glia cell line-1; ROS, reactive oxygen species; SEM, standard error of the mean; Stat3, signal transducer and activator of transcription-3; TLR2, Toll-like receptor-2; TNF, tumor necrosis factor; Vim, vimentin
Received 10.6.13; revised 09.7.13; accepted 15.7.13; Edited by A Verkhratsky

However, divergent data exist and various reports attribute TNF also a role in the promotion of neurodegeneration (reviewed in detail[22,23]). Blocking TNF in a glaucoma model of retinal ganglion cell (RGC) death, for example, had beneficial effects on RGC survival.[28–30] In contrast, increased survival of RGCs after axotomy of the optic nerve required elevated and not decreased TNF levels.[31]

In addition to NFκB, TNF has been shown to activate the p38 mitogen-activated protein kinase (MAPK) pathway in a variety of models, and a small number of genes have been identified that are regulated through p38 MAPK after TNF induction.[27] However, similar to TNF, no consensus exists on the anti- or pro-apoptotic effects of p38 MAPK activity in neuronal tissues. Active p38 MAPK signaling has been shown to contribute to RGC death after ischemia or optic nerve axotomy.[32,33] In contrast, recent findings suggest that p38 MAPK activity is important for RGC survival after ischemia/reperfusion injury,[34,35] and that active crosstalk between NFκB and p38 MAPK pathways may be an important aspect of this neuroprotection.[35]

To date, the effects of TNF and p38 MAPK on photoreceptor protection and their possible role in the regulation of neuroprotective factors in the retina have not been studied. To gain insight into the mechanisms that regulate LIF-mediated neuroprotection, we investigated the contributions of TNF and p38 MAPK to *Lif* expression both *in vitro* and *in vivo*, and tested the relevance of the findings in the model of light-induced retinal degeneration (LIRD) *in vivo*. The results show that p38 MAPK activity is neuroprotective and required to upregulate expression of *Lif* in the injured retina.

Results

TNF upregulates *Lif* expression through p38 MAPK in cultured Muller cells *in vitro*. Previously, it has been shown that treatment with recombinant TNF induces upregulation of *Lif* expression in fibroblasts and other cells.[20,21] Since LIF is crucial for endogenous neuroprotection in the retina and is expressed by a subset of Muller cells upon photoreceptor injury, we tested whether Muller cells upregulate *Lif* in response to TNF administration *in vitro*. When cultured rat Muller cells (rMC-1)[36] were treated with TNF, *Lif* and *Tnf* were simultaneously upregulated 10.7- and 21-fold, respectively (Figure 1). This transcriptional response was fast and reached its peak at 1 h before it gradually decreased towards basal levels even though TNF was still present in the culture medium. This suggests a transcriptional induction by TNF followed by suppression of expression. The transient upregulation of *Lif* and *Tnf* in Muller cells is consistent with results from previously studied models.[20,21] We also tested expression of genes that are known to be upregulated in activated Muller cells including *Gfap*, ciliary neurotrophic factor (*Cntf*) and *Fgf2*.[1] However, none of these genes was activated by TNF demonstrating a specificity of TNF for the regulation of *Lif* expression in rMC-1 (Figure 1).

Stimulation of cells with TNF has been previously shown to induce p38 MAPK signaling. Thus, we determined the role of p38 MAPK in the regulation of *Lif* expression. Since the expression of *Lif* in cultured Muller cells was robust, we first

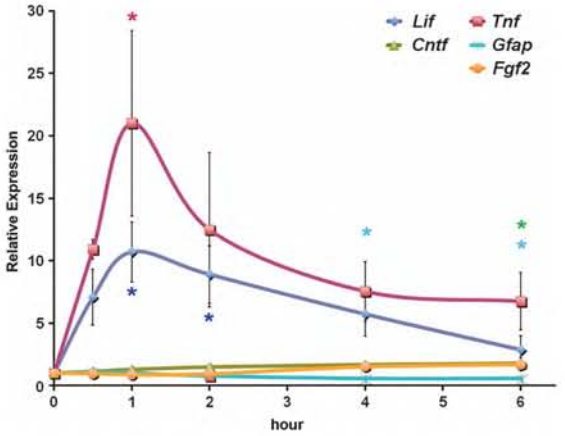

Figure 1 TNF treatment transiently upregulates *Lif* expression in Muller cells *in vitro*. Real-time PCR analysis of gene expression in rMC-1 cells before (0 h) or at various timepoints during TNF treatment as indicated. TNF (10 ng/ml) treatment resulted in a strong upregulation of *Lif* expression as early as 30 min. Peak of expression was at 1 h. *Tnf* expression was upregulated similarly to *Lif*. In contrast, expression of *Cntf*, *Gfap* and *Fgf2* was not affected by TNF. Shown are means ± S.E.M. of $N=3$. ANOVA with Dunnett's post-tests was used to compare control levels (at '0') with expression levels of each gene at all timepoints after TNF treatment. Note that the color of the stars indicating significance match the color of the respective gene. $^*P<0.05$

tested the effect of p38 MAPK activity on basal *Lif* expression in the absence of TNF by using two specific chemical inhibitors for p38 MAPK activity, SB239063 and SB202190.[37,38] Treatment with either SB compound downregulated *Lif* expression in a dose-dependent manner within 1 h of treatment and at a similar concentration range (Figures 2a and b). As expected, inhibitor treatment did not block phosphorylation of p38 MAPK (see also Figures 5b and c) but prevented its activity reducing activation of downstream targets like heat shock protein-27 (data not shown). The effect of p38 MAPK inhibition was specific for *Lif* as the expression of *Gfap*, *Cntf* and *Fgf2* was not reduced (Figures 2a and b).

To analyze whether TNF-mediated upregulation of *Lif* expression also involves p38 MAPK signaling, we co-treated Muller cells with TNF and SB239063. Consistent with our results above (Figure 1), TNF treatment induced *Lif* expression (Figure 3a). However, inhibition of p38 MAPK activity by SB239063 completely blocked *Lif* upregulation in the presence of TNF (Figure 3a), suggesting that p38 MAPK activity is crucial not only for basal *Lif* expression but also for TNF-induced *Lif* upregulation.

Another signaling pathway known to be activated by TNF centers around NFκB. Since multiple potential binding sites for NFκB are located in the *Lif* promoter region (not shown) and NFκB was identified to bind the *Lif* promoter upon stimulation of cells with Toll-like receptor-2 (TLR2) agonists,[39] we determined the activation of NFκB in Muller cells upon TNF treatment using a luciferase reporter vector that contains NFκB binding elements. Treatment with TNF strongly increased luciferase levels suggesting that NFκB was activated in Muller cells under these conditions (Figure 3b). Importantly, addition of the p38 MAPK inhibitor SB202190

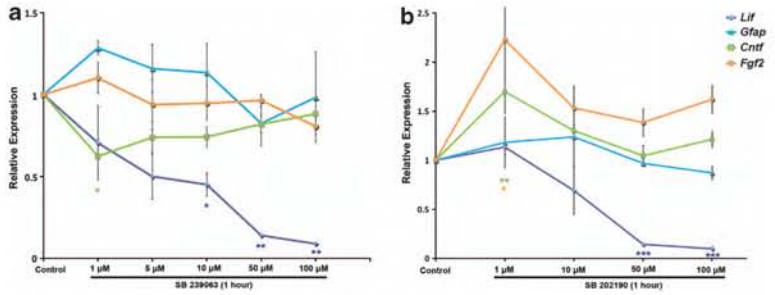

Figure 2 Inhibition of p38 MAPK activity downregulates *Lif* expression in Muller cells *in vitro*. Real-time PCR analysis of gene expression in rMC-1 cells before (control) or at 1 h of treatment with various concentrations (as indicated) of p38 MAPK inhibitors SB239063 (**a**) or SB202190 (**b**). Expression levels of *Lif* inversely correlated with the concentration of p38 MAPK inhibitors. Expression levels of *Cntf*, *Gfap* and *Fgf2* were not affected. Shown are means ± S.E.M. of $N=3$. ANOVA with Dunnett's post-tests was used to compare control levels with expression levels of each gene after inhibitor treatment. Note that the color of the stars indicating significance match the color of the respective gene. $^{*}P<0.05$; $^{**}P<0.01$; $^{***}P<0.005$

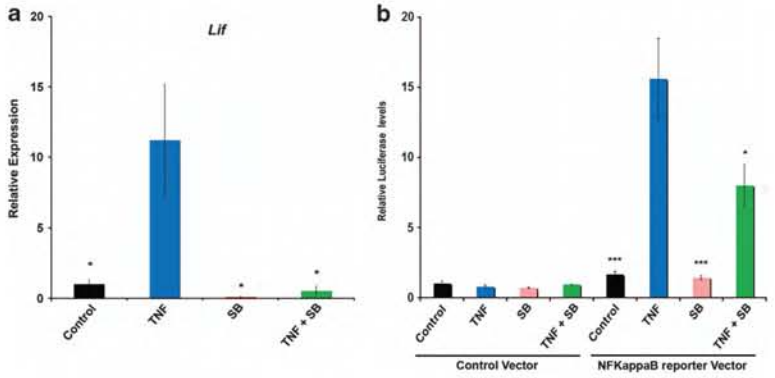

Figure 3 Inhibition of p38 MAPK activity prevents TNF-induced upregulation of *Lif* expression in Muller cells *in vitro*. (**a**) RT PCR analysis of *Lif* expression in rMC-1 cells before (control, black bar) or at 1 h of treatment with TNF (10 ng/ml, blue bar), p38 MAPK inhibitor SB239063 (SB, 100 μM, pink bar) or a combination of both (green bar). Inhibition of p38 MAPK activity downregulated basal *Lif* expression and blocked TNF-induced *Lif* upregulation. Shown are means ± S.E.M. of $N=3$. ANOVA with Dunnett's post-tests was used to compare *Lif* levels after TNF injection with control levels or levels after SB or SB + TNF treatment. (**b**) Luciferase levels in rMC-1 cells transfected with a control vector or an NFκB reporter vector. Cells were treated for 6 h with TNF (10 ng/ml, blue bars), p38 MAPK inhibitor SB202190 (SB, 100 μM, pink bars), or a combination of both (green bars). Controls (black bars) were not treated. NFκB-mediated luciferase expression was upregulated by TNF treatment. The TNF-mediated upregulation was partially blocked by the inhibitor of p38 MAPK activity. ANOVA with Dunnett's post-tests was used to compare luciferase levels after TNF injection with levels of other treatments. Statistics were calculated seperately for the 'control vector' group and the 'NFκB vector' group. Shown are means ± S.E.M. of $N=4$

completely inhibited TNF-induced *Lif* upregulation (Figure 3a), but reduced TNF-induced NFκB activity only by 49% leaving it still fivefold above control levels (Figure 3b). This indicates that, although p38 MAPK and NFκB pathways may interact, increased NFκB activity may not be sufficient to induce *Lif* expression in Muller cells in response to TNF treatment (Figure 3b) *in vitro*.

Regulation of *Lif* expression in the neuronal retina *in vivo*. Our results show that TNF induces *Lif* expression via the p38 MAPK pathway in Muller cells *in vitro*. To determine whether *Lif* expression is similarly regulated in the healthy or injured neuronal retina *in vivo*, we injected TNF, a water-soluble p38 MAPK inhibitor (SB220025 trihydrochloride),[40] or a combination of both into the vitreous of wild-type mice that were or were not exposed to damaging levels of white light (Figures 4–7).

Similar to our observations in cultured Muller cells, TNF injections increased the expression of *Lif* and *Tnf* in the retina within 1 – 2 h before levels gradually decreased again (Figure 4). Since *Fgf2*, *End2* and *Stat3* are part of the LIF-controlled endogenous neuroprotective signaling system,[1,12] we also analyzed their expression pattern after TNF injections. Expression of all three genes was significantly upregulated and peaked at around 12 h after injection and thus with a slight delay compared with *Lif* (Figure 4). Although not directly tested, this suggests that LIF may also be important for *Fgf2*, *End2* and *Stat3* expression after TNF injections, as it is in the injured retina.[1,12] Similarly, expression of *Gfap*, which has also been shown to depend on LIF signaling,[1] was upregulated with a similar delay (Figure 4). In contrast, expression of paired box protein-6 (*Pax6*), *Lif* receptor (*Lifr*) and *Cntf*, genes that may not depend on LIF signaling, was not comparably regulated. Although CNTF

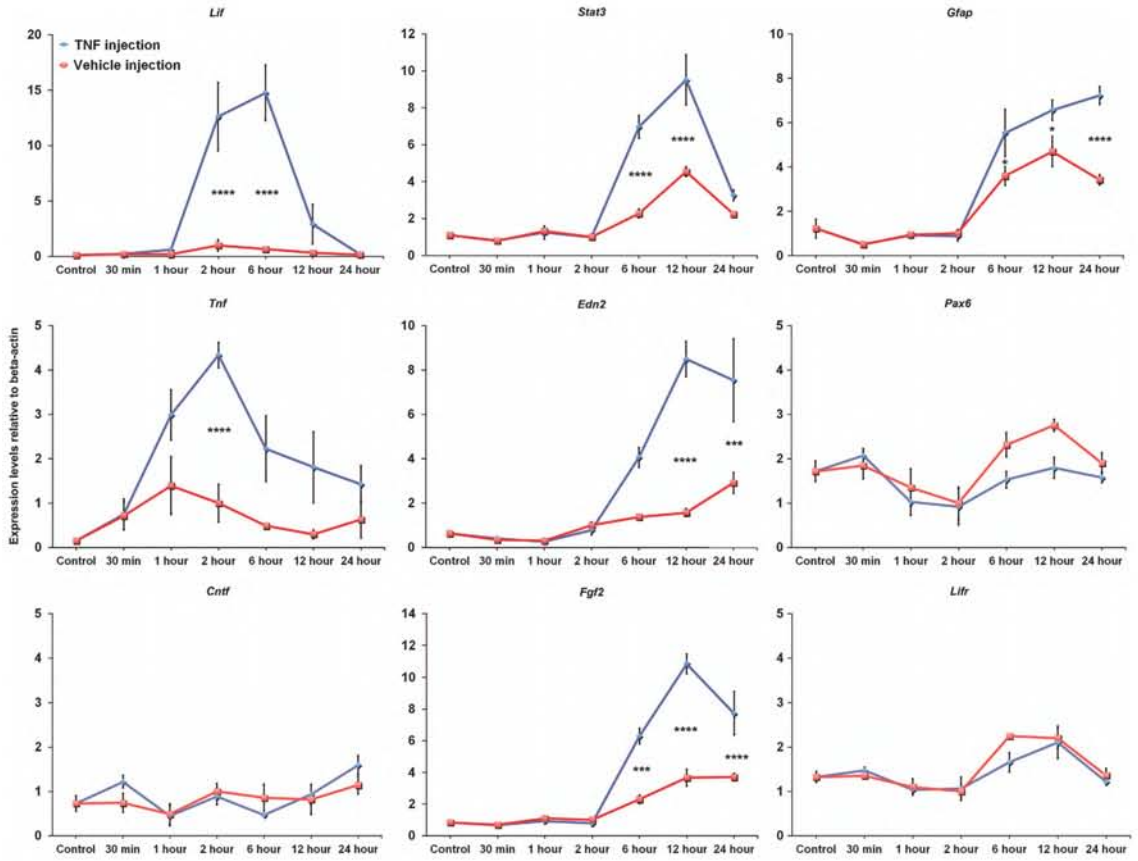

Figure 4 Intravitreal injection of TNF induces Lif gene expression in the neuronal retina *in vivo*. Real-time PCR analysis of gene expression in retinas of C67BL/6 mice before (control) or at indicated timepoints after intravitreal injection of TNF (blue lines) or vehicle (maroon lines). *Lif* and *Tnf* were upregulated as early as 1 h (*Tnf*) or 2 h (*Lif*) after injection, before levels of *Stat3, Edn2, Fgf2* and *Gfap* started to increase at 6 h. Expression of *Cntf, Lifr* and *Pax6* was not remarkably affected by the injections. Shown are means ± S.E.M. of $N = 3-4$ per timepoint and treatment. Two-way ANOVA with Bonferroni post-test was used to test for statistical significance between treatments at each timepoint. $^{*}P<0.05$; $^{***}P<0.005$; $^{****}P<0.001$

is strongly neuroprotective in the retina[2,3] and belongs to the same interleukin-6 (IL-6) family of cytokines as LIF, consequences of TNF injections were thus rather specific for the *Lif* gene.

To determine whether p38 MAPK is also involved in TNF-induced *Lif* expression in the retina *in vivo*, we analyzed gene expression at 2 and 6 h after intravitreal injection of TNF and/or the p38 MAPK inhibitor SB220025. As expected, injection of TNF caused increased *Lif* RNA levels at both timepoints (Figure 5a). However, when SB220025 was co-injected with TNF, upregulation of *Lif* expression was reduced by 78 and 73% at the 2 and 6 h timepoints, respectively. Injection of vehicle or SB220025 alone slightly upregulated *Lif* expression probably due to injection-inflicted retinal injury (Figure 5a). Western blots of retinal extracts showed an approximately 7.5-fold increase in phosphorylation levels of p38 MAPK at 2 h after TNF injection as compared with controls, suggesting that TNF increases p38 MAPK activity in the retina (Figures 5b and c). Injection of the p38 MAPK inhibitor (which does not block phosphorylation but the activity of p38 MAPK)[40] either alone or in combination with TNF also resulted in increased p38 phosphorylation levels which may suggest an attempt of inhibitor-treated retinal cells to increase p38 MAPK activity by a positive feedback. Since vehicle injections upregulated phospho-p38 MAPK levels by 3.5-fold, intravitreal injections *per se* may generate a stress response and activate p38 MAPK to a certain degree (Figures 5b and c). In summary, these data imply that the p38 MAPK pathway is also important for TNF-mediated *Lif* regulation in the neuronal retina *in vivo*.

p38 MAPK is an important regulator for increased *Lif* expression after exposure to damaging light *in vivo*. We showed that TNF-induced *Lif* upregulation depends on p38 MAPK activity in the healthy wild-type retina. To test whether *Lif* regulation depends on p38 MAPK also in a disease model, we exposed dark-adapted mice to high-intensity white light that has been shown to cause photoreceptor degeneration and to upregulate *Lif* expression in Muller cells.[1] Six hours after light exposure, *Lif* levels were increased 62-fold

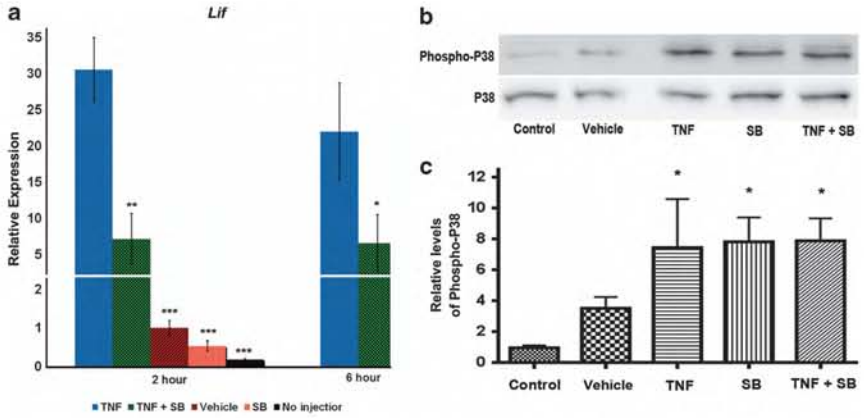

Figure 5 Activation of p38 MAPK is essential for TNF-induced upregulation of *Lif* expression in the neuronal retina *in vivo*. (**a**) RT PCR analysis of gene expression in retinas of C67BL/6 mice before (no injection, black bars) or at 2 and 6 h after intravitreal injection of TNF (blue bars), p38 MAPK inhibitor SB220025 (SB, pink bar), TNF + p38 MAPK inhibitor SB220025 (TNF + SB, green bar) or vehicle (maroon bar). TNF-mediated upregulation of *Lif* expression was significantly attenuated by the p38 MAPK inhibitor. Shown are means ± S.E.M. of $N = 3-4$ per timepoint and treatment. ANOVA with Bonferroni post-tests was used to compare expression levels after TNF injection with levels of remaining groups at the 2-h timepoint. Student's *t*-test was used to compare expression at 6 h. $^{*}P<0.05$; $^{**}P<0.01$; $^{***}P<0.005$. (**b**) Detection of phospho-p38 MAPK (upper panel) and p38 MAPK (lower panel) by western blot of protein extracts from retinas before (control) or at 2 h after injection of vehicle, TNF, p38 MAPK inhibitor SB220025 (SB), or TNF + p38 MAPK inhibitor SB220025 (TNF + SB) as indicated. Injection of TNF, SB and TNF + SB increased levels of phospho-p38 MAPK compared with vehicle and uninjected retinas. Shown are representative blots. (**c**) Quantification of signals detected by western blot in (**b**) using Bio1D software. Phospho-p38 MAPK levels were highest after injection of TNF, of p38 MAPK inhibitor SB220025 (SB) and of TNF + p38 MAPK inhibitor SB220025 (TNF + SB). Shown are means ± S.E.M. of $N = 3$–9 per treatment. ANOVA with Bonferroni post-tests was used to compare levels to control. $^{*}P<0.05$

(Figure 6). Intravitreal injection of vehicle immediately after light exposure slightly further increased *Lif* levels. Importantly, however, injection of p38 MAPK inhibitor SB220025 reduced *Lif* levels by 57% compared with vehicle injections. Similarly to observations made before (Figure 5a), vehicle injection induced *Lif* expression also in non-exposed mice (dark controls). As in the light-exposed retinas, injection of SB220025 reduced this induction by about 63% (Figure 6).

SB-mediated inhibition of *Lif* expression in the light-exposed retina was not as strong as in TNF + SB-injected retinas (Figure 5a), most probably because the SB inhibitor was injected for experimental reasons 2 h after the start of light exposure and thus only after the *Lif*-inducing signaling cascade had been activated by the light stimulus. Cardiotrophin-like cytokine (*Clc*) is another member of the IL-6 family of cytokines that is upregulated in response to light damage.[12] Similarly to *Lif*, induction of *Clc* was partially inhibited by SB treatment (Figure 6). Analysis of *Cntf*, *Gfap* and vimentin (*Vim*), which are expressed in Muller cells,[41–43] did not show any significant changes as a result of SB treatment (Figure 6). These results imply that p38 MAPK is involved in controlling *Lif* upregulation after light-induced photoreceptor injury *in vivo*.

p38 MAPK activity is neuroprotective in the model of light-induced photoreceptor degeneration. If p38 MAPK is indeed important for regulation of neuroprotective *Lif* in the injured retina, inhibition of its activity should increase photoreceptor damage after light exposure. To directly test this hypothesis, we quantified cell death in the retina at 40 h after exposure of wild-type mice to high levels of white light. Although intravitreal injections had a protective effect in general (vehicle), inhibition of p38 MAPK by SB220025 significantly increased cell death as compared with vehicle injections (compare 'SB' to 'vehicle'). In contrast, TNF injections reduced cell death almost to dark control levels (Figure 7). Importantly, cell death showed a distinct negative correlation with levels of *Lif* mRNA after no, SB, vehicle or TNF injections (Figures 5a and 7), corroborating earlier findings that showed that dosage and timing of *Lif* expression is an important factor for retinal physiology and neuroprotection.[13,44,45] These results strongly argue that LIF-mediated endogenous neuroprotection after light damage depends on p38 MAPK signaling in the retina.

Discussion

Regulation of *Lif* expression in Muller cells. Our results demonstrate that p38 MAPK signaling is required for the regulation of *Lif* expression in Muller cells *in vitro* and in the retina *in vivo*. We also show that inhibition of p38 MAPK activity reduces *Lif* expression and increases cell death in a model of photoreceptor injury supporting a direct role for p38 MAPK in LIF-mediated neuroprotection in the retina. Furthermore, treatment with recombinant TNF was sufficient to activate p38 MAPK, to increase *Lif* expression *in vitro* and *in vivo*, and to protect against light damage *in vivo*. However, whether endogenous TNF is involved in regulating *Lif* expression in the injured retina *in vivo* needs still to be determined, even though *Tnf* expression is induced early after light exposure in the eyecup.[46]

p38 MAPK activity has been shown to be one of the most important stress response factors by regulating the expression of several genes through activation of transcription factors such as ATF2, CHOP, CREB and ELK1.[22] Additionally, p38 MAPK affects gene expression at the

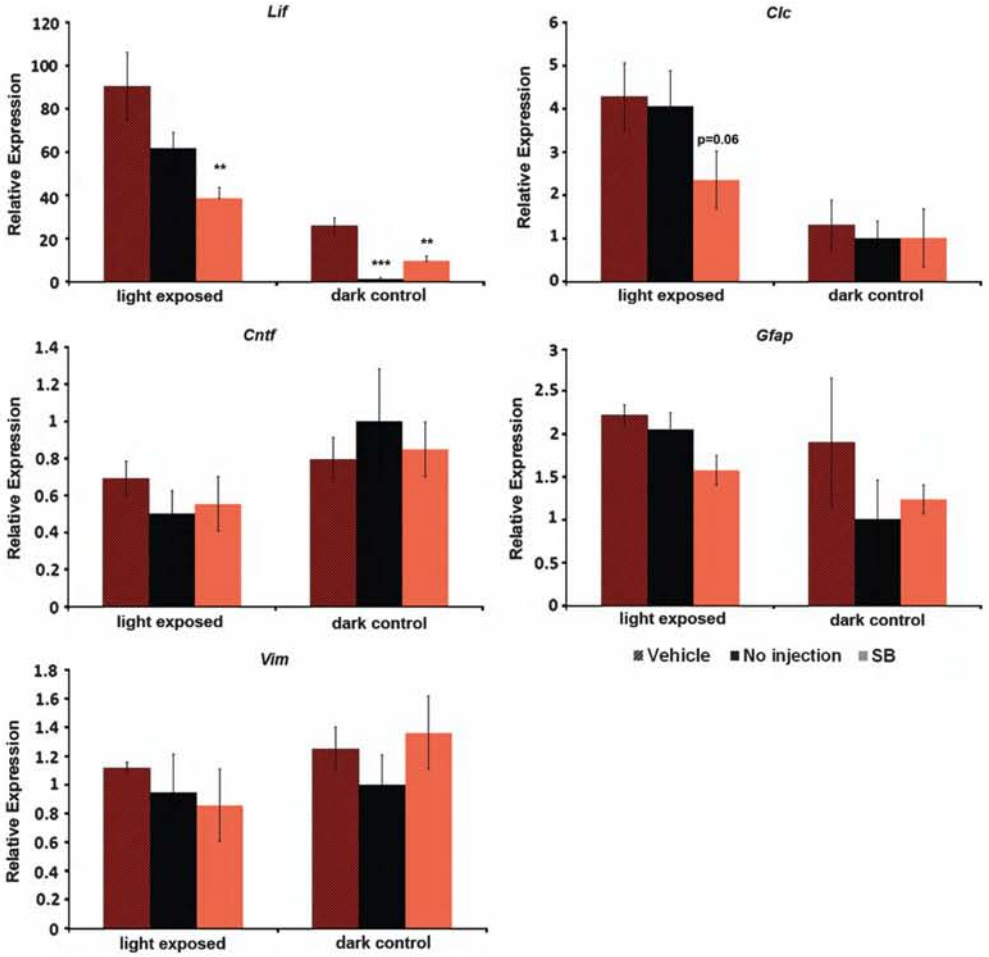

Figure 6 p38 MAPK is involved in light-induced *Lif* upregulation *in vivo*. Real-time PCR analysis of retinal gene expression before (dark controls) or at 6 h after exposure to 2 h of 13 000 lux of white light. Vehicle (maroon bars) or p38 MAPK inhibitor SB220025 (SB, pink bars) was injected into the vitreous immediately after the end of light exposure. Injections in dark-exposed control mice were done at a similar timepoint during the day to control for potential circadian alterations in gene expression. Light exposure significantly upregulated *Lif* expression in non-injected (black bars) and vehicle-injected eyes. Upregulation was prevented by SB injections. Note that *Lif* levels in light-exposed mice after SB injections were not different from dark control mice after vehicle injections. Expression of *Clc* was regulated similarly to *Lif*. Levels of *Cntf*, *Vim* and *Gfap* were not affected by light exposure or injections. Shown are means ± S.E.M. of $N = 3$–7 per treatment. ANOVA with Bonferroni post-tests was used to compare levels after vehicle injection to levels after SB injections and to levels of mice that received no injection. Statistics were calculated seperately for the light-exposed groups and the control groups. $^{**}P < 0.01$; $^{***}P < 0.005$

post-transcriptional level by enhancing the stability of target mRNAs containing AU-rich elements in their 3′ UTRs.[47] In our experimental systems, however, we focused on the effects of p38 MAPK signaling on the regulation of *Lif* expression at the transcriptional level *in vitro* and *in vivo*.

Activation (phosphorylation) of p38 MAPK by TNF was rapid, as was upregulation of *Lif* expression. The fast upregulation of *Lif* levels was blocked by an inhibitor of p38 MAPK activity, suggesting that the initial role of p38 MAPK involves transcriptional activation of *Lif* expression. Transcription factors involved in this regulatory pathway have not been defined and their identification will need further investigations. However, NFκB is a candidate factor that was upregulated by TNF treatment in a p38 MAPK-dependent manner (Figure 3), and NFκB binding to the *Lif* promoter has recently been shown in response to TLR2 agonists.[39] Furthermore, a connection between p38 MAPK, NFκB and cytokine regulation has been suggested[48] and TNF-mediated activation of p38 MAPK is well documented.[22] Nevertheless, the contribution of NFκB to TNF-mediated *Lif* upregulation may not be major, or else may depend on p38 MAPK. In the presence of TNF and the p38 MAPK inhibitor SB202190, Müller cells retain 50% of NFκB activity but completely lack *Lif* upregulation (Figures 3a and b), at least *in vitro*.

Regulation of *Lif* expression may additionally include a second level of complexity. The fast increase in expression

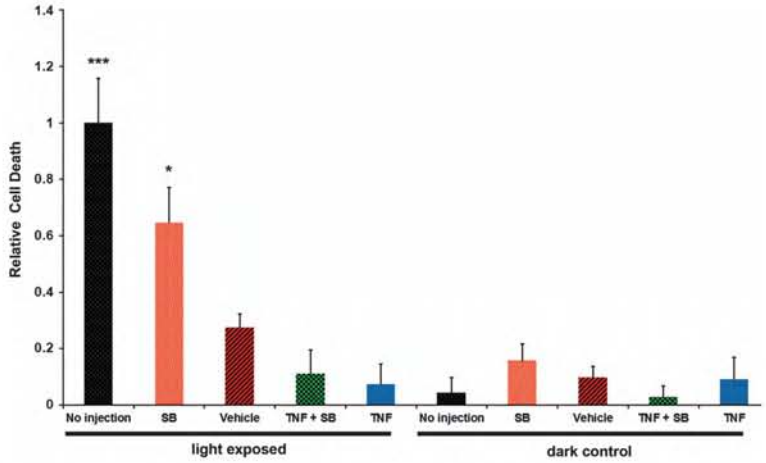

Figure 7 Inhibition of p38 MAPK activity increases cell death in the retina after light exposure *in vivo*. Quantification of cell death in retinas of non-exposed SV129S6 mice (dark controls) or in retinas of mice at 40 h after exposure to 2 h of 13 000 lux of white light (light damage). Twenty hours before light exposure, mice received an intravitreal injection of TNF (blue bars), p38 MAPK inhibitor SB220025 (SB, pink bars), TNF + p38 MAPK inhibitor SB220025 (TNF + SB, green bars) or vehicle (maroon bars). No-injection controls (black bars) were treated equally but did not receive intravitreal injections. The highest level of retinal cell death after light exposure was observed in non injected mice. Vehicle injections induced a protection, which was further strengthened by injection of TNF. p38 MAPK inhibitor SB220025 increased cell death almost to the level of non-injected control mice. Shown are means ± S.E.M. of $N = 3$–7 per treatment. ANOVA with Bonferroni post-tests was used to compare levels of cell death of the various groups to vehicle control. Statistics were calculated seperately for the light damage and the dark control group. $^{*}P < 0.05$; $^{***}P < 0.005$

after TNF treatment *in vitro* (Figure 1) or after light exposure *in vivo*,[11] was followed by a rapid decline of *Lif* mRNA levels towards basal levels. This argues for the presence of a regulatory feedback loop and that transcriptional activation of *Lif* expression might be followed by transcriptional inhibition or by a reduction of *Lif* mRNA stability, or both.

Neuroprotective role of p38 MAPK activity and *Lif* expression. Depending on the concept and experimental setup, activation of p38 MAPK has been shown to promote cell survival or apoptosis. Whereas inhibition of p38 MAPK activity has been reported to protect 661W photoreceptor cells against light damage *in vitro*,[49] our results indicate that inhibition of p38 MAPK activity accelerates light damage *in vivo*. This discrepancy may be due to the lack of intercellular communication between photoreceptors, RPE and Muller cells in the *in vitro* cell culture system. Photoreceptor degeneration induced *in vivo* by high levels of white light depends on RPE65 in the RPE and on the regeneration kinetics of the bleached chromophore in the visual cycle.[50,51] Hence mechanisms of light-induced death in isolated 661W cells *in vitro* and photoreceptors *in vivo* differ and the two experimental systems cannot be directly compared. Of additional importance, photoreceptors injured by light or other stimuli signal to Muller cells, which induce expression of *Lif* to ignite a neuroprotective response in the retina leading to increased photoreceptor survival.[1,8] This intercellular communication is not possible in the cell culture system, and effects of p38 MAPK inhibition in 661W cells may thus not accurately reflect the *in vivo* situation where p38 MAPK activity seems important in Muller cells to upregulate expression of neuroprotective *Lif*.

Despite the neuroprotective role of p38 MAPK, inhibition of its activity in the presence of TNF was still protective against LIRD, in contrast to inhibitor injections alone (Figure 7). Protection correlated with increased levels of *Lif* in retinas of eyes injected with a combination of TNF and inhibitor, and with decreased *Lif* levels after injection of the p38 MAPK inhibitor alone (Figure 5a). This suggests that injection of the p38 MAPK inhibitor was not sufficient to completely block the strong *Lif*-inducing activity of TNF and raises the possibility that a mechanism for TNF-induced *Lif* upregulation in addition to p38 MAPK may be present *in vivo*. Alternatively, TNF may potentially have protective effects through other mechanisms such as NFκB activation and its downstream targets, or the regulation of heat shock proteins.[52] It is interesting to note that p38 MAPK inhibitors only partially blocked TNF-induced NFκB activation whereas they completely abolished *Lif* induction, at least *in vitro* (Figure 5). This may argue that TNF could regulate the fate of photoreceptor cells via several mechanisms.

Due to the inhibition of pro-inflammatory gene expression, inhibitors of p38 MAPK are discussed as potential therapeutic agents in inflammatory diseases like psoriasis and rheumatoid arthriis.[53] Moreover, p38 MAPK inhibitors were shown to block tumor growth and metastases formation.[54] However, our results demonstrating that inhibition of p38 MAPK activity may be detrimental to injured photoreceptor cells ask for precautions when developing p38 MAPK inhibitors for therapeutic use. In cases of open or hidden retinal disease conditions, application of p38 MAPK inhibitors to patients may have adverse effects on vision due to its negative effect on *Lif* expression and LIF-dependent survival factors in the retina. Similar adverse effects may possibly be observed in other neurodegenerative diseases where LIF has a reported protective activity.[55–57] Thus, as a safety measure, p38 MAPK inhibitors may be designed not to cross retina – blood or brain – blood barriers, which may prevent potential neurodegenerative effects.

TNF signaling in the retina. Although most reports attribute TNF a devastating role in the retina and retinal diseases through the modulation of an inflammatory response,[28,29] our results demonstrate that intravitreal injection of TNF before light exposure did not accelerate degeneration. Rather, TNF reduced the relative average cell death by almost fourfold (0.27 ± 0.049 S.E.M., $N=6$ for vehicle *versus* 0.074 ± 0.07 S.E.M. for TNF, $N=5$). Even though these values did not reach statistical significance when tested in context of the additional experimental paradigms using analysis of variance (ANOVA), they showed a tendency for TNF-mediated protection of photoreceptors against light-induced degeneration (Figure 7). At least part of this effect may be explained by increased expression of *Lif* which leads to the upregulation of neuroprotective factors like *Fgf2*, *End2* and *Stat3* (Figure 4).[1,12]

Emerging evidence indicates that TNF may be a signaling molecule of general importance that has differential effects on disease outcome depending on the interaction with its receptors. In a retinal ischemia-reperfusion model, TNF-R2 signaling was neuroprotective whereas TNF-R1 increased neuronal death.[58] Moreover, a recent report suggests that TNF expression in dying photoreceptors and Muller cells is important for Muller cell proliferation and photoreceptor regeneration in a zebrafish model of LIRD.[19,59] Although the mammalian retina diverges from zebrafish in several ways including its limited proliferation and regeneration capacity of Muller cells,[60,61] these results together with our findings may nevertheless indicate a possible role of TNF for the protection of function in the stressed or injured mammalian retina. Clearly, further studies are warranted to elucidate the role of TNF signaling during photoreceptor degeneration in detail.

Materials and Methods

Animals. All experimental protocols were accepted by the Veterinary Authorities of Zurich and experiments were conducted in accordance with the statement of 'The Association for Research in Vision and Ophthalmology' for the use of animals in research. All mice had access to food and water *ad libitum* and were housed in a light–dark cycle of 12 : 12 h with 60 lux at cage level. All experimental conditions and time points were tested with a minimum of $N=3$ mice. All experimental mice were on a C57BL/6 background except for the light damage experiments in which mice of the SV129/S6 strain were used (Figure 7). For intravitreal injections after light exposure Rlbp::GFP mice[62] on a C57BL/6 background were used (Figure 6).

Cell culture assays

TNF and p38 MAPK inhibitor treatment rMC-1 cells[35] were cultured in Dulbecco's modified Eagle's medium (Life Technologies, Grand Island, NY, USA) supplemented with 10% fetal bovine serum (Life Technologies), 100 U/ml penicillin and 100 μg/ml streptomycin (Life Technologies), and grown in a humidified 5% CO_2 incubator as described in Sarthy *et al.*[35] Rat recombinant TNF (R&D Systems, Minneapolis, MN, USA) was dissolved in PBS containing 0.1% bovine serum albumin (BSA) (Sigma Aldrich, St Louis, MO, USA), the p38 MAPK inhibitors SB202190 and SB239063 (Sigma Aldrich) were dissolved in water or in DMSO (Sigma Aldrich), respectively. Compounds were added alone or in combinations directly to growth media at concentrations and times indicated in the Results section.

Luciferase assay rMC-1 cells were transfected using FuGENE6 reagent (Promega, Madison, WI, USA). Renilla luciferase expressing vector, pRL-CMV (Promega), was used as an internal control to normalize the transfection efficiency. Transfection solution was prepared in 91 μl Optimem (Life Technologies) media using 3 μg/ml of total plasmid DNA and 9 μl of FuGENE6 reagent according to manufacturer's instructions. The ratio of renilla to firefly plasmids was 1 : 9. Ten thousand cells in 100 μl growth media were seeded on a 96-well plate and each well was transfected with 3.3 μl of transfection solution after attachment. An EGFP reporter vector, EGFP-C1 (Clontech, Mountain View, CA, USA), was used to assess the transfection efficiency of rMC-1 cells, which was between 15 and 20%. Cells were transfected either with a control vector, pTAL-luc (Clontech), or with an NFκB reporter vector, pNFκB-luc (Clontech). TNF, SB202190 and TNF + SB202190 treatments were performed for 6 h starting at 24 h after transfection. TNF and SB202190 had final concentrations of 10 ng/ml and 100 μM, respectively. Each treatment was performed in triplicates in four independent experiments. Luciferase levels were measured using the Dual Luciferase kit (Promega).

Immunoblotting. Protein homogenates were prepared by sonication (Branson sonifier, 10 strokes of 0.3 s with 30% output) of isolated retinas in Tris-HCl (100 mM, pH 7.5 or pH 8.0). Protein concentrations were determined by Bradford using BSA as standard. Homogenates were mixed with an equal volume of 4X Laemmli sample buffer and a total of 40 μg/ml protein was loaded in each lane of 10% SDS-polyacrylamide gels. Samples were electrophoresed, blotted and probed as described previously in Bürgi *et al.*[12] To detect phospho-p38 MAPK (cat no. 840771; R&D Systems) and p38 MAPK (cat no. 9212; Cell Signaling, Danvers, MA, USA) primary antibodies were used at a dilution of 1 : 500 and 1 : 1000, respectively. The secondary antibody, anti-rabbit IgG peroxidase-linked (cat no. NA934; GE Healthcare, Pittsburgh, PA, USA), was used at a dilution of 1 : 10 000. We have used WesternBright Sirius HRP substrate (Advansta, Menlo Park, CA, USA) for chemiluminescence reaction. Fusion FX7 Advance imaging system (Vilber Lourmat, Torcy, France) with a CCD camera was used for digital signal detection. Recordings were taken at the dynamic range of exposure without binning. Calculations for exposure levels were performed using BioD1 software (Vilber Lourmat) without background subtractions.

RT-PCR analysis. Retinas were collected through a slit in the cornea, and total RNA was prepared and analyzed by real-time PCR (RT-PCR) as described previously in Bürgi *et al.*[12] Briefly, 10 ng cDNA was amplified in a LightCycler instrument (Roche Diagnostics, Basel, Switzerland) using appropriate primer pairs (Table 1) and SybrGreen Master mix (Roche). *Actb* was used as reference gene. For the analysis of gene expression in rMC-1 cells, total RNA was extracted using the Megamax RNA isolation kit (Life Technologies) according to manufacturer's instructions. cDNA was prepared using the high-capacity cDNA reverse transcription kit (Life Technologies). Real-time PCR reactions were conducted using appropriate primer pairs (Table 1) and *Actb* as internal control. Additional internal controls, *Gapdh* and *Rpl32*, were used for each new treatment. Real-time PCR reactions were performed in a StepOne Real-Time PCR system with Fast SybrGreen master mix (Life Technologies). The comparative cycle threshold method was used to calculate relative transcript levels for both mouse and rat experiments.

Intravitreal injections. Intravitreal injections were performed as previously described in Joly *et al.*[1] Rat recombinant TNF (R&D Systems) was reconstituted in sterile PBS containing 0.1% BSA (Sigma Aldrich) and injected at a concentration of 10 μg/ml. SB220025 trihydrochloride (Sigma Aldrich) was dissolved in water and adjusted to 6 mM using sterile PBS containing 0.1% BSA for injections. Sterile PBS containing 0.1% BSA was used for vehicle control injections. For the injection of TNF + SB220025, stock solutions for SB220025 and TNF were mixed and diluted with PBS containing 0.1% BSA to reach final injection concentrations of 10 μg/ml/ml and 6 mM for TNF and SB220025, respectively. Injection volume was 1 μl.

Light damage and cell death assay. Light damage and quantification of cell death by an ELISA-based cell death assay (Roche Diagnostics, Basel, Switzerland) were performed essentially as previously described in Bürgi *et al.*[12] and Samardzija *et al.*[10] with minor modifications. White light intensity for light damage was set to 13 000 lux, and 6–10-week-old animals with dilated pupils[12] were exposed for 2 h. Animals were kept in darkness overnight before and after light exposure. Animals were sacrificed and retinas were isolated for cell death assay at 40 h after light exposure.

Data analysis. Statistical analysis was performed using ANOVA with Dunnett's Multiple Comparison tests where multiple comparisons were made to a single value. ANOVA with Bonferroni post-test was performed for multiple

Table 1 Real-time PCR primer sequences

Gene	Species	Forward primer	Reverse primer
Cntf	Rn	CTCTGTAGCCGTTCTATCTG	GGTACACCATCCACTGAGTC[Rn/Mm]
Fgf2	Rn	GGCTGCTGGCTTCTAAGTGT	TCCGTGACCGGTAAGTGTTG
Gapdh	Rn	ATGACTCTACCCACGGCAAG	GGAAGATGGTGATGGGTTTC
Gfap	Rn	AGTGGTATCGGTCCAAGTTTGC	TGGCGGCGATAGTCATTAGC
Lif	Rn	ATGAAGGTCTTGGCCACAGG	GTATGGCGCAGGTGGCATT
Tnf	Rn	CCACGCTCTTCTGTCTACTGA[RN/MM]	GGCCATGGAACTGATGAGAGG
Rpl32[21]	Rn	AAGCGAAACTGGCGGAAAC	TAACCGATGTTGGGCATCAG
Actb	Rn/Mm	CAACGGCTCCGGCATGTGC[Rn/Mm]	CTCTTGCTCTGGGCCTCG[Rn/Mm]
Clc	Mm	CCCTGGCCCCTCCATCCAGAAA	TGCCCCCAGTCGAGGAGGATTG
Cntf	Mm	CTCTGTAGCCGCTCTATCTG	GGTACACCATCCACTGAGTC[Rn/Mm]
Edn2	Mm	AGACCTCCTCCGAAAGCTG	CTGGCTGTAGCTGGCAAAG
Fgf2	Mm	TGTGTCTATCAAGGGAGTGTGTGC	ACCAACTGGAGTATTTCCGTGACCG
Gapdh	Mm	CAGCAATGCATCCTGCACC	TGGACTGTGGTCATGAGCCC
Gfap	Mm	CCACCAAACTGGCTGATGTCTAC	TTCTCTCCAAATCCACACGAGC
Lif	Mm	AATGCCACCTGTGCCATACG	CAACTTGGTCTTCTCTGTCCCG
Lifr	Mm	ACTGAAGTGGAACGACAGAGG	CTTTACCACTCAGCATTGTGTTG
Pax6	Mm	AGTTCTTCGCAACCTGGCTA	CATCTGAGCTTCATCCGAGT
Stat3	Mm	CAAAACCCTCAAGAGCCAAGG	TCACTCACAATGCTTCTCCGC
Tnf	Mm	CCACGCTCTTCTGTCTACTGA[Rn/Mm]	CCACGCTCTTCTGTCTACTGA
Vim	Mm	TACAGGAAGCTGCTGGAAGG	TGGGTGTCAACCAGAGGAA

Rn, *Rattus norvegicus*; Mm, *Mus musculus*
Primers used for both rat and mouse samples are marked (Rn/Mm)

comparisons against independent controls. Student's *t*-tests were used for individual pairwise comparisons. *P*-values lower than 0.05 were considered to be significant. Error bars represent the standard error of the mean (S.E.M.). We also used the ROUT algorithm, with the coefficient Q value of 0.1, to detect possible outliers related to intravitreal injections. Graph Pad 6 software or Prism 5 (GraphPad Inc., San Diego, CA, USA) were used for all statistical analyses.

Conflict of Interest

The authors declare no conflict of interest.

Acknowledgements. We thank Dr. Vijay Sarthy (Northwestern University, Chicago, IL, USA) for providing rMC-1 cells. We also thank the members of the Institute of Laboratory Animal Science, University Hospital Zurich, for support in animal care. We wish to thank Swiss National Science Foundation and Velux Foundation for financial support to CG and CA. CA and CG designed the experiments. CA, AG, GT, CB, CI, DA, CC and CG performed the experiments. CA and CG wrote the manuscript.

1. Joly S, Lange C, Thiersch M, Samardzija M, Grimm C. Leukemia inhibitory factor extends the lifespan of injured photoreceptors *in vivo*. *J Neurosci* 2008; **28**: 13765–13774.
2. Leibinger M, Muller A, Andreadaki A, Hauk TG, Kirsch M, Fischer D. Neuroprotective and axon growth-promoting effects following inflammatory stimulation on mature retinal ganglion cells in mice depend on ciliary neurotrophic factor and leukemia inhibitory factor. *J Neurosci* 2009; **29**: 14334–14341.
3. Azadi S, Johnson LE, Paquet-Durand F, Perez MT, Zhang Y, Ekstrom PA *et al*. CNTF+BDNF treatment and neuroprotective pathways in the rd1 mouse retina. *Brain Res* 2007; **1129**: 116–129.
4. Campochiaro PA, Nguyen QD, Shah SM, Klein ML, Holz E, Frank RN *et al*. Adenoviral vector-delivered pigment epithelium-derived factor for neovascular age-related macular degeneration: results of a phase I clinical trial. *Hum Gene Ther* 2006; **17**: 167–176.
5. Frigg R, Wenzel A, Grimm C, Reme CE. [Survival factors in the treatment of hereditary retinal degeneration]. *Ophthalmologe* 2005; **102**: 757–763.
6. Grimm C, Wenzel A, Groszer M, Mayser H, Seeliger M, Samardzija M *et al*. HIF-1-induced erythropoietin in the hypoxic retina protects against light-induced retinal degeneration. *Nat Med* 2002; **8**: 718–724.
7. Sahel JA. Saving cone cells in hereditary rod diseases: a possible role for rod-derived cone viability factor (RdCVF) therapy. *Retina* 2005; **25**(8 Suppl): S38–S39.
8. Rattner A, Nathans J. The genomic response to retinal disease and injury: evidence for endothelin signaling from photoreceptors to glia. *J Neurosci* 2005; **25**: 4540–4549.
9. Schaeferhoff K, Michalakis S, Tanimoto N, Fischer MD, Becirovic E, Beck SC *et al*. Induction of STAT3-related genes in fast degenerating cone photoreceptors of cpfl1 mice. *Cell Mol Life Sci* 2010; **67**: 3173–3186.
10. Samardzija M, Wariwoda H, Imsand C, Huber P, Heynen SR, Gubler A *et al*. Activation of survival pathways in the degenerating retina of rd10 mice. *Exp Eye Res* 2012; **99**: 17–26.
11. Samardzija M, Wenzel A, Aufenberg S, Thiersch M, Reme C, Grimm C. Differential role of Jak-STAT signaling in retinal degenerations. *FASEB J* 2006; **20**: 2411–2413.
12. Burgi S, Samardzija M, Grimm C. Endogenous leukemia inhibitory factor protects photoreceptor cells against light-induced degeneration. *Mol Vis* 2009; **15**: 1631–1637.
13. Ueki Y, Wang J, Chollangi S, Ash JD. STAT3 activation in photoreceptors by leukemia inhibitory factor is associated with protection from light damage. *J Neurochem* 2008; **105**: 784–796.
14. Chollangi S, Wang J, Martin A, Quinn J, Ash JD. Preconditioning-induced protection from oxidative injury is mediated by leukemia inhibitory factor receptor (LIFR) and its ligands in the retina. *Neurobiol Dis* 2009; **34**: 535–544.
15. Groeger G, Mackey AM, Pettigrew CA, Bhatt L, Cotter TG. Stress-induced activation of Nox contributes to cell survival signaling via production of hydrogen peroxide. *J Neurochem* 2009; **109**: 1544–1554.
16. Bhatt L, Groeger G, McDermott K, Cotter TG. Rod and cone photoreceptor cells produce ROS in response to stress in a live retinal explant system. *Mol Vis* 2010; **16**: 283–293.
17. Mackey AM, Sanvicens N, Groeger G, Doonan F, Wallace D, Cotter TG. Redox survival signaling in retina-derived 661W cells. *Cell Death Differ* 2008; **15**: 1291–1303.
18. Groeger G, Quiney C, Cotter TG. Hydrogen peroxide as a cell-survival signaling molecule. *Antioxid Redox Signal* 2009; **11**: 2655–2671.
19. Nelson CM, Ackerman KM, O'Hayer P, Bailey TJ, Gorsuch RA, Hyde DR. Tumor necrosis factor-alpha is produced by dying retinal neurons and is required for muller glia proliferation during zebrafish retinal regeneration. *J Neurosci* 2013; **33**: 6524–6539.
20. Lorenzo JA, Jastrzebski SL, Kalinowski JF, Downie E, Korn JH. Tumor necrosis factor alpha stimulates production of leukemia inhibitory factor in human dermal fibroblast cultures. *Clinical Immunol Immunopathol* 1994; **70**: 260–265.
21. Hao S, Baltimore D. The stability of mRNA influences the temporal order of the induction of genes encoding inflammatory molecules. *Nature Immunol* 2009; **10**: 281–288.
22. Wajant H, Pfizenmaier K, Scheurich P. Tumor necrosis factor signaling. *Cell Death Differ* 2003; **10**: 45–65.
23. Figiel I. Pro-inflammatory cytokine TNF-alpha as a neuroprotective agent in the brain. *Acta Neurobiol Exp* 2008; **68**: 526–534.
24. Dolga AM, Granic I, Blank T, Knaus HG, Spiess J, Luiten PG *et al*. TNF-alpha-mediates neuroprotection against glutamate-induced excitotoxicity via NF-kappaB-dependent up-regulation of K2.2 channels. *J Neurochem* 2008; **107**: 1158–1167.
25. Saha RN, Liu X, Pahan K. Up-regulation of BDNF in astrocytes by TNF-alpha: a case for the neuroprotective role of cytokine. *J Neuroimmune Pharmacol* 2006; **1**: 212–222.
26. Tamatani M, Che YH, Matsuzaki H, Ogawa S, Okado H, Miyake S *et al*. Tumor necrosis factor induces Bcl-2 and Bcl-x expression through NFkappaB activation in primary hippocampal neurons. *J Biol Chem* 1999; **274**: 8531–8538.
27. Viemann D, Goebeler M, Schmid S, Klimmek K, Sorg C, Ludwig S *et al*. Transcriptional profiling of IKK2/NF-kappa B- and p38 MAP kinase-dependent gene expression in TNF-alpha-stimulated primary human endothelial cells. *Blood* 2004; **103**: 3365–3373.
28. Nakazawa T, Nakazawa C, Matsubara A, Noda K, Hisatomi T, She H *et al*. Tumor necrosis factor-alpha mediates oligodendrocyte death and delayed retinal ganglion cell loss in a mouse model of glaucoma. *J Neurosci* 2006; **26**: 12633–12641.

29. Roh M, Zhang Y, Murakami Y, Thanos A, Lee SC, Vavvas DG *et al.* Etanercept, a widely used inhibitor of tumor necrosis factor-alpha (TNF-alpha), prevents retinal ganglion cell loss in a rat model of glaucoma. *PLoS One* 2012; **7**: e40065.
30. Tezel G, Li LY, Patil RV, Wax MB. TNF-alpha and TNF-alpha receptor-1 in the retina of normal and glaucomatous eyes. *Invest Ophthalmol Vis Sci* 2001; **42**: 1787–1794.
31. Diem R, Meyer R, Weishaupt JH, Bähr M. Reduction of potassium currents and phosphatidylinositol 3-kinase-dependent AKT phosphorylation by tumor necrosis factor-(alpha) rescues axotomized retinal ganglion cells from retrograde cell death *in vivo*. *J Neurosci* 2001; **21**: 2058–2066.
32. Roth S, Shaikh AR, Hennelly MM, Li Q, Bindokas V, Graham CE. Mitogen-activated protein kinases and retinal ischemia. *Invest Ophthalmol Vis Sci* 2003; **44**: 5383–5395.
33. Kikuchi M, Tenneti L, Lipton SA. Role of p38 mitogen-activated protein kinase in axotomy-induced apoptosis of rat retinal ganglion cells. *J Neurosci* 2000; **20**: 5037–5044.
34. Drexler JC, Barone FC, Shaikh AR, Du E, Roth S. Mitogen-activated protein kinase p38alpha and retinal ischemic preconditioning. *Exp Eye Res* 2009; **89**: 782–790.
35. Jiang SY, Zou YY, Wang JT. p38 mitogen-activated protein kinase-induced nuclear factor kappa-light-chain-enhancer of activated B cell activity is required for neuroprotection in retinal ischemia/reperfusion injury. *Mol Vis* 2012; **18**: 2096–2106.
36. Sarthy VP, Brodjian SJ, Dutt K, Kennedy BN, French RP, Crabb JW. Establishment and characterization of a retinal Muller cell line. *Invest Ophthalmol Vis Sci* 1998; **39**: 212–216.
37. Underwood DC, Osborn RR, Kotzer CJ, Adams JL, Lee JC, Webb EF *et al.* SB 239063, a potent p38 MAP kinase inhibitor, reduces inflammatory cytokine production, airways eosinophil infiltration, and persistence. *J Pharmacol Exp Ther* 2000; **293**: 281–288.
38. Fox T, Coll JT, Xie X, Ford PJ, Germann UA, Porter MD *et al.* A single amino acid substitution makes ERK2 susceptible to pyridinyl imidazole inhibitors of p38 MAP kinase. *Protein Sci* 1998; **7**: 2249–2255.
39. Wang J, Zhang J, Ash JD. Leukemia inhibitory factor expression can be induced by agonist of TLR-2 or gp130, and may require NFkB or STAT3 binding to promoter elements. *ARVO* 2013; abstract 3251.
40. Jackson JR, Bolognese B, Hillegass L, Kassis S, Adams J, Griswold DE *et al.* Pharmacological effects of SB 220025, a selective inhibitor of P38 mitogen-activated protein kinase, in angiogenesis and chronic inflammatory disease models. *J Pharmacol Exp Ther* 1998; **284**: 687–692.
41. Bignami A, Dahl D. The radial glia of Muller in the rat retina and their response to injury. An immunofluorescence study with antibodies to the glial fibrillary acidic (GFA) protein. *Exp Eye Res* 1979; **28**: 63–69.
42. Kivela T, Tarkkanen A, Virtanen I. Intermediate filaments in the human retina and retinoblastoma. An immunohistochemical study of vimentin, glial fibrillary acidic protein, and neurofilaments. *Invest Ophthalmol Vis Sci* 1986; **27**: 1075–1084.
43. Ju WK, Lee MY, Hofmann HD, Kirsch M, Chun MH. Expression of CNTF in Muller cells of the rat retina after pressure-induced ischemia. *Neuroreport* 1999; **10**: 419–422.
44. Graham DR, Overbeek PA, Ash JD. Leukemia inhibitory factor blocks expression of Crx and Nrl transcription factors to inhibit photoreceptor differentiation. *Invest Ophthalmol Vis Sci* 2005; **46**: 2601–2610.
45. Ash J, McLeod DS, Lutty GA. Transgenic expression of leukemia inhibitory factor (LIF) blocks normal vascular development but not pathological neovascularization in the eye. *Mol Vis* 2005; **11**: 298–308.
46. Joly S, Francke M, Ulbricht E, Beck S, Seeliger M, Hirrlinger P *et al.* Cooperative phagocytes: resident microglia and bone marrow immigrants remove dead photoreceptors in retinal lesions. *Am J Pathol* 2009; **174**: 2310–2323.
47. Dean JL, Sully G, Clark AR, Saklatvala J. The involvement of AU-rich element-binding proteins in p38 mitogen-activated protein kinase pathway-mediated mRNA stabilisation. *Cell Signal* 2004; **16**: 1113–1121.
48. Craig R, Larkin A, Mingo AM, Thuerauf DJ, Andrews C, McDonough PM *et al.* p38 MAPK and NF-kappa B collaborate to induce interleukin-6 gene expression and release. Evidence for a cytoprotective autocrine signaling pathway in a cardiac myocyte model system. *J Biol Chem* 2000; **275**: 23814–23824.
49. Yang LP, Zhu XA, Tso MO. Role of NF-kappaB and MAPKs in light-induced photoreceptor apoptosis. *Invest Ophthalmol Vis Sci* 2007; **48**: 4768–4776.
50. Grimm C, Wenzel A, Hafezi F, Yu S, Redmond TM, Reme CE. Protection of Rpe65-deficient mice identifies rhodopsin as a mediator of light-induced retinal degeneration. *Nature Genet* 2000; **25**: 63–66.
51. Wenzel A, Reme CE, Williams TP, Hafezi F, Grimm C. The Rpe65 Leu450Met variation increases retinal resistance against light-induced degeneration by slowing rhodopsin regeneration. *J Neurosci* 2001; **21**: 53–58.
52. Tezel G. TNF-alpha signaling in glaucomatous neurodegeneration. *Prog Brain Res* 2008; **173**: 409–421.
53. Cohen P. Targeting protein kinases for the development of anti-inflammatory drugs. *Curr Opin Cell Biol* 2009; **21**: 317–324.
54. Marengo B, De Ciucis CG, Ricciarelli R, Furfaro AL, Colla R, Canepa E *et al.* p38MAPK inhibition: a new combined approach to reduce neuroblastoma resistance under etoposide treatment. *Cell Death Dis* 2013; **4**: e589.
55. Zigmond RE. gp130 cytokines are positive signals triggering changes in gene expression and axon outgrowth in peripheral neurons following injury. *Front Mol Neurosci* 2011; **4**: 62.
56. Bauer S, Rasika S, Han J, Mauduit C, Raccurt M, Morel G *et al.* Leukemia inhibitory factor is a key signal for injury-induced neurogenesis in the adult mouse olfactory epithelium. *J Neurosci* 2003; **23**: 1792–1803.
57. Cheema SS, Richards L, Murphy M, Bartlett PF. Leukemia inhibitory factor prevents the death of axotomised sensory neurons in the dorsal root ganglia of the neonatal rat. *J Neurosci Res* 1994; **37**: 213–218.
58. Fontaine V, Mohand-Said S, Hanoteau N, Fuchs C, Pfizenmaier K, Eisel U. Neurodegenerative and neuroprotective effects of tumor Necrosis factor (TNF) in retinal ischemia: opposite roles of TNF receptor 1 and TNF receptor 2. *J Neurosci* 2002; **22**: RC216.
59. Thomas JL, Nelson CM, Luo X, Hyde DR, Thummel R. Characterization of multiple light damage paradigms reveals regional differences in photoreceptor loss. *Exp Eye Res* 2012; **97**: 105–116.
60. Yurco P, Cameron DA. Responses of Muller glia to retinal injury in adult zebrafish. *Vis Res* 2005; **45**: 991–1002.
61. Ooto S, Akagi T, Kageyama R, Akita J, Mandai M, Honda Y *et al.* Potential for neural regeneration after neurotoxic injury in the adult mammalian retina. *Proc Natl Acad Sci USA* 2004; **101**: 13654–13659.
62. Vazquez-Chona FR, Clark AM, Levine EM. Rlbp1 promoter drives robust Muller glial GFP expression in transgenic mice. *Invest Ophthalmol Vis Sci* 2009; **50**: 3996–4003.

Curriculum Vitae

Christian Caprara

Curriculum Vitae

Personal Information

Date of Birth	31 December 1983
Nationality	Swiss
Address	Schaufelbergerstrasse 44, 8055 Zürich
E-mail	christian.caprara@uzh.ch
Phone	0041 79 611 36 96

Education and Research Experience

- 2009 – 2013: **PhD student at the Lab for Retinal Cell Biology, Dept of Ophthalmology, University Hospital Zürich, Switzerland**

  PhD Thesis: “Role of Hypoxia-Inducible Factor 1a and Erythropoietin in Retinal Physiology and Development”

  Supervised by Prof. Dr. Christian Grimm

  PhD Program in Integrative Molecular Medicine (imMed), Life Science Zürich Graduate School

- 2007 – 2008: **Master of Science (M.sc.) UZH in Biology, Molecular and Cellular Biology University of Zurich, Switzerland**

  Master Thesis: "Role of Palmitoylation and Ubiquitination for the Trafficking of the Cation-Dependent Mannose-6-Phosphate Receptor"

  Supervised by Prof. Dr. Jack Rohrer

- 2004 - 2007: **Bachelor of Science (B.sc) UZH in Biology, minor subject Biochemistry**
  University of Zurich, Switzerland

- 09.1999 - 06.2003 Liceo Cantonale, Bellinzona, Switzerland

Conferences

Oral Presentations

- Swiss Eye Research Meeting (SERM)
  January 24-25, **2013**
  Biel, Switzerland
  Intrinsically photosensitive retinal ganglion cells are resistant to N-methyl-D-aspartic acid excitotoxicity

- XX Biennial Meeting of the International Society for Eye Research (ISER)
  July 21-25, **2012**
  Berlin, Germany
  Invited Speaker
  Hypoxia-Inducible Factors in retinal angiogenesis and neuroprotection

- Swiss Eye Research Meeting (SERM)
  January 27-28, **2011**
  Biel, Switzerland
  HIF1A is essential for the development of the retinal vasculature

Poster Presentations

- 9th Symposium of the Zürich Center for Integrative Human Physiology (ZIHP)
  August 23, **2013**
  Zürich, Switzerland
  The Erythropoietin Receptor is not required for retinal function, development, and survival

- 12th Day of Clinical Research, University Hospital Zürich
  April 4, **2013**
  Zürich, Switzerland
  The Erythropoietin Receptor in retinal physiology, development and its implication in neuroprotection

- 7th Symposium of the Zürich Center for Integrative Human Physiology (ZIHP)
  August 28, **2011**
  Zürich, Switzerland
  HIF1A is essential for the development of the intermediate plexus of the retinal vasculature

- 6th retreat of the PhD Program in Integrative Molecular Medicine (ImMed)
  June 15-16, **2011**
  Kleine Scheidegg/Jungfraujoch, Switzerland
  HIF1A is essential for the development of the intermediate plexus of the retinal vasculature

- 10th Day of Clinical Research, University Hospital Zürich
  June 9, **2011**
  Zürich, Switzerland
  HIF1A is essential for the development of the intermediate plexus of the retinal vasculature

- Annual Meeting of the Association for Research in Vision and Ophthalmology (ARVO)
  May 2-6, **2010**
  Fort Lauderdale (FL), USA
  HIF1A is required for the development of the retinal vasculature

- 9th Day of Clinical Research, University Hospital Zürich
  April 8, **2010**
  Zürich, Switzerland
  HIF1A is required for the development of the retinal vasculature

Publications

Original Research Articles

- Caprara C, Britschgi C, Samardzija M, Grimm C. The erythropoietin receptor is dispensable for retinal physiology and development. Sent for publication to Mol. Vis. **2013**

- Agca C, Gubler A, Traber G, Beck C, Imsand C, Ail D, Caprara C, Grimm C. p38 MAPK signalling acts upstream of LIF-dependant neuroprotection during photoreceptor degeneration. Cell Death Dis. **2013**, Sep 5;4:e785

- Heynen SR, Meneau I, Caprara C, Samardzija M, Imsand C, Levine EM, Grimm C. CDC42 is required for tissue lamination and cell survival in the mouse retina. PLoS One. **2013**;8(1):e53806.

- DeParis S, Caprara C, Grimm C. Intrinsically photosensitive retinal ganglion cells are resistant to N-methyl-D-aspartic acid excitotoxicity. Mol Vis. **2012**;18:2814-27

- Lange C, Heynen SR, Tanimoto N, Thiersch M, Le YZ, Meneau I, Seeliger MW, Samardzija M, Caprara C, Grimm C. Normoxic activation of hypoxia-inducible factors in photoreceptors provides transient protection against light-induced retinal degeneration. Invest Ophthalmol Vis Sci. **2011** Jul 29;52(8):5872-80

- Caprara C, Thiersch M, Lange C, Joly S, Samardzija M, Grimm C. HIF1A is essential for the development of the intermediate plexus of the retinal vasculature. Invest Ophthalmol Vis Sci. **2011** Apr 4;52(5):2109-17

- Lange C, Caprara C, Tanimoto N, Beck S, Huber G, Samardzija M, Seeliger M, Grimm C. Retina-specific activation of a sustained hypoxia-like response leads to severe retinal degeneration and loss of vision. Neurobiol Dis. **2011** Jan;41(1):119-30

Review Articles

- Caprara C, Grimm C. From oxygen to erythropoietin: relevance of hypoxia for retinal development, health and disease. Prog Retin Eye Res. **2012** Jan;31(1):89-119.

Teaching Duties

- Tutorship at the practical course in physiology II for medicine student (B.sc.) **2010**

- Tutorship at the practical course in inorganic chemistry for biology students (B.sc.) **2005/6**

Courses

- WS 2009/2010: LTK module 1E: Introductory Course to Animal Science
- SS 2010: Mouse Physiology and Pathophysiology
- FS 2011: BIO 431: Advanced Physiology
- FS 2011: Scientific Writing
- HS 2011: Introduction in Neurosciences Part I
- HS 2012: Project Management for Research

Acknowledgements

I am grateful to many people, which have helped me in one or another way during my PhD.

First, I would like to acknowledge the members of my PhD committee Prof. Stephan Neuhauss, Prof. Max Gassmann, Dr. Botond Roska and Prof. Christian Grimm, for their precious and constructive advices during committee meetings and for reviewing my thesis.

In particular, I would like to give very special thanks to my PhD supervisor, Prof. Christian Grimm, for giving me the opportunity to conduct my PhD in his laboratory and thereby gain research experience. I would also like to thank him for the constant support, availability to discuss project outlines and results, and willingness to revise manuscripts. I would also like to thank Dr. Marijana Samardzija and Dr. Markus Thiersch, who have introduced me to most of the laboratory techniques and were always extremely helpful.

Additionally, I am very grateful to the current (Divya Ail, Marijana Samardzija, Jadwiga Oczos, Andrea Gubler, Christel Beck, Cornelia Imsand) and previous (Markus Thiersch, Cavit Agca, Christina Lange, Ghislaine Traber, Sandrine Joly, Corinne Britschgi, Véronique Wettstein, Sara Willcox, Hedwig Wariwoda, Philip Huber, Isabelle Meneau, Philipp Geiger) members of the laboratory for all the great times we spent together.

I am also thankful for the collaboration with the group of Prof. Mathias Seeliger (Gesine Huber, Susanne Beck, Naoyuki Tanimoto, Marina Garcia Garrido, Vithiyanjali Sothilingam) and their involvement in my projects.

Finally, I would like to thank my family, my friends and especially my girlfriend Alice for encouraging, supporting and motivating me during difficult times of my PhD.